NUTRITION, DISEASE, ENVIRONMENTAL STRESS, AND MICROORGANISMS IN CRUSTACEAN AQUACULTURE

EDITED BY: Yangfang Ye, Xiangli Tian, Chris Hauton and Ying Liu

PUBLISHED IN: Frontiers in Marine Science

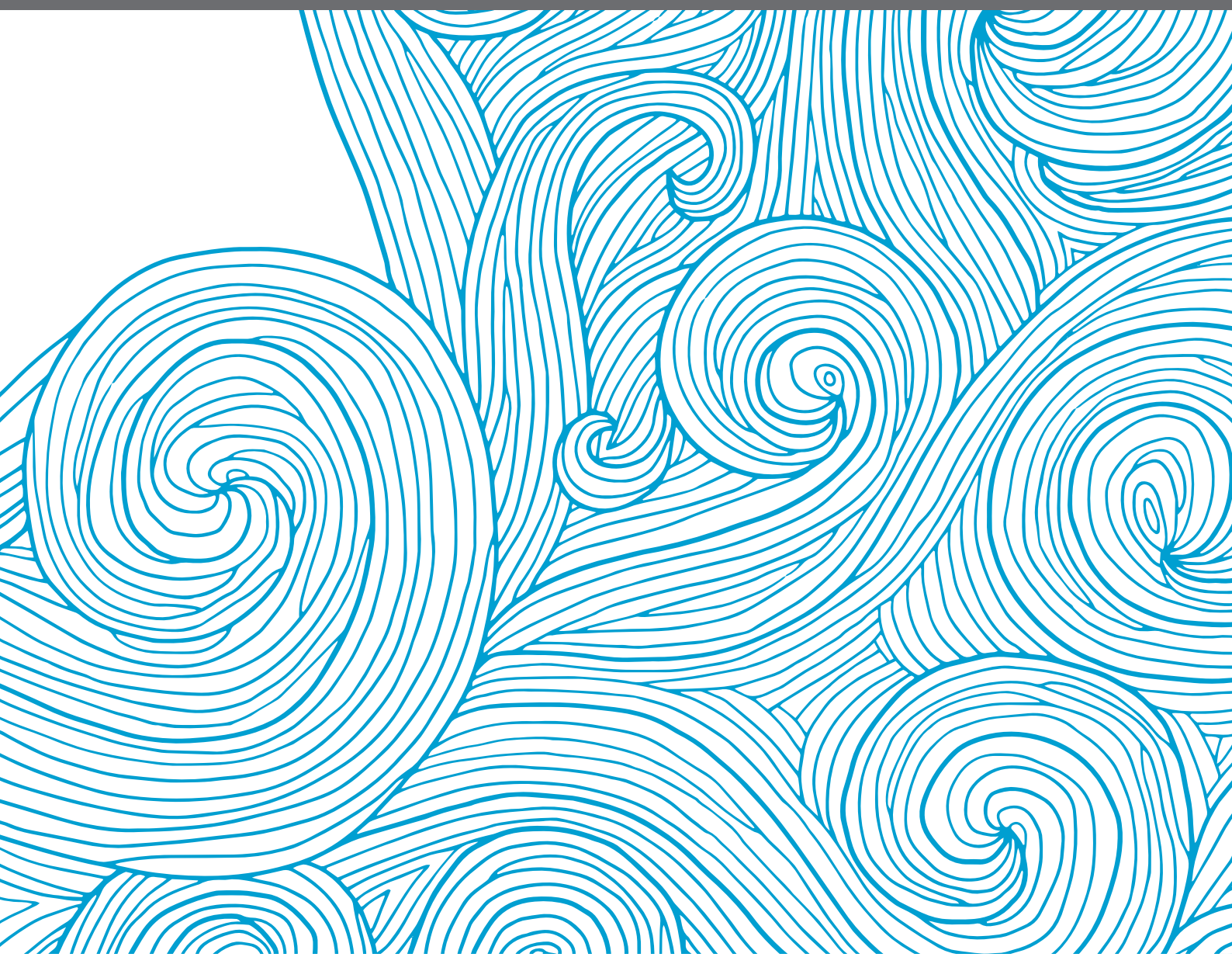

frontiers Research Topics

ISSN 1664-8714
ISBN 978-2-83250-351-5
DOI 10.3389/978-2-83250-351-5

About Frontiers

Frontiers is more than just an open-access publisher of scholarly articles: it is a pioneering approach to the world of academia, radically improving the way scholarly research is managed. The grand vision of Frontiers is a world where all people have an equal opportunity to seek, share and generate knowledge. Frontiers provides immediate and permanent online open access to all its publications, but this alone is not enough to realize our grand goals.

Frontiers Journal Series

The Frontiers Journal Series is a multi-tier and interdisciplinary set of open-access, online journals, promising a paradigm shift from the current review, selection and dissemination processes in academic publishing. All Frontiers journals are driven by researchers for researchers; therefore, they constitute a service to the scholarly community. At the same time, the Frontiers Journal Series operates on a revolutionary invention, the tiered publishing system, initially addressing specific communities of scholars, and gradually climbing up to broader public understanding, thus serving the interests of the lay society, too.

Dedication to Quality

Each Frontiers article is a landmark of the highest quality, thanks to genuinely collaborative interactions between authors and review editors, who include some of the world's best academicians. Research must be certified by peers before entering a stream of knowledge that may eventually reach the public - and shape society; therefore, Frontiers only applies the most rigorous and unbiased reviews.
Frontiers revolutionizes research publishing by freely delivering the most outstanding research, evaluated with no bias from both the academic and social point of view. By applying the most advanced information technologies, Frontiers is catapulting scholarly publishing into a new generation.

What are Frontiers Research Topics?

Frontiers Research Topics are very popular trademarks of the Frontiers Journals Series: they are collections of at least ten articles, all centered on a particular subject. With their unique mix of varied contributions from Original Research to Review Articles, Frontiers Research Topics unify the most influential researchers, the latest key findings and historical advances in a hot research area! Find out more on how to host your own Frontiers Research Topic or contribute to one as an author by contacting the Frontiers Editorial Office: frontiersin.org/about/contact

NUTRITION, DISEASE, ENVIRONMENTAL STRESS, AND MICROORGANISMS IN CRUSTACEAN AQUACULTURE

Topic Editors:
Yangfang Ye, Ningbo University, China
Xiangli Tian, Ocean University of China, China
Chris Hauton, University of Southampton, United Kingdom
Ying Liu, Zhejiang University, China

Citation: Ye, Y., Tian, X., Hauton, C., Liu, Y., eds. (2022). Nutrition, Disease, Environmental Stress, and Microorganisms in Crustacean Aquaculture. Lausanne: Frontiers Media SA. doi: 10.3389/978-2-83250-351-5

Table of Contents

frontiers | Frontiers in Marine Science

TYPE Editorial
PUBLISHED 12 October 2022
DOI 10.3389/fmars.2022.1056109

OPEN ACCESS

EDITED AND REVIEWED BY
Yngvar Olsen,
Norwegian University of Science and Technology, Norway

*CORRESPONDENCE
Yangfang Ye
yeyangfang@nbu.edu.cn

SPECIALTY SECTION
This article was submitted to Marine Fisheries, Aquaculture and Living Resources, a section of the journal Frontiers in Marine Science

RECEIVED 28 September 2022
ACCEPTED 04 October 2022
PUBLISHED 12 October 2022

CITATION
Ye Y (2022) Editorial: Nutrition, disease, environmental stress, and microorganisms in crustacean aquaculture. *Front. Mar. Sci.* 9:1056109. doi: 10.3389/fmars.2022.1056109

Editorial: Nutrition, disease, environmental stress, and microorganisms in crustacean aquaculture

Yangfang Ye*

School of Marine Sciences, Ningbo University, Ningbo, China

KEYWORDS

crustacean, nutrition, disease, environmental stress, aquaculture

Editorial on the Research Topic
Nutrition, disease, environmental stress, and microorganisms in crustacean aquaculture

According to Food and Agriculture Organization (FAO, 2022), global aquaculture production of crustaceans retained its growth trend in 2020 and reached 11.2 million tons, valued 81.5 billion US dollars. With the rapid expansion of aquaculture production of crustaceans (mainly shrimp and crabs), factors as nutrition, disease, and environmental stress are an existing constraint to the sustainability and growth of the global crustacean aquaculture industry (Asche et al., 2021). For a long time, the focus of traditional crustacean aquaculture studies has been primarily on crustaceans themselves (Ye et al., 2014; Ye et al., 2016; Chen and He, 2019; Ye et al., 2020; He et al., 2022), but nowadays the microbial communities hosted by the crustaceans have drawn attention of researchers.

In recent years, it is becoming increasingly clear that animals can no longer be considered as autonomous entities but rather as holobionts, encompassing the host plus its associated microbiota (McFall-Ngai et al., 2013; Bordenstein and Theis, 2015). This recognition has opened up a new field in biology and caused researchers to reexamine the questions on crustacean aquaculture. Therefore, it is crustaceans and their associated microbiotas that pull together to face factors as nutrition, disease, and environmental stress. Correspondingly, the field of crustacean microbiology has remarkably advanced in terms of information on the microbial functions in the nutrient digestion, disease defense, and stress response of the host.

Nutrients are critical in supporting the survival, development, and growth of crustaceans. Both live food and formulated diet should be digested before absorption by crustaceans. It is generally recognized that the gut microbiota provides the crustaceans with a complementary enzymatic arsenal for food ingestion (Dempsey and Kitting, 1987; Pinn et al., 1999; Lau et al., 2002; Oxley et al., 2002; Zbinden and Cambon-Bonavita, 2003). For example, bacteria and fungi in the hindgut assist digestion of wood fragments

for *Munidopsis andamanica* (Hoyoux et al., 2009). Further, the proteasome metabolic capacity of the intestinal bacteria may facilitate the feed protein utilization of *Litopenaeus vannamei* (Duan et al., 2020) while a more complex and cooperative gut eukaryotic interspecies interaction may facilitate nutrient acquisition efficiency of shrimp (Dai et al., 2017). However, every coin has two sides. Microorganisms such as viruses, bacteria, and fungi could be pathogens for crustaceans. Diverse diseases, such as emulsification disease of swimming crab (Wang et al., 2006) and white faeces syndrome of shrimp (Hou et al., 2018), have occurred in crustacean farming. The innate immune of crustaceans is vital for disease control. However, probiotics are considered as a practical alternative in disease prevention of crustaceans through immune enhancement, disease resistance, modulation of the gut microbiota, and competitive exclusion of pathogens (Castex et al., 2008; Talpur et al., 2012). For example, dietary supplementation of lactic acid bacteria (*Enterococcus faecalis* Y17 and *Pediococcus pentosaceus* G11) could modulate the immune system of mud crab and protect the host against *Vibrio parahaemolyticus* infection (Yang et al., 2019). Thus, the healthy gut microbiome affects the colonization, growth, and virulence of invading pathogens (Sassone-Corsi and Raffatellu, 2015; Bäumler and Sperandio, 2016; Xiong et al., 2019), which is vital for the fitness of host.

Crustaceans have been challenged with a variety of biotic and abiotic factors. The associated microbes of crustaceans have also been challenged and respond phylogenetically and functionally (Zheng et al., 2016; Shi et al., 2019; Lin et al., 2020; Lu et al., 2022). For example, the acute hepatopancreatic necrosis in diseased shrimp caused a gastrointestinal microbiota imbalance highlighted by the enrichment of *Vibrio* and the significantly increased gene abundances of the NOD receptor signaling pathway, *Vibrio* infection, and *Vibrio* pathogenic cycle function (Dong et al., 2021). Thus, changes in the microbial community could determine the ability of the crustacean to cope with biotic and abiotic stress, subsequently leading to resistance, resilience, disease, or acclimatization of crustacean holobiont upon stress.

In summary, this Research Topic delivers new ideas for crustacean aquaculture accomplished up to date. We also note that it is timely to scale up the crustacean concept from the simple autonomous entity to the complex holobiont, to further understand the nutrition, disease, and environmental stress in crustacean aquaculture.

Author contributions

The author confirms being the sole contributor of this work and has approved it for publication.

Funding

This work was funded by the National Natural Science Foundation of China (32073024), the earmarked fund for CARS-48, and K. C. Wong Magna Fund in Ningbo University.

Conflict of interest

The author declares that the research was conducted in the absence of any commercial or financial relationships that could be construed as a potential conflict of interest.

Publisher's note

References

Asche, F., Anderson, J. L., Botta, R., Kumar, G., Abrahamsen, E. B., Nguyen, L. T., et al. (2021). The economics of shrimp disease. *J. Invertebr. Pathol.* 186, 107397. doi: 10.1016/j.jip.2020.107397

Bäumler, A. J., and Sperandio, V. (2016). Interactions between the microbiota and pathogenic bacteria in the gut. *Nature* 535, 85–93. doi: 10.1038/nature18849

Bordenstein, S. R., and Theis, K. R. (2015). Host biology in light of the microbiome: ten principles of holobionts and hologenomes. *PloS Biol.* 13, e1002226. doi: 10.1371/journal.pbio.1002226

Castex, M. L., Chim, D., Pham, P., Lemaire, N., Wabete, J. L., Nicolas, P., et al. (2008). Probiotic p. acidilactici application in shrimp *Litopenaeus stylirostris* culture subject to vibriosis in new Caledonia. *Aquaculture* 275, 182–193. doi: 10.1016/j.aquaculture.2008.01.011

Chen, Y. H., and He, J. G. (2019). Effects of environmental stress on shrimp innate immunity and white spot syndrome virus infection. *Fish Shellfish Immun.* 84, 744–755. doi: 10.1016/j.fsi.2018.10.069

Dai, W., Yu, W., Zhang, J., Zhu, J., Tao, Z., and Xiong, J. (2017). The gut eukaryotic microbiota influences the growth performance among cohabitating shrimp. *Appl. Microbiol. Biotechnol.* 101 (16), 6447–6457. doi: 10.1007/s00253-017-8388-0

Dempsey, A. C., and Kitting, C. L. (1987). Characteristics of bacteria isolated from penaeid shrimp. *Crustaceana* 52 (1), 90–94. doi: 10.1163/156854087X00105

Dong, P., Guo, H., Wang, Y., Wang, R., and Zhang, D. (2021). Gastrointestinal microbiota imbalance is triggered by the enrichment of *Vibrio* in subadult *Litopenaeus vannamei* with acute hepatopancreatic necrosis disease. *Aquaculture* 533, 736199. doi: 10.1016/j.aquaculture.2020.736199

Duan, Y., Huang, J., Wang, Y., and Zhang, J. (2020). Characterization of bacterial community in intestinal and rearing water of *Penaeus monodon* differing growth performances in outdoor and indoor ponds. *Aquac. Res.* 51 (10), 4279–4289. doi: 10.1111/are.14770

FAO (2022). *The state of world fisheries and aquaculture 2022. towards blue transformation* (Rome: FAO).

He, Y., Lin, W., Shi, C., Li, R., Mu, C., Wang, C., et al. (2022). Accumulation, detoxification, and toxicity of dibutyl phthalate in the swimming crab. *Chemosphere* 289, 133183. doi: 10.1016/j.chemosphere.2021.133183

Hou, D., Huang, Z., Zeng, S., Liu, J., Wei, D., Deng, X., et al. (2018). Intestinal bacterial signatures of white feces syndrome in shrimp. *Appl. Microbiol. Biotechnol.* 102, 3701–3709. doi: 10.1007/s00253-018-8855-2

Hoyoux, C., Zbinden, M., Samadi, S., Gaill, F., and Compère, P. (2009). Wood-based diet and gut microflora of a galatheid crab associated with pacific deep-sea wood falls. *Mar. Bio.* 156, 2421–2439. doi: 10.1007/s00227-009-1266-2

Lau, W. W. Y., Jumars, P. A., and Armbrust, E. V. (2002). Genetic diversity of attached bacteria in the hindgut of the deposit-feeding shrimp *Neotrypaea* (formerly *Callianassa*) *californiensis* (Decapoda: Thalassinidae). *Microb. Ecol.* 43, 455–466. doi: 10.1007/s00248-001-1043-3

Lin, W., Ren, Z., Mu, C., Ye, Y., and Wang, C. (2020). Effects of elevated pCO_2 on survival and growth of *Portunus trituberculatus*. *Front. Physiol.* 11, 750. doi: 10.3389/fphys.2020.00750

Lu, J., Li, X., Qiu, Q., Chen, J., and Xiong, J. (2022). Gut interkingdom predator-prey interactions are key determinants of shrimp health. *Aquaculture* 546, 737304. doi: 10.1016/j.aquaculture.2021.737304

McFall-Ngai, M., Hadfield, M. G., Bosch, T. C., Carey, H. V., Domazet-Lošo, T., Douglas, A. E., et al. (2013). Animals in a bacterial world, a new imperative for the life sciences. *PNAS* 110, 3229–3236. doi: 10.1073/pnas.1218525110

Oxley, A. P., Shipton, W., Owens, L., and McKay, D. (2002). Bacterial flora from the gut of the wild and cultured banana prawn, *Penaeus merguiensis*. *J. Appl. Microbiol.* 93 (2), 214–223. doi: 10.1046/j.1365-2672.2002.01673.x

Pinn, E., Nickell, L., Rogerson, A., and Atkinson, R. J. A. (1999). Comparison of gut morphology and gut microflora of seven species of mud shrimp (Crustacea: Decapoda: Thalassinidea). *Mar. Biol.* 133, 103–114. doi: 10.1007/s002270050448

Sassone-Corsi, M., and Raffatellu, M. (2015). No vacancy: how beneficial microbes cooperate with immunity to provide colonization resistance to pathogens. *J. Immunol.* 194, 4081–4087. doi: 10.4049/jimmunol.1403169

Shi, C., Xia, M., Li, R., Mu, C., Zhang, L., Liu, L., et al. (2019). *Vibrio alginolyticus* infection induces coupled changes of bacterial community and metabolic phenotype in the gut of swimming crab. *Aquaculture* 499, 251–259. doi: 10.1016/j.aquaculture.2018.09.031

Talpur, A. D., Memon, A. J., Khan, M. I., Ikhwanuddin, M., Daniel, M. M. D., and Abol- Munafi, A. B. (2012). Control of *Vibrio harveyi* infection in blue swimming crab, *Portunus pelagicus* larvae by the gut isolated lactic acid bacteria under challenge bioassay. *Pak. Vet. J.* 32, 408–411.

Wang, G. L., Jin, S., Chen, Y., and Li, Z. (2006). Study on pathogens and pathogenesis of emulsification disease of *Portunus trituberculatus*. *Adv. Mar. Sci.* 24 (4), 526–531. doi: 10.3969/j.issn.1671-6647.2006.04.015

Xiong, J. B., Nie, L., and Chen, J. (2019). Current understanding on the roles of gut microbiota in fish disease and immunity. *Zool Res.* 40, 70–76. doi: 10.24272/j.issn.2095-8137.2018.069

Yang, Q., Lü, Y., Zhang, M., Gong, Y., Li, Z., Tran, N. T., et al. (2019). Lactic acid bacteria, *Enterococcus faecalis* Y17 and *Pediococcus pentosaceus* G11, improved growth performance, and immunity of mud crab (*Scylla paramamosain*). *Fish Shellfish Immun.* 93, 135–143. doi: 10.1016/j.fsi.2019.07.050

Ye, Y., An, Y., Li, R., Mu, C., and Wang, C. (2014). Strategy of metabolic phenotype modulation in *Portunus trituberculatus* exposed to low salinity. *J. Agr. Food Chem.* 62 (15), 3496–3503. doi: 10.1021/jf405668a

Ye, Y., Lin, W., Ren, Z., Mu, C., and Wang, C. (2020). Effects of ocean acidification on crabs. *Acta Hydrobiologica Sin.* 44 (4), 920–928. doi: 10.7541/2020.109

Ye, Y., Xia, M., Mu, C., Li, R., and Wang, C. (2016). Acute metabolic response of *Portunus trituberculatus* to *Vibrio alginolyticus* infection. *Aquaculture* 463, 201–208. doi: 10.1016/j.aquaculture.2016.05.041

Zbinden, M., and Cambon-Bonavita, M. (2003). Occurrence of *Deferribacterales* and *Entomoplasmatales* in the deep-sea alvinocarid shrimp *Rimicaris exoculata* gut. *FEMS Microbiol. Ecol.* 46 (1), 23–30. doi: 10.1016/S0168-6496(03)00176-4

Zheng, Y., Yu, M., Liu, Y., Su, Y., Xu, T., Yu, M., et al. (2016). Comparison of cultivable bacterial communities associated with pacific white shrimp (*Litopenaeus vannamei*) larvae at different health statuses and growth stages. *Aquaculture* 451, 163–169. doi: 10.1016/j.aquaculture.2015.09.020

frontiers in Marine Science

ORIGINAL RESEARCH
published: 23 September 2021
doi: 10.3389/fmars.2021.744281

Effects of *Bacillus velezensis* Supplementation on the Growth Performance, Immune Responses, and Intestine Microbiota of *Litopenaeus vannamei*

Lizhu Chen[1†], Chengjie Lv[2,3†], Bin Li[1], Huawei Zhang[1], Lihua Ren[1], Qianqian Zhang[2,3], Xiaoli Zhang[2,3], Jiqing Gao[1], Chunxiao Sun[1] and Shunxin Hu[1]*

[1] Shandong Provincial Key Laboratory of Marine Ecological Restoration, Shandong Marine Resource and Environment Research Institute, Yantai, China, [2] Muping Coastal Environment Research Station, Yantai Institute of Coastal Zone Research, Chinese Academy of Sciences, Yantai, China, [3] Research and Development Center for Efficient Utilization of Coastal Bioresources, Yantai Institute of Coastal Zone Research, Chinese Academy of Sciences, Yantai, China

OPEN ACCESS

Edited by:
Yangfang Ye,
Ningbo University, China

Reviewed by:
Bin Xia,
Qingdao Agricultural University, China
Yanjiao Zhang,
Ocean University of China, China
Yancui Zhao,
Ludong University, China

***Correspondence:**
Shunxin Hu
hushunxin001@163.com

[†]These authors have contributed equally to this work

Specialty section:
This article was submitted to Marine Fisheries, Aquaculture and Living Resources, a section of the journal Frontiers in Marine Science

Received: 20 July 2021
Accepted: 23 August 2021
Published: 23 September 2021

Citation:
Chen L, Lv C, Li B, Zhang H, Ren L, Zhang Q, Zhang X, Gao J, Sun C and Hu S (2021) Effects of Bacillus velezensis Supplementation on the Growth Performance, Immune Responses, and Intestine Microbiota of Litopenaeus vannamei. Front. Mar. Sci. 8:744281. doi: 10.3389/fmars.2021.744281

In the present study, *Bacillus velezensis* (BV007, CGMCC No. 20039) was isolated from the gut of *Litopenaeus vannamei*, and the effects of BV007 on the growth performance, immune responses, and intestine microbiota of the shrimp were investigated. A total of 1,200 healthy shrimp (3.0 ± 0.3 cm, 0.32 ± 0.8 g) were randomly divided into four groups, and fed diets supplemented with different levels of BV007 (C: 0; BV1: 1×10^5 CFU/g; BV2: 1×10^7 CFU/g; and BV3: 1×10^9 CFU/g) for 8 weeks. The results showed a significantly increased final body length (FBL), length gain rate (LGR), final body weight (FBW), weight gain rate (WGR), plumpness index (PI), and specific growth rate (SGR) in shrimp fed with BV007 for 42 days compared with shrimp fed with control diet. The activity of α-amylase in hepatopancreas was also significantly increased in the BV007-administered groups. After 42 days of growth trial, the challenge test with *Vibrio parahaemolyticus* was conducted for 2 weeks. The enhanced immune responses were exhibited by shrimp fed with BV007 after *V. parahaemolyticus* challenge, particularly in respiratory bursts and superoxide dismutase, catalase, and alkaline phosphatase activities. Moreover, the administration of BV007 could considerably increase the abundance of potential probiotics (*Bacillus*) and reduced the abundances of potential pathogenic bacteria (*Vibrio*) in shrimp intestines. In conclusion, the dietary supplementation with *B. velezensis* BV007 could promote the growth performance, enhance the immune responses, and modulate the intestine microbiota of shrimp, and 10^7 CFU/g feed was recommended to be used as a feed additive to enhance the growth and health status of shrimp.

Keywords: *Litopenaeus vannamei, Bacillus velezensis*, growth performance, innate immunity, intestinal health

INTRODUCTION

The Pacific white shrimp *Litopenaeus vannamei* is one of the major cultivated aquaculture crustacean species worldwide. In recent years, shrimp aquaculture has developed rapidly and intensively, but the low growth rates and disease have occurred more frequently, causing considerable economic losses (Neiland et al., 2001). The use of hormones and antibiotics as a traditional way to prevent and treat infectious diseases has led to the evolution of pathogenic bacteria and environmental pollution. Great effort has been invested to develop the potential alternatives to antibiotics to avoid the creation of bacterial resistance and high antibiotic residues. Currently, probiotics, prebiotics, and medicinal herbs have shown to be a vital alternative additive for the improvement of host health (Raman et al., 2019; Dawood et al., 2020; Zhang et al., 2021).

Probiotics are valuable in animal production due to their improvement of feed value, enzymatic contribution to digestion, and activation of the immune responses (Gao et al., 2018; Wang Y. et al., 2019; Qin et al., 2020). For example, oral administration of *Bacillus* PC465 enhanced the growth performance and survival rate of *L. vannamei* (Chai et al., 2016). Dietary supplementation with *B. licheniformis* at 10^5 CFU/ml for 8 weeks enhanced abalones growth and enhanced disease resistance to *Vibrio parahemolyticus* (Gao et al., 2018). Moreover, the activities of glutamic-pyruvic transaminase (GPT) and glutamic oxaloacetic transaminase (GOT) were significantly lower in shrimp fed with *Enterococcus faecalis* supplemented groups as compared with control shrimp (Wang Y. et al., 2019). In addition, dietary *Bacillus amyloliquefaciens* A23 at 10^8 CFU/g significantly enhanced the intestinal microbial diversity of *Procambarus clarkii* (Xu et al., 2021). Besides the promotion of *Lac. pentosus,* BD6 feeding can increase the relative abundance of beneficial bacteria and reduce the abundance of harmful pathogenic bacteria in the gut flora of shrimp, thus regulating the host immune system (Lin et al., 2017).

Although many studies suggest that *B. subtilis* possesses a number of beneficial traits when used as a supplement in the shrimp diets (Liu et al., 2010; Fu et al., 2011; Zokaeifar et al., 2012, 2014; Interaminense et al., 2018, 2019), few studies have investigated the appropriate dose of *B. velezensis* in *L. vannamei* farming. Therefore, the current study aimed to find the optimum supplementation level of *B. velezensis* and to investigate the potential effect on the growth performance, feed utilization, immune responses, and gut microbiota of *L. vannamei*.

MATERIALS AND METHODS

Bacterial Strain and Diet Preparation

Bacillus velezensis (named as BV007) was previously isolated from healthy *L. vannamei* intestines. The intestines were immersed in sterile phosphate buffered saline (PBS) (0.05 M, pH 7.4), shook, and eluted at 30°C for 30 min. Spread the eluate on LB nutrient agar (Beijing Land Bridge Tech. Co. Ltd.) plates with gradient dilution and incubated at 30°C for 24 h. After picking a single colony and streaking for purification, the strain 007 with a wide range of enzyme-producing abilities was obtained. The genetic characterization of *B. velezensis* was accomplished by using 16S rDNA sequence analysis, and the strain was deposited by the China General Microbiological Culture Center (CGMCC no. 20039).

In the diet preparation, the bacterial strains were inoculated in nutrient broth, collected in sterilized water, and adjusted to 10^9 CFU/ml before feed production. The ingredients of the basal diet were measured to contain 41.35% crude protein and 7.67% crude lipid with fish meal, corn gluten meal, and soybean meal as the fundamental protein source whereas the main lipid sources were soybean oil and soy lecithin oil. Three experimental diets were supplemented with different levels of BV007: 10^5 CFU/g (BV1), 10^7 CFU/g (BV2), and 10^9 CFU/g (BV3). The group without BV007 was served as a control (C). The bacterial amounts of experimental diets were also confirmed by the plate count method, and the colonies that emerged on the plates were counted. The four formulated experimental diets were extruded through a 1.2-mm die. The resulting pellets were dried at 25°C with the aid of an air conditioner. After drying, all diets were stored at 4°C until usage.

Experimental Design and Daily Management

Healthy *L. vannamei* (body length: 3.0 ± 0.3 cm, body weight: 0.32 ± 0.8 g) were purchased from a local farm (Yantai, Shandong Province, China) and acclimated at 25–27°C and 30% of salinity for 2 weeks before processing. The shrimp were randomly dispersed into 12 fiberglass tanks (60 L), each containing 100 shrimp. The shrimp were fed four times daily (06:00, 12:00, 17:00, and 22:00) at 6% of body weight. The cumulative mortality of the shrimp was recorded daily. After 42 days of feeding, the total number of shrimp and the weight in each tank was quantified to calculate the survival rate (SR, in percentage), final body weight (FBW), final body length (FBL), plumpness index (PI), specific growth rate (SGR, %/d) according to the methods described previously (Velmurugan et al., 2015; Amoah et al., 2019b).

Sample Collection

Hemolymph samples (eight replicates were tested in each treatment, and three shrimps were tested in each replicate [$n = 24$]) were individually withdrawn from the pericardial cavity of the shrimp using a 1-ml sterile syringe containing an anticoagulant (30 mM trisodium citrate, 0.34 M sodium chloride, and 10 mM EDTA at pH 7.55 with an osmolality adjusted to 780 mOsm/kg with glucose). The volume ratio of anticoagulant to hemolymph was 1:1. The harvested hemocytes were centrifuged at 4°C, 4,000 rpm/min for 10 min, collected, and adjusted to 10^6 cells/ml with PBS (0.05 M, pH 7.4) for the phagocytic activity and respiratory burst assays. In addition, the hepatopancreas was collected for the assay of digestive, antioxidant, and immune-related enzyme activities, eight replicates were tested in each treatment, and three shrimps were tested in each replicate ($n = 24$). The middle intestines and hepatopancreas of each group were collected sterile into 4% paraformaldehyde and stored at 4°C for the analysis of microorganisms (three parallel assays).

Phagocytosis Assay

The phagocytosis assay was adapted from the method of Delaporte (Delaporte et al., 2003) with minor modifications. Briefly, the hemolymph was mixed with 2.3% yellow-green FluoSpheres (diameter 2.0 μm, Polyscience, Eppelheilm, Germany), and incubated in the dark at 18 °C for 1 h with rotation. After incubation, the hemocytes were analyzed by flow cytometry (BD Accuri C6 Plus, BD Biosciences, America) using the FL-1 tunnel to detect hemocytes containing fluorescent beads. The phagocytosis rates were expressed as the percentage of hemocytes that engulfed three or more beads.

Respiratory Burst Activity

Respiratory burst activity was analyzed according to the protocols described by Kalgraff et al., 2011. Briefly, hemocytes (1×10^6 cells/ml) were challenged by phorbol 12-myristate 13-acetate (PMA; final concentration of 0.1 μg/ml) for 10 min. Subsequently, dihydrorhodamine 123 (DHR 123) was added to a final concentration of 2 μg/ml and then incubated for 30 min prior to flow cytometry analysis. The flow cytometry analyses were done on a BD FACSCalibur flow cytometer equipped with a 15 mW 488 nm argon ion laser. Further data analyses were done using FCS Express 3 software (De Novo Software, CA, USA).

Assay of Digestive and Immune-Related Enzymes

The digestive enzymes and immune enzymes were measured as described by Cao et al. (2012). Briefly, the digestive enzymes included α-amylase (AMS), trypsin (TRP), lipase (LPS), gltamic-pyruvic transaminase (GPT), glutamic oxaloacetic transaminase (GOT), and the immune enzymes included catalase (CAT), superoxide dismutase (SOD), acid phosphatase (ACP), and alkaline phosphatase (AKP). The enzymatic activities were quantified with corresponding commercial detection kits (C016-1-1, A080-2-2, A054-1-1, C009-2-1, C010-2-1, A007-1-1, A001-3-2, A001-3-1, and A060-2-1, Nanjing Jiancheng Bioengineering Institute, P.R. China) according to the instructions of the manufacturer.

Real-Time PCR Analysis

Total RNA was isolated from hepatopancreas of different treatments using RNAiso (TaKaRa, Japan) reagent. cDNA synthesis was performed according to Promega M-MLV RT Usage information. The temporal expression profiles were carried out with an Applied Biosystem 7500 fast real-time PCR system (Applied Biosystems, MA, USA) using SYBR Green I (Biotek, VT, USA). The PCR amplification program was 95°C for 10 min, then 40 cycles of 95°C for 15 s, 60°C for 1 min, followed by 95°C for 15 s, 60°C for 1 min, and 95°C for 15 s. At the end of each PCR, a dissociation curve analysis of amplification products was performed to confirm the purity of the PCR product. The $2^{-\Delta\Delta CT}$ method was used to analyze the expression levels (Livak and Schmittgen, 2001). All data were given in terms of relative mRNA expressed as mean ± SD ($N = 6$). The primers for qRT-PCR of genes for antioxidant-related genes (*cat* and *sod*), antibacterial peptides genes (*crustin* and *penaiedin 3a*), pattern recognition receptors (*lgbp* and *lec*), along with the housekeeping gene β-*actin*, are shown in **Table 1**.

Histopathological Examination of the Intestine and Hepatopancreas

Three similar-sized shrimp from each tank were sampled and dissected to obtain the midgut and the hepatopancreas (5 mm^3). The fixed intestinal and hepatopancreas samples were dehydrated in a graded series of ethyl alcohol and embedded in paraffin. Then, the paraffin blocks were sliced transversely into 5-μm thick sections and stained with H&E. The villus length of intestinal slice and the cell type of hepatopancreas slice were measured by a light microscope with a computerized image system (Olympus, DP73, Tokyo, Japan).

Intestinal Microbial Composition

The intestinal community of the micro-organisms was performed according to Suo (Suo et al., 2017) with slight changes. The total DNA of microbes in the intestine was extracted directly with the E.Z.N.A. Stool DNA Kit (Omega Bio-tek, Inc., GA, USA) (Xin et al., 2015). The amplification and sequencing of the hypervariable region (V4 + V5) of the bacterial 16S DNA gene was performed for the sequencing analysis and species identification. High-throughput sequencing was performed on the IonS5TMXL platform (Novogene, China). The sequencing reads were assigned to each sample according to the individual unique barcode. The sequences were analyzed with the QIIME software package (Quantitative Insights Into Microbial Ecology) and the UPARSE pipeline (Caporaso et al., 2011). The reads were first filtered and clustered into operational taxonomic units (OTUs) at an identity threshold of 97%. The alpha and beta diversity analyses were then performed as described by Amoah et al. (2019b).

Vibrio Parahaemolyticus Challenge

Vibrio parahaemolyticus was used for the challenge experiment (Amoah et al., 2019b). At the end of the culture experiment, 30 shrimps from each tank were injected with *V. parahaemolyticus* (final concentration 2×10^7 CFU). In each tank, 20 shrimps were used for cumulative mortality assay, which was recorded daily for 14 days. The other 10 shrimps were cultured for immunoassays and 1 week after bacterial challenge, both the hemocytes and hepatopancreas were sampled and analyzed as described above. In addition, each treatment group was continuously fed with the experimental diets. The cumulative mortality rate was calculated following the formula of Liu et al. (2017).

Statistical Analysis

The experimental data are presented as the mean ± SE. The data were statistically analyzed for significance using a one-way ANOVA, and then the differences among the means at $P < 0.05$ were tested with Duncan's multiple range test using SPSS 23.0 (SPSS Inc., 2005, IL, USA).

TABLE 1 | Primers used to amplify immune-related genes in the present study.

Primer	Sequence information	Accession number
cat F	CATCCAGGATCGAGCAATCAA	AY518322
cat R	TGAAGCCTGGCTCATCTTTATC	
sod F	TGCCACCTCTCAAGTATGATTTC	AB108065
sod R	TCAACCAACTTCTTCGTAGCG	
crustin F	GAGGGTCAAGCCTACTGCTG	AY488497
crustin R	ACTTATCGAGGCCAGCACAC	
pen 3α F	CTCGTGGTCTGCCTGGTCTTCTTG	Y14926
pen 3α R	CAGGGCAACCGTTGTATGGA	
lgbp F	TGGACGCTTATGTCACCTAC	AY249858
lgbp R	CTTCTACTTCATCTGTTGCT	
lec F	GATCGAGGACTGCGAAACCT	BF024206
lec R	CCCCAGAAAGGTACACCCTG	
β-*actin* F	GAGCAACACGGAGTTCGTTGT	AF300705
β-*actin* R	CATCACCAACTGGGACGACATGGA	

pen 3α, penaeidin 3α; lgbp. Lipopolysaccharide and β-1, 3-glucan binding protein; lec, lectin.

TABLE 2 | Effects of different supplementation levels of *B. velezensis* BV007 on the growth performance and survival of *L. vannamei*.

Items	Treatments			
	C	BV 1	BV 2	BV 3
FBL (cm)	9.25±0.36^{b}	9.95±0.41^{a}	9.9±0.45^{a}	9.87±0.40^{a}
LGR (%)	167.96±15.15^{b}	181.63±10.42^{a}	183.63±18.25^{a}	181.64±9.92^{a}
FBW (g)	4.78±1.22^{b}	5.59±0.40^{a}	5.58±0.37^{a}	5.68±0.29^{a}
WGR (%)	1481.41±112.47^{b}	1781.66±85.52^{a}	1849.82±122.80^{a}	1837.64±83.66^{a}
SGR (%)	16.60±0.30^{b}	17.21±0.26^{a}	17.37±0.23^{a}	17.35±0.23^{a}
PI (g/cm)	0.52±0.03^{b}	0.57±0.02^{a}	0.57±0.03^{a}	0.58±0.02^{a}
SR (%)	84.71±10.24	86.64±4.07	80.41±1.76	78.53±2.27

IBL, initial body length; FBL, final body length; LGR, length gain rate; IBW, initial body weight; FBW, final body weight; WGR, weight gain rate; SGR, specific growth rate; PI, plumpness index; SR, survival rate; and CMR, cumulative mortality rate after infection. The values (mean of 10 replicates ± SE) with different letters (a, b, c) represent statistically significant differences based on the LSD method ($P < 0.05$, one-way ANOVA).

RESULT

Growth Performance and Survival

The growth performance and survival of *L. vannamei* fed experimental diets are shown in **Table 2**. The results showed that FBL, FBW, PI, and SGR were significantly improved by the different levels of probiotics supplementation, whereas no significant differences were observed in SR among the control and probiotic diets.

Phagocytic and Respiratory Burst Activity

After 42 days of feeding, there was a significant increase in the phagocytic activity of shrimp fed diets supplemented with *B. velezensis* as compared to the control group (**Figure 1A**). However, no significant increase in the rates of phagocytosis was found in either the probiotics-supplemented or non-supplemented shrimps after the *V. parahaemolyticus* challenge (**Figure 1B**). Compared with the control group, significantly reduced reactive oxygen species (ROS) production was observed in the BV3 group, but not in the BV1 or BV2 groups (**Figure 1C**). In contrast, the production of ROS by hemocytes decreased statistically in the BV1, BV2, and BV3 groups when shrimp were challenged with *V. parahaemolyticus* ($P < 0.01$; **Figure 1D**).

Digestive Enzyme Activities

As shown in **Table 3**, the specific activity of the α-amylase enzyme was enhanced in *B. velezensis*-supplemented groups. As compared with the control group, the AMS activity was enhanced significantly in shrimp fed BV1, BV2, and BV3 diets with the highest activity observed in the BV2 group ($P < 0.01$). However, no significant differences were observed in TRP or LPS activities among any of the groups. In addition, the GOT and GPT activities were significantly reduced in the BV3 and BV1 groups as compared with the control group, respectively ($P < 0.05$).

Immune-Related Enzyme Activities

The activities of ACP showed no differences among the tested groups after being challenged with *V. parahaemolyticus* (**Table 4**). Similarly, no significant difference in AKP activity

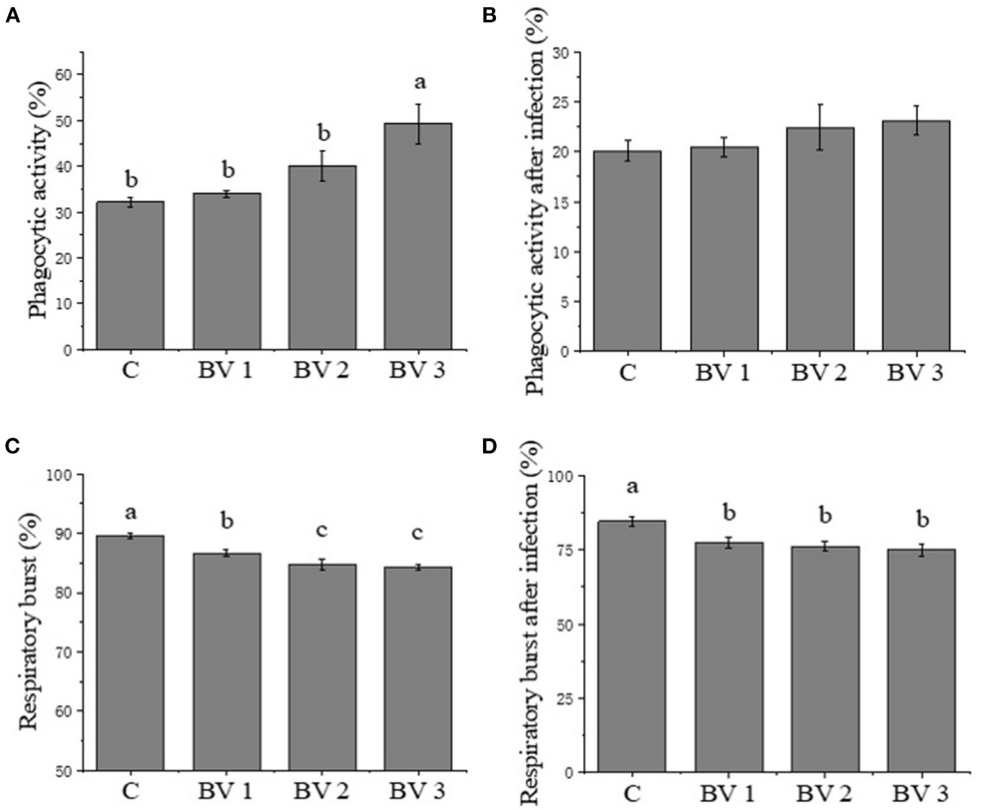

FIGURE 1 | (A-D) Phagocytic activity and respiratory burst activity of hemocytes in *Litopenaeus vannamei* fed diets containing *Bacillus velezensis* concentration of 0 CFU/g (C), 10^5 CFU/g (BV1), 10^7 CFU/g (BV2), and 10^9 CFU/g (BV3) for 6 weeks and then infected with *Vibrio parahaemolyticus* for 1 week. Error bars with different letters (a, b, c) represent statistically significant differences based on the least significant difference (LSD) method ($P < 0.05$, one-way ANOVA). The results were shown as mean ± SE ($N = 12$).

TABLE 3 | Digestive enzyme activities in the hepatopancreas of *L. vannamei* fed diets containing 0 CFU/g (C), 10^5 CFU/g (BV1), 10^7 CFU/g (BV2), 10^9 CFU/g (BV3) *B. velezensis* for 6 weeks.

Items	Treatments			
	C	BV 1	BV 2	BV 3
LPS (U/gprot)	57.02±4.33	57.28±7.00	57.28±7.00	54.16±5.20
TRP (U/gprot)	117.57±16.39^{b}	122.62±10.35^{ab}	157.98±12.32^{a}	153.88±13.88^{a}
AMS (U/gprot)	5.21±0.15^{b}	5.62±0.09^{ab}	5.94±0.12^{a}	5.23±0.17^{b}
GPT (U/mgprot)	97.61±11.49^{a}	53.52±6.07^{b}	66.93±9.80^{b}	76.91±12.88^{ab}
GOT (U/mgprot)	38.86±2.37^{a}	34.42±3.83^{ab}	29.81±4.51^{ab}	26.94±1.76^{b}

The values (mean of 8 replicates ± SD) with different letters (a, b, c) represent statistically significant differences based on LSD method ($P < 0.05$, one-way ANOVA). LPS, lipase; TRP, trypsin; AMS, α-amylase; GPT, gltamic-pyruvic transaminase; COT, glutamic oxaloacetic transaminase.

was detected among the BV1, BV2, and BV3 groups. However, the AKP activity was enhanced significantly after *V. parahaemolyticus* challenge among the tested groups ($P < 0.01$; **Table 4**). Both the CAT and SOD activities were enhanced in *B. velezensis*-supplemented groups and in the groups challenged with pathogenic bacteria (**Table 4**). The highest SOD and CAT activities were observed in the BV2 ($P < 0.01$; **Table 4**) and BV3 ($P < 0.01$; **Table 4**) groups.

Expression of Immune-Related Genes

As revealed in **Figure 2**, the feeding dosage of *B. velezensis* had a significant effect on the expression levels of immune-related genes. The expression levels of *cat* were significantly induced in BVs groups ($P < 0.05$, **Figure 2A**). After *V. parahaemolyticus* challenge, the *cat* transcripts in BV1 group were significantly higher than other groups ($P < 0.05$, **Figure 2A**). As concerned to *sod* expression, the higher expression levels were observed in BV2 and BV3 groups compared with C and BV1 groups, while

TABLE 4 | Immune-related enzyme activities in the hepatopancreas of *L. vannamei* fed diets containing 0 CFU/g (C), 10^5 CFU/g (BV1), 10^7 CFU/g (BV2), or 10^9 CFU/g (BV3) *B. velezensis* for 6 weeks and then, infected with 10^7 CFU/ml *V. parahaemolyticus* for one week (use words with a superscript comma).

Items	Treatments			
	C	BV 1	BV 2	BV 3
SOD (U/mgprot)	23.25±1.20^{b}	25.48±0.92^{b}	29.09±0.79^{a}	29.50±0.83^{a}
SOD′ (U/mgprot)	17.99±1.56^{b}	21.05±0.85^{ab}	23.57±1.57^{a}	21.64±0.77^{a}
CAT (U/mgprot)	29.14±2.37^{b}	44.26±9.96^{ab}	71.69±5.30^{a}	58.39±3.37^{a}
CAT′ (U/mgprot)	23.62±2.43^{b}	49.70±6.64^{a}	59.82±5.75^{a}	51.05±8.50^{a}
AKP (U/gprot)	22.77±3.83^{b}	28.55±5.19^{ab}	36.39±3.76^{a}	29.30±4.32^{ab}
AKP′ (U/gprot)	65.31±2.38^{b}	88.13±7.26^{ab}	93.37±7.59^{a}	86.79±7.47^{ab}
ACP (U/gprot)	168.51±12.48	183.43±22.56	200.06±23.97	152.77±15.12
ACP′ (U/gprot)	115.39±3.83^{a}	123.18±8.77^{a}	138.98±10.48^{a}	101.72±12.43^{b}

The values (mean of 8 replicates ± SD) with different letters (a, b, c) represent statistically significant differences based on the LSD method ($P < 0.05$, one-way ANOVA). SOD, superoxide dismutase; CAT, catalase; AKP, alkaline phosphatase; ACP, acid phosphatase.

the levels were significantly upregulated in BV1 and BV2 groups after the bacterial challenge ($P < 0.05$, **Figure 2B**). No significant changes in the expression levels of antibacterial peptides (*crustin* and *penaeidin 3α*) were observed among C, BV1, BV2, and BV3 groups. After the bacterial challenge, the expression levels of *crustin* and *penaeidin 3α* in BV2 were significantly higher than the other groups ($P < 0.05$, Figures 2C,D). In addition, the expression levels of *lgbp* and *lec* were highly enhanced regardless of whether the shrimp were bacterial challenged, especially in BV1 and BV2 groups ($P < 0.05$, **Figures 2E,F**).

Intestinal and Hepatopancreas Morphology

The intestinal and hepatopancreas morphometric parameters were presented in **Figure 3** and **Table 5**. The liver tubule of hepatopancreas in the BV addition groups are arranged relatively tightly and significantly generally star-shaped or polygonal ($P < 0.05$), while the lumen of the control group is mostly circular. Besides, the control group distributed many differentiated E cells (embryonic cells), while the BV addition group distributed more B cells (secreting cells), F cells (fibrocyte), and R cells (absorbing cells). The shrimps from all dietary treatments had an intact epithelial barrier with extensive mucosal folds and abundant Microvilli. The mucosal structure of the control group was slightly loose, the length of intestinal villi was significantly shorter ($P < 0.05$), and the number of mucosal epithelial cells was less. The intestinal tissue structures of the BV addition groups were relatively complete, and the length of the intestinal villi was increased and closely connected with the intestinal wall.

Microbiota

Richness and Diversity of Intestinal Microflora

The alpha diversity was calculated using the Shannon and Simpson indices and the Chao1, ACE, and PD whole tree estimators (**Table 6**). The nonparametric species-richness estimator Chao1 showed a minimum OTUs count of 287 in the BV1 group and a maximum count of 730 in the BV2 group ($P < 0.05$). The highest level of supplemented probiotics (10^9 CFU/g) also had a higher OTU count than the control group ($P < 0.05$). The number of observed species, Shannon index, and ACE showed similar trends with BV3 exhibiting significantly higher values than the other groups. Phylogenetic diversity was measured using the PD whole tree estimator, which ranged from 26.50 to 52.64. All these indices suggested that the BV2 and BV3 groups had a higher microbial diversity in their intestines, whether measured *via* richness or evenness. A Venn diagram was constructed to identify the OTUs held in common or unique to shrimp under different diets. In this regard, 961 OTUs were shared among all the shrimp gut samples (**Figure 4**). In contrast, 43, 49, 197, and 245 OTUs were unique to the C, BV1, BV2, and BV3 diets, respectively. This observation suggests that the exposure of shrimp to different graded probiotics led to the selection of unique microbial populations.

Bacterial Composition of Intestinal Microflora

The bacterial composition at the genus level in the intestine of *L. vannamei* is represented in **Figure 5**. The most abundant genera in the shrimp intestine were *Candidatus Bacilloplasma*, *Vibrio*, *Pseudoalteromonas*, *Bacillus,* and *Tenacibaculum*. After 42 days of feeding, the relative abundance of the predominant genera differed between the control and the groups fed with the BV2 and BV3 diets. In particular, the proportions of *Vibrio* and *Pseudoalteromonas* in the BV2 group (11.7 and 5.7%) were decreased compared with the C group (30.2 and 10.9%), BV1 group (15.2 and 10.7%), and BV3 group (17.9 and 8.8%). In addition, the proportion of *Bacillus* in the BV2 group (7.7%) was significantly higher than that in the C group (0.2%, $P < 0.05$).

Challenge Test

After the 2-weeks challenge with *V. parahaemolyticus*, the cumulative mortality rates of *L. vannamei* were shown in **Figure 6**. It was observed that the cumulative mortality was significantly lower in the treated groups than in the untreated ones, that is, 97.2, 61.1, 30.6, and 51.4% for shrimps fed with the C, BV1, BV2, and BV3, respectively.

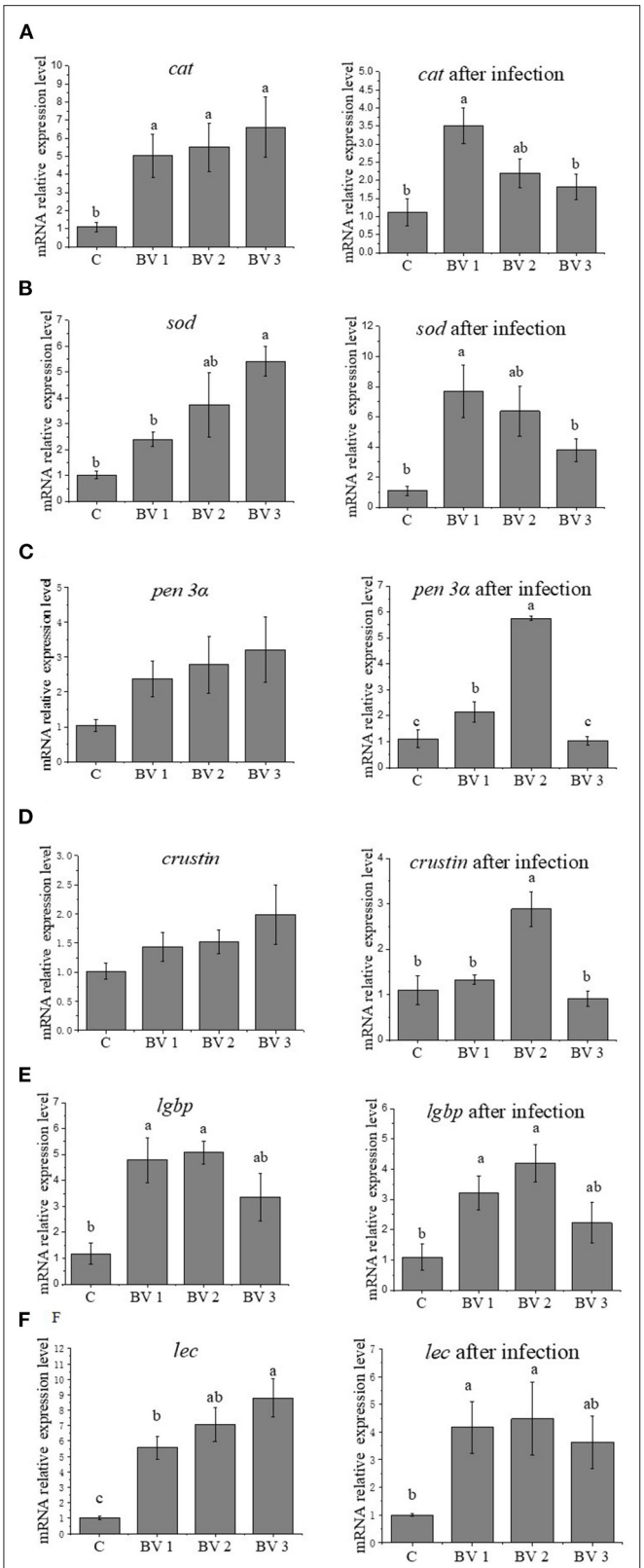

FIGURE 2 | Effects of different levels of dietary *B. velezensis* on the relative expression of *cat* **(A)**, *sod* **(B)**, *pen 3α* **(C)**, *crustin* **(D)**, *lgbp* **(E)**, and *lec* **(F)** in hepatopancreas. Error bars with different letters (a, b, c) represent statistically significant differences based on the LSD method ($P < 0.05$, one-way ANOVA). The results were shown as mean ± SE ($N = 6$).

DISCUSSION

Many strains of some *Bacillus* sp. are currently used as probiotic dietary supplements in aquatic animal feeds (Foysal and Lisa, 2018; Kewcharoen and Srisapoome, 2019; Kuebutornye et al., 2019; Zhai et al., 2019; Zhou et al., 2019; Liu et al., 2020). These probiotics not only produce certain essential micronutrients that promote better growth and feed utilization of the hosts (Xie et al., 2019) but also participate in the digestion processes that break down nutrients, such as carbohydrates, proteins, and lipids by producing extracellular enzymes (e.g., amylase, trypsin, lipase) (Wang et al., 2007; Zhang et al., 2020). In this study, a basal diet with continuous supplementation of *B. velezensis* was shown to increase the growth performance of shrimp, which is consistent with the results of previous studies in tilapia (Galagarza et al., 2018; Hassaan et al., 2018), carp (Fan et al., 2018; Jiang et al., 2019), and grouper (Li et al., 2019b). The observed improvement in growth performance could be ascribed to the enhanced intestinal digestive enzyme activities (Bokkenheuser et al., 1988; Xu et al., 2003; Fu et al., 2018). In the present study, the digestive enzymes, such as α-amylase (known to catalyze the hydrolysis of starch into sugars), lipase (known to catalyze the hydrolysis of fats and lipids), and trypsin (catalyzing the hydrolysis of proteins into smaller peptides) significantly increased in the treated groups compared with the untreated shrimp (Rawlings and Barrett, 1994; Svendsen, 2000). Similar observations were recorded in *Apostichopus japonicus* and *Salmo salar L.* that were fed diets supplemented with *B. velezensis* (Wang et al., 2018; Wang J. et al., 2019). It was also noted that *Bacillus* genus might secrete a wide range of exoenzymes that aid in the nutritional enhancement of the host. As a result, the increase in digestive enzyme activities can be linked to the elevated beneficial bacteria in the *Bacillus*-treated groups since they secrete chemical compounds, such as protease, amylases, and β-galactosidases. Notably, the GPT and GOT activities were reduced in the *B. velezensis*-supplemented groups, indicating that no hepatopancreas tissue damage or dysfunction was induced by the addition of probiotics (Cao et al., 2012).

The modulation of immune responses and disease resistance is a major function induced by probiotics. As a result, both cellular and humoral immunity are stimulated in response to a pathogenic challenge (Goulart et al., 2019; Ng et al., 2019; Wang G. et al., 2019). In this study, the phagocytosis of *L. vannamei* hemocytes was increased with the addition of *B. velezensis*. Similarly, Rengpipat et al. (2000) found that the use of *Bacillus* S11 could activate cellular immune defenses of *Penaeus monodon*. During phagocytosis, respiratory bursts were used to kill bacterial pathogens, relying in particular on ROS, but their overproduction can cause damage to biomolecules, such as lipids, proteins, and nucleic acids, and generate oxidative stress (Spencer et al., 2019). After infection, BVs groups significantly reduced the damage of ROS to the body, possibly by modulation of the internal antioxidants and antioxidative systems (Chen et al., 2015). The SOD and CAT are considered to be molecular biomarkers for evaluating the oxidative stress status of aquatic organisms (Valavanidis et al., 2006; Yang et al., 2015). After the bacterial challenge, the activities of SOD and CAT showed similar trends, increasing slightly at first and then decreasing,

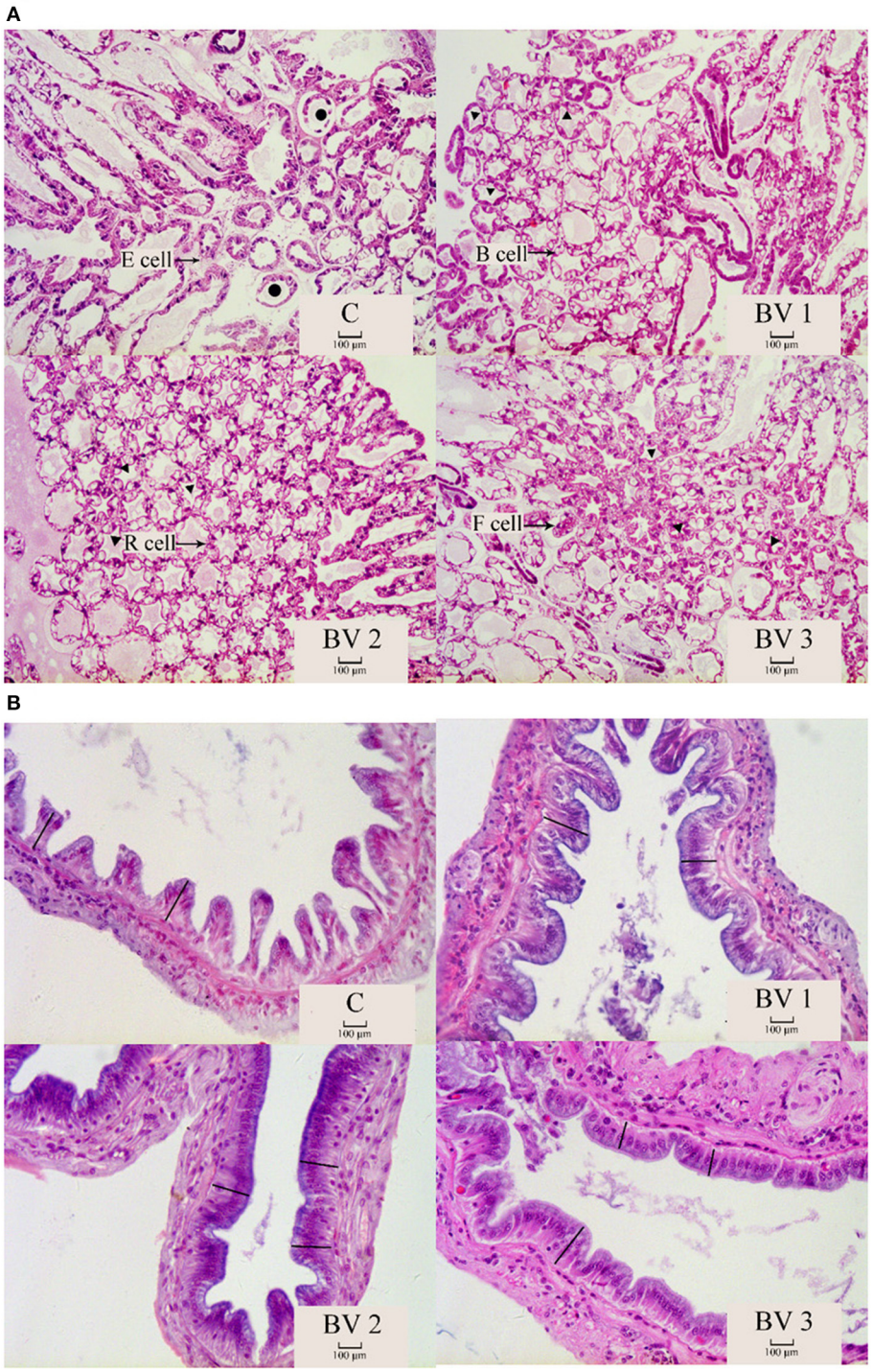

FIGURE 3 | The morphological structure of hepatopancreas **(A)** and intestine **(B)**. C, 0 CFU/g; BV1, 10^5 CFU/g group; BV2, 10^7 CFU/g group; BV3, 10^9 CFU/g group. •: liver tubules are round; ▲: the liver tubules are star-like or polygonal. -: intestinal villus.

which suggest that dietary supplemented probiotics improved the hepatopancreas antioxidant capacity of shrimp. ACP and AKP are necessary for phosphorylation and dephosphorylation, which are very important to the crustacean immune system (Yang et al., 2007). In the present study, the AKP activities in *B. velezensis*-supplemented groups were significantly higher than that in the control group. Similar results have also been found by Amoah and Cai (Amoah et al., 2019b; Cai et al.,

TABLE 5 | Statistics of the morphology and structure of hepatopancreas and midgut of *L. vannamei* fed diets containing 0 CFU/g (C), 10^5 CFU/g (BV1), 10^7 CFU/g (BV2), and 10^9 CFU/g (BV3) *B. velezensis* for 6 weeks.

Items	Treatments			
	C	BV 1	BV 2	BV 3
Star-shaped or polygonal liver tubule	52.00±8.19^b	93.00±14.47^a	100.00±15.25^a	81.00±9.49^a
Circular liver tubule	10.00±2.64^a	7.00±2.45^{ab}	1.75±2.06^b	2.50±1.73^b
Intestinal villi (μm)	94.71±34.65^b	130.37±27.00^a	127.83±35.15^a	123.80±47.36^a

The values (mean of 8 replicates ± SD) with different letters (a, b, c) represent statistically significant differences based on the LSD method ($P < 0.05$, one-way ANOVA).

TABLE 6 | Operational taxonomic unit (OTU) numbers, species richness, and diversity indices for the intestinal microbial community diversity analysis of *L. vannamei* fed different levels of *B. velezensis* BV007.

Sample name	C	BV1	BV2	BV3
OUT numbers	316.00±3.00^{ab}	286.33±27.51^b	573.00±137.41^a	587.00±74.06^a
Observed_species	273.50±12.50^{ab}	237.67±29.13^b	523.67±137.87^a	518.00±77.01^{ab}
Shannon	2.74±0.01	2.65±0.65	4.58±1.02	4.39±0.81
Simpson	0.69±0.031	0.66±0.13	0.79±0.10	0.84±0.06
Chao1	290.91±4.74^{ab}	287.26±29.45^b	606.81±136.92^a	593.92±54.11^a
ACE	302.08±9.728^{ab}	300.43±24.48^b	587.27±123.42^a	582.96±67.67^a
PD_whole_tree	34.70±1.07^{ab}	25.48±2.86^b	53.34±11.39^a	52.64±5.33^a

The values (mean of 3 replicates ± SE) with different letters (a, b, c) represent statistically significant differences based on the LSD method ($P < 0.05$, one-way ANOVA).

2019). The results suggested that dietary supplementation of *Paenibacillus polymyxa, B. licheniformis, and Bacillus flexus* enhanced the growth, hepatopancreas immune, and antioxidant activities of shrimps. In addition, the expressions of immune-related genes were highly induced in BVs groups. Among them, *crustin* and *penaeidin 3α* are vital antibacterial peptides in shrimps, powerful for the elimination of *Vibrio* (Cuthbertson et al., 2002, 2005; Muñoz et al., 2002; Arockiaraj et al., 2013). The enhanced expression of these genes contributes to resist invading bacteria and improve non-specific immunity (Muñoz et al., 2002; Arockiaraj et al., 2013; Cuthbertson et al., 2005). Overall, the dietary supplemented *B. velezensis* BV007 could boost the innate immunity of shrimp at an appropriate level.

The intestinal microbiota of shrimp plays an essential role in mediating immunity, nutrient metabolism, and energy homeostasis (Zhang et al., 2020). The previous studies have shown that probiotics in the shrimp diet could effectively modulate the intestinal microbiota, improve growth performance, and enhance disease resistance (Yang et al., 2015; Suo et al., 2017; Amoah et al., 2019a; Xie et al., 2019). In the present study, a greater diversity of bacterial species was found in the BV007 supplemented groups than that in the control group. The reason may lie in the changed metabolic activities or beneficial effects on gut microbiota regulated by *B. velezensis* (He et al., 2019; Li et al., 2019a). Notably, the *Vibrio* species are severe pathogens in aquatic organisms (Hsu and Chen, 2007). In 2013, severe acute hepatopancreatic necrosis disease (AHPND) was induced by *V. parahaemolyticus* (Tran et al., 2013) causing mass mortality of shrimps specifically in the affected Southeast Asian countries (Hsu and Chen, 2007). In this study, cumulative mortality of the probiotics treated groups was significantly lower

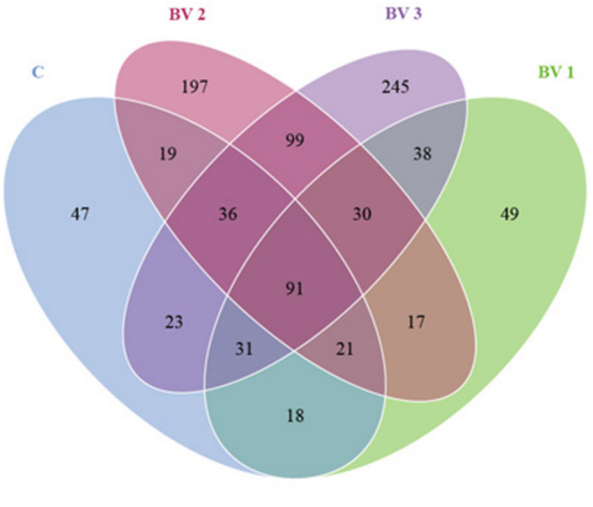

FIGURE 4 | A Venn diagram showing the unique and shared operational taxonomic units (OTUs) among groups of *L. vannamei* fed diets containing 0 CFU/g (C), 10^5 CFU/g (BV1), 10^7 CFU/g (BV2), or 10^9 CFU/g (BV3) *B. velezensis*.

than the untreated group after *V. parahaemolyticus* challenge. It suggested that *B. velezensis* 007 could improve the disease resistance of *L. vannamei*. Similar results were also proved by Zokaeifar et al. (2012) and Amoah et al. (2019b). They suggested that *Bacillus subtilis* and *Bacillus coagulans* ATCC 7050 enhanced the anti-disease ability in shrimp. The results might be attributed to the increased abundances of beneficial genus bacteria *Bacillus*

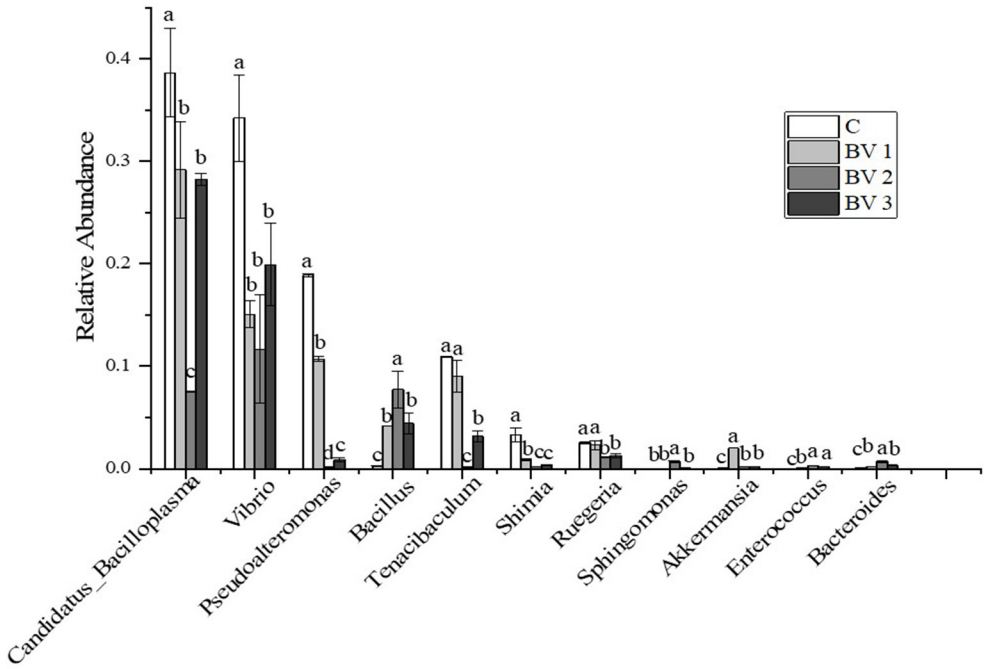

FIGURE 5 | Relative abundance of the top 10 classes at the genus level of intestinal microflora of *L. vannamei* fed diets containing 0 CFU/g (C), 10^5 CFU/g (BV1), 10^7 CFU/g (BV2), or 10^9 CFU/g (BV3) *B. velezensis*. Error bars with different letters (a, b, c) represent statistically significant differences based on the LSD method ($P < 0.05$, one-way ANOVA). The results were shown as mean ± SE ($N = 3$).

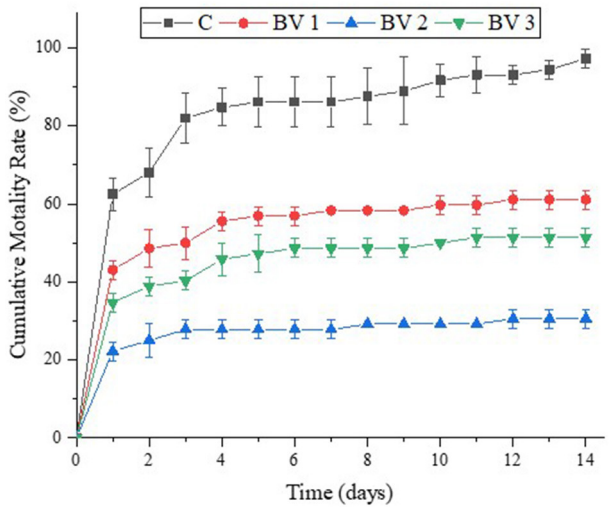

FIGURE 6 | Effects of dietary administration of *B. velezensis* on the cumulative mortality percentage of *L. vannamei* after infection with *V. parahaemolyticus*.

and enhanced immune responses in the treated groups (Amoah et al., 2019b).

The present study showed that diet supplementation with the potential probiotic *B. velezensis* BV007 could significantly promote growth performance, enhance immune response, and disease resistance in *L. vannamei*. Based on these findings, we conclude that a dose of 10^7 CFU/g feed provides health and growth benefits by improving the digestive enzyme activities, immune responses, intestinal development, and gut microflora.

DATA AVAILABILITY STATEMENT

The datasets presented in this study can be found in online repositories. The names of the repository/repositories and accession number(s) can be found in the article/supplementary material.

AUTHOR CONTRIBUTIONS

SH conceived and designed the experiments. LC and CL conducted the experiments. BL, HZ, and QZ analyzed the data. LR, XZ, CS, and JG contributed reagents, materials, and analytical tools. LC, CL, and SH wrote the manuscript. All authors contributed to the article and approved the submitted version.

FUNDING

This research was supported by grants from the Key Research and Development Project of Shandong (No. 2020CXGC011404), the Natural Science Foundation of Shandong Province (ZR2020QD097), and the Key Research and Development Project of Yantai (2019XDHZ105).

REFERENCES

Amoah, K., Huang, Q.-C., Dong, X.-H., Tan, B.-P., Zhang, S., Chi, S.-Y., et al. (2019a). *Paenibacillus polymyxa*, improves the growth, immune and antioxidant activity, intestinal health, and disease resistance in *Litopenaeus vannamei* challenged with *Vibrio parahaemolyticus*. *Aquaculture* 518:734563. doi: 10.1016/j.aquaculture.2019.734563

Amoah, K., Huang, Q.-C., Tan, B.-P., Zhang, S., Chi, S.-Y., Yang, Q.-H., et al. (2019b). Dietary supplementation of probiotic *Bacillus coagulans* ATCC 7050, improves the growth performance, intestinal morphology, microflora, immune response, and disease confrontation of Pacific white shrimp, *Litopenaeus vannamei*. *Fish Shellfish Immunol.* 87, 796–808. doi: 10.1016/j.fsi.2019.02.029

Arockiaraj, J., Gnanam, A. J., Muthukrishnan, D., Gudimella, R., Milton, J., Singh, A., et al. (2013). Crustin, a WAP domain containing antimicrobial peptide from freshwater prawn *Macrobrachium rosenbergii*: immune characterization. *Fish Shellfish Immunol.* 34, 109–118. doi: 10.1016/j.fsi.2012.10.009

Bokkenheuser, V. D., Shackleton, C., and Winter, J. (1988). Hydrolysis of dietary flavonoid glycosides by strains of intestinal *Bacteroides* from humans. *Biochem. J.* 248, 953–956. doi: 10.1042/bj2480953

Cai, Y., Yuan, W., Wang, S., Guo, W., Li, A., Wu, Y., et al. (2019). *In vitro* screening of putative probiotics and their dual beneficial effects: to white shrimp (*Litopenaeus vannamei*) postlarvae and to the rearing water. *Aquaculture* 498, 61–71. doi: 10.1016/j.aquaculture.2018.08.024

Cao, J. M., Yan, J., Wang, G. X., Huang, Y. H., Zhang, R. B., Zhou, T. L., et al. (2012). Effects of replacement of fish meal with housefly maggot meal on digestive enzymes, transaminases activities and hepatopancreas histological structure of *Litopenaeus vannamei*. *South China Fish. Sci.* 8, 72–79. doi: 10.3969/j.issn.2095-0780.2012.05.011

Caporaso, J., Lauber, C., Walters, W., Berg-Lyons, D., Lozupone, C., Turnbaugh, P., et al. (2011). Global patterns of 16S rRNA diversity at a depth of millions of sequences per sample. *Proc. Natl. Acad. Sci. USA.* 108 Suppl 1, 4516–4522. doi: 10.1073/pnas.1000080107

Chai, P.-C., Song, X.-L., Chen, G.-F., Xu, H., and Huang, J. (2016). Dietary supplementation of probiotic *Bacillus* PC465 isolated from the gut of *Fenneropenaeus chinensis* improves the health status and resistance of *Litopenaeus vannamei* against white spot syndrome virus. *Fish Shellfish Immunol.* 54, 602–611. doi: 10.1016/j.fsi.2016.05.011

Chen, Y. Y., Lee, P.-C., Wu, Y.-L., and Liu, L.-Y. (2015). In *vivo* effects of free form astaxanthin powder on anti-oxidation and lipid metabolism with high-cholesterol diet. *PLoS ONE* 10:e0134733. doi: 10.1371/journal.pone.0134733

Cuthbertson, B. J., Shepard, E. F., Chapman, R. W., and Gross, P. S. (2002). Diversity of the penaeidin antimicrobial peptides in two shrimp species. *Immunogenetics* 54, 442–445. doi: 10.1007/s00251-002-0487-z

Cuthbertson, B. J., Yang, Y., Bachère, E., Büllesbach, E. E., and Aumelas, A. J. J., o. B. C. (2005). Solution structure of synthetic penaeidin-4 with structural and functional comparisons with penaeidin-3. *J. Biol. Chem.* 280, 16009–16018. doi: 10.1074/jbc.M412420200

Dawood, M., Abo-Al-Ela, H. G., and Hasan, M. T. (2020). Modulation of transcriptomic profile in aquatic animals: probiotics, prebiotics and synbiotics scenarios. *Fish Shellfish Immunol.* 97, 268–282. doi: 10.1016/j.fsi.2019.12.054

Delaporte, M., Soudant, P., Moal, J., Lambert, C., Quéré, C., Miner, P., et al. (2003). Effect of a mono-specific algal diet on immune functions in two bivalve species—*Crassostrea gigas* and *Ruditapes philippinarum*. *J. Exp. Biol.* 206, 3053–3064. doi: 10.1242/jeb.00518

Fan, Y., Liu, L., Zhao, L., Wang, X., Wang, D., Huang, C., et al. (2018). Influence of *Bacillus subtilis* ANSB060 on growth, digestive enzyme and aflatoxin residue in *Yellow River carp* fed diets contaminated with aflatoxin B1. *Food Chem. Toxicol.* 113, 108–114. doi: 10.1016/j.fct.2018.01.033

Foysal, M. J., and Lisa, A. K. (2018). Isolation and characterization of *Bacillus* sp. strain BC01 from soil displaying potent antagonistic activity against plant and fish pathogenic fungi and bacteria. *J. Genet. Eng. Biotechnol.* 16, 387–392. doi: 10.1016/j.jgeb.2018.01.005

Fu, L.-L., Wang, Y., Wu, Z.-C., and Li, W.-F. (2011). In *vivo* assessment for oral delivery of *Bacillus subtilis* harboring a viral protein (VP28) against white spot syndrome virus in *Litopenaeus vannamei*. *Aquaculture* 322–323, 33–38. doi: 10.1016/j.aquaculture.2011.09.036

Fu, S., Wang, L., Tian, H., Wei, D., and Liu, Y. (2018). Pathogenicity and genomic characterization of *Vibrio parahaemolyticus* strain PB1937 causing shrimp acute hepatopancreatic necrosis disease in China. *Ann. Microbiol.* 68, 175–184. doi: 10.1007/s13213-018-1328-0

Galagarza, O. A., Smith, S. A., Drahos, D. J., Eifert, J. D., Williams, R. C., and Kuhn, D. D. (2018). Modulation of innate immunity in Nile tilapia (*Oreochromis niloticus*) by dietary supplementation of *Bacillus subtilis* endospores. *Fish Shellfish Immunol.* 83, 171–179. doi: 10.1016/j.fsi.2018.08.062

Gao, X., Zhang, M., Li, X., Han, Y., Wu, F., and Liu, Y. (2018). Effects of a probiotic (*Bacillus licheniformis*) on the growth, immunity, and disease resistance of *Haliotis discus hannai* Ino. *Fish Shellfish Immunol.* 76, 143–152. doi: 10.1016/j.fsi.2018.02.028

Goulart, C., Rodriguez, D., Kanno, A. I., Silva, J. L. S. C., and Leite, L. C. C. (2019). Early pneumococcal clearance in mice induced by systemic immunization with recombinant BCG PspA-PdT prime and protein boost correlates with cellular and humoral immune response in bronchoalveolar fluids (BALF). *Vaccine: X* 4:100049. doi: 10.1016/j.jvacx.2019.100049

Hassaan, M. S., Soltan, M. A., Mohammady, E. Y., Elashry, M. A., El-Haroun, E. R., and Davies, S. J. (2018). Growth and physiological responses of Nile tilapia, *Oreochromis niloticus* fed dietary fermented sunflower meal inoculated with *Saccharomyces cerevisiae* and *Bacillus subtilis*. *Aquaculture* 495, 592–601. doi: 10.1016/j.aquaculture.2018.06.018

He, G., Dong, Y., Huang, J., Wang, X., Zhang, S., Wu, C., et al. (2019). Alteration of microbial community for improving flavor character of Daqu by inoculation with *Bacillus velezensis* and *Bacillus subtilis*. *LWT* 111, 1–8. doi: 10.1016/j.lwt.2019.04.098

Hsu, S.-W., and Chen, J.-C. (2007). The immune response of white shrimp *Penaeus vannamei* and its susceptibility to *Vibrio alginolyticus* under sulfide stress. *Aquaculture* 271, 61–69. doi: 10.1016/j.aquaculture.2007.05.028

Interaminense, J., Vogeley, J., Gouveia, C., Portela, R., Oliveira, J., Andrade, H., et al. (2018). In *vitro* and in *vivo* potential probiotic activity of *Bacillus subtilis* and *Shewanella algae* for use in *Litopenaeus vannamei* rearing. *Aquaculture* 488, 114–122. doi: 10.1016/j.aquaculture.2018.01.027

Interaminense, J. A., Vogeley, J. L., Gouveia, C. K., Portela, R. S., Oliveira, J. P., Silva, S. M. B. C., et al. (2019). Effects of dietary *Bacillus subtilis* and *Shewanella algae* in expression profile of immune-related genes from hemolymph of *Litopenaeus vannamei* challenged with *Vibrio parahaemolyticus*. *Fish Shellfish Immunol.* 86, 253–259. doi: 10.1016/j.fsi.2018.11.051

Jiang, Y., Zhou, S., and Chu, W. (2019). The effects of dietary *Bacillus cereus* QSI-1 on skin mucus proteins profile and immune response in Crucian Carp (*Carassius auratus gibelio*). *Fish Shellfish Immunol.* 89, 319–325. doi: 10.1016/j.fsi.2019.04.014

Kalgraff, C. A. K., Wergeland, H. I., and Pettersen, E. F. (2011). Flow cytometry assays of respiratory burst in Atlantic salmon (*Salmo salar L.*) and in Atlantic cod (*Gadus morhua L.*) leucocytes. *Fish Shellfish Immunol.* 31, 381–388. doi: 10.1016/j.fsi.2011.05.028

Kewcharoen, W., and Srisapoome, P. (2019). Probiotic effects of Bacillus spp. from Pacific white shrimp (*Litopenaeus vannamei*) on water quality and shrimp growth, immune responses, and resistance to *Vibrio parahaemolyticus* (AHPND strains). *Fish Shellfish Immunol.* 94, 175–189. doi: 10.1016/j.fsi.2019.09.013

Kuebutornye, F. K. A., Abarike, E. D., and Lu, Y. (2019). A review on the application of *Bacillus* as probiotics in aquaculture. *Fish Shellfish Immunol.* 87, 820–828. doi: 10.1016/j.fsi.2019.02.010

Li, A., Wang, Y., Pei, L., Mehmood, K., Li, K., Qamar, H., et al. (2019a). Influence of dietary supplementation with *Bacillus velezensis* on intestinal microbial diversity of mice. *Microb. Pathog.* 136:103671. doi: 10.1016/j.micpath.2019.103671

Li, J., Wu, Z.-B., Zhang, Z., Zha, J.-W., Qu, S.-Y., Qi, X.-Z., et al. (2019b). Effects of potential probiotic *Bacillus velezensis* K2 on growth, immunity and resistance to *Vibrio harveyi* infection of hybrid grouper (*Epinephelus lanceolatus*♂ × E. fuscoguttatus♀). *Fish Shellfish Immunol.* 93, 1047–1055. doi: 10.1016/j.fsi.2019.08.047

Lin, H. L., Shiu, Y. L., Chiu, C. S., Huang, S. L., and Liu, C. H. (2017). Screening probiotic candidates for a mixture of probiotics to enhance the growth performance, immunity, and disease resistance of asian seabass, *lates calcarifer* (bloch), against *aeromonas hydrophila*. *Fish Shellfish Immunol.* 60, 474–482. doi: 10.1016/j.fsi.2016.11.026

Liu, H., Wang, S., Cai, Y., Guo, X., Cao, Z., Zhang, Y., et al. (2017). Dietary administration of *Bacillus subtilis* HAINUP40 enhances growth, digestive enzyme activities, innate immune responses and disease resistance of tilapia, *Oreochromis niloticus*. *Fish Shellfish Immunol.* 60, 326–333. doi: 10.1016/j.fsi.2016.12.003

Liu, K.-F., Chiu, C.-H., Shiu, Y.-L., Cheng, W., and Liu, C.-H. (2010). Effects of the probiotic, *Bacillus subtilis* E20, on the survival, development, stress tolerance, and immune status of white shrimp, *Litopenaeus vannamei* larvae. *Fish Shellfish Immunol.* 28, 837–844. doi: 10.1016/j.fsi.2010.01.012

Liu, S., Wang, S., Cai, Y., Li, E., Ren, Z., Wu, Y., et al. (2020). Beneficial effects of a host gut-derived probiotic, *Bacillus pumilus*, on the growth, non-specific immune response and disease resistance of juvenile golden pompano, *Trachinotus ovatus*. *Aquaculture* 514:734446. doi: 10.1016/j.aquaculture.2019.734446

Livak, K. J., and Schmittgen, T. (2001). Analysis of relative gene expression data using real-time quantitative PCR and the $2^{-\Delta\Delta CT}$ method. *Methods* 25, 402–408. doi: 10.1006/meth.2001.1262

Muñoz, M., Vandenbulcke, F., Saulnier, D., and Bachère, E. J. E. J. (2002). Expression and distribution of penaeidin antimicrobial peptides are regulated by haemocyte reactions in microbial challenged shrimpandnbsp. 269, 2678–2689. doi: 10.1046/j.1432-1033.2002.02934.x

Neiland, A. E., Soley, N., Varley, J. B., and Whitmarsh, D. J. (2001). Shrimp aquaculture: economic perspectives for policy development. *Mar. Policy* 25, 265–279. doi: 10.1016/S0308-597X(01)00017-3

Ng, K.-H., Zhang, S. L., Tan, H. C., Kwek, S. S., Sessions, O. M., Chan, C.-Y., et al. (2019). Persistent dengue infection in an immunosuppressed patient reveals the roles of humoral and cellular immune responses in virus clearance. *Cell Host Microbe* 26, 601–605.e603. doi: 10.1016/j.chom.2019.10.005

Qin, L., Xiang, J., Xiong, F., Wang, G., Zou, H., Li, W., et al. (2020). Effects of Bacillus licheniformis on the growth, antioxidant capacity, intestinal barrier and disease resistance of grass carp (*Ctenopharyngodon idella*). *Fish Shellfish Immunol.* 97, 344–350. doi: 10.1016/j.fsi.2019.12.040

Raman, M., Ambalam, P., and Doble, M. (2019). Probiotics, prebiotics, and fibers in nutritive and functional beverages. *Nutr. Beverag.* 2019, 315–367. doi: 10.1016/B978-0-12-816842-4.00009-5

Rawlings, N. D., and Barrett, A. J. (1994). "Families of serine peptidases," in *Methods in Enzymology, vol. 244* (New York, NY: Academic Press), 19–61. doi: 10.1016/0076-6879(94)44004-2

Rengpipat, S., Rukpratanporn, S., Piyatiratitivorakul, S., and Menasaveta, P. (2000). Immunity enhancement in black tiger shrimp (*Penaeus monodon*) by a probiont bacterium (*Bacillus* S11). *Aquaculture* 191, 271–288. doi: 10.1016/S0044-8486(00)00440-3

Spencer, S. P., Fragiadakis, G. K., and Sonnenburg, J. L. (2019). Pursuing Human-Relevant Gut Microbiota-Immune Interactions. *Immunity* 51, 225–239. doi: 10.1016/j.immuni.2019.08.002

Suo, Y., Li, E., Li, T., Jia, Y., Qin, J. G., Gu, Z., et al. (2017). Response of gut health and microbiota to sulfide exposure in Pacific white shrimp *Litopenaeus vannamei*. *Fish Shellfish Immunol.* 63, 87–96. doi: 10.1016/j.fsi.2017.02.008

Svendsen, A. (2000). Lipase protein engineering. *Biochim. Biophys. Acta Protein Struct. Mol. Enzymol.* 1543, 223–238. doi: 10.1016/S0167-4838(00)00239-9

Tran, L., Nunan, L., Redman, R. M., Mohney, L. L., Pantoja, C. R., Fitzsimmons, K., et al. (2013). Determination of the infectious nature of the agent of acute hepatopancreatic necrosis syndrome affecting penaeid shrimp. *Dis. Aquat. Org.* 105, 45–55. doi: 10.3354/dao02621

Valavanidis, A., Vlachogianni, T., Dassenakis, M., and Scoullos, M. (2006). Molecular biomarkers of oxidative stress in aquatic organisms in relation to toxic environmental pollutants. *Ecotoxicol. Environ. Saf.* 64, 178–189. doi: 10.1016/j.ecoenv.2005.03.013

Velmurugan, S., Palanikumar, P., Velayuthani, P., Donio, M. B. S., Babu, M. M., Lelin, C., et al. (2015). Bacterial white patch disease caused by *Bacillus cereus*, a new emerging disease in semi-intensive culture of *Litopenaeus vannamei*. *Aquaculture* 444, 49–54. doi: 10.1016/j.aquaculture.2015.03.017

Wang, C., Liu, Y., Sun, G., Li, X., and Liu, Z. (2018). Growth, immune response, antioxidant capability, and disease resistance of juvenile Atlantic salmon (*Salmo salar L.*) fed *Bacillus velezensis* V4 and Rhodotorula mucilaginosa compound. *Aquaculture* 500, 65–74. doi: 10.1016/j.aquaculture.2018.09.052

Wang, G., Na, S., and Qin, L. (2019). Uncovering the cellular and humoral immune responses of *Antheraea pernyi* hemolymph to *Antheraea pernyi* nucleopolyhedrovirus infection by transcriptome analysis. *J. Invertebr. Pathol.* 166:107205. doi: 10.1016/j.jip.2019.107205

Wang, J., Li, B., Wang, Y., Liao, M., Rong, X., and Zhang, Z. (2019). Influences of immersion bathing in *Bacillus velezensis* DY-6 on growth performance, non-specific immune enzyme activities and gut microbiota of *Apostichopus japonicus*. *J. Oceanol. Limnol.* 37, 1449–1459. doi: 10.1007/s00343-019-8119-8

Wang, Q., Garrity, G., Tiedje, J. R., and Cole's, J. (2007). Naïve Bayesian classifier for rapid assignment of rRNA sequences into the new bacterial taxonomy. *Appl. Environ. Microbiol.* 73, 5261–5267. doi: 10.1128/AEM.00062-07

Wang, Y.-C., Hu, S.-Y., Chiu, C.-S., and Liu, C.-H. (2019). Multiple-strain probiotics appear to be more effective in improving the growth performance and health status of white shrimp, *Litopenaeus vannamei*, than single probiotic strains. *Fish Shellfish Immunol.* 84, 1050–1058. doi: 10.1016/j.fsi.2018.11.017

Xie, J., Liu, Q., Liao, S., Fang, H., Yin, P., Xie, S., et al. (2019). Effects of dietary mixed probiotics on growth, non-specific immunity, intestinal morphology and microbiota of juvenile pacific white shrimp, *Litopenaeus vannamei*. *Fish Shellfish Immunol.* 90, 456–465. doi: 10.1016/j.fsi.2019.04.301

Xin, Y., Xiaohe, G., Tingting, Y., Hongyu, W., Xiali, G., and Xi, Z. (2015). Study of enteropathogenic bacteria in children with acute diarrhoea aged from 7 to 10 years in Xuzhou, China. *Microb. Pathog.* 91, 41–45. doi: 10.1016/j.micpath.2015.11.027

Xu, J., Bjursell, M., Himrod, J., Deng, S., Carmichael, L., Chiang, H., et al. (2003). A genomic view of the Human–Bacteroides thetaiotaomicron symbiosis. *Science* 299, 2074–2076. doi: 10.1126/science.1080029

Xu, L., Yuan, J., Chen, X., Zhang, S., and Wu, Z. (2021). Screening of intestinal probiotics and the effects of feeding probiotics on the digestive enzyme activity, immune, intestinal flora and *wssv* resistance of *procambarus clarkii*. *Aquaculture* 540:736748. doi: 10.1016/j.aquaculture.2021.736748

Yang, C., Kong, J., Wang, Q., Liu, Q., Tian, y., and Luo, K. (2007). Heterosis of haemolymph analytes of two geographic populations in Chinese shrimp *Fenneropenaeus chinensis*. *Fish Shellfish Immunol.* 23, 62–70. doi: 10.1016/j.fsi.2006.09.005

Yang, H., Yang, M., Sun, J.-J., Guo, F., Lan, J., Wang, X., et al. (2015). Catalase eliminates reactive oxygen species and influences the intestinal microbiota of shrimp. *Fish Shellfish Immunol.* 47, 63–73. doi: 10.1016/j.fsi.2015.08.021

Zhai, J., Jiumu, L., Cong, L., Wu, Y., Dai, L., Zhang, Z., et al. (2019). Reed decomposition under *Bacillus subtilis* addition conditions and the influence on water quality. *Ecohydrol. Hydrobiol.* 20, 504–512. doi: 10.1016/j.ecohyd.2019.11.003

Zhang, J., Chen, H., Luo, L., Zhou, Z., and Wu, M. (2021). Structures of fructan and galactan from *polygonatum cyrtonema* and their utilization by probiotic bacteria. *Carbohydr. Polym.* 267:118219. doi: 10.1016/j.carbpol.2021.118219

Zhang, M., Shan, C., Tan, F., Limbu, S. M., Chen, L., and Du, Z.-Y. (2020). Gnotobiotic models: powerful tools for deeply understanding intestinal microbiota–host interactions in aquaculture. *Aquaculture* 517:734800. doi: 10.1016/j.aquaculture.2019.734800

Zhou, S., Song, D., Zhou, X., Mao, X., Zhou, X., Wang, S., et al. (2019). Characterization of *Bacillus subtilis* from gastrointestinal tract of hybrid Hulong grouper (*Epinephelus fuscoguttatus* × *E. lanceolatus*) and its effects as probiotic additives. *Fish Shellfish Immunol.* 84, 1115–1124. doi: 10.1016/j.fsi.2018.10.058

Zokaeifar, H., Babaei, N., Saad, C. R., Kamarudin, M. S., Sijam, K., and Balcazar, J. L. (2014). Administration of *Bacillus subtilis* strains in the rearing water enhances the water quality, growth performance, immune response, and resistance against *Vibrio harveyi* infection in juvenile white shrimp, *Litopenaeus vannamei*. *Fish Shellfish Immunol.* 36, 68–74. doi: 10.1016/j.fsi.2013.10.007

Zokaeifar, H., Balcazar, J., Saad, C., Kamarudin, M. S., Sijam, K., Arshad, A. B., et al. (2012). Effects of *Bacillus subtilis* on the growth performance, digestive enzymes, immune gene expression and disease resistance of white shrimp, *Litopenaeus vannamei*. *Fish Shellfish Immunol.* 33, 683–689. doi: 10.1016/j.fsi.2012.05.027

Conflict of Interest: The authors declare that the research was conducted in the absence of any commercial or financial relationships that could be construed as a potential conflict of interest.

Publisher's Note: All claims expressed in this article are solely those of the authors and do not necessarily represent those of their affiliated organizations, or those of the publisher, the editors and the reviewers. Any product that may be evaluated in this article, or claim that may be made by its manufacturer, is not guaranteed or endorsed by the publisher.

frontiers in Marine Science

ORIGINAL RESEARCH
published: 28 September 2021
doi: 10.3389/fmars.2021.730569

Development of a Quantitative PCR Method for Specific and Quantitative Detection of *Enterocytospora artemiae*, a Microsporidian Parasite of Chinese Grass Shrimp (*Palaemonetes sinensis*)

*Hongbo Jiang†, Jie Bao†, Jinghui Liu, Yuwen Chen, Chengcheng Feng, Xiaodong Li, Shuai Huang and Qijun Chen**

Key Laboratory of Livestock Infectious Diseases in Northeast China, Ministry of Education, Key Laboratory of Zoonosis, Shenyang Agricultural University, Shenyang, China

OPEN ACCESS

Edited by:
Xiangli Tian,
Ocean University of China, China

Reviewed by:
Shihao Li,
Institute of Oceanology, Chinese Academy of Sciences (CAS), China
Ha Thanh Dong,
Asian Institute of Technology, Thailand

***Correspondence:**
Qijun Chen
qijunchen759@syau.edu.cn;
syaucqj@126.com

† These authors have contributed equally to this work

Specialty section:
This article was submitted to Marine Fisheries, Aquaculture and Living Resources, a section of the journal Frontiers in Marine Science

Received: *25 June 2021*
Accepted: *09 September 2021*
Published: *28 September 2021*

Citation:
Jiang H, Bao J, Liu J, Chen Y, Feng C, Li X, Huang S and Chen Q (2021) Development of a Quantitative PCR Method for Specific and Quantitative Detection of Enterocytospora artemiae, a Microsporidian Parasite of Chinese Grass Shrimp (Palaemonetes sinensis). Front. Mar. Sci. 8:730569. doi: 10.3389/fmars.2021.730569

Enterocytospora artemiae (EAM) mainly parasitizes the hepatopancreas of Palaemonetes sinensis. Serious infection leads to hepatopancreatic lesions, which greatly reduce the vitality of *P. sinensis*. Currently, EAM is detected via conventional PCR methods. However, conventional PCR has low sensitivity and cannot be used for accurate quantitative detection of EAM or its parasitic activity in host tissues. In this study, we designed a pair of specific primers based on the sequence of the ribosomal protein S9 gene (RPS9; GenBank accession number: MZ420734) to establish and optimize a SYBR Green I real-time fluorescent quantitative PCR detection method for EAM. Only EAM appeared as a bright and single target band, whereas other microorganisms did not, indicating that the primer for RPS9 had high specificity. This method displayed optimum amplification effects at an annealing temperature of 55°C, and the melting curve of the product produced a single peak. The established method showed a good linear relationship from 2.2×10^8 to 2.2×10^1 copies/μL. The relationship between the number of cycle thresholds (Ct) and the logarithm of the initial template amount (x) conformed to $Ct = -3.281 \log x + 36.543$ ($R^2 = 0.998$). Amplification efficiency was 101.737%, and the lower limit of detection sensitivity was 2.2×10^1 copies/μL. Good intra- and inter-group repeatability was observed within the linear range. The sensitivity of this method was more than 200 times higher than that of nested PCR. Thus, detection data obtained using this method may be useful as a technical reference for rapid and accurate identification of EAM infection and for the prevention and control of EAM during *P. sinensis* breeding.

Keywords: ***Palaemonetes sinensis*, *Enterocytospora artemiae*, qPCR detection method, RPS9, specific and quantitative detection**

INTRODUCTION

Microsporidia are a group of common fungal intracellular parasites consisting of over 200 genera and 1600 species (Stentiford et al., 2016). This group has a wide range of hosts, including almost all lower invertebrates, as well as higher vertebrates. Microsporidia are opportunistic pathogens, which easily infect patients receiving immunosuppressive therapy for congenital immune disorders (Pol et al., 1993; Didier and Weiss, 2011). Currently, 17 microsporidia species belonging to nine genera are known for their ability to infect humans (Pan et al., 2018). In addition to causing harm to human health, many microsporidia cause economic damage to important animal and plant industries (Kent and Speare, 2005; Higes et al., 2013). For example, the pepper disease of silkworms, which plagued the silkworm industry for more than two centuries, is caused by *Nosema bombycis*, a microsporidian (Nageswara Rao et al., 2004). Decapoda, an order of crustaceans that hosts microsporidia, has been studied for more than 100 years. As early as the end of the nineteenth century, French researchers reported that *Thelohania* infects *Palaemon rectirostris*, *P. serratus*, *Crangon vulgaris*, *Procambarus clarkii*, and *Astacus fluviatilis* as well as other shrimp (Stentiford and Dunn, 2014). Reportedly, the infection rate as well as the transmission range of *Enterocytozoon hepatopenaei* (EHP) in *Litopenaeus vannamei* has been increasing annually, making it one of three major pathogens endangering healthy *L. vannamei* cultures (Biju et al., 2016; Chaijarasphong et al., 2020).

Enterocytospora artemiae (EAM) was first discovered in *Artemia* in 2013. It was considered as an obligate parasite of *Artemia* that was confined to Europe and America (Rode et al., 2013). However, in 2020, it was found that this microsporidian had spread to Asia and was infecting the economically important Chinese grass shrimp, *Palaemonetes sinensis* (Jiang et al., 2020). EAM mainly parasitizes the hepatopancreas of *P. sinensis* (Jiang et al., 2020). Serious EAM infections lead to hepatopancreatic lesions and greatly reduce the vitality of *P. sinensis*. Although the mortality rate is not high, absorption of host nutrition by these microsporidia leads to increased breeding costs. Microsporidia are minute and do not cause obvious symptoms after infecting a host. Therefore, it is necessary to establish a rapid and accurate method to detect these parasites. Currently, only conventional PCR methods are used to detect EAM (Rode et al., 2013; Jiang et al., 2020). However, conventional PCR has low sensitivity and cannot be used for accurate, quantitative detection of EAM or its parasitic activity in host tissues. When the number of microsporidia infecting a host is low, observation via traditional staining followed by microscopy or electron microscopy becomes ineffective, preventing various species of microsporidia from being accurately determined. In contrast, real-time fluorescence quantitative PCR (qPCR), which is associated with advantages such as high specificity as well as high sensitivity, consumes less time and allows the copy number of the initial DNA template in the sample to be quantitated. The qPCR detection process is completed in a relatively closed and independent system, which prevents cross contamination of the sample and environment (Kotková et al., 2018; Li et al., 2019). In this study, we designed a nested PCR method, leading to the establishment of a qPCR protocol that detects EAM using SYBR Green I fluorescent dye. We compared the sensitivity and detection efficacy of conventional PCR, nested PCR, and qPCR to ensure rapid and accurate identification of EAM infections to control and prevent infection during *P. sinensis* breeding.

MATERIALS AND METHODS

Sample Collection of *Palaemonetes sinensis*

P. sinensis was collected from farms 1, 2, and 3 in Panjin, Liaoning province. These shrimp were transported to Shenyang Agricultural University for temporary cultivation. During the temporary cultivation period, 30 shrimp were randomly selected from each farm to detect the prevalence via different methods. During sampling, the live shrimp were anesthetized on ice for 5 min, and the hepatopancreases were removed quickly and placed in a centrifuge tube containing 100% alcohol for further analysis.

DNA Extraction

DNA was extracted from the tissues of *P. sinensis* in strict accordance with the instructions of the TIANamp Marine Animals DNA Kit (Tiangen, Beijing). The extracted DNA was diluted to 50 ng/μL after determination of DNA concentration with an ultra-microspectrophotometer (K5500, Beijing Kaiao Technology Development Co., Ltd.), and then was stored at −20°C.

Conventional PCR Amplification and Nested PCR Primer Design

Previously reported universal 18S rDNA primers, V1F and 1492R, were used for PCR amplification (Rode et al., 2013). The V1F and 1492R sequences are listed in **Table 1**. The amplification procedure was as follows: denaturation at 94°C for 3 min; 35 cycles (denaturation at 94°C for 45 s, annealing at 45°C for 30 s, and extension at 72°C for 90 s); and a final extension at 72°C for 5 min. The PCR reaction system contained a total of 15 μL, with 13 μL of 2 × Taq Plus Master Mix, 0.5 μL of Primer-F, 0.5 μL of Primer-R, and 1 μL of DNA template.

Primers, V1F, and 1492R were used for the first round of nested PCR amplification. The second-round primers, YW-F and YW-R, are shown in **Table 1**. The target segment was 322 bp. The

TABLE 1 | Primer sequences and PCR product size.

Primer name	Primer sequence (5′–3′)	Product size (bp)
V1F	CACCAGGTTGATTCCTGAC	1295
1492R	GGTTACCTTGTTACGACTT	
YW-F	GAAATGGCGAACGGCTCA	322
YW-R	TGCTGGCACCAAACTTGC	
RPS9-F	AGGATCTGTTTATGCTGCTA	206
RPS9-R	AACGGTATGATTTCTGGTAT	

amplification procedure was as follows: denaturation at 94°C for 3 min; 35 cycles (denaturation at 94°C for 30 s, annealing at 55°C for 45 s, and extension at 72°C for 45 s); and a final extension at 72°C for 5 min. The PCR reaction system was the same as in the first round of nested PCR amplification, and DNA samples were taken from the first round of PCR and diluted 1000 times.

Preparation of Plasmid Standard

Conventional PCR amplification: Using the EAM-positive samples as the template, the ribosomal protein S9 (RPS9) primers were used for amplification. The primers specific for RPS9 (GenBank accession number: MZ420734), RPS9-F, and RPS9-R, were designed using Primer 5.0 (**Supplementary File 1**). The RPS9-F and RPS9-R primer sequences are shown in **Table 1**. The PCR procedure was as follows: pre-denaturation at 94°C for 3 min; 35 cycles (denaturation at 94°C for 30 s, annealing at 55°C for 30 s, and extension at 72°C for 30 s); and a final extension at 72°C for 5 min. The PCR reaction system was the same as that described for nested PCR.

Purification and recovery of DNA fragments: The PCR product was dispensed into the well of a 1.5% agarose gel, which was then transferred to an electrophoresis apparatus and run at 100 V for 38 min. After electrophoresis, a strong, positive single strip of 206 bp was rapidly excised from the gel, and the gel containing the target strip was placed in a centrifuge tube, following which DNA was recovered using a FastPure Gel DNA Extraction Mini Kit (Vazyme, Nanjing, China).

Vector recombination: A reaction solution (5 μL total volume) composed of pMD-19-T vector (1 μL), extracted DNA samples (1 μL), and ddH_2O (3 μL) was prepared. Next, 5 μL of solution I was added to the prepared reaction solution and left to stand overnight at 4°C.

Strain screening: A mixture of vector solution and *Escherichia coli* DH5α competent cells was added to a 1.5 mL centrifuge tube, placed on ice for 30 min, heated at 42°C for 45 s, and placed on ice for 1 min. Subsequently, 890 μL of LB medium was added, and the mixture was shaken at 37°C for 60 min. Selection plates were made by adding 35 μL of X-gal and 5 μL of IPTG to LB agar medium containing ampicillin (AMP). Next, 100 μL of bacterial solution was spread on the selection plate, and the plate was placed in an incubator at 37°C overnight after sealing with parafilm. A single white colony was picked from the plate using a pipette tip and dissolved in 100 μL of ddH_2O. One microliter of the plasmid DNA sample was verified via sequencing (Sangon, Shanghai, China). The remaining liquid was poured into a centrifuge tube containing 10 mL of AMP-LB liquid and placed in an orbital shaker for approximately 4 h until the liquid was turbid. Plasmids were extracted using a FastPure Plasmid Mini Kit (Vazyme, Nanjing, China).

Optimization of the Quantitative PCR Amplification Conditions

The initial concentration of the plasmid was 7.3 ng/μL. According to the formula copies/μL = initial concentration (ng/μL) × 6.02×10^{14}/[(base number of vector fragment + base number of target gene) × 660], the copy number of the recombinant plasmid was 2.2×10^9 copies/μL. The recombinant plasmid was diluted using a 10-fold serial dilution with DEPC-treated water, and a 2.2×10^8–2.2×10^1 copies/μL plasmid standard was used as a template for qPCR amplification. The recombinant plasmid gradient was used as the standard, and the total reaction system volume was 20 μL. The PCR reaction system contained 10.0 μL of 2 × ChamQ Universal SYBR qPCR Master Mix, 0.4 μL of RPS9-F, 0.4 μL of RPS9-R, 8.2 μL of ddH_2O, and 1 μL of recombinant plasmid. The blank group was treated with ddH_2O instead of DNA samples. The amplification reaction was performed in the Applied Biosystems QuantStudio 3 (Thermo Fisher Scientific, Waltham, MA, United States). After pre-denaturation at 95°C for 30 s, 40 cycles of amplification at 95°C for 10 s, X°C for 30 s (X was the annealing temperature gradient and the set range was 50–65°C) and 72°C for 30 s were carried out to select the best annealing temperature. The data analysis was performed using QuantStudio Design and Analysis Software v1.4 (Applied Biosystems). The optimum annealing temperature was 55°C, and the reaction procedure was as follows: pre-denaturation at 95°C for 30 s and 40 cycles (95°C for 10 s; 55°C for 30 s; 72°C for 30 s).

Plotting of Quantitative PCR Standard Curve for *Enterocytospora artemiae*

The recombinant plasmid was diluted via a 10-fold serial dilution, which yielded a dilution series of 8 concentrations ranging from 2.2×10^8 to 2.2×10^1 copies/μL. The standard curve of the relationship between the logarithm of the initial quantity of the standard template (x) and the cycle threshold number (Ct) of the amplification products was established. The quality of the standard curve was determined by analyzing the correlation coefficient and amplification efficiency.

Sensitivity Comparison, Specificity Analysis, and Stability Evaluation of Quantitative PCR Primer RPS9

The sensitivity of qPCR and conventional PCR (RPS9), indicated by recombinant plasmids with a concentration of 2.2×10^8–2.2×10^1 copies/μL, and detection limits for qPCR and conventional PCR were analyzed by determining whether showing an S-shaped amplification curves and whether the target bands appeared separately. Furthermore, qPCR, nested PCR (V1F/1492R—YW-F/YW-R), and conventional PCR (V1F/1492R) were used to detect the 90 shrimp hepatopancreas samples simultaneously.

DNA from the hepatopancreases of healthy *P. sinensis* was used as the negative control, and microsporidia (EHP, *Hepatospora eriocheir* and *Microsporidia* sp.), viruses (white spot syndrome), bacteria (*Pseudomonas putida* and *Vibrio parahaemolyticus*), and fungi (*Metschnikowia bicuspidata*) were detected simultaneously. These pathogens were obtained from our laboratory. Specificity was analyzed using conventional PCR (RPS9) and qPCR.

To determine the stability of qPCR, serially diluted positive plasmid DNA (2.2×10^8–2.2×10^1 copies/μL) was used for qPCR templates, in which three replicates were set for each

template concentration. Stability assessment consisted of two parts: intra-group repetition (in the same experiment) and inter-group repetition (in the same group). For intra-group repetition, the mean value, standard deviation, and coefficient of variation were calculated using the *Ct* value of three replicates (Liu et al., 2016). For inter-group repetition, the experiment was repeated thrice. The mean value, standard deviation, and coefficient of variation were calculated using the *Ct* value of three experiments (Ding et al., 2017).

Tissue Tropisms and Detection of Potential *Enterocytospora artemiae* Carriers by Quantitative PCR

Tissue tropisms: 10 shrimp were randomly selected from the temporary container for tissue tropism detection. The selected tissues included the hepatopancreas, gut, gill, muscle, and stomach.

Potential carriers: Biological and water samples were collected from the rice field of infected *P. sinensis*. The biological samples included fish, two *Chanodichthys erythropterus* and five *Pseudorasbora parva*; shrimp, five *Macrobrachium nipponense* and four *Neocaridina denticulate*; five cladocerans; and five copepods. The hepatopancreas tissues of fish and shrimp and the whole cladocerans and copepods were used for DNA extraction. The water samples from the rice field were filtered using a 0.22 μM filter membrane. The filter membrane was then washed with distilled water, the supernatant was discarded after centrifugation (8000 rpm, 10 min), and the precipitate was used to extract DNA. The extracted DNA was diluted to 50 ng/μL, and then was detected by qPCR and nested PCR. PCR amplification products of nested PCR

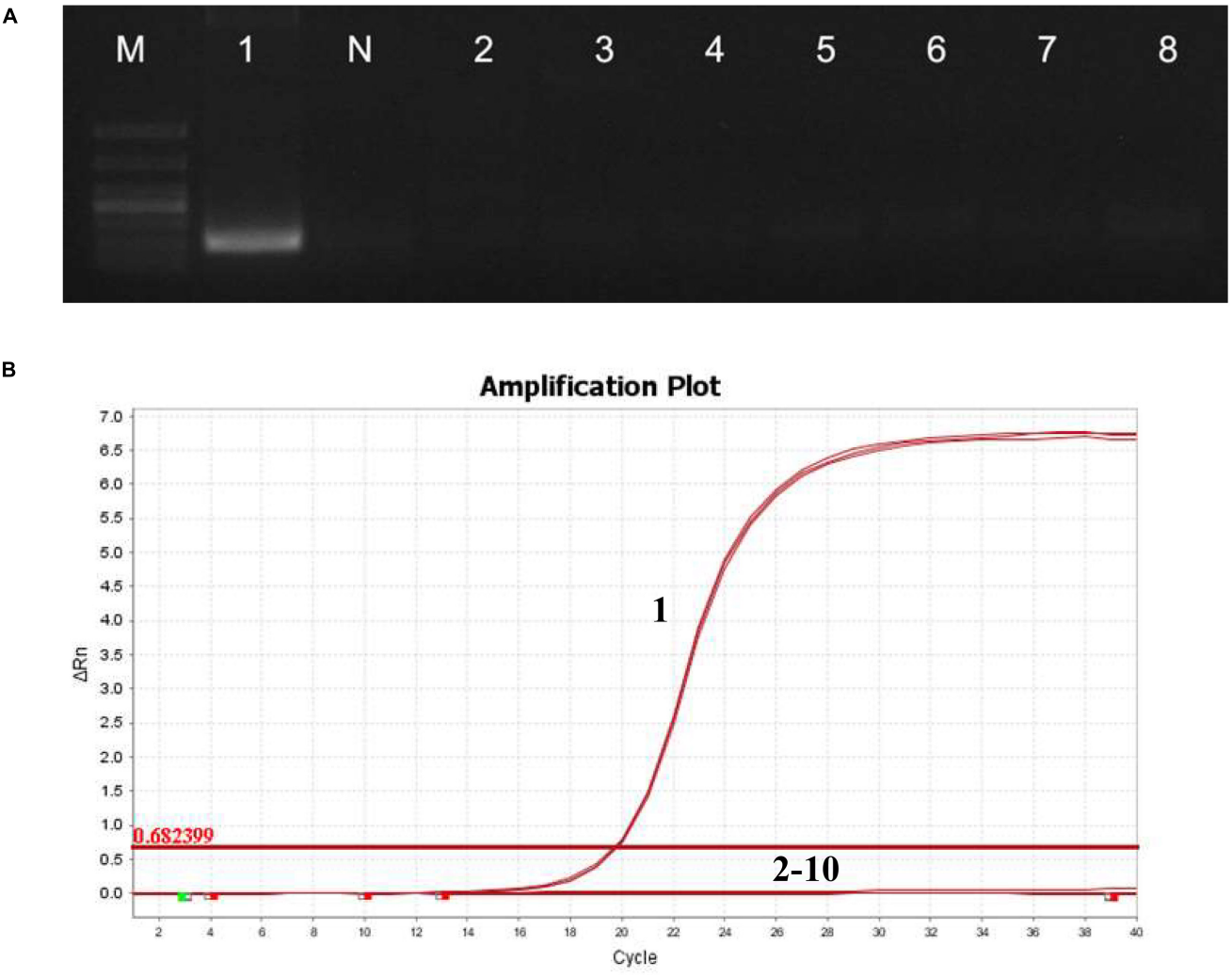

FIGURE 1 | Specificity of detection of RPS9. **(A)** Electrophoresis of PCR products amplified using primer RPS9. M: DL1000; 1: EAM; N: healthy shrimp hepatopancreas DNA; 2: *E. hepatopenaei*; 3: *H. eriocheir*; 4: *M. bicuspidata*; 5: *Microsporidia* sp.; 6: *P. putida*; 7: *V. parahaemolyticus*; and 8: white spot syndrome virus. **(B)** Specificity of qPCR amplification curve of RPS9. 1: EAM; 2: *E. hepatopenaei*; 3: *H. eriocheir*; 4: *M. bicuspidata*; 5: *Microsporidia* sp.; 6: *P. putida*; 7: *V. parahaemolyticus*; 8: white spot syndrome virus; 9: healthy shrimp hepatopancreas DNA; and 10: water.

positive samples were verified EAM via sequencing (Sangon, Shanghai, China).

RESULTS

Specificity Analysis

The specificity of qPCR primers was analyzed by detecting other microsporidia, fungi, bacteria, and viruses. Only the hepatopancreatic DNA of EAM-infected shrimp appeared as a bright, single target band (**Figure 1A**), indicating that the primer RPS9 had high specificity. In addition, the qPCR amplification curve showed that only samples with positive EAM showed amplification curves, whereas no fluorescence signal was detected for non-target genes (**Figure 1B**), further indicating that the primer showed excellent specificity.

Construction of Quantitative PCR Standard Curve

The established qPCR system for EAM was used to amplify eight standard templates (2.2×10^8–2.2×10^1 copies/μL) with 10-fold gradient dilution, and the standard curve of the relationship between the threshold *Ct* value and the logarithm of the initial quantity of standard templates (x) was established. The qPCR results showed a strong fluorescence signal from 2.2×10^8 to 2.2×10^1 copies/μL (**Figure 2A**). The relationship was $Ct = -3.281 \log x + 36.543$ (**Figure 2B**). The correlation coefficient R^2 was 0.998, and the amplification efficiency was 101.737%.

Melting curve analysis (**Figure 2C**) showed that the curves of three parallel amplification products in each gradient group merged to produce a single melting peak at 82.4°C, with overlapping positions. This unique melting peak indicated that there was no non-specific amplification or primer dimer formation during the amplification process.

Stability Assessment

Six concentrations of plasmid (2.2×10^8–2.2×10^1 copies/μL) were selected, and a repeatability analysis was conducted using three parallel samples of the same gradient within the group. The coefficient of variation of *Ct* was much less than 1% (**Table 2**), indicating that intra-group repeatability was very good. All coefficients of variation between groups were less than 2% (**Table 2**), indicating that the method showed good repeatability, thereby ensuring the stability and reliability of the test results.

Comparison of Sensitivity Between Quantitative PCR and Conventional PCR

Standard plasmid templates (2.2×10^8–2.2×10^1 copies/μL) were used for conventional PCR and qPCR. The amplified

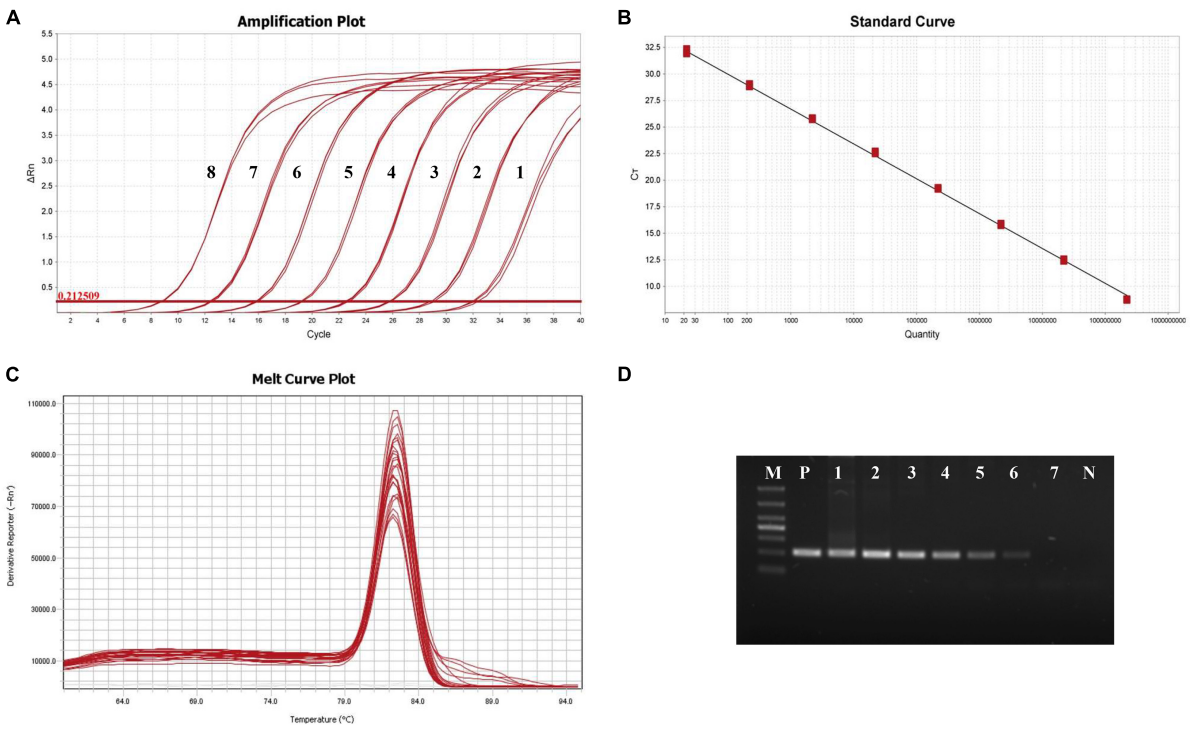

FIGURE 2 | Amplification of the standard samples. **(A)** The amplification curve of RPS9-qPCR. 1: 2.2×10^1 copies/μL; 2: 2.2×10^2 copies/μL; 3: 2.2×10^3 copies/μL; 4: 2.2×10^4 copies/μL; 5: 2.2×10^5 copies/μL; 6: 2.2×10^6 copies/μL; 7: 2.2×10^7 copies/μL; and 8: 2.2×10^8 copies/μL. **(B)** Standard curve of qPCR-RPS9. **(C)** Melting curve of qPCR-RPS9. **(D)** Agarose electrophoresis of conventional PCR-RPS9. M: DL1000; P: EAM; N: Hepatopancreas DNA of healthy shrimp; 1: 2.2×10^7 copies/μL; 2: 2.2×10^6 copies/μL; 3: 2.2×10^5 copies/μL; 4: 2.2×10^4 copies/μL; 5: 2.2×10^3 copies/μL; 6: 2.2×10^2 copies/μL; and 7: 2.2×10^1 copies/μL.

TABLE 2 | Repeatability of detection of EAM by RPS9-qPCR.

Template quantity	*Ct* values intra-group		*Ct* values between groups	
	Average value ± standard deviation	Coefficient of variation (%)	Average value ± standard deviation	Coefficient of variation (%)
2.2×10^8	8.76 ± 0.06	0.68	8.80 ± 0.12	1.36
2.2×10^7	12.46 ± 0.10	0.80	12.51 ± 0.08	0.64
2.2×10^6	15.83 ± 0.08	0.51	15.84 ± 0.10	0.63
2.2×10^5	19.22 ± 0.07	0.36	19.09 ± 0.17	0.89
2.2×10^4	22.60 ± 0.11	0.49	22.61 ± 0.07	0.31
2.2×10^3	25.80 ± 0.08	0.31	25.74 ± 0.14	0.54
2.2×10^2	28.90 ± 0.15	0.52	29.03 ± 0.40	1.38
2.2×10^1	32.11 ± 0.23	0.72	31.62 ± 0.51	1.61

products of conventional PCR were analyzed by electrophoresis on a 1.5% agarose gel. The primer, RPS9, was detected by conventional PCR at 2.2×10^2 copies/μL, and at this concentration, the electrophoresis band was dim and almost invisible to the eye (**Figure 2D**).

With qPCR, the fluorescence signal could be detected from 2.2×10^1 to 2.2×10^8 copies/μL (**Figure 2A**). When the template concentration was 2.2×10^1 copies/μL, the cycle threshold was 32.11 and had good S-shaped amplification curves, indicating that the detection limit of qPCR was 2.2×10^1 copies/μL and that sensitivity was over 10 times that of conventional PCR.

Detection of Samples by Nested PCR and Quantitative PCR for *Enterocytospora artemiae*

Nested PCR showed that, of the 90 *P. sinensis* hepatopancreas samples, 56 were positive, indicating a detection rate of 62.22% (56/90). The ratio of PCR samples negative in the first round to PCR samples positive in the second round was 37/56 (66.07%), and the ratio of positives in both rounds was 19/56 (33.93%). The qPCR results showed that 73 shrimp samples were positive, with a detection rate of 81.11% (73/90). *Ct* was substituted in the established formula $Ct = -3.281 \log x + 36.543$. The *E. artemiae* content ranged from 4.4×10^1 to 6.3×10^7 copies/μL. EAM could be detected only when the level of 1.4×10^5 copies/μL was exceeded in the first round of PCR. When the copy number of EAM small subunit (SSU) rRNA was lower than 4.6×10^3 copies/μL, the results for nested PCR were negative, whereas the limit of qPCR for EAM was 2.2×10^1 copies/μL. This indicates that the sensitivity of qPCR for EAM was over 200 times higher than that of nested PCR for detecting *P. sinensis* in hepatopancreas samples.

Tissue Tropisms and Potential Carrier Detection by Quantitative PCR for *Enterocytospora artemiae*

The EAM load in the five tissues differed (**Table 3**). It was highest in the hepatopancreas, followed by the gut, gill, stomach, and muscle. However, there was no difference in the positive rate of EHP among the five tissues, all of which were 80%.

The water samples collected from the rice field of infected *P. sinensis* were all positive by qPCR detection. Some samples of fish and shrimp in the collected aquatic biological samples were positive by PCR detection, and the positive rate of cladocerans and copepods reached 80% (**Table 4**). However, *C. erythropterus and M. nipponense* was not detected by nested PCR (**Table 4**). Nested PCR positive samples were confirmed as EAM after sequencing and blast analysis, indicating that qPCR detection method had high sensitivity.

DISCUSSION

Rapid and accurate identification of pathogens is the basis of aquatic animal disease control. Microscopic examination is a rapid method. However, microsporidia can be observed under high magnification only when infection is severe. In addition, it is difficult to accurately identify microsporidia only by appearance due to inconsistencies during different developmental stages. Therefore, it is impossible to obtain accurate information regarding *E. artemiae* infection via microscopic examination. Based on this, highly sensitive molecular methods, such as PCR (Tang et al., 2015), nested PCR (Jaroenlak et al., 2016), qPCR (Liu et al., 2018; Piamsomboon et al., 2019), loop-mediated isothermal amplification (Suebsing et al., 2013; Cai et al., 2018), and recombinase polymerase amplification (Ma et al., 2021), are used instead of microscopic methods. Compared with conventional PCR, qPCR has the advantages of high sensitivity, good repeatability and quantification. Furthermore, qPCR reduces non-specific amplification and shortens detection time. Two common qPCR methods are the TaqMan probe and the SYBR Green I fluorescent dye method. Although the TaqMan probe method shows higher specificity, its cost of detection is also high, limiting its practical use. The SYBR Green I fluorescence method has the advantages of low cost and easy implementation and is more suitable for rapid detection. Notably, qPCR is often used in the detection of microsporidia and is considered to be more sensitive than conventional PCR (Naung et al., 2020). Wang et al. (2020) used qPCR to detect the polar tube protein 2 gene when quantitatively analyzing EHP in infected shrimp and reported that sensitivity was increased by at least two orders of magnitude compared with that of conventional PCR. Phelps and Goodwin (2007) used the same technology to detect *Notemigonus crysoleucas* and reported that the minimum gene copy number that could be detected in each reaction was as low

TABLE 3 | Tissue tropisms of EAM in *P. sinensis*.

	Hepatopancreas	Gut	Muscle	Gill	Stomach
Log (EAM copies)/50 ng DNA	5.73 ± 0.79	3.67 ± 0.58	2.51 ± 0.46	3.17 ± 0.77	2.88 ± 0.71
Positive percentage (%)	80	80	80	80	80

TABLE 4 | Detection rate of EAM in samples from rice field of infected *P. sinensis* by qPCR and nested PCR.

Samples	Number	*Ct* value	Positive number by qPCR	Positive rate by qPCR (%)	Positive number by nested PCR	Positive rate by nested PCR (%)
Pseudorasbora parva	5	24.80 ± 3.74	3	60	2	40
Chanodichthys erythropterus	2	30.12	1	50	0	0
Macrobrachium nipponense	5	29.03 ± 0.29	2	40	0	0
Neocaridina denticulate	4	–	0	0	0	0
Cladocerans	5	23.52 ± 3.99	4	80	3	60
Copepods	5	25.88 ± 2.80	4	80	2	40
Water	5	23.80 ± 1.17	5	100	5	100

as 10. Because the SSU rRNA gene of microsporidium is not a single-copy gene, ultrasonic treatment of spores can be used to extract DNA, which improves detection sensitivity, enabling 0.14 spores to be detected at the lowest level in each reaction (Phelps and Goodwin, 2007). In this study, the sensitivity of qPCR for detecting EAM was higher than that of conventional PCR and nested PCR. With real samples, nested PCR did not detect target DNA fragments below 4.6×10^3 copies/μL, and the sensitivity was only approximately 1/200 of that of qPCR for EAM. In contrast, in a batch of real samples, the detection rate of qPCR for EAM (81.11%) was significantly higher than that of nested PCR (62.22%). Meanwhile, the qPCR method was used to detect EAM tissue tropism and the carriers in the culture environment. The tissue tropism detection found that the content in the hepatopancreas was the highest, indicating that it was the main location of EAM, which was consistent with previous research (Rode et al., 2013; Jiang et al., 2020). At the same time, EAM was also detected in the gut, gill, stomach and muscle, and the same results have been obtained with EHP (Santhoshkumar et al., 2017; Cheng et al., 2018). Although EAM was detectable in these tissues in this study, whether EAM can infect the cells of these tissues needs to be further studied. Furthermore, the same infection rates were obtained in different tissues, which may be related to the high content of EAM in *P. sinensis*. Certainly, hepatopancreatic tissue was preferred because the load was the highest (**Table 4**). However, when hepatopancreas tissue is used for the determination of other indexes in research, tissues such as the gut can be considered as an alternative for detecting infection. Environmental detection found EAM in some biological samples, except for *Neocaridina denticulata*, and the detection rate in water was 100%. Sequencing showed that the positive sample of nested PCR was EAM, but the detection rate was significantly lower than qPCR, indicating that qPCR method has high sensitivity and can find carriers in the environment. This can provide guidance for transmission route research and prevent EAM infection.

Researchers have attempted to use qPCR to detect different microsporidia genes, such as those encoding the SSU rRNA, the polar tube protein, tubulin, and the spore wall protein (Jaroenlak et al., 2016; Han et al., 2018; Piamsomboon et al., 2019; Wang et al., 2020). Of these, the SSU rRNA gene carries the most commonly used detection target sequence. However, this gives rise to false positive results and shows high similarity with SSU rRNA genes of different species, leading to false detections (Lucchi et al., 2012; Tangprasittipap et al., 2013; Hitakarun et al., 2014). Sequence alignment showed that the EAM SSU rDNA gene (GenBank No. MT 645708) had 94% shared homology with the SSU rRNA gene of *Globulispora mitoporans* (GenBank No. KT762153), which shared more than 85% identity with five other species (Jiang et al., 2020). Therefore, we selected a specific target to modify the SYBR Green I qPCR detection method to detect microsporidia in *P. sinensis*. In this study, we established a qPCR method for the detection of EAM using *RPS9* and established a minimum copy number of 22 copies/μL, indicating a highly sensitive diagnostic standard. *RPS9* is widely distributed in yeast, bacteria, parasites, mammals, and humans. Studies have shown that *RPS9* is a highly conserved gene, which plays a role in DNA repair, self-translation regulation, development regulation, malignant transformation of normal cells as well as in other undetected functions and is often used for pathogen detection (Lindström and Zhang, 2008; Lindström and Nistér, 2010; Araújo et al., 2012). In addition, whereas three species of microsporidia were detected using this study, no specific bands or interference reactions pertaining to other shrimp pathogens were found (**Figure 2**), indicating that the qPCR-RPS9 method showed high specificity.

Establishment of a qPCR method specifically for microsporidium not only enabled microsporidia to be detected sensitively and efficiently, but also allowed quantification. Analyzing microsporidium load is extremely important when conducting research on the prevention and control of microsporidia. Liu et al. (2016) reported that EHP load was negatively correlated with the growth of *L. vannamei*. When the relative copy number of EHP SSU rDNA in the hepatopancreas exceeded 10^3 copies/ng hepatopancreatic DNA, the growth of the shrimp was significantly slower, indicating that the effect of EHP on shrimp growth had reached a high-risk level

(Liu et al., 2016). Thus, detection of microsporidium load enables better breeding strategies to be formulated. A serious microsporidium infection in *P. sinensis* causes body color turbidity and hepatopancreatic lesions, seriously reducing aquaculture yields (Jiang et al., 2020). Therefore, establishment of a rapid and quantitative detection method may help determine the severity of infection. In addition, this method may be useful for clarifying the relationship between EAM load and growth, leading to productive *P. sinensis* cultivation.

CONCLUSION

Serious EAM infection leads to hepatopancreatic lesions, which greatly reduce the vitality of *P. sinensis*. Conventional PCR has low sensitivity and cannot be used for accurate quantitative detection of EAM. In this study, a SYBR Green I real-time fluorescent quantitative PCR detection method based on the sequence of the ribosomal protein S9 gene was established and optimized. This method had high specificity and stability and was more than 200 times more sensitive than nested PCR. Thus, detection data obtained using this method may be useful as a technical reference for rapid and accurate identification of EAM infection and for the prevention and control of EAM during *P. sinensis* breeding.

DATA AVAILABILITY STATEMENT

The datasets presented in this study can be found in online repositories. The names of the repository/repositories and accession number(s) can be found in the article/ **Supplementary Material**.

ETHICS STATEMENT

The animal study was reviewed and approved by the Animal Experiments Ethics Committee of Shenyang Agricultural University.

AUTHOR CONTRIBUTIONS

HJ, JB, and QC were involved in designing of the research and wrote the manuscript. HJ, JB, JL, YC, and SH performed the majority of the experiment, data processing, analysis, and interpretation. CF and XL assisted in sample collection and wrote the manuscript. All authors contributed to the article and approved the submitted version.

FUNDING

This work was supported by the Liaoning province Department of Education fund item (LSNQN202002), the China Agriculture Research System of MOF and MARA (CARS-48), the Liaoning Science and Technology Mission Project (2020JH 5/10400147 and 2020JH5/10400115), and the Liaoning Province Key R&D Planning Guidance Plan Project (2019JH8/102 00018).

SUPPLEMENTARY MATERIAL

The Supplementary Material for this article can be found online at: https://www.frontiersin.org/articles/10.3389/fmars.2021.730569/full#supplementary-material

REFERENCES

Araújo, H. F., Campos, P. C., Camargo, D. R., Pereira, F. N., Samuel, M. L., Oliveira, M. A., et al. (2012). Immune response and protective efficacy of S9 ribosomal protein of *Streptococcus pneumoniae* in a model of sepsis. *Can. J. Microbiol.* 58, 1055–1062. doi: 10.1139/w2012-083

Biju, N., Sathiyaraj, G., Raj, M., Shanmugam, V., Baskaran, B., Govindan, U., et al. (2016). High prevalence of *Enterocytozoon hepatopenaei* in shrimps *Penaeus monodon* and *Litopenaeus vannamei* sampled from slow growth ponds in India. *Dis. Aquat. Organ.* 120, 225–230. doi: 10.3354/dao03036

Cai, S. X., Kong, F. D., Xu, S. F., and Yao, C. L. (2018). Real-time loop-mediated isothermal amplification for rapid detection of *Enterocytozoon hepatopenaei*. *PeerJ* 6:e5993. doi: 10.7717/peerj.5993

Chaijarasphong, T., Munkongwongsiri, N., Stentiford, G. D., Aldama-Cano, D. J., Thansa, K., Flegel, T. W., et al. (2020). The shrimp microsporidian *Enterocytozoon hepatopenaei* (EHP): biology, pathology, diagnostics and control. *J. Invertebr. Pathol.* 2020:107458. doi: 10.1016/j.jip.2020.107458

Cheng, D. Y., Qiu, L., Song, Z. L., Wan, X. Y., Dong, X., Xie, G. S., et al. (2018). Differences between populations and tissues of *Litopenaeus vannamei* infected with *Enterocytozoon hepatopenaei*. *Prog. Fishery Sci.* 39, 83–92. doi: 10.19663/j.issn2095-9869.20170426001

Didier, E. S., and Weiss, L. M. (2011). Microsporidiosis: not just in AIDS patients. *Curr. Opin. Infect. Dis.* 24, 490–495. doi: 10.1097/QCO.0b013e32834aa152

Ding, Z. F., Chen, J. Q., Lin, J., Zhu, X. S., Xu, G. H., Wang, R. L., et al. (2017). Development of In situ hybridization and real-time PCR assays for the detection of *Hepatospora eriocheir*, a microsporidian pathogen in the Chinese mitten crab *Eriocheir sinensis*. *J. Fish Dis.* 40, 919–927. doi: 10.1111/jfd.12573

Han, J. E., Tang, K., and Hyung, K. J. (2018). The use of beta-tubulin gene for phylogenetic analysis of the microsporidian parasite *Enterocytozoon hepatopenaei* (EHP) and in the development of a nested PCR as its diagnostic tool. *Aquaculture* 495, 899–902. doi: 10.1016/j.aquaculture.2018.06.059

Higes, M., Meana, A., Bartolomé, C., Botías, C., and Martín-Hernández, R. (2013). *Nosema ceranae* (Microsporidia), a controversial 21st century honey bee pathogen. *Environ. Microbiol. Rep.* 5, 17–29. doi: 10.1111/1758-2229.12024

Hitakarun, A., Tan-ariya, P., Siripattanapipong, S., Mungthin, M., Piyaraj, P., Naaglor, T., et al. (2014). Comparison of PCR methods for detection of *Leishmania siamensis* infection. *Parasit. Vectors* 7:458. doi: 10.1186/s13071-014-0458-x

Jaroenlak, P., Sanguanrut, P., Williams, B. A., Stentiford, G. D., Flegel, T. W., Sritunyalucksana, K., et al. (2016). A nested PCR assay to avoid false positive detection of the microsporidian *Enterocytozoon hepatopenaei* (EHP) in environmental samples in shrimp farms. *PLoS One* 11:e0166320. doi: 10.1371/journal.pone.0166320

Jiang, H., Chen, Y., Bao, J., Li, X., Feng, C., Xing, Y., et al. (2020). Isolation of the parasite *Enterocytospora artemiae* from Chinese grass shrimp (*Palaemonetes sinensis*)-first report in Asia. *Front. Cell. Infect. Microbiol.* 10:580088. doi: 10.3389/fcimb.2020.580088

Kent, M. L., and Speare, D. J. (2005). Review of the sequential development of Loma salmonae (Microsporidia) based on experimental infections of rainbow trout (*Oncorhynchus mykiss*) and Chinook salmon (*O. tshawytscha*). *Folia Parasitol.* 52, 63–68. doi: 10.14411/fp.2005.009

Kotková, M., Sak, B., and Kváč, M. (2018). Differences in the intensity of infection caused by *Encephalitozoon cuniculi* genotype II and III - Comparison using

quantitative real-time PCR. *Exp. Parasitol.* 192, 93–97. doi: 10.1016/j.exppara.2018.07.019

Li, P., Mi, R., Zhao, R., Li, X., Zhang, B., Yue, D., et al. (2019). Quantitative real-time PCR with high-throughput automatable DNA preparation for molecular screening of *Nosema* spp. in *Antheraea pernyi*. *J. Invertebr. Pathol.* 164, 16–22. doi: 10.1016/j.jip.2019.04.003

Lindström, M. S., and Nistér, M. (2010). Silencing of ribosomal protein S9 elicits a multitude of cellular responses inhibiting the growth of cancer cells subsequent to p53 activation. *PLoS One* 5:e9578. doi: 10.1371/journal.pone.0009578

Lindström, M. S., and Zhang, Y. (2008). Ribosomal protein S9 is a novel B23/NPM-binding protein required for normal cell proliferation. *J. Biol. Chem.* 283, 15568–15576. doi: 10.1074/jbc.M801151200

Liu, Y. M., Qiu, L., Sheng, A. Z., Wan, X. Y., Cheng, D. Y., and Huang, J. (2018). Quantitative detection method of *Enterocytozoon hepatopenaei* using TaqMan probe real-time PCR. *J. Invertebr. Pathol.* 151, 191–196. doi: 10.1016/j.jip.2017.12.006

Liu, Z., Zhang, Q. L., Wan, X. Y., Ma, F., and Huang, J. (2016). Development of real-time PCR assay for detecting microsporidian *Enterocytozoon hepatopenaei* and the application in shrimp samples with different growth rates. *Prog. Fishery Sci.* 37, 119–126. doi: 10.11758/yykxjz.20150512003

Lucchi, N. W., Poorak, M., Oberstaller, J., DeBarry, J., Srinivasamoorthy, G., Goldman, I., et al. (2012). A new single-step PCR assay for the detection of the zoonotic malaria parasite Plasmodium knowlesi. *PLoS One* 7:e31848. doi: 10.1371/journal.pone.0031848

Ma, C., Fan, S., Wang, Y., Yang, H., Qiao, Y., Jiang, G., et al. (2021). Rapid detection of *Enterocytozoon hepatopenaei* infection in shrimp with a real-time isothermal recombinase polymerase amplification assay. *Front. Cell. Infect. Microbiol.* 11:631960. doi: 10.3389/fcimb.2021.631960

Nageswara Rao, S., Muthulakshmi, M., Kanginakudru, S., and Nagaraju, J. (2004). Phylogenetic relationships of three new microsporidian isolates from the silkworm, *Bombyx mori*. *J. Invertebr. Pathol.* 86, 87–95. doi: 10.1016/j.jip.2004.05.004

Naung, M., Webster, T., Lloyd, R., Leaniz, C., and Consuegra, S. (2020). A novel qPCR assay for the rapid detection and quantification of the lumpfish (*Cyclopterus lumpus*) microsporidian parasite *Nucleospora cyclopteri*. *Aquaculture* 531:735779. doi: 10.1016/j.aquaculture.2020.735779

Pan, G., Bao, J., Ma, Z., Song, Y., Han, B., Ran, M., et al. (2018). Invertebrate host responses to microsporidia infections. *Dev. Comp. Immunol.* 83, 104–113. doi: 10.1016/j.dci.2018.02.004

Phelps, N. B., and Goodwin, A. E. (2007). Validation of a quantitative PCR diagnostic method for detection of the microsporidian *Ovipleistophora ovariae* in the cyprinid fish *Notemigonus crysoleucas*. *Dis. Aquat. Organ.* 76, 215–221. doi: 10.3354/dao076215

Piamsomboon, P., Choi, S. K., Hanggono, B., Nuraini, Y. L., Wati, F., Tang, K., et al. (2019). Quantification of *Enterocytozoon hepatopenaei* (EHP) in penaeid shrimps from Southeast Asia and Latin America using TaqMan probe-based quantitative PCR. *Pathogens* 8:233. doi: 10.3390/pathogens8040233

Pol, S., Romana, C. A., Richard, S., Amouyal, P., Desportes-Livage, I., Carnot, F., et al. (1993). Microsporidia infection in patients with the human immunodeficiency virus and unexplained cholangitis. *N. Engl. J. Med.* 328, 95–99. doi: 10.1056/NEJM199301143280204

Rode, N. O., Landes, J., Lievens, E. J., Flaven, E., Segard, A., Jabbour-Zahab, R., et al. (2013). Cytological, molecular and life cycle characterization of *Anostracospora rigaudi* n. g., n. sp. and *Enterocytospora artemiae* n. g., n. sp., two new microsporidian parasites infecting gut tissues of the brine shrimp Artemia. *Parasitology* 140, 1168–1185. doi: 10.1017/S0031182013000668

Santhoshkumar, S., Sivakumar, S., Vimal, S., Abdul Majeed, S., Taju, G., Haribabu, P., et al. (2017). Biochemical changes and tissue distribution of *Enterocytozoon hepatopenaei* (EHP) in naturally and experimentally EHP-infected whiteleg shrimp, *Litopenaeus vannamei* (Boone, 1931), in India. *J. Fish Dis.* 40, 529–539. doi: 10.1111/jfd.12530

Stentiford, G. D., Becnel, J. J., Weiss, L. M., Keeling, P. J., Didier, E. S., Williams, B. A. P., et al. (2016). Microsporidia - emergent pathogens in the global food chain. *Trends Parasitol.* 32, 336–348. doi: 10.1016/j.pt.2015.12.004

Stentiford, G. D., and Dunn, A. M. (2014). "Microsporidia in aquatic invertebrates," in *Microsporidia: Pathogens of Opportunity*, eds L. M. Weiss and J. J. Becnel (Hoboken, NJ: John Wiley & Sons, Inc), 579–604. doi: 10.1002/9781118395264.ch23

Suebsing, R., Prombun, P., Srisala, J., and Kiatpathomchai, W. (2013). Loop-mediated isothermal amplification combined with colorimetric nanogold for detection of the microsporidian *Enterocytozoon hepatopenaei* in penaeid shrimp. *J. Appl. Microbiol.* 114, 1254–1263. doi: 10.1111/jam.12160

Tang, K. F., Pantoja, C. R., Redman, R. M., Han, J. E., Tran, L. H., and Lightner, D. V. (2015). Development of in situ hybridization and PCR assays for the detection of *Enterocytozoon hepatopenaei* (EHP), a microsporidian parasite infecting penaeid shrimp. *J. Invertebr. Pathol.* 130, 37–41. doi: 10.1016/j.jip.2015.06.009

Tangprasittipap, A., Srisala, J., Chouwdee, S., Somboon, M., Chuchird, N., Limsuwan, C., et al. (2013). The microsporidian *Enterocytozoon hepatopenaei* is not the cause of white feces syndrome in whiteleg shrimp Penaeus (Litopenaeus) vannamei. *BMC Vet. Res.* 9:139. doi: 10.1186/1746-6148-9-139

Wang, L., Lv, Q., He, Y., Gu, R., Zhou, B., Chen, J., et al. (2020). Integrated qPCR and staining methods for detection and quantification of *Enterocytozoon hepatopenaei* in shrimp *Litopenaeus vannamei*. *Microorganisms* 8:1366. doi: 10.3390/microorganisms8091366

Conflict of Interest: The authors declare that the research was conducted in the absence of any commercial or financial relationships that could be construed as a potential conflict of interest.

Publisher's Note: All claims expressed in this article are solely those of the authors and do not necessarily represent those of their affiliated organizations, or those of the publisher, the editors and the reviewers. Any product that may be evaluated in this article, or claim that may be made by its manufacturer, is not guaranteed or endorsed by the publisher.

frontiers in Marine Science

ORIGINAL RESEARCH
published: 07 December 2021
doi: 10.3389/fmars.2021.771630

Sustainable Marine Aquaponics: Effects of Shrimp to Plant Ratios and C/N Ratios

*Yu-Ting Chu and Paul B. Brown**

Department of Forestry and Natural Resources, Purdue University, West Lafayette, IN, United States

Integrated aquaponic food production systems are capable of producing more food on less land using less water than conventional food systems, and marine systems offer the potential of conserving freshwater resources. However, there have been few evaluations of species combinations or operational parameters in marine aquaponics. The goal of this experiment was evaluation of stocking density ratio of Pacific whiteleg shrimp (*Litopenaeus vannamei*) to three edible halophytes (*Atriplex hortensis*, *Salsola komarovii*, and *Plantago coronopus*) with two C/N ratios in a 3 × 2 factorial design. There were three stocking density ratios (shrimp: plant), 2:1, 3:1, and 5:1; and two C/N ratios, 12 and 15. The results indicated that stocking density ratio exerted a significant impact on shrimp growth. Shrimp reared in 2:1 and 3:1 treatments had better growth performance. In contrast, plants were affected by both stocking density ratio and C/N ratio. Halophytes grown in stocking density ratios of 3:1 and 5:1 with a C/N ratio of 15 had better growth performance and nutrient content. The concentrations of TAN and NO_2^- were below 0.2 mg/ L throughout the experiment, including the higher stocking density ratio treatments. In conclusion, the stocking density ratio of 3:1 with a C/N ratio of 15 was suggested as the optimal condition for the operation of marine aquaponics in which whiteleg shrimp and the three halophytes are target crops.

Keywords: marine aquaponics, shrimp to plant ratio, C/N ratio, *Litopenaeus vannamei*, halophytic plants, biofloc, sustainable food production, water pumpless system design

OPEN ACCESS

Edited by:
Xiangli Tian,
Ocean University of China, China

Reviewed by:
Nathalie Rose Le François,
Montreal Biodome, Canada
Li Li,
Ocean University of China, China

***Correspondence:**
Paul B. Brown
pb@purdue.edu

Specialty section:
This article was submitted to Marine Fisheries, Aquaculture and Living Resources, a section of the journal Frontiers in Marine Science

Received: *06 September 2021*
Accepted: *15 November 2021*
Published: *07 December 2021*

Citation:
Chu Y-T and Brown PB (2021) Sustainable Marine Aquaponics: Effects of Shrimp to Plant Ratios and C/N Ratios. Front. Mar. Sci. 8:771630. doi: 10.3389/fmars.2021.771630

INTRODUCTION

Integrated aquaponic food production systems are capable of producing more food, on less land, using less water and a lower environmental impact than conventional food production systems (Somerville et al., 2014; Alshrouf, 2017; Goddek et al., 2019). Adopting a salt-, or brackish water aquaponics system significantly increases the potential animal species that could be raised, and many of the potential species have good name recognition and demand in the marketplace. Further, marine aquaponics reduces the reliance on freshwater resources. Water usage in a marine recirculating aquaculture system can be as low as 16 L per kg of seafood produced, while usage in freshwater recirculating aquaculture system is approximately 50 L per kg of production (Klinger and Naylor, 2012). Marine systems rely on saltwater for initial fill and replacement of evaporative losses, given the system is near a natural source of saltwater (Klinger and Naylor, 2012). Freshwater would only be needed in these situations to adjust salinity to desired levels. Additionally, marine and/or brackish water species tend to have lower FCR (on average) and grow faster than freshwater species (Fry et al., 2018). Of the potential animal species, the Pacific whiteleg shrimp

(*Litopenaeus vannamei*) appears to have potential in the short-term as global production was second highest among aquaculture industries in 2018 (FAO, 2020) (4966.2 thousand metric tons) and they display rapid growth (FAO, 2006), high market price (Ross et al., 2017) and strong global demand (FAO, 2020). Whiteleg shrimp are tolerant of a wide range of salinities (Gao et al., 2016; Ray and Lotz, 2017; Pinheiro et al., 2020; Chu and Brown, 2021) and stocking densities (Otoshi et al., 2007; Krummenauer et al., 2011; Araneda et al., 2020) (90 to 600 shrimp/m^2) making them strong candidates for marine aquaponics. Further, shrimp might alleviate the "economic drain" of fish raised in freshwater aquaponic systems (Quagrainie et al., 2018). However, the complex interaction between marine aquaponic subsystems and taxa has received little attention in the scientific literature.

Halophytes (salt-tolerant plants) only represent 2% of terrestrial plant species and most of them are not common commodities; however, they have been used for many purposes such as food and forage crops, oilseeds, phytoremediation and medicinal purposes (Glenn et al., 1998, 1999; Ventura and Sagi, 2013; Panta et al., 2014; Panth et al., 2016; Kim et al., 2017). Red orache (*Atriplex hortensis*), okahijiki (*Salsola komarovii*), and minutina (*Plantago coronopus*) are edible halophytes that possess high nutrient concentrations (protein, amino acids, vitamins, and minerals) and have been successfully raised in marine aquaponics (Chu and Brown, 2021). However, the ratio of subsystem components, which will impact the flow of nutrients and health of subsystem taxa, has not been evaluated in marine aquaponic food production systems.

Several broad generalizations have been developed to help conceptualize the sizing and ratios of aquaponic subsystems. For example, current recommendations include 60 to 100 grams of fish feed/d/m^2 of plant growing area, a 1:2 ratio of fish tank volume to hydroponic media, a 7.3:1 ratio of plant-bed surface to fish-tank surface area, and a 3:1 ratio of hydroponic tank volume to fish production tank volume (Rakocy, 2012; Somerville et al., 2014; Lam et al., 2015). Generalized ratios fail to acknowledge the biological variability associated with potential species combinations. For example, feed consumption varies between species of fish and crustacean, dietary formulations contain varying concentrations of crude protein and amino acids, nutrient needs of plants vary as a function of growth stage (vegetative vs. fruiting), plant nutrient uptake is influenced by environmental conditions (pH, temperature and the microbiome in the rhizosphere), and the recommendations assume the space and nutritional needs of the system microbiome are adequate. The ratio of specific animals to plants might be a more realistic view of the physiological interactions and flow of nutrients that must occur in an integrated system. Consequently, the ratio of animals to plants must be understood for economical and sustainable operation.

Biofloc technology (BFT) has been used for decades to manage and control the water quality at safe ranges for target organisms in high density aquaculture (Avnimelech, 1999). Biofloc technology is an agglomeration of diverse microbes, which includes heterotrophic and autotrophic bacteria, algae, zooplankton, fungi, and viruses. The major function of BFT is to assimilate and mineralize toxic metabolites such as total ammonia nitrogen (TAN) and nitrite (NO_2^-) in the water (Panigrahi et al., 2018; Luo et al., 2020). Biofloc technology requires the addition of organic carbon to manipulate the C/N ratio and accelerate the development of the microbial communities. A C/N ratio between 10 and 20 is recommended for aquaculture (Xu et al., 2016, 2018; Panigrahi et al., 2018), while the recommendation for aquaponic systems is lacking. Moreover, inoculating probiotics is a promising approach to ensure the dominant bacteria are beneficial organisms (Crab et al., 2012). While it is common to amend the growing environment for better plant nutrient uptake and a higher yield, there is little information about the optimal C/N ratio in nutrient solutions for plant cultivation (Rodríguez-Kábana, 1986; Schenck, 2001; White, 2012; Pyakurel et al., 2019; Li et al., 2020).

The goal of this project was to evaluate critical ratios of crop density in aquaculture and hydroponics subsystems and provide operational guidelines for marine aquaponics. Specific objectives were to evaluate stocking densities and the C/N ratio on growth and production of whiteleg shrimp and three halophytes.

MATERIALS AND METHODS

Aquaponic System Design

Eighteen individual aquaponic systems were constructed at the Aquaculture Research Lab, Purdue University. The following are the components of each system; an aquaculture tank (113.6L), a hydroponic tank (102.2L), and a biofilter tank (18.9 L; **Figure 1**). To avoid shrimp escape and algal growth, plastic mesh, and lids were placed on the top of aquaculture tanks and hydroponic tanks, respectively. The lids on the top of hydroponic tanks were used to inhibit light into the tank, and also used as the floating rafts to support plants. Every biofilter tank was equipped with a 25-micron filter bag and bio-balls (surface area 98 ft^2/ft^3; Pentair Aquatic Eco-Systems, Inc., Apopka, FL, United States). Bio-balls in the biofilter tank were used to provide high surface area for attachment and colony expansion of microbes, and the filter bag was used to filter water from shrimp culture to prevent plant roots from clogging by biofloc. Air stones were installed in aquaculture tanks, hydroponic tanks, and biofilter tanks to maintain dissolved oxygen (DO) level above 6 mg/ L. To maintain the water temperature within the optimal range 26–28°C for shrimp, submersible heaters (300w; Aqueon, Wisconsin, United States) were used in aquaculture tanks. Light source for plant growth was provided via LED light tubes (40w, 5000 lumens, 4000K daylight white; Kihung LED, Guangdong, China), that were suspended at a height of 16.5 cm over the plant growth bed. Quantum sensor (MQ-500 Full-Spectrum Quantum Meter; Apogee Instruments, Inc., UT, United States) was used to measure light intensity. The photosynthetically active radiation averaged 234 $\mu molm^{-2}s^{-1}$. The photoperiod was 14 h light and 10 h dark.

Biological Material

Shrimp

Pacific whiteleg shrimp were purchased from a commercial shrimp farm (RDM Aquaculture, Fowler, IN, United States), and transported to the Aquaculture Research Lab. Water temperature

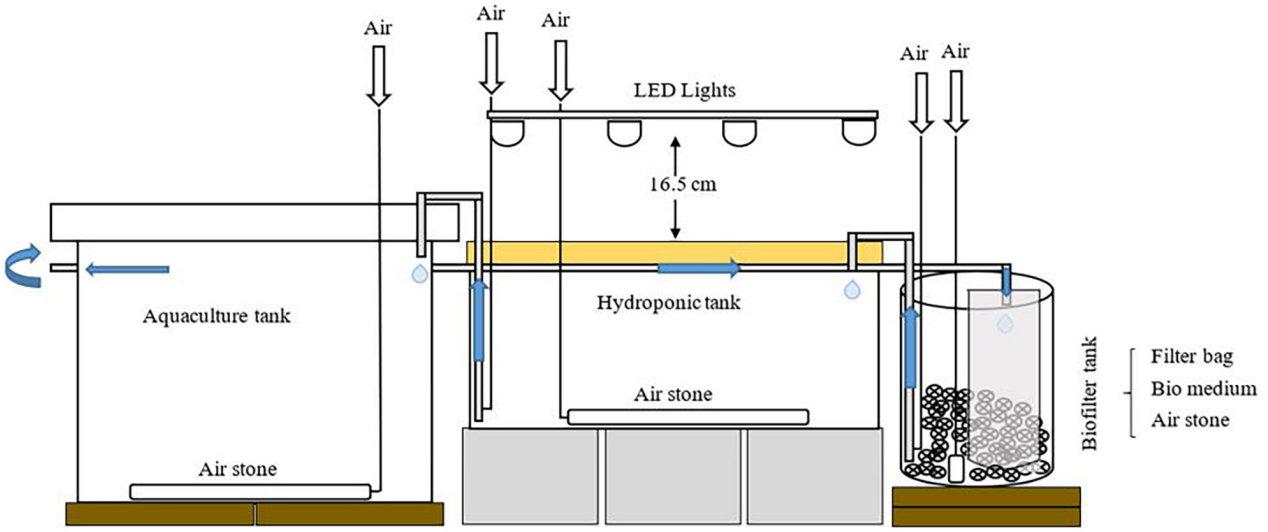

FIGURE 1 | Schematic diagram of an aquaponics system unit (adapted from Chu and Brown (2021); https://creativecommons.org/licenses/by/4.0/).

during transport was 24°C and salinity was 15 ppt. Shrimp were separated into three 700 L tanks, and quarantined for 1 week before moving into aquaponic systems. During quarantine, shrimp were fed a commercial shrimp feed (Zeigler Brothers, Gardners, PA, United States) twice a day at 8 a.m. and 5 p.m., with a total daily amount of 3.0% of body weight divided into equal aliquots.

Plants

Seeds of red orache, okahijiki, and minutina, were purchased from a commercial source (Johnny's Selected Seeds, Winslow, ME, United States) and sowed in horticubes, soilless foam medium (OASIS® Grower Solutions, Kent, OH, United States). Fresh water was used for plant irrigation in the first week of germination. To prevent osmotic shock on plants, salinity was increased at a rate of 2–3 ppt every 48 h from the second week until the desired salinity (15 ppt) was reached.

Experimental Design and System Management

A 3 × 2 experimental design was established in this study; 3 ratios of shrimp to plants (2:1, 3:1 or 5:1) and 2 C/N ratios (12 or 15). Treatments were designated 2:1–12 (stocking density ratio 2:1 with C/N ratio 12), 2:1–15, 3:1–12, 3:1–15, 5:1–12, and 5:1–15. Treatments were randomly assigned to three replicate experimental systems. The study was conducted for 4 weeks, from July 4 to August 1, 2020. Before the experiment started, all experimental systems were seeded with *Bacillus* spp. (EZ-Bio; Zeigler Brothers, Gardners, PA, United States), and inoculated water from established systems used in prior research. Sea salt (Instant Ocean®, Blacksburg, VA, United States) was used to adjust the salinity to 15 ppt. One week prior to the experiment, shrimp were weighed and placed in aquaculture tanks to produce nutrients for plants. The stocking density of shrimp was 200 shrimp/ m^2 (40 shrimp/ tank), 300 shrimp/ m^2 (60 shrimp/ tank), or 500 shrimp/ m^2 (100 shrimp/ tank). The average weight of individual shrimp was 1.50 g. The stocking density of plants was 100 plants/ m^2, which was equivalent to 24 plants (8 plants per species) in each hydroponic tank. Commercial shrimp feed (Zeigler Brothers, Gardners, PA, United States) was provided twice a day at 8 a.m. and 5 p.m., with a total daily amount of 3.0% of body weight divided into equal aliquots. Guaranteed analysis of the feed was 35% protein, 7% fat, and a maximum of 2% fiber.

Probiotics (EZ-Bio; Zeigler Brothers, Gardners, PA, United States) were used to manage water quality and the microbial community within every system. EZ-bio (*Bacillus* spp.) was inoculated at 10 mg/ L into every system once a week prior to starting the experiment. As soon as shrimp were moved into aquaculture tanks, additional doses of probiotics were added every other day in the first week, twice per week in the second week, and once per week beginning in the third week continuing until the end of the experiment (Crab et al., 2010; Chu, 2014). Molasses (Hawthorne Gardening Co., Vancouver, WA, United States) was added to aquaculture tank as an organic carbon source to adjust the C/N ratio in the water with the same frequency of the probiotic inoculations. The amount of molasses added was based on the carbon-nitrogen content of shrimp feed and the carbon content of the molasses to adjust the C/N ratio to 12 or 15 (Xu et al., 2016). Potassium bicarbonate was added to maintain the alkalinity above 60 mg/L, and 10% sulfuric acid was applied to keep the pH below 8. Throughout the 4-week experiment, there was no water discharged or exchanged except for replacement due to evaporation.

Measurement of Water Quality

During the experiment, dissolved oxygen, temperature (OxyGuard Handy Polaris DO meter, Farum, Denmark), and pH (pHTestr^{TM} 10 Pocket pH Tester, Vernon Hills, IL, United States) were measured twice per day at 8 a.m. and 5 p.m. before feeding. Salinity (Vital Sine^{TM} Salinity Refractometer,

Pentair Aquatic Eosystems, Apopka, FL, United States) was measured once per day at 8 a.m. Water samples were collected twice per week from the aquaculture tank before feeding, to determine the concentrations of total ammonia nitrogen (TAN), nitrite-N (NO_2^-), nitrate-N (NO_3^-), phosphate (PO_4^{3-}), and alkalinity using HACH reaction kits (HACH, Loveland, CO, United States). Total suspended solids (TSSs) and volatile suspended solids (VSSs) were measured once a week by United States EPA method 1684.

Growth Performance

Shrimp

Response parameters for shrimp included survival, weight gain, specific growth rate (SGR), and feed conversion ratio (FCR) The following formulae were used:

$$\text{Survival (\%)} = \frac{\text{Final number of shrimp}}{\text{Initial number of shrimp}} \times 100;$$

$$\text{Weight gain (\%)} = \frac{(\text{Final biomass (g)} - \text{Initial biomass (g)})}{\text{Initial biomass}} \times 100;$$

$$\text{Specific growth rate(\%)} = \frac{[\text{Ln (Final biomass (g))} - \text{Ln (Initial biomass (g))}]}{\text{day}} \times 100; \text{ and,}$$

$$\text{Feed conversion ratio} = \frac{\text{Total feed intake (g)}}{(\text{Final biomass (g)} - \text{Initial biomass (g)})}$$

Plants

Only edible parts of individual plants were collected and weighed at the beginning and end of the experiment. Initial plant samples were obtained from the extra plant seedlings and chosen those that were similar to the seedlings transplanted into systems. Initial plant samples were weighed on the same day of the transplantation. Initial and final fresh weights were used to calculate relative growth rate (RGR). Dry weight was measured after plant samples were dried in an oven at 100 °C until constant weight. The water content (WC) in plants was determined through final fresh weights and final dry weights. Formulae used to calculate plant growth and water content are shown below. In addition, dried plant samples were ground and sieved (with a 10-mesh screen) and kept in 50 ml centrifuge tubes for nutrient analysis. Plant tissue analysis was conducted by the Midwest Laboratory (Omaha, NE, United States).

$$\text{Relative growth rate(\%)} = \frac{[\text{Ln (Final biomass (g))} - \text{Ln (Initial biomass (g))}]}{\text{day}} \times 100; \text{ and,}$$

$$\text{Water content(\%)} = \frac{(\text{Final fresh weight (g)} - \text{Final dry weight (g)})}{\text{Final fresh weight}} \times 100$$

Statistical Analysis

Shrimp and plant growth performance, nutrient content in plants, and water quality parameters were analyzed using JMP v14.0 (SAS Institute Inc., Cary, NC, United States). Treatment means were compared by two-way analysis of variance (ANOVA). Statistical differences between means was determined by Tukey's honestly significant difference test (HSD) at $p \leq 0.05$.

RESULTS

Shrimp Growth

The survival of shrimp in all treatments was above 95% and there were no significant ($p > 0.05$) differences among treatments. The growth of shrimp was significantly ($p < 0.05$) impacted by stocking density, but not by the C/N ratio or the interaction of factors (**Table 1**). Shrimp raised in 2:1–12 treatment had better growth performances (final weight, weight gain, and SGR) and a lower FCR. The mean values of final weight, weight gain, and SGR were significantly greater ($p < 0.05$) in the treatment 2:1–12, averaging 2.68g, 73.9%, and 1.97, respectively, compared to 5:1–12 and 5:1–15 treatments, yet, values were not significantly ($p > 0.05$) different from that of the 2:1–15, 3:1–12, and 3:1–15 treatments. Similarly, FCR was significantly lower ($p < 0.05$) in shrimp raised in 2:1–12 treatment compared to shrimp raised in 5:1–12 and 5:1–15 treatments, whereas it was not significantly ($p > 0.05$) different from the other treatments.

Plants

Survival of red orache, okahijiki, and minutina was 100% in all treatments. Stocking density ratio significantly ($p < 0.05$) affected the growth of all plants, and C/N ratio significantly ($p < 0.05$) affected water content (WC) of red orache (**Table 2**), the final fresh weight (FFW), final dry weight (FDW), RGR and WC of okahijiki (**Table 3**), and the FFW and RGR of minutina (**Table 4**). The interaction of the two factors exerted no significant ($p > 0.05$) effect on growth of plants.

Yield and Mineral Nutrient Content

According to the result of two-way ANOVA (**Table 5**), the yield, and the concentration of N, P, K, Mg, Ca, and S were significantly ($p < 0.05$) affected by plant species and stocking density ratio. The C/N ratio significantly ($p < 0.05$) affected the yield and the concentration of Mg. The interactions between plant species and stocking density ratio significantly ($p < 0.05$) affected the results of yield and the concentration of N, P, K, Mg, and Ca.

The 5:1–15 treatment had better plant production among treatments (**Table 5**). Red orache and okahijiki had significantly higher ($p < 0.05$) yield in 5:1–15 treatment. The yield was about twice that of red orache, while around 1.5 to 2 times higher than 2:1–12 and 3:1–12 treatments in okahijiki. Minutina had a better yield among the three species. Its production was also higher in 5:1–15 treatment, whereas, the production in the 5:1–15 treatment was only higher than that of 2:1–12 treatment.

In general, the concentrations of N, P, K in plants were increased with the increasing stocking density and C/N ratio (**Table 5**). In contrast, the concentration of Mg and Ca displayed an opposite trend. The treatment with lower stocking density ratio and C/N ratio had a higher concentration of Mg and Ca, while the concentrations of S and Na in plants were not significantly ($p > 0.05$) different among treatments.

Water Quality

During the experiment, temperature and dissolved oxygen (DO) were maintained at 28–29°C and 6.1–7.3 mg/ L in all treatments, respectively. The salinity was monitored and controlled every day

TABLE 1 | Response of shrimp in marine aquaponics at three stocking density ratios (SD ratio) of shrimp to plant and two C/N ratios for 4 weeks.

Treatment		Initial weight (g)	Final weight (g)	Weight gain (%)	SGR	FCR	Survival (%)
SD ratio	**C/N ratio**						
2:1	12	1.51 ± 0.07	2.68 ± 0.25 a	73.9 ± 10.9 a	1.97 ± 0.22 a	1.50 ± 0.22 c	100 ± 0.0
	15	1.50 ± 0.26	2.59 ± 0.27 ab	71.3 ± 12.0 ab	1.92 ± 0.25 ab	1.55 ± 0.24 bc	99.2 ± 1.4
3:1	12	1.51 ± 0.09	2.38 ± 0.22 b	58.0 ± 5.2 abc	1.63 ± 0.12 abc	1.89 ± 0.17 abc	99.4 ± 1.0
	15	1.50 ± 0.09	2.55 ± 0.14 ab	64.8 ± 1.6 abc	1.78 ± 0.03 abc	1.67 ± 0.03 bc	97.2 ± 2.5
5:1	12	1.49 ± 0.09	2.37 ± 0.17 b	50.2 ± 3.8 c	1.45 ± 0.09 c	2.14 ± 0.15 a	95.7 ± 2.3
	15	1.49 ± 0.12	2.39 ± 0.15 b	53.2 ± 3.2 bc	1.52 ± 0.07 bc	2.01 ± 0.12 ab	96.3 ± 1.5
P		ns	**	**	**	**	ns
ANOVA							
SD ratio		ns	***	***	***	***	**
C/N ratio		ns	ns	ns	ns	ns	ns
SD ratio*C/N ratio		ns	ns	ns	ns	ns	ns

Values are means ± SD (n = 40, 60, and 100 for stocking density 200, 300, and 500, respectively). Means within column followed by different letters are significantly different based on Tukey's honestly significant difference (HSD) test (α = 0.05).
*ns, **, *** mean no significant or significant at $p \leq 0.01$, or 0.001, respectively.*

TABLE 2 | Initial fresh weight (IFW), initial dry weight (IDW), final fresh weight (FFW), final dry weight (FDW), relative growth rate (RGR), and water content (WC) of red orache cultivated in marine aquaponics at three stocking density ratios (SD ratio) of shrimp to plant and two C/N ratios for 4 weeks.

Treatment		IFW(g/plant)	IDW(g/plant)	FFW(g/plant)	FDW(g/plant)	RGR(%)	WC(%)
SD ratio	**C/N ratio**						
2:1	12	0.19 ± 0.01	0.016 ± 0.002	5.3 ± 1.2 b	0.63 ± 0.12 b	11.8 ± 0.8 b	87.9 ± 0.9 c
	15	0.19 ± 0.01	0.016 ± 0.002	6.0 ± 1.5 b	0.69 ± 0.18 b	12.2 ± 0.9 b	88.3 ± 0.7 bc
3:1	12	0.19 ± 0.01	0.016 ± 0.002	6.0 ± 0.9 b	0.69 ± 0.11 b	12.3 ± 0.5 b	88.5 ± 0.5 b
	15	0.19 ± 0.01	0.016 ± 0.002	6.0 ± 1.6 b	0.67 ± 0.18 b	12.2 ± 1.0 b	88.8 ± 0.6 b
5:1	12	0.19 ± 0.01	0.016 ± 0.002	10.6 ± 2.5 a	1.06 ± 0.23 a	14.2 ± 0.9 a	89.9 ± 0.5 a
	15	0.19 ± 0.01	0.016 ± 0.002	10.9 ± 1.2 a	1.06 ± 0.13 a	14.4 ± 0.4 a	90.3 ± 0.4 a
P		ns	ns	***	***	***	***
ANOVA							
SD ratio		ns	ns	***	***	***	***
C/N ratio		ns	ns	ns	ns	ns	**
SD ratio*C/N ratio		ns	ns	ns	ns	ns	ns

Values are means ± SD (n = 24). Means within column followed by different letters are significantly different based on Tukey's honestly significant difference (HSD) test (α = 0.05).
*ns, **, *** mean no significant or significant at $p \leq 0.01$, or 0.001, respectively.*

to maintain at the desired level, 15 ppt. The alkalinity in all treatments was not significantly different ($p > 0.05$) among each other. There were no significant differences ($p > 0.05$) found in the concentrations of total suspended solids (TSS) or volatile suspended solids (VSS) (**Table 6**). The pH was affected by the stocking density ratio, the lower stocking density ratio tended to have a higher pH than the higher stocking density ratio. Starting on day 9, the value was significantly higher ($p < 0.05$) in the stocking ratio of 2:1–12 and 2:1–15 treatment than that of 5:1–12 and 5:1–15 (**Figure 2**).

The concentrations of TAN, and NO_2^-, which are toxic to aquatic animals and plants, remained at safe and low concentrations (both were below 0.2 mg/ L) throughout the experiment in all treatments, although the treatments with higher stocking density ratio, 5:1–12 and 5:1–15, had significantly higher ($p < 0.05$) concentrations than that of lower stocking density ratio, 2:1–12 and 2:1–15 (**Figures 3A,B**). On the other hand, concentrations of NO_3^- and PO_4^{3-} continued increasing throughout the experiment. In general, 5:1–12 and 5:1–15 treatments had significantly higher ($p < 0.05$) concentrations of NO_3^- and PO_4^{3-} than 2:1–12 and 2:1–15 treatments (**Figures 3C,D**).

DISCUSSION

Shrimp Growth

The results of this study indicate that an increase in stocking density ratio was a negative factor on shrimp growth. In addition, the FCR increased with the increasing stocking density, which increases the cost of production. Similar results were observed in other studies that investigated the effect of stocking density on shrimp production (Moss and Moss, 2004; Esparza-Leal et al., 2010; Neal et al., 2010; Krummenauer et al., 2011; Sookying et al., 2011; Façanha et al., 2016; Araneda et al., 2020; Fleckenstein et al., 2020). However, survival of shrimp in our experiment was above 95%, while other researchers reported that survival decreased with increasing density (Neal et al., 2010; Krummenauer et al., 2011; Araneda et al., 2020).

TABLE 3 | Initial fresh weight (IFW), initial dry weight (IDW), final fresh weight (FFW), final dry weight (FDW), relative growth rate (RGR), and water content (WC) of okahijiki cultivated in marine aquaponics at three stocking density ratios (SD ratio) of shrimp to plant and two C/N ratios for 4 weeks.

Treatment		IFW(g/plant)	IDW(g/plant)	FFW(g/plant)	FDW(g/plant)	RGR(%)	WC(%)
SD ratio	**C/N ratio**						
2:1	12	0.18 ± 0.01	0.015 ± 0.002	1.6 ± 0.5 c	0.17 ± 0.05 c	7.7 ± 1.1 c	89.5 ± 1.4 c
	15	0.18 ± 0.01	0.015 ± 0.002	2.0 ± 0.8 bc	0.21 ± 0.07 bc	8.4 ± 1.5 bc	89.9 ± 1.6 bc
3:1	12	0.18 ± 0.01	0.015 ± 0.002	2.0 ± 0.5 c	0.21 ± 0.05 bc	8.4 ± 0.9 bc	89.3 ± 1.1 c
	15	0.18 ± 0.01	0.015 ± 0.002	3.0 ± 1.4 ab	0.28 ± 0.12 ab	9.7 ± 1.7 ab	90.8 ± 0.8 ab
5:1	12	0.18 ± 0.01	0.015 ± 0.002	2.1 ± 1.1bc	0.21 ± 0.09 bc	8.4 ± 2.0 bc	89.7 ± 1.9 bc
	15	0.18 ± 0.01	0.015 ± 0.002	3.6 ± 1.9 a	0.31 ± 0.14 a	10.2 ± 2.1 a	91.0 ± 1.0 a
P		ns	ns	***	***	**	***
ANOVA							
SD ratio		ns	ns	***	**	**	**
C/N ratio		ns	ns	***	***	***	***
SD ratio*C/N ratio		ns	ns	ns	ns	ns	ns

Values are means ± SD (n = 24). Means within column followed by different letters are significantly different based on Tukey's honestly significant difference (HSD) test (α = 0.05).
*ns, **, *** mean no significant or significant at p ≤ 0.01, or 0.001, respectively.*

TABLE 4 | Initial fresh weight (IFW), initial dry weight (IDW), final fresh weight (FFW), final dry weight (FDW), relative growth rate (RGR), and water content (WC) of minutina cultivated in marine aquaponics at three stocking density ratios (SD ratio) of shrimp to plant and two C/N ratios for 4 weeks.

Treatment		IFW (g/plant)	IDW (g/plant)	FFW (g/plant)	FDW (g/plant)	RGR (%)	WC (%)
SD ratio	**C/N ratio**						
2:1	12	0.08 ± 0.01	0.006 ± 0.001	18.3 ± 4.5 b	1.38 ± 0.40	19.3 ± 0.9 b	92.5 ± 0.7 b
	15	0.08 ± 0.01	0.006 ± 0.001	21.3 ± 5.2 ab	1.62 ± 0.40	19.8 ± 0.9 ab	92.5 ± 0.4 b
3:1	12	0.08 ± 0.01	0.006 ± 0.001	18.9 ± 6.1 b	1.43 ± 0.49	19.3 ± 1.2 b	92.4 ± 0.3 b
	15	0.08 ± 0.01	0.006 ± 0.001	20.6 ± 5.2 ab	1.52 ± 0.37	19.7 ± 0.9 ab	92.6 ± 0.4 ab
5:1	12	0.08 ± 0.01	0.006 ± 0.001	21.2 ± 4.6 ab	1.48 ± 0.31	19.8 ± 0.9 ab	93.0 ± 0.5 a
	15	0.08 ± 0.01	0.006 ± 0.001	23.7 ± 4.4 a	1.64 ± 0.34	20.2 ± 0.6 a	93.0 ± 0.4 a
P		ns	ns	*	ns	**	***
ANOVA							
SD ratio		ns	ns	*	ns	*	***
C/N ratio		ns	ns	**	ns	**	ns
SD ratio*C/N ratio		ns	ns	ns	ns	ns	ns

Values are means ± SD (n = 24). Means within column followed by different letters are significantly different based on Tukey's honestly significant difference (HSD) test (α = 0.05).
*ns, *, **, *** mean no significant or significant at p ≤ 0.05, 0.01, or 0.001, respectively.*

The reduced survival and growth of shrimp at higher stocking densities can be related to several factors including the availability of space for growth, competition for feed, cannibalism, and increased waste excretion leading to degraded water quality (Arnold et al., 2006; Wang and Gu, 2010; Ferreira et al., 2020; Luo et al., 2020). The high survival at high stocking density in this study might be attributed to the application of probiotics and molasses, because probiotics improve the resistance to adverse environments and the ability to tolerate stress (Martínez Cruz et al., 2012; Buruiană et al., 2014; Nemutanzhela et al., 2014; Olmos et al., 2020). The use of molasses increased the C/N ratio in the environment, which provided a beneficial environment for probiotics to assimilate nitrogenous waste (Avnimelech, 1999; Crab, 2010; Crab et al., 2012) and compete with pathogens, such as *Vibrio* spp. (Panigrahi et al., 2018). The increased C/N ratio also led to the generation of biofloc, which can be a supplementary food for shrimp (Avnimelech, 1999; Browdy et al., 2012; Crab et al., 2012). Moreover, the application of molasses improved the ability of plants to uptake nutrients from the water column (White, 2012). The combined effect from the application of probiotics and molasses maintained the water quality and led to higher survival in the present study, albeit, with reduced growth. It is unclear if the increased density and potential increases in marketable shrimp would offset the slower growth and increased feed costs associated with super-high-density culture, but this possibility needs to be explored.

Plants

In general, the growth performance of the three halophytes was better with the increasing stocking ratio and C/N ratio. The nutrient balance is one of the key factors to the success of aquaponics; too few animals (inadequate nitrogen) is limiting to plants, and excessive animal density will result in nitrogen excretion in excess of the plants' ability to uptake

TABLE 5 | Average yield and mineral nutrient concentrations of the three halophytic plants cultivated in marine aquaponics at three stocking density ratios (SD ratio) of shrimp to plant and two C/N ratios for 4 weeks.

Plant species	Treatment		Yield (kg/m^2)	N (%)	P (%)	K (%)	Mg (%)	Ca (%)	S (%)	Na (%)
	SD ratio	C/N ratio								
Red orache	2:1	12	0.55 c	3.15 b	0.36 ab	1.50	2.64 a	0.79 a	0.27	11.18
	2:1	15	0.61 bc	3.12 b	0.34 b	1.46	2.39 a	0.70 ab	0.27	10.66
	3:1	12	0.60 bc	3.14 b	0.35 b	1.47	2.42 a	0.73 ab	0.24	10.60
	3:1	15	0.64 bc	3.20 b	0.36 ab	1.44	2.41 a	0.71 ab	0.25	10.73
	5:1	12	0.98 ab	3.80 a	0.43 ab	1.71	2.32 ab	0.70 ab	0.27	10.28
	5:1	15	1.20 a	4.02 a	0.46 a	1.64	2.04 b	0.66 b	0.26	10.39
P			**	***	**	ns	**	*	ns	ns
Okahijiki	2:1	12	0.18 c	3.79 c	0.99 ab	3.66 b	1.79	0.99 ab	0.31	6.11
	2:1	15	0.28 abc	3.78 c	0.98 b	4.28 ab	1.60	1.04 a	0.30	6.22
	3:1	12	0.22 bc	3.69 c	1.01 ab	3.75 b	1.90	0.88 ab	0.30	6.30
	3:1	15	0.33 ab	3.93 bc	1.00 ab	4.14 b	1.68	0.81 b	0.31	6.60
	5:1	12	0.26 abc	4.32 ab	1.18 a	4.99 ab	1.55	0.94 ab	0.34	5.77
	5:1	15	0.36 a	4.34 a	1.17 a	5.45 a	1.58	0.89 ab	0.35	6.06
P			*	*	*	**	ns	*	ns	ns
Minutina	2:1	12	1.99 b	3.89	0.64 b	1.80	1.28 a	1.29	0.54	8.04
	2:1	15	2.27 ab	3.69	0.79 ab	1.83	1.27 a	1.25	0.58	8.06
	3:1	12	2.06 ab	3.65	0.79 ab	2.02	1.24 ab	1.28	0.59	8.15
	3:1	15	2.17 ab	3.87	0.91 ab	1.85	1.18 ab	1.27	0.55	8.07
	5:1	12	2.26 ab	3.78	1.12 a	1.88	1.25 ab	1.31	0.65	8.66
	5:1	15	2.52 a	3.67	1.11 a	1.90	1.14 b	1.28	0.58	8.21
P			*	ns	*	ns	*	ns	ns	ns
ANOVA										
Plant Species			***	***	***	***	***	***	***	***
Table 5 cont'd										
SD ratio			***	***	***	***	***	*	**	ns
C/N ratio			**	ns	ns	ns	*	ns	ns	ns
Plant Species*SD ratio			*	***	*	***	***	**	ns	ns
Plant Species* C/N ratio			ns	ns	ns	*	ns	ns	ns	ns
SD ratio* C/N ratio			ns	ns	ns	ns	ns	ns	ns	ns
Plant Species* SD ratio* C/N ratio			ns	ns	ns	ns	ns	ns	ns	ns

*Means within a column of each plant species followed by different letters are significantly different based on Tukey's honestly significant difference (HSD) test (α = 0.05). ns, *, **, *** mean no significant or significant at p ≤ 0.05, 0.01, or 0.001, respectively.*

TABLE 6 | Mean water quality values (range) for marine aquaponics at three stocking density ratios (SD ratio) of shrimp to plant and two C/N ratios for 4 weeks.

Treatment		Temperature (°C)	DO (mg/ L)	Alkalinity (mg/ L)	TSS (mg/ L)	VSS (mg/ L)
SD ratio	C/N ratio					
2:1	12	28.5 ± 0.3 (28.0–28.9)	6.8 ± 0.2 (6.2–7.3)	71.1 ± 11.5 (60–100)	40.9 ± 5.9 (32.0–51.0)	26.1 ± 6.9 (12.5–37.0)
	15	28.6 ± 0.2 (28.1–29.0)	6.8 ± 0.2 (6.2–7.3)	74.8 ± 11.9 (60–100)	41.2 ± 8.4 (29.0–56.0)	25.6 ± 6.6 (16.5–35.0)
3:1	12	28.5 ± 0.3 (28.0–28.9)	6.8 ± 0.2 (6.2–7.3)	72.6 ± 12.6 (60–100)	40.8 ± 7.5 (28.5–52.0)	24.9 ± 6.2 (14.0–33.5)
	15	28.5 ± 0.3 (28.0–28.9)	6.8 ± 0.3 (6.1–7.3)	71.1 ± 11.5 (60–100)	41.4 ± 6.3 (29.5–51.5)	27.0 ± 5.6 (16.5–34.0)
5:1	12	28.7 ± 0.2 (28.1–29.0)	6.8 ± 0.2 (6.2–7.3)	66.7 ± 9.6 (60–80)	43.9 ± 5.9 (34.5–55.5)	28.8 ± 6.2 (18.5–42.0)
	15	28.5 ± 0.2 (28.0–28.8)	6.7 ± 0.2 (6.1–7.2)	79.3 ± 10.4 (60–100)	40.3 ± 5.8 (33.5–52.0)	25.6 ± 5.7 (17.0–33.0)

Values are means ± SD.

compounds, and may lead to chronic or even acute toxicity to both animals and plants (Somerville et al., 2014).

In our study, plants were benefiting from a higher shrimp stocking density, in which more nutrients are provided for plants. All plants had greater yield in treatment 5:1 (**Table 5**). A similar trend was also reported by Shete et al. (2015); the plant production was higher in fish to plant ratio of 1:1, followed by1:2 and then 1:3. Furthermore, the concentration of macronutrients (N, P, and K) in plant tissues were also higher in both 5:1 treatments than the other stocking density ratio treatments. The higher concentrations of TAN, NO_2^-, NO_3^-, and PO_4^{3-} found in the 5:1 treatment was likely the result of the higher feed inputs into those treatments. The steady increase in NO_3^-, and PO_4^{3-}

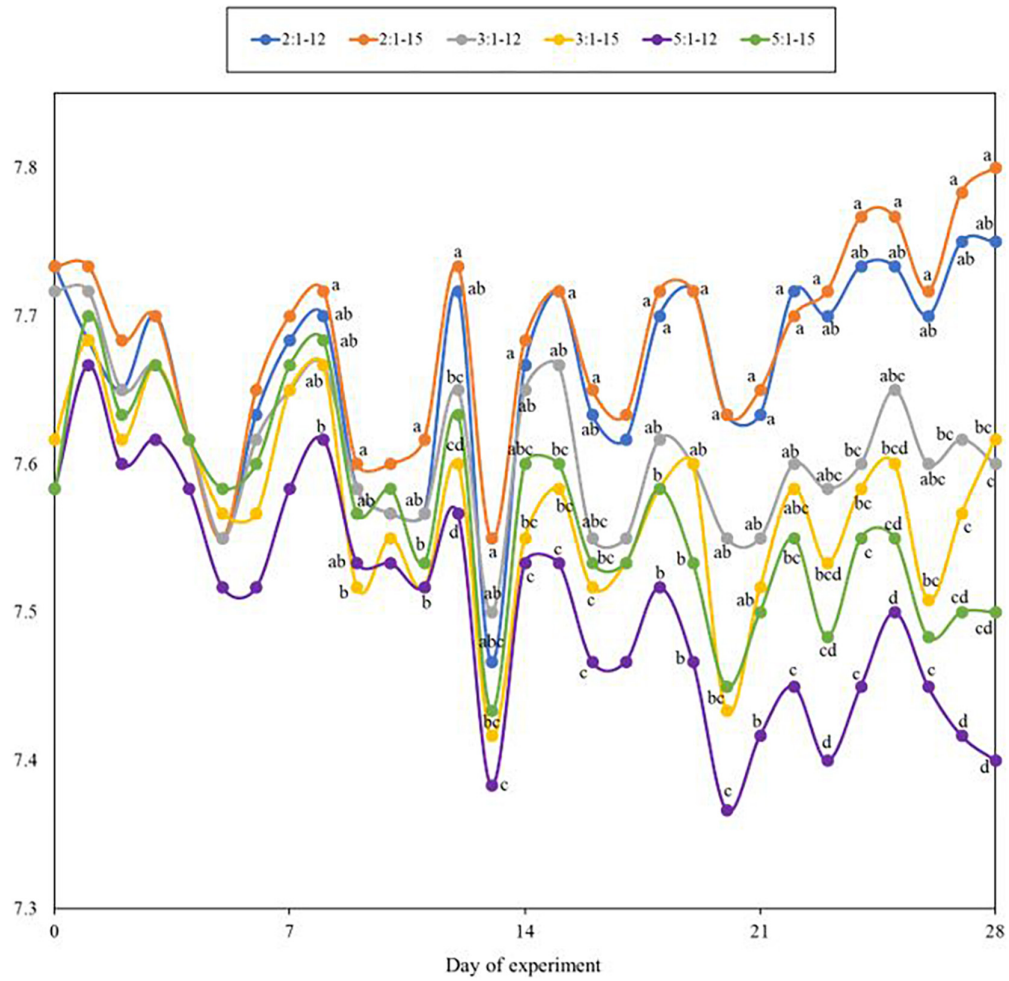

FIGURE 2 | Dynamic change of pH measured during the 4-week experiment. Each point represents the means of 3 replicates, and lower-case alphabet letters represent significant differences, followed by one-way ANOVA and Tukey's HSD test ($\alpha = 0.05$).

in all treatments may indicate the saturation of plant's assimilation limits. Further research is needed to evaluate a longer culture duration or a different strategy on plant harvest (sequential stocking) since the concentration of all N- and P-compounds in the water will likely increase after every harvest (Yang and Kim, 2020b), which might be a concern for shrimp culture.

While not as pronounced as the effect of shrimp stocking density, the C/N ratio also exerted an impact on plant production characteristics. Additional carbon for amending the growing environment improves nutrient uptake by plants, increases crop yield, and alleviates phytotoxicity, caused by trace metals, salinity, pesticides, phytotoxins, or allelochemicals (Rodríguez-Kábana, 1986; Schenck, 2001; White, 2012; Pyakurel et al., 2019; Li et al., 2020). Overall, the effect of C/N ratio on plant growth, yield, and mineral nutrient concentrations in plants was relatively minor compared to stocking density.

Water Quality

To manage the water quality well, a robust microbial community is indispensable in aquaponics. Promoting the establishment of microbial flora by inoculation of probiotics or inoculations from mature water, used-biomedia, or biofloc from stabilized systems to new systems are efficient practices (Otoshi et al., 2011; Xu and Pan, 2012; Pinheiro et al., 2020; Chu and Brown, 2021). Xu and Pan (2012) inoculated bioflocs, characterized by *Bacillus* sp. as the predominant bacteria, into experimental tanks before their study. The concentrations of toxic nitrogenous waste, TAN and NO_2^-, in their study were maintained below 0.51 mg/ L and 1.25 mg/ L, respectively. In the present study, the concentration of TAN and NO_2^- remained lower than 0.2 mg/ L throughout the experiment, even in the high stocking density treatments. Additional research needs to be conducted examining the frequency of probiotic application and varying harvest scenarios, as after every plant harvest, the TAN and NO_2^- will likely increase (Yang and Kim, 2020b).

Concentrations of TAN and NO_2^- were higher in the higher C/N treatments while the NO_3^- concentrations were lower. Similar results were also reported in other studies (Xu et al., 2016, 2018). The additional organic carbon facilitates growth of heterotrophic bacteria, which compete for nutrients and space inside the biofilm or biomedia with the nitrifying bacteria (NB), which are composed of ammonia-oxidizing bacteria (AOB) and nitrite-oxidizing bacteria

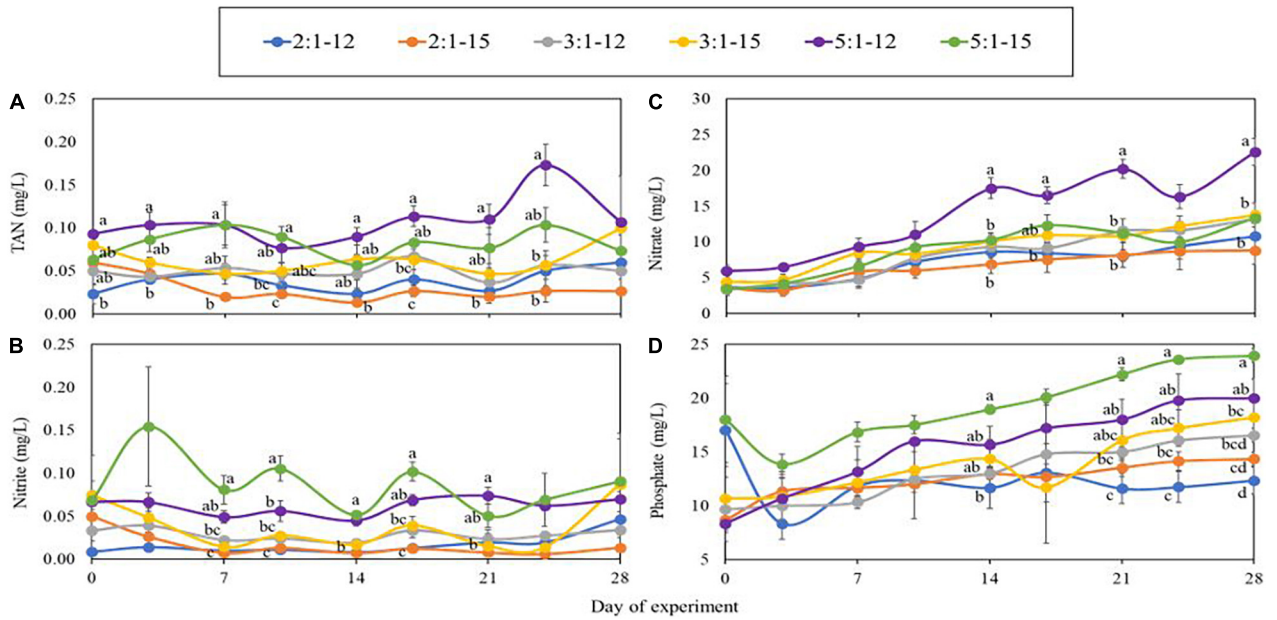

FIGURE 3 | Concentrations of TAN **(A)**, nitrite **(B)**, nitrate **(C)**, and phosphate **(D)** measured during the 4-week experiment. Each point represents the means of 3 replicates ± standard error. Lower-case alphabet letters represent significant differences, followed by one-way ANOVA and Tukey's HSD test ($\alpha = 0.05$).

(NOB). The rate of reproduction of heterotrophic bacteria is much faster than NB, while the reproduction rate of AOB is faster than NOB (Hu et al., 2015). Due to the competition with heterotrophic bacteria, and the slower growth rate of AOB and NOB, the efficiency of nitrification decreases with the increasing C/N ratio, resulting in a decrease in TAN removal rate and NO_3^- productivity (Zhu and Chen, 2001; Michaud et al., 2006; Luo et al., 2020). However, in our study, all nitrogenous waste products remained below concentrations considered toxic. The concentrations of PO_4^{3-} continued to accumulate throughout the experiment, similar to previous results (Boxman et al., 2018; Yang and Kim, 2019, 2020a,b; Chu and Brown, 2021; Huang et al., 2021), and was higher in the treatments with the higher stocking densities and C/N ratio, likely due to higher feed inputs. Another explanation could be the higher C/N ratios resulted in bioflocs dominated by heterotrophic bacteria and less algae (Xu et al., 2016). Moreover, the accumulation of PO_4^{3-} suggests the saturation of plant's assimilation ability. PO_4^{3-}, one of the compounds that causes eutrophication, is an issue for aquaponics; hence, more research is required to improve the management of PO_4^{3-} in aquaponics and determine how to improve plant's ability to assimilate PO_4^{3-}.

In aquaponics, pH is another vital parameter that can be affected by nitrification, nutrient assimilation by plants and heterotrophic bacteria, and CO_2 excretion by aquatic animals, as well as other factors (Yang and Kim, 2019; Li et al., 2020). The process of nitrification and nitrogenous waste assimilation by bacteria, and CO_2 released through the respiration of aquatic animals and microorganisms tends to decrease the pH. Conversely, CO_2 removal and nutrient assimilation by plant tends to raise the pH (Ebeling et al., 2006; White, 2012; Somerville et al., 2014). This may explain why the pH level was lowest at the stocking density of 5:1, followed by 3:1, then 2:1. Also, the lower pH can be another possible reason for a better plant growth in higher stocking density treatments, because nutrient availability increases with the decreasing pH (Somerville et al., 2014).

CONCLUSION

The stocking density ratio and C/N ratio exerted significant impacts on the performance of shrimp and plants in marine aquaponics. Shrimp performed better in the stocking density of 2:1 and 3:1, with no impact from the C/N ratio. Conversely, plants performed better in the stocking density of 3:1 and 5:1 with the C/N ratio at 15. Therefore, a stocking density ratio of 3:1 with a C/N ratio at 15 is suggested as the optimal condition for shrimp and the three halophytes in an indoor marine aquaponic food production system. Inoculating the water with biofloc and applying probiotics regularly can enhance the management of water quality and the health of shrimp and plants in aquaponics. Although water quality was maintained at safe levels for shrimp and halophytes during the experiment, more studies with a longer period of cultivation are needed for a better understanding of marine aquaponics using these species.

DATA AVAILABILITY STATEMENT

The original contributions presented in the study are included in the article/supplementary material, further inquiries can be directed to the corresponding author.

AUTHOR CONTRIBUTIONS

Y-TC: conceptualization, methodology, investigation, validation, formal analysis, data curation, and writing – original draft

preparation and editing. PB: resources, supervision, project administration, funding acquisition, and writing – review and editing. Both authors have read and agreed to the published version of the manuscript.

FUNDING

Funding for this project was provided by the Purdue University Department of Forestry and Natural Resources, the College of Agriculture, and the US Department of Agriculture.

ACKNOWLEDGMENTS

We would like to thank Zeigler Bros., Inc for their donation of commercial shrimp feed and EZ-bio. We would like to thank the manager, Robert Rode, of the Aquaculture Research Lab for his help and support for the study.

REFERENCES

Alshrouf, A. (2017). Hydroponics, aeroponic and aquaponic as compared with conventional farming. *Am. Sci. Res. J. Eng. Technol. Sci.* 27, 247–255.

Araneda, M., Gasca-Leyva, E., Vela, M. A., and Domínguez-May, R. (2020). Effects of temperature and stocking density on intensive culture of Pacific white shrimp in freshwater. *J. Therm. Biol.* 94:102756. doi: 10.1016/j.jtherbio.2020.102756

Arnold, S. J., Sellars, M. J., Crocos, P. J., and Coman, G. J. (2006). Intensive production of juvenile tiger shrimp *Penaeus monodon*: an evaluation of stocking density and artificial substrates. *Aquaculture* 261, 890–896. doi: 10.1016/j.aquaculture.2006.07.036

Avnimelech, Y. (1999). Carbon/nitrogen ratio as a control element in aquaculture systems. *Aquaculture* 176, 227–235. doi: 10.1016/S0044-8486(99)00085-X

Boxman, S. E., Nystrom, M., Ergas, S. J., Main, K. L., and Trotz, M. A. (2018). Evaluation of water treatment capacity, nutrient cycling, and biomass production in a marine aquaponic system. *Ecol. Eng.* 120, 299–310. doi: 10.1016/j.ecoleng.2018.06.003

Browdy, C. L., Ray, A. J., Leffler, J. W., and Avnimelech, Y. (2012). "Biofloc-based aquaculture systems," in *Aquaculture Production Systems*, ed. J. Tidwell (Oxford: Johy Wiley & Sons, Inc), 278–307. doi: 10.1002/9781118250105.ch12

Buruiană, C. T., Profir, A. G., and Vizireanu, C. (2014). Effects of probiotic Bacillus species in aquaculture – an overview. *Ann. Univ. Dunarea Jos Galati Fascicle VI Food Technol.* 38, 9–17. doi: 10.1016/j.fsi.2021.07.007

Chu, Y.-T. (2014). *Effects of Different Probiotics on Water Qualities and Growth in Close Culture System of Litpenaeus vannamei*. Master's Thesis. Keelung: National Taiwan Ocean University.

Chu, Y.-T., and Brown, P. B. (2021). Evaluation of Pacific whiteleg shrimp and three halophytic plants in marine aquaponic systems under three salinities. *Sustainability* 13:269. doi: 10.3390/su13010269

Crab, R. (2010). *Bioflocs Technology: An Integrated System for the Removal of Nutrients and Simultaneous Production of Feed in Aquaculture.* Ph.D. Thesis. Brusseis: Ghen Unversity.

Crab, R., Chielens, B., Wille, M., Bossier, P., and Verstraete, W. (2010). The effect of different carbon sources on the nutritional value of bioflocs, a feed for *Macrobrachium rosenbergii* postlarvae. *Aquac. Res.* 41, 559–567. doi: 10.1111/j.1365-2109.2009.02353.x

Crab, R., Defoirdt, T., Bossier, P., and Verstraete, W. (2012). Biofloc technology in aquaculture: beneficial effects and future challenges. *Aquaculture* 35, 351–356. doi: 10.1016/j.aquaculture.2012.04.046

Ebeling, J. M., Timmons, M. B., and Bisogni, J. J. (2006). Engineering analysis of the stoichiometry of photoautotrophic, autotrophic, and heterotrophic removal of ammonia-nitrogen in aquaculture systems. *Aquaculture* 257, 346–358. doi: 10.1016/j.aquaculture.2006.03.019

Esparza-Leal, H. M., Ponce-Palafox, J. T., Aragón-Noriega, E. A., Arredondo-Figueroa, J. L., García-Ulloa Gómez, M., and Valenzuela-Quiñonez, W. (2010). Growth and performance of the whiteleg shrimp *Penaeus vannamei* (boone) cultured in low-salinity water with different stocking densities and acclimation times. *Aquac. Res.* 41, 878–883. doi: 10.1111/j.1365-2109.2009.02367.x

Façanha, F. N., Oliveira-Neto, A. R., Figueiredo-Silva, C., and Nunes, A. J. P. (2016). Effect of shrimp stocking density and graded levels of dietary methionine over the growth performance of *Litopenaeus vannamei* reared in a green-water system. *Aquaculture* 463, 16–21. doi: 10.1016/j.aquaculture.2016.05.024

FAO (2006). *Cultured Aquatic Species Information Programme Penaeus vannamei*. Rome: FAO.

FAO (2020). *The State of World Fisheries and Aquaculture 2020. Sustainability in Action., Nature and Resources*. Rome: FAO.

Ferreira, G. S., Silva, V. F., Martins, M. A., da Silva, A. C. C. P., Machado, C., Seiffert, W. Q., et al. (2020). Strategies for ammonium and nitrite control in *Litopenaeus vannamei* nursery systems with bioflocs. *Aquac. Eng.* 88:102040. doi: 10.1016/j.aquaeng.2019.102040

Fleckenstein, L. J., Kring, N. A., Tierney, T. W., Fisk, J. C., Lawson, B. C., and Ray, A. J. (2020). The effects of artificial substrate and stocking density on Pacific white shrimp (*Litopenaeus vannamei*) performance and water quality dynamics in high tunnel-based biofloc systems. *Aquac. Eng.* 90:102093. doi: 10.1016/j.aquaeng.2020.102093

Fry, J. P., Mailloux, N. A., Love, D. C., Milli, M. C., and Cao, L. (2018). Feed conversion efficiency in aquaculture: do we measure it correctly? *Environ. Res. Lett.* 13:024017. doi: 10.1088/1748-9326/aaa273

Gao, W., Tian, L., Huang, T., Yao, M., Hu, W., and Xu, Q. (2016). Effect of salinity on the growth performance, osmolarity and metabolism-related gene expression in white shrimp *Litopenaeus vannamei*. *Aquac. Reports* 4, 125–129. doi: 10.1016/j.aqrep.2016.09.001

Glenn, E. P., Brown, J. J., and Blumwald, E. (1999). Salt tolerance and crop potential of halophytes. *CRC. Crit. Rev. Plant Sci.* 18, 227–255. doi: 10.1080/07352689991309207

Glenn, E. P., Brown, J. J., and Leary, J. W. O. (1998). Irrigating crops with seawater. *Sci. Am.* 279, 76–81. doi: 10.1038/scientificamerican0898-76

Goddek, S., Joyce, A., Kotzen, B., and Butnell, G. M. (2019). "Nutrient cycling in aquaponics systems," in *Aquaponics Food Production Systems*, 1st Edn, eds S. Goddek, A. Joyce, B. Kotzen, and G. M. Butnell (Cham: Springer), doi: 10.1007/978-3-030-15943-6_9

Hu, Z., Lee, J. W., Chandran, K., Kim, S., Brotto, A. C., and Khanal, S. K. (2015). Effect of plant species on nitrogen recovery in aquaponics. *Bioresour. Technol.* 188, 92–98. doi: 10.1016/j.biortech.2015.01.013

Huang, C. C., Lu, H. L., Chang, Y. H., and Hsu, T. H. (2021). Evaluation of the water quality and farming growth benefits of an intelligence aquaponics system. *Sustain.* 13, 1–15. doi: 10.3390/su13084210

Kim, J. H., Suk, S., Jang, W. J., Lee, C. H., Kim, J. E., Park, J. K., et al. (2017). *Salicornia* extract ameliorates salt-induced aggravation of nonalcoholic fatty liver disease in obese mice fed a high-fat diet. *J. Food Sci.* 82, 1765–1774. doi: 10.1111/1750-3841.13777

Klinger, D., and Naylor, R. (2012). Searching for solutions in aquaculture: charting a sustainable course. *Annu. Rev. Environ. Resour.* 37, 247–276. doi: 10.1146/annurev-environ-021111-161531

Krummenauer, D., Peixoto, S., Cavalli, R. O., Poersch, L. H., and Wasielesky, W. (2011). Superintensive culture of white shrimp, *Litopenaeus vannamei*, in a biofloc technology system in Southern Brazil at different stocking densities. *J. World Aquac. Soc.* 42, 726–733. doi: 10.1111/j.1749-7345.2011.00507.x

Lam, S. S., Ma, N. L., Jusoh, A., and Ambak, M. A. (2015). Biological nutrient removal by recirculating aquaponic system: optimization of the dimension ratio between the hydroponic & rearing tank components. *Int. Biodeterior. Biodegrad.* 102, 107–115. doi: 10.1016/j.ibiod.2015.03.012

Li, S., Zhao, X., Ye, X., Zhang, L., Shi, L., Xu, F., et al. (2020). The effects of condensed molasses soluble on the growth and development of rapeseed through seed germination, hydroponics and field trials. *Agriculture* 10, 1–20. doi: 10.3390/agriculture10070260

Luo, G., Xu, J., and Meng, H. (2020). Nitrate accumulation in biofloc aquaculture systems. *Aquaculture* 520:734675. doi: 10.1016/j.aquaculture.2019.734675

Martínez Cruz, P., Ibáñez, A. L., Monroy Hermosillo, O. A., and Ramírez Saad, H. C. (2012). Use of probiotics in aquaculture. *ISRN Microbiol.* 2012, 1–13. doi: 10.5402/2012/916845

Michaud, L., Blancheton, J. P., Bruni, V., and Piedrahita, R. (2006). Effect of particulate organic carbon on heterotrophic bacterial populations and nitrification efficiency in biological filters. *Aquac. Eng.* 34, 224–233. doi: 10.1016/j.aquaeng.2005.07.005

Moss, K. R. K., and Moss, S. M. (2004). Effects of artificial substrate and stocking density on the nursery production of Pacific white shrimp Litopenaeus vannamei. *J. World Aquac. Soc.* 35, 537–542. doi: 10.1111/j.1749-7345.2004.tb00121.x

Neal, R. S., Coyle, S. D., Tidwell, J. H., and Boudreau, B. M. (2010). Evaluation of stocking density and light level on the growth and survival of the pacific white shrimp, *Litopenaeus vannamei*, reared in zero-exchange systems. *J. World Aquac. Soc.* 41, 533–544. doi: 10.1111/j.1749-7345.2010.00393.x

Nemutanzhela, M. E., Roets, Y., Gardiner, N., and Lalloo, R. (2014). "The use and benefits of *Bacillus* based biological agents in aquaculture," in *Sustainable Aquaculture Techniques*, eds M. Hernandez-Vergara and C. Perez-Rostro (Rijeka: Intech Publishing), 1–34. doi: 10.1016/j.colsurfa.2011.12.014

Olmos, J., Acosta, M., Mendoza, G., and Pitones, V. (2020). *Bacillus subtilis*, an ideal probiotic bacterium to shrimp and fish aquaculture that increase feed digestibility, prevent microbial diseases, and avoid water pollution. *Arch. Microbiol.* 202, 427–435. doi: 10.1007/s00203-019-01757-2

Otoshi, C. A., Naguwa, S. S., Falesch, F. C., and Moss, S. M. (2007). Shrimp behavior may affect culture performance at super-intensive stocking densities. *Glob. Aquac. Advocate* 2, 67–69.

Otoshi, C. A., Rodriguez, N., and Moss, S. M. (2011). Establishing nitrifying bacteria in super-intensive biofloc shrimp production. *Glob. Aquac. Advocate* 14, 24–26.

Panigrahi, A., Saranya, C., Sundaram, M., Vinoth Kannan, S. R., Das, R. R., Satish Kumar, R., et al. (2018). Carbon: nitrogen (C:N) ratio level variation influences microbial community of the system and growth as well as immunity of shrimp (*Litopenaeus vannamei*) in biofloc based culture system. *Fish Shellfish Immunol.* 81, 329–337. doi: 10.1016/j.fsi.2018.07.035

Panta, S., Flowers, T., Lane, P., Doyle, R., Haros, G., and Shabala, S. (2014). Halophyte agriculture: success stories. *Environ. Exp. Bot.* 107, 71–83. doi: 10.1016/j.envexpbot.2014.05.006

Panth, N., Park, S. H., Kim, H. J., Kim, D. H., and Oak, M. H. (2016). Protective effect of *Salicornia europaea* extracts on high salt intake-induced vascular dysfunction and hypertension. *Int. J. Mol. Sci.* 17:1176. doi: 10.3390/ijms17071176

Pinheiro, I., Carneiro, R. F. S., Vieira, F., do, N., Gonzaga, L. V., Fett, R., et al. (2020). Aquaponic production of *Sarcocornia ambigua* and Pacific white shrimp in biofloc system at different salinities. *Aquaculture* 519, 1–9. doi: 10.1016/j.aquaculture.2019.734918

Pyakurel, A., Dahal, B. R., and Rijal, S. (2019). Effect of molasses and organic fertilizer in soil fertility and yield of Spinach in Khotang. *Nepal. Int. J. Appl. Sci. Biotechnol.* 7, 49–53. doi: 10.3126/ijasbt.v7i1.23301

Quagrainie, K. K., Flores, R. M. V., Kim, H. J., and McClain, V. (2018). Economic analysis of aquaponics and hydroponics production in the U.S. Midwest. *J. Appl. Aquac.* 30, 1–14. doi: 10.1080/10454438.2017.1414009

Rakocy, J. E. (2012). "Aquaponics — Integrating fish and plant culture," in *Aquaculture Production Systems*, ed. J. Tidwell (Oxford: Johy Wiley & Sons, Inc), 343–386. doi: 10.1002/9781118250105.ch14

Ray, A. J., and Lotz, J. M. (2017). Comparing salinities of 10, 20, and 30‰ in intensive, commercial-scale biofloc shrimp (*Litopenaeus vannamei*) production systems. *Aquaculture* 476, 29–36. doi: 10.1016/j.aquaculture.2017.03.047

Rodríguez-Kábana, R. (1986). Organic and inorganic nitrogen amendments to soil as nematode suppressants. *J. Nematol.* 18, 129–134.

Ross, W., Gallaudet, R. T., and Oliver, C. (2017). *Fisheries of the United States, 2017. U.S. Department of Commerce, NOAA Current Fishery Statistics No. 2017*. Washington, DC: NOAA.

Schenck, S. (2001). *Molasses Soil Amendment for Crop Improvement and Nematode Management*. Honolulu, HI: Hawaii Agriculture. Reserch. Center, 1–7.

Shete, A. P., Verma, A. K., Chadha, N. K., Prakash, C., and Chandrakant, M. H. (2015). A comparative study on fish to plant component ratio in recirculating aquaponic system with common carp and mint. *J. Env. Bio-Sci* 29, 323–329.

Somerville, C., Cohen, M., Pantanella, E., Stankus, A., and Lovatelli, A. (2014). *Small-Scale Aquaponic Food Production. Integrated fish and Plant Farming. Fisheries and Aquaculture Technical Paper, No 589*. Rome: FAO, 262.

Sookying, D., Silva, F. S. D., Davis, D. A., and Hanson, T. R. (2011). Effects of stocking density on the performance of Pacific white shrimp *Litopenaeus vannamei* cultured under pond and outdoor tank conditions using a high soybean meal diet. *Aquaculture* 319, 232–239. doi: 10.1016/j.aquaculture.2011.06.014

Ventura, Y., and Sagi, M. (2013). Halophyte crop cultivation: the case for salicornia and sarcocornia. *Environ. Exp. Bot.* 92, 144–153. doi: 10.1016/j.envexpbot.2012.07.010

Wang, Y., and Gu, Q. (2010). Effect of probiotics on white shrimp (*Penaeus vannamei*) growth performance and immune response. *Mar. Biol. Res.* 6, 327–332. doi: 10.1080/17451000903300893

White, P. J. (2012). "Ion uptake mechanisms of individual cells and roots: short-distance transport," in *Marschner's Mineral Nutrition of Higher Plants*, ed. P. Marschner (Cambridge, MA: Academic Press), 7–47. doi: 10.1016/B978-0-12-384905-2.00002-9

Xu, W. J., Morris, T. C., and Samocha, T. M. (2016). Effects of C/N ratio on biofloc development, water quality, and performance of *Litopenaeus vannamei* juveniles in a biofloc-based, high-density, zero-exchange, outdoor tank system. *Aquaculture* 453, 169–175. doi: 10.1016/j.aquaculture.2015.11.021

Xu, W. J., Morris, T. C., and Samocha, T. M. (2018). Effects of two commercial feeds for semi-intensive and hyper-intensive culture and four C/N ratios on water quality and performance of *Litopenaeus vannamei* juveniles at high density in biofloc-based, zero-exchange outdoor tanks. *Aquaculture* 490, 194–202. doi: 10.1016/j.aquaculture.2018.02.028

Xu, W. J., and Pan, L. Q. (2012). Effects of bioflocs on growth performance, digestive enzyme activity and body composition of juvenile *Litopenaeus vannamei* in zero-water exchange tanks manipulating C/N ratio in feed. *Aquaculture* 356–357, 147–152. doi: 10.1016/j.aquaculture.2012.05.022

Yang, T., and Kim, H. J. (2019). Nutrient management regime affects water quality, crop growth, and nitrogen use efficiency of aquaponic systems. *Sci. Hortic.* 256:108619. doi: 10.1016/j.scienta.2019.108619

Yang, T., and Kim, H. J. (2020b). Comparisons of nitrogen and phosphorus mass balance for tomato-, basil-, and lettuce-based aquaponic and hydroponic systems. *J. Clean. Prod.* 274:122619. doi: 10.1016/j.jclepro.2020.122619

Yang, T., and Kim, H. J. (2020a). Characterizing nutrient composition and concentration in tomato-, basil-, and lettuce-based aquaponic and hydroponic systems. *Water* 12:1259. doi: 10.3390/W12051259

Zhu, S., and Chen, S. (2001). Effects of organic carbon on nitrification rate in fixed film biofilters. *Aquac. Eng.* 25, 1–11. doi: 10.1016/S0144-8609(01)00071-1

Conflict of Interest: The authors declare that the research was conducted in the absence of any commercial or financial relationships that could be construed as a potential conflict of interest.

Publisher's Note: All claims expressed in this article are solely those of the authors and do not necessarily represent those of their affiliated organizations, or those of the publisher, the editors and the reviewers. Any product that may be evaluated in this article, or claim that may be made by its manufacturer, is not guaranteed or endorsed by the publisher.

frontiers in Marine Science

ORIGINAL RESEARCH
published: 09 December 2021
doi: 10.3389/fmars.2021.797241

Physiological and Molecular Responses in the Gill of the Swimming Crab *Portunus trituberculatus* During Long-Term Ammonia Stress

*Jingyan Zhang[1,2], Mengqian Zhang[2,3], Nishad Jayasundara[4], Xianyun Ren[4,5], Baoquan Gao[4,5], Ping Liu[4,5], Jian Li[4,5] and Xianliang Meng[2,3]**

[1] National Demonstration Center for Experimental Fisheries Science Education (Shanghai Ocean University), Shanghai, China, [2] Key Laboratory of Aquatic Genomics, Ministry of Agriculture and Rural Affairs, Yellow Sea Fisheries Research Institute, Chinese Academy of Fishery Sciences, Qingdao, China, [3] Laboratory for Marine Fisheries Science and Food Production Processes, Qingdao National Laboratory for Marine Science and Technology, Qingdao, China, [4] Nicholas School of the Environment, Duke University, Durham, NC, United States, [5] Key Laboratory of Sustainable Development of Marine Fisheries, Ministry of Agriculture and Rural Affairs, Yellow Sea Fisheries Research Institute, Chinese Academy of Fishery Sciences, Qingdao, China

OPEN ACCESS

Edited by:
Yangfang Ye,
Ningbo University, China

Reviewed by:
Hongbo Jiang,
Shenyang Agricultural University, China
Bin Xia,
Qingdao Agricultural University, China

***Correspondence:**
Xianliang Meng
xlmeng@ysfri.ac.cn

Specialty section:
This article was submitted to Marine Fisheries, Aquaculture and Living Resources, a section of the journal Frontiers in Marine Science

Received: 18 October 2021
Accepted: 18 November 2021
Published: 09 December 2021

Citation:
Zhang J, Zhang M, Jayasundara N, Ren X, Gao B, Liu P, Li J and Meng X (2021) Physiological and Molecular Responses in the Gill of the Swimming Crab Portunus trituberculatus During Long-Term Ammonia Stress. Front. Mar. Sci. 8:797241. doi: 10.3389/fmars.2021.797241

Ammonia is a common environmental stressor encountered during aquaculture, and is a significant concern due to its adverse biological effects on vertebrate and invertebrate including crustaceans. However, little information is available on physiological and molecular responses in crustaceans under long-term ammonia exposure, which often occurs in aquaculture practices. Here, we investigated temporal physiological and molecular responses in the gills, the main ammonia excretion organ, of the swimming crab *Portunus trituberculatus* following long-term (4 weeks) exposure to three different ammonia nitrogen concentrations (2, 4, and 8 mg l^{-1}), in comparison to seawater (ammonia nitrogen below 0.03 mg l^{-1}). The results revealed that after ammonia stress, the ammonia excretion and detoxification pathways were initially up-regulated. These processes appear compromised as the exposure duration extended, leading to accumulation of hemolymph ammonia, which coincided with the reduction of adenosine 5′-triphosphate (ATP) and adenylate energy charge (AEC). Considering that ammonia excretion and detoxification are highly energy-consuming, the depression of these pathways are, at least partly, associated with disruption of energy homeostasis in gills after prolonged ammonia exposure. Furthermore, our results indicated that long-term ammonia exposure can impair the antioxidant defense and result in increased lipid peroxidation, as well as induce endoplasmic reticulum stress, which in turn lead to apoptosis through p53-bax pathway in gills of the swimming crab. The findings of the present study further our understanding of adverse effects and underlying mechanisms of long-term ammonia in decapods, and provide valuable information for aquaculture management of *P. trituberculatus*.

Keywords: long-term, ammonia, crab, gill, physiology

INTRODUCTION

Ammonia is a common environmental stressor in aquatic ecosystem, and is also of significant concern to the aquaculture industry. In intensive aquaculture systems, ammonia is mostly derived from the decomposition of uneaten feed and from the brachial excretion of the cultured animals (Romano and Zeng, 2007). As aquaculture is moving toward more intensive systems with high stocking density and feed supply, there has been rising concerns on ammonia levels in crustacean aquaculture industry. In recent years, an increasing number of studies have been performed to understand the adverse effects and defensive mechanisms in crustaceans (Zhao et al., 2020). However, most of these studies focused on acute ammonia exposure, and there has been limited information available on stress responses in crustaceans under long-term exposure (Liang et al., 2019; Liu F. et al., 2020). Previous studies in fish showed that the detrimental effects of ammonia is largely influenced by the duration of exposure (Brinkman et al., 2009). In addition, during aquaculture practice, ammonia may accumulate over time due to excessive feeding, and culture animals may be exposed at HEA for a long period, leading to high rates of mortality. Therefore, it is of great significance to study the stress responses of crustaceans under long-term ammonia stress.

Ammonia is present in water in two forms, unionized (NH_3) and ionized (NH_4^+) (in this study, the term "ammonia" refers to the sum of NH_3 and NH_4^+). The unionized NH_3 is more toxic because it is diffusible through phospholipid bilayers of the gill epithelial cells (Benli et al., 2008). High environmental ammonia (HEA) may result in accumulation of internal ammonia, and in turn, cause a board range of adverse effects in aquatic animals. At the organismal level, ammonia can lead to reduction in growth (Lemarié et al., 2004; Foss et al., 2009), decreased resistance to diseases (Ackerman et al., 2006; Zhang et al., 2019), histopathological changes in tissues (Romano and Zeng, 2007; Liang et al., 2016), and even death (Romano and Zeng, 2010; Henry et al., 2017). At the physiological and molecular levels, ammonia can alter hormonal regulation (Cui et al., 2017; Zhang X. et al., 2020), influence ionic balance (Romano and Zeng, 2010; Henry et al., 2012), affect energy metabolism (Racotta and Herna′ndez-Herrera, 2000; Shan et al., 2019), induce oxidative stress and endoplasmic reticulum (ER) stress (Ching et al., 2009; Liang et al., 2016), and trigger apoptosis (Cheng et al., 2015; Zhang T. et al., 2020).

To protect against ammonia stress, various excretory and defense mechanisms have been reported in aquatic animals including in crustaceans (Ip et al., 2001; Weihrauch et al., 2004; Zhao et al., 2020). As ammonotelic animals, crustaceans can excrete ammonia actively against an inwardly directed gradient. Gills are considered to act as the predominant excretory organs for ammonia in aquatic crustaceans (Henry et al., 2012). Previous studies have shown that ammonia can be transported through the gills *via* several transport proteins, including Rhesus (Rh) glycoprotein, Na^+-K^+-ATPase (NKA), $Na^+/K^+/2Cl^-$-cotransporter (NKCC), and Na^+/H^+-exchanger (NHE) (Lucu et al., 1989; Weihrauch et al., 2017; Weihrauch and Allen, 2018). Furthermore, ammonia can also be excreted from the gills with a microtubule dependent mechanism with vacuolar-type H^+-ATPase (VAT) and vesicle associated membrane protein (VAMP) (Weihrauch et al., 2002). There are evidences that crustaceans possess ammonia detoxifying mechanisms involving the conversion of ammonia to glutamine through the combined action of glutamate dehydrogenase (GDH) and glutamine synthetase (GS) (Murray et al., 2003), and to less-toxic urea by the ornithine-urea cycle (OUC) (Liu et al., 2014).

The swimming crab *Portunus trituberculatus* (Crustacea: Decapoda: Brachyura) is widely distributed in the estuary and coastal areas of Korea, Japan, China, and Southeast Asia (Dai et al., 1986). This species dominates the swimming crab fishery around the world, and is an important aquaculture species in China with a production of 116,251 tons in 2018 (China Agriculture Press, 2020). In intensive aquaculture systems, the swimming crabs are often exposed to elevated ammonia in coastal ponds. Although several studies reported the physiological responses of this species to acute ammonia (Ren et al., 2015; Pan et al., 2018; Si et al., 2018), there has been no report describing the stress responses under prolonged ammonia exposure, a common occurrence in aquaculture operations. In this study, we investigated the temporal responses associated with ammonia excretion and detoxification, energy metabolism, antioxidant defense, unfolded protein responses (UPR), and apoptosis in the gills, the major excretory organs for ammonia, of *P. trituberculatus* during long-term ammonia stress. The results provide a better understanding of detrimental effects during long-term ammonia exposure and the underlying mechanisms in the swimming crab, and valuable information for improving aquaculture management.

MATERIALS AND METHODS

Animals and Experimental Setup

Adult female *P. trituberculatus* with an average weight of 213.84 ± 21.55 g (means ± S.D.) were obtained from Haifeng company (Weifang, China). After transferring to the laboratory, crabs without visible damage were reared for 2 weeks at ambient temperature of 14.0 ± 0.8°C, that is considered the optimum temperatures for these organisms. Water was well-aerated and the pH was 7.6 ± 0.2, salinity was 30.3 ± 0.6, ammonia nitrogen concentration was below 0.03 mg l^{-1} and the photoperiod was set as 12 h of light: 12 h of dark. One half of water was exchanged in each tank daily, and the crabs were fed *ad libitum* everyday with fresh clams *Ruditapes philippinarum*.

After acclimation, eighty crabs were randomly allocated into four recirculating systems, each system contains twenty 10-L tanks. To avoid cannibalism, each tank only has one individual. Based on the results from our survey on seawater quality in culture ponds, the highest ammonia level in the seawater near sediments was ∼4 mg l^{-1}. In this study, four concentrations of ammonia nitrogen were chosen for the different groups, below 0.03 mg l^{-1} (seawater) for the control group, 2.0 mg l^{-1} for the low-ammonia (LA) group, 4.0 mg l^{-1} for the medium-ammonia (MA) group, and 8.0 mg l^{-1} for the high-ammonia (HA) group. The ammonia-nitrogen concentrations for the treatment groups

were achieved by infusion of calculated amount of ammonium chloride (NH_4Cl) stock solutions that was prepared with filtered seawater (pH was 7.8, salinity was 30.8). Ammonia nitrogen concentration in these groups was monitored using salicylic acid method with spectrophotometer, and it was adjusted with freshly prepared stock solution daily to ensure consistency.

At the end of each week during the total experiment period (4 weeks), five individuals from each group were anesthetized for hemolymph and gill collection. The gills from each crab were collected, snap frozen in liquid nitrogen, and stored in −80°C. Hemolymph samples were obtained by puncturing the arthrodial membrane at the base of the swimming leg with a sterilized syringe containing equal volume of the anti-coagulant, and then centrifuged at 1,500 g at 4°C for 10 min. The supernatant was collected as the plasma sample and frozen at -80°C until analysis. The animal experiment was approved by the Institutional Animal Care and Use Committee of Yellow Sea Fisheries Research Institute.

Physiological Assay

The levels of adenosine 5′-triphosphate (ATP), adenosine 5′-diphosphate (ADP) and adenosine 5′-monophosphate (AMP) in the gill samples were determined by liquid chromatography as described in Lu et al. (2015). The gills from each sample were ground in liquid nitrogen and homogenized in 9 volumes of ice-cold 0.9 mol l^{-1} perchloric acid. After centrifugation at 4 °C and 7,000 g for 5 min, the supernatant was neutralized to pH 6.5–7.0 with 3.75 M potassium carbonate. Precipitated potassium perchlorate was removed with a second centrifugation, and the homogenate was filtered through a 0.45 μm HV-Millipore filter. The aliquots of 20 μl were injected into an Agilent 1100 high-performance liquid chromatography (HPLC, Agilent Corp., United States) system for analyzing ATP, ADP, and AMP contents on an Ultimate AQ-C18 column (4.6 × 250 mm) at 254 nm, using phosphate buffer (40 mmol l^{-1} KH_2PO_4 and 60 mmol l^{-1} K_2HPO_4, pH 6.50) as the mobile phases. Flow rate of 1.0 ml min^{-1}, and column temperature was constantly at 35°C. The elution time was 24 min. The concentration of the adenylate was calculated from the measured peak areas and standard curves, which were made from standards of known concentrations (ATP, 0–0.8 mmol/L; ADP, 0–1.2 mmol/L; AMP, 0–1.5 mmol/L). The adenylate energy charge (AEC) was calculated as follow:

$$AEC = ([ATP] + 0.5 \times [ADP])/([ATP] + [ADP] + [AMP])$$

The levels of hemolymph ammonia and urea, and the activity of the enzymes involved in ammonia detoxification, including glutamate dehydrogenase (GDH), glutamine synthase (GS), arginase (ARG), were determined with assay kits from Nanjing Jiancheng Bioengineering Institute (Nanjing, China) (ammonia, A086-1-1; urea, C013-2-1; GDH, A125-1-1; GS, A047-1-1) and BioAssay Systems (Hayward, United States) (Arginase, DARG-100).

To study the effects of ammonia on energy metabolism in gills, the activities of hexokinase (HK), pyruvate kinase (PK), and succinate dehydrogenase (SDH) were measured using commercial diagnostic kits purchased from Nanjing Jiancheng Bioengineering Institute (Nanjing, China) (HK, A077-3-1; PK, A076-1-1; SDH, A022-1-1).

The activities of antioxidant enzymes, including superoxide dismutase (SOD), catalase (CAT), and glutathione peroxidase (GPX) and were analyzed with assay kits (Nanjing Jiancheng Bioengineering Institute, Nanjing, China) (SOD, A001-3-2; CAT, A007-1-1; GPX, A005-1-2). Malondialdehyde (MDA) was measured to assess oxidative damage to lipids. MDA concentrations were determined using assay kit (Solarbio Life Science, Beijing, China) (MDA, BC0025).

Gene Expression Analysis

Total RNA of the samples was isolated using TransZol UP Plus RNA Kit (TransGen Biotech, China). A sample of 0.8 μg of total RNA was used as the template for synthesis of the first strand of cDNA with PrimeScript RT reagent kit (Takara, China). The PCR reactions were run in ABI 7500 fast real-time PCR system (Applied Biosystems, United States) using SYBR Green Premix Pro Taq HS qPCR Kit (Accurate Biology, China). The PCR was performed in a total volume of 20 μl, containing 10 μl of 2X SYBR Green Pro Taq HS Premix II, 2 μl of diluted cDNA, 0.8 μl each of 10 mM each primer and 7.2 μl DNase-free water. The PCR program comprised a 95°C activation step for 30 min, followed by 40 cycles of 95°C for 5 s (denaturation) and 60°C for 30 s (annealing and extension). The β-*actin* was used as the reference gene to normalize expression levels of the target genes. All the specific primers used are listed in **Table 1**. The relative expression levels were calculated using the $2^{-\Delta\Delta Ct}$ method (Livak and Schmittgen, 2001).

Statistical Analysis

All the data were analyzed with SPSS 20.0. The levels of physiological parameters and gene expression among different groups at each sample point were analyzed with one-way ANOVA after checking tests of normality and homogeneity of variance. When significant differences were found, Duncan's-test was used to identify the differences between treatments. The correlation among physiological parameters and gene expression was analyzed using Spearman correlation analysis using the OmicShare tools. Significant differences were considered at $P < 0.05$.

RESULTS

Energy Metabolism

The levels of adenylates (ATP, AMP, ADP), ADP/ATP, AMP/ATP, and AEC significantly changed during the long-term ammonia exposure (**Table 2**). For the 4 mg l^{-1} (MA group) and 8 mg l^{-1} (HA group) groups, the contents of AMP and ADP, as well as the ratio of ADP/ATP and AMP/ATP showed significant increase, whereas ATP and AEC decreased significantly from 2 week to the end of the experiment ($P < 0.05$). For the 2 mg l^{-1} (LA group), ATP content and AEC exhibited significant decrease at the end of the 4 weeks ($P < 0.05$). The expression of *AMPK*α and

TABLE 1 | The primers used in this study.

Primer	Primer sequences	Functional category
AMPKα-F	CAAGCCCTTTCAAACCACAT	Energy metabolism
AMPKα-R	ACGTTTCCCTGGAGTTCCTT	Energy metabolism
NKA-F	CTGGCTTGGAAACTGGAGAG	Ammonia excretion
NKA-R	AGCATCCAGCCAATGGTAAC	Ammonia excretion
VAT-F	GTGACTTCCCTGAGCTGGAG	Ammonia excretion
VAT-R	GTGTGATGCCGGTGTAGATG	Ammonia excretion
NHE-F	CTCCGTAATGGGTTGCCTTA	Ammonia excretion
NHE-R	GCTTCTGCCATGAGGAATGT	Ammonia excretion
NKCC-F	CGCGGAAAGATGAGAAGAAG	Ammonia excretion
NKCC-R	GTGCTGCAGGATGGTAGGAT	Ammonia excretion
VAMP-F	TCACTTCTACGGGAAATGTCA	Ammonia excretion
VAMP-R	GGACCACCAACGATTTCAC	Ammonia excretion
Rh-F	CGTGGACCATGTCAAACTTCT	Ammonia excretion
Rh-R	CATGATAGGCACCGTATTTCTG	Ammonia excretion
UT-F	ATTCTTGGTGGTTCTCCTCTG	Urea excretion
UT-R	CAGTCCCAGTGCTATCCTACC	Urea excretion
Bip-F	TGTCCAGCATGACATCCAGT	Unfolded protein response
Bip-R	CCGAGATAAGCCTCAGCAAC	Unfolded protein response
ATF-6-F	TACCACAGCTGACACACGC	Unfolded protein response
ATF-6-R	GCAGCAGGTTCGTCTCCAT	Unfolded protein response
IRE1-F	CCTGCTGTGGACTCTTGAGA	Unfolded protein response
IRE1-R	ACTGCTGTGTTGAGTGAGGT	Unfolded protein response
XBP1-F	GTGATGGACTCTGCACTGC	Unfolded protein response
XBP1-R	GGGTTCCAGGACTGTTGCT	Unfolded protein response
eIF2α-F	TGAAATGTCCACCAACGAGA	Unfolded protein response
eIF2α-R	CACATCCGTCACAATCTTGG	Unfolded protein response
ATF-4-F	AAGGCACCATCTTCCAACTG	Unfolded protein response
ATF-4-R	TGCTGGAAGTGGACAGACAG	Unfolded protein response
p53-F	GAGGATGAAACTGCGGCTGA	Apoptosis
p53-R	AACTCTGTCCCTCCCACTAC	Apoptosis
bax-F	ATCGCAGGAACCACAGTGA	Apoptosis
bax-R	GTTGTGTGGGTCATGGCTG	Apoptosis
caspase-3-F	TGGCAGTGGTGGCTTGTCT	Apoptosis
caspase-3-R	CGTGGCTTGTTGAGCAGTG	Apoptosis

The primers for VAMP, Rh, UT, and caspase-3 were from Meng et al. (2014) and Ren et al. (2015).

activity of HK, PK, and SDH in the MA and HA groups were significantly elevated at 1 week, after which their levels decreased as exposure time increased and become lower than the control at 4 week (**Figure 1**).

Hemolymph Ammonia and Urea Contents

During the entire period of ammonia exposure, the levels of hemolymph ammonia of the three treatment groups remained lower than that of external medium, which indicated that the swimming crab has the capacity to excrete and detoxify ammonia under long-term ammonia (**Table 3**). However, the hemolymph ammonia contents in all the treatment groups showed an increasing trend as the exposure duration extended. Hemolymph ammonia concentrations in the MA and HA groups increased to 0.98 ± 0.28 mg l^{-1} and 1.96 ± 0.56 mg l^{-1} which were significantly higher than the control group (0.42 ± 0.14 mg l^{-1}) at 1 week after exposure ($P < 0.05$), and further increased in a stepwise fashion during the remaining exposure period. Hemolymph ammonia in LA group increased gradually, and reached the level ($P < 0.05$) significantly higher than the control group at four week. Similarly, the hemolymph urea contents in MA and HA groups became significantly higher than that in the control at 1 week, and increased gradually afterward. Despite a slight increase at 4 week, no significant increase of urea in LA group was found.

Ammonia Excretion

Significant differences in expression of *NKA*, *NHE*, *Rh*, *VAMP*, and *VAT* were observed in the swimming crabs under the long-term ammonia exposure ($P < 0.05$), while no obvious change was found in *NKCC* expression (**Figure 2**). The expression of *NKA*, *NHE*, *Rh*, *VAMP*, and *VAT* showed a similar pattern during the exposure. For the MA and HA groups, their expression reached the highest levels at 1 or 2 week, and then decreased gradually to the levels comparable or lower than the control group. For the LA group, the expression of these genes rose with the exposure duration, and exhibited significant up-regulation at 2 or 3 week, and returned to the control level.

Ammonia Detoxification

The activity of the ammonia detoxifying enzymes, including GDH, GS, and ARG, was significantly elevated after exposure in MA group and HA group for 1 week ($P < 0.05$), and then decreased to the control level at 2 (GS and ARG) and 3 week (GDH), respectively, and remained stable to the end of exposure (**Figure 3**). A similar pattern was also observed in the expression of *urea transporter* (*UT*). There was a significant up-regulation in *UT* expression in the MA and HA groups at 1 week ($P < 0.05$), followed by a sharp decrease at week 2. No significant difference in activity of GDH, GS, and ARG, and expression of *UT* was found in LA group during the exposure.

Antioxidant Defense and Oxidative Damage

The activity of the antioxidant enzymes were significantly altered during the long-term ammonia exposure (**Figure 4**). Compared with the control group, SOD activity in the MA and HA groups were constantly higher in the exposure period ($P < 0.05$), while CAT activity showed a gradual decrease after a slight increase at 1 week, and GPX activity decreased significantly at 4 week ($P < 0.05$). MDA levels in all the treatment groups exhibited an increasing trend as exposure time extended, and significantly elevated levels of MDA were observed in the MA and HA groups from 2 to 4 week ($P < 0.05$).

Endoplasmic Reticulum Stress and Unfolded Protein Response

Gene expression analysis showed that mRNA levels of *Bip*, *IRE1*, *XBP1*, *ATF-4*, and *ATF-6* were significantly altered after ammonia

TABLE 2 | Adenine nucleotides in the gills of *P. trituberculatus* in different groups during long-term ammonia stress.

Time	Group	ATP (μ mol/g)	ADP (μ mol/g)	AMP (μ mol/g)	ADP/ATP	AMP/ATP	AEC
1W	*Control*	697 ± 108.68^{a}	270 ± 83.61^{a}	71.63 ± 12.04^{a}	0.41 ± 0.18^{a}	0.11 ± 0.03^{a}	0.8 ± 0.05^{a}
	LA	557 ± 46.6^{a}	325.33 ± 63.89^{a}	88.53 ± 12.17^{ab}	0.59 ± 0.16^{a}	0.16 ± 0.03^{ab}	0.74 ± 0.03^{ab}
	MA	538.67 ± 111.63^{a}	352.67 ± 48.09^{a}	85.3 ± 13.04^{ab}	0.69 ± 0.25^{a}	0.16 ± 0.02^{ab}	0.73 ± 0.04^{ab}
	HA	507.67 ± 99.79^{a}	321.33 ± 38.14^{a}	94.3 ± 6.4^{b}	0.64 ± 0.07^{a}	0.19 ± 0.04^{b}	0.72 ± 0.03^{b}
2W	*Control*	640 ± 65.48^{a}	233.67 ± 30.02^{a}	65.13 ± 6.85^{a}	0.37 ± 0.09^{a}	0.1 ± 0.01^{a}	0.81 ± 0.02^{a}
	LA	600 ± 118.44^{a}	337.67 ± 35.8^{ab}	80.43 ± 15.82^{ab}	0.58 ± 0.17^{a}	0.14 ± 0.03^{a}	0.75 ± 0.03^{a}
	MA	368.33 ± 103.98^{b}	385 ± 82.49^{b}	99 ± 11.95^{b}	1.13 ± 0.51^{b}	0.28 ± 0.09^{b}	0.66 ± 0.05^{b}
	HA	333.67 ± 65.53^{b}	389.33 ± 84.2^{b}	101.13 ± 15.41^{b}	1.17 ± 0.21^{b}	0.31 ± 0.09^{b}	0.64 ± 0.02^{b}
3W	*Control*	661 ± 140.72^{a}	257.67 ± 18.93^{a}	64.07 ± 10.87^{a}	0.41 ± 0.11^{a}	0.1 ± 0.02^{a}	0.8 ± 0.03^{a}
	LA	507.67 ± 63.07^{ab}	305.67 ± 45.35^{ab}	96.57 ± 7.31^{b}	0.6 ± 0.08^{ab}	0.19 ± 0.02^{b}	0.73 ± 0.02^{b}
	MA	311.67 ± 71.84^{bc}	433.67 ± 57.07^{b}	149.83 ± 18.62^{c}	1.45 ± 0.44^{bc}	0.5 ± 0.16^{c}	0.59 ± 0.04^{c}
	HA	337.33 ± 82.28^{c}	416.67 ± 127.79^{b}	171.3 ± 15.55^{c}	1.33 ± 0.63^{c}	0.52 ± 0.09^{c}	0.59 ± 0.04^{c}
4W	*Control*	678 ± 84.34^{a}	272.67 ± 34.27^{a}	75.7 ± 12.76^{a}	0.41 ± 0.07^{a}	0.11 ± 0.01^{a}	0.79 ± 0.02^{a}
	LA	430.67 ± 68.6^{b}	255 ± 18.52^{a}	104.07 ± 10.56^{ab}	0.6 ± 0.12^{a}	0.25 ± 0.07^{a}	0.71 ± 0.04^{b}
	MA	276 ± 44.84^{c}	308 ± 72.02^{a}	139.97 ± 20.01^{c}	1.13 ± 0.29^{b}	0.52 ± 0.15^{b}	0.59 ± 0.04^{c}
	HA	225.67 ± 57.35^{c}	328.33 ± 73.87^{a}	133.83 ± 24.86^{bc}	1.48 ± 0.21^{b}	0.62 ± 0.2^{b}	0.56 ± 0.04^{c}

Values are means ± SD (n = 3). Values with different letters in the same column at each time point are significantly different (P < 0.05).

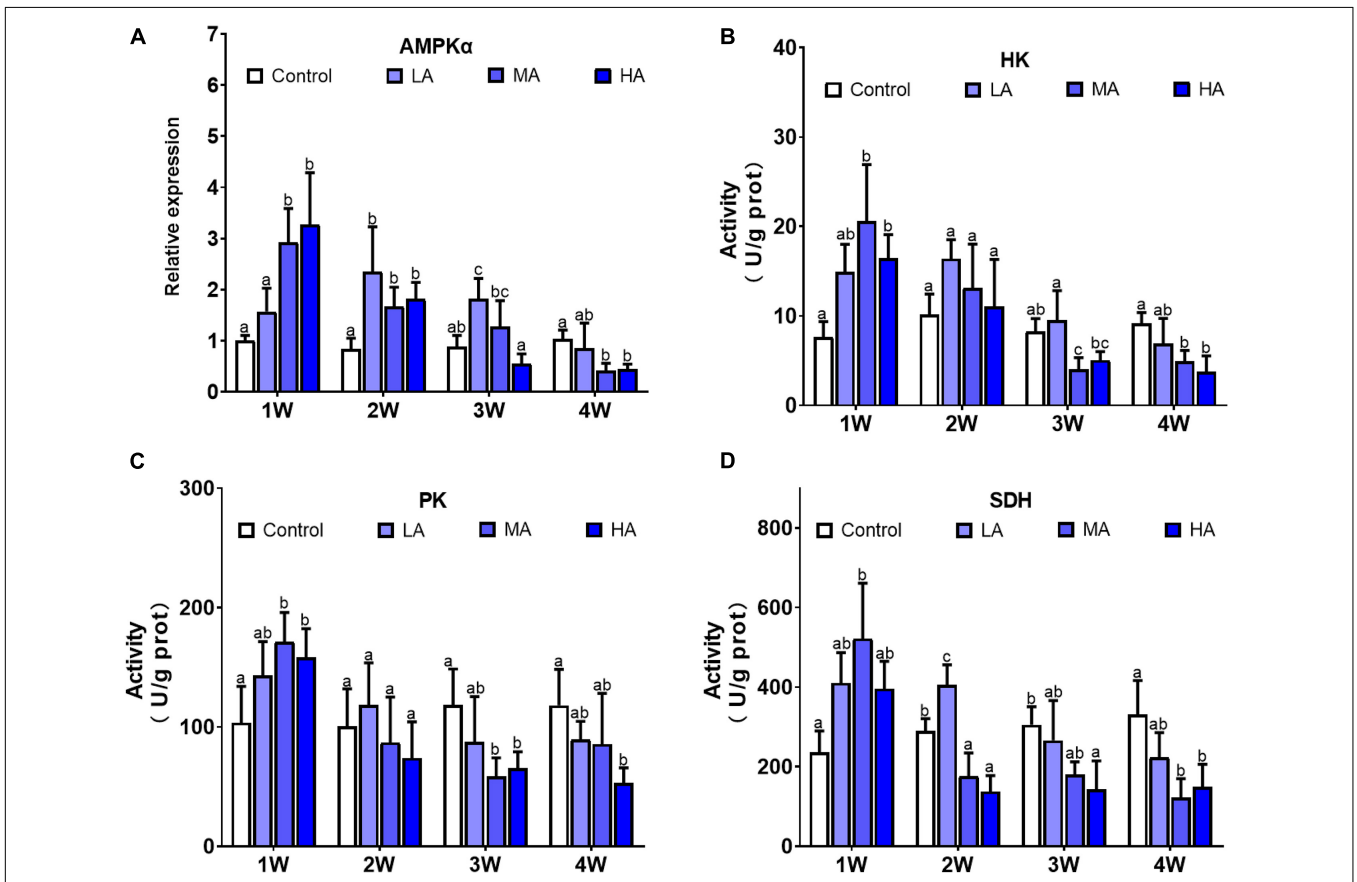

FIGURE 1 | Expression of AMPKα **(A)** and activities of HK **(B)**, PK **(C)**, and SDH **(D)** in different treatments during long-term ammonia stress. Values are means ± S.D (*n* = 3). Different letters represent significant differences among different groups (*P* < 0.05).

exposure, while no significant difference was found in *eIF2α* expression (**Figure 5**). Up-regulation of *Bip*, *IRE1*, *XBP1*, *ATF-4*, and *ATF-6* was observed in the MA and HA groups from 1 to 3 week ($P < 0.05$). However, their expression decreased to the levels similar to (*IRE1*, *XBP1*, *ATF-4*, and *ATF-6*) or lower than (*Bip*) the control at 4 week post exposure.

TABLE 3 | Hemolymph ammonia and urea contents in different groups during long-term ammonia stress.

		1W	2W	3W	4W
Hemolymph ammonia (mg l^{-1})	*Control*	0.03 ± 0.01^{a}	0.02 ± 0.01^{a}	0.03 ± 0.01^{a}	0.02 ± 0.01^{a}
	LA	0.06 ± 0.01^{b}	0.06 ± 0.01^{b}	0.07 ± 0.02^{b}	0.1 ± 0.01^{b}
	MA	0.07 ± 0.02^{b}	0.12 ± 0.03^{b}	0.14 ± 0.04^{c}	0.16 ± 0.02^{b}
	HA	0.14 ± 0.04^{c}	0.24 ± 0.08^{c}	0.27 ± 0.05^{d}	0.3 ± 0.07^{c}
Hemolymph urea (mg l^{-1})	*Control*	555.25 ± 94.52^{a}	546.83 ± 51.58^{a}	552.82 ± 103.62^{a}	623.36 ± 143.83^{a}
	LA	655.29 ± 60.37^{ab}	715.49 ± 143.2^{ab}	675.92 ± 124.21^{a}	720.23 ± 57.02^{a}
	MA	716.34 ± 62.31^{bc}	832.56 ± 106.01^{b}	799.36 ± 97.25^{a}	984.57 ± 114^{b}
	HA	829.76 ± 88.84^{c}	1070.58 ± 153.11^{c}	1066.09 ± 195.48^{b}	1190.45 ± 126.31^{b}

Values are means ± SD (n = 3). Values with different letters in the same column are significantly different ($P < 0.05$).

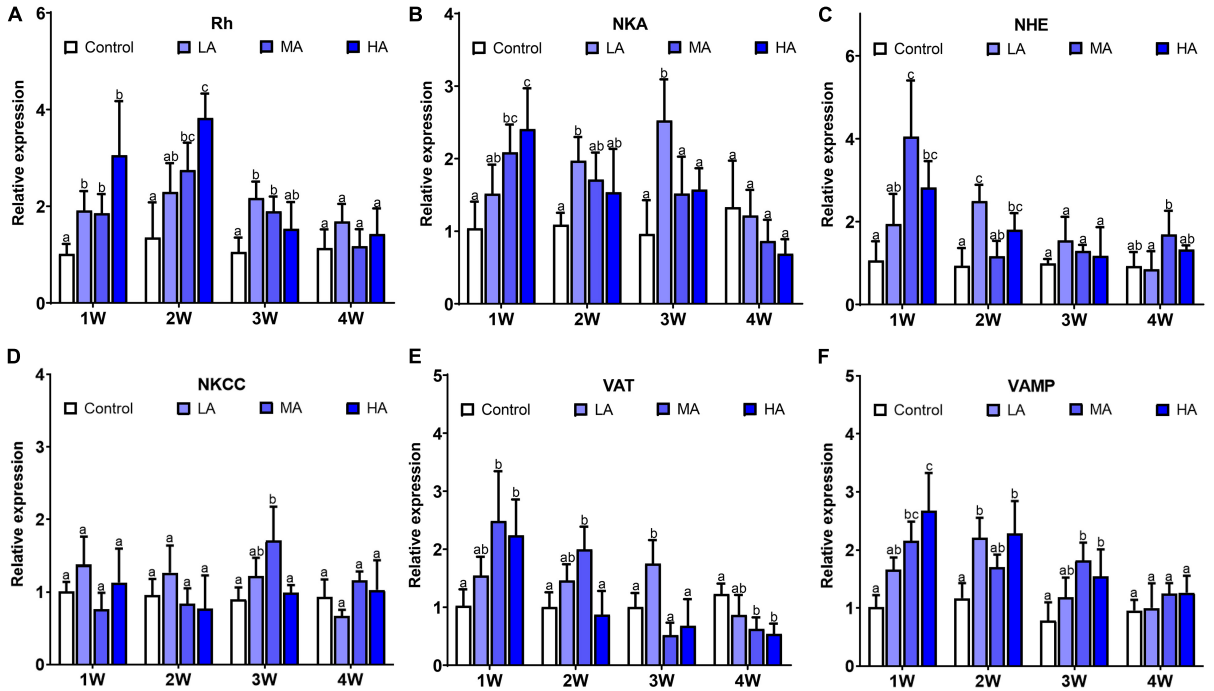

FIGURE 2 | Expression of NKA **(A)**, Rh **(B)**, NHE **(C)**, NKCC **(D)**, VAT **(E)**, and VA MP **(F)** in different treatments during long-term ammonia stress. Values are means ± S.D ($n = 3$). Different letters represent significant differences among different groups ($P < 0.05$).

Apoptosis

As shown in **Figure 6**, there was significant differences in expression of *caspase-3*, *bax*, and *bcl-2* in all the treatment groups, while *p53* only showed differential expression in MA group at week 2. Compared with the control group, *caspase-3* and *bax* exhibited higher expression in the MA and HA groups from 1 week ($P < 0.05$). In contrast, expression of *bcl-2* was lower in the MA and HA groups ($P < 0.05$). For the LA group, expression of *caspase-3* increased significantly after 3 and 4 weeks of exposure ($P < 0.05$).

DISCUSSION

Although many studies have been conducted on stress responses to acute ammonia stress in crustaceans, there has been limited information regarding their physiological and molecular responses under long-term exposure. In this study, we investigated alteration of energy metabolism, ammonia excretion and detoxification, antioxidant and UPR, and apoptosis in gills, the main excretory organ, of the swimming crab during prolonged ammonia exposure.

Energy Homeostasis

Energy metabolism plays a central role in restoring and maintaining cellular homeostasis under environmental stress (Sokolova et al., 2012), including ammonia stress (Sinha et al., 2012; Shan et al., 2019). Under ammonia exposure, energy demand associated with ammonia excretion and detoxification, and cellular stress responses may increase substantially. A recent study in *Penaeus vannamei* showed that acute ammonia exposure at 32.11 mg l^{-1} (∼half of LC50) resulted in significant reduction

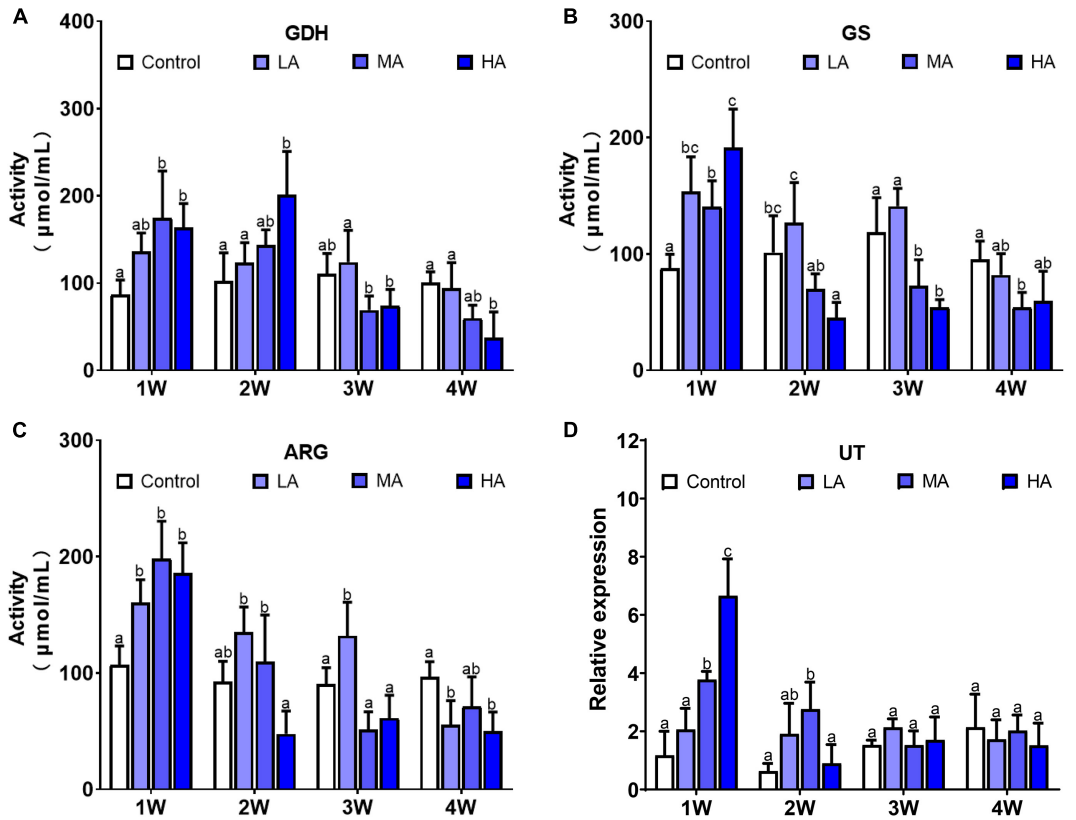

FIGURE 3 | Activities of GDH **(A)**, GS **(B)**, ARG **(C)**, and expression of UT **(D)** in different treatments during long-term ammonia stress. Values are means ± S.D ($n = 3$). Different letters represent significant differences among different groups ($P < 0.05$).

in ATP, the universal currency of free energy, and AEC, an indicator of cellular energy status, indicating that acute HEA perturbs energy homeostasis (Wang et al., 2021). In the present study, the levels of ATP and AEC in gills of all the treatment groups decreased significantly after 4-week exposure, indicating that long-term ammonia challenge, even at the concentration of 2 mg l^{-1} (LA group), can disrupt energy homeostasis in the gills of *P. trituberculatus*.

AMP-activated protein kinase (AMPK) is a key regulator of cellular energy balance (Hardie et al., 2012). Once activated by low energy status (AMP/ATP or ADP/ATP), AMPK initiates downstream signaling and switches on catabolic pathways such as glycolysis and oxidative metabolism, to enhance ATP production (Herzig and Shaw, 2018). It was reported that acute ammonia exposure stimulates AMPK signaling in gills of *P. vannamei* (Wang et al., 2021). Consistent with that result, significant upregulation of the expression of *AMPK*α, as well as activities of HK, PK, and SDH, were observed in MA and HA groups at 1 week post exposure, indicating that AMPK signaling was activated after a short-term ammonia exposure and thereby promotes glycolysis and oxidative phosphorylation, to meet increased energy requirement for defending against ammonia stress. However, as exposure time increase, there was a general trend of decline in *AMPK*α expression accompanied by decrease in activities of the metabolic enzymes in MA and HA groups, though the ATP levels in those groups remained lower than those in control group. These results suggest that long-term ammonia stress likely directly or indirectly inhibits AMPK signaling, that contributes to energy deprivation in gills of the swimming crab. Since most of the ammonia excretion and detoxification pathways, and cellular stress responses are energy-consuming, the energy imbalance is likely to have significant adverse consequences as outlined next.

Ammonia Excretion and Hemolymph Ammonia

Benthic species employ a variety of ammonia excretion pathways to survive the HEA (Weihrauch et al., 2009; Ip and Chew, 2010). In crustaceans, ammonia excretion is accomplished mainly at the gill epithelium through several transporters, such as *Rh*, *NKA*, *VAT*, and *NHE*, as well as a microtubule-dependent vesicular excretion mechanism (Weihrauch et al., 2002). Numerous investigations in decapods have shown that, under acute ammonia stress, these excretion pathways are activated to maintain hemolymph ammonia concentration (Si et al., 2018; Zhang X. et al., 2020). However, little is known about the alteration of ammonia excretion pathways and hemolymph ammonia during long-term ammonia stress. During the 4-week exposure period in this study, the levels of hemolymph

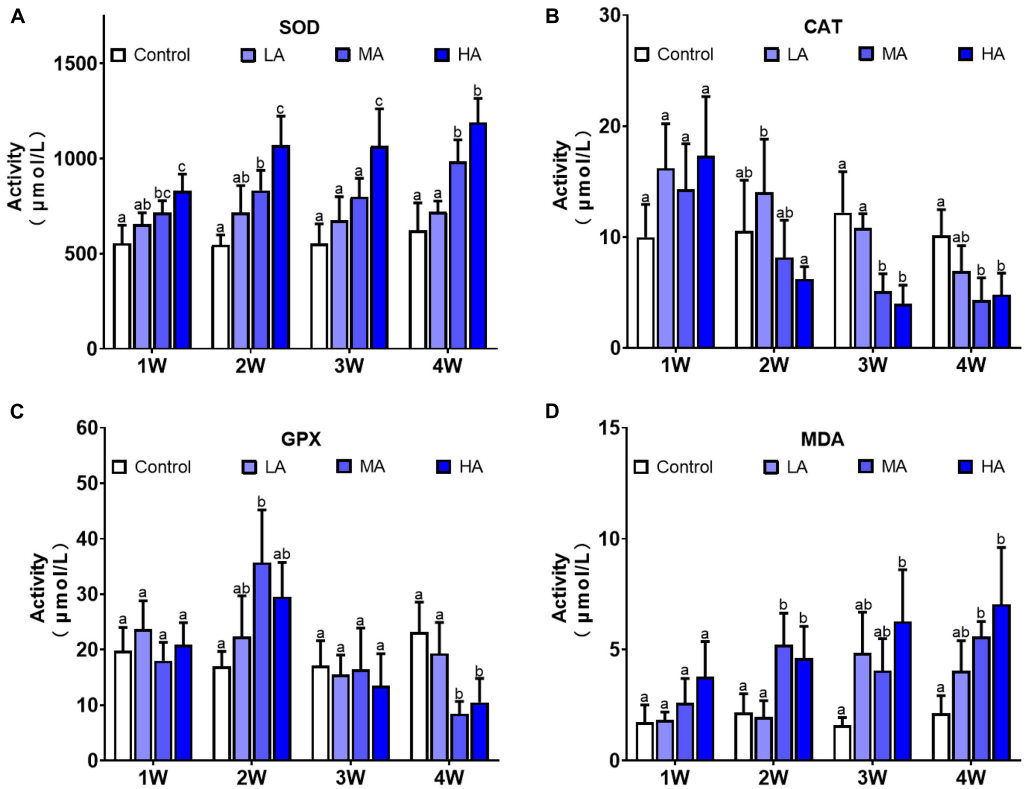

FIGURE 4 | Activities of SOD **(A)**, CAT **(B)**, GPX **(C)**, and levels of MDA **(D)** in different treatments during long-term ammonia stress. Values are means ± S.D ($n = 3$). Different letters represent significant differences among different groups ($P < 0.05$).

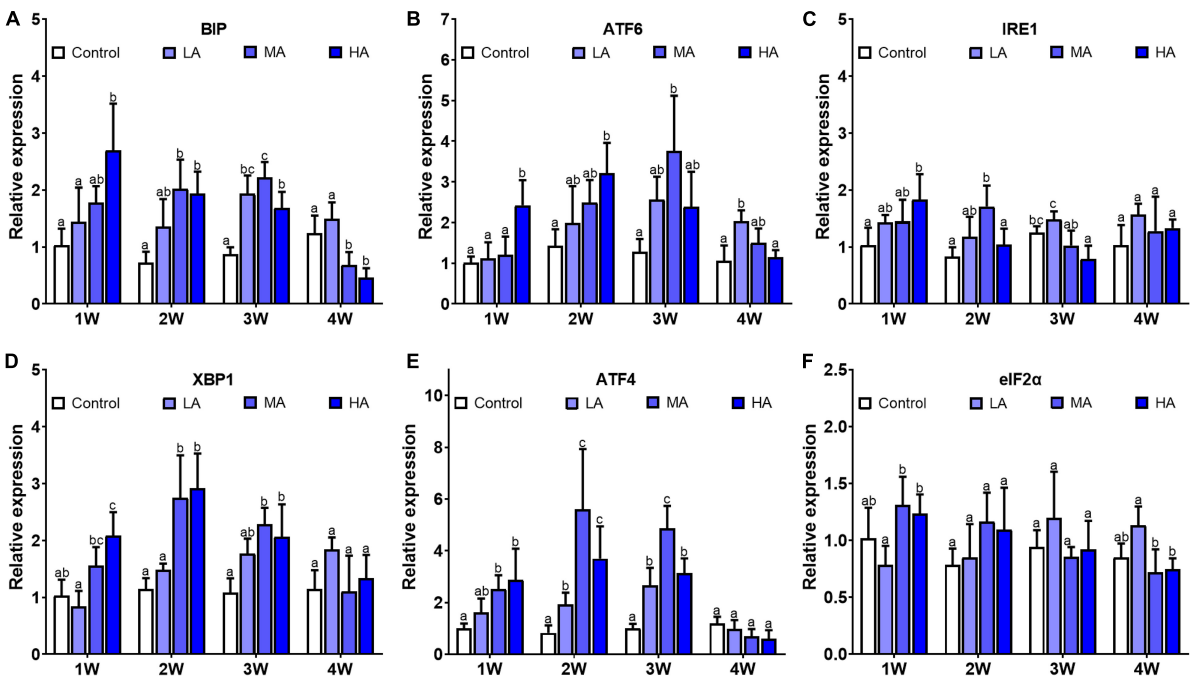

FIGURE 5 | Expression of BIP **(A)**, ATF-6 **(B)**, IRE1 **(C)**, XBP1 **(D)**, ATF-4 **(E)**, and eIF2α **(F)** in different treatments during long-term ammonia stress. Values are means ± S.D ($n = 3$). Different letters represent significant differences among different groups ($P < 0.05$).

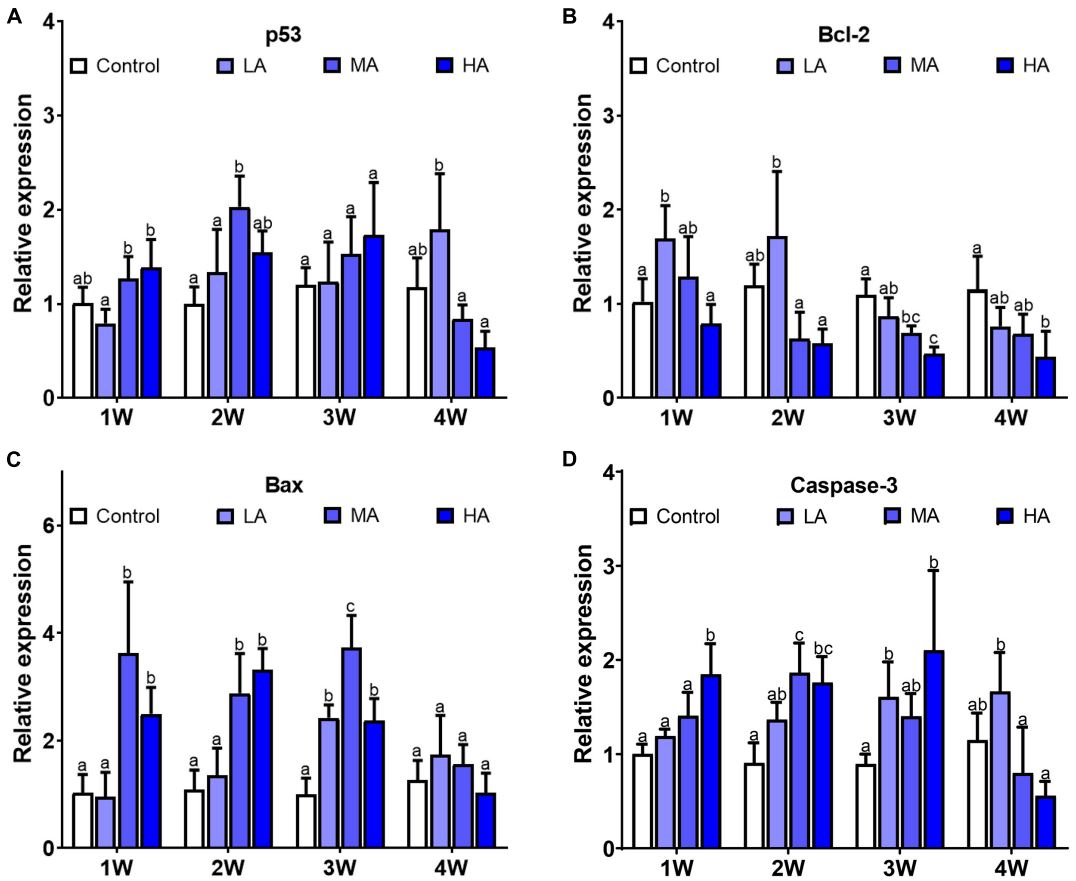

FIGURE 6 | Expression of p53 **(A)**, bcl-2 **(B)**, bax **(C)**, and caspase-3 **(D)** in different treatments during long-term ammonia stress. Values are means ± S.D ($n = 3$). Different letters represent significant differences among different groups ($P < 0.05$).

ammonia in all the treatment groups were below those in ambient seawater, suggesting that active ammonia excretion continued to counteract ammonia influx. Nevertheless, hemolymph ammonia concentrations in all the exposure groups showed an increasing trend as exposure duration increased, and is potentially a result of gradually decreasing expression of ammonia excretion genes. Similar results were also observed in the Dungeness crab *Metacarcinus magister* (Martin et al., 2011). These results indicated that efficient branchial ammonia excretion can only last for a certain time period, and prolonged exposure depresses the excretion mechanisms, leading to accumulation of internal ammonia in the swimming crab.

It is noteworthy that the expression of *NKA* and *VAT* in MA and HA groups decreased to the control level earlier than the other genes involved in ammonia excretion. NKA and VAT are the major ATP-requiring participants in the ammonia excretion mechanisms (Weihrauch et al., 2002). The decrease of NKA and VAT expression coincided with the reduction in ATP contents. It is possible that the down-regulation of *NKA* and *VAT* is due to the disruption of energy homeostasis due to the prolonged ammonia exposure. Both NKA and VAT are key proteins in the transepithelial ammonia transport processes (Gonçalves et al., 2006; Henry et al., 2012). NKA, localized in basolateral membrane, transports ammonia from the hemolymph into the epithelial cell. VAT is distributed in cytoplasm and is critical in microtubule-dependent vesicular excretion through diffusion of NH_3 into vesicles (Allen and Weihrauch, 2021). Considering their importance in the excretion, the depression expression of *NKA* and *VAT* may severely impair the ammonia excretion process in gills and is perhaps a result of declining overall cellular health.

Ammonia Detoxification and Hemolymph Urea

Aside from excreting ammonia directly, crustaceans have detoxification strategies *via* converting ammonia into other compounds to protect against HEA (Romano and Zeng, 2013). One of the detoxification strategies is conversion of ammonia to glutamate by GDH and then to glutamine by GS which can be stored in tissues and used as an oxidative substrate when returned to normal condition (Weihrauch et al., 1999; Hong et al., 2007). It is well-documented that this strategy is important for decapods to mitigate acute ammonia stress. In this study, both GDH and GS activities in MA and HA groups were significantly elevated at the initial stage, followed by a

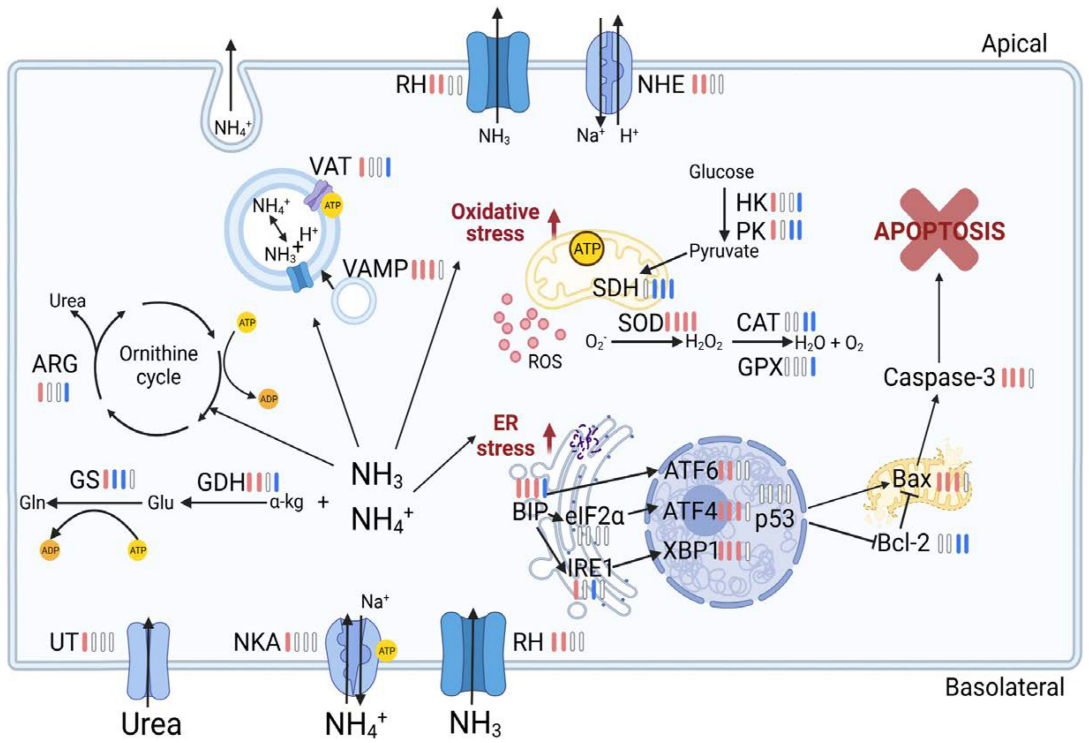

FIGURE 7 | Overview of physiological and molecular responses in the gill of the swimming crab Portunus trituberculatus during long-term ammonia stress. The different colors of the bars indicate the changes of physiological parameters and gene expression in HA group (8 mg l^{-1}). Red bars represent significant up-regulation, blue bars represent significant down-regulation and white bars represent no significant difference, compared with the control group. The figure is created in BioRender.

decrease to the levels comparable with or lower than the control group at later stages. This confirms that glutamine synthesis is important for detoxification under short-term ammonia, however, this detoxification pathway may be inhibited after long-term exposure. Although glutamine formation is considered to be an effective ammonia detoxification mechanism in crustaceans, it is a highly energy-consuming processes (Newsholme et al., 2003), where the conversion of glutamate and ammonia to glutamine, catalyzed by GS, is an ATP-dependent reaction. Results from the present study showed that GS activity decreased concurrently with the reduction of ATP. Moreover, correlation analysis revealed that GS activity was positively correlated with ATP level (**Supplementary Figure 1**). These results indicated that the depression of glutamine conversion after long-term exposure could be attributed to limited energy available.

It has been reported that converting ammonia into less toxic urea *via* ornithine-urea cycle (OUC) is an important pathway for ammonia detoxification in crustaceans (Liu et al., 2014; Geng et al., 2020). Similar to the detoxification *via* glutamate synthesis, urea production from ammonia is also energetically costly, and it requires at least 2 mol of ATP for synthesizing 1 mol urea (Wood, 1993). In the present study, the activity of ARG, a key enzyme in OUC, shared a similar temporal pattern with that of GS, and decreased paralleled with ATP content. This further indicate that the depressed energy-consuming detoxification pathways in gills after prolonged exposure is likely due to the lack of ATP. Despite the reduction of ARG activity in gill after long-term exposure, the level of hemolymph urea increased significantly. This might be related to increased urea production in hepatopancreas, and many studies have reported that hepatopancreas is another organ for converting ammonia into urea (Pan et al., 2018). Therefore, another possibility is that the swimming crabs were unable to excrete urea efficiently as evidenced by no increment in expression of *UT*, the specific transporter that facilitates urea transport across the gills (You et al., 1993). Urea accumulation without increased excretion capacity was also observed in largemouth bass, and it was speculated that it may be a strategy to avoid the loss of metabolic carbon fuel (Egnew et al., 2019). On the other hand, urea is toxic, though less than ammonia (Randall and Tsui, 2002). To date, its exact toxicity in crustacean is still unclear. Further work is required to understand the physiological consequences of urea accumulation in the swimming crab under ammonia stress.

Oxidative Stress, Endoplasmic Reticulum Stress, and Apoptosis

A number of studies in decapods have reported that acute ammonia stress can induce reactive oxygen species (ROS) generation, leading to oxidative damage to biomolecules including lipids (Zhang et al., 2015; Liang et al., 2016). Our data showed that MDA, an index of lipid peroxidation, accumulated

in gills in a time- and dose-dependent manner following long term ammonia exposure. The build-up of MDA is probably associated with the alteration of antioxidant defense system. SOD, CAT, and GPx are key enzymes in antioxidant system, and represents the first line of defense against oxidative stress (McCord, 2000). For MA and HA group, a significant increase in SOD activity was observed after exposure, while CAT and GPx activities showed a gradual decrease during the exposure. SOD catalyzes the dismutation of superoxide ions (O_2^-) to hydrogen peroxide (H_2O_2), and CAT and GPx convert H_2O_2 to water (Xie et al., 2016). Increment of SOD activity can result in elevated levels of H_2O_2, and reduction of CAT and GPx activity can lead to accumulation of H_2O_2, and then this build-up of H_2O_2 can oxidatively damaged lipids and other biomolecules (Magdalan et al., 2011; Meng et al., 2014).

Oxidative stress is usually coupled with ER stress during which protein folding is overwhelmed, and leads to accumulation of unfold and misfold proteins in ER (Todd et al., 2008). To restore ER homeostasis, cells activate several signaling pathways, collectively called the unfolded protein response (UPR), aiding protein folding and eliminating terminally misfolded protein (Hetz, 2012). Results of this study showed that *Bip*, the master regulator of UPR, was significantly upregulated in all the treatment groups, indicating that long-term ammonia exposure can cause ER stress and induce UPR in the swimming crab. The activation of the UPR involves three signaling pathways, including PERK/ATF4, IRE1/XBP1 and ATF6 (Kim et al., 2006). Previous studies in *Litopenaeus vannamei* showed that short-term HEA (20∼42 mg l^{-1}) can activate PERK/ATF4 and IRE1/XBP1 pathways in hepatopancreas tissue (Liang et al., 2016; Wang et al., 2020). In this study, upregulation of *ATF4*, *ATF6*, *IRE1*, and *XBP1* indicated that all the three UPR signaling pathways were initiated to alleviate ER stress in gills after ammonia stress. Notably, the expression of *ATF4*, *ATF6*, *IRE1*, and *XBP1* in MA and HA groups decreased, accompanied by *Bip*, to the levels similar to the control group at 4 week. This result suggested that prolonged ammonia exposure can compromise UPR signaling, which may lead to aggravation of ER stress and cell death (Sano and Reed, 2013).

It is well-documented that both oxidative stress and ER stress can interfere with cell function and activate pro-apoptotic signaling (Chandra et al., 2000; Tabas and Ron, 2011). Moreover, oxidative stress and ER stress could accentuate each other in a positive feedback loop, which further perturbs cellular homeostasis and elicit apoptotic cell death (Liu X. et al., 2020). Expression analysis revealed that *caspase-3*, the executioner of apoptosis, was significantly up-regulated in all the treatment groups, indicating that long-term ammonia stress, even at the concentration as low as 2 mg l^{-1} (LA group), can induce apoptosis in gills of the swimming crab. Recent studies in fish showed that ammonia induced apoptosis in hepatopancreas *via* p53-Bax signaling pathway (Cheng et al., 2015; Jia et al., 2015). In this pathway, activation of p53 down-regulates anti-apoptotic genes, such as *bcl-2*, and up-regulates pro-apoptotic genes including the *bax*, which causes activation of caspases and eventually apoptosis (Schuler and Green, 2001). In the present study, enhanced *bax* expression and reduced *bcl-2* expression were observed after ammonia exposure. However, there was only slight increase in *p53* expression, which is possibly because p53 is activated through post-translational modifications (Xu, 2003). Collectively, our results indicate that ammonia-induces apoptosis in gills of *P. trituberculatus* likely *via* the p53-Bax pathway.

CONCLUSION

In summary, this study investigated stress responses in the gills of the swimming crab *P. trituberculatus* following long-term ammonia stress over a temporal scale (**Figure 7**). The results revealed that prolonged ammonia impaired energy homeostasis possibly through inhibiting AMPK signaling, and depressed ammonia excretion and detoxification machinery. This likely leads to hemolymph ammonia accumulation, which was, at least in part, due to the mismatch in the increased energy demand and reduced ATP generation. Furthermore, the long-term exposure resulted in oxidative damage and ER stress, and elicited apoptosis in gills of the crabs, even for those at low ammonia concentration (2 mg l^{-1}). The findings of the present study further our understanding of detrimental effects and mechanisms of long-term ammonia in swimming crabs, and provide valuable information for aquaculture management.

DATA AVAILABILITY STATEMENT

The original contributions presented in the study are included in the article/**Supplementary Material**, further inquiries can be directed to the corresponding author/s.

AUTHOR CONTRIBUTIONS

JZ and XM: conceptualization. JZ and MZ: methodology and investigation. XM, JZ, XR, and BG: software, validation, formal analysis, data curation, and original draft. NJ, JZ, and XM: writing, review, and editing. PL and JL: resources, supervision, and project administration. XM: funding acquisition. All authors contributed to the article and approved the submitted version.

FUNDING

This research was funded by the National Key Research and Development Plan (2019YFD0900402), the Qingdao Shinan District Science and Technology Program (2020-2-001-QT), the Central Public-interest Scientific Institution Basal Research Fund, CAFS (2020TD46), and the China Agriculture Research System of MOF and MARA.

SUPPLEMENTARY MATERIAL

The Supplementary Material for this article can be found online at: https://www.frontiersin.org/articles/10.3389/fmars.2021.797241/full#supplementary-material

REFERENCES

Ackerman, P. A., Wicks, B. J., Iwama, G. K., and Randall, D. J. (2006). Low levels of environmental ammonia increase susceptibility to disease in Chinook salmon smolts. *Physiol*. Biochem. Zool. 79, 695–707. doi: 10.1086/504615

Allen, G. J. P., and Weihrauch, D. (2021). Exploring the versatility of the perfused crustacean gill as a model for transbranchial transport processes. *Comp. Biochem. Physiol. B.* 254:110572. doi: 10.1016/j.cbpb.2021.110572

Benli, A. ÇK., Köksal, G., and Özkul, A. (2008). Sublethal ammonia exposure of Nile tilapia (*Oreochromis niloticus* L.): effects on gill, liver and kidney histology. *Chemosphere* 72, 1355–1358. doi: 10.1016/j.chemosphere.2008.04.037

Brinkman, S. F., Woodling, J. D., Vajda, A. M., and Norris, D. O. (2009). Chronic toxicity of ammonia to early life stage rainbow trout. *Trans. Am. Fish. Soc.* 138, 433–440. doi: 10.1577/T07-224.1

Chandra, J., Samali, A., and Orrenius, S. (2000). Triggering and modulation of apoptosis by oxidative stress. *Free. Radical. Biol. Med.* 29, 323–333. doi: 10.1016/S0891-5849(00)00302-6

Cheng, C. H., Yang, F. F., Ling, R. Z., Liao, S. A., Miao, Y. T., Ye, C. X., et al. (2015). Effects of ammonia exposure on apoptosis, oxidative stress and immune response in pufferfish (*Takifugu obscurus*). *Aquat. Toxicol.* 164, 61–71. doi: 10.1016/j.aquatox.2015.04.004

China Agriculture Press (2020). *China Fishery Statistical Yearbook*. Beijing: China Agriculture Press, 24–34.

Ching, B., Chew, S. F., Wong, W. P., and Ip, Y. K. (2009). Environmental ammonia exposure induces oxidative stress in gills and brain of *Boleophthalmus boddarti* (mudskipper). *Aquat.Toxicol.* 95, 203–212. doi: 10.1016/j.aquatox.2009.09.004

Cui, Y., Ren, X., Li, J., Zhai, Q., Feng, Y., Xu, Y., et al. (2017). Effects of ammonia-N stress on metabolic and immune function via the neuroendocrine system in *Litopenaeus vannamei*. *Fish. Shellfish Immunol.* 64, 270–275. doi: 10.1016/j.fsi.2017.03.028

Dai, A., Yang, S., and Song, Y. (1986). *Marine Crabs In China Sea*. Beijing: Marine press, 194–196.

Egnew, N., Renukdas, N., Ramena, Y., Yadav, A. K., Kelly, A. M., Lochmann, R. T., et al. (2019). Physiological insights into largemouth bass (*Micropterus salmoides*) survival during long-term exposure to high environmental ammonia. *Aquat. Toxicol.* 207, 72–82. doi: 10.1016/j.aquatox.2018.11.027

Foss, A., Imsland, A. K., Roth, B., Schram, E., and Stefansson, S. O. (2009). Effects of chronic and periodic exposure to ammonia on growth and blood physiology in juvenile turbot (*Scophthalmus maximus*). *Aquaculture* 296, 45–50. doi: 10.1016/j.aquaculture.2009.07.013

Geng, Z., Liu, Q., Wang, T., Ma, S., and Shan, H. (2020). Changes in physiological parameters involved in glutamine and urea synthesis in Pacific white shrimp, *Litopenaeus vannamei*, fed *Ampithoe* sp. meal and exposed to ammonia stress. *Aquac. Res.* 51, 2725–2734. doi: 10.1111/are.14611

Gonçalves, R. R., Masui, D. C., McNamara, J. C., Mantelatto, F. L., Garçon, D. P., Furriel, R. P., et al. (2006). A kinetic study of the gill (Na+, K+)-ATPase, and its role in ammonia excretion in the intertidal hermit crab, *Clibanarius vittatus*. *Comp. Biochem. Physiol. A* 145, 346–356. doi: 10.1016/j.cbpa.2006.07.007

Hardie, D. G., Ross, F. A., and Hawley, S. A. (2012). AMPK: a nutrient and energy sensor that maintains energy homeostasis. *Nat. Rev. Mol. Cell. Biol.* 13, 251–262. doi: 10.1038/nrm3311

Henry, R. P., Lucu, C., Onken, H., and Weihrauch, D. (2012). Multiple functions of the crustacean gill: osmotic/ionic regulation, acid-base balance, ammonia excretion, and bioaccumulation of toxic metals. *Front. Physiol.* 3:431. doi: 10.3389/fphys.2012.00431

Henry, Y., Piscart, C., Charles, S., and Colinet, H. (2017). Combined effect of temperature and ammonia on molecular response and survival of the freshwater crustacean *Gammarus pulex*. *Ecotoxicol. Environ. Saf.* 137, 42–48. doi: 10.1016/j.ecoenv.2016.11.011

Herzig, S., and Shaw, R. J. (2018). AMPK: guardian of metabolism and mitochondrial homeostasis. *Nat. Rev. Mol. Cell. Biol.* 19, 121–135. doi: 10.1038/nrm.2017.95

Hetz, C. (2012). The unfolded protein response: controlling cell fate decisions under ER stress and beyond. *Nat. Rev. Mol. Cell. Biol.* 13, 89–102. doi: 10.1038/nrm3270

Hong, M., Chen, L., Sun, X., Gu, S., Zhang, L., and Chen, Y. (2007). Metabolic and immune responses in Chinese mitten-handed crab (*Eriocheir sinensis*) juveniles exposed to elevated ambient ammonia. *Comp. Biochem. Physiol. C* 145, 363–369. doi: 10.1016/j.cbpc.2007.01.003

Ip, Y. K., and Chew, S. F. (2010). Ammonia production, excretion, toxicity, and defense in fish: a review. *Front. Physiol.* 1:134. doi: 10.3389/fphys.2010.00134

Ip, Y., Chew, S., and Randall, D. J. (2001). Ammonia toxicity, tolerance, and excretion. *Fish. Physiol.* 20, 109–148. doi: 10.1016/S1546-5098(01)20005-3

Jia, R., Han, C., Lei, J. L., Liu, B. L., Huang, B., Huo, H. H., et al. (2015). Effects of nitrite exposure on haematological parameters, oxidative stress and apoptosis in juvenile turbot (*Scophthalmus maximus*). *Aquat.Toxicol.* 169, 1–9. doi: 10.1016/j.aquatox.2015.09.016

Kim, R., Emi, M., Tanabe, K., and Murakami, S. (2006). Role of the unfolded protein response in cell death. *Apoptosis* 11, 5–13. doi: 10.1007/s10495-005-3088-0

Lemarié, G., Dosdat, A., Covès, D., Dutto, G., Gasset, E., and Person-Le Ruyet, J. (2004). Effect of chronic ammonia exposure on growth of European seabass (*Dicentrarchus labrax*) juveniles. *Aquaculture* 229, 479–491. doi: 10.1016/s0044-8486(03)00392-2

Liang, C., Liu, J., Cao, F., Li, Z., and Chen, T. (2019). Transcriptomic analyses of the acute ammonia stress response in the hepatopancreas of the kuruma shrimp (*Marsupenaeus japonicus*). *Aquaculture* 513:734328. doi: 10.1016/j.aquaculture.2019.734328

Liang, Z., Liu, R., Zhao, D., Wang, L., Sun, M., Wang, M., et al. (2016). Ammonia exposure induces oxidative stress, endoplasmic reticulum stress and apoptosis in hepatopancreas of pacific white shrimp (*Litopenaeus vannamei*). *Fish. Shellfish Immunol.* 54, 523–528. doi: 10.1016/j.fsi.2016.05.009

Liu, F., Li, S., Yu, Y., Sun, M., Xiang, J., and Li, F. (2020). Effects of ammonia stress on the hemocytes of the Pacific white shrimp *Litopenaeus vannamei*. *Chemosphere* 239:124759. doi: 10.1016/j.chemosphere.2019.124759

Liu, S., Pan, L., Liu, M., and Yang, L. (2014). Effects of ammonia exposure on nitrogen metabolism in gills and hemolymph of the swimming crab *Portunus trituberculatus*. *Aquaculture* 432, 351–359. doi: 10.1016/j.aquaculture.2014.05.029

Liu, X., Zhang, E., Yin, S., Zhao, C., Fan, L., and Hu, H. (2020). Activation of the IRE1α arm, but not the PERK arm, of the unfolded protein response contributes to fumonisin B1-induced hepatotoxicity. *Toxins* 12:55. doi: 10.3390/toxins12010055

Livak, K., and Schmittgen, T. (2001). Analysis of relative gene expression data using real-time quantitative PCR and the 2 (-MC (T)) Method. *Methods* 25, 402–408. doi: 10.1006/meth.2001.1262

Lu, Y., Wang, F., and Dong, S. (2015). Energy response of swimming crab *Portunus trituberculatus* to thermal variation: implication for crab transport method. *Aquaculture* 441, 64–71. doi: 10.1016/j.aquaculture.2015.02.022

Lucu, Č, Devescovi, M., and Siebers, D. J. (1989). Do amiloride and ouabain affect ammonia fluxes in perfused *Carcinus gill* epithelia? *J. Exp. Zool.* 249, 1–5. doi: 10.1002/jez.1402490102

Magdalan, J., Piotrowska, A., Gomułkiewicz, A., Sozański, T., Szeląg, A., and Dziegiêl, P. (2011). Influence of commonly used clinical antidotes on antioxidant systems in human hepatocyte culture intoxicated with α-amanitin. *Hum. Exp. Toxicol.* 30, 38–43. doi: 10.1177/0960327110368418

Martin, M., Fehsenfeld, S., Sourial, M. M., and Weihrauch, D. (2011). Effects of high environmental ammonia on branchial ammonia excretion rates and tissue Rh-protein mRNA expression levels in seawater acclimated Dungeness crab *Metacarcinus magister*. *Comp. Biochem. Physiol. A* 160, 267–277. doi: 10.1016/j.cbpa.2011.06.012

McCord, J. M. (2000). The evolution of free radicals and oxidative stress. *Am. J. Med.* 108, 652–659. doi: 10.1016/S0002-9343(00)00412-5

Meng, X. L., Liu, P., Li, J., Gao, B. Q., and Chen, P. (2014). Physiological responses of swimming crab Portunus trituberculatus under cold acclimation: antioxidant defense and heat shock proteins. *Aquaculture* 434, 11–17. doi: 10.1016/j.aquaculture.2014.07.021

Murray, B. W., Busby, E. R., Mommsen, T. P., and Wright, P. A. (2003). Evolution of glutamine synthetase in vertebrates: multiple glutamine synthetase genes expressed in rainbow trout (*Oncorhynchus mykiss*). *J. Exp. Biol.* 206, 1511–1521. doi: 10.1242/jeb.00283

Newsholme, P., Procopio, J., Lima, M. M. R., Pithon-Curi, T. C., and Curi, R. (2003). Glutamine and glutamate-their central role in cell metabolism and function. *Cell. Biochem. Funct.* 21, 1–9. doi: 10.1002/cbf.1003

Pan, L., Si, L., Liu, S., Liu, M., and Wang, G. (2018). Levels of metabolic enzymes and nitrogenous compounds in the swimming crab *Portunus trituberculatus* exposed to elevated ambient ammonia-N. *J. Ocean. Univ. China* 17, 957–966. doi: 10.1007/s11802-018-3574-y

Racotta, I. S., and Herna′ndez-Herrera, R. (2000). Metabolic responses of the white shrimp, *Penaeus vannamei*, to ambient ammonia. *Comp. Biochem. Physiol. A* 125, 437–443. doi: 10.1016/S1095-6433(00)00171-9

Randall, D. J., and Tsui, T. K. (2002). Ammonia toxicity in fish. *Mar. Pollut. Bull.* 45, 17–23.

Ren, Q., Pan, L., Zhao, Q., and Si, L. (2015). Ammonia and urea excretion in the swimming crab *Portunus trituberculatus* exposed to elevated ambient ammonia-N. *Comp. Biochem. Physiol. A* 187, 48–54. doi: 10.1016/j.cbpa.2015.04.013

Romano, N., and Zeng, C. (2007). Ontogenetic changes in tolerance to acute ammonia exposure and associated gill histological alterations during early juvenile development of the blue swimmer crab, *Portunus pelagicus*. *Aquaculture* 266, 246–254. doi: 10.1016/j.aquaculture.2007.01.035

Romano, N., and Zeng, C. (2010). Survival, osmoregulation and ammonia-N excretion of blue swimmer crab, P*ortunus pelagicus*, juveniles exposed to different ammonia-N and salinity combinations. *Comp. Biochem. Physiol. C* 151, 222–228. doi: 10.1016/j.cbpc.2009.10.011

Romano, N., and Zeng, C. (2013). Toxic effects of ammonia, nitrite, and nitrate to decapod crustaceans: a review on factors influencing their toxicity, physiological consequences, and coping mechanisms. *Rev. Fish. Sci.* 21, 1–21. doi: 10.1080/10641262.2012.753404

Sano, R., and Reed, J. C. (2013). ER stress-induced cell death mechanisms. *Biochim. Biophys. Acta Mol. Cell. Res.* 1833, 3460–3470. doi: 10.1016/j.bbamcr.2013.06.028

Schuler, M., and Green, D. (2001). Mechanisms of p53-dependent apoptosis. *Biochem. Soc. Trans.* 29, 684–688. doi: 10.1042/bst0290684

Shan, H., Geng, Z., Ma, S., and Wang, T. (2019). Comparative study of the key enzymes and biochemical substances involved in the energy metabolism of Pacific white shrimp, *Litopenaeus vannamei*, with different ammonia-N tolerances. *Comp. Biochem. Physiol. C* 221, 73–81. doi: 10.1016/j.cbpc.2019.04.001

Si, L., Pan, L., Wang, H., and Zhang, X. (2018). Identification of the role of Rh protein in ammonia excretion of the swimming crab *Portunus trituberculatus*. *J. Exp. Biol.* 221, jeb184655. doi: 10.1242/jeb.184655

Sinha, A. K., Liew, H. J., Diricx, M., Blust, R., and De Boeck, G. (2012). The interactive effects of ammonia exposure, nutritional status and exercise on metabolic and physiological responses in gold fish (*Carassius auratus* L.). *Aquat. Toxicol.* 109, 33–46. doi: 10.1016/j.aquatox.2011.11.002

Sokolova, I. M., Frederich, M., Bagwe, R., Lannig, G., and Sukhotin, A. A. (2012). Energy homeostasis as an integrative tool for assessing limits of environmental stress tolerance in aquatic invertebrates. *Mar. Environ. Res.* 79, 1–15. doi: 10.1016/j.marenvres.2012.04.003

Tabas, I., and Ron, D. (2011). Integrating the mechanisms of apoptosis induced by endoplasmic reticulum stress. *Nat. Cell. Biol.* 13, 184–190. doi: 10.1038/ncb0311-184

Todd, D. J., Lee, A. H., and Glimcher, L. H. (2008). The endoplasmic reticulum stress response in immunity and autoimmunity. *Nat. Rev. Immunol.* 8, 663–674. doi: 10.1038/nri2359

Wang, T., Li, W., Shan, H., and Ma, S. (2021). Responses of energy homeostasis and lipid metabolism in Penaeus vannamei exposed to ammonia stress. *Aquaculture* 544:737092. doi: 10.1016/j.aquaculture.2021.737092

Wang, T., Shan, H. W., Geng, Z. X., Yu, P., and Ma, S. (2020). Dietary supplementation with freeze-dried *Ampithoe* sp. enhances the ammonia-N tolerance of *Litopenaeus vannamei* by reducing oxidative stress and endoplasmic reticulum stress and regulating lipid metabolism. *Aquacult. Rep.* 16:100264. doi: 10.1016/j.aqrep.2019.100264

Weihrauch, D., and Allen, G. J. J. (2018). Ammonia excretion in aquatic invertebrates: new insights and questions. *J. Exp. Biol.* 221:jeb169219. doi: 10.1242/jeb.169219

Weihrauch, D., Becker, W., Postel, U., Luck-Kopp, S., and Siebers, D. (1999). Potential of active excretion of ammonia in three different haline species of crabs. *J. Comp. Physiol.* 169, 25–37. doi: 10.1007/s003600050190

Weihrauch, D., Fehsenfeld, S., and Quijada-Rodriguez, A. (2017). "Nitrogen excretion in aquatic crustaceans," in *Acid-Base Balance and Nitrogen Excretion in Invertebrates*, eds D. Weihrauch and M. O'Donnell (Cham: Springer), 1–24. doi: 10.1007/978-3-319-39617-0_1

Weihrauch, D., Morris, S., and Towle, D. W. (2004). Ammonia excretion in aquatic and terrestrial crabs. *J. Exp. Biol.* 207, 4491–4504. doi: 10.1242/jeb.01308

Weihrauch, D., Wilkie, M. P., and Walsh, P. J. (2009). Ammonia and urea transporters in gills of fish and aquatic crustaceans. *J. Exp. Biol.* 212, 1716–1730. doi: 10.1242/jeb.024851

Weihrauch, D., Ziegler, A., Siebers, D., and Towle, D. W. (2002). Active ammonia excretion across the gills of the green shore crab *Carcinus maenas*: participation of Na+/K+-ATPase, V-type H+-ATPase and functional microtubules. *J. Exp. Biol.* 205, 2765–2775. doi: 10.1242/jeb.205.18.2765

Wood, C. M. (1993). "Ammonia and urea metabolism and excretion," in *The Physiology of Fishes*, ed. D. H. Evans (Boca Raton: CRC Press), 379–425.

Xie, Z. Z., Liu, Y., and Bian, J. S. (2016). Hydrogen sulfide and cellular redox homeostasis. *Oxid. Med. Cell. Longev.* 2016:6043038. doi: 10.1155/2016/6043038

Xu, Y. (2003). Regulation of p53 responses by post-translational modifications. *Cell. Death Differ.* 10, 400–403. doi: 10.1038/sj.cdd.4401182

You, G., Smith, C. P., Kanai, Y., Lee, W. S., Stelzner, M., and Hediger, M. A. (1993). Cloning and characterization of the vasopressin-regulated urea transporter. *Nature* 365, 844–847. doi: 10.1038/365844a0

Zhang, T., Yan, Z., Zheng, X., Wang, S., Fan, J., and Liu, Z. (2020). Effects of acute ammonia toxicity on oxidative stress, DNA damage and apoptosis in digestive gland and gill of Asian clam (*Corbicula fluminea*). *Fish Shellfish Immunol.* 99, 514–525. doi: 10.1016/j.fsi.2020.02.046

Zhang, W., Jiang, Q., Liu, X., Pan, D., Yang, Y., and Yang, J. (2015). The effects of acute ammonia exposure on the immune response of juvenile freshwater prawn, *Macrobrachium nipponense*. *J. Crustacean. Biol.* 35, 76–80. doi: 10.1163/1937240X-00002292

Zhang, W., Li, J., Chen, Y., Si, Q., Tian, J., Jiang, Q., et al. (2019). Exposure time relevance of response to nitrite exposure: insight from transcriptional responses of immune and antioxidant defense in the crayfish, *Procambarus clarkii*. *Aquat. Toxicol.* 214:105262. doi: 10.1016/j.aquatox.2019.105262

Zhang, X., Pan, L., Wei, C., Tong, R., Li, Y., Ding, M., et al. (2020). Crustacean hyperglycemic hormone (CHH) regulates the ammonia excretion and metabolism in white shrimp, *Litopenaeus vannamei* under ammonia-N stress. *Sci. Total Environ.* 723:138128. doi: 10.1016/j.scitotenv.2020.138128

Zhao, M., Yao, D., Li, S., Zhang, Y., and Aweya, J. J. (2020). Effects of ammonia on shrimp physiology and immunity: a review. *Rev. Aquacult.* 12, 2194–2211. doi: 10.1111/raq.12429

Conflict of Interest: The authors declare that the research was conducted in the absence of any commercial or financial relationships that could be construed as a potential conflict of interest.

Publisher's Note: All claims expressed in this article are solely those of the authors and do not necessarily represent those of their affiliated organizations, or those of the publisher, the editors and the reviewers. Any product that may be evaluated in this article, or claim that may be made by its manufacturer, is not guaranteed or endorsed by the publisher.

frontiers in Marine Science

REVIEW
published: 14 January 2022
doi: 10.3389/fmars.2021.809759

Emerging Diseases and Epizootics in Crabs Under Cultivation

*Christopher J. Coates**† and Andrew F. Rowley**†

Department of Biosciences, Faculty of Science and Engineering, Swansea University, Swansea, United Kingdom

While most crab production for human consumption worldwide comes from capture fisheries, there is increasing production of selected species using aquaculture-based methods. This is both for the purpose of stock replacement and direct yield for human consumption. Disease has limited the ability to produce larval crabs in commercial hatcheries and this together with suitable feeds, are major hurdles in the sustainable development of cultivation methods. Juvenile and adult crabs are also subject to a range of diseases that can cause severe economic loss. Emerging pathogens/parasites are of major importance to crab aquaculture as they can cause high levels of mortality and are difficult to control. Diseases caused by viruses and bacteria receive considerable attention but the dinoflagellate parasites, *Hematodinium* spp., also warrant concern because of their wide host range and lack of control methods to limit their spread. This concise review examines the emerging diseases in several crabs that have been selected as candidates for aquaculture efforts including Chinese mitten crabs (*Eriocheir sinensis*), mud crabs (*Scylla* spp.), swimming crabs (*Portunus* spp.), blue crabs (*Callinectes sapidus*) and shore crabs (*Carcinus maenas*). The latter is also a prolific invasive species known to harbour diverse macro- and micro-parasites that can affect commercially important bivalves and crustaceans.

Keywords: *Hematodinium* spp., vibriosis, mud crabs, Chinese mitten crabs, *Portunus* spp., *Callinectes sapidus*, reoviruses, *Scylla* spp.

OPEN ACCESS

Edited by:
Yangfang Ye,
Ningbo University, China

Reviewed by:
Carlos Rosas,
National Autonomous University of Mexico, Mexico
Meng Li,
Key Laboratory of Marine Ecology and Environmental Sciences, Institute of Oceanology, Chinese Academy of Sciences (CAS), China

***Correspondence:**
Christopher J. Coates
c.j.coates@swansea.ac.uk
Andrew F. Rowley
a.f.rowley@swansea.ac.uk

†These authors have contributed equally to this work

Specialty section:
This article was submitted to Marine Fisheries, Aquaculture and Living Resources, a section of the journal Frontiers in Marine Science

Received: *05 November 2021*
Accepted: *14 December 2021*
Published: *14 January 2022*

Citation:
Coates CJ and Rowley AF (2022) Emerging Diseases and Epizootics in Crabs Under Cultivation. Front. Mar. Sci. 8:809759. doi: 10.3389/fmars.2021.809759

INTRODUCTION

The infraorder Brachyura contains over 7,000 species of true crabs making them one of the largest groups within the sub-phylum Crustacea. These crabs are found in marine, brackish and fresh waters with some species adapted to life in terrestrial habitats. The derivation of the term Brachyura literally means short-tail as during the larval stage the abdomen becomes reduced and folded underneath the developing crab—a process termed brachyurization (Cui et al., 2021).

Capture fisheries of brachyurans contribute substantially to food production globally as these have high protein, low saturated fat and micronutrients not abundant in diets based on the consumption of terrestrial animals (Azra et al., 2021; Golden et al., 2021). The gazami crab, *Portunus trituberculatus* is the most widely fished crab worldwide with landings in the Indo-Pacific region of over 500,000 t in 2015 (Stevens and Miller, 2020). In northern Europe, the edible or brown crab (*Cancer pagurus*) fishery, although much smaller in tonnage landed, has an annual production of over 45,000 t (valued at >€50 million per annum to Ireland and the United Kingdom markets; Johnson et al., 2016). Similarly, Tanner (*Chionoecetes bairdi*) and snow crabs (*C. opilio*) in Alaskan and Canadian fisheries have yielded *ca.* 90,00 and 147,000 t p.a., respectively, in recent

years (Stevens and Miller, 2020). However, some of these and other fisheries are now unsustainable due to overfishing and environmental changes (e.g., Mullowney and Baker, 2020), and may not be sufficient to feed the rising global population (Costello et al., 2020; Foehlich et al., 2021). To address the limitations of capture fishing, aquaculture-based cultivation can provide larval-juvenile crabs for restocking purposes (e.g., Le Vay et al., 2008) and/or for producing marketable sized animals for human consumption. As many species of crabs have lengthy life history (developmental) cycles lasting several years, this makes it problematic to grow these through to a market size. Hence, those crabs with high market value and with rapid growth are more likely to be candidates for aquaculture-based cultivation.

Portunid crabs belonging to the family Portunidae are a large group of over 700 species including a few fast-growing crabs and some with high market value because of their taste and consistency of meat content. These "swimming crabs" often have large paddle-like limbs that facilitate their locomotory behaviour. As well as capture fisheries, there is also a market for soft-shell swimming crabs (i.e., post-moult individuals) as these attract a higher price and several short-term holding methods have been developed taking pre-moult crabs from the fishery, holding these in various water systems, and waiting for these to moult (Hungria et al., 2017). Crabs including *Callinectes sapidus*, *Scylla* spp. and *Portunus* spp. are sold as soft-shell crabs (Tavares et al., 2018).

The Chinese mitten crab, *Eriocheir sinensis* has a long history of cultivation stretching back to the 1960s when declines in wild caught crabs in China due to overfishing and obstructive engineering of waterways, triggered initial developments in hatchery techniques (Cheng et al., 2018). As a result of improved hatchery rearing methods, large scale production has become possible and the annual returns of mitten crabs in China rose from 17,500 t in 1993 to 796,535 t in 2014 (Cheng et al., 2018). By 2018, 8% of global crustacean aquaculture production was mitten crabs behind whiteleg shrimp, *Penaeus vannamei* and red swamp crayfish, *Procambarus clarkii* at 53 and 18%, respectively (FAO, 2020).

Disease is a key problem in aquaculture regardless of the type of production or the species targeted. For instance, major obstacles to larval production in hatcheries include diseases caused by opportunistic pathogens, such as vibrios (Sui et al., 2011; Zhang et al., 2014), a lack of knowledge of suitable diets (e.g., Holme et al., 2008; Waiho et al., 2018; Basford et al., 2021) and the cannibalistic behaviour of some crab species (Romano and Zeng, 2017). High stocking densities, poor water quality and other environmental parameters/stressors (e.g., temperature) can tip the balance in favour of the pathogen resulting in disease outbreaks (Coates and Söderhäll, 2021). Emerging diseases–usually defined as diseases that are new or are increasing in prevalence in new areas–can often appear when species are cultivated or moved into new geographical locations. These can cause high mortalities and appear in cycles or episodic events. Shellfish aquaculture (notably penaeid shrimp) are subject to "boom and bust" cycles in which disease–linked to inbreeding depression–is considered the major proximal cause in the "busted" industry (You and Hedgecock, 2019).

In this text we provide a succinct overview of the main diseases that threaten the establishment of crab aquaculture worldwide. We focus on several key species including the Chinese mitten crab (*E. sinensis*), mud crabs (*Scylla* spp.), swimming crabs (*Portunus* spp.), the Atlantic blue crab (*C. sapidus*), and the European shore crab (*Carcinus maenas*).

CHINESE MITTEN CRABS, *Eriocheir sinensis*

The mitten crab, *E. sinensis*, so-called because the males' hairy outgrowths on its claws resembling mittens, is native to East Asia. It lives in fresh water but moves into estuarine–coastal areas to breed. *E. sinensis* is a highly invasive crab and has spread into North America and Northern Europe where it can cause environmental damage because of its burrowing behaviour leaving riverbanks unstable. In the United Kingdom, it was first seen in the River Thames in 1935 (Ingle, 1986) with numbers increasing dramatically in the 1990s in several rivers throughout England (Clark et al., 1998; Herborg et al., 2005). Aquaculture production of this crab in China is important where it is viewed as a delicacy steamed with ginger and vinegar, and hence it has a high commercial value. Since the 1980's there has been a dramatic increase in hatchery production in China to 9 billion megalopa larvae by 2005 (Sui et al., 2011). In the first year, juvenile crabs are grown in ponds often in polyculture conditions. The grow out phase in year 2 brings them to market size often in ponds, lakes, pens, and paddy fields (Cheng et al., 2018).

Chinese mitten crabs under high stocking density culture conditions are subject to a range of diseases that have been found to cause high levels of mortality and hence production loss. These include white spot, tremor disease, hepatopancreatic necrosis disease, and milky disease (**Table 1**). White spot is a serious condition of shrimp that has decimated their production over the last few decades (Dhar et al., 2022). It is caused by a virus, the white spot syndrome virus, mainly found to affect shrimp production. An epidemic of this disease was reported in China by Ding et al. (2015) with high mortality. Tremor disease, a serious condition of cultured Chinese mitten crabs, was originally thought to be caused by rickettsia-like organisms (RLOs; Wang and Gu, 2002) but the infectious agent was later identified as a novel species of *Spiroplasma*, *S. eriocheiris* (Wang et al., 2011). It mainly occurs from May to October and causes high levels of mortality, but this bacterial disease can be treated with oxytetracycline (Liang et al., 2009). A further condition, termed hepatopancreatic necrosis disease is characterised by lesion development in the hepatopancreas, reduction in feeding activity and subsequent death (Ding et al., 2016, 2018). According to Ding et al. (2016), it is caused by the microsporidian parasite *Hepatospora eriocheir*, and interestingly, the first report of this disease was not in crabs in culture but in invasive crabs caught in the Thames estuary (Stentiford et al., 2011) implying both its wide geographical presence and as a potential biological control of these animals. Bateman et al. (2016) believe that *Hepatospora* spp., most likely belonging to the same species (*eriocheiris*) may be widespread in several species of crabs including edible crabs

TABLE 1 | Key diseases of Chinese mitten crabs, *Eriocheir sinensis* in cultivation.

Disease	Source	Causative agent	Mortality (%)	Pathology	References
White spot	China	Viral, White spot syndrome virus	80–100	Acute viral disease, virus multiplies in haemolymph and hindgut wall cells	Ding et al., 2015, 2017
Tremor disease	China	Bacterial, *Spiroplasma eriocheiris*	30–90	Tremors, lethargy, loss of appetite. Infection spread by haemocytes in which they multiply intracellularly, to nervous, muscular and connective tissue	Wang and Gu, 2002; Wang et al., 2004, 2011
Hepatopancreatic necrosis disease	(1). FW pond culture, China	Microsporidian, *Hepatospora eriocheir* (1, 2) or a non-infectious disease (3)	40–50	Reduction in locomotory behaviour, white focal patches in hepatopancreas, muscle necrosis	Ding et al., 2016
	(2). River Thames, United Kingdom (wild)		N/A		Stentiford et al., 2011
	(3). Aquarium-based experiment		?		Shen G. et al., 2021
Milky disease	Northern China	Fungal, *Metschnikowia bicuspidata*	>20	White haemolymph with reduced clotting, white muscle, leg loss	Bao et al., 2021; Ma et al., 2021

(*C. pagurus*) and parasitic pea crabs (*Pinnotheres pisum*). There is still some debate, however, on the aetiology of hepatopancreatic necrosis disease as some consider it to be an example of a non-infectious disease probably caused by environmental residues including insecticides (Shen G. et al., 2021) and meta-transcriptomic analyses suggest that environmental factors may result in microbial dysbiosis in the hepatopancreas leading to disease (Shen Z. et al., 2021).

Non-native *E. sinensis* found in Holland have been shown to harbour the serious oomycete pathogen, *Aphanomyces astaci*, the causative agent of the crayfish plague (Tilmans et al., 2014). To our knowledge, there have been no published reports of infection in *E. sinensis* under cultivation caused by *Hematodinium* spp. which are common disease-causing agents of many species of decapods (Stentiford and Shields, 2005; Small, 2012). It is probable that its presence in fresh water rather than more haline conditions results in this lack of infection as infective dinospores of *Hematodinium* spp. do not survive low salinity conditions (Coffey et al., 2012). However, *Hematodinium* sp. has been observed in invasive *E. sinensis* in the River Thames in the United Kingdom (Kerr and Bateman personal communication, December 2021) showing that they are vulnerable to infection presumably depending on environmental salinity levels.

MUD CRABS (MANGROVE CRABS) *Scylla* spp.

There are four species of mud crabs that are important in food production. These include the Indo-Pacific swamp crab (mangrove crab), *Scylla serrata* found in Southeast Africa, India, China, Indonesia, Thailand, and Northeast Australia, and *S. olivacea*, *S. paramamosain*, and *S. tranquebarica*. The identification of these four species can be difficult (Keenan et al., 1998) and hence some fisheries data and reports of diseases for particular species may be inaccurate (FishStat, Li et al., 2018; FAO, 2020). The form of mud crab cultivation ranges from simple fattening and grow on using crabs/crablets collected from the wild through to larval hatchery production and subsequent grow on in ponds using monoculture and/or polyculture approaches (see Shelley and Lovatelli, 2011; Waiho et al., 2018; Syafaat et al., 2021a for reviews of culture methods). Around 95% of aquaculture production of *Scylla* spp. relies on wild caught crabs (Stevens and Miller, 2020). Growth rates for mud crabs are high meaning they can be brought to market quickly and they have a good market value usually as live crabs (Paterson and Mann, 2011). Global aquaculture production of mud crabs rose to 89,390 t in 2016 (FishStat). By 2019, cultivation of *S. serrata* in Viet Nam, Indonesia and the Philippines reached 71,757, 39,900, and 20,772 t, respectively (OECD.stat). In southeast China, where mud crab cultivation is also of importance, unpublished data reported in Liu et al. (2011) revealed a loss of production due to disease in 2006 of *ca*. 14% worth an estimated US$ 32 million.

Because of the active culture of mud crabs in several countries including Bangladesh, China, Indonesia, The Philippines, Thailand and Viet Nam, several disease conditions have been reported and the causative agents fully characterised. **Table 2** presents some of the main diseases found in *S. serrata* and *S. paramamosain* during cultivation–restricted to diseases where the causative agents have been identified. The reader should note that other disease conditions including those probably caused by bacteria (e.g., shell disease syndrome, red sternum syndrome) and protistans (e.g., egg infestation caused by *Haliphthoros*-like oomycete; Leaño, 2002) have been described (see Shelley and Lovatelli, 2011 and Santhanam, 2018 for reviews of these). For example, red sternum disease of *S. serrata* from crab farms in Thailand is associated with several morphotypes of bacteria seen in the tissues yet no definite causative agent has been elucidated (Areekijseree et al., 2010). The characteristics of this disease include progressive reddening of the ventral carapace and cloudiness of the haemolymph (probably caused by sepsis). Similarly, there are reports of cuticular abnormalities classified within the collective group of diseases termed shell disease syndrome, that may have a bacterial aetiology. Both

of these are probably dysbiotic conditions where adverse environmental states cause changes in the cuticular (shell disease) and haemolymph (red sternum syndrome) microbiomes resulting in lesion development and septicaemia. Such diseases are unlikely to conform with Koch's postulates and so their cause(s) remain uncertain.

Viral diseases are prominent in mud crab cultivation and several of these have been identified in crab farms in China (**Table 2**). The three main viral conditions of current importance and associated with sleeping disease are caused by a reovirus, mud crab reovirus (MCRV), a dicistrovirus, mud crab dicistrovirus (MCDV) and finally a mud crab tombus-like virus (MCTV) as a co-infection with other reoviruses. The first of these, MCRV, a double stranded RNA virus, was first described in China in farms in 2007 (Weng et al., 2007) infecting *Scylla* sp. (*S. paramamosain*?) from a farm in Zhuhai, China experiencing sleeping disease. Viruses were found in the cytoplasm of unidentified connective tissue cells within the hepatopancreas and experimental infection of crabs either by injection or bath exposure with infected tissues caused 100% mortality (Weng et al., 2007). The second of these viruses associated with sleeping sickness is MCDV (=MCDV-1), a single stranded RNA containing dicistrovirus that also causes high mortality in mud crabs under cultivation (Zhang et al., 2011). This is distinct to the other viruses that infect mud crabs. Finally, mud crabs appear to be susceptible to infection by white spot syndrome virus, a well-known pathogen of penaeids. The virus can be found in several tissues of *S. serrata* but replication appears to mainly occur in the epithelial cells below the cuticle in the gill (Liu et al., 2009). Mud crabs may contract the virus by spillover from viraemic shrimp.

Several bacterial diseases of *Scylla* spp. have been reported (**Table 2**) including a recent report of a chitinolytic bacterium, *Aquimarina hainanensis* that caused high mortality in larvae in a crab hatchery (Midorikawa et al., 2020). It is closely related to other crustacean pathogens, such as *Aquimarina penaei*. This bacterium is also highly pathogenic to larvae of other crustaceans including *P. trituberculatus*, yet its virulence mechanisms remain unexplored. A second bacterial infection has been attributed to *Photobacterium damselae* subsp. *damselae,* also found to be highly pathogenic in many species of marine fishes and cetaceans (Rivas et al., 2013). Moreover, strains of this zoonotic bacterium can cause necrotising fasciitis in humans.

SWIMMING CRABS *Portunus pelagicus* (BLUE SWIMMING CRABS, BLUE SWIMMER CRABS) AND *Portunus trituberculatus* (THE GAZAMI CRAB, THE HORSE CRAB, JAPANESE BLUE CRAB)

Swimming crabs belonging to the genus *Portunus* are important commercial species in both fisheries and aquaculture. *Portunus pelagicus* is recognised as a species complex consisting of *P. pelagicus*, *P. reticulatus*, *P. segnis* and *P. armatus* that are morphologically, genetically, and geographically distinct (Lai et al., 2010). The two commercially important species of this group include *P. armatus* that is distributed in Australia and New Caledonia while *P. pelagicus* is mainly found in the West Pacific Ocean. World production of *P. pelagicus* was 265,869 and 29 t by capture fisheries and aquaculture, respectively, in 2016

TABLE 2 | Key diseases of mud crabs (*Scylla serrata* and *S. paramamosain*) in cultivation.

Disease	Source	Causative agent	Mortality (%)	Pathology	References
Sleeping sickness	Guangdong Province, China	Viral, mud crab reovirus (MCRV)	80–100 (in infection trials)	Sluggish behaviour, loss of feeding, atrophy of hepatopancreas, empty intestine, and yellow gills	Weng et al., 2007; Huang et al., 2012
"	*S. paramamosain*, Zhuhai, Guangdong Province, China	Viral, mud crab dicistrovirus (MCDV)	100 by 7 days (in infection trials)	Viral multiplication in most tissues	Zhang et al., 2011; Guo et al., 2013
"	*S. paramamosain*, Guangdong Province, China	Viral, mud crab tombus-like virus (MCTV)	?	Co-infection with other reoviruses	Gao et al., 2019
White spot	Zhejiang Province, China	Viral, WSSV	34	Epithelial cells of gills, cuticle infected	Liu et al., 2009, 2011
Vibriosis	*S. paramamosain*, China	Bacterial, *Vibrio parahaemolyticus*	?		Xie et al., 2021a
–	*S. paramamosain,* Zhejiang Province, China	Bacterial, *Photobacterium damselae* subsp. *damselae*	20	Lethargy, lack of feeding behaviour, darkened gills, pale hepatopancreas, muscle necrosis	Xie et al., 2021b
–	*S. serrata* larvae in hatchery in Ishigaki Island, Japan	Bacterial, *Aquimarina hainanensis*	Mass mortality	Tissue necrosis with accompanying melanisation	Dan and Hamasaki, 2015; Midorikawa et al., 2020
Milky disease	*S. serrata* in Guangdong Province, China	Dinoflagellate, *Hematodinium* sp.	Acute epizootics	Cooked appearance, lethargy, milky haemolymph, atrophy of epithelial cells in hepatopancreas, coagulative necrosis in heart	Li et al., 2008

TABLE 3 | Key diseases of *Portunus trituberculatus* in cultivation.

Disease	Source	Causative agent	Mortality (%)	Pathology	References
Vibriosis	China	Bacterial, *Vibrio alginolyticus*	?	–	Liu et al., 2007
Vibriosis	Megalopa in commercial hatchery, China	*Vibrio harveyi*	Not given, described as "mass mortality"	"weak," pale red bodies	Zhang et al., 2014
Vibriosis	Jiansgu Province, China	*Vibrio metschnikovii*	30–40	Lethargy, disturbed swimming movement, dark pigmentation in carapace, turbid haemolymph	Wan et al., 2011
Vibriosis	Juvenile crabs from Jiansgu Province, China	*Vibrio natriegens*	>85%	Lethargy, decreased feeding	Bi et al., 2016
Microsporidiosis (toothpaste crab disease)	Jiangsu Province, China	Microsporidian, *Ameson portunus*	?	Chalky white muscle, toothpaste appearance, numerous spores found in muscle	Wang Y. et al., 2017
–	Zhejiang Province, China	Ciliate, *Mesanophrys* sp.	>80	Slow swimming, reduced food intake, ciliates found in haemolymph, gills, hepatopancreas and muscle	Liu et al., 2020; Perveen et al., 2021
–	Polyculture in Qingdao, Shandong Province, China	Dinoflagellate, *Hematodinium perezi*	>90	Trophont stages develop in a range of tissues including muscle, haemolymph and gills	Wang J.F. et al., 2017; Huang et al., 2021

(FAO, 2020). The gazami crab, *P. trituberculatus* is found along the Eastern coast of India, Japan, the South China Sea through to Australia. Global captive production in 2016 was 557,728 t (FAO FishStat; FAO, 2020) making it the most widely fished species of crab in the world. Depletion of localised crab stocks in some regions has resulted in aquaculture-based production designed to facilitate stock enhancement, restoration, and restocking, as well as human consumption. Cultivation methods are diverse as already described for mud crab aquaculture. Attempts to produce *P. pelagicus* in suspended net cages in Indonesia in a mixed polyculture system is a promising development (Kasmawati et al., 2020).

Vibriosis is an important disease of portunid crabs in cultivation. Various species of vibrios have been linked to disease including. *V. alginolyticus*, *V. harveyi*, V. *metschnikovii, V. natriegens,* and *V. parahaemolyticus* (**Table 3**). Crabs can become infected both in hatcheries during their larval phases as well as in later cultivation as juveniles/adults. Such diseases can cause high levels of mortality. Poor water quality and a lack of temperature control are likely to be contributory factors in such diseases.

A key pathogen of *P. trituberculatus* in China is *Hematodinium perezi* causing significant disease outbreaks in polyculture raised crabs with subsequent loss of production (Li et al., 2013, 2021; Wang J.F. et al., 2017; Huang et al., 2021). Infections peak during summer months when the environmental temperature is high (>30°C). There is evidence that wild mud crabs, *Helice tientsinensis* in the vicinity of rearing areas for *P. trituberculatus* may be sinks/reservoirs for the parasite (Huang et al., 2021).

Of further note is the finding that *P. trituberculatus* is also a host for a variant of the Wenzhou shark flavivirus (Parry and Asgari, 2019)—indicating horizontal transfer of the virus from crabs to sharks or *vice versa*. While there is evidence of a host response to the multiplication of the virus in crab tissues, no pathology is currently available and so its importance as a driver of crab mortality both in the wild and in cultivation is unknown.

Moult death syndrome is a commonly observed phenomenon in several crustaceans including *P. pelagicus*. This fatal condition is characterised by animals in moult becoming trapped inside their old exoskeleton (i.e., dysecdysis). While the causes(s) of this is/are unclear, nutritional deficiency is a potential contributory factor and recent work has found that adding cholesterol to formulated diets significantly reduces this (Noordin et al., 2020).

BLUE CRABS *Callinectes sapidus*

The Atlantic blue crab, *C. sapidus*, has a wide range running along the Atlantic coast from Nova Scotia in the north to Argentina in the south. It is fished commercially and recreationally in many locations, e.g., Chesapeake Bay region and the Gulf of Mexico. In the former area, winter dredge surveys have been used to estimate crab abundance and these data have shown a general reduction in stock from over 800 million crabs in 1993 to *ca*. 260 million by 2007 but with yearly variances. Following conservation measures, by 2020 an estimated abundance of 405 million individuals of all ages was reported (Chesapeake Bay Blue Crab Advisory Report).[1] Commercial production of soft-shell blue crabs in the United States has taken place for nearly two centuries (Tavares et al., 2018) making it one of the oldest forms of aquaculture in North America. There are two main production systems namely open (flow through)–reliant on local water supplies and with no control of environmental variables, and closed systems based on

[1]https://www.fisheries.noaa.gov/species/blue-crab

recirculating technology. Closed systems offer better biosecurity and crabs have improved survival rates (Spitznagel et al., 2019). For example, peeler blue crab mortality in a commercial flow through system was found to be 33%, while in a recirculating system it was less than half, 16% (Spitznagel et al., 2019).

There is an extensive literature on the diseases of *C. sapidus* particularly in the Chesapeake Bay region of the United States that supports a large fishery (Jesse et al., 2021). Diseases include those caused by viruses (Johnson and Bodammer, 1975; Johnson and Lightner, 1988), bacteria (Krantz et al., 1969; Messick, 1998; Sullivan and Neigel, 2018), the parasitic dinoflagellate *Hematodinium perezi* (Messick and Shields, 2000; Huchin-Mian et al., 2017), various protistans, trematodes and ribbon worms (Messick, 1998; Shields, 2022). Because holding of crabs in soft-shell production facilities is short term (>14 days) there is little time for them to become infected with new parasites and pathogens and hence diseases come from pre-existing conditions gained in the wild. The process of moulting is recognised as stressful to crustaceans in general (due to the major physiological expense) and this together with capture and handling stress, can result in mortality. It is probable that some of the deaths recorded in such facilities may be linked to infectious or non-infectious diseases. In a small survey of diseases encountered at a shedding facility in Louisiana, United States, the authors found tissue infestations by the commensal gill ciliate, *Lagenophrys callinectes*, *H. perezi* (by PCR alone), vibrios in haemolymph, reoviruses, the microsporidian, *Ameson michaelis* and shell disease (Rogers et al., 2015). They concluded that crab mortality seen in the facility could not be attributed with any certainty to any of these potential parasites and pathogens alone. More recently, there has been a great deal of emphasis placed on viral diseases in blue crab shedding facilities as these may be drivers of mortality (Spitznagel et al., 2019). Johnson (1977) was the first to record a novel viral disease in blue crabs that she observed mainly developing in the circulating haemocytes and in haematopoietic tissue but also in epithelial cells and the gill. This virus was originally referred to as reo-like virus (RLV) but later given the name *C. sapidus* reovirus 1 (CsRV1; Bowers et al., 2010; Flowers et al., 2016a,b). CsRV1 is like some other reoviruses in brachyuran crabs including *S. serrata, E. sinensis* and *P. trituberculatus* (Flowers et al., 2016b; Zhao et al., 2021). CsRV1 has been reported in *ca*. 20% of capture fished *C. sapidus* (Flowers et al., 2016a) and at a variable prevalence across its host's geographic range from Northeast Atlantic through to Uruguay (Zhao et al., 2020). High CsRV1 loads in shedding facilities are associated with high crab mortality. For instance, infection by this virus is a significant predictor of mortality of pre-moult crabs and viral loads are highest in those crabs that die in these facilities (Spitznagel et al., 2019). The heightened presence of CsRV1 in crabs collected close to shedding plants (Flowers et al., 2018) may also suggest release of the virus from such areas and the authors considered that the potential practice of discarding dead crabs from such facilities may be a factor in these higher levels of infection. Finally, crabs held in recirculating systems, which also have enhanced biosecurity potential, have fewer diseases than those in flow through systems (Spitznagel et al., 2019).

SHORE CRABS (EUROPEAN SHORE CRAB, GREEN CRAB, EUROPEAN GREEN CRAB) *Carcinus maenas*

The European shore crab is an iconic inhabitant of the intertidal zone in northern European shores often found in rock pools to the delight of generations of children "crabbing" with nets and buckets. Its native range is from northern Africa in the south through to Iceland and Norway in the north. *C. maenas* is a hardy crab capable of withstanding changes in salinity, and tolerant to perturbations in temperature and oxygenation (Young and Elliott, 2020). Over the last two centuries it has become established in North America, Australia, and South America. In many of these regions it is considered a pest species damaging native fisheries (e.g., Cohen et al., 1995; Grosholz et al., 2000; Walton et al., 2002). Shore crabs are of limited commercial value as food both in their native and non-native environments although projects have expounded its culinary use in non-native areas as a way of controlling its population (Parks and Thanh, 2019). One important use of shore crabs is as a bait where soft post-moult crabs from pre-moult peelers are highly prized by recreational fishers targeting bass and cod.[2] There have been pilot projects in the United Kingdom to determine the feasibility of collecting shore crabs from the wild and growing these on in flow through systems to produce soft crabs for the bait industry but, to our knowledge, none are currently in active commercial production.

There is a plethora of reports of diseases in shore crabs both in their native (Stentiford and Feist, 2005; Edwards et al., 2019; Davies et al., 2020a,b) and non-native (Goddard et al., 2005; Bojko et al., 2017, 2018; Blakeslee et al., 2020; Frizzera et al., 2021) ranges (**Figure 1**). Disease causing agents include viruses (Bojko et al., 2019; Bateman et al., 2021), bacteria (Spindler-Barth, 1976; Eddy et al., 2007), fungi (Davies et al., 2020a), microsporidians (Bojko et al., 2017), dinoflagellates (Chatton and Poisson, 1931; Stentiford and Feist, 2005; Hamilton et al., 2007, 2009; Davies et al., 2019), haplosporidians (Davies et al., 2020b), nematodes (Stentiford and Feist, 2005), acanthocephalans (Zetlmeisl et al., 2011), digeneans (Stentiford and Feist, 2005; Zetlmeisl et al., 2011; Blakeslee et al., 2015, 2020), and parasitic barnacles, *Sacculina carcini* (Mouritsen and Jensen, 2006; Powell and Rowley, 2008; Lützen et al., 2018; Mouritsen et al., 2018; Rowley et al., 2020). The extensive literature makes shore crabs one of the most highly studied decapods in terms of disease prevalence. In a recent survey of shore crab diseases in South Wales, United Kingdom a key endemic condition was found to be caused by the parasitic dinoflagellate, *Hematodinium* sp. with an overall prevalence of *ca*. 14% (Davies et al., 2019). Other disease conditions included those caused by two novel species of haplosporidians (Davies et al., 2020b) and *S. carcini* (Rowley et al., 2020) but these were of lower prevalence and hence of less importance within crab populations.

Eddy et al. (2007) examined a novel disease of shore crabs in a pilot plant designed to grow on wild caught animals

[2]https://britishseafishing.co.uk/peeler-crab/

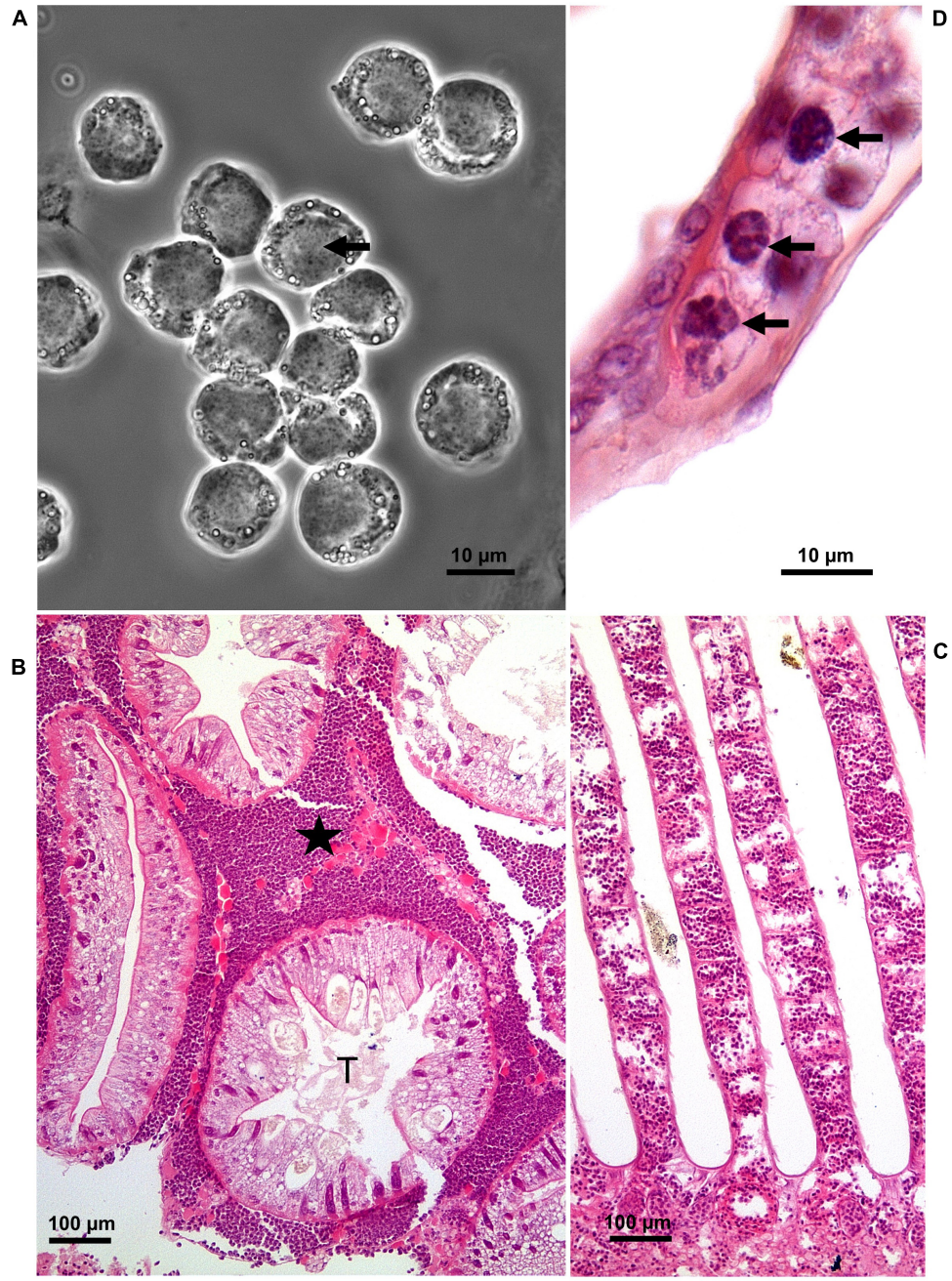

FIGURE 1 | *Hematodinium* infection of shore crab, *Carcinus maenas*. **(A)** Phase contrast micrograph of haemolymph replete with trophont stages of *Hematodinium* sp. The nuclei contain chromatin with a granular appearance (arrow) and the cytoplasm has many phase-bright droplets. **(B)** Histological section of hepatopancreas from a crab with a high severity infection. The interstitial spaces between the tubules (T) are swollen and replete with *Hematodinium* parasites (*). **(C)** Section through the gill region of a heavily infected crab with numerous *Hematodinium* parasites in the lumen of swollen gill filaments. **(D)** High power micrograph of a histological section of gills showing the appearance of *Hematodinium* parasites with highly characteristic chromatin (arrows). Panels **(B–D)** are histological sections stained with haematoxylin and eosin.

for the bait market. They found that during the summer months with high water temperatures (>25°C) that over 20% of crabs developed a condition that they described as "milky disease" as the haemolymph (blood) was milk colour. The cause of this was found to be a previously undescribed α-proteobacterium related to the order Rhodobacteriales that resulted in septicaemia. This disease has also been reported at low prevalence in wild caught shore crabs (Eddy et al., 2007; Bojko et al., 2018) but was absent in a recent (2018–2019) large survey of shore crabs (∼1,200) from two locations in

South Wales, United Kingdom (unpublished observations by the authors).

COMMON PATHOGENS AND THEIR GLOBAL RISK TO CRAB CULTURE

While there are many common pathogens and parasites that can adversely affect crab production worldwide, the dinoflagellate parasites, *Hematodinium* spp. are perhaps some of the most notable. These parasites are host generalists in that they can infect a wide range of decapods worldwide and are endemic in several populations (Small, 2012; Shields, 2022). In some cases, such as velvet swimming crabs, *Necora puber* in France (Wilhelm and Mialhe, 1996) and snow crabs, *Chionoecetes opilio* in North America (Shields et al., 2005, 2007) they have caused epidemics that adversely affected fisheries. Furthermore, as already described, *H. perezi* infections of *P. trituberculatus* in China, have resulted in economic loss (Li et al., 2013; Wang J.F. et al., 2017) showing that these parasites are important in both fishery and aquaculture production of crabs. The life cycle of *Hematodinium* spp. is thought not to involve reservoirs and carriers outside the Decapoda. Motile dinospores are released from infected crabs as a cloud of infective stages and these penetrate susceptible animals resulting in infection that is localised in tissues including the haemolymph, hepatopancreas, gills and muscle (**Figure 1**; Stentiford and Shields, 2005; Shields, 2022). Ultimately, the trophont stage of parasites develop in the haemolymph with a concomitant decline in haemocyte number and the heavily affected animals become metabolically "exhausted" as the parasites utilise the host's resources (Stentiford et al., 2001; Shields et al., 2003). The timescale of initial infection through to death of the host varies from days to nearly a year and this is determined by a combination of the host species, the strain of parasite and the environmental conditions–especially the water temperature (see Smith and Rowley, 2015 for an overview). Apart from improvements in biosecurity, there are no prophylactic approaches available to control this infection.

Viral infections are common in crabs and an increasing number of pathogenic viruses have been identified in wild and cultured species of crustaceans (Bateman and Stentiford, 2017). Although particular emphasis has been placed on viral diseases of shrimp, a greater understanding of such agents has been achieved in mud crabs, *Scylla* spp. in culture (Weng et al., 2007; Jithendran et al., 2010; Zhang et al., 2011; Huang et al., 2012; Guo et al., 2013; Gao et al., 2019), blue crabs both in capture fisheries and aquaculture systems (Flowers et al., 2016a,b, 2018) and shore crabs, *C. maenas* in the wild (Bojko et al., 2019; Bateman et al., 2021). While the pathology and structure of the disease-causing viruses is often well-studied, the host range, potential reservoirs of disease and the effect of disease on wild populations, is less clear. The control and treatment of viral diseases in crustaceans, as in invertebrates in general, is still in its infancy.

Vibriosis is a common infection of many aquatic invertebrates. However, there are relatively few definitive reports of such infections in crabs either in the wild or under captive cultivation except for *Scylla paramamosain* (**Table 2**) and *Portunus* spp. (**Table 3**). Identification of vibrios down to species level can be difficult requiring additional methods other than just general 16S RNA sequencing (e.g., Nagpal et al., 1998) and so some older reports on the identification of disease-causing vibrios based on biochemical (phenotypic) markers together with these alone can be misleading. Bacteria, including vibrios, remain important disease-causing agents in hatcheries (Valente and Wan, 2021) and together with the development of suitable diets are key challenges in crab cultivation (Dan and Hamasaki, 2015; Azra and Ikhwanuddin, 2016). Zoea and megalopa stages show rapid moulting and immature immune systems leaving them highly susceptible to chance infections. While antimicrobials including antibiotics, are commonly employed to control such diseases, their continued use is not sustainable due to environmental and heightened antibiotic resistance, so alternate strategies need to be explored to control these. Improvement in water quality (pH, nitrogenous wastes, sterility *via* ozonation) and novel therapeutants (e.g., prebiotics, probiotics, immune stimulants, bacteriophages) are all potential strategies for development (Dan and Hamasaki, 2015; Ayisi et al., 2017; Doss et al., 2017; Culot et al., 2019; Valente and Wan, 2021; Rowley, 2022).

Crustaceans, especially those in wild stocks, are subject to parasitisation by macroparasites (e.g., microphallid digeneans and parasitic barnacles) but their importance in limiting production during cultivation is unclear. Removal of crabs from the wild for "fattening" is likely to introduce these conditions into farms but because such diseases have relatively long generation times their effect is probably limited unless they detract from the growth and/or market value of the product. Digenean parasites generally use crabs as their second intermediate hosts with molluscs as the primary intermediate hosts, and both fish and sea birds are the definitive host. Rearing crabs in polyculture systems will undoubtedly lead to infection if the primary intermediate hosts are present. The metacercarial stage of digeneans found in crustaceans may cause mortality by increased predation (e.g., Mouritsen and Jensen, 1997) and parasitic barnacles can limit fecundity in both male and female crabs resulting in losses of wild populations needed for broodstock and larvae for aquaculture-based cultivation (Waiho et al., 2021). Improved biosecurity measures are the only practical approach to limit the potential effects of these macroparasites as disease-free stocks of various crabs are not currently available.

ENVIRONMENTAL FACTORS AND DISEASE

It is well-established that disease outbreaks in both shellfish and fish are often linked to environmental perturbations/stressors. These include changes in (usually elevated) temperature, toxins, such as those from harmful algal blooms, metals, nitrogenous waste products and changes in pH (reviewed by Coates and Söderhäll, 2021). Aquatic animals because of their constant and intimate association with water, are highly vulnerable to such factors that can cause disease and trauma, i.e., non-infectious or sterile inflammation, on their own (Coates, 2022). Temperature is a major driver of disease, and although there is extensive

literature on the mechanisms of how these impact on the host (e.g., Le Moullac and Haffner, 2000), pathogen (e.g., Baker-Austin et al., 2012; Le Roux et al., 2015; Sullivan and Neigel, 2018) and other environmental factors (e.g., Sullivan and Neigel, 2018) the temperature tolerance range for many crabs has not been widely explored and even then laboratory-based experiments may not fully reflect the intricacy of the real environment. Syafaat et al. (2021b) explored the thermal tolerance of early stages of mud crab, *S. paramamosain* in terms of growth, survival, moult frequency and gill health. The optimum temperature for the megalopa stage of these crabs was found to be between 28 and 30°C. Gill health as measured by morphological changes, also showed paler gills at both low (24°C) and high (32°C) temperatures accompanied with changes in the thickness of the gill lamellae. However, how the parameters measured may impact on resistance to microbial disease was not studied. Shields (2019) also compared the thermal range of several species of crustaceans including *C. sapidus* with that of the parasitic dinoflagellate, *H. perezi*. Using the thermal ranges of the host and parasite, he concluded that the parasite could overcome the host defences at the higher margins of the thermal tolerance values resulting in faster multiplication of this parasite to the detriment of host tissues. There is extensive literature on the effect of climate change (largely temperature driven) on vibrios although most refers to human pathogens including *V. cholerae*, *V. parahaemolyticus*, and *V. vulnificus* (e.g., Vezzulli et al., 2013; Baker-Austin et al., 2017). Higher water temperatures generally favour faster growth of most vibrios and the enhanced production of virulence factors (e.g., Kimes et al., 2012; Feng et al., 2016; Lages et al., 2019; López-Cervantes et al., 2021) leaving them more likely to cause disease. It is the combination of temperature-driven immune dysregulation of the host and enhanced microbial growth that results in disease episodes caused by vibrios.

DISEASE SURVEILLANCE AND EMERGING DISEASES OF CRABS

To our knowledge, with the exception of white spot syndrome virus, none of the disease-causing agents currently reviewed here are included in the Aquatic Animal Health Code (2021) of diseases adopted by the OIE, the World Organisation for Animal Health[3] and so their surveillance and reporting may not be widely available in the public domain. Hence, it is difficult, if not impossible, to predict future epizootics of relevance to those species described herein. Improvements in biosecurity are difficult in aquaculture facilities where holding water is in direct contact with the environment and crabs are not from disease-free stocks. While recirculating aquaculture systems (RAS) offer improved biosecurity, they have economic and social needs that leave them as unviable alternatives to some current production approaches. For an overview of disease surveillance of relevance to crab aquaculture, the reader is referred to the excellent review by Bondad-Reantaso et al. (2021).

Overall, a broad lack of temporal data on disease prevalence in crabs subject to cultivation hampers the accurate prediction, and management, of future epizootics, which should be addressed as a matter of urgency.

AUTHOR CONTRIBUTIONS

CC and AR researched, drafted, and edited the manuscript. Both authors contributed to the article and approved the submitted version.

FUNDING

AR and CC were supported by the BBSRC/NERC ARCH-UK network grant (BB/P017215/1).

ACKNOWLEDGMENTS

We thank Rose Kerr and Kelly Bateman of Cefas (Weymouth, United Kingdom) for sharing with us their unpublished observations of *Hematodinium* infections in Chinese mitten crabs.

[3] https://www.oie.int/en/what-we-do/standards/codes-and-manuals/aquatic-code-online-access/?id=169&L=1&htmfilechapitre_diseases_listed.htm

REFERENCES

Areekijseree, M., Chuen-Im, T., and Panyarachun, B. (2010). Characterization of red sternum syndrome in mud crab farms from Thailand. *Biologia* 65, 150–156. doi: 10.2478/s11756-009-0228-y

Ayisi, C. L., Apraku, A., and Afriye, G. (2017). A review of probiotics, prebiotics, and synbiotics in crab: present research, problems and future perspectives. *J. Shellf. Res.* 36, 799–806. doi: 10.2983/035.036.0329

Azra, M. N., and Ikhwanuddin, M. (2016). A review of maturation diets for mud crab genus *Scylla* broodstock: Present research, problems and future perspective. *Saudi. J. Biol. Sci.* 23, 257–267.

Azra, M. N., Okomoda, V. T., Tabatabaei, M., Hassan, M., and Ikhwanuddin, M. (2021). The contributions of shellfish aquaculture to global food security: Assessing its characteristics from a future food perspective. *Front. Mar. Sci.* 8:654897. doi: 10.3389/fmars.2021.654897

Baker-Austin, C., Trinanes, J. A., Taylor, N. G. H., Hartnell, R., Siitonen, A., and Martinez-Urtaza, J. (2012). Emerging *Vibrio* risk at high latitudes in response to ocean warming. *Nat. Clim. Chan.* 3, 73–77. doi: 10.1038/nclimate1628

Baker-Austin, C., Trinanes, J., Gonzalez-Escalona, N., and Martinez-Urtaza, J. (2017). Non-cholera vibrios: The microbial barometer of climate change. *Trends Microbiol.* 25, 76–84. doi: 10.1016/j.tim.2016.09.008

Bao, J., Jiang, H., Shen, H., Xing, Y., Feng, C., Li, X., et al. (2021). First description of milky disease in the Chinese mitten crab *Eriocheir sinensis* caused by the yeast *Metschnikowia bicuspidata*. *Aquaculture* 532:735984. doi: 10.1016/j.aquaculture.2020.735984

Basford, A. J., Makings, N., Mos, B., White, C. A., and Dworjanyn, S. (2021). Greenwater, but not live feed enrichment, promotes development, survival, and growth of larval *Portunus armatus*. *Aquaculture* 534:736331. doi: 10.1016/j.aquaculture.2020.736331

Bateman, K. S., and Stentiford, G. D. (2017). A taxonomic review of viruses infecting crustaceans with an emphasis on wild hosts. *J. Invertebr. Pathol.* 147, 86–110. doi: 10.1016/j.jip.2017.01.010

Bateman, K. S., Wiredu-Boakye, D., Kerr, R., Williams, B. A. P., and Stentiford, G. D. (2016). Single and multi-gene phylogeny of *Hepatospora* (Microsporidia)–a generalist pathogen of farmed and wild crustacean hosts. *Parasitology* 143, 971–982. doi: 10.1017/S0031182016000433

Bateman, K. S., Kerr, R., Stentiford, G. D., Bean, T. P., Hooper, C., Van Eynde, B., et al. (2021). Identification and full characterisation of two novel crustacean infecting members of the family Nudiviridae provides support for two subfamilies. *Viruses* 13:1694. doi: 10.3390/v13091694

Bi, K., Zhang, X., Yan, B., Gao, H., Gao, X., and Sun, J. (2016). Isolation and molecular identification of *Vibrio natriegens* from diseased *Portunus trituberculatus* in China. *J. World Aquacult. Soc.* 47, 854–861.

Blakeslee, A. M. H., Keogh, C. L., Fowler, A. E., and Griffen, B. D. (2015). Assessing the effects of trematode infection on invasive green crabs in eastern North America. *PLoS One* 10:e0128674. doi: 10.1371/journal.pone.0128674

Blakeslee, A. M. H., Barnard, R. B., Matheson, K., and McKenzie, C. H. (2020). Host-switching among crabs: species introduction results in a new target host for native parasites. *Mar. Ecol. Prog. Ser.* 636, 91–106. doi: 10.3354/meps13214

Bojko, J., Clark, F., Bass, D., Dunn, A. M., Stewart-Clark, S., Stebbing, P. D., et al. (2017). *Parahepatospora carcini* n. gen., n. sp., a parasite of invasive *Carcinus maenas* with intermediate features of sporogony between the Enterocytozoon clade and other microsporidia. *J. Invertebr. Pathol.* 143, 124–134. doi: 10.1016/j.jip.2016.12.006

Bojko, J., Stebbing, P. D., Dunn, A. M., Bateman, K. S., Clark, F., Kerr, R. C., et al. (2018). Green crab *Carcinus maenas* symbiont profiles along a North Atlantic invasion route. *Dis. Aquat. Org.* 128, 147–168. doi: 10.3354/dao03216

Bojko, J., Subramaniam, K., Waltzek, T. B., Stentiford, G. D., and Behringer, D. C. (2019). Genomic and developmental characterisation of a novel bunyavirus infecting the crustacean *Carcinus maenas*. *Sci. Rep.* 9, 1–10. doi: 10.1038/s41598-019-49260-4

Bondad-Reantaso, M. G., Fejzic, N., MacKinnon, B., Huchzermeyer, D., Seric-Haracic, S., Mardones, F. O., et al. (2021). A 12-point checklist for surveillance of diseases of aquatic organisms: a novel approach to assist multidisciplinary teams in developing countries. *Rev. Aquacult.* 13, 1469–1487. doi: 10.1111/raq.12530

Bowers, H., Messick, G., Hanif, A., Jagus, R., Carrion, L., Zmora, O., et al. (2010). Physicochemical properties of double-stranded RNA used to discover a reo-like virus from blue crab *Callinectes sapidus*. *Dis. Aquat. Org.* 93, 17–29. doi: 10.3354/dao02280

Clark, P. F., Rainbow, P. S., Robbins, R. S., et al. (1998). The alien Chinese mitten crab, *Eriocheir sinensis* (Crustacea: Decapoda: Brachyura) in the thames catchment. *J. Mar. Biol. Assoc. UK* 78, 1215–1221. doi: 10.1017/s002531540004443x

Chatton, E., and Poisson, R. (1931). Sur l'existence, dans le sang des crabes, de Péridiniens parasites: *Hematodinium perezi* n. g., n. sp. (Syndinidae). *CR Séances Soc. Biol. Paris*. 105, 553–557.

Cheng, Y., Wu, X., and Li, J. (2018). "Chinese mitten crab culture: current status and recent progress towards sustainable development," in *Aquaculture in China: Success Stories and Modern Trends*, eds J.-F. Gui, Q. Tang, Z. Li, J. Liu, and S.S. De Silva (Hoboken: John Wiley and Sons), 197–217.

Coates, C. J. (2022). "Host defences of invertebrates to non-communicable diseases," in *Invertebrate Pathology*, eds A. F. Rowley, C. J. Coates, and M. M. A. Whitten (Oxford: Oxford University Press), 41–60. in press

Coates, C. J., and Söderhäll, K. (2021). The stress–immunity axis in shellfish. *J. Invertebr. Pathol.* 186:107492. doi: 10.1016/j.jip.2020.107492

Coffey, A. H., Li, C. W., and Shields, J. D. (2012). The effect of salinity on experimental infections of a *Hematodinium* sp. in blue crabs, *Callinectes sapidus*. *J. Parasitol.* 98, 536–542. doi: 10.1645/GE-2971.1

Cohen, A. N., Carlton, J. T., and Fountain, M. C. (1995). Introduction, dispersal and potential impacts of the green crab *Carcinus maenas* in San Francisco Bay. *Mar. Biol.* 122, 225–237.

Costello, C., Cao, L., Gelcich, S., Cisneros-Mata, M. A., Free, C. M., Froelich, H. E., et al. (2020). The future of food from the sea. *Nature* 588, 95–100. doi: 10.1038/s41586-020-2616-y

Cui, Z., Liu, Y., Yuan, J., Zhang, X., Ventura, T., Ma, K. Y., et al. (2021). The Chinese mitten crab genome provides insights into adaptive plasticity and developmental regulation. *Nat. Commun.* 12:2395. doi: 10.1038/s41467-021-22604-3

Culot, A., Grosset, N., and Gautier, M. (2019). Overcoming the challenges of phage therapy for industrial aquaculture: A review. *Aquaculture* 513:734423. doi: 10.1016/j.aquaculture.2019.734423

Dan, S., and Hamasaki, K. (2015). Evaluation of the effects of probiotics in controlling bacterial necrosis symptoms in larvae of the mud crab *Scylla serrata* during mass seed production. *Aquacult. Int.* 23, 277–296. doi: 10.1007/s10499-014-9815-1

Davies, C. E., Batista, F. M., Malkin, S. H., Thomas, J. E., Bryan, C. C., Crocombe, P., et al. (2019). Spatial and temporal disease dynamics of the parasite *Hematodinium* sp. in shore crabs, *Carcinus maenas*. *Paras. Vect.* 12:472. doi: 10.1186/s13071-019-3727-x

Davies, C. E., Malkin, S. H., Thomas, J. E., Batista, F. M., Rowley, A. F., and Coates, C. J. (2020a). Mycosis is a disease state encountered rarely in shore crabs, *Carcinus maenas*. *Pathogens* 9:462. doi: 10.3390/pathogens9060462

Davies, C. E., Bass, D., Ward, G. M., Batista, F. M., Malkin, S. H., Thomas, J. E., et al. (2020b). Diagnosis and prevalence of two new species of haplosporidians infecting shore crabs *Carcinus maenas*: *Haplosporidium carcini* n. sp., and *H. cranc* n. sp. *Parasitology* 147, 1229–1237. doi: 10.1017/S0031182020000980

Dhar, A. K., Cruz-Flores, R., and Bateman, K. S. (2022). "Viral diseases of crustaceans," in *Invertebrate Pathology*, eds A. F. Rowley, C. J. Coates, and M. M. A. Whitten (Oxford: Oxford University Press), 368–399. in press

Ding, Z., Yao, Y., Zhang, F., Wan, J., Sun, M., Liu, H., et al. (2015). The first detection of white spot syndrome virus in naturally infected cultured Chinese mitten crabs, *Eriocheir sinensis* in China. *J. Virol. Methods* 220, 49–54. doi: 10.1016/j.jviromet.2015.04.011

Ding, Z., Meng, Q., Liu, H., Yuan, S., Zhang, F., Sun, M., et al. (2016). First case of hepatopancreatic necrosis disease in pond-reared Chinese mitten crab, *Eriocheir sinensis*, associated with microsporidian. *J. Fish Dis.* 39, 1043–1051. doi: 10.1111/jfd.12437

Ding, Z., Wang, S., Zhu, X., Pan, J., and Xue, H. (2017). Temporal and spatial dynamics of white spot syndrome virus in the Chinese mitten crab, *Eriocheir sinensis*. *Aquac. Res.* 48, 2528–2537. doi: 10.1111/are.13089

Ding, Z., Pan, J., Huang, H., Jiang, G., Chen, J., Zhu, X., et al. (2018). An integrated metabolic consequence of *Hepatospora eriocheir* infection in the Chinese mitten crab *Eriocheir sinensis*. *Fish Shellf. Immunol.* 72, 443–451. doi: 10.1016/j.fsi.2017.11.028

Doss, J., Culbertson, K., Hahan, D., Camacho, J., and Barekzi, N. (2017). A review of phage therapy against bacterial pathogens of aquatic and terrestrial organisms. *Viruses* 9:50. doi: 10.3390/v9030050

Eddy, F., Powell, A., Gregory, S., Numan, L. M., Lightner, D. V., Dyson, P. J., et al. (2007). A novel bacterial disease of the European shore crab, *Carcinus maenas* molecular pathology and epidemiology. *Microbiology* 153, 2839–2849. doi: 10.1099/mic.0.2007/008391-0

Edwards, M., Coates, C. J., and Rowley, A. F. (2019). Host range of the mikrocytid parasite *Paramikrocytos canceri* in decapod crustaceans. *Pathogens* 8:e252. doi: 10.3390/pathogens8040252

FAO (2020). *The State of World Fisheries and Aquaculture 2020. Sustainability in Action*. Rome: FAO. doi: 10.4060/ca9229en

Feng, B., Guo, Z., Zhang, W., Pan, Y., and Zhao, Y. (2016). Metabolome response to temperature-induced virulence gene expression in two genotypes of pathogenic *Vibrio parahaemolyticus*. *BMC Microbiol.* 16:75. doi: 10.1186/s12866-016-0688-5

Flowers, E. M., Simmonds, K., Messick, G. A., Sullivan, L., and Schott, E. J. (2016a). PCR-based prevalence of a fatal reovirus of the blue crab, *Callinectes sapidus* (Rathbun) along the northern Atlantic coast of the USA. *J. Fish Dis.* 39, 705–714. doi: 10.1111/jfd.12403

Flowers, E. M., Bachvaroff, T. R., Warg, J. V., et al. (2016b). Genome sequence analysis of CsRV1: A pathogenic reovirus that infects the blue crab *Callinectes sapidus* across its trans-hemispheric range. *Front. Microbiol.* 7:126. doi: 10.3389/fmicb.2016.00126

Flowers, E. M., Johnson, A. F., Aguilar, R., and Schott, E. J. (2018). Prevalence of the pathogenic virus *Callinectes sapidus* reovirus 1 near flow-through blue crab aquaculture in Chesapeake Bay. *USA Dis. Aquat. Org.* 129, 135–144. doi: 10.3354/dao03232

Frizzera, A., Bojko, J., Cremonte, F., and Vázquez, N. (2021). Symbionts of invasive and native crabs, in Argentina: The most recently invaded area on the Southwestern Atlantic coastline. *J. Invertebr. Pathol.* 184:107650. doi: 10.1016/j.jip.2021.107650

Foehlich, H. E., Couture, J., Falconer, L., et al. (2021). Mind the gap between ICES nations' future seafood consumption and aquaculture production. *ICES J. Mar. Sci*. 78, 468–477. doi: 10.1093/icesjms/fsaa006

Gao, Y., Liu, S., Huang, J., Wang, Q., Li, K., He, J., et al. (2019). Cryo-electron microscopy structures of novel viruses from mud crab *Scylla paramamosain* with multiple infections. *J. Virol*. 93, e2255–e2218. doi: 10.1128/JVI.02255-18

Goddard, J. H., Torchin, M. E., Kuris, A. M., and Lafferty, K. D. (2005). Host specificity of *Sacculina carcini*, a potential biological control agent of the introduced European green crab *Carcinus maenas* in California. *Biol. Inv*. 7, 895–912. doi: 10.1007/s10530-003-2981-0

Golden, C. D., Koehn, J. Z., Shepon, A., Passarelli, S., Free, C. M., Viana, D. F., et al. (2021). Aquatic foods to nourish nations. *Nature* 598, 315–320. doi: 10.1038/s41586-021-03917-1

Grosholz, E. D., Ruiz, G. M., Dean, C. A., Shirley, K. A., Maron, J. L., and Connors, P. G. (2000). The impacts of a nonindigenous marine predator in a California bay. *Ecology* 81, 1206–1224.

Guo, Z.-X., He, J.-G., Xu, H.-D., and Weng, S.-P. (2013). Pathogenicity and complete genome sequence analysis of the mud crab dicistrovirus-1. *Virus Res*. 171, 8–14. doi: 10.1016/j.virusres.2012.10.002

Hamilton, K. M., Morritt, D., and Shaw, P. W. (2007). Molecular and histological identification of the crustacean parasite *Hematodinium* sp. (Alveolata, Syndinea) in the shore crab *Carcinus maenas*. *Acta Protozool.* 46, 183–192.

Hamilton, K. M., Shaw, P. W., and Morritt, D. (2009). Prevalence and seasonality of *Hematodinium* (Alveolata: Syndinea) in a Scottish crustacean community. *ICES J. Mar. Sci*. 66, 1837–1845. doi: 10.1093/icesjms/fsp152

Herborg, L. M., Rushton, S. P., Clare, A. S., and Bentley, M. G. (2005). The invasion of the Chinese mitten crab (*Eriocheir sinensis*) in the United Kingdom and its comparison to continental Europe. *Biol. Invas.* 7, 959–968. doi: 10.1007/s10530-004-2999-y

Holme, M.-H., Zeng, C., and Southgate, P. C. (2008). A review of recent progress toward development of a formulated microbound diet for mud crab, *Scylla serrata*, larvae and their nutritional requirements. *Aquaculture* 286, 164–175. doi: 10.1016/j.aquaculture.2008.09.021

Huang, Q., Li, M., Wang, F., Song, S., and Li, C. (2021). Transmission pattern of the parasitic dinoflagellate *Hematodinium perezi* in polyculture ponds of coastal China. *Aquaculture* 538:736549. doi: 10.1016/j.aquaculture.2021.736549

Huang, Z., Deng, X., Li, Y., et al. (2012). Structural insights into the classification of mud crab reovirus. *Virus Res.* 166, 116–120. doi: 10.16/j.virusres.2012.02.025

Huchin-Mian, J. P., Small, H. J., and Shields, J. D. (2017). Patterns in the natural transmission of the parasitic dinoflagellate *Hematodinium perezi* in American blue crabs, *Callinectes sapidus* from a highly endemic area. *Mar. Biol*. 164:153. doi: 10.1007/s00227-017-3185-y

Hungria, D. B., Tavares, C. P., Pereira, L. A., daSilva, U. D. A. T., and Ostrensky, A. (2017). Global status of production and commercialization of soft-shell crabs. *Aquacult. Int*. 25, 2213–2226. doi: 10.1007/s10499-017-0183-5

Ingle, R. W. (1986). The Chinese mitten crab *Eriocheir sinensis* H. Milne Edwards – a contentious immigrant. *London Nat.* 65, 101–105.

Jesse, J. A., Agnew, M. V., Arai, K., Armstrong, C. T., Hood, S. M., Kachmar, M. L., et al. (2021). Effects of infectious diseases on population dynamics of marine organisms in Chesapeake Bay. *Estuar. Coasts* 2021:915. doi: 10.1007/s122237-021-00915-4

Jithendran, K. P., Poornima, M., Balasubbramanian, C. P., and Kulasekarandian, S. (2010). Diseases of mud crabs (*Scylla* spp.): an overview. *Ind. J. Fish*. 57, 55–63.

Johnson, L., Coates, C. J., Albalat, A., Todd, K., and Neil, D. (2016). Temperature-dependent morbidity of 'nicked' edible crab, *Cancer pagurus*. *Fish. Res.* 175, 127–131. doi: 10.1016/j.fishres.2015.11.024

Johnson, P. T. (1977). A viral disease of the blue crab, *Callinectes sapidus*: histopathology and differential diagnosis. *J. lnvertebr. Pathol*. 29, 201–209. doi: 10.1016/0022-2011(77)90194-X

Johnson, P. T., and Bodammer, J. E. (1975). A disease of the blue crab, *Callinectes sapidus*, of possible viral etiology. *J. Invertebr. Pathol*. 26, 141–143.

Johnson, P. T., and Lightner, D. V. (1988). Rod-shaped nuclear viruses of crustaceans: gut-infecting species. *Dis. Aquat. Org*. 5, 123–141.

Kasmawati, I., Asni, A., Ernaningsih, A., and Adimu, H. E. (2020). Aquaculture management of blue swimming crab (*Portunus pelagicus*) using integrated submerged net cage in Pangkep Regency waters, South Sulawesi, Indonesia. *AACL Bioflux*. 13, 3279–3286.

Keenan, C. P., Davie, P. J. F., and Cannon, L. R. G. (1998). A revision of the genus *Scylla* de Haan, 1833 (Crustacea: Decapoda: Brachyura: Portunidae). *Raffles Bull. Zool*. 46, 217–245.

Kimes, N., Grim, C., Johnson, W., Hasan, N. A., Tall, B. D., Kothary, M. H., et al. (2012). Temperature regulation of virulence factors in the pathogen *Vibrio coralliilyticus*. *ISME J.* 6, 835–846. doi: 10.1038/ismej.2011.154

Krantz, G. E., Colwell, R. R., and Lovelace, E. (1969). *Vibrio parahaemolyticus* from the blue crab *Callinectes sapidus* in Chesapeake Bay. *Science* 164, 1286–1287.

Lai, J. C. Y., Ng, P. K. L., and Davie, P. J. F. (2010). A revision of the *Portunus pelagicus* (Linnaeus 1758) species complex (Crustacea:Brachyura:Portunidae), with the recognition of four species. *Raffles Bull. Zool*. 58, 199–237.

Lages, M. A., Balado, M., and Lemos, M. L. (2019). The expression of virulence factors in *Vibrio anguillarum* is dually regulated by iron levels and temperature. *Front. Microbiol*. 10:2335. doi: 10.3389/fmicb.2019.02335

Le Moullac, G., and Haffner, P. (2000). Environmental factors affecting immune responses in Crustacea. *Aquaculture* 191, 121–131. doi: 10.1016/S0044-8486(00)00422-1

Le Roux, F., Wegner, K. M., Baker-Austin, C., Vezzulli, L., Osorio, C. R., Amaro, C., et al. (2015). The emergence of *Vibrio* pathogens in Europe: ecology, evolution and pathogenesis. *Front. Microbiol*. 6:830. doi: 10.3389/fmicb.2015.00830

Leaño, E. M. (2002). *Haliphthoros* spp. from spawned eggs of captive mud crab, *Scylla serrata*, broodstocks. *Fung. Diver*. 9, 93–103.

Le Vay, L., Lebata, M. J. H., Walton, M., Primavera, J., Quinitio, E., Lavilla-Pitogo, C., et al. (2008). Approaches to stock enhancement in mangrove-associated crab fisheries. *Rev. Fish. Sci.* 16, 72–80. doi: 10.1080/10641260701727285

Li, C. W., Song, S. Q., Liu, Y., and Chen, T. T. (2013). *Hematodinium* infections in cultured Chinese swimming crab, *Portunus trituberculatus*, in northern China. *Aquaculture* 396, 59–65. doi: 10.1016/j.aquaculture.2013.02.022

Li, C., Li, M., and Huang, Q. (2021). The parasitic dinoflagellate *Hematodinium* infects marine crustaceans. *Mar. Life Sci. Technol*. 3, 313–325. doi: 10.1007/s42995-020-00061-z

Li, Y., Ai, C., and Liu, L. (2018). "Mud crab, *Scylla paramamosain* China's leading maricultured crab," in *Aquaculture in China: Success Stories and Modern Trends*, eds J.-F. Giu, Q. Tang, A. Li, J. Liu, and S.S. De Silva (Hoboken: John Wiley), 226–233. doi: 10.1002/9781119120759.ch3_4

Li, Y. Y., Xia, X. A., Wu, Q. Y., Liu, W. H., and Lin, Y. S. (2008). Infection of *Hematodinium* sp. in mud crabs *Scylla serrata* cultured in low salinity water in southern China. *Dis. Aquat. Org*. 82, 145–150. doi: 10.3354/dao01988

Liang, T., Feng, Q., Wu, T., Gu, W., and Wang, W. (2009). Use of oxytetracycline for the treatment of tremor disease in the Chinese mitten crab *Eriocheir sinensis*. *Dis. Aquat. Org*. 84, 243–250. doi: 10.3354/dao02052

Liu, Q., Li, H. Y., Wang, Q., Liu, P., Dai, F. Y., and Li, J. (2007). Identification and phylogenetic analysis of a strain of *Vibrio alginolyticus*, a pathogen in *Portunus trituberculatus* with toothpaste disease. *Mar. Freshwater Res*. 28, 9–13.

Liu, W., Dong, Q., QingQing, P., and Xiaojun, Y. (2009). Studies on pathogenicity of the white spot syndrome virus and effect on hemolymph enzymes activities changes in mud crab *Scylla serrata* (Forskal). *Acta Hydrobiol. Sinica* 33, 1112–1117.

Liu, W., Qian, D., and Yan, X. J. (2011). Studies on pathogenicity and prevalence of white spot syndrome virus in mud crab, *Scylla serrata* (Forskal), in Zhejiang Province, China. *J. Fish. Dis*. 34, 131–138. doi: 10.1111/j.1365-2761.2010.01221.x

Liu, X., Lei, Y., Ren, Z., et al. (2020). Isolation, characterization and virulence of *Mesanophrys* sp. (Ciliophora: Orchitophyryidae) in farmed swimming crab (*Portunus trituberculatus*) in eastern China. *J. Fish. Dis*. 43, 1419–1429. doi: 10.1111/jfd.13248

López-Cervantes, G., Álvarez-Ruiz, P., Luna-Suárez, S., Luna-González, A., Esparza-Leal, H. M., Castro-Martínez, C., et al. (2021). Temperature and salinity modulate virulence and PirA gene expression of *Vibrio parahaemolyticus*, the causative agent of AHPND. *Aquacult. Int*. 29, 743–756. doi: 10.1007/s10499-021-00654-0

Lützen, J., Jensen, K. H., and Glenner, H. (2018). Life history of *Sacculina carcini* Thompson, 1836 (Cirripedia: Rhizocephala: Sacculinidae) and the intermoult cycle of its host, the shore crab *Carcinus maenas* (Linnaeus, 1758) (Decapoda: Brachyura: Carcinidae). *J. Crust. Biol*. 38, 413–419. doi: 10.1093/jcbiol/ruy044

Ma, H., Lu, X., Liu, J., Guo, S., Zhao, X., and Ye, S. (2021). *Metschnikowia bicuspidata* isolated from milky diseased *Eriocheir sinensis*: Phenotypic and

genetic characterization, antifungal susceptibility and challenge models. *J. Fish. Dis.* 2021, 1–9. doi: 10.1111/jfd.13530

Messick, G. A. (1998). Diseases, parasites, and symbionts of blue crabs (*Callinectes sapidus*) dredged from Chesapeake Bay. *J. Crust. Biol.* 18, 533–548. doi: 10.1163/193724098X00368

Messick, G. A., and Shields, J. D. (2000). Epizootiology of the parasitic dinoflagellate *Hematodinium* sp. in the American blue crab *Callinectes sapidus*. *Dis. Aquat. Org.* 43, 139–152. doi: 10.3354/dao043139

Midorikawa, Y., Shimizu, T., Sanda, T., Hamasaki, K., Dan, S., Lai, M. T. B. M., et al. (2020). Characterization of *Aquimarina hainanensis* isolated from diseased mud crab *Scylla serrata* larvae in a hatchery. *J. Fish Dis.* 43, 541–549. doi: 10.1111/jfd.13151

Mouritsen, K. N., and Jensen, T. (1997). Parasite transmission between soft-bottom invertebrates: temperature mediated infection rates and mortality in *Corophium volutator*. *Mar. Ecol. Prog. Ser.* 151, 123–134.

Mouritsen, K. N., and Jensen, T. (2006). The effect of *Sacculina carcini* infections on the fouling, burying behaviour and condition of the shore crab. *Carcinus maenas*. *Mar. Biol. Res.* 2, 270–275. doi: 10.1080/17451000600874752

Mouritsen, K. N., Geyti, S. N., Lützen, J., Høeg, J. T., and Glenner, H. (2018). Population dynamics and development of the rhizocephalan *Sacculina carcini*, parasitic on the shore crab *Carcinus maenas*. *Dis. Aquat. Org.* 131, 199–211. doi: 10.3354/dao03290

Mullowney, D. R. J., and Baker, K. D. (2020). Gone to shell: Removal of a million tonnes of snow crab since cod moratorium in the Newfoundland and Labrador fishery. *Fish. Res.* 230:105680. doi: 10.1016/j.fishres.2020.105680

Nagpal, M. L., Fox, K. F., and Fox, A. (1998). Utility of 16S–23S rRNA spacer region methodology: how similar are interspace regions within a genome and between strains for closely related organisms? *J. Micro. Meth.* 33, 211–219. doi: 10.1016/S0167-7012(98)00054-2

Noordin, N. M., Zeng, C., and Southgate, P. C. (2020). Survival, molting pattern, and growth of early blue swimmer crab, *Portunus pelagicus*, juveniles fed diets containing varying levels of cholesterol. *J. World Aquacult. Soc.* 51, 255–265. doi: 10.1111/jwas.12623

Parks, M., and Thanh, T. (2019). *The Green Crab Cookbook: An Invasive Species Meets a Culinary Solution*. Massachusetts: Greencrab.org.

Parry, R., and Asgari, S. (2019). Discovery of novel crustacean and cephalopod flaviviruses: insights into the evolution and circulation of flaviviruses between marine invertebrate and vertebrate hosts. *J. Virol.* 93, e432–e419. doi: 10.1128/JVI.00432-19

Paterson, B. D., and Mann, D. L. (2011). "Mud crab aquaculture," in *Recent Advances and New Species in Aquaculture*, eds R. K. Fotedar and B. F. Phillips (Oxford: Wiley-Blackwell), 115–135.

Perveen, S., Lei, Y., Yin, F., and Wang, C. (2021). Effect of environmental factors on survival and population growth of ciliated parasite, *Mesanophrys* sp. (Ciliophora: Scuticociliatia) infecting *Portunus trituberculatus*. *Parasitology* 148, 477–485. doi: 10.1017/S0031182020002127

Powell, A., and Rowley, A. F. (2008). Tissue changes in the shore crab *Carcinus maenas* as a result of infection by the parasitic barnacle *Sacculina carcini*. *Dis. Aquat. Org.* 80, 75–79. doi: 10.3354/dao01930

Rivas, A. J., Lemos, M. L., and Osorio, C. R. (2013). *Photobacterium damselae* subsp. *damselae*, a bacterium pathogenic for marine animals and humans. *Front. Microbiol.* 25:283. doi: 10.3389/fmicb.2013.00283

Rogers, H. A., Taylor, S. S., Hawke, J. P., Schott, E. J., and Anderson Lively, J. A. (2015). Disease, parasite and commensal prevalences for blue crab *Callinectes sapidus* at shedding facilities in Louisiana, USA. *Dis. Aquat. Org.* 112, 207–217. doi: 10.3354/dao02803

Romano, N., and Zeng, C. (2017). Cannibalism of decapod crustaceans and implications for their aquaculture: A review of its prevalence, influencing factors, and mitigating methods. *Rev. Fish. Sci. Aquacult.* 25, 42–69. doi: 10.1080/23308249.2016.1221379

Rowley, A. F. (2022). "Bacterial diseases of crustaceans," in *Invertebrate Pathology*, eds A. F. Rowley, C. J. Coates, and M. M. A. Whitten (Oxford: Oxford University Press), 400–435. in press

Rowley, A. F., Davies, C. E., Malkin, S. H., Bryan, C. C., Thomas, J. E., Batista, F. M., et al. (2020). Prevalence and histopathology of the parasitic barnacle, *Sacculina carcini* in shore crabs, *Carcinus maenas*. *J. Invertebr. Pathol.* 171:107338. doi: 10.1016/j.jip.2020.107338

Santhanam, R. (2018). *Biology and Culture of Portunid Crabs of World Seas*. Oakville: Apple Academic Press/CRC Press.

Shelley, C., and Lovatelli, A. (2011). *Mud Crab Aquaculture – A Practical Manual. FAO Fisheries and Aquaculture Technical Paper. No. 567*. Rome: FAO.

Shen, G., Shui, Y., Zhang, X., Song, K., Wang, Y., Xu, Z., et al. (2021). Hepatopancreatic necrosis disease (HPND) in Chinese mitten crab *Eriocheir sinensis* tightly linked to low concentration of two insecticides. *Aquacult. Res.* 52, 2294–2304. doi: 10.1111/are.15081

Shen, Z., Kumar, D., Liu, X., Yan, B., Fang, P., Gu, Y., et al. (2021). Metatranscriptomic analysis reveals an imbalance of hepatopancreatic flora of Chinese mitten crab *Eriocheir sinensis* with hepatopancreatic necrosis disease. *Biology* 10:462. doi: 10.3390/biology10060462

Shields, J. D. (2019). Climate change enhances disease processes in crustaceans: case studies in lobsters, crabs, and shrimps. *J. Crust. Biol.* 39, 673–683. doi: 10.1093/jcbiol/ruz072

Shields, J. D. (2022). "Parasitic diseases of crustaceans," in *Invertebrate Pathology*, eds A. F. Rowley, C. J. Coates, and M. M. A. Whitten (Oxford: Oxford University Press), 458–502. in press

Shields, J. D., Scanlon, C., and Volety, A. (2003). Aspects of the pathophysiology of blue crabs, *Callinectes sapidus*, infected with the parasitic dinoflagellate *Hematodinium perezi*. *Bull. Mar. Sci.* 72, 519–535.

Shields, J. D., Taylor, D. M., and Pardy, A. L. (2005). Epidemiology of bitter crab disease (*Hematodinium* sp.) in snow crabs *Chionoecetes opilio* from Newfoundland, Canada. *Dis. Aquat. Org.* 64, 253–264. doi: 10.3354/dao064253

Shields, J. D., Taylor, D. M., O'Keefe, P. G., Colbourne, E., and Hynick, E. (2007). Epidemiological determinants in outbreaks of bitter crab disease (*Hematodinium* sp.) in snow crabs *Chionoecetes opilio* from Conception Bay, Newfoundland, Canada. *Dis. Aquat. Org.* 77, 1616–1580. doi: 10.3354/dao01825

Small, H. J. (2012). Advances in our understanding of the global diversity and distribution of *Hematodinium* spp. – Significant pathogens of commercially exploited crustaceans. *J. Invertebr. Pathol.* 110, 234–246. doi: 10.1016/j.jip.2012.03.012

Smith, A. L., and Rowley, A. F. (2015). Effects of experimental infection of juvenile edible crabs *Cancer pagurus* with the parasitic dinoflagellate *Hematodinium* sp. *J. Shellf. Res.* 34, 511–519. doi: 10.2983/035.034.0236

Spindler-Barth, M. (1976). A bacterial infection in the common shore crab *Carcinus maenas* and the fiddler crab *Uca pugilator*. *Mar. Biol.* 36, 1–4.

Spitznagel, M. I., Small, H. J., Lively, J. A., Shields, J. D., and Schott, E. J. (2019). Investigating risk factors for mortality and reovirus infection in aquaculture production of soft-shell blue crabs (*Callinectes sapidus*). *Aquaculture* 502, 289–295. doi: 10.1016/j.aquaculture.2018.12.051

Stentiford, G. D., Chang, E. S., Chang, S. A., and Neil, D. M. (2001). Carbohydrate dynamics and the crustacean hyperglycemic hormone (CHH): effects of parasitic infection in Norway lobsters (*Nephrops norvegicus*). *Gen. Comp. Endocrinol.* 121, 13–22. doi: 10.1006/gcen.2000.7575

Stentiford, G. D., and Feist, S. W. (2005). A histopathological survey of shore crab (*Carcinus maenas*) and brown shrimp (*Crangon crangon*) from six estuaries in the United Kingdom. *J. Invertebr. Pathol.* 88, 136–146. doi: 10.1016/j.jip.2005.01.006

Stentiford, G. D., and Shields, J. D. (2005). A review of the parasitic dinoflagellates *Hematodinium* species and *Hematodinium*-like infections in marine crustaceans. *Dis. Aquat. Org.* 66, 47–70. doi: 10.3354/dao066047

Stentiford, G. D., Bateman, K. S., Dubuffet, A., Chambers, E., and Stone, D. M. (2011). *Hepatospora eriocheir* (Wang and Chen, 2007) gen. et comb. nov. infecting invasive Chinese mitten crabs (*Eriocheir sinensis*) in Europe. *J. Invertebr. Pathol.* 108, 156–166. doi: 10.1016/j.jip.2011.07.008

Stevens, B. G., and Miller, T. J. (2020). "Crab fisheries," in *The Natural History of the Crustacea, Fisheries and Aquaculture*, eds G. Lovrich and M. Thiel (Oxford: Oxford University Press), doi: 10.1093/0s0/9780190865627.003.0002

Sullivan, T. J., and Neigel, J. E. (2018). Effects of temperature and salinity on prevalence and intensity of infection of blue crabs, *Callinectes sapidus*, by *Vibrio cholerae*, *V. parahaemolyticus*, and *V. vulnificus* in Louisiana. *J. Invertebr. Pathol.* 151, 82–90. doi: 10.1016/j.jip.2017.11.004

Sui, L., Wille, M., Cheng, Y., Wu, X., and Sorgeloos, P. (2011). Larviculture techniques for Chinese mitten crab *Eriocheir sinensis*. *Aquaculture* 315, 16–19. doi: 10.1016/j.aquaculture.2010.06.021

Syafaat, M. N., Azra, M. N., Waiho, K., Fazhan, H., Abol-Munafi, A. B., Ishak, S. D., et al. (2021a). A review of the nursery culture of mud crabs, genus *Scylla*: Current progress and future directions. *Animals* 11:2034. doi: 10.3390/ani11072034

Syafaat, M. N., Azra, M. N., Mohamad, F., Che-Ismail, C. Z., Amin-Safwan, A., Asmat-Ullah, M., et al. (2021b). Thermal tolerance and physiological changes in mud crab, *Scylla paramamosain* crablet at different water temperatures. *Animals* 11:1146. doi: 10.3390/1ni11041146

Tavares, C. P. S., Silva, U. A. T., Pereira, L. A., and Ostrensky, A. (2018). Systems and techniques used in the culture of soft-shell swimming crabs. *Rev. Aquacult.* 10, 913–923. doi: 10.1111/raq.12207

Tilmans, M., Mrugała, A., Svoboda, J., Engelsma, M. Y., Petie, M., Soes, D. M., et al. (2014). Survey of the crayfish plague pathogen presence in the Netherlands reveals a new *Aphanomyces astaci* carrier. *J. Invertebr. Pathol.* 120, 74–79. doi: 10.1016/j.jip.2014.06.002

Valente, C. D. S., and Wan, A. H. L. (2021). Vibrio and major commercially important vibriosis diseases in decapod crustaceans. *J. Invertebr. Pathol.* 181:107527. doi: 10.1016/j.jip.2020.107527

Vezzulli, L., Colwell, R. R., and Pruzzo, C. (2013). Ocean warming and spread of pathogenic vibrios in the aquatic environment. *Microb. Ecol.* 65, 817–825. doi: 10.1007/s00248-012-0163-2

Waiho, K., Fazhan, H., Quinitio, E. T., et al. (2018). Larval rearing of mud crab (*Scylla*): What lies ahead? *Aquaculture* 493, 37–50. doi: 10.1016/j.aquaculture.2018.04.047

Waiho, K., Glenner, H., Miroliubov, A., Noever, C., Hassan, M., Ikhwanuddin, M., et al. (2021). Rhizocephalans and their potential impact on crustacean aquaculture. *Aquaculture* 531:735876. doi: 10.1016/j.aquaculture.2020.735876

Walton, W. C., MacKinnon, C., Rodriguez, L. F., Proctor, C., and Ruiz, G. M. (2002). Effect of an invasive crab upon a marine fishery: green crab, *Carcinus maenas*, predation upon a venerid clam, *Katelysia scalarina*, in Tasmania (Australia). *J. Exp. Mar. Biol. Ecol.* 272, 171–189. doi: 10.1016/S0022-0981(02)00127-2

Wan, X., Shen, H., Wang, L., and Cheng, Y. (2011). Isolation and characterization of *Vibrio metschnikovii* causing infection in farmed *Portunus trituberculatus* in China. *Aquacult. Int.* 19, 351–359. doi: 10.1007/s10499-011-9422-3

Wang, J. F., Li, M., Xiao, J., Xu, W. J., and Li, C. W. (2017). *Hematodinium* spp. infections in wild and cultured populations of marine crustaceans along the coast of China. *Dis. Aquat. Org.* 124, 181–191. doi: 10.3354/dao03119

Wang, W., and Gu, Z. (2002). Rickettsia-like organism associated with tremor disease and mortality of the Chinese mitten crab *Eriocheir sinensis*. *Dis. Aquat. Org.* 11, 149–153. doi: 10.3354/dao048149

Wang, W., Wen, B., Gasparich, G. E., Zhu, N., Rong, L., Chen, J., et al. (2004). A spiroplasma associated with tremor disease in the Chinese mitten crab (*Eriocheir sinensis*). *Microbiology* 150, 3035–3040. doi: 10.1099/mic.0.26664-0

Wang, W., Gu, W., Gasparich, G. E., Bi, K., Ou, J., Meng, Q., et al. (2011). Spiroplasma eriocheiris sp. nov., associated with mortality in the Chinese mitten crab, *Eriocheir sinensis*. *Int. J. Syst. Evol. Microbiol.* 61, 703–708.

Wang, Y., Li, X. C., Fu, G., Zhao, S., Chen, Y., Wang, H., et al. (2017). Morphology and phylogeny of *Ameson portunus* n. sp. (Microsporidia) infecting the swimming crab *Portunus trituberculatus* from China. *Eur. J. Protistol.* 61, 122–136. doi: 10.1016/j.ejop.2017.09.008

Weng, S.-P., Guo, Z.-X., Sun, J.-J., Chan, S.-M., and He, J.-G. (2007). A reovirus disease in cultured mud crab, *Scylla serrata*, in southern China. *J. Fish. Dis.* 30, 133–139. doi: 10.1111/j.1365-2761.2007.00794.x

Wilhelm, G., and Mialhe, E. (1996). Dinoflagellate infection associated with the decline of *Necora puber* crab populations in France. *Dis. Aquat. Org.* 26, 213–219.

Xie, J., Mei, H., JIn, S., Bu, L., Wang, X., Wang, C., et al. (2021a). Outbreak of vibriosis associated with *Vibrio parahaemolyticus* in the mud crab *Scylla paramamosain* cultured in China. *Dis. Aquat. Org.* 144, 187–196. doi: 10.3354/dao03587

Xie, J., Mei, H., Jin, S., Bu, L., Wang, X., Wang, C., et al. (2021b). First report of *Photobacterium damselae* subsp. *damselae* infection in the mud crab *Scylla paramamosain* cultured in China. *Aquaculture* 530:73588. doi: 10.16/j.aquaculture.2020.735880

You, W., and Hedgecock, D. (2019). Boom-and-bust production cycles in animal seafood aquaculture. *Rev. Aquac.* 11, 1045–1060. doi: 10.1111/are.15377

Young, A. M., and Elliott, J. A. (2020). Life history and population dynamics of green crabs (*Carcinus maenas*). *Fishes* 5:4. doi: 10.3390/fishes5010004

Zetlmeisl, C., Hermann, J., Petney, T., Glenner, H., Griffiths, C., and Taraschewski, H. (2011). Parasites of the shore crab *Carcinus maenas* (L.): implications for reproductive potential and invasion success. *Parasitology* 138, 394–401. doi: 10.1017/S0031182010001344

Zhang, R., He, J., Su, H., Dong, C., Guo, Z., Ou, Y., et al. (2011). Identification of the structural proteins of VP1 and VP2 of a novel mud crab dicistrovirus. *J. Virol. Meth.* 171, 323–328. doi: 10.1016/j.jviromet.2010.09.010

Zhang, X. J., Bai, X. S., Yan, B. L., Bi, K. R., and Qin, L. (2014). *Vibrio harveyi* as a causative agent of mass mortalities of megalopa in the seed production of swimming crab *Portunus trituberculatus*. *Aquacult. Int.* 22, 661–672. doi: 10.1007/s10499-013-9695-9

Zhao, M., Behringer, D., Bojko, J., Kough, A. S., Plough, L., Tavares, C. P. D. S., et al. (2020). Climate and season are associated with prevalence and distribution of trans-hemispheric blue crab reovirus (*Callinectes sapidus* reovirus 1). *Mar. Ecol. Prog. Ser.* 647, 123–133. doi: 10.3354/meps13405

Zhao, M., Tavares, C. P. D. S., and Schott, E. J. (2021). Diversity and classification of reoviruses in crustaceans: A proposal. *J. Invertebr. Pathol.* 182:107568. doi: 10.1016/j.jip.2021.107568

Conflict of Interest: The authors declare that the research was conducted in the absence of any commercial or financial relationships that could be construed as a potential conflict of interest.

Publisher's Note: All claims expressed in this article are solely those of the authors and do not necessarily represent those of their affiliated organizations, or those of the publisher, the editors and the reviewers. Any product that may be evaluated in this article, or claim that may be made by its manufacturer, is not guaranteed or endorsed by the publisher.

frontiers in Marine Science

ORIGINAL RESEARCH
published: 31 January 2022
doi: 10.3389/fmars.2022.816932

The Mechanism of Carbonate Alkalinity Exposure on Juvenile *Exopalaemon carinicauda* With the Transcriptome and MicroRNA Analysis

Kunpeng Shi[1,2,3†], Mingdong Li[1,2†], Zhen Qin[1,2], Jiajia Wang[1,2], Ping Liu[1,2], Jian Li[1,2] and Jitao Li[1,2]*

[1] Key Laboratory for Sustainable Utilization of Marine Fisheries Resources, Ministry of Agriculture and Rural Affairs, Yellow Sea Fisheries Research Institute, Chinese Academy of Fishery Sciences, Qingdao, China, [2] Function Laboratory for Marine Fisheries Science and Food Production Processes, Qingdao National Laboratory for Marine Science and Technology, Qingdao, China, [3] Institute of Biomedical Engineering, College of Life Sciences, Qingdao University, Qingdao, China

OPEN ACCESS

Edited by:
Xiangli Tian,
Ocean University of China, China

Reviewed by:
Xiaodan Wang,
East China Normal University, China
Huan Wang,
Ningbo University, China

***Correspondence:**
Jitao Li
lijt@ysfri.ac.cn

[†] These authors share first authorship

Specialty section:
This article was submitted to Marine Fisheries, Aquaculture and Living Resources, a section of the journal Frontiers in Marine Science

Received: 17 November 2021
Accepted: 03 January 2022
Published: 31 January 2022

Citation:
Shi K, Li M, Qin Z, Wang J, Liu P, Li J and Li J (2022) The Mechanism of Carbonate Alkalinity Exposure on Juvenile Exopalaemon carinicauda With the Transcriptome and MicroRNA Analysis. Front. Mar. Sci. 9:816932. doi: 10.3389/fmars.2022.816932

Saline-alkali water is distributed all over the world and affects the development of fisheries. The ridge tail white prawn *Exopalaemon carinicauda* is an economically important shrimp in China, which has excellent environmental tolerance. However, due to its complex genetic structure, there have been few studies on its alkalinity-adaptation mechanisms. In order to explore the molecular mechanisms of *E. carinicauda* in adapting to the alkaline water, mRNA and miRNA transcriptomes from the gills of *E. carinicauda* were determined. The results showed that after alkalinity stress, the structures of the gill and hepatopancreas were disorganized; however, *E. carinicauda* could still maintain vital signs. Transcriptome results showed that ATP binding protein and carbonic anhydrase played an important role in alkalinity-adaptation. At the same time, a large number of immune-related genes were up-regulated, which protect *E. carinicauda* from bacterial infection. MiRNAs also played an important role in alkalinity-adaptation. A total of 24 miRNAs were identified as differentially expressed after alkalinity stress, and up-regulated miRNAs might active the GnRH signaling pathway and accelerate the synthesis and secretion of aldosterone, which might maintain the balance of osmotic pressure in *E. carinicauda* to adapt to alkaline environment. These results provide a better understanding of the alkalinity-adaptation mechanism of economic aquatic animals and provide theoretical basis for breeding in the future.

Keywords: alkalinity stress, *Exopalaemon carinicauda*, microRNA, adaptation mechanism, aquaculture

INTRODUCTION

Saline-alkali water is distributed all over the world with high alkalinity, high salinity, high pH, and complex ion composition. There were 45.87 million hm^2 of saline-alkali water in China, which is distributed across 19 provinces and autonomous regions. Generally, most aquatic animals cannot grow and reproduce in saline-alkali water, which makes saline-alkali waters a global low-yielding

water resource, which greatly hinders the utilization of saline-alkali water resources. In order to make the best use of saline-alkali water resources, an increasing amount of saline-alkali water has been used for fisheries. To date, underground brackish water, brackish water, and surface brackish water have been used for aquaculture of prawns, freshwater fish, sea cucumbers, and flatfish in China's Yellow River Delta, Liao River Delta, Hebei, Tianjin, Jilin, Inner Mongolia, and other inland saline-alkali water areas. To effectively use saline-alkali water resources, it is urgent to breed more saline-alkali-resistant aquaculture species and study the saline-alkali stress mechanism of aquatic organisms.

Exopalaemon carinicauda, an important economic shrimp in China, has great adaptive capacity to extreme environments, especially for pH and carbonate alkalinity (Xu et al., 2010; Liu et al., 2018; Ge et al., 2019), and has been recognized as an excellent model for both physiological and evolutionary studies of saline-alkali adaptation in crustaceans. At present, *E. carinicauda* has been successfully cultivated in coastal saline-alkali waters in Cangzhou, Hebei Province (approximate carbonate alkalinity 3.5–13.0 mmol/L, salinity 5-15, pH 8.3–9.2) and Dongying, Shandong province (approximate carbonate alkalinity 1.4–8.0 mmol/L, salinity 5–8, pH 8.5–10.0). However, the mechanism of alkalinity tolerance in *E. carinicauda* remained unknown. To date, comparative transcriptome studies on *E. carinicauda* adapted to thermal stress and viral infection have been performed, and significant differential gene expression that encoded modulators of stress adaptation and tolerance, including heat shock proteins (e.g., heath shock protein 70, heat shock protein 90, heat shock protein 40, and heat shock protein 10), pattern recognition proteins (e.g., lectins, lipopolysaccharide β-1,3-glucan binding protein, and β-1,3-glucan binding protein), antioxidant enzymes (e.g., glutathione-*S*-transferase, glutamine synthetase, glutathione peroxidase, and copper/zinc superoxide dismutase) (Ge et al., 2017). These results revealed that there are substantial gene expression changes that allow *E. carinicauda* to adapt to extreme environments. However, the mechanism of alkalinity tolerance has remained unclear in recent years.

MicroRNAs (miRNAs) were well-studied small single-stranded RNAs that regulated gene expression by base-pairing with target mRNAs, which leaded to translational repression and exonucleolytic mRNA decay (Kim et al., 2009; Berezikov, 2011; Urbarova et al., 2018; Liu et al., 2019). MiRNAs were initially transcribed as RNA polymerase II transcripts and then processed by RNases Drosha and Dicer into precursor miRNAs and mature miRNAs, respectively (Gregory et al., 2005; Bartel, 2009). Crustacean miRNAs appeared to contain plant-like features in post-transcriptional gene silencing, and expression profiling indicated that miRNAs were involved in environmental stress and gonadal development (Moran et al., 2014; Meng et al., 2018; Liu et al., 2019). However, few studies were currently available concerning miRNAs during acute carbonate alkalinity stress in *E. carinicauda*.

High-throughput RNA sequencing was widely used to explore stress resistance mechanisms in aquatic animals (Collins et al., 2015; Hu et al., 2015; Liu et al., 2018; Chen et al., 2019; Shi et al., 2019, 2020; Zhang et al., 2019; Shang et al., 2021). Identification and characterization of the miRNAs and differentially expressed genes (DEGs) in *E. carinicauda* was an important step for a thorough understanding of the adaptation mechanism to acute carbonate alkalinity stress. In this study, we investigated the mRNA and miRNA transcriptomes from the gills of *E. carinicauda* using Illumina deep sequencing technology and found 96 and 272 DEGs after 24 h and 48 h alkalinity stress respectively. At the same time, a total of 24 miRNAs were identified as differentially expressed after alkalinity stress. This study provided a better understanding of the function of mRNA and miRNAs after acute carbonate alkalinity stress in *E. carinicauda*.

MATERIALS AND METHODS

Sampling and Histology

Two hundreds *E. carinicauda*, weighting 0.51 ± 0.18 g, were obtained from Haichen Aquaculture Co., Ltd., in Rizhao, China. Before the experiment, the prawns were acclimated at a salinity of 30 and temperature of 23 ± 0.5°C aerated seawater for one week, and 50% of the water was renewed once daily. The prawns were checked every day to confirm that no prawns died before the experiment.

During the experimental process, the carbonate alkalinity of water was maintained at 8.26 mmol/L according to previous study (Qin et al., 2021), adjusted by $NaHCO_3$, and determined by acid titration (Millero et al., 1993). The experiment involved three tanks with 30 prawns per tank (**Figure 1**). Samples were taken at 0, 24, and 48 h under stress after the carbonate alkalinity of water was adjusted to 8.26 mmol/L. At each time point, four prawns were taken from each tank, and the gill tissues were dissected and mixed into one sample. Then, all samples were rapidly frozen in liquid nitrogen and stored at −80°C until RNA extraction. Thus, nine samples were prepared for the RNA-seq experiments. At the same time, one prawn was taken from each tank at 0, 24, and 48 h, and the gill and hepatopancreas tissues were dissected and placed in 4% paraformaldehyde in PBS for gill and hepatopancreas histology for 24 h. The samples were dehydrated with ethanol (70, 90, 95, and 100%), embedded in paraffin wax serially, obtained a solid paraffin block after cooling, and sectioned at 5 μm. Then, the slide sections were stained with hematoxylin and eosin and observed using a Nikon ECLIPSE microscope (Nikon, Tokyo, Japan).

RNA Isolation, Sequencing, and Library Preparation

Total RNA was extracted from the gills using TRIzol reagent according to the manufacturer's instructions (Invitrogen, United States). A 1% agarose gel was used to detect RNA degradation and contamination. RNA purity was determined using a NanoPhotometer® spectrophotometer (Implen, CA, United States). RNA concentration was measured using a Qubit® 2.0 fluorometer (Life Technologies, CA, United States) using the Qubit® RNA detection kit. RNA Nano 6000 detection kit from Agilent Bioanalyzer 2100 System (Agilent Technologies, CA, United States) was used to assess RNA integrity.

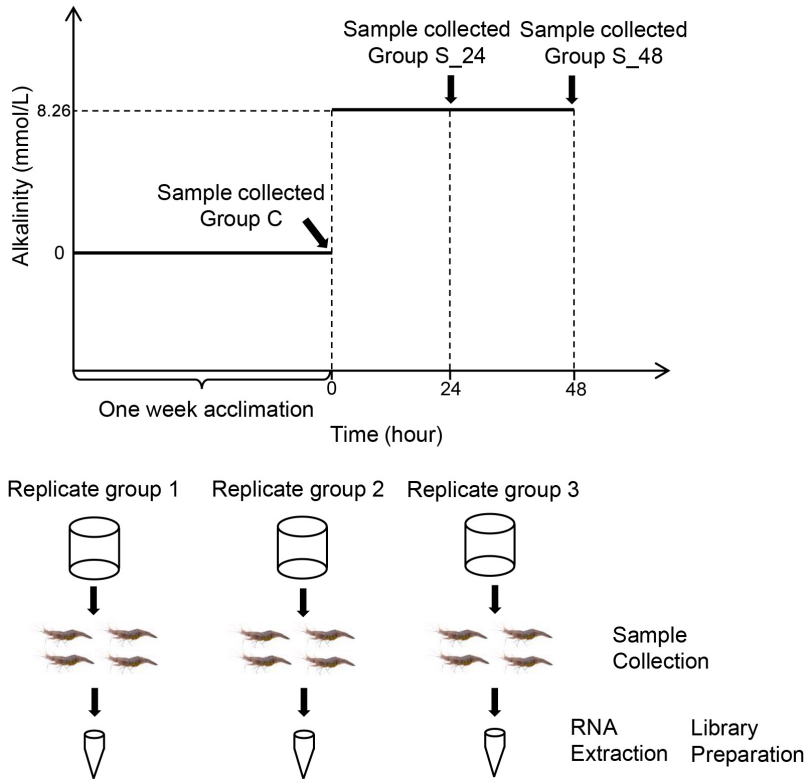

FIGURE 1 | Schematic representation of the acute saline-alkali stress experiment and sample collection, the saline-alkali stress concentration as 10 mmol/L. Samples were collected before the experiment (control group), at 24 h (24 h of saline-alkali stress), and at 48 h (48 h of saline-alkali stress).

The sequencing library was generated using the NEB Next® Ultra™ RNA Library Preparation Kit from Illumina® (NEB, Boston, MA, United States), as recommended by the manufacturer. The mRNA and sRNA-seq libraries were sequenced on an Illumina Novae 6000 and were constructed according to the manuals provided by Illumina by Neogene Company (Beijing, China). Library quality was assessed on an Agilent Bioanalyzer 2100 (Agilent Technologies, CA, United States) using DNA High Sensitivity Chips. All original transcriptome data were deposited in the National Center for Biotechnology Information (NCBI), with the accession number PRJNA782370.

Bioinformatic Analysis

The initial raw reads for Illumina sequencing were filtered to remove adaptor sequences and low-quality reads, and Q20, Q30, and GC content were calculated. All downstream analyses were based on high-quality, clean reads. The clean reads of each RNA-seq library were aligned to the reference transcriptome in a previous study using STAR (version 2.5.0b) to obtain a perfect match and only one mismatch read for further annotation and analysis. The false discovery rate (FDR)-corrected P value was corrected using the EBseq package version 1.24.0, and corrected P value < 0.05, and $|\log_2(\text{fold change})| \geq 1$ was set as the threshold for significant differential expression.

Gene ontology (GO) function and KEGG pathway enrichment analyses were performed on all DEGs in each comparison using the R packages of GOseq and KOBAS software version 3.3.0. Only the GO terms and KEGG pathways were identified as highly expressed in DEGs with the corrected P value < 0.05.

All clean reads were searched against the Rfam and GenBank databases to exclude rRNAs, tRNAs, snRNAs, and snoRNAs. The distribution of small RNA read lengths was determined and reads within the range of 18–35 nt were selected for the following analysis. Then, the conserved miRNAs were identified using the miRBase database (version 21.0[1]). Additionally, the Mirdeep2 software tool was used to analyze potential novel miRNAs (Friedlnder et al., 2012).

The sequences over the length of 18 bp were submitted to Mirdeep2 to get the mapping sequences for further analysis. To obtain the differentially expressed miRNAs between samples, the expression levels of miRNAs were normalized as previously described (Liu et al., 2019). Audic-Claverie was used to analyze differentially expressed miRNAs (DEMs) among libraries (Tiňo, 2009). The criteria for significant expression were defined as $P < 0.05$, and transcripts per million > 2.

ORF Finder[2] was used to identify the 5′ UTR, 3′ UTR, and protein-coding regions. Potential target genes of the

[1]http://www.mirbase.org/

[2]https://www.ncbi.nlm.nih.gov/orffinder/

DEMs were analyzed using Miranda software ($S \geq 150$, $\Delta G \leq -30$ kcal/mol) using 3′UTR data extracted from the transcriptomes of *E. carinicauda* (John et al., 2004). In addition, GO enrichment analysis (corrected P value < 0.05) and KEGG pathway analysis ($P < 0.05$) were conducted to categorize the function and to analyze the pathway of putative target genes of DEMs.

Quantitative Real-Time-PCR Analysis

To further validate our DEG library, qRT-PCR analysis was performed on RNA samples originally used for transcriptome sequencing. Six genes with large expression differences were selected, including acetaldehyde dehydrogenase (ALDH), ATP citrate lyase (ACL), actin (ACT), sarcoplasmic reticulum Ca^{2+}-ATP enzyme (SER2a), blood coagulating protein (BC), DEAD-box (DEA), and Premier v5 (Premier Biosoft International, Palo Alto, CA, United States) to design specific primer pairs. The first strand of cDNA was synthesized from 1 mg of RNA using the Prime-Script^{TM} RT Reagent Kit with gDNA Eraser (Takara, Japan). qPCR was performed using SYBR Premix Ex Taq (TaKaRa, Japan) on the ABI PRISM 7500 Sequence Detection system (Applied Biosystems, United States) according to the manufacturer's instructions, and, 18s rRNA (GenBank accession number: GQ369794) was used to detect the expression level of genes, and all experiments were repeated three times (Ge et al., 2017). The PCR program was set at 95°C for 30 s, then 40 cycles of 95°C for 5 s and 60°C for 34 s, followed by 1 cycle of 95°C for 15 s, 60°C for 1 min, and 95°C for 15 s. The fold change in target gene expression level was calculated using a relative quantitative method. Data were statistically analyzed using SigmaStat software (Jandel Scientific, San Rafael, CA, United States). One-way analyses of variance were assessed between-group comparisons, followed by Student-Newman-Keuls tests. Values with $P < 0.05$ were considered statistically significant.

RESULTS

Gill and Hepatopancreas Morphology

The results of hematoxylin-eosin staining of gill and hepatopancreas sections from *E. carinicauda* are shown in **Figure 2**. Normal gill tissue of the *E. carinicauda* was phyllodes, the gill filaments were arranged in order with clear structure, the cuticle was smooth and flat, and the epithelial cells were regular, the gap at the end of branchial filament was flat or round, and there were blood cells in the microvasculature (**Figure 2A**). After 24 h of alkalinity stress, the gill filaments were enlarged, the cuticle was deformed, and the space under the cuticle was expanded. At the same time, the epithelial cells were damaged and the number of blood cells were decreased (**Figure 2B**). After 48 h of alkaline stress, the gill filaments were arranged disorderly, the cuticle and epithelial cells were necrotic and exfoliated, the space under the stratum corneum was seriously deformed, and the structure of the capillary network was ruptured (**Figure 2C**). The hepatopancreatic tissues of *E. carinicauda* showed that normal hepatopancreatic cells were closely packed and structurally intact with small vacuoles (**Figure 2D**). After 24 h of alkaline stress, the hepatopancreas was loosely arranged, and the vacuoles were enlarged (**Figure 2E**). After 48 h of alkaline stress, the vacuoles in the hepatopancreas was enlarged and the hepatopancreas cells lost its basic structure (**Figure 2F**).

Raw Sequencing Data and Quality Statistics

To identify the differences in gene expression of *E. carinicauda* after exposure to alkalinity stress, nine cDNA libraries were constructed using the Illumina HiSeq 4000 sequencing platform. A total of 543,504,644 clean reads filtered from 54,547,064 paired-end raw reads were identified, with Q30 (%) above 93.74% (**Supplementary Table 1**). After mapping these clean reads to

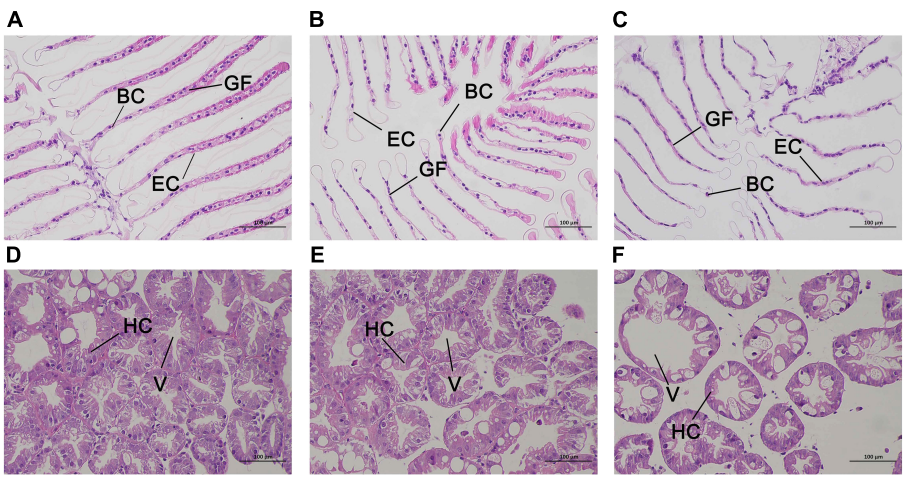

FIGURE 2 | Representative HE staining and TEM photomicrographs of *Exopalaemon carinicauda* gill **(A–C)** and hepatopancreas **(C–E)** after saline-alkali stress. Among them, panels **(A,D)** were control group, panels **(B,E)** were saline- alkali stress for 24 h, panels **(C,F)** were saline-alkali stress for 48 h. BC, blood cell; GF, gill filament; EC, epithelial cell; HC, hepatopancreatic cells; V, vacuole.

reference sequences of *E. carinicauda*, an average of 55,460,344 (63.01%), 62,453,121 (63.14%), and 63, 254, and 750 (68.37%) were found to be unique matches for groups C, S24, and S48, respectively (**Supplementary Table 2**). A total of 14,112 unigenes with a total length of 41,067,851 bp, ranging from 92 to 10,458 bp (with an average of 2,910 bp) were obtained (**Figure 3A**).

The potential functions of transcripts were annotated using BLAST against the nr databases with an E-value cutoff of $1 e^{-5}$. Of the 13, 704 transcripts, 12, 383 (90.36%) matched nr proteins, and the rest had no match (**Supplementary Table 3**). The highest matched species was *Penaeus vannamei* with 70.34% of the sequences, while only 5.87% were similar to the available *E. carinicauda* (**Figure 3B**). This result could be explained by the fact that the *P. vannamei* genome was completely sequenced (ASM378908v1).

Analysis of Differentially Expressed Genes

A total of 10,431 annotated transcripts were classified into the GO categories (**Supplementary Table 3**). The top four categories of molecular function were cellular process (32.77%), metabolic process, biological regulation, and localization (**Figure 3C**). A total of 7,788 annotated transcripts were classified into the KEGG categories (**Figure 3D** and **Supplementary Table 3**). Candidate genes involved in alkalinity stress responses were identified from DEGs that significantly enriched GO terms and KEGG pathways.

A total of 368 genes were identified as differentially expressed in pairwise comparisons (C vs. S24, and C vs. S48, $\log_2$[fold change] > 1, corrected P value < 0.05). Among all DEGs, 96 DEGs were identified after 24 h of alkaline stress; among them, 59 genes were up-regulated and 40 genes were down-regulated; 272 DEGs were identified after 48 h of alkalinity stress, among which 147 genes were up-regulated and 125 genes were down regulated (**Figure 4A**). A Venn diagram of DEGs at each time point is shown in **Figure 4B**. There were 25 genes were significantly expressed at both 24 and 48 h alkalinity stress.

Gene Ontology Analysis of Significant Differentially Expressed Genes

Differentially expressed genes were enriched in 20 GO terms after 24 and 48 h of alkalinity stress (corrected P < 0.05). Of these GO terms, hemolymph coagulation, humoral immune response, coagulation, hemostasis, and regulation of body fluid levels were significantly enriched after 24 h of alkaline stress (**Figure 4C**). Hemolymph coagulation, humoral immune response, coagulation, hemostasis, immune response, immune system process, defense response, and regulation of body fluid levels were significantly enriched after 48 h of alkaline stress (**Figure 4D**).

Computational Identification of MicroRNA From sRNA Libraries

The length distribution of the identified miRNAs showed a similar pattern, and the predominant length of miRNAs was 22 nt (**Supplementary Figure 1**). To obtain the details of the matching sRNA, all the sRNAs were compared with the sequence in the specified range of miRBase, and a total of 22 mature miRNAs and

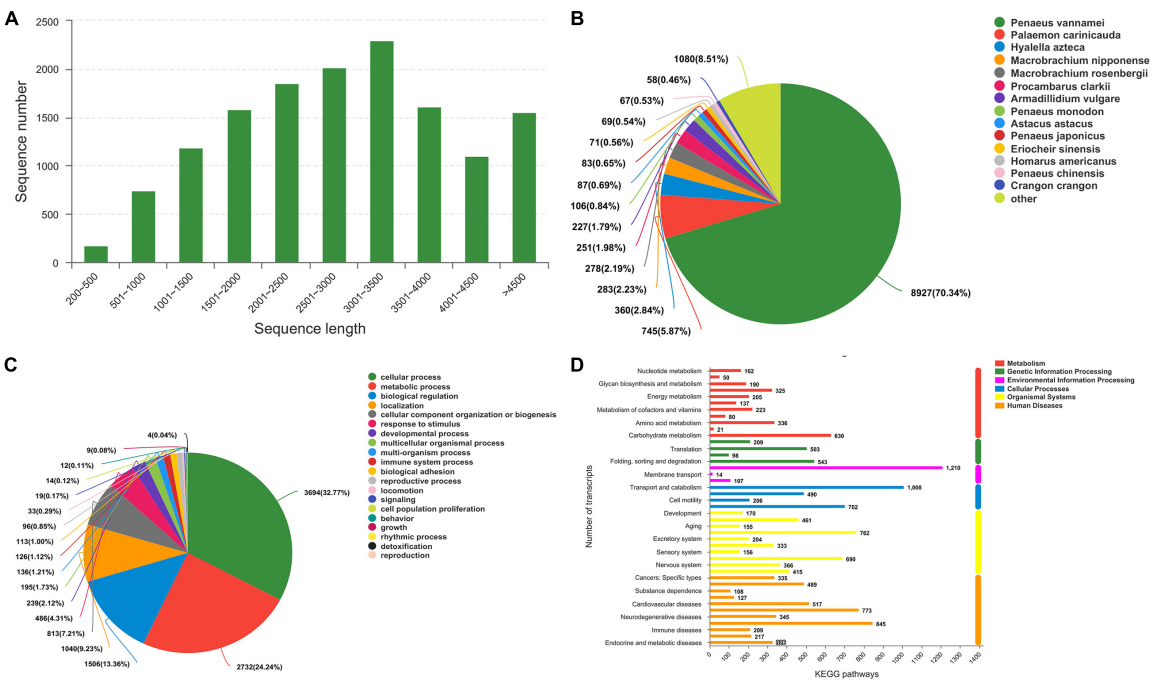

FIGURE 3 | Transcriptome sequence length distribution and annotation. **(A)** Sequence length distribution. **(B)** Species Distribution. **(C)** GO Classification_BP. **(D)** Histogram of KEGG.

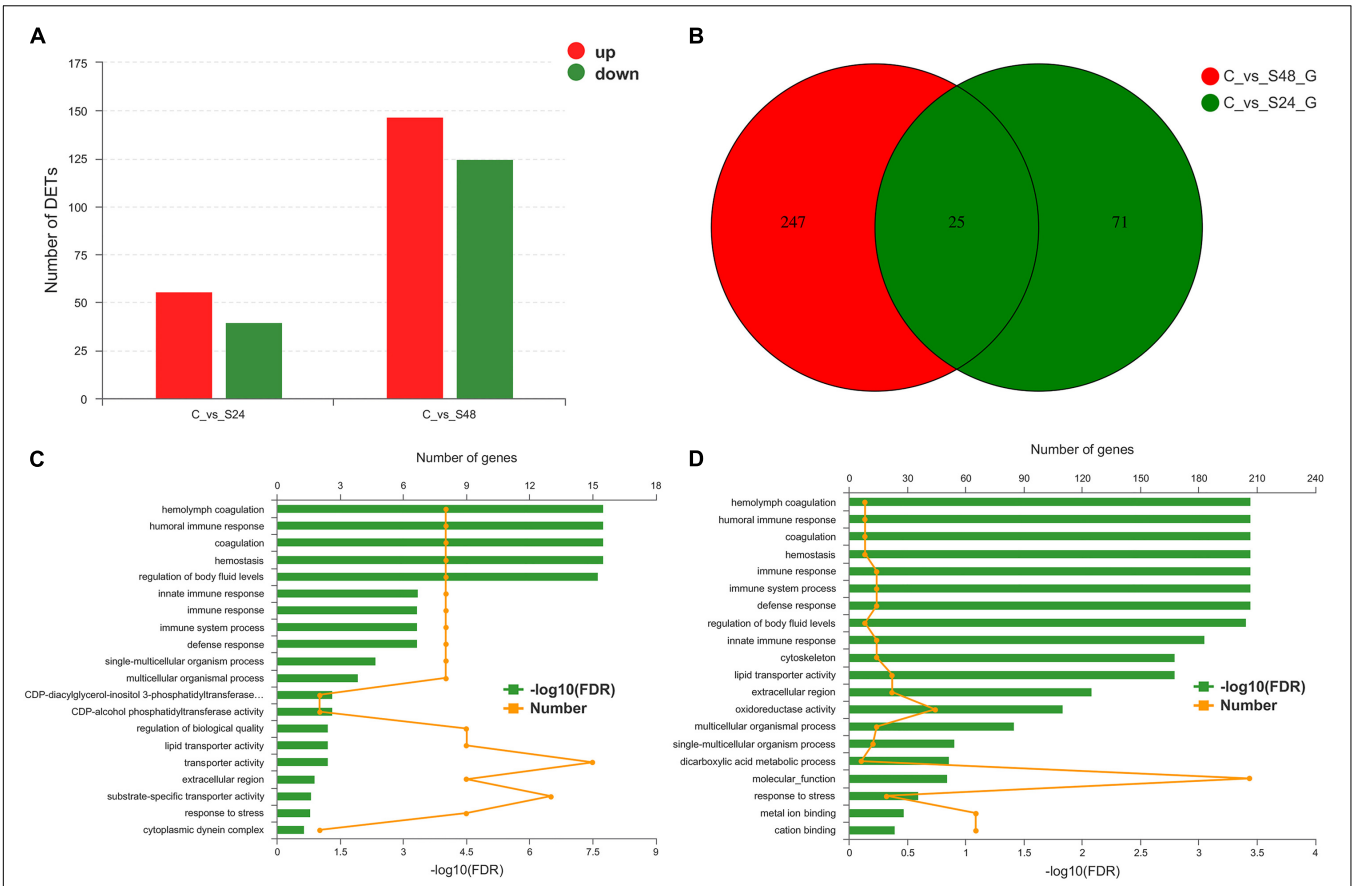

FIGURE 4 | Statistical analysis of differentially expressed genes. **(A)** Differentially expressed genes statistics in group C vs. S24 and C vs. S48 (C, control group; S24, acute saline-alkali stress for 24 h; S48 acute saline-alkali stress for 48 h). **(B)** DEGs number and Venn diagram of overlap of the different group. **(C,D)** The most enriched Gene Ontology (GO) term analysis and function classifications of differentially expressed genes after 24 h **(C)** and 48 h **(D)** acute heat stress.

23 precursor miRNAs were obtained (**Supplementary Table 4**). All sRNAs were compared and annotated; among them, the proportion of known sRNAs in all sRNAs ranged from 16 to 50% (**Supplementary Figure 2**). Then, the distribution preferences of the bases in different locations were analyzed. Among them, most of the miRNA bases were initiated by U and ended by G (**Supplementary Figure 3**). Subsequently, the signature hairpin structure of the miRNA precursor was used to predict new miRNAs, and a total of 69 mature RNAs and 70 precursor RNAs were predicted (**Supplementary Table 5**). The expression levels of miRNAs were analyzed using miRDeep2. The top 10 expressed miRNAs are shown in **Figure 5A**, and dre-miR-100-5p had the highest expression level. Principal component analysis (PCA) showed that alkalinity stress was an effective factor for miRNA expression (**Figure 5B**).

Identification of Differentially Expressed MicroRNAs

A total of 24 miRNAs were identified as differentially expressed in pairwise comparisons (C vs. S24, and C vs. S48, $\log_2$[fold change] > 1, corrected *P* value < 0.05). Among all differentially expressed miRNAs, only 4 miRNAs were identified after 24 h of alkalinity stress; among them, three miRNAs were up-regulated and one miRNA was down-regulated; 20 DEGs were identified after 48 h of alkalinity stress, among which 13 miRNAs were up-regulated and 7 miRNAs were down regulated (**Figure 5C**). The details of the differentially expressed miRNAs are shown in **Table 1**. Among them, 11 differentially expressed miRNAs were identified. The target genes for differentially expressed miRNAs were analyzed to understand the molecular functions of miRNAs after alkaline stress. KEGG analysis results are shown in **Figures 5D,E**, where the predicted target genes of 24 differentially expressed miRNAs were involved in various pathways, among which Vitamin B6 metabolism, phenylalanine metabolism, tyrosine metabolism, methane metabolism, and monobactam biosynthesis were the top five pathways of predicted target genes after 24 h of alkalinity stress, and selenocompound metabolism was the top pathway of predicted target genes after 48 h of alkalinity stress.

Quantitative Real-Time-PCR Analysis

According to the importance of potential gene function, six DEGs (ALDH, acetaldehyde dehydrogenase; ACL, ATP citrate lyase; ACT, actin; SER2a, sarcoplasmic reticulum

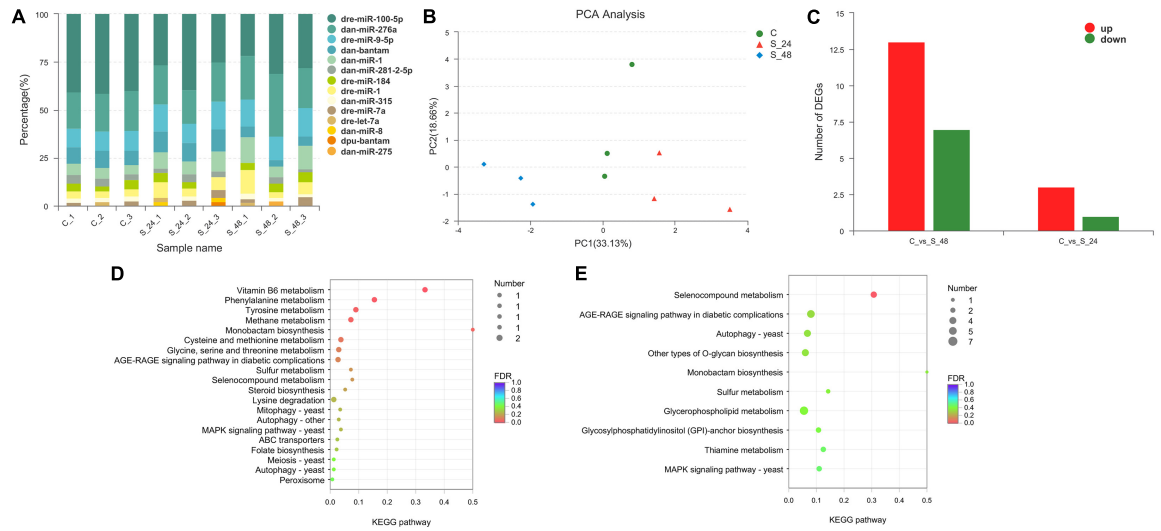

FIGURE 5 | Analysis of the miRNAs in *Exopalaemon carinicauda*. **(A)** Top10 expressed miRNAs in different experiment group. **(B)** Principal component analysis plot of the expression quality of different experiment group. The green circle showed the control group, and the red triangle showed the group after 24 h saline-alkali stress, while the blue rhombus showed the group after 48 h saline-alkali stress. **(C)** Differentially expressed miRNAs statistics in group C vs. S24 and C vs. S48 (C, control group; S24, acute saline-alkali stress for 24 h; S48 acute saline-alkali stress for 48 h). **(D)** KEGG analysis of the target genes for differentially expressed miRNAs after 24 h saline-alkali stress. **(E)** KEGG analysis of the target genes for differentially expressed miRNAs after 48 h saline-alkali stress.

Ca^{2+}-ATPase; BC, blood coagulating protein; DEA, DEAD-box) were selected for further validation using qRT-PCR. The results of quantitative real-time PCR showed that all up-regulated and down-regulated genes showed the same trend as the high-throughput sequencing data (**Figure 6**).

TABLE 1 | The detail of differentially expressed miRNAs.

miRNA name	S_48/C Significant|regulate	S_24/C Significant|regulate
NW_020872269.1_20886	Yes|up	No|up
dre-miR-1	Yes|up	No|up
NW_020872269.1_20898	Yes|up	No|up
dan-miR-276b	Yes|up	No|up
dan-miR-276a	Yes|up	No|down
dre-let-7e	Yes|up	No|up
dre-miR-9-5p	Yes|up	No|up
NW_020869651.1_8727	Yes|up	No|no change
dan-miR-1	Yes|up	No|up
dpu-miR-1	Yes|up	No|up
NW_020869557.1_8224	Yes|up	No|down
NW_020871162.1_18254	Yes|up	No|up
NW_020871162.1_18253	Yes|up	No|up
dre-miR-200b-3p	Yes|down	No|up
NW_020871955.1_20175	Yes|down	No|up
dre-let-7b	Yes|down	No|up
dre-let-7i	Yes|down	No|up
tcf-miR-193	Yes|down	No|up
dre-miR-199-3p	Yes|down	No|up
NW_020869540.1_8121	Yes|down	No|down
NW_020870701.1_15705	No|up	Yes|up
dan-miR-iab-4-5p	No|up	Yes|up
NW_020869014.1_4411	No|up	Yes|up
NW_020868837.1_3328	No|up	Yes|down

DISCUSSION

The gill and hepatopancreas are important metabolic organs of *E. carinicauda*. The main function of gill tissue is to exchange gas and maintain ionic equilibrium (Henry et al., 2012), which is vulnerable to toxic substances (Bhavan and Geraldine, 2000). The results of this study showed that the gill tissue of *E. carinicauda* was damaged under alkaline stress, the gill filaments arranged disorderly, the stratum corneum epithelial cells were necrotic and shedding, and the capillary network ruptured with increasing alkalinity stress, which seriously affected the osmotic pressure regulation function of the gill tissue and eventually resulted in the death of *E. carinicauda*. The histological lesions in gills may result of the stress within short period of time. The similar results were found that when *Chalcalburnus tarichi* migrate from alkaline water to fresh water, which indicate that these damage in gill tissue may due to the changing alkaline (Oguz, 2015). At the same time, the hepatopancreas was also damaged under alkaline stress, which influences the function of detoxification, excretion, and metabolism of *E. carinicauda* (Caceci et al., 1988). Previous study also showed the result of epithelium disorganization in the hepatopancreas tubules, and hepatopancreas cells suffer from oxidative damage with high pH stress, which indicated the stress of carbonate alkalinity might have the same mechanism with pH stress (Wang et al., 2018).

There was limited study concerning the adaptation mechanism of crustacean alkalinity in previous studies. In this study, the genes including ATP binding protein kinase

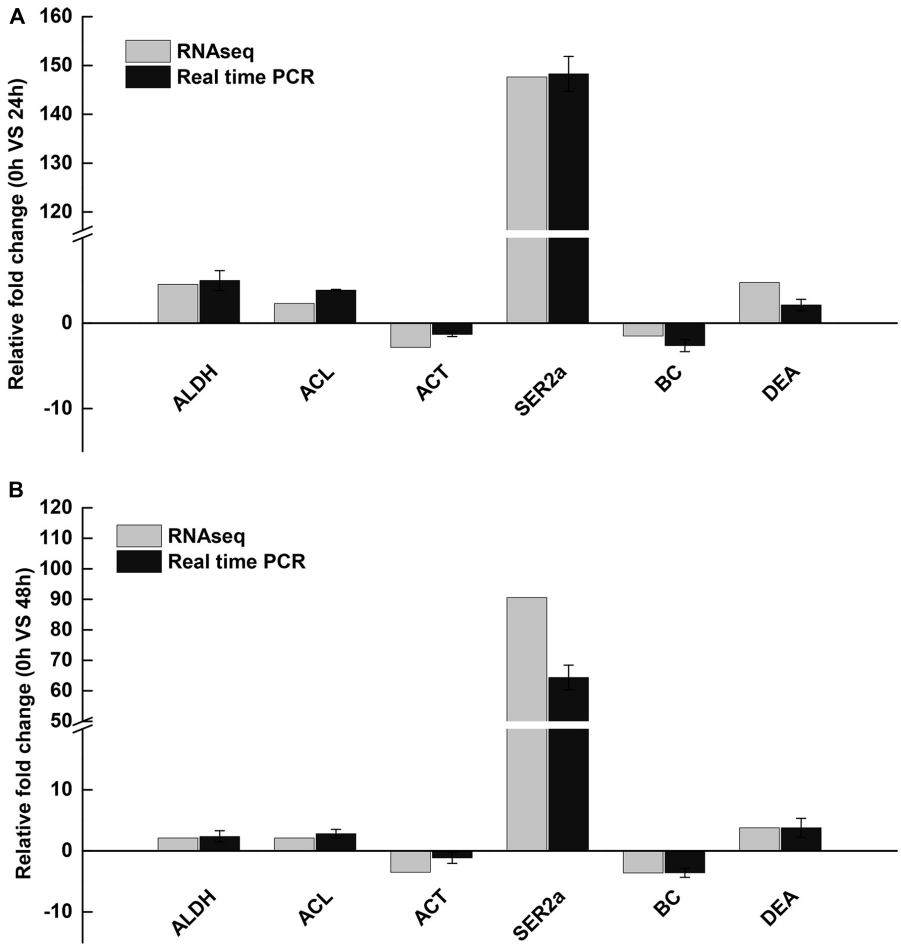

FIGURE 6 | Validation of RNA-Seq results using qRT-PCR. **(A)** 24 h saline-alkali stress, **(B)** 48 h saline-alkali stress. ALDH, acetaldehyde dehydrogenase; ACL, ATP citrate lyase; ACT, actin; SER2a, sarcoplasmic reticulum Ca^{2+}-ATPase; BC, blood coagulating protein; DEA, DEAD-box.

and carbonic anhydrase were significantly up-regulated in *E. carinicauda*, and these genes played a key role in the response to alkalinity stress in *E. carinicauda*. Carbonic anhydrase, a Zn-containing metal enzyme, played an important role in the regulation of osmotic pressure and ion transport in aquatic animals (Shang et al., 2021). The main role of carbonic anhydrase was to provide H^+ for the neutral exchange of Na^+/H^+ and participates in Cl^-/HCO_3^- transportation (Jillette et al., 2010). Ali et al. (2015) found through transcriptome sequencing that carbonic anhydrase played an important role in red crayfish after pH stress. Ge et al. (2019) found that the carbonic anhydrase gene was significantly up-regulated after pH stress in *E. carinicauda*, which proved that carbonic anhydrase played an important role in the regulation of osmotic pressure in *E. carinicauda*. At the same time, carbonic anhydrase played an important role in salinity and pH stress in previous studies on *L. vannamei* and *Portunus trituberculatus* (Liu et al., 2015; Pan et al., 2016). In this study, the up-regulated carbonic anhydrase and ATP binding protein kinase might accelerate ion excretion of *E. carinicauda*, which help *E. carinicauda* to adapt to the alkalinity environment as soon as possible.

Alkalinity stress may also affect the immune system of aquatic animals (Zhao et al., 2020). In this study, some immune-related genes, like T-cell immunomodulatory protein, HSP90, antimicrobial peptide type 2, zinc finger protein were up-regulated after alkalinity exposure. Transcriptome analysis also revealed that the NOD-receptor signaling pathway and IL-17 signaling pathway were significant enrichment after alkalinity exposure. One explanation was that the alkalinity exposure of *E. carinicauda* triggered the immune response of the prawn, and up-regulated immune-related genes to protect the prawn from infection. In addition, alkalinity exposure may affect the diet of organism and trigger the intestinal inflammation, then resulting in the change of immune network (Shang et al., 2021).

Gene ontology enrichment analysis of the DEGs of *E. carinicauda* after alkalinity stress showed that after 24 h of alkalinity stress, hemolymph coagulation, humoral immune response, hemostasis, and humoral regulation were significantly enriched, after 48 h of alkalinity stress, immune response, and

stress response were significantly enriched. Many immune-related genes of *E. carinicauda* were up-regulated after alkalinity stress, including chitinase-related protein genes and antibacterial peptides. Chitinase not only participates in molting and digestion, but also has immune functions (Gayathri et al., 2018). Antimicrobial peptides are natural antibiotics with antibacterial potential and are also used for immune regulation by activating mast cells (Amparyup et al., 2020). Zhao et al. (2020) analyzed the changes in the transcriptome of Nile tilapia under alkaline stress and found that the immune-related genes cytosolic 5-nucleotidase, L-threonine dehydrogenase, and transmembrane superfamily members were significantly up-regulated. Acute carbonate alkalinity stress breaks the balance between the individual and the environment of *E. carinicauda*, which leads to a disorder in its physiological function. Up-regulation of immune-related genes could be interpreted as an attempt to improve the immune system to adapt to highly alkaline environments, which was consistent with the results of this study (Gao et al., 2021). The results suggested that in order to maintain the stability of the internal environment and normal life activities, the over-expression of immune-related genes was a protective mechanism.

In this study, we obtained 22 known and 69 novel miRNAs using high-throughput sequencing. In these miRNAs, we focused on DEMs to determine the adaptation mechanism of *E. carinicauda*. We found that dme-mir-9a-5p and dme-mir-1-3p were up-regulated after 24 and 48 h of alkaline stress, indicating that they may be closely related to the alkalinity adaptation of *E. carinicauda*. To gain insight into the potential function of DEMs, the predicted target genes of these miRNAs were subjected to KEGG pathway analyses. KEGG enrichment analysis of the target genes of the differentially expressed miRNAs of *E. carinicauda* after alkalinity stress showed that the main enriched pathways were the cholinergic synaptic pathway, the GnRH signaling pathway, and the synthesis and secretion of aldosterone. Among them, the expression of most miRNAs was up-regulated in the synthesis and secretion pathways of aldosterone, indicating that it might be related to the alkali-tolerance mechanism of *E. carinicauda*. The main function of aldosterone is to regulate the excretion and secretion of Na^+ and K^+ and maintain the balance of osmotic pressure in the organism, which is of positive significance for *E. carinicauda* in dealing with a highly alkaline environment (Rash and Lillywhite, 2019). In addition, the GnRH signaling pathway also has a great function in the adaptation of the alkalinity environment in crustaceans. Previous studies have shown that the GnRH signaling pathway played an important role in the reproduction of *Macrobrachium rosenbergii* (Suwansa-Ard et al., 2016), *Penaeus japonicus* (Amano et al., 2009), *Penaeus monodon* (Ngernsoungnern et al., 2008), *Eriocheir sinensis* (Yuan et al., 2019) and *Procambarus clarkii* (Guan et al., 2014). Based on this, we speculate that the miRNA enriched in the aldosterone synthesis and secretion pathway in this pathway may play a key role in the alkali resistance mechanism o*f E. carinicauda*, and the specific functions need to be verified later.

CONCLUSION

Under alkaline stress, the *E. carinicauda* gill transcriptome results showed that 96 DEGs were identified after 24 h of alkaline stress and 272 DEGs were identified after 48 h of alkalinity stress. ATP binding protein, carbonic anhydrase and a large number of immune-related genes were up-regulated, which played an important role in alkalinity-adaptation of *E. carinicauda*. A total of 24 miRNAs were identified as differentially expressed after alkalinity stress, among which 11 differentially expressed miRNAs were newly discovered. Up-regulated miRNAs might active the GnRH signaling pathway and accelerate the synthesis and secretion of aldosterone, which might maintain the balance of osmotic pressure in *E. carinicauda* to adapt to alkaline environment. These results provide a better understanding of the alkalinity-adaptation mechanism of *E. carinicauda*.

DATA AVAILABILITY STATEMENT

The datasets presented in this study can be found in online repositories. The names of the repository/repositories and accession number(s) can be found below: NCBI SRA BioProject, accession no: PRJNA782370.

ETHICS STATEMENT

The animal study was reviewed and approved by Institutional Animal Care and Use Committee of Yellow Sea Fisheries Research Institute. Written informed consent was obtained from the owners for the participation of their animals in this study.

AUTHOR CONTRIBUTIONS

JnL, PL, and JtL designed the research. KS and ML conducted the experiment, preformed the statistical and bioinformatics analyses, and wrote the manuscript. KS, ML, ZQ, and JW obtained the data. All authors reviewed the manuscript.

FUNDING

This research was supported by the National Key R&D Program of China (2018YFD0901302), National Natural Science Foundation of China (32072974), China Agriculture Research System of MOF and MARA (CARS-48), and the Central Public-interest Scientific Institution Basal Research Fund, CAFS (2020TD46).

SUPPLEMENTARY MATERIAL

The Supplementary Material for this article can be found online at: https://www.frontiersin.org/articles/10.3389/fmars.2022.816932/full#supplementary-material

REFERENCES

Ali, M. Y., Pavasovic, A., Mather, P. B., and Prentis, P. J. (2015). Transcriptome analysis and characterisation of gill-expressed carbonic anhydrase and other key osmoregulatory genes in freshwater crayfish *Cherax quadricarinatus*. *Data Brief.* 5, 187–193. doi: 10.1016/j.dib.2015.08.018

Amano, M., Okumura, T., Okubo, K., Amiya, N., and Oka, Y. (2009). Biochemical analysis and immunohistochemical examination of a GnRH-like immunoreactive peptide in the central nervous system of a decapod crustacean, the kuruma prawn *(Marsupenaeus japonicus)*. *Zoolog. Sci.* 26, 840–845. doi: 10.2108/zsj.26.840

Amparyup, P., Charoensapsri, W., Samaluka, N., Chumtong, P., Yocawibun, P., and Imjongjirak, C. (2020). Transcriptome analysis identifies immune-related genes and antimicrobial peptides in Siamese fighting fish (*Betta splendens*). *Fish Shellfish Immun.* 99, 403–413. doi: 10.1016/j.fsi.2020.02.030

Bartel, D. P. (2009). MicroRNAs: target recognition and regulatory functions. *Cell* 136, 215–233.

Berezikov, E. (2011). Evolution of microRNA diversity and regulation in animals. *Nat. Rev. Genet.* 12, 846–860. doi: 10.1038/nrg3079

Bhavan, P. S., and Geraldine, P. (2000). Histopathology of the hepatopancreas and gills of the prawn *Macrobrachium malcolmsonii* exposed to endosulfan. *Aquat. Toxicol.* 50, 331–339. doi: 10.1016/s0166-445x(00)00096-5

Caceci, T., Neck, K. F., Lewis, D. D. H., and Sis, R. F. (1988). Ultrastructure of the hepatopancreas of the Pacific white shrimp, *Penaeus vannamei*. *J. Mar. Biol. Assoc. U. K.* 68, 323–337. doi: 10.1017/s002531540005222x

Chen, B. H., Xu, J., Cui, J., Pu, F., Peng, W. Z., Chen, L., et al. (2019). Transcriptional differences provide insight into environmental acclimatization in wild amur ide (*Leuciscus waleckii*) during spawning migration from alkalized lake to freshwater river. *Genomics* 111, 267–276. doi: 10.1016/j.ygeno.2018.11.007

Collins, J. E., Wali, N., Sealy, I. M., Morris, J. A., and Busch-Nentwich, E. M. (2015). High-throughput and quantitative genome-wide messenger RNA sequencing for molecular phenotyping. *BMC Genomics* 16:578. doi: 10.1186/s12864-015-1788-6

Friedlnder, M. R., Mackowiak, S. D., Li, N., Chen, W., and Nikolaus, R. (2012). miRDeep2 accurately identifies known and hundreds of novel microRNA genes in seven animal clades. *Nucleic Acids. Res.* 40, 37–52. doi: 10.1093/nar/gkr688

Gao, H., Ma, H. K., Sun, J. Q., Xu, W. Y., Gao, W., Lai, X. F., et al. (2021). Expression and function analysis of crustacyanin gene family involved in resistance to heavy metal stress and body color formation in *Exopalaemon carinicauda*. *J. Exp. Zool. Parta.* 336, 352–363. doi: 10.1002/jez.b.23025

Gayathri, R., Venkatesh, K., Arun, M., Arunkumar, D., and Aziz, A. (2018). Bactericidal and fungistatic activity of peptide derived from GH18 domain of prawn chitinase 3 and its immunological functions during biological stress. *Int. J. Biol. Macromol.* 106, 1014–1022. doi: 10.1016/j.ijbiomac.2017.08.098

Ge, Q. Q., Li, J., Wang, J. J., Li, J. T., Ge, H. X., and Zhai, Q. Q. (2017). Transcriptome analysis of the hepatopancreas in *Exopalaemon carinicauda* infected with an AHPND-causing strain of Vibrio parahaemolyticus. *Fish Shellfish Immunol.* 67, 620–633. doi: 10.1016/j.fsi.2017.06.047

Ge, Q. Q., Li, J., Wang, J. J., Li, Z., and Li, J. (2019). Characterization, functional analysis, and expression levels of three carbonic anhydrases in response to pH and saline-alkaline stresses in the ridgetail white prawn *Exopalaemon carinicauda*. *Cell Stress Chaperones* 24, 503–515. doi: 10.1007/s12192-019-00987-z

Gregory, R. I., Chendrimada, T. P., Cooch, N., and Shiekhattar, R. (2005). Human RISC couples microRNA biogenesis and posttranscriptional gene silencing. *Cell* 123, 631–640. doi: 10.1016/j.cell.2005.10.022

Guan, Z. B., Shui, Y., Liao, X. R., Xu, Z. H., and Zhou, X. (2014). Primary structure of a novel gonadotropin-releasing hormone in the ovary of red swamp crayfish *Procambarus clarkii*. *Aquaculture* 418, 67–71. doi: 10.1016/j.aquaculture.2013.10.010

Henry, R. P., Lucu, C., Onken, H., and Weihrauch, D. (2012). Multiple functions of the crustacean gill: osmotic/ionic regulation, acid-base balance, ammonia excretion, and bioaccumulation of toxic metals. *Front. Physiol.* 3:431. doi: 10.3389/fphys.2012.00431

Hu, D. X., Pan, L. Q., Zhao, Q., and Ren, Q. (2015). Transcriptomic response to low salinity stress in gills of the Pacific white shrimp, *Litopenaeus vannamei*. *Mar. Genom.* 24, 297–304. doi: 10.1016/j.margen.2015.07.003

Jillette, N., Cammack, L., Lowenstein, M., and Henry, R. P. (2010). Down-regulation of activity and expression of three transport-related proteins in the gills of the euryhaline green crab, *Carcinus maenas*, in response to high salinity acclimation. *Comp. Pestic. Biochem. Phys.* 158, 189–193. doi: 10.1016/j.cbpa.2010.10.024

John, B., Enright, A. J., Aravin, A., Tuschl, T., Sander, C., and Marks, D. S. (2004). Human MicroRNA Targets. *PLoS Biol.* 2:e363. doi: 10.1371/journal.pbio.0020363

Kim, V. N., Han, J., and Siomi, M. C. (2009). Biogenesis of small RNAs in animals. *Nat. Rev. Mol. Cell. Biol.* 10, 126–139. doi: 10.1038/nrm2632

Liu, M., Liu, S., Hu, Y., and Pan, L. (2015). Cloning and expression analysis of two carbonic anhydrase genes in white shrimp *Litopenaeus vannamei*, induced by pH and salinity stresses. *Aquaculture* 448, 391–400. doi: 10.1016/j.aquaculture.2015.04.038

Liu, X., Luo, B. Y., Feng, J. B., Zhou, L. X., Ma, K. Y., and Qiu, G. F. (2019). Identification and profiling of microRNAs during gonadal development in the giant freshwater prawn *Macrobrachium rosenbergii*. *Sci. Rep U. K.* 9, 2406. doi: 10.1038/s41598-019-38648-x

Liu, Y., Xin, Z. Z., Song, J., Zhu, X. Y., Liu, Q. N., Zhang, D. Z., et al. (2018). Transcriptome analysis reveals potential antioxidant defense mechanisms in *Antheraea pernyi* in response to zinc stress. *J. Agr. Food. Chem.* 66, 8132–8141. doi: 10.1021/acs.jafc.8b01645

Meng, X. L., Zhang, X. H., Li, J., and Liu, P. (2018). Identification and comparative profiling of ovarian and testicular microRNAs in the swimming crab *Portunus trituberculatus*. *Gene* 640, 6–13. doi: 10.1016/j.gene.2017.10.026

Millero, F. J., Zhang, J. Z., Lee, K., and Campbell, D. M. (1993). Titration alkalinity of seawater. *Mar. Chem.* 44, 153–165. doi: 10.1016/0304-4203(93)90200-8

Moran, Y., Fredman, D., Praher, D., Li, X. Z., Wee, L. M., Rentzsch, F., et al. (2014). Cnidarian microRNAs frequently regulate targets by cleavage. *Genome Res.* 24, 651–663. doi: 10.1101/gr.162503.113

Ngernsoungnern, P., Ngernsoungnern, A., Kavanaugh, S., Sobhon, P., Sower, S. A., and Sretarugsa, P. (2008). The presence and distribution of gonadotropin-releasing hormone-liked factor in the central nervous system of the black tiger shrimp, *Penaeus monodon*. *Gen. Comp. Endocr.* 155, 613–622. doi: 10.1016/j.ygcen.2007.08.012

Oguz, A. R. (2015). Histological changes in the gill epithelium of endemic Lake Van Fish (*Chalcalburnus tarichi*) during migration from alkaline water to freshwater. *North West J. Zool.* 11, 51–57.

Pan, L., Hu, D., Liu, M., and Hu, Y. (2016). Molecular cloning and sequence analysis of two carbonic anhydrase in the swimming crab *Portunus trituberculatus* and its expression in response to salinity and pH stress. *Gene* 576, 347–357. doi: 10.1016/j.gene.2015.10.049

Qin, Z., Ge, Q. Q., Wang, J. J., Li, M. D., Liu, P., Li, J., et al. (2021). Comparative transcriptomic and proteomic analysis of *Exopalaemon carinicauda* in response to alkalinity stress. *Front. Mar. Sci.* 8:759923. doi: 10.3389/fmars.2021.759923

Rash, R., and Lillywhite, H. B. (2019). Drinking behaviors and water balance in marine vertebrates. *Mar. Biol.* 166:122.

Shang, X. C., Geng, L. W., Yang, J., Zhang, Y. T., and Xu, W. (2021). Transcriptome analysis reveals the mechanism of alkalinity exposure on spleen oxidative stress, inflammation and immune function of *Luciobarbus capito*. *Ecotoxicol. Environ. Saf.* 225:112748. doi: 10.1016/j.ecoenv.2021.112748

Shi, K. P., Dong, S. L., Zhou, Y. G., Li, Y., Gao, Q. F., and Sun, D. J. (2019). RNA-seq reveals temporal differences in the transcriptome response to acute heat stress in the Atlantic salmon (*Salmo salar*). *Comp. Biophys. D* 30, 169–178. doi: 10.1016/j.cbd.2018.12.011

Shi, K. P., Li, J. T., Lv, J. J., Liu, P., Li, J., and Li, S. D. (2020). Full-length transcriptome sequences of ridgetail white prawn *Exopalaemon carinicauda* provide insight into gene expression dynamics during thermal stress. *Sci. Total. Environ.* 747:141238. doi: 10.1016/j.scitotenv.2020.141238

Suwansa-Ard, S., Zhao, M., Thongbuakaew, T., Chansela, P., Ventura, T., Cummins, S. F., et al. (2016). Gonadotropin-releasing hormone and adipokinetic hormone/corazonin-related peptide in the female prawn. *Gen. Comp. Endocr.* 236, 70–82. doi: 10.1016/j.ygcen.2016.07.008

Tiňo, P. (2009). Basic properties and information theory of Audic-Claverie statistic for analyzing cDNA arrays. *BMC Bioinformatics* 10:310. doi: 10.1186/1471-2105-10-310

Urbarova, I., Patel, H., Foret, S., Karlsen, B. O., Jorgensen, T. E., Hall-Spencer, J. M., et al. (2018). Elucidating the small regulatory RNA repertoire of the sea

anemone *Anemonia viridis* based on whole genome and small RNA sequencing. *Genome Biol. Evol.* 10, 410–426. doi: 10.1093/gbe/evy003

Wang, Z., Cai, C. F., Cao, X. M., Zhu, J. M., He, J., Wu, P., et al. (2018). Supplementation of dietary astaxanthin alleviated oxidative damage induced by chronic high pH stress, and enhanced carapace astaxanthin concentration of Chinese mitten crab *Eriocheir sinensis*. *Aquaculture* 483, 230–237. doi: 10.1016/j.aquaculture.2017.10.006

Xu, W. J., Xie, J. J., Shi, H., and Li, C. W. (2010). Hematodinium infections in cultured ridgetail white prawns, *Exopalaemon carinicauda*, in eastern China. *Aquaculture* 300, 25–31.

Yuan, L. J., Peng, C., Liu, B. H., Feng, J. B., and Qiu, G. F. (2019). Identification and characterization of a luteinizing hormone receptor (LHR) homolog from the Chinese Mitten Crab *Eriocheir sinensis*. *Int. J. Mol. Sci.* 20:1736.

Zhang, Y., Li, Z. Y., Kholodkevich, S., Sharov, A., Feng, Y. J., Ren, N. Q., et al. (2019). Cadmium-induced oxidative stress, histopathology, and transcriptome changes in the hepatopancreas of freshwater crayfish (*Procambarus clarkii*). *Sci. Total Environ.* 666, 944–955. doi: 10.1016/j.scitotenv.2019.02.159

Zhao, Y., Zhang, C., Zhou, H., Song, L., Wang, J., and Zhao, J. (2020). Transcriptome changes for Nile tilapia (*Oreochromis niloticus*) in response to alkalinity stress. *Comp. Biochem. Physiol. Part D Genom. Proteom.* 33:100651. doi: 10.1016/j.cbd.2019.100651

Conflict of Interest: The authors declare that the research was conducted in the absence of any commercial or financial relationships that could be construed as a potential conflict of interest.

Publisher's Note: All claims expressed in this article are solely those of the authors and do not necessarily represent those of their affiliated organizations, or those of the publisher, the editors and the reviewers. Any product that may be evaluated in this article, or claim that may be made by its manufacturer, is not guaranteed or endorsed by the publisher.

frontiers in Marine Science

ORIGINAL RESEARCH
published: 11 February 2022
doi: 10.3389/fmars.2022.817868

Aquaporins in Pacific White Shrimp (*Litopenaeus vannamei*): Molecular Characterization, Expression Patterns, and Transcriptome Analysis in Response to Salinity Stress

Zhongkai Wang, Yigeng Chen, Cong Wang, Nannan Zhao, Zhihao Zhang, Zhitong Deng, Yanting Cui, Renjie Wang and Yuquan Li**

School of Marine Science and Engineering, Qingdao Agricultural University, Qingdao, China

OPEN ACCESS

Edited by:
Yangfang Ye,
Ningbo University, China

Reviewed by:
Mengqiang Wang,
Ocean University of China, China
Zhenlu Wang,
Guizhou University, China
Xiaoxi Zhang,
Institute of Oceanology, Chinese Academy of Sciences (CAS), China

***Correspondence:**
Zhongkai Wang
zkwang@qau.edu.cn
Yuquan Li
jiangfangqian@163.com

Specialty section:
This article was submitted to Marine Fisheries, Aquaculture and Living Resources, a section of the journal Frontiers in Marine Science

Received: *18 November 2021*
Accepted: *24 January 2022*
Published: *11 February 2022*

Citation:
Wang Z, Chen Y, Wang C, Zhao N, Zhang Z, Deng Z, Cui Y, Wang R and Li Y (2022) Aquaporins in Pacific White Shrimp (Litopenaeus vannamei): Molecular Characterization, Expression Patterns, and Transcriptome Analysis in Response to Salinity Stress. Front. Mar. Sci. 9:817868. doi: 10.3389/fmars.2022.817868

Aquaporins (AQPs) are integral membrane proteins that facilitate the transport of water and small solutes across cell membranes. These proteins are vital for maintaining water homeostasis in living organisms. In mammals, thirteen aquaporins have been characterized, but in crustaceans, especially penaeid shrimp, the diversity, structure, and substrate specificity of these membrane channel proteins are largely unknown. We here presented the three types of AQPs from *Litopenaeus vannamei* based on genome and transcriptome sequencing. Phylogenetic analysis showed that each AQP separately represented members of aquaglyceroporins, classical aquaporins, and unorthodox aquaporins, thus they were named as LvAQP3, LvAQP4, and LvAQP11. The *LvAqp4* was mostly expressed in hepatopancreas, stomach, and gill, meanwhile *LvAqp3* and *LvAqp11* were separately predominantly expressed in intestine and muscle, respectively. To investigate possible roles of aquaporins in osmoregulation, mRNA expression changes in mainly expressed tissues were analyzed after acute exposure or long-term acclimation to different salinities. The results revealed that the expression levels of aquaporins genes were significantly decreased in most tissues (except hepatopancreas) under salinity stress, though the expression patterns were variable among isoforms and tissues. Moreover, comparative transcriptome analysis indicated the combination roles of aquaglyceroporin and amino acid metabolism related genes and pathways in response to acute salinity changes in the intestine. This study opened new windows for future investigations and provided new insights into the role of aquaporins in osmoregulation in *L. vannamei*.

Keywords: aquaporin, aquaglyceroporin, salinity, osmoregulation, shrimp

INTRODUCTION

Aquaporins (AQPs), also referred to as Major Intrinsic Proteins (MIPs), are small transmembrane channel proteins that mainly facilitate water and solute permeation across cellular membranes and have been identified in organisms spanning all kingdoms of life (Abascal et al., 2014; Finn and Cerdà, 2015). AQPs present as tetramers in cell membranes, and each monomer forms a

pore composed of six transmembrane domains (TMDs) connected by five loops (two intracellular and three extracellular), with the N- and C-termini facing the cytoplasm (Bienert et al., 2012). The pore is regulated by two conserved selectivity filters. One is formed by two asparagine-proline-alanine (NPA) motifs that establish hydrogen bonds with the water molecule and create an electrostatic repulsion of protons (Murata et al., 2000; Sui et al., 2001). The other selectivity filter is aromatic/arginine (Ar/R) domain, which usually consists of four amino acids including an aromatic amino acid and an arginine, creating the narrowest section of the pore and recognize diverse substrates (Fu et al., 2000). Extensive studies have reported the involvement of AQPs in various physiological processes in animals. To date, 12–15 mammalian AQPs have been identified to cluster into 13 subfamilies (AQP0–12) and divide into three groups according to their selective permeability and tertiary structure: the classical AQPs (AQP0, 1, 2, 4, 5, 6, and 8) that are considered primarily selective to water, the aquaglyceroporins (AQP3, 7, 9, and 10), which mediate the transport of glycerol, urea, and other small non-charged solutes beside water due to their larger pore size, and the unorthodox AQPs (also called superaquaporins) (AQP11 and 12), the pore selectivity and function of which are still under investigation (Benga, 2012; Ishibashi et al., 2017). Crustaceans represent another excellent animal models for investigating the regulation of AQPs expression due to their wide distribution in waters of different salinities, including freshwater, marine, estuarine, and intertidal habitats with some decapod species able to move among ecotypes within their own life times (Zhang et al., 2019; Cui et al., 2021). Therefore, efficient osmoregulation is the main physiological mechanism that maintains the hydromineral homeostasis of these animals. In decapods, the roles of ion transporters and ion channels in coping with environmental stressors are heavily studied, such as V-type H^+ ATPase, Na^+/K^+-ATPase, Na^+ channel, Na^+-K^+-$2Cl^-$ cotransporter, and Cl^-/HCO_3^- exchanger (McNamara and Faria, 2012; Thabet et al., 2017). Nevertheless, studies focusing on the function of AQPs in responses to osmotic challenge were only carried out in limited crustacean species (Gao, 2009; Chung et al., 2012; Boyle et al., 2013; Foguesatto et al., 2017, 2019; Moshtaghi et al., 2018).

The Pacific white shrimp (*Litopenaeus vannamei*) is one of the most important farmed penaeid shrimps in the world. As a typical euryhaline penaeid species with strong osmoregulatory capacity, *L. vannamei* can inhabit waters of salinity around 0.5–78 (Zhang et al., 2019; Li et al., 2020). Nowadays, it has become not only an emerging aquaculture species in low-salinity water in inland but also a popular cultivar in high-salinity water (40–70‰) along the coast of Shandong province in China (Cheng et al., 2006; Shen et al., 2020). Thus, it can serve as a good model to investigate salinity adaptation mechanisms of euryhaline crustaceans. However, extensive studies on the salinity adaptation of *L. vannamei* also mainly focusing on the function of ion transporters and ion channels in osmoregulation (Pan et al., 2014; Liu M. et al., 2015). Therefore, many aspects regarding the functions and osmoregulation of aquaporins remain to be elucidated in *L. vannamei*. In addition, several studies have used transcriptomic and proteomic approaches to reveal the involvement of genes and pathways during the osmoregulation in the gill, hepatopancreas, and muscle of *L. vannamei* (Chen et al., 2015; Hu et al., 2015; Wang et al., 2015; Xu et al., 2017; Li et al., 2020). Beyond that, the intestine of crustaceans is also an osmoregulatory organ responsible for regulating the flow of water and ions (Croghan, 1958; McGaw and Curtis, 2013). Nonetheless, few studies have explored the pathways and genes that are required for the osmoregulation in the intestine of *L. vannamei* under salinity stress.

The current study is aimed at investigating the putative roles of AQPs in the salinity adaption of *L. vannamei*. We first screened putative *Aqp* genes based on genome and transcriptome data and provided the expression profiles of *Aqp* mRNAs in different tissues. To further clarify the responses of AQPs to salinity stress, their expression changes under salinity stress were detected in tissues with higher *Aqp* expression levels. Moreover, we employed high-throughput RNA sequencing (RNA-seq) technology to examine transcriptomic responses of the intestine from shrimp exposed to acute salinity stress. This study provided valuable information for understanding the mechanism of AQPs in osmoregulation in decapod shrimps and highlighted the genes and pathways related to salinity stress in the intestine of *L. vannamei*.

MATERIALS AND METHODS

Experimental Maintenance of *L. vannamei*

Juvenile shrimp (3.0 ± 0.5 g; 8.6 ± 0.3 cm) were obtained from a farm in Binzhou, China. They were transported to the School of Marine Science and Engineering, Qingdao Agricultural University. The shrimp were acclimated to laboratory culture conditions in plastic tanks (200 L) containing aerated natural seawater (salinity 30‰, pH 8.0) at 28 ± 0.5°C for 10 days. They were fed four times a day (8:30, 13:00, 18:00, and 22:30) with dry pellets. Dissolved oxygen was maintained above 6.0 mg/L. The culture water was exchanged at a daily rate of 1/3 tank volume. The feces and uneaten feed were removed daily with a siphon tube. All treatments in this study were strictly in accordance with the guidelines of the Animal Experiment Ethics Committee of Qingdao Agriculture University, which also approved the protocol.

Salinity Exposure Experiments and Tissue Sampling

Before the salinity exposure experiment, six individuals acclimated at 30‰ salinity were randomly selected as the control group (CTR) and different tissues (intestine, hepatopancreas, muscle, epidermis, gill, and stomach) were dissected, flash frozen in liquid nitrogen, and kept in -80°C for further analysis.

For the acute salinity exposure experiment, 180 shrimps were divided into two groups (90 shrimp per group) and each group had three replicates (30 shrimp per replicate). Then, the two groups were directed transferred from natural seawater of 30‰ salinity to artificial seawater of 10 or 50‰ salinity. The pH (pH 8.0) and water temperature (28 ± 0.5°C) of the artificial

seawater was set consistently with the natural seawater during the experimental period. Six shrimp (2 shrimp/replicate × 3 replicates) per group were randomly selected and the tissues described above were sampled at 2, 4, 8, 12, and 24 h (hours) after salinity challenge, respectively.

For the long-term salinity stress experiment, 480 shrimp were also randomly divided into two groups, which were separately acclimated from natural seawater of 30 to 50‰ through daily four increments in salinity by the addition of artificial high-salinity seawater and from 30 to 10‰ through daily four decrements in salinity by the addition of freshwater. Each group had 240 shrimp with three biological replicates (each replicate having 80 individuals). All treatment groups reached the experimental salinity on the fifth day (5 d) after salinity challenge. The pH and water temperature of the high- or low-salinity seawater were kept constant as described above. Six shrimp (2 shrimp/replicate × 3 replicates) per treatment were sampled at 5, 15, 25, and 35 days after salinity challenge, respectively.

RNA Extraction and cDNA Synthesis

Total RNA was extracted from the sampled tissues by using TRIzol Reagent (Vazyme, China). The purity and concentration of the extracted RNA were determined by OD260/OD280 value obtained with a NanoDrop 2000 spectrophotometer (Thermo Fisher Scientific, United States). RNA integrity was checked on a 1% agarose gel. RNA samples of the two individuals per replicate were pooled together in equal amounts to generate one mixed sample for each replicate and three mixed samples for each group. Then, first-strand cDNA was generated from 1 μg mixed RNA of each replicate with PrimeScript^{TM} RT Reagent Kit with gDNA Eraser (Vazyme, China).

Identification of *LvAqp* Genes

Unigenes annotated as AQPs were first identified by screening the previously generated Illumina transcriptome (SRA accession No. PRJNA649598) from our laboratory using human and *Drosophila* AQPs as the query sequences. Then, amplification primers were designed to verify the open reading frames (ORFs) (**Supplementary Table 1**). The complete coding regions of the *LvAqp* genes were amplified and Sanger-sequenced. The gene structures of *LvAqp* were further analyzed based on the genome of *L. vannamei* database using the BLASTX and BLASTN program[1] and illustrated by IBS software (Liu W. et al., 2015).

Bioinformatics Analysis of *LvAqp* Genes

For the naming process of the *L. vannamei* AQPs (LvAQPs), phylogenetic trees were generated by the maximum likelihood method with 1,000 bootstrap replications in MEGA X software (Kumar et al., 2018). We used ModelGenerator (Keane et al., 2006) to choose the best model for generating phylogenetic tree. The conserved motifs of protein sequences were analyzed with the program Multiple Em for Motif Elicitation (MEME; version 5.3.3) at http://meme-suite.org/tools/meme. Then, the phylogenetic tree and conserved MEME domains were visualized using Interactive Tree of Life (iTOL) version 6 (Letunic and Bork, 2021). Additionally, multiple alignment of crustacean AQPs sequences was built using MUSCLE method in MEGA X software and visualized through Jalview software (Waterhouse et al., 2009). Transmembrane regions were predicted with TMHMM 2.0.[2] Protein structures were simulated by Phyre2[3] and visually edited by Chimera 1.15 software (Pettersen et al., 2004).

qPCR Analysis of *LvAqp* mRNAs Under Salinity Exposure

The specific primer sequences of the target and reference genes were designed using Primer Premier 5.0, and were listed in **Supplementary Table 1**. The tissue distribution of *LvAqp* mRNAs was first examined, and then their expression changes under salinity stress were detected in tissues with high *LvAqp* expression levels. qPCR was performed in a 96-well plate, and the reaction mixture (10 μL volume) consisted of 5.0 μL of 2 × ChamQ Universal SYBR qPCR Master Mix (Vazyme, China), 1.0 μL of cDNA (10 ng/μL), 0.2 μL each of 10 μM forward and reverse primers, and 3.6 μL of RNase-free water. qPCR was carried out on a CFX96 Touch Real-Time PCR Detection System (Bio-Rad, United States) as follows: 95°C (30 s) for pre-incubation, followed by 40 cycles at 95°C (10 s) and 60°C (30 s). Finally, the melting curve was analyzed to verify amplification specificity. The accumulation of fluorescence signals from the SYBR Green dye was recorded in the 60°C (30 s) phase during each cycle. A negative control (no-template reaction) was included throughout. Each sample was analyzed in triplicate, along with the two reference genes *ubiquitin* (*Ub*) and *ribosomal protein S12* (*S12*) according to previous studies (Li et al., 2022), and the expression level was normalized to the geometric mean of the two reference genes (Vandesompele et al., 2002). The relative gene expression levels were calculated by the comparative Ct method using the formula $2^{-\Delta\Delta Ct}$ (Livak and Schmittgen, 2001). qPCR data were statistically evaluated by one-way analysis of variance (ANOVA), followed by Tukey's *post-hoc* test in SPSS 21.0 (SPSS, IL, United States), wherein $p < 0.05$ denoted a statistically significant difference.

Transcriptome Sequencing of Intestine Under Acute Salinity Stress

The RNA integrity of intestine tissues sampled at 2 h after salinity exposure was assessed using the RNA Nano 6000 Assay Kit and the Agilent Bioanalyzer 2100 system (Agilent Technologies, United States) and was expressed as an RNA Integrity Number (RIN). According to the results, RNA samples with high quality (OD260/OD280 = 2.0–2.2, OD260/OD230 ≥ 2.0, RIN ≥ 8.0, and 28S:18S ≥ 1.0) were used for library construction. For the RNA sample preparation, 3 μg of RNA per sample was used as input material (3 replicates per group at salinity 10, 30, and 50‰, named S10, S30, and S50 group). Sequencing libraries were

[1]http://www.ncbi.nlm.nih.gov/BLAST/

[2]http://www.cbs.dtu.dk/services/TMHMM

[3]http://www.sbg.bio.ic.ac.uk/phyre2

generated using NEBNext® Ultra™ RNA Library Prep Kit (NEB, United States), and were then sequenced on an Illumina HiSeq 2500 platform.

Functional Analysis of Differentially Expressed Genes

Raw reads in fastq format were initially processed using Perl scripts. Clean reads were obtained by the removal of reads containing adapters, reads containing poly-N, and low-quality reads from the raw data. At the same time, Q20, Q30, and GC contents of the clean data were calculated. Reference genome and gene model annotation files for *L. vannamei* were downloaded from genome website.[4] An index of the reference genome was built and clean reads were mapped to the reference genome using Hisat2 v2.2.4 (Kim et al., 2015). The mapped reads of each sample were assembled by StringTie v1.3.1 (Pertea et al., 2015, 2016). Then, the fragment per kilobase of transcript per million mapped reads (FPKM) of each gene was calculated to quantify its expression abundance and variations.

Differential expression analysis of genes was performed between the two groups by DESeq2 R package (1.16.1) (Love et al., 2014). The resulting *p*-values were adjusted by the Benjamini–Hochberg procedure. Genes with an adjusted *p*-value < 0.05 and $|\log_2(\text{Fold Change})| > 1.0$ were regarded as differentially expressed. To assess changes in gene expression patterns upon two types of salinity stress, expression pattern analysis was performed using Short Time-series Expression Miner (STEM, version 1.3.8) (Ernst and Bar-Joseph, 2006) based on all Differentially Expressed Genes (DEGs). Gene Ontology (GO) and Kyoto Encyclopedia of Genes and Genomes (KEGG) enrichment analyses of DEGs were implemented by means of the clusterProfiler R package, in which gene length bias was corrected (Yu et al., 2012). GO terms or KEGG pathways with corrected *p*-value less than 0.05 were considered significantly enriched in a set of DEGs. To validate the Illumina sequencing data, twelve DEGs were chosen for qPCR analysis by using the same RNA samples for transcriptome sequencing.

RESULTS

Molecular Characteristic and Evolutionary Analysis of *LvAqp* Genes

Three *L. vannamei* aquaporins (LvAqps) with complete ORFs were identified and further confirmed by PCR, cloning, and sequencing. Those mRNA sequences were submitted to GenBank with the accession numbers MW915485, MW915486, and MW915487. The complete ORFs and derived amino acid sequences were shown in **Supplementary Figure 1**. Phylogenetic tree analysis based on the amino acid sequences of vertebrate and invertebrate AQPs illustrated that one belonged to the water specific AQPs within the classical aquaporins subfamily (named LvAQP4), one belonged to the aquaglyceroporins (named LvAQP3), and the last one belonged to the unorthodox aquaporins (named LvAQP11) (**Figure 1**). A total of six conserved motifs were predicted in those AQPs protein sequences *via* MEME with a length of 6–50 amino acid residues. The classical aquaporins had three motifs (motif 1, 3, and 4), the aquaglyceroporins harbored four motifs (motif 1, 3, 4, and 6), and the unorthodox aquaporins shared three motifs (motif 1, 2, and 5). Therefore, the classification of AQPs by conserved motifs was consistent with phylogenetic tree clustering (**Figure 1**).

The genomic organization of the aquaporins genes revealed that *LvAqp3* and *LvAqp4* genes were separately located at two independent scaffolds and both were single copy gene in the genome, whereas two *LvAqp11* genes were found to be arranged in a tandem array locate at one scaffold (**Figure 2**). Online BLAST of the mRNA sequences against the scaffolds showed that *LvAqp3* gene consisted of eight exons with the first exon mapped into scaffold604 and other exons mapped into scaffold3120 (**Figure 2A**). Besides the *LvAqp3* transcript identified above, alternative splicing of partial sequence of exon 1 and whole exon 7 resulted in another *LvAqp3* transcript, which had been presented in the annotated genome database (named *LvAqp3-2*). Nevertheless, the ORFs of *LvAqp3-1* and *LvAqp3-2* mRNA are still the same (**Figure 2A**). Similar alternative splicing was also found for *LvAqp11* gene. Both *LvAqp11* genes identified from the genome had the same coding regions with seven exons and are transcribed as three splice variants. In both cases the variation occurs at the N-terminus whereby only one exon of the first three exons was retained. We therefore named these isoforms *LvAqp11-1*, *LvAqp11-2,* and *LvAqp11-3*, respectively. The sequence of *LvAqp11-2* was the same as the obtained transcript in this study. Nevertheless, the ORFs of the three *LvAqp11* transcripts were located at the last four exons and encoding the same protein (**Figure 2C**). In contrast with the *LvAqp3* and *LvAqp11* genes, alternative splicing was not found in *LvAqp4* gene. The *LvAqp4* gene was composed of seven exons with the first exon mapped into scaffold3009 and other exons mapped into scaffold1754, and the ORFs was located at the first five exons (**Figure 2B**).

Analysis of the Conserved Structural Features of LvAQP

Multiple sequence alignments among the decapod AQPs showed that their sequences, especially for the NPA motifs, were conserved. In contrast to other subtypes of AQPs, the unorthodox aquaporins had non-canonical NPA motifs, with the N-terminal cysteine-proline-tyrosine (CPY) and C-terminal asparagine-proline-valine (NPV) motifs (**Figure 3A**). Positions for the four amino acids in the Ar/R constriction motif in the crustacean AQPs were identified based on protein alignments. The fourth amino acid residue of constriction motif is considered as the most highly conserved position, while all decapod AQPs, except AQP11 subfamily, is an arginine at this site. All decapod AQPs have an aromatic amino acid at the first position of constrict motif, except in some AQP4 proteins where it was a valine. The amino acid residues at the second and third positions

[4]https://www.ncbi.nlm.nih.gov/genome/?term=penaeus+vannamei

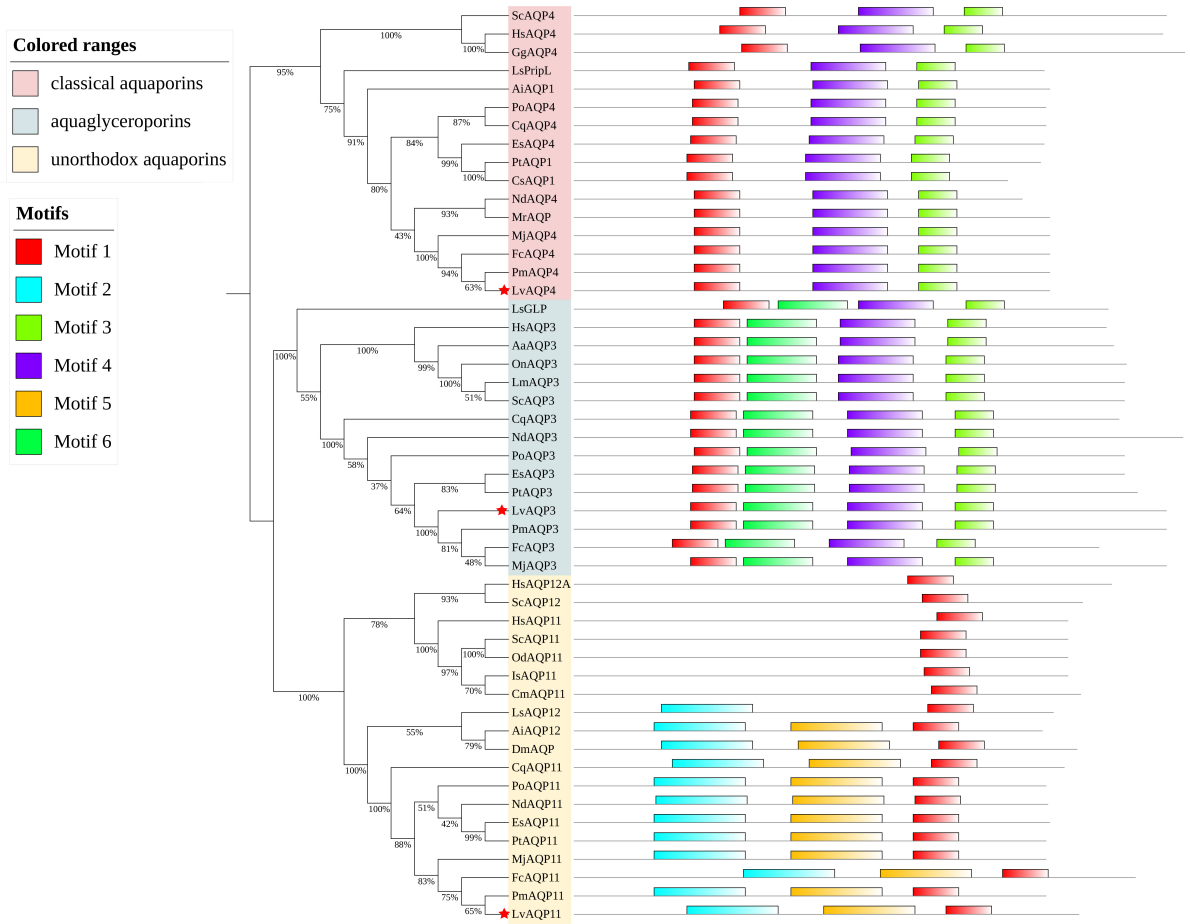

FIGURE 1 | Molecular phylogenetic classification of the aquaporins and MEME motif distribution of each protein. A phylogenetic tree based on the amino acid sequences of the AQPs from multiple vertebrates and invertebrates was constructed by using MUSCLE and the maximum likelihood method of MEGA X. The node value indicates the percentage of 1,000 bootstrap replicates. Red stars indicate the LvAQP3, LvAQP4, and LvAQP11. Other AQPs used in the phylogenetic analysis were obtained by blast against the genome and transcriptome assemblies at NCBI database or CAT Database. The sources and accession numbers of the AQPs were listed in **Supplementary Table 2**.

varied among three decapod AQPs subfamilies. In the second position, the AQP3 subfamily had a glycine, the AQP4 subfamily had a histidine, and the AQP11 subfamily had a valine. The amino acid at the third position was a tyrosine, serine or alanine, and glycine for the AQP3, AQP4, and AQP11 subfamily, respectively (**Figure 3A**).

Results from TMHMM prediction indicated that LvAQP3 and LvAQP4 contained six potential transmembrane helices and five connecting loops. However, in the case of LvAQP11, the probability scores for some of the helices were weak. Thus, four potential transmembrane helices and three connecting loops were found in LvAQP11 (**Figure 3A**). In order to obtain tertiary structures of LvAQPs, *in silico* homology models were built for each protein. All LvAQPs showed structural features that are typical of known AQP pore channels (**Figure 3B**). The highly conserved dual NPA motifs were symmetrically distributed in LvAQP3 and LvAQP4 for pore structure formation (**Figure 3B**). Besides, the two predicted weak helices still formed transmembrane helices in the tertiary structure for LvAQP11, with the non-canonical CPY and NPV motifs similar to the pore structure formation function of the NPA motifs (**Figure 3B**).

Tissue Distribution of *LvAqp* mRNAs

qPCR analyses characterized the tissue specific expression patterns of *LvAqp3*, *LvAqp4*, and *LvAqp11* mRNAs in juvenile *L. vannamei* at intermolt stage. The expression patterns of *LvAqp3-1* and *LvAqp3-2* mRNAs were first examined together with a pair of primers because the ORFs of both mRNAs were identical. Therefore, the total expression levels of *LvAqp3-1* and *LvAqp3-2* were regarded as the expression of *LvAqp3* gene, and significantly higher levels of expression was observed in intestine (**Figure 4A**). Further analysis showed that the *LvAqp3-1* mRNA was the predominant isoform expressed in intestine (**Supplementary Figure 2A**). The *LvAqp4* could be detected in all examined tissues with varied expression levels in different tissues, and significantly higher levels of expression were observed in hepatopancreas, stomach, and gill (**Figure 4B**). In the case of *LvAqp11*, the three alternative spliced transcripts were quantified

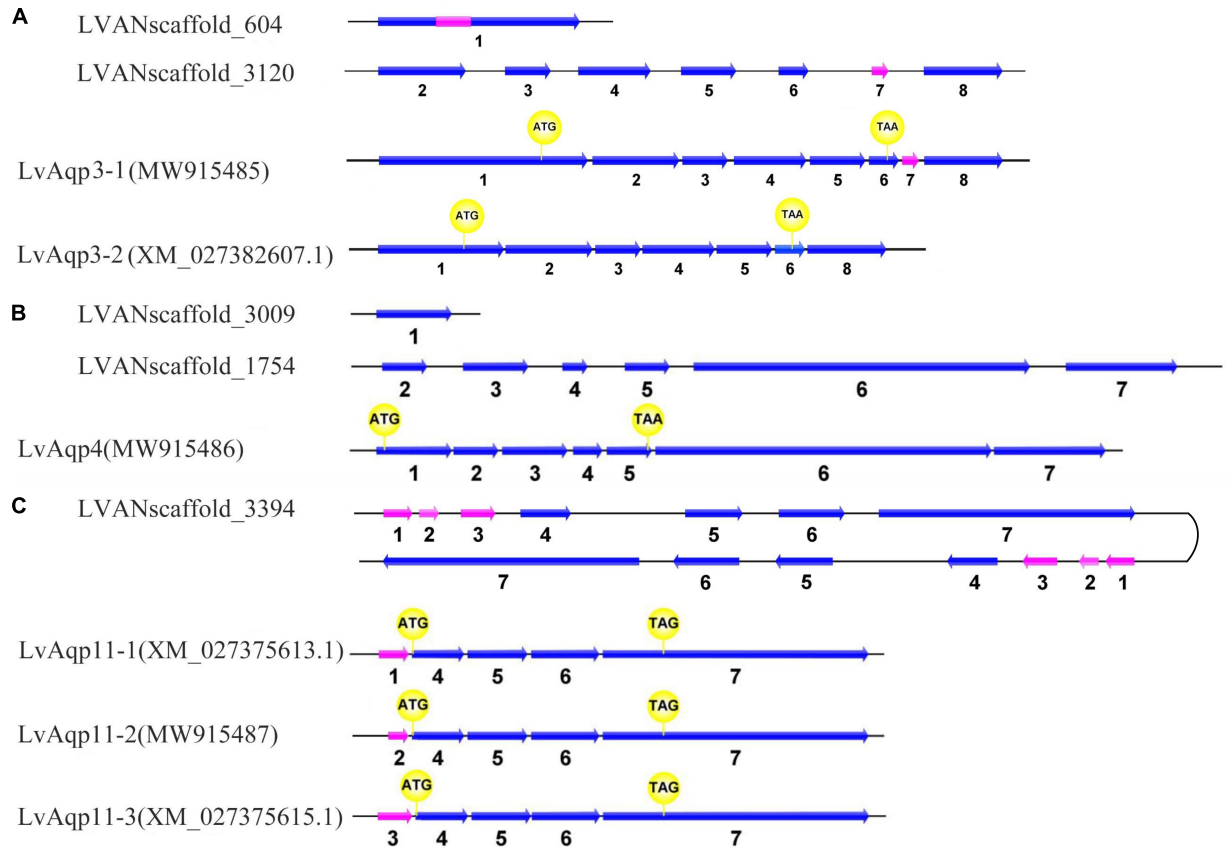

FIGURE 2 | Gene structures of the *LvAqp3* **(A)**, *LvAqp4* **(B)**, and *LvAqp11* **(C)**. Exons were indicated in arrows and introns by thin lines. The alternative spliced exons were indicated by pink arrows. The start and stop codons were marked in yellow circles.

together and showed the extremely high expression level in muscle (**Figure 4C**). In addition, the *LvAqp11-2* mRNA was the predominant isoform expressed in muscle (**Supplementary Figure 2B**). The total levels of two *LvAqp3* mRNAs and three *LvAqp11* mRNAs was used to represent the expression of *LvAqp3* and *LvAqp11* genes in the following studies, respectively.

Differential Expression of *LvAqps* After Salinity Stress

As the *LvAqp3* and *LvAqp11* were separately predominantly expressed in intestine and muscle, suggesting that the two genes primarily function in intestine and muscle, respectively. Thus, we selected intestine and muscle to separately detect the expression profiles of *LvAqp3* and *LvAqp11* under salinity stress. In addition, the expression of *LvAqp4* was mostly expressed in hepatopancreas, stomach, and gill. Thus, the hepatopancreas was first chosen to detect the expression of *LvAqp4* under salinity stress and the gill was also selected because it is an important osmoregulatory tissue. Compared with the shrimp of control group at salinity 30‰, qPCR analysis showed that in the intestine, the expression level of *LvAqp3* significantly decreased at 2 h and remained at low levels from 2 to 24 h, regardless of whether they were under acute low- or high-salinity stress (**Figure 5A**). The significantly lower expression of *LvAqp3* was also detected in the intestine when the shrimp were exposed to long-term low- or high-salinity stress (**Figure 5B**). On the contrary, the expression levels of *LvAqp4* in the hepatopancreas were significantly up-regulated after acute salinity stress. It was significantly increased at 4 h, then consistently elevated and reached the peak at 24 h under acute low-salinity stress (**Figure 5C**). Meanwhile, the expression was significantly higher at 2 h, and no significant changes were found in the following time points at acute high-salinity stress (**Figure 5C**). However, the elevated expression of *LvAqp4* in the hepatopancreas was not observed under long-term salinity stress. It was not significantly altered after 15 days of low salinity stress, while it decreased and stayed at a lower level compared to control under high salinity stress (**Figure 5D**). The expression profiles of *LvAqp4* in the gill showed a similar expression pattern compared to *LvAqp3* (**Figures 5E,F**). Yet, two major differences were noted. First, no significant changes in the expression of *LvAqp4* in the gill were observed since the initial decrease at 2 h after acute salinity stress (**Figure 5E**). Second, the reduction was larger in the expression levels of *LvAqp3* than that observed in *LvAqp4* in the gill after long-term salinity stress (**Figure 5F**). Moreover, the acute salinity stress caused a gradual decrease in the expression level of *LvAqp11* in muscle (**Figure 5G**). The expression of

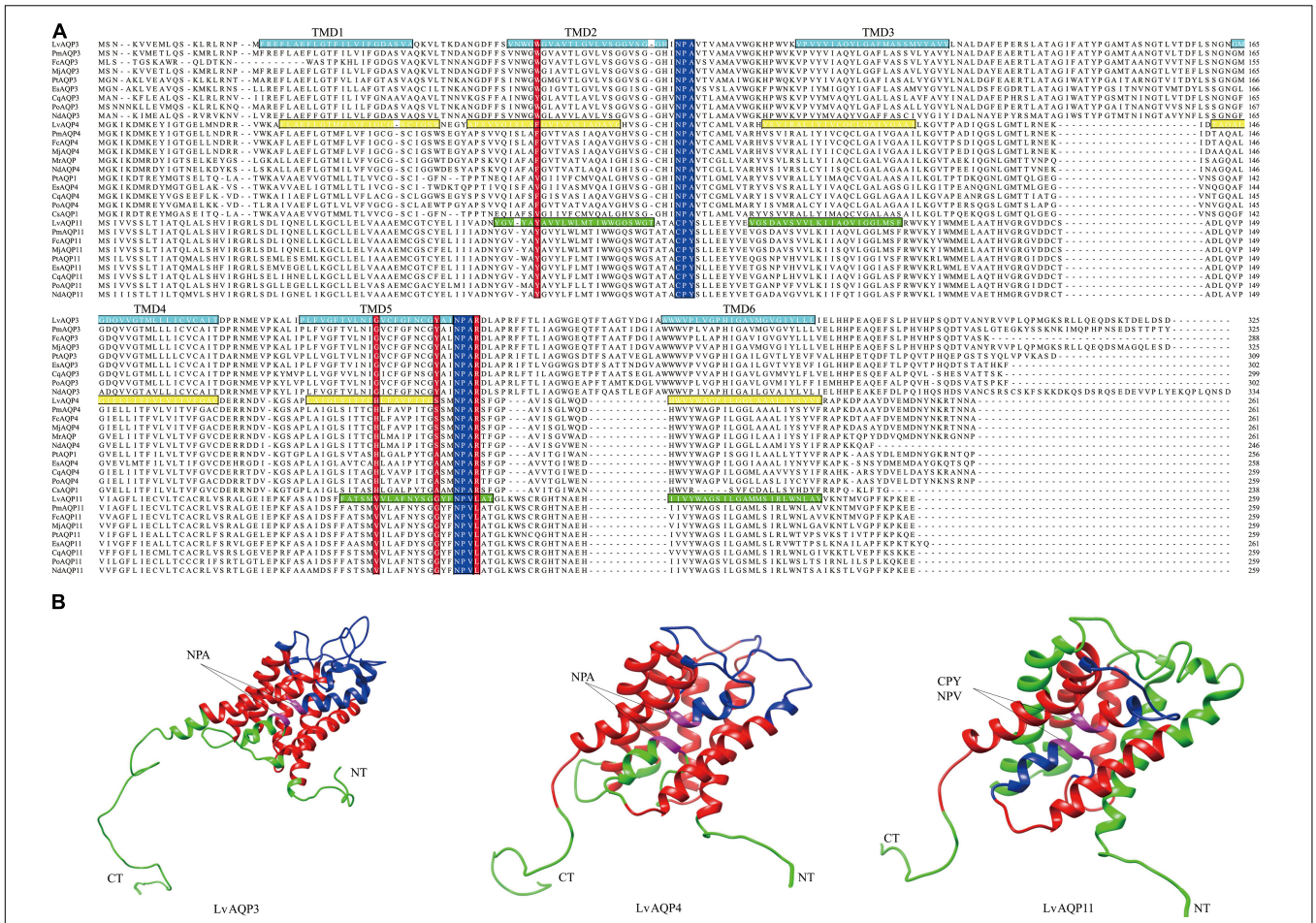

FIGURE 3 | The conserved structural features of LvAQPs. **(A)** Protein alignments of the aquaporins in crustaceans. The two NPA motifs (or the variants thereof) were indicated with blue boxes, and the four amino acids in the constriction site were indicated with red boxes. The sequences of the transmembrane spanning regions (TMDs), based on TMHMM predictions of LvAQP3, LvAQP4, andLvAQP11, were indicated with indigo, yellow, and green boxes, respectively. **(B)** Analysis of the tertiary structural features of LvAQP3, LvAQP4, and LvAQP11. Blue region: outside of the membrane. Green region: inside of the membrane. Red region: transmembrane helix. CT: carboxyl terminal. NT: amino terminal. Pink region: NPA/CPY/NPV motifs. The sequence features of the proteins were illustrated based on the prediction results from TMHMM. Thus, the two predicted weak helices of LvAQP11 formed as transmembrane helices were still painted as green.

LvAqp11 was also down-regulated during the long-term salinity stress (**Figure 5H**).

Functional Analysis of Differentially Expressed Genes in the Intestine After Acute Salinity Stress

Nine intestine RNA samples of high quality (three replicates in each group) were used for the creation of cDNA libraries, followed by sequencing. The details were listed in **Supplementary Table 3**. A total of 440,033,298 paired-end reads with 150-bp read length were generated and 437,955,694 clean reads were selected after removing the reads containing adapters and/or poly-N, and low-quality reads. The average Q20, Q30, and GC% were 97.45, 93.16, and 44.63%, respectively. Next, clean reads were aligned to the *L. vannamei* genome using Hisat2 and the average mapping rate was 82.65% among the samples. Raw reads were archived in the NCBI SRA (accession No. PRJNA772775). In total, 1,964 DEGs between different groups were chosen by means of the following criteria: an adjusted p-value < 0.05 and $|\log_2$ Fold Change$| > 1.0$. A number of genes were found to be significantly up-regulated in S30 compared to S50 (711) and in S30 compared to S10 (213). The corresponding numbers of down-regulated genes were 661 and 614, respectively. The qPCR analysis of nine selected DEGs were compared with the results of the differential expression analysis. Overall, the differential expression of these genes was confirmed by the qPCR analysis, indicating the reliability and accuracy of our differential expression analysis (**Supplementary Figure 3**). In addition, to get expression patterns of DEGs upon different salinity stresses, STEM was performed to classify all the DEGs according to their abundance changes. The DEGs were classified into eight clusters according to their expression patterns, while only three gene expression profiles were significant ($p < 0.05$) (**Figure 6**). Down-regulated profile and up-regulated profile under both salinity stresses contained 596

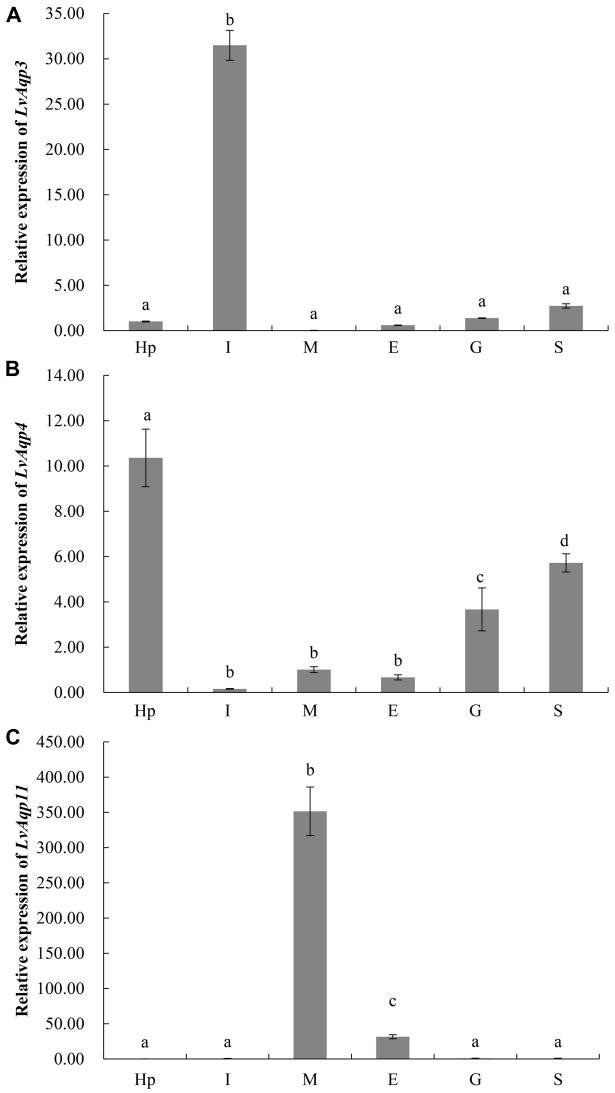

FIGURE 4 | Tissue distribution of *LvAqp3* **(A)**, *LvAqp4* **(B)**, and *LvAqp11* **(C)** in different tissues. Hp, hepatopancreas; I, intestine; M, muscle; E, epidermis; G, gill; S, stomach. The data are presented as mean ± *SD* ($n = 3$). Means labeled with different letters are significantly different ($p < 0.05$).

and 435 DEGs, while 331 DEGs in another profile were elevated at the high salinity stress and not significant changed at low salinity stress. The results were in accordance with the patterns shown in the heatmap (**Figure 6**). Moreover, for the purpose of the study, we checked the expression of osmoregulatory genes. The results showed that the 10 highest expressed genes were hardly significantly changed under acute salinity stresses (**Supplementary Table 4**).

In total, 31 and 21 GO terms were significantly enriched in the intestine of the two comparisons (S30 vs. S10 and S30 vs. S50), respectively (corrected $p < 0.05$; **Supplementary Tables 5**, **6**). The top significantly enriched GO terms were shown in **Figure 7A**. Among the significantly enriched terms, half were belonged to biological processes, including alpha-amino acid metabolic process (GO: 1901605), cellular amino acid metabolic process (GO: 0006520), aromatic amino acid family metabolic process (GO: 0009072), L-phenylalanine metabolic process (GO: 0006558), and erythrose 4-phosphate/phosphoenolpyruvate family amino acid metabolic process (GO: 1902221) enriched in both comparisons. In addition, similar results were also found for the enriched terms of cellular component, such as Golgi stack (GO: 0005975), Golgi cisterna (GO: 0031985), Golgi subcompartment (GO: 0098791), and extracellular region (GO: 0005576); molecular function, such as catalytic activity (GO: 0003824), sulfotransferase activity (GO: 0008146), transferase activity, transferring sulfur-containing groups (GO: 0016782), and prenol kinase activity (GO: 0052673).

Thirteen and 11 KEGG pathways were significantly enriched in the intestine of the two comparisons, respectively (corrected $p < 0.05$; **Supplementary Tables 7**, **8**) and were shown in **Figure 7B**. Most of the significantly enriched pathways belonged to the metabolism pathway class. Moreover, the results demonstrated that there were seven pathways enriched in both comparisons: amino acid metabolism (Tyrosine metabolism, Phenylalanine metabolism, and Phenylalanine, tyrosine and tryptophan biosynthesis), carbohydrate metabolism (Amino sugar and nucleotide sugar metabolism), global and overview maps (Metabolic pathways), and glycan biosynthesis and metabolism (Glycosaminoglycan biosynthesis-keratan sulfate and Mucin type O-glycan biosynthesis) (**Figure 7B**).

DISCUSSION

Evolution of Aquaporins in *L. vannamei*

Based on biological characteristics, molecular phylogeny, and permeation selectivity to water, glycerol, or other substance, 13 members of human AQP family are divided into three subfamilies: classical aquaporins, aquaglyceroporins, and unorthodox aquaporins (Benga, 2012; Ishibashi et al., 2017). Although only three types of AQPs were identified in *L. vannamei*, phylogenetic analysis revealed that the categorization of LvAQPs is consistent with the previous classification of human AQPs, with each LvAQP corresponding to a subfamily. Moreover, as we obtained more decapod AQPs by blast against the NCBI or CAT Database (Nong et al., 2020), it seems that this classification is common for decapod species. Apart from the above subfamilies, the classical aquaporins still includes an arthropod specific subfamily, big brain (BIB) protein (Finn and Cerdà, 2015), which is not characterized in this study. Thus, further elucidation and verification of other subgroups are warranted.

In this study, the three splice variants of *LvAqp11* encoded proteins with identical sequences. This is also the case for *LvAqp3*. Alternative splicing of aquaporins has been reported in crustacean salmon louse (*Lepeophtheirus salmonis*) (Stavang et al., 2015) and barnacle (*Balanus improvise*) (Lind et al., 2017). Furthermore, we analyzed the available genomes of three crustacean species, and found that transcripts of *aquaporin-11-like* genes from the *Penaeus monodon* (Gene ID: 119593716), *Penaeus japonicus* (Gene ID: 122256039), and

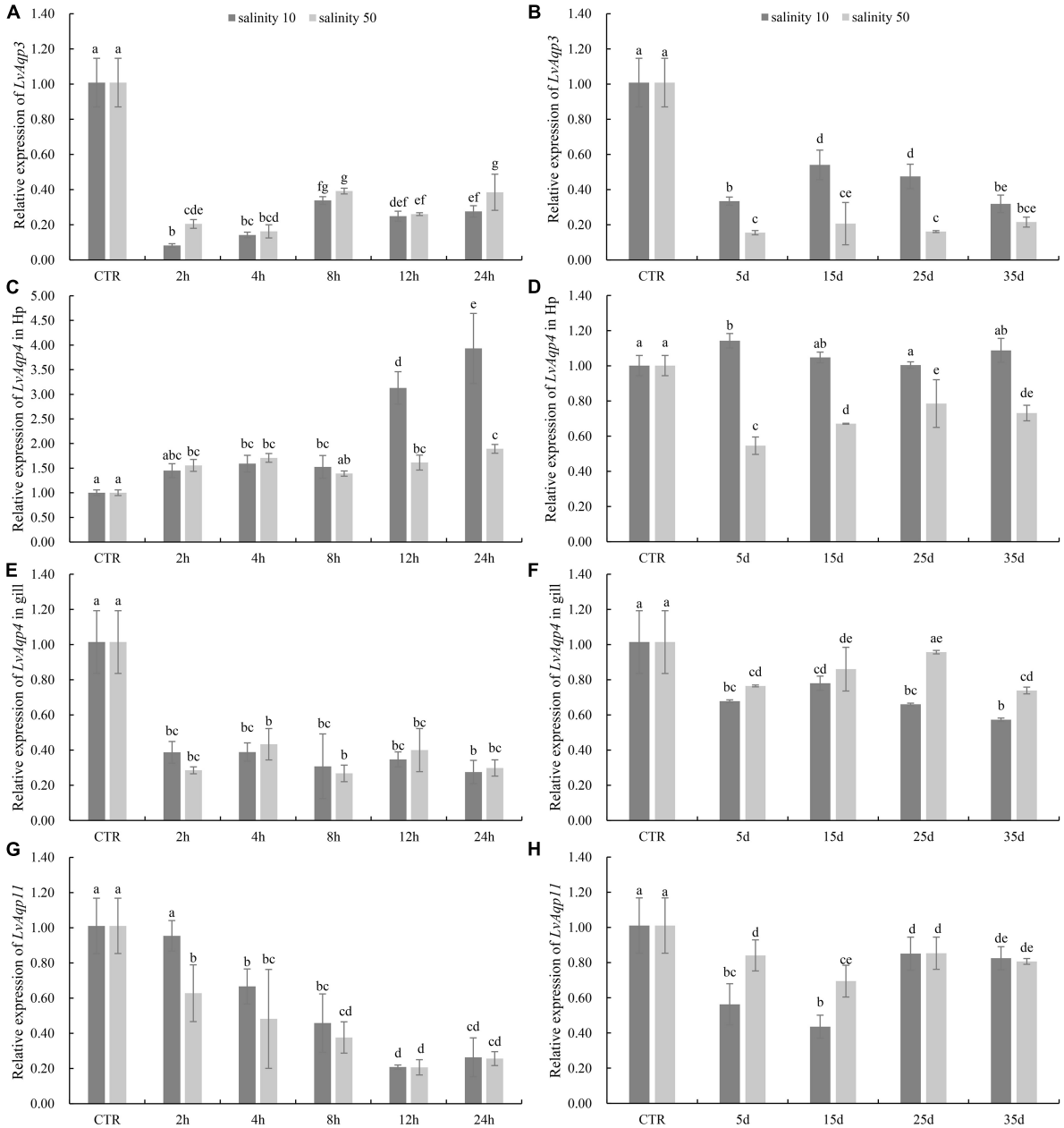

FIGURE 5 | Differential expression of *LvAqps* after salinity challenge. Expression profiles of *LvAqp3* in intestine **(A,B)**, *LvAqp4* in hepatopancreas and gill **(C–F)**, and *LvAqp11* in muscle **(G,H)** under acute and long-term salinity stress, respectively. The data are presented as mean ± *SD* ($n = 3$). Means labeled with different lower case letters are significantly different ($p < 0.05$).

Homarus americanus (Gene ID: 121855104) also have N-terminal splice variants with identical ORFs sequences, created by a similar splicing mechanism as occurs for the *LvAqp11* transcripts. Such conserved splicing mechanism indicate that the splice variants might have some important function. Nevertheless, only *LvAqp3-1* and *LvAqp11-2* were predominantly expressed in the intestine and muscle, respectively. Aquaporins variants are expressed sex-specifically in a copepod, *Caligus rogercresseyi* (Farlora et al., 2014) and in an insect *Anopheles gambiae* (Tsujimoto et al., 2013). As we do not detect the expression of splice variants in gonads, it is possible that they might have functions in sex-related organs.

The NPA motifs are the most common conserved signature of AQPs and play a critical role in the formation of a pore structure (Ishibashi et al., 2017). Sequence analysis showed that the identified decapod AQP3 and APQ4 proteins all have the two conserved NPA motifs. Instead, the AQP11 proteins contain CPY and NPV motifs. The variations of the NPA motifs in the decapod unorthodox AQPs are not unusual in comparison to unorthodox

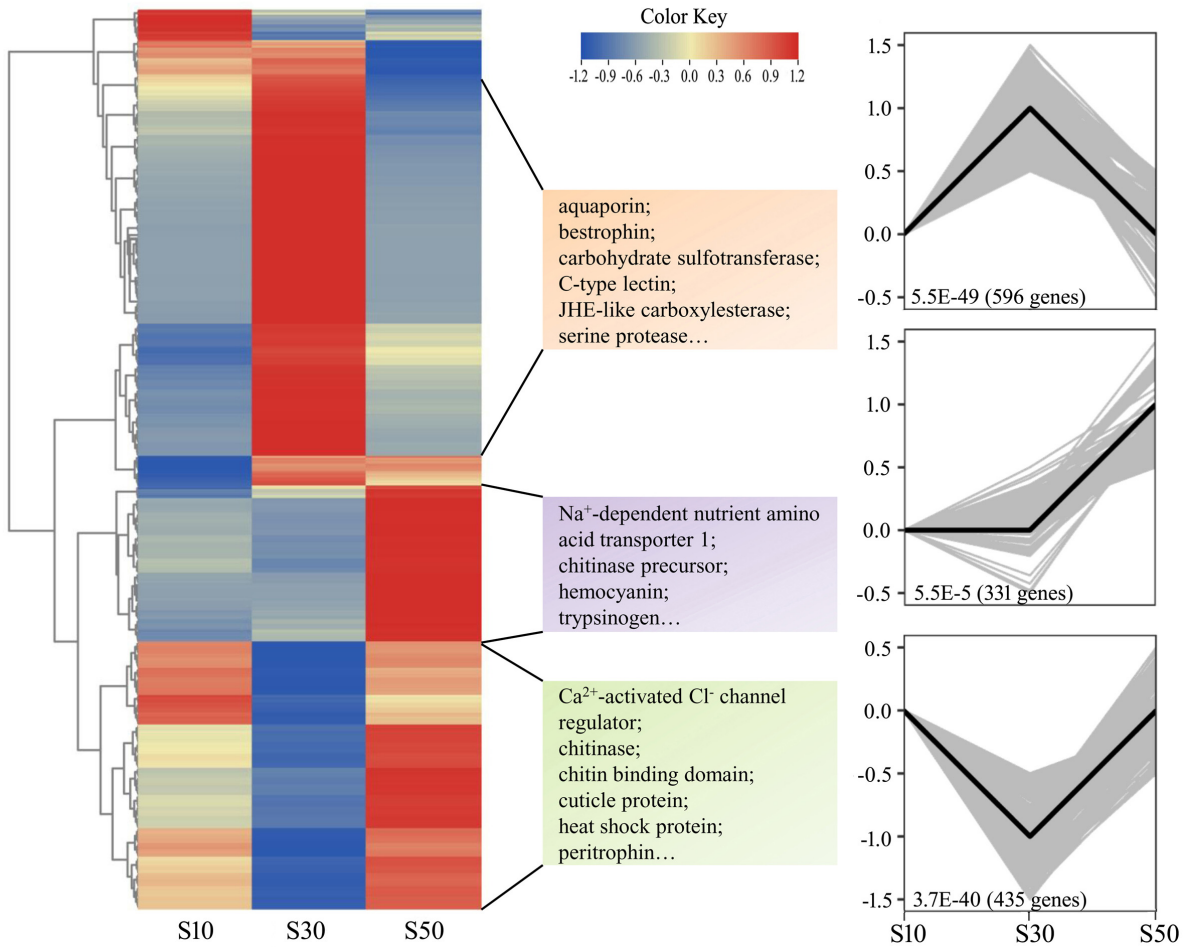

FIGURE 6 | Hierarchical clustering of DEGs in the intestine. The heatmap of all DEGs was drawn by TBtools (Chen et al., 2020). Colors represent relative mRNA expression as indicated in the color key. The red color shows high expression, and the blue color represents lower levels of expression. The color from red to blue represents the $\log_2$ (FPKM + 1) from large to small. The clustering indicates similar expression patterns among the groups. The DEGs were grouped into three main clusters according to their expression patterns. The *p*-value and numbers of DEGs are shown at the bottom of the square. For each cluster, several enriched genes in each profile are listed.

AQPs from other species. The same substitutions are found in AQP12L1 and AQP12L2 from *L. salmonis* (Stavang et al., 2015). Moreover, the CPY substitution has been reported in AQP12 from *B. improvise* (Lind et al., 2017), while the NPV substitution in AQP of *Rhodnius prolixus* has been shown to be functional in *in vitro* assays (Staniscuaski et al., 2013).

Involvement of Aquaporins in Osmoregulation

The regulation of AQPs under salinity stress has been well-reported in fish, where it has also been shown that the expression patterns and levels of AQPs in different species, tissues, and environments vary (Madsen et al., 2015). Nevertheless, the osmoregulatory role of AQPs is little known in crustaceans. Earlier investigation of the osmoregulatory function of AQPs is mainly dependent on the findings of transcriptome study in crustaceans, especially in decapods. The expression of *Aqps* decreased in the gills of *Portunus trituberculatus* during 3 days of acute low salinity stress (Gao et al., 2019) and after 10 days of hypo-osmotic and hyper-osmotic stress (Lv et al., 2013). The results were in accordance with the expression patterns of *LvAqp4*, which was down-regulated in the gill under acute and long-term salinity challenges. Similar expression patterns of *Aqps* were also reported in *Crassostrea gigas* (Meng et al., 2013) and *B. improvise* (Lind et al., 2017) under long-term salinity stress. These results indicate that salinity stresses could induce a reduction of AQPs activities to avoid cell swelling or shrinkage as a consequence of water influx or efflux. In contrast, opposite changes in the expressions of *LvAqp4* were found in the hepatopancreas under acute salinity stresses. Gao et al. (2017) has reported the up-regulation of *LvAqp4* in the hepatopancreas under acute high salinity stress, whereas its expression was not significantly changed under acute low salinity stress. It was not completely consistent with our results. Instead, we observed no significant changes of *LvAqp4* in

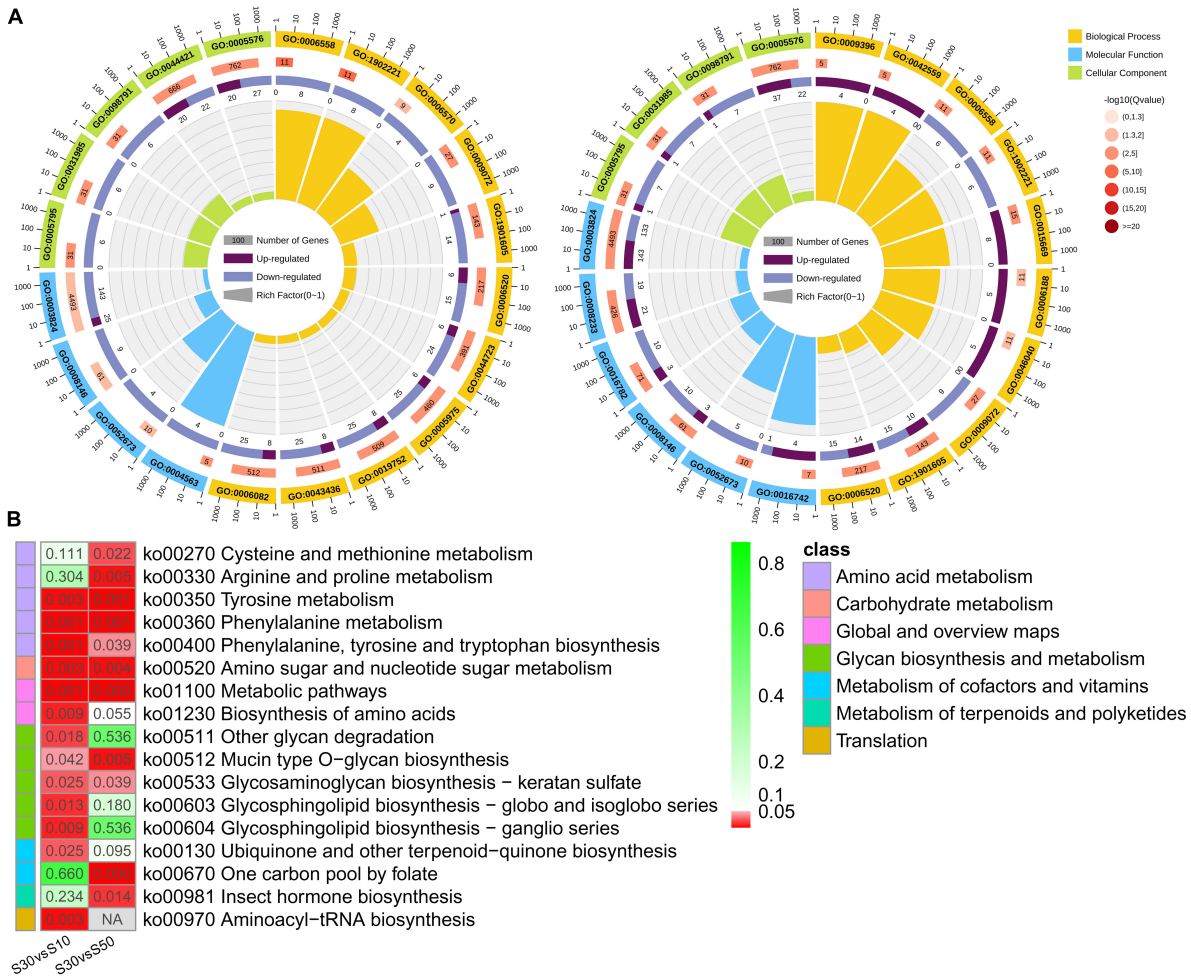

FIGURE 7 | Functional enrichment of DEGs. **(A)** Circular map of the top enriched GO terms in S30 vs. S10 and S30 vs. S50. **(B)** Comparison of enriched pathways that were predicted by DEGs with different comparisons.

the hepatopancreas under long-term low salinity stress. This deviation is probably due to the developmental stage of the shrimp. Juvenile shrimp are used in this study, which are much smaller than the sub-adult shrimp in their study. It is widely accepted that larval or juvenile shrimp are more tolerable to salinity stresses in aquaculture practices. In blue crab *C. sapidus*, the expression of *Aqp1-like* gene was shown to be related to developmental stages, and it was transcriptionally up-regulated at early larval stages in the exposure of hypo-salinity (Chung et al., 2012).

The unorthodox aquaporin of *LvAqp11* is mostly expressed in the muscle, whereas its orthologs are mainly expressed in the mammalian kidney and pancreas (Li and Wang, 2017). As unorthodox aquaporins are most recently identified, still less is known about this subfamily than other AQP subfamilies. Its unique intracellular localization, specifically in the ER of mammalian cells has made its functional studies challenging (Ishibashi et al., 2021). To date, functional studies on unorthodox aquaporins in crustacean has been only reported in salmon louse, the unorthodox aquaporins of which are localized intracellularly and difficult to be expressed in *Xenopus* oocytes as is the case with mammalian unorthodox aquaporins (Stavang et al., 2015). In addition, the few studies on unorthodox aquaporins in fish have reported that these molecules significantly induce water or glycerol permeability in medaka and zebrafish oocytes (Tingaud-Sequeira et al., 2010; Kim et al., 2014). The significantly reduced levels of *LvAqp11* indicate that it is sensitive to relative salinity changes. Further immunohistochemistry studies would be needed to investigate the spatial expression of LvAQP11 in order to better understand their biological functions on osmoregulation.

Four members of aquaglyceroporins subgroup (AQP3, 7, 9, and 10) have been identified in vertebrate (Ishibashi et al., 2017, 2020). Nevertheless, we only obtained one aquaglyceroporin from *L. vannamei* and other decapod species. In addition, the number of members in aquaglyceroporins subfamily differs in crustaceans. The barnacle has two, while salmon louse has three and *Daphnia* has six (Lind et al., 2017). In *L. vannamei*,

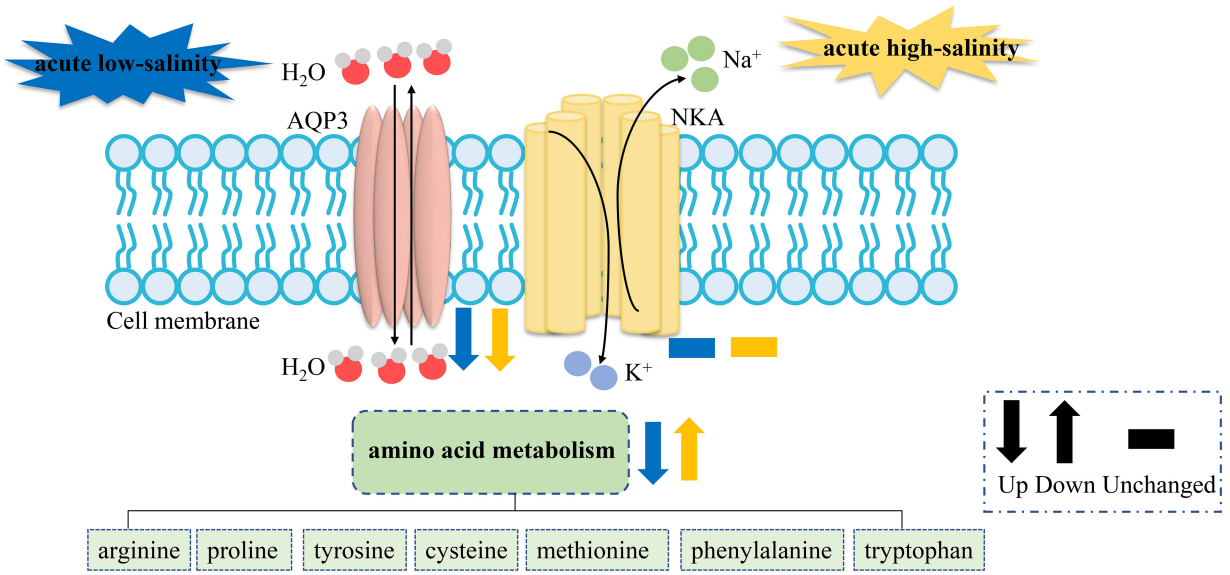

FIGURE 8 | The hypothetical model based on the expression changes of genes and pathways from the intestine transcriptome challenged with acute low- or high-salinity stress. NKA stands for the ion transporters and ion channels, the expression of which are not significantly changed.

the *LvAqp3* is predominantly expressed in the intestine. Such expression pattern of aquaglyceroporins have been observed in its human counterpart AQP10, which is mainly expressed in the gastrointestinal tract (Li and Wang, 2017). The AQP10 isoform is also dominantly detected in the intestine of teleost zebrafish (Hamdi et al., 2009) and medaka (Kim et al., 2014). Moreover, the lower intestinal mRNA level of *LvAqp3* under high salinity stress is consistent with the trend shown by the *Aqp10* ortholog in medaka (Kim et al., 2014) and mandarin fish (Shen et al., 2021). The results suggest the possible osmoregulatory roles of aquaglyceroporins in the intestinal organoids.

Taken together, the presences of *LvAqps* are quite ubiquitously and sometimes are predominantly expressed at specific tissues. Our study further showed the effects of acute exposure and long-term acclimation to different salinities on the expression levels of *LvAqp3*, *LvAqp4*, and *LvAq11* in the predominantly or mainly expressed osmoregulatory tissues. The results revealed that although the influences of environmental salinities on *LvAqps* expression varied among isoforms and tissues, their expression levels were significantly decreased in most cases. As to the salinity-dependent patterns of *LvAqp4* in hepatopancreas not in accordance with that observed in gill, we hypothesized that the function of *LvAqp4* may be tissue-specific during the osmoregulation. Moreover, the synthesis of these findings suggest that all the LvAQP isoforms collaborate to maintain water balance within the shrimp and reduce cellular damage resulted from water shifts.

Osmoregulation of Intestine Under Acute Salinity Stresses

It is considered that knock-down or overexpression experiment is required to verify the function of genes. However, it is difficult to overexpress LvAQPs in mRNA level or protein level in shrimp due to the lack of suitable shrimp cell line. Nevertheless, the sharply decreased levels of *LvAqp3* mRNA in intestine under acute salinity stress provided a good model to perform gene expression assays with *LvAqp3* gene, comparable to the effect of knock-down. Therefore, transcriptome analysis of intestine under acute salinity stress was conducted to reveal the role of *LvAqp3* during the osmoregulation in intestine. Osmoregulation requires not only permeation of water but also the transport of ions. However, although several ion transporters and ion channels are significantly changed under salinity stresses, the 10 highest expressed osmoregulatory genes were hardly changed, including Na^+/K^+-ATPase (NKA), carbonic anhydrase (CA), and Ca^{2+} activated Cl^- channel regulator 2/4. NKA and CA have been shown to play crucial roles during salinity adaptation in *L. vannamei* (Pan et al., 2014; Liu M. et al., 2015). It is possible that as they are important regulatory molecules for maintaining ion balance, their expression will not dramatically change in the intestine at the initial stage during the acute salinity stress. On the contrary, qPCR analysis has revealed the sharply decreased expression of *LvAqp3* at the initial stages during the acute salinity stress. This result suggested a possible role of LvAQP3 as a coordinator of water and ion transport in the cell membrane. As described above, the down-regulated *LvAqp3* may be related to the reduced activities of LvAQP3 to protect against cell swelling or shrinkage caused by water influx or efflux. The above results suggest the relative stable of intracellular ion concentration and water volume. However, this raises the question which osmolytes are used in the intestine cell for maintaining osmotic balance. Further enrichment analysis indicates similar GO terms and KEGG pathways related to amino acid metabolism in the intestine under acute low- and high-salinity stresses, which is similar to the previous findings in

crustaceans (Li et al., 2014; Wang et al., 2015; Yuan et al., 2021). The finding in this study further corroborates the notion that free amino acids are important intracellular osmotic effectors in crustaceans (Cobb et al., 1975; McNamara et al., 2004; Augusto et al., 2007, 2009). Nevertheless, the enriched DEGs are quite different in those terms and pathways under acute low- or high-salinity stress. Most of the enriched DEGs are down-regulated at low salinity, whereas more enriched DEGs are up-regulated at high salinity (**Supplementary Tables 5–8**). It is possible that changes in the gene expression may lead to changes in free amino acid concentration. The concentrations of arginine, proline, and alanine were elevated significantly with increasing salinity in *Eriocheir sinensis* (Wang et al., 2012). We speculate that the down-regulated gene expression levels may result in the decreased concentrations of free amino acid and then reduce the intracellular osmotic pressure under acute low-salinity stress. In turn, the concentrations of free amino acid would be elevated to increase the intracellular osmotic pressure under acute high-salinity stress. Further metabolome study is needed to confirm the changes in free amino acid concentration under low- or high-salinity stress. Thus, based on transcriptomic results, we establish a hypothetical model of the components involved in salinity responses in the intestine of *L. vannamei*. When exposed to salinity stress, the activities of LvAQP3 will first be inhibited to stabilize the cell morphology, and then the free amino acid concentrations are adjusted by regulating the expression of amino acid metabolism related genes and pathways to maintain osmotic balance between intracellular region and external environment in the intestine (**Figure 8**). Furthermore, transcriptome analysis would supply new references and benefit future studies on the function of other *LvAqp* genes for better understanding their involvements in salinity adaptation of this euryhaline species.

CONCLUSION

Our analyses first reported three types of aquaporins in *L. vannamei*, where two of them, *LvAqp3* and *LvAqp11*, have splice variants with identical ORFs. The relative gene expression profiles of three aquaporins revealed remarkable differences and some consistent expression patterns of those genes over an experimental time frame under different salinity stresses. On the whole, the expression of *LvAqps* was decreased and may probably contribute to protect cell by preventing the water shifts that lead to cellular damage in intestine, gill, and muscle upon salinity challenge. Moreover, we proposed the combination roles of aquaglyceroporin and amino acid metabolism in responses to acute salinity changes in the intestine based on the comparative transcriptome analysis. These findings shed new insights into the investigation regarding the osmoregulation of AQPs in the decapod species.

DATA AVAILABILITY STATEMENT

The datasets presented in this study can be found in online repositories. The names of the repository/repositories and accession number(s) can be found below: SRA, PRJNA772775; GenBank, MW915485, MW915486, MW915487.

AUTHOR CONTRIBUTIONS

ZW: conceptualization, methodology, investigation, funding acquisition, formal analysis, and writing—review and editing. YGC: investigation, formal analysis, resources, and data curation. CW, ZZ, NZ, and RW: investigation and resources. ZD: investigation. YTC: funding acquisition, investigation, and methodology YL: conceptualization, supervision, project administration, funding acquisition, and writing—review and editing. All authors contributed to the article and approved the submitted version.

FUNDING

This work was supported by the National Science Foundation of China (31802269), the Shrimp and Crab Innovation Team of Shandong Agriculture Research System (SDAIT-15-011), the Major Applied Technology Innovation Project of agriculture in Shandong Province (SD2019YY001), the High-level Talents Research Fund of Qingdao Agricultural University (663/1119054 and 663/1120027), and the "First Class Fishery Discipline" program in Shandong Province.

ACKNOWLEDGMENTS

We thank Gene *Denovo* corporation in assistance with sequencing analysis.

SUPPLEMENTARY MATERIAL

The Supplementary Material for this article can be found online at: https://www.frontiersin.org/articles/10.3389/fmars.2022.817868/full#supplementary-material

REFERENCES

Abascal, F., Irisarri, I., and Zardoya, R. (2014). Diversity and evolution of membrane intrinsic proteins. *BBA Gen. Sub.* 1840, 1468–1481. doi: 10.1016/j.bbagen.2013.12.001

Augusto, A., Greene, L. J., Laure, H. J., and McNamara, J. C. (2007). Adaptive shifts in osmoregulatory strategy and the invasion of freshwater by brachyuran crabs: evidence from Dilocarcinus pagei (Trichodactylidae). *J. Exp. Zoo. Part A* 307A, 688–698. doi: 10.1002/jez.a.422

Augusto, A., Silva Pinheiro, A., Greene, L., Laure, H., and McNamara, J. C. (2009). Evolutionary transition to freshwater by ancestral marine palaemonids: evidence from osmoregulation in a tide pool shrimp. *Aquat. Biol.* 7, 113–122. doi: 10.3354/ab00183

Benga, G. (2012). On the definition, nomenclature and classification of water channel proteins (aquaporins and relatives). *Mol. Aspects Med.* 33, 514–517. doi: 10.1016/j.mam.2012.04.003

Bienert, G. P., Cavez, D., Besserer, A., Berny, M. C., Gilis, D., Rooman, M., et al. (2012). A conserved cysteine residue is involved in disulfide bond formation

between plant plasma membrane aquaporin monomers. *Biochem. J.* 445, 101–111. doi: 10.1042/BJ20111704

Boyle, R. T., Oliveira, L. F., Bianchini, A., and Souza, M. M. (2013). The effects of copper on Na+/K+-ATPase and aquaporin expression in two euryhaline invertebrates. *Bull. Environ. Contam. Toxicol.* 90, 387–390. doi: 10.1007/s00128-012-0949-4

Chen, C., Chen, H., Zhang, Y., Thomas, H. R., Frank, M. H., He, Y., et al. (2020). TBtools: an integrative toolkit developed for interactive analyses of big biological data. *Mol. Plant* 13, 1194–1202. doi: 10.1016/j.molp.2020.06.009

Chen, K., Li, E., Li, T., Xu, C., Wang, X., Lin, H., et al. (2015). Transcriptome and molecular pathway analysis of the hepatopancreas in the Pacific white shrimp Litopenaeus vannamei under chronic low-salinity stress. *PLoS One* 10:e0131503. doi: 10.1371/journal.pone.0131503

Cheng, K., Hu, C., Liu, Y., Zheng, S., and Qi, X. (2006). Effects of dietary calcium, phosphorus and calcium/phosphorus ratio on the growth and tissue mineralization of Litopenaeus vannamei reared in low-salinity water. *Aquaculture* 251, 472–483. doi: 10.1016/j.aquaculture.2005.06.022

Chung, J. S., Maurer, L., Bratcher, M., Pitula, J. S., and Ogburn, M. B. (2012). Cloning of aquaporin-1 of the blue crab, Callinectes sapidus: its expression during the larval development in hyposalinity. *Aquat. Biosyst.* 8:21. doi: 10.1186/2046-9063-8-21

Cobb, B. F., Conte, F. S., and Edwards, M. A. (1975). Free amino acids and osmoregulation in penaeid shrimp. *J. Agric. Food Chem.* 23, 1172–1174. doi: 10.1021/jf60202a015

Croghan, P. C. (1958). The mechanism of osmotic regulation in Artemia Salina (L.): the physiology of the gut. *J. Exp. Biol.* 35, 243–249. doi: 10.1242/jeb.35.1.243

Cui, Z., Liu, Y., Yuan, J., Zhang, X., Ventura, T., Ma, K. Y., et al. (2021). The Chinese mitten crab genome provides insights into adaptive plasticity and developmental regulation. *Nat. Commun.* 12, 2395. doi: 10.1038/s41467-021-22604-3

Ernst, J., and Bar-Joseph, Z. (2006). STEM: a tool for the analysis of short time series gene expression data. *BMC Bioinform.* 7:191. doi: 10.1186/1471-2105-7-191

Farlora, R., Araya-Garay, J., and Gallardo-Escárate, C. (2014). Discovery of sex-related genes through high-throughput transcriptome sequencing from the salmon louse Caligus rogercresseyi. *Mar. Genom.* 15, 85–93. doi: 10.1016/j.margen.2014.02.005

Finn, R. N., and Cerdà, J. (2015). Evolution and functional diversity of aquaporins. *Biol. Bull.* 229, 6–23. doi: 10.1086/BBLv229n1p6

Foguesatto, K., Bastos, C. L. Q., Boyle, R. T., Nery, L. E. M., and Souza, M. M. (2019). Participation of Na+/K+-ATPase and aquaporins in the uptake of water during moult processes in the shrimp Palaemon argentinus (Nobili, 1901). *J. Comp. Physiol. B* 189, 523–535. doi: 10.1007/s00360-019-01232-w

Foguesatto, K., Boyle, R. T., Rovani, M. T., Freire, C. A., and Souza, M. M. (2017). Aquaporin in different moult stages of a freshwater decapod crustacean: expression and participation in muscle hydration control. *Comp. Biochem. Phys. A* 208, 61–69. doi: 10.1016/j.cbpa.2017.03.003

Fu, D., Libson, A., Miercke, L. J., Weitzman, C., Nollert, P., Krucinski, J., et al. (2000). Structure of a glycerol-conducting channel and the basis for its selectivity. *Science* 290, 481–486. doi: 10.1126/science.290.5491.481

Gao, B., Sun, D., Lv, J., Ren, X., Liu, P., and Li, J. (2019). Transcriptomic analysis provides insight into the mechanism of salinity adjustment in swimming crab Portunus trituberculatus. *Genes Genom.* 41, 961–971. doi: 10.1007/s13258-019-00828-4

Gao, Y. (2009). *Cloning and Expression of Aquaporin in the Antennal Gland of Crayfish, Procambarus Clarkii*. Dayton: Wright State University.

Gao, Y., Hu, C., Ren, C., Qian, J., He, X., Jiang, X., et al. (2017). Molecular cloning of aquaporin-4 (AQP4) gene in the Pacific white shrimp (Litopenaeus vannamei) and the effect of salinity stress on its expression in hepatopancreas. *Mar. Sci.* 41, 61–70.

Hamdi, M., Sanchez, M. A., Beene, L. C., Liu, Q., Landfear, S. M., Rosen, B. P., et al. (2009). Arsenic transport by zebrafish aquaglyceroporins. *BMC Mol. Biol.* 10:104. doi: 10.1186/1471-2199-10-104

Hu, D., Pan, L., Zhao, Q., and Ren, Q. (2015). Transcriptomic response to low salinity stress in gills of the Pacific white shrimp, Litopenaeus vannamei. *Mar. Genom.* 24, 297–304. doi: 10.1016/j.margen.2015.07.003

Ishibashi, K., Morishita, Y., and Tanaka, Y. (2017). The evolutionary aspects of aquaporin family. *Adv. Exp. Med. Biol.* 969, 35–50. doi: 10.1007/978-94-024-1057-0_2

Ishibashi, K., Tanaka, Y., and Morishita, Y. (2020). "Chapter One - Perspectives on the evolution of aquaporin superfamily" in *Vitamins and Hormones*. ed. G. Litwack (United States: Academic Press). 1–27. doi: 10.1016/bs.vh.2019.08.001

Ishibashi, K., Tanaka, Y., and Morishita, Y. (2021). The role of mammalian superaquaporins inside the cell: an update. *BBA Biomembranes* 1863:183617. doi: 10.1016/j.bbamem.2021.183617

Keane, T. M., Creevey, C. J., Pentony, M. M., Naughton, T. J., and McLnerney, J. O. (2006). Assessment of methods for amino acid matrix selection and their use on empirical data shows that ad hoc assumptions for choice of matrix are not justified. *BMC Evol. Biol.* 6:29. doi: 10.1186/1471-2148-6-29

Kim, D., Langmead, B., and Salzberg, S. L. (2015). HISAT: a fast spliced aligner with low memory requirements. *Nat. Methods* 12, 357–360. doi: 10.1038/nmeth.3317

Kim, Y. K., Lee, S. Y., Kim, B. S., Kim, D. S., and Nam, Y. K. (2014). Isolation and mRNA expression analysis of aquaporin isoforms in marine medaka Oryzias dancena, a euryhaline teleost. *Comp. Biochem. Phys. A* 171, 1–8. doi: 10.1016/j.cbpa.2014.01.012

Kumar, S., Stecher, G., Li, M., Knyaz, C., and Tamura, K. (2018). MEGA X: molecular evolutionary genetics analysis across computing platforms. *Mol. Biol. Evol.* 35, 1547–1549. doi: 10.1093/molbev/msy096

Letunic, I., and Bork, P. (2021). Interactive Tree Of Life (iTOL) v5: an online tool for phylogenetic tree display and annotation. *Nucleic. Acids. Res.* 49, W293–W296. doi: 10.1093/nar/gkab301

Li, C., Li, N., Dong, T., Fu, Q., Cui, Y., and Li, Y. (2020). Analysis of differential gene expression in Litopenaeus vannamei under high salinity stress. *Aquacult. Rep.* 18:100423. doi: 10.1016/j.aqrep.2020.100423

Li, C., and Wang, W. (2017). "Molecular Biology of Aquaporins" in *Aquaporins*. ed. B. Yang (Dordrecht: Springer). 1–34. doi: 10.1007/978-94-024-1057-0_1

Li, E., Wang, S., Li, C., Wang, X., Chen, K., and Chen, L. (2014). Transcriptome sequencing revealed the genes and pathways involved in salinity stress of Chinese mitten crab, Eriocheir sinensis. *Physiol. Genomics* 46, 177–190. doi: 10.1152/physiolgenomics.00191.2013

Li, Y., Chen, Y., Cui, Y., Shen, M., Wang, R., and Wang, Z. (2022). Transcriptome analysis of Pacific white shrimp (Litopenaeus vannamei) under prolonged high-salinity stress. *J. Ocean Univ. China* 21, 1–15. doi: 10.1007/s11802-022-4882-9

Lind, U., Järvå, M., Alm Rosenblad, M., Pingitore, P., Karlsson, E., Wrange, A.-L., et al. (2017). Analysis of aquaporins from the euryhaline barnacle Balanus improvisus reveals differential expression in response to changes in salinity. *PLoS One* 12:e0181192. doi: 10.1371/journal.pone.0181192

Liu, M., Liu, S., Hu, Y., and Pan, L. (2015). Cloning and expression analysis of two carbonic anhydrase genes in white shrimp Litopenaeus vannamei, induced by pH and salinity stresses. *Aquaculture* 448, 391–400. doi: 10.1016/j.aquaculture.2015.04.038

Liu, W., Xie, Y., Ma, J., Luo, X., Nie, P., Zuo, Z., et al. (2015). IBS: an illustrator for the presentation and visualization of biological sequences. *Bioinformatics* 31, 3359–3361. doi: 10.1093/bioinformatics/btv362

Livak, K. J., and Schmittgen, T. D. (2001). Analysis of relative gene expression data using real-time quantitative PCR and the 2-ΔΔCT method. *Methods* 25, 402–408. doi: 10.1006/meth.2001.1262

Love, M. I., Huber, W., and Anders, S. (2014). Moderated estimation of fold change and dispersion for RNA-seq data with DESeq2. *Genome Biol.* 15, 550. doi: 10.1186/s13059-014-0550-8

Lv, J., Liu, P., Wang, Y., Gao, B., Chen, P., and Li, J. (2013). Transcriptome analysis of Portunus trituberculatus in response to salinity stress provides insights into the molecular basis of osmoregulation. *PLoS One* 8:e82155. doi: 10.1371/journal.pone.0082155

Madsen, S. S., Engelund, M. B., and Cutler, C. P. (2015). Water transport and functional dynamics of aquaporins in osmoregulatory organs of fishes. *Biol. Bull.* 229, 70–92. doi: 10.1086/BBLv229n1p70

McGaw, I. J., and Curtis, D. L. (2013). A review of gastric processing in decapod crustaceans. *J. Comp. Physiol. B* 183, 443–465. doi: 10.1007/s00360-012-0730-3

McNamara, J. C., and Faria, S. C. (2012). Evolution of osmoregulatory patterns and gill ion transport mechanisms in the decapod Crustacea: a review. *J. Comp. Physiol. B* 182, 997–1014. doi: 10.1007/s00360-012-0665-8

McNamara, J. C., Rosa, J. C., Greene, L. J., and Augusto, A. (2004). Free amino acid pools as effectors of osmostic adjustment in different tissues of the freshwater shrimp Macrobrachium olfersii (Crustacea, Decapoda) during long-term salinity acclimation. *Mar. Freshw. Behav. Phy.* 37, 193–208. doi: 10.1080/10236240400006208

Meng, J., Zhu, Q., Zhang, L., Li, C., Li, L., She, Z., et al. (2013). Genome and transcriptome analyses provide insight into the euryhaline adaptation mechanism of Crassostrea gigas. *PLoS One* 8:e58563. doi: 10.1371/journal.pone.0058563

Moshtaghi, A., Rahi, M. L., Mather, P. B., and Hurwood, D. A. (2018). An investigation of gene expression patterns that contribute to osmoregulation in Macrobrachium australiense: assessment of adaptive responses to different osmotic niches. *Gene Rep.* 13, 76–83. doi: 10.1016/j.genrep.2018.09.002

Murata, K., Mitsuoka, K., Hirai, T., Walz, T., Agre, P., Heymann, J. B., et al. (2000). Structural determinants of water permeation through aquaporin-1. *Nature* 407, 599–605. doi: 10.1038/35036519

Nong, W., Chai, Z. Y. H., Jiang, X., Qin, J., Ma, K. Y., Chan, K. M., et al. (2020). A crustacean annotated transcriptome (CAT) database. *BMC Genomics* 21:32. doi: 10.1186/s12864-019-6433-3

Pan, L., Liu, H., and Zhao, Q. (2014). Effect of salinity on the biosynthesis of amines in Litopenaeus vannamei and the expression of gill related ion transporter genes. *J. Ocean Univ. China* 13, 453–459. doi: 10.1007/s11802-014-2013-y

Pertea, M., Kim, D., Pertea, G. M., Leek, J. T., and Salzberg, S. L. (2016). Transcript-level expression analysis of RNA-seq experiments with HISAT, StringTie and Ballgown. *Nat. Protoc.* 11, 1650–1667. doi: 10.1038/nprot.2016.095

Pertea, M., Pertea, G. M., Antonescu, C. M., Chang, T.-C., Mendell, J. T., and Salzberg, S. L. (2015). StringTie enables improved reconstruction of a transcriptome from RNA-seq reads. *Nat. Biotechnol.* 33, 290–295. doi: 10.1038/nbt.3122

Pettersen, E. F., Goddard, T. D., Huang, C. C., Couch, G. S., Greenblatt, D. M., Meng, E. C., et al. (2004). UCSF Chimera—A visualization system for exploratory research and analysis. *J. Comput. Chem.* 25, 1605–1612. doi: 10.1002/jcc.20084

Shen, M., Cui, Y., Wang, R., Dong, T., Ye, H., Wang, S., et al. (2020). Acute response of Pacific white shrimp Litopenaeus vannamei to high-salinity reductions in osmosis-, metabolism-, and immune-related enzyme activities. *Aquacult. Int.* 28, 31–39. doi: 10.1007/s10499-019-00441-y

Shen, Y., Li, H., Zhao, J., Tang, S., Zhao, Y., Gu, Y., et al. (2021). Genomic and expression characterization of aquaporin genes from Siniperca chuatsi. *Comp. Biochem. Phys. D* 38:100819. doi: 10.1016/j.cbd.2021.100819

Staniscuaski, F., Paluzzi, J.-P., Real-Guerra, R., Carlini, C. R., and Orchard, I. (2013). Expression analysis and molecular characterization of aquaporins in Rhodnius prolixus. *J. Insect Physiol.* 59, 1140–1150. doi: 10.1016/j.jinsphys.2013.08.013

Stavang, J. A., Chauvigné, F., Kongshaug, H., Cerdà, J., Nilsen, F., and Finn, R. N. (2015). Phylogenomic and functional analyses of salmon lice aquaporins uncover the molecular diversity of the superfamily in Arthropoda. *BMC Genomics* 16:618. doi: 10.1186/s12864-015-1814-8

Sui, H., Han, B.-G., Lee, J. K., Walian, P., and Jap, B. K. (2001). Structural basis of water-specific transport through the AQP1 water channel. *Nature* 414, 872–878. doi: 10.1038/414872a

Thabet, R., Ayadi, H., Koken, M., and Leignel, V. (2017). Homeostatic responses of crustaceans to salinity changes. *Hydrobiologia* 799, 1–20. doi: 10.1007/s10750-017-3232-1

Tingaud-Sequeira, A., Calusinska, M., Finn, R. N., Chauvigné, F., Lozano, J., and Cerdà, J. (2010). The zebrafish genome encodes the largest vertebrate repertoire of functional aquaporins with dual paralogy and substrate specificities similar to mammals. *BMC Evol. Biol.* 10:38. doi: 10.1186/1471-2148-10-38

Tsujimoto, H., Liu, K., Linser, P. J., Agre, P., and Rasgon, J. L. (2013). Organ-specific splice variants of aquaporin water channel AgAQP1 in the malaria vector Anopheles gambiae. *PLoS One* 8:e75888. doi: 10.1371/journal.pone.0075888

Vandesompele, J., De Preter, K., Pattyn, F., Poppe, B., Van Roy, N., De Paepe, A., et al. (2002). Accurate normalization of real-time quantitative RT-PCR data by geometric averaging of multiple internal control genes. *Genome Biol.* 3:research0034.1. doi: 10.1186/gb-2002-3-7-research0034

Wang, X., Wang, S., Li, C., Chen, K., Qin, J. G., Chen, L., et al. (2015). Molecular pathway and gene responses of the Pacific white shrimp Litopenaeus vannamei to acute low salinity stress. *J. Shellfish Res.* 34, 1037–1048. doi: 10.2983/035.034.0330

Wang, Y., Li, E., Yu, N., Wang, X., Cai, C., Tang, B., et al. (2012). Characterization and expression of glutamate dehydrogenase in response to acute salinity stress in the Chinese mitten crab. Eriocheir sinensis. *PLoS One* 7:e37316. doi: 10.1371/journal.pone.0037316

Waterhouse, A. M., Procter, J. B., Martin, D. M. A., Clamp, M., and Barton, G. J. (2009). Jalview Version 2–a multiple sequence alignment editor and analysis workbench. *Bioinformatics* 25, 1189–1191. doi: 10.1093/bioinformatics/btp033

Xu, C., Li, E., Liu, Y., Wang, X., Qin, J. G., and Chen, L. (2017). Comparative proteome analysis of the hepatopancreas from the Pacific white shrimp Litopenaeus vannamei under long-term low salinity stress. *J. Proteomics* 162, 1–10. doi: 10.1016/j.jprot.2017.04.013

Yu, G., Wang, L.-G., Han, Y., and He, Q.-Y. (2012). clusterProfiler: an R package for comparing biological themes among gene clusters. *OMICS* 16, 284–287. doi: 10.1089/omi.2011.0118

Yuan, J., Zhang, X., Wang, M., Sun, Y., Liu, C., Li, S., et al. (2021). Simple sequence repeats drive genome plasticity and promote adaptive evolution in penaeid shrimp. *Commun. Biol.* 4:186. doi: 10.1038/s42003-021-01716-y

Zhang, X., Yuan, J., Sun, Y., Li, S., Gao, Y., Yu, Y., et al. (2019). Penaeid shrimp genome provides insights into benthic adaptation and frequent molting. *Nat. Commun.* 10:356. doi: 10.1038/s41467-018-08197-4

Conflict of Interest: The authors declare that the research was conducted in the absence of any commercial or financial relationships that could be construed as a potential conflict of interest.

Publisher's Note: All claims expressed in this article are solely those of the authors and do not necessarily represent those of their affiliated organizations, or those of the publisher, the editors and the reviewers. Any product that may be evaluated in this article, or claim that may be made by its manufacturer, is not guaranteed or endorsed by the publisher.

frontiers in Marine Science

ORIGINAL RESEARCH
published: 24 February 2022
doi: 10.3389/fmars.2022.824973

Optimal Dietary Crude Protein in Commercial Feeds for Shrimp and Halophytes in Marine Aquaponic Biofloc Systems

*Yu-Ting Chu and Paul B. Brown**

Department of Forestry and Natural Resources, Purdue University, West Lafayette, IN, United States

Formulated diets for animals is the primary source of nutrients in aquaponic systems that need to maintain beneficial bacteria as well as for plants. Dietary protein is one of the expensive macronutrients in fish diets, especially when fishmeal is used, and it is the source of nitrogen (N) for other biotic components. Biofloc has the potential to serve as the supplement diet for shrimp and reduce the need of expensive protein. However, it is not clear if low dietary protein will be adequate to support the three organisms (animals, plants, and bacteria) in an aquaponic system operated with biofloc technology. The aim of the present study was to investigate the effect of shrimp feed with different protein concentrations (30, 35, or 40%) on water quality and the growth performance of Pacific whiteleg shrimp (*Litopenaeus vannamei*) and three edible halophytic plants (*Atriplex hortensis*, *Salsola komarovii*, and *Plantago coronopus*) in biofloc-based marine aquaponics. The experiment was conducted for 12 weeks, the plants were harvested and seedlings transplanted every 4 weeks. Dietary protein content did not influence shrimp growth in the current study, indicating that feeds with lower protein concentrations can be used in biofloc-based marine aquaponic systems. During the early and mid-stages of cultivation, plants grew better when supplied diets with higher protein concentration, whereas no differences were observed for later harvests. Hence, for maximum production with mature systems or in the scenario of high concentration of nitrate, providing a higher protein concentration feed in the early stages of system start-up, and switching to a lower protein concentration feed in later stages of cultivation was recommended.

Keywords: marine aquaponics, crude protein concentration, nutrient management, *Litopenaeus vannamei*, halophytic plants, biofloc, sustainable food production

OPEN ACCESS

Edited by:
Xiangli Tian,
Ocean University of China, China

Reviewed by:
Nor Azman Kasan,
University of Malaysia Terengganu, Malaysia
Nicholas Romano,
University of Arkansas at Pine Bluff, United States

***Correspondence:**
Paul B. Brown
pb@purdue.edu

Specialty section:
This article was submitted to Marine Fisheries, Aquaculture and Living Resources, a section of the journal Frontiers in Marine Science

Received: *29 November 2021*
Accepted: *02 February 2022*
Published: *24 February 2022*

Citation:
Chu Y-T and Brown PB (2022) Optimal Dietary Crude Protein in Commercial Feeds for Shrimp and Halophytes in Marine Aquaponic Biofloc Systems. Front. Mar. Sci. 9:824973. doi: 10.3389/fmars.2022.824973

INTRODUCTION

The primary source of nutrients into aquaponic systems is the feed for the animal. Bacteria and plants then rely on waste excretions from the animal, solubilization of nutrients from uneaten feed and feces, and/or conversion of nutrients by bacteria as their primary nutrient sources. Among the macronutrients, protein is the main source of nitrogen (N). Dietary crude protein and the constituent essential amino acids are vital for the growth and health of animals and waste N is

excreted primarily as ammonia-N (NH_3) across the gills of aquatic animals. Excreted NH_3 can be metabolized by bacterial colonies within the system to nitrite-N (NO_2^-) and nitrate-N (NO_3^-), which plants use as their N source. Several aspects of nutrient input into aquaponic systems have been evaluated, such as feeding frequency, feeding regime, feed amount to plant area ratio, animal to plant ratio, water retention time, and subsystem ratio (Rakocy, 2012; Liang and Chien, 2013; Lam et al., 2015; Yang and Kim, 2019, 2020a; Chu and Brown, 2021a). However, the effects of the dietary protein concentration on aquaponics have not been fully evaluated.

Meeting the nutritional needs of target crops is vital for successful operation. Insufficient dietary crude protein concentrations will result in reduced growth of animals, lower NH_3 excretion and potentially inadequate concentrations of NO_2^- and NO_3^- for plants. However, an excessive concentration of dietary crude protein could result in the accumulation of toxic nitrogen compounds. Dietary protein in aquatic animal diets is generally considered one of the macronutrients that influence the price of feeds; thus, the complex N flow through aquaponic subsystems is a significant economic consideration. One of the basic tenets in nutrition is quantification of the minimum concentration of nutrient that results in maximum response. This fundamental concept has not been fully explored in integrated systems where both animal and plant nutrition is important.

Pacific whiteleg shrimp (*Litopenaeus vannamei*) are the largest crustacean aquaculture industry globally (FAO, 2020), can potentially produce 3–4 marketable crops per year, display high market demand and value, are tolerant of a wide range of salinities and stocking densities (FAO, 2016; Gao et al., 2016; Ross et al., 2017; Araneda et al., 2020) and may alleviate the "economic drain" associated with fish raised in freshwater aquaponic systems (Quagrainie et al., 2018). The optimal dietary crude protein concentration for shrimp varies as a function of several factors, and one of them that influence protein requirement is biofloc. It is generally considered to be in the range of 25–45% of the diet (Xu et al., 2012; Xu and Pan, 2014; Yun et al., 2016; Lee and Lee, 2018; Panigrahi et al., 2019). The three plant crops (*Atriplex hortensis*, *Salsola komarovii*, and *Plantago coronopus*) we have been working with have high nutrient concentrations (Carlsson and Clarke, 1983; Zhao and Feng, 2001; Koyro, 2006) and have been successfully grown in marine aquaponics with Pacific whiteleg shrimp (Chu and Brown, 2021a,b).

Biofloc technology (BFT) is one of the sustainable approaches used in high-density aquaculture to manage water quality, especially for shrimp farming (Avnimelech, 1999, 2006; Browdy et al., 2012). The BFT system deviated from the strictly recirculating culture systems by relying on heterotrophic bacteria to help degrade waste products instead of attempting to maintain nearly pure cultures of chemolithotrophs. Additional organic carbon input is commonly required to maintain healthy heterotrophic populations (Crab, 2010; Browdy et al., 2012; Crab et al., 2012; Xu et al., 2016). Ecosystem services provided by these diverse microbial communities include the recycling of waste material and nutrient supply to the target crop (Avnimelech, 1999; Crab, 2010; Browdy et al., 2012; Crab et al., 2012). Several reports indicated lower concentrations of dietary crude protein did not significantly affect shrimp growth in biofloc systems (Xu et al., 2012; Yun et al., 2016). However, it is not clear if low dietary crude protein will be adequate in an aquaponic system operated with biofloc technology.

The objective of this study was evaluation of varying concentrations of dietary crude protein in practical diets fed to shrimp raised in biofloc aquaponic saltwater systems.

MATERIALS AND METHODS

Aquaponic System Design

Nine experimental systems were designed, constructed, and used in this research. Systems were located at the Aquaculture Research Lab (ARL), Purdue University, West Lafayette, IN, United States (40° 25′ 26.4″ N, 86° 55′ 44.4″ W). Systems were described previously (Chu and Brown, 2021b). Briefly, each aquaponic system had 113.6 L aquaculture tank, a 102.2 L hydroponic tank, and an 18.9 L biofilter tank. Air stones were placed in every aquaculture, hydroponic and biofilter tank. Water temperature was maintained within the range of 26–28°C using submersible heaters (300w; Aqueon, WI, United States). The airlift system moved water at a rate of 3 L/min. LED lights (40w, 5,000 lumens, 4,000K daylight white; Kihung LED, Guangdong, China) were suspended at a height of 6.5 inches over the plant growth bed. Photosynthetic photon flux density (PPFD) was determined by a quantum sensor (MQ-500 Full-Spectrum Quantum Meter; Apogee Instruments, Inc., Logan, UT, United States). The photosynthetically active radiation (PAR) averaged 239 $\mu molm^{-2}s^{-1}$. The photoperiod during the experiment was set as 14 h light (6:00 am–8:00 pm) and 10 h dark (8:00 pm–6:00 am).

Biological Material

Shrimp

Juvenile Pacific whiteleg shrimp (*Litopenaeus vannamei*) were transported from a private producer (RDM Aquaculture, Fowler, IN, United States) to the ARL in water of 24°C and salinity of 15 ppt. Shrimp were separated into three 700 L tanks and quarantined for a week before moving into experimental units. Shrimp were fed twice a day (8:00 a.m. and 5:00 p.m.) with commercial shrimp feed (Zeigler Brothers, Gardners, PA, United States) during quarantine. Daily feeding amount was 3.0% of total biomass, divided into aliquots.

Plants

Seeds of three halophytic plants, red orache (*Atriplex hortensis*), okahijiki (*Salsola komarovii*), and minutina (*Plantago cornonpus*), were obtained from a commercial source (Johnny's Selected Seeds, Winslow, ME, United States). Seeds were sowed in horticubes, soilless foam medium (OASIS Grower Solutions, Kent, OH, United States), and irrigated with fresh water for a week while germinating. Beginning the 2nd week, sea salt (Instant Ocean, Blacksburg, VA, United States) was added to increase the salinity in the irrigation water at a rate of 2–3 ppt every 2 days to a final salinity of 15 ppt.

Experimental Design and System Management

The experiment was conducted for 12 weeks (October 17, 2020 to January 9, 2021). Growth assay of shrimp and the three halophytes was determined as a function of three different commercial diets containing 30% (P30), 35% (P35), or 40% (P40) crude protein (**Supplementary Figure 1**). Specific ingredients concentrations were proprietary, but all three diets are commercially available. One week prior to the experiment, shrimp were weighed and placed in aquaculture tanks to produce nutrients for plants. The stocking density of shrimp was 300 shrimp/m^2 (60 shrimp/tank, 600 shrimp/m^3), with an initial average weight of 1.46 g. A total of 24 plants (8 plants per species) were stocked in each hydroponic tank, which was equivalent to a density of 100 plants/m^2. Shrimp were fed three times per day at 8:00 a.m., 1:00 p.m., and 6:00 p.m., with a total daily amount of 3.0% of bodyweight divided into aliquots. Plants were harvested every 4 weeks and new seedlings were transplanted.

Initial water in all experimental systems remained from prior experiments. In the interim between experiments, evaporative losses were replaced with well water, constant aeration was provided to all subsystems and probiotics (EZ-Bio, *Bacillus* spp., Zeigler Brothers, Gardners, PA, United States) were added weekly at a dose of 10 ppm EZ-bio once a week. Once shrimp moved into experimental units, additional doses of probiotics were added every other day in the 1st week, twice per week in the 2nd week, and once per week beginning in the 3rd week continuing until the end of the experiment (Crab et al., 2010; Chu, 2014; Chu and Brown, 2021b). Molasses (Hawthorne Gardening Co., Vancouver, WA, United States) was provided as an organic carbon source for the adjustment of C/N ratio. The amount of molasses added was based on the C/N content of shrimp feed and the carbon content of the molasses to raise the C/N ratio to 15 (**Table 1**). If alkalinity decreased below 75 mg/L, or pH lower than 7.2, potassium bicarbonate was added to adjust environmental conditions. If pH rose above 8.0, 10% sulfuric acid was applied.

The nine aquaponic systems used for this experiment were each randomly assigned to one of three treatments (n = 3). Throughout the 12-week experiment, no water was discharged or exchanged, only added to replace evaporative losses.

Measurement of Water Quality

Dissolved oxygen (DO) and temperature (OxyGuard Handy Polaris DO meter, Farum, Denmark), pH (pHTestr 10 Pocket pH Tester, Vernon Hills, IL, United States) were measured and recorded in each system twice daily at 8:00 a.m. and 6:00 p.m. before feeding. Salinity (Vital Sine Salinity Refractometer, Pentair Aquatic Eosystems, Apopka, FL, United States) was determined once per day at 8 a.m. Water samples were collected twice weekly from aquaculture tanks before feeding, to determine the concentrations of total ammonia-nitrogen (TAN), nitrite-N (NO_2^-), nitrate-N (NO_3^-), phosphate (PO_4^{3-}), and alkalinity. TAN, NO_2^-, NO_3^-, and PO_4^{3-} were measured using Hach methods 8155, 8507, 8039, and 8048, respectively, using a Hach DR3900 spectrophotometer (HACH, Loveland, CO, United States). Alkalinity was determined with Hach kit (HACH, Loveland, CO, United States). Total suspended solids (TSS) and volatile suspended solids (VSS) were measured once weekly following United States EPA method 1684.

TABLE 1 | The amount of molasses needed to get C/N ratio to 15 for the three commercial shrimp feed.

Product	Protein content (%)	Total carbon (%)	C/N ratio	Amount of molasses needed (g/g feed)
SI-30	30	42.1	8.7	0.85
HI-35	35	41.8	7.1	1.2
PL-40	40	42.0	6.9	1.5
Molasses	–	35.0	–	–

Growth Performance

Shrimp

Weights and numbers of shrimp were collected at the beginning and end of the experiment. Feed input was recorded every day and summed. The following formulae were used to calculate shrimp responses:

$$\text{Survival (\%)} = \frac{\text{Final number of shrimp}}{\text{Initial number of shrimp}} \times 100;$$

$$\text{Weight gain (\%)} = \frac{\text{(Final biomass (g)} - \text{Initial biomass (g))}}{\text{Initial biomass}} \times 100; \text{ and}$$

$$\text{Specific growth rate (\%)} = \frac{\text{[Ln (Final biomass (g))} - \text{Ln (Initial biomass (g))]}}{\text{day}} \times 100.$$

Plants

Edible parts of all plants were collected and weighed individually at the beginning and end of the experiment. Plant samples were dried in an oven at 100°C until constant weight and then measured as dry weight. In addition, dried plant samples were ground and filtered through a 10-mesh sieve and stored in plastic vials for nutrient analysis. Plant tissue analysis was done by the Midwest laboratory (Omaha, NE, United States). Formula used to calculate plant growth indices and nitrogen use efficiency were:

$$\text{Relative growth rate (\%)} = \frac{\text{[Ln (Final biomass (g))} - \text{Ln (Initial biomass (g))]}}{\text{day}} \times 100;$$

$$\text{Water content (\%)} = \frac{\text{(Final fresh weight (g)} - \text{Final dry weight (g))}}{\text{Final fresh weight}} \times 100; \text{ and,}$$

$$\text{Nitrogen use efficiency (NUE)} = \frac{\text{g N absorbed}}{\text{g N supplied}} \times 100.$$

Statistical Analysis

Shrimp and plant responses, nutrient concentrations in plants, and water quality parameters were subjected to analysis of variance (ANOVA) using JMP Pro 16.0 (SAS Institute Inc., Cary, NC, United States). Interactions between treatment and plant species or harvest time were tested by two-way ANOVA. Statistical difference between means were determined by Tukey's honestly significant difference test (HSD) at $p \leq 0.05$.

RESULTS

Shrimp Response

There were no significant differences in final weight, weight gain (WG), or specific growth rate (SGR) of shrimp among dietary treatments (**Table 2**). Shrimp mortality increased in the last 2 weeks of the experiment (**Figure 1**), and most carcasses were soft-shelled and had traces of being eaten. The average survival of P30, P35, and P40 treatments was 72.8, 66.1, and 49.4%, respectively (**Table 2**). To alleviate shrimp mortality and the increasing TAN, feeding was reduced to 1/3 of the original amount from week 10 until the end of the experiment.

Plant Response

Plant growth parameters of all three plants were significantly ($p < 0.05$) affected by harvest time. Only okahijiki was also affected by dietary crude protein concentration and the interaction of dietary crude protein and harvest time (**Figure 2**). In general, dietary crude protein concentrations significantly ($p < 0.05$) affected the growth performance of red orache and okahijiki in the first and second harvest, while there were no significant ($p > 0.05$) differences among treatments in the third harvest. Red orache and okahijiki had better final fresh weight and final dry weight in the P35 treatment in the first two harvests. In the third harvest, although there was no difference among treatments, red orache had relatively better performance in P40 than other treatments, whereas, okahijiki still performed better in the P35 treatment. The growth performance of minutina was increased with the increasing protein level, yet there were no significant ($p > 0.05$) differences among treatments. The growth of the three plants was significantly ($p < 0.05$) increased with harvest time (**Figure 2**). Red orache and minutina's fresh weight and dry weight were 1.5 to twofold greater in the second and third harvests, and okahijiki's fresh weight and dry weight were 2–3 times as great as the first harvest.

The interaction of plant species and treatment exerted no significant effect on yield, NUE, or the concentration of N, P, and K (**Table 3**). However, the yield, and the concentrations of N, P, and K were significantly ($p < 0.05$) affected by plant species, and NUE was significantly ($p < 0.05$) affected by plant species, and treatment. The production of each plant species was not significantly ($p > 0.05$) different among treatments. When comparing the three plant species in each treatment, the yield and NUE of okahijiki was significantly lower ($p < 0.05$) than that of red orache and minutina regardless of protein level; however, okahijiki contained the highest concentrations of N, P, and K in tissues. NUE declined with increasing crude protein concentration, and the lowest NUE of all three plant species was in the P40 treatment.

TABLE 2 | Growth parameters and survival of *Litopenaeus vannamei* fed with three levels of dietary protein in marine aquaponics for 12 weeks.

Parameter	Treatment			
	P30	P35	P40	*P*
Initial weight (g)	1.46 ± 0.01	1.45 ± 0.01	1.46 ± 0.01	ns
Final weight (g)	9.41 ± 0.68	9.46 ± 1.21	10.41 ± 0.73	ns
WG (%)	546.7 ± 47.1	551.8 ± 83.9	615.0 ± 51.2	ns
SGR (%)	2.22 ± 0.09	2.22 ± 0.15	2.34 ± 0.09	ns
Survival (%)	72.8 ± 2.5	66.1 ± 5.4	49.4 ± 20.2	ns

Each value represents means ± SD.
ns means no significant at p > 0.05.

Water Quality

During the 12-week experiment, temperature and dissolved oxygen (DO) were maintained at 26–28°C and 6.4–7.1 mg/L in all treatments, respectively. The salinity was monitored and controlled every day to maintain at 15 ppt. There were no significant differences ($p > 0.05$) in alkalinity, TSS, VSS, or environmental pH among treatments (**Figure 3** and **Table 4**). The pH in the three treatments decreased over time, but the decrease was consistent across all treatment (**Figure 3**).

The concentrations of TAN, nitrite-N, nitrate-N, and phosphate are shown in **Figure 4**. The concentration of TAN and nitrite-N slightly increased after every harvest (day 28 and day 56), but remained below 0.9 and 0.4 ppm, respectively (**Figures 4A,B**). However, the concentration of TAN increased to around 2 ppm in P35 and P40 treatments, and 1.5 ppm in P30 treatment on day 73 (**Figure 4A**). The concentration of nitrite-N in the P35 and P40 treatments was higher than that in P30 treatment after day 35 (**Figure 4B**). Similar to TAN and nitrite-N, the concentration of nitrate-N was higher in the higher protein treatment. However, nitrate-N concentrations decreased over time in all three treatments (**Figure 4C**). Unlike the fluctuation in nitrogenous compounds, the concentration of phosphate steadily increased over time (**Figure 4D**).

DISCUSSION

Shrimp Growth

Based on these data, dietary crude protein concentrations higher than 30% do not appear to confer additional benefit to whiteleg shrimp grown in aquaponic systems with biofloc. Lower dietary crude protein concentrations commonly results in lower costs

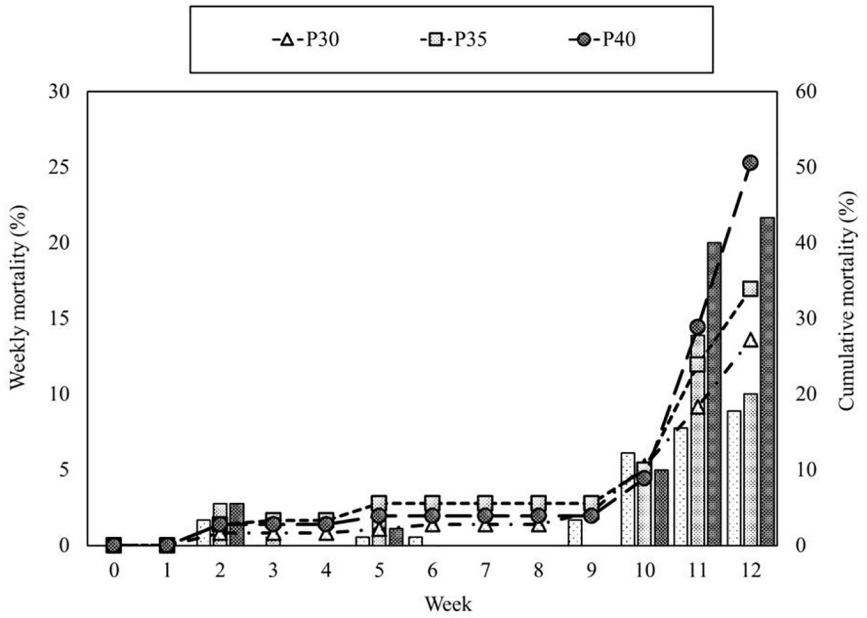

FIGURE 1 | Weekly (bar) and cumulative mortality (line) of *Litopenaeus vannamei* fed with three levels of dietary protein in marine aquaponics for 12 weeks.

diets. If there is no benefit feeding higher concentrations of crude protein, this potentially results in improved economic efficiency. Several studies have demonstrated that shrimp experience better growth performance and lower FCR when fed higher protein diets (Xia et al., 2010; Shahkar et al., 2014; Jana et al., 2021); however, daily exchanges of water occurred in these studies. In contrast, other researchers reported that there is the possibility of reducing dietary crude protein concentration in shrimp feed without affecting growth performance when BFT is applied (Xu et al., 2012; Panigrahi et al., 2019). The present study also implemented BFT and showed similar results to previous research. These results could be attributed to the microbial proteins, which serve as a source of supplemental protein for shrimp in this kind of system (Ballester et al., 2010; Browdy et al., 2012).

The high mortality rate that occurred at the late stage of the present study might be related to competition for space, cannibalism, pH decrease, insufficient ions, or increased nitrogenous compounds (Abdussamad and Thampy, 1994; Wheatly, 1999; Nga et al., 2005; Arnold et al., 2006). In crustaceans, molting is associated with growth, and they are vulnerable at postmolt, which has been viewed as a period conducive to disease and dysfunction (Lemos and Weissman, 2021). In the postmolt period, the new cuticle is predominantly mineralized with external calcium. Furthermore, Zanotto and Wheatly (1995) reported that the uptake of calcium by shrimp was reduced by 60% under low pH conditions. Insufficient calcium in the water or a low pH can retard the calcification of the cuticle and delay recovery from molting, leading to mortality and cannibalism (Zanotto and Wheatly, 1993; Wheatly, 1999). In the present study, pH decreased with time, which might have contributed to low Ca uptake and soft-shelled shrimp, along with high mortality in the later stage of cultivation. Additionally, shrimp without a hard shell are subject to attacks from fellow shrimp, and toxic substances (TAN or nitrite-N) are also more likely to penetrate the membrane into the body and cause poisoning and death (Lemos and Weissman, 2021). This might be an explanation for the relatively lower survival in higher protein treatments. More research is needed to investigate the feeding and calcium management, and determine the optimal pH range for shrimp-based aquaponics.

Plants

Similar to the results with shrimp, there were no significant benefits of feeding higher dietary crude protein concentrations to yield and NUE of plants. The goal of food production systems is to optimize nutrient use efficiency in order to increase production yields while reducing inputs (USDA, 2007). In the present study, plants provided with 40% dietary crude protein did not return with higher growth and yield but resulted in low NUE, which suggested excessive N was provided. Yield was numerically higher in systems offered 35% dietary crude protein. More importantly, yield increased over time.

Nutrient requirements for optimal growth of plants varies by species, growth stage, temperature, pH, and other environmental factors (Hawkesford et al., 2011; Abbasi et al., 2017; Prieto et al., 2017). The yield of all three plant species increased significantly ($p < 0.05$) with each harvest (**Figure 2**), which was similar to the result published by Yang and Kim (2020b). They suggested the increased production was related to the maturity of the system. Furthermore, the ratio of NH_4^+ to NO_3^- and pH decrease in the present study might also play a role in this result. Plants grow better when provided a mixed supply of

ANOVA	Red orache	Okahijiki	Minutina
Treatment	ns	***	ns
Harvest time	***	***	***
Treatment × Harvest time	ns	*	ns

FIGURE 2 | Plant growth parameters of red orache, okahijiki, and minutina at three harvest times. Each value represents means. Values within rows followed by different uppercase alphabet letters indicate significant differences ($p < 0.05$) between treatments. Values within columns with different lowercase alphabet letters indicate significant differences ($p < 0.05$) between harvest times. ns, *, *** means no significant or significant at $p \leq 0.05$, or 0.0001, respectively.

NH_4^+ and NO_3^-, while the optimal ratio varies from species to species, common ratio of NH_4^+: NO_3^- are 1:9, 1:3, or 1:1 (Hawkesford et al., 2011; Zhang et al., 2019; Yang et al., 2020; Zhu et al., 2021). At the early stage of the present study, the concentration of NO_3^- (>10 ppm) was relatively higher than that of TAN (<0.5 ppm) and was the main source of N for plants in the water. This could be the potential reason for lower growth at the early stage, because NO_3^- assimilation consumes more energy than ammonium assimilation. Before plant assimilation, NO_3^- has to be reduced to nitrite and then ammonium by nitrate reductase and nitrite reductase, respectively (Hawkesford et al., 2011). The concentration of TAN slowly increased over time, whereas that of nitrate-N presented in an opposite trend (**Figures 4A,C**), which resulted in a mixed nutrient in the middle and late stages of the cultivation, and this could contribute to the improvement of plant growth in

TABLE 3 | Average nutrient content, yield, and nitrogen use efficiency (NUE) of red orache, okahijiki, and minutina from the three harvests.

Treatment	Plant species	N (%)	P (%)	K (%)	Yield (kg/m^2)	NUE (%)
P30	Red orache	4.52 ± 0.50a	0.58 ± 0.14c	1.77 ± 0.28c	1.45 ± 0.40a	13.88 ± 2.74a
	Okahijiki	4.97 ± 0.38a	1.79 ± 0.24a	6.17 ± 0.53a	0.62 ± 0.38b	5.03 ± 1.61c
	Minutina	3.87 ± 0.39b	1.38 ± 0.18b	2.31 ± 0.22b	1.82 ± 0.28a	10.54 ± 2.99b
	P	***	***	***	***	***
P35	Red orache	4.79 ± 0.38a	0.64 ± 0.15c	1.75 ± 0.20c	1.55 ± 0.28a	13.71 ± 2.69a
	Okahijiki	5.05 ± 0.32a	1.67 ± 0.14a	6.77 ± 0.79a	0.78 ± 0.36b	5.70 ± 0.53c
	Minutina	3.87 ± 0.34b	1.35 ± 0.15b	2.54 ± 0.17b	1.93 ± 0.72a	9.43 ± 1.60b
	P	***	***	***	***	***
P40	Red orache	4.80 ± 0.41a	0.65 ± 0.16c	1.77 ± 0.14c	1.51 ± 0.31a	11.70 ± 1.69a
	Okahijiki	5.03 ± 0.31a	1.63 ± 0.21a	6.56 ± 0.61a	0.67 ± 0.34b	4.25 ± 0.97c
	Minutina	3.82 ± 0.38b	1.41 ± 0.19b	2.45 ± 0.23b	1.92 ± 0.64a	8.36 ± 1.38b
	P	***	***	***	***	***
ANOVA						
Plant species		***	***	***	***	***
Treatment		*ns*	*ns*	*ns*	*ns*	**
Plant species*Treatment		*ns*	*ns*	*ns*	*ns*	*ns*

Each value represents means ± SD. Values in same columns of each treatment with different lowercase alphabet letters are significantly different ($p < 0.05$).
*ns, **, *** mean no significant or significant at $p \leq 0.01$, or 0.001, respectively.*

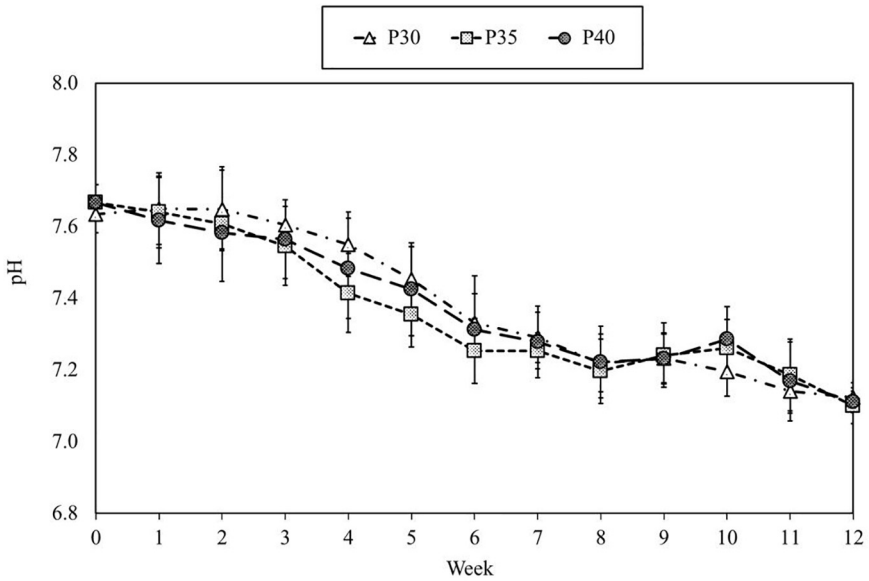

FIGURE 3 | Dynamic of pH in marine aquaponics provided with varying concentrations of protein feeds for 12 weeks. Each point represents the means (±SD) of three replicates in each treatment.

TABLE 4 | Average concentrations of water-quality parameters (range) in marine aquaponics provided with varying concentrations of protein feeds for 12 weeks.

Treatment	Temperature (°C)	DO (mg/L)	Alkalinity (mg/L)	TSS (mg/L)	VSS (mg/L)
P30	27.4 ± 0.2	6.9 ± 0.2	96.0 ± 15.0	38.8 ± 12.1	24.1 ± 9.3
	(26.9–28.0)	(6.4–7.1)	(73–120)	(22.2–63.7)	(12.7–42.8)
P35	27.4 ± 0.2	6.9 ± 0.2	95.7 ± 19.8	36.5 ± 10.8	22.4 ± 8.1
	(27.0–27.8)	(6.4–7.1)	(67–133)	(26.3–66.3)	(15.0–43.0)
P40	27.4 ± 0.2	6.8 ± 0.2	104.5 ± 22.3	55.0 ± 22.7	33.8 ± 16.0
	(27.0–27.8)	(6.4–7.1)	(73–140)	(28.0–105.9)	(14.8–67.2)

Each value represents means ± SD (range).

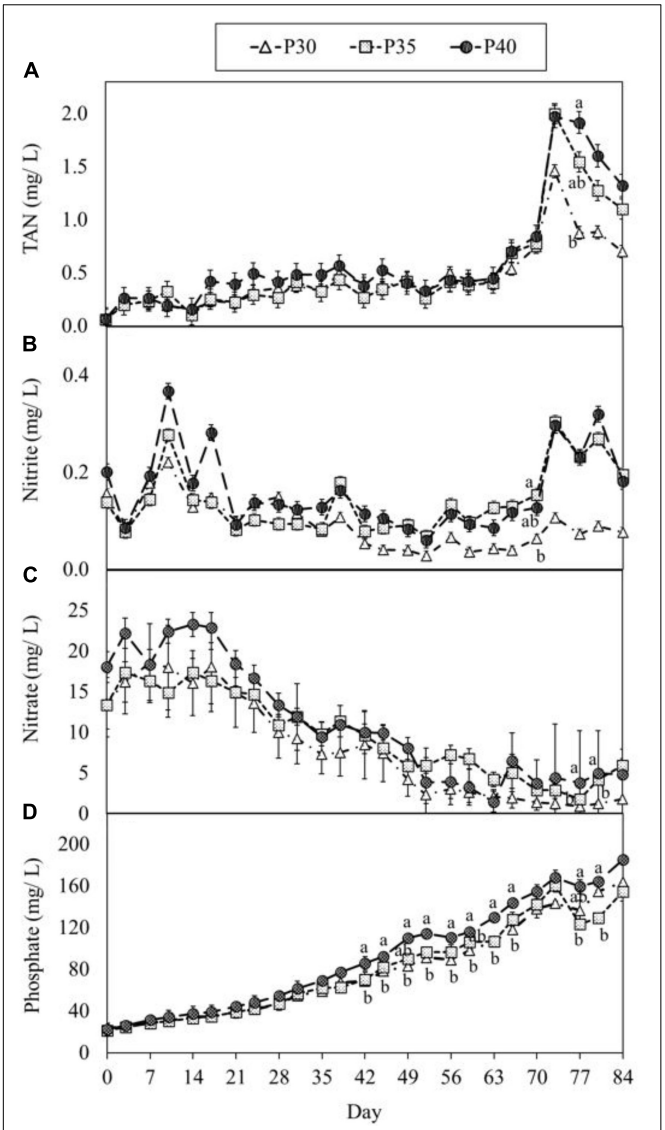

FIGURE 4 | The change of TAN **(A)**, nitrite **(B)**, nitrate **(C)**, and phosphate **(D)**, concentrations in marine aquaponics provided with varying concentration of protein feeds for 12 weeks. Values are means (± SD) of three replicates. Lower-Case alphabet letters represent significant differences, followed by one way ANOVA and Turkey's HSD test ($\alpha = 0.05$).

the last two harvests. In addition, the availability of nutrient elements is higher when pH is lower (Somerville et al., 2014; Goddek et al., 2019). Therefore, the better growth performance and production of the three plants in the second and third harvest might be explained by the mixed factors mentioned above. More research is needed on successive harvests from aquaponic systems.

Plank and Kissel (1989) reported the critical concentrations of N, P, and K in plant tissue are 2.75, 0.3, and 2.0%, respectively. The result of the plant tissue analysis (**Table 3**) indicated the concentrations of N, P, and K were above those values, and indicated that the plants were not N, P or K limited.

Stoyanova et al. (2019) reported that higher protein content in fish feed was related to a higher concentration of nitrogenous compounds and phosphate in the water and contributed to better production of lettuce. In general, the growth performance of the three plants in the present study were higher in P35 and P40 treatments than those grown in P30 treatment (**Figure 2**). This result aligned with their findings.

Water Quality

The concentration of TAN remained below 0.9 ppm until day 70, while nitrite-N remained below 0.4 ppm the during the course of this experiment; however, pH decreased. The change in pH is likely due to increasing biomass, increasing feed input and increased CO_2 excretion. The decreased pH affects the activity of nitrifying bacteria and further impacts the process of nitrification (Jadhav et al., 2010; Satapute et al., 2012). In general, optimal pH range for ammonia-oxidizing bacteria (AOB) is 7.0–8.0, and optimal pH for nitrite-oxidizing bacteria (NOB) is 7.5–8.0. Because of these phenomena, the concentration of TAN and NO_2^- increased at the late stage of cultivation. In addition, the efficiency of calcium absorption and utilization by shrimp decreases with decreasing pH and likely contributed to the mortality in this study.

In the present study, the concentrations of toxic substances (TAN and nitrite-N) remained at acceptable ranges for shrimp culture, and this could be attributed to the use of probiotics and introducing mature water and bio-media from a stable system. This result aligned with the findings reported by other researchers (Otoshi et al., 2011; Xu and Pan, 2012; Cerozi and Fitzsimmons, 2016; Chu and Brown, 2021a,b). TAN can be stabilized and remain below 0.1 mg/L within 3 weeks in new systems *via* inoculating probiotics on a regular basis (Cerozi and Fitzsimmons, 2016; Chu and Brown, 2021b). Xu and Pan (2012) demonstrated that the concentrations of TAN and NO_2^- remained under 0.51ppm and 1.25 mg/L, respectively, by introducing biofloc from an established system prior to the experiment. Chu and Brown (2021a) reused the water and bio-media from previous experiment, and the toxic compounds, TAN and NO_2^-, remained below 0.2 ppm the entire research period.

Steadily increased nitrate-N is commonly occurred in matured aquaponics and has been reported by other researchers (Nozzi et al., 2016; Boxman et al., 2017, 2018; Yang and Kim, 2019; Pinheiro et al., 2020). However, the concentration of nitrate-N in the present study decreased with experiment time. The potential factor for this phenomena was the dominance of heterotrophic bacteria (HB) in the water, which facilitated by the inoculation of probiotics and additional organic carbon (Xu and Pan, 2012; Cerozi and Fitzsimmons, 2016; Chu and Brown, 2021a,b). The dominance of HB hinders the growth of AOB and NOB and affects the process of nitrification (Zhu and Chen, 2001; Michaud et al., 2006). Along with the absorption by plants, this can explain the steady decrease of NO_3^- in the present study. More research is needed to investigate environmental pH, and the effect of applying commercial probiotics.

Among the research in aquaponics, some researchers reported low concentrations of PO_4^{3-}, about 1–17 mg/L in the systems

(Seawright et al., 1998; Al-Hafedh et al., 2008; Endut et al., 2010; Huang et al., 2021). However, in the present study, the concentration of PO_4^{3-} accumulated with the experiment time, which aligned with other studies, and this can be attributed to several factors, including heterotrophic bacteria dominated in biofloc results in fewer algae present to absorb P (Xu et al., 2016), the presence of Na and Cl impacts P assimilation (Nozzi et al., 2016), and daily P provided from aquafeed exceeds plant's ability to assimilate (Yang and Kim, 2020a). Due to its scarcity and finite supply, phosphorus is an expensive component in hydroponic solutions (Hawkesford et al., 2011; Goddek et al., 2015). Between 30 and 85% of the dietary P input ends up as uneaten feed, fish excretion, and feces, which is the primary source of environmental contamination (Wu, 1995; Seawright et al., 1998; Schneider et al., 2005). Therefore, growing plants with aquaculture effluent could address the issues in both aquaculture and hydroponics. However, the accumulation of PO_4^{3-} needs to be addressed, both from an environmental viewpoint as well as the potential ability to produce more plant crops.

CONCLUSION

Among the findings of the present study, it was found that shrimp growth was not affected by the protein content of the feed, suggesting that it is possible to use feeds with lower protein concentration when culturing shrimp in biofloc-based marine aquaponics. However, plants grew better in the treatments with higher protein content feed in the early and middle stages of the operation. Hence, for a longer period of shrimp cultivation, providing a higher protein content feed (35%) until the middle stage and switching to a lower protein content feed (30%) at the late stage of cultivation might be feasible. Yet, more research is needed to study the feeding scheme in biofloc-based marine aquaponics to provide better guidelines for managing water quality for successful operation and better production.

DATA AVAILABILITY STATEMENT

The original contributions presented in the study are included in the article/**Supplementary Material**, further inquiries can be directed to the corresponding author.

AUTHOR CONTRIBUTIONS

Y-TC: conceptualization, methodology, investigation, validation, formal analysis, data curation, writing-original draft preparation, and editing. PB: resources, supervision, project administration, funding acquisition, and writing – review and editing. Both authors have read and agreed to the published version of the manuscript.

FUNDING

Funding for this project was provided by the Purdue University Department of Forestry and Natural Resources, the College of Agriculture, and the United States Department of Agriculture. Publication of this article was funded in part by Purdue University Libraries Open Access Publishing Fund.

ACKNOWLEDGMENTS

We would like to thank Zeigler Bros., Inc., for their donation of commercial shrimp feed and EZ-bio. We also would like to thank Robert Rode, Aquaculture Research Lab for his help and support for the study.

SUPPLEMENTARY MATERIAL

The Supplementary Material for this article can be found online at: https://www.frontiersin.org/articles/10.3389/fmars.2022.824973/full#supplementary-material

REFERENCES

Abbasi, H. N., Vasileva, V., and Lu, X. (2017). The influence of the ratio of nitrate to ammonium nitrogen on nitrogen removal in the economical growth of vegetation in hybrid constructed wetlands. *Environments* 4:24. doi: 10.3390/environments4010024

Abdussamad, E. M., and Thampy, D. M. (1994). Cannibalism in the tiger shrimp Penaeus monodon Fabricius in nursery rearing phase. *J. Aquacult. Trop.* 9, 67–75. doi: 10.1111/j.1749-7345.1994.tb00189.x

Al-Hafedh, Y. S., Alam, A., and Beltagi, M. S. (2008). Food production and water conservation in a recirculating aquaponic system in Saudi Arabia at different ratios of fish feed to plants. *J. World Aquac. Soc.* 39, 510–520. doi: 10.1111/j.1749-7345.2008.00181.x

Araneda, M., Gasca-Leyva, E., Vela, M. A., and Domínguez-May, R. (2020). Effects of temperature and stocking density on intensive culture of Pacific white shrimp in freshwater. *J. Therm. Biol.* 94:102756. doi: 10.1016/j.jtherbio.2020.102756

Arnold, S. J., Sellars, M. J., Crocos, P. J., and Coman, G. J. (2006). An evaluation of stocking density on the intensive production of juvenile brown tiger shrimp (Penaeus esculentus). *Aquaculture* 256, 174–179. doi: 10.1016/j.aquaculture.2006.01.032

Avnimelech, Y. (1999). Carbon/Nitrogen ratio as a control element in aquaculture systems. *Aquaculture* 176, 227–235. doi: 10.1016/S0044-8486(99)00085-X

Avnimelech, Y. (2006). Bio-filters: the need for an new comprehensive approach. *Aquac. Eng.* 34, 172–178. doi: 10.1016/j.aquaeng.2005.04.001

Ballester, E. L. C., Abreu, P. C., Cavalli, R. O., Emerenciano, M., de Abreu, L., and Wasielesky, W. (2010). Effect of practical diets with different protein levels on the performance of Farfantepenaeus paulensis juveniles nursed in a zero exchange suspended microbial flocs intensive system. *Aquac. Nutr.* 16, 163–172. doi: 10.1111/j.1365-2095.2009.00648.x

Boxman, S. E., Nystrom, M., Capodice, J. C., Ergas, S. J., Main, K. L., and Trotz, M. A. (2017). Effect of support medium, hydraulic loading rate and plant density on water quality and growth of halophytes in marine aquaponic systems. *Aquac. Res.* 48, 2463–2477. doi: 10.1111/are.13083

Boxman, S. E., Nystrom, M., Ergas, S. J., Main, K. L., and Trotz, M. A. (2018). Evaluation of water treatment capacity, nutrient cycling, and biomass production in a marine aquaponic system. *Ecol. Eng.* 120, 299–310. doi: 10.1016/j.ecoleng.2018.06.003

Browdy, C. L., Ray, A. J., Leffler, J. W., and Avnimelech, Y. (2012). "Biofloc-based aquaculture systems," in *Aquaculture Production Systems*, ed. J. Tidwell (Oxford, UK: Johy Wiley & Sons, Inc.), 278–307. doi: 10.1002/9781118250105.ch12

Carlsson, R., and Clarke, E. M. W. (1983). Atriplex hortensis L. as a leafy vegetable, and as a leaf protein concentrate plant. *Qual. Plant. Plant Foods Hum. Nutr.* 33, 127–133. doi: 10.1007/bf01091298

Cerozi, B. D. S., and Fitzsimmons, K. (2016). Use of Bacillus spp. to enhance phosphorus availability and serve as a plant growth promoter in aquaponics systems. *Sci. Hortic.* 211, 277–282. doi: 10.1016/j.scienta.2016.09.005

Chu, Y. T. (2014). *Effects of Different Probiotics on Water Qualities and Growth in Close Culture System of Litpenaeus vannamei*. Keelung: National Taiwan Ocean University. [PhD thesis].

Chu, Y. T., and Brown, P. B. (2021a). Evaluation of Pacific whiteleg shrimp and three halophytic plants in marine aquaponic systems under three salinities. *Sustainability* 13:269. doi: 10.3390/su13010269

Chu, Y. T., and Brown, P. B. (2021b). Sustainable marine aquaponics: effects of shrimp to plant ratio and C/N ratios. *Front. Mar. Sci.* 8:771630. doi: 10.3389/fmars.2021.771630

Crab, R. (2010). *Bioflocs Technology: an Integrated System for the Removal of Nutrients and Simultaneous Production of Feed in Aquaculture*.[PhD thesis]. Ghent: Ghent University.

Crab, R., Chielens, B., Wille, M., Bossier, P., and Verstraete, W. (2010). The effect of different carbon sources on the nutritional value of bioflocs, a feed for Macrobrachium rosenbergii postlarvae. *Aquac. Res.* 41, 559–567. doi: 10.1111/j.1365-2109.2009.02353.x

Crab, R., Defoirdt, T., Bossier, P., and Verstraete, W. (2012). Biofloc technology in aquaculture: beneficial effects and future challenges. *Aquaculture* 35, 351–356. doi: 10.1016/j.aquaculture.2012.04.046

Endut, A., Jusoh, A., Ali, N., Wan Nik, W. B., and Hassan, A. (2010). A study on the optimal hydraulic loading rate and plant ratios in recirculation aquaponic system. *Bioresour. Technol.* 101, 1511–1517. doi: 10.1016/j.biortech.2009.09.040

FAO (2016). *The State of World Fisheries and Aquaculture 2016. Contributing to Food Security and Nutrition for All*. Rome: FAO.

FAO (2020). *The State of World Fisheries and Aquaculture 2020. Sustainability in Action*. Rome: FAO.

Gao, W., Tian, L., Huang, T., Yao, M., Hu, W., and Xu, Q. (2016). Effect of salinity on the growth performance, osmolarity and metabolism-related gene expression in white shrimp Litopenaeus vannamei. *Aquac. Rep.* 4, 125–129. doi: 10.1016/j.aqrep.2016.09.001

Goddek, S., Delaide, B., Mankasingh, U., Ragnarsdottir, K. V., Jijakli, H., and Thorarinsdottir, R. (2015). Challenges of sustainable and commercial aquaponics. *Sustainability* 7, 4199–4224. doi: 10.3390/su7044199

Goddek, S., Joyce, A., Kotzen, B., and Butnell, G. M. (2019). *Aquaponics Food Production Systems*, 1st Edn. Denmark: Cham Springer.

Hawkesford, M., Horst, W., Kichey, T., Lambers, H., Schjoerring, J., Møller, I. S., et al. (2011). "Functions of Macronutrients," in *Marschner's Mineral Nutrition of Higher Plants* (Ed)M. Horst, (Amsterdam: Elsevier Ltd), 135–189. doi: 10.1016/B978-0-12-384905-2.00006-6

Huang, C. C., Lu, H. L., Chang, Y. H., and Hsu, T. H. (2021). Evaluation of the water quality and farming growth benefits of an intelligence aquaponics system. *Sustainability* 13:4210. doi: 10.3390/su13084210

Jadhav, G. G., Salunkhe, D. S., Nerkar, D. P., and Bhadekar, R. K. (2010). Isolation and characterization of salt-tolerant nitrogen-fixing microorganisms from food. *Eur. Asian J. Biosci.* 4, 33–40. doi: 10.5053/ejobios.2010.4.0.5

Jana, P., Prasad Sahu, N., Sardar, P., Shamna, N., Varghese, T., Dharmendra Deo, A., et al. (2021). Dietary protein requirement of white shrimp, Penaeus vannamei (Boone, 1931) juveniles, reared in inland ground water of medium salinity. *Aquac. Res.* 52, 2501–2517. doi: 10.1111/are.15100

Koyro, H. W. (2006). Effect of salinity on growth, photosynthesis, water relations and solute composition of the potential cash crop halophyte Plantago coronopus (L.). *Environ. Exp. Bot.* 56, 136–146. doi: 10.1016/j.envexpbot.2005.02.001

Lam, S. S., Ma, N. L., Jusoh, A., and Ambak, M. A. (2015). Biological nutrient removal by recirculating aquaponic system: optimization of the dimension ratio between the hydroponic & rearing tank components. *Int. Biodeterior. Biodegrad.* 102, 107–115. doi: 10.1016/j.ibiod.2015.03.012

Lee, C., and Lee, K. J. (2018). Dietary protein requirement of Pacific white shrimp Litopenaeus vannamei in three different growth stages. *Fish. Aquat. Sci.* 21:30. doi: 10.1186/s41240-018-0105-0

Lemos, D., and Weissman, D. (2021). Moulting in the grow-out of farmed shrimp: a review. *Rev. Aquac.* 13, 5–17. doi: 10.1111/raq.12461

Liang, J. Y., and Chien, Y. H. (2013). Effects of feeding frequency and photoperiod on water quality and crop production in a tilapia-water spinach raft aquaponics system. *Int. Biodeterior. Biodegrad.* 85, 693–700. doi: 10.1016/j.ibiod.2013.03.029

Michaud, L., Blancheton, J. P., Bruni, V., and Piedrahita, R. (2006). Effect of particulate organic carbon on heterotrophic bacterial populations and nitrification efficiency in biological filters. *Aquac. Eng.* 34, 224–233. doi: 10.1016/j.aquaeng.2005.07.005

Nga, B. T., Lürling, M., Peeters, E. T. H. M., Roijackers, R., Scheffer, M., and Nghia, T. T. (2005). Chemical and physical effects of crowding on growth and survival of Penaeus monodon Fabricius post-larvae. *Aquaculture* 246, 455–465. doi: 10.1016/j.aquaculture.2005.02.026

Nozzi, V., Parisi, G., Di Crescenzo, D., Giordano, M., and Carnevali, O. (2016). Evaluation of Dicentrarchus labrax meats and the vegetable quality of Beta vulgaris var. Cicla farmed in freshwater and saltwater aquaponic systems. *Water* 8:423. doi: 10.3390/w8100423

Otoshi, C. A., Rodriguez, N., and Moss, S. M. (2011). Establishing nitrifying bacteria in super-intensive biofloc shrimp production. *Glob. Aquac. Advocate* 14, 24–26.

Panigrahi, A., Sundaram, M., Saranya, C., Satish Kumar, R., Syama Dayal, J., Saraswathy, R., et al. (2019). Influence of differential protein levels of feed on production performance and immune response of pacific white leg shrimp in a biofloc–based system. *Aquaculture* 503, 118–127. doi: 10.1016/j.aquaculture.2018.12.036

Pinheiro, I., Carneiro, R. F. S., Vieira, F., do, N., Gonzaga, L. V., Fett, R., et al. (2020). Aquaponic production of *Sarcocornia ambigua* and Pacific white shrimp in biofloc system at different salinities. *Aquaculture* 519:734918. doi: 10.1016/j.aquaculture.2019.734918

Plank, C. O., and Kissel, D. E. (1989). *Plant Analysis Handbook for Georgia*. [PhD thesis]. Georgia: University of Georgia College of Agricultural Extension Service.

Prieto, K. R., Echaide-Aquino, F., Huerta-Robles, A., Valério, H. P., Macedo-Raygoza, G., Prado, F. M., et al. (2017). "Endophytic bacteria and rare earth element; promising candidates for nutrient use efficiency in plants," in *Plant Macronutrient Use Efficiency*, eds M. A. Hossain, T. Kamiya, D. J. Burritt, L.-S. P. Tran, and T. Fujiwara (Cambridge: Academic Press), 285–306. doi: 10.1081/e-ess3-120015983

Quagrainie, K. K., Flores, R. M. V., Kim, H. J., and McClain, V. (2018). Economic analysis of aquaponics and hydroponics production in the U.S. *Midwest. J. Appl. Aquac.* 30, 1–14. doi: 10.1080/10454438.2017.1414009

Rakocy, J. E. (2012). "Aquaponics — Integrating fish and plant culture," in *Aquaculture Production Systems*, ed. J. Tidwell (Oxford, UK: Johy Wiley & Sons, Inc.), 343–386. doi: 10.1002/9781118250105.ch14

Ross, W., Gallaudet, R. T., and Oliver, C. (2017). *Fisheries of the United States, 2017. U.S. Department of Commerce, NOAA Current Fishery Statistics No. 2017*. Available online at: https://www.fisheries.noaa.gov/feature-story/fisheries-united-states-2017. (accessed on Feb 04, 2022).

Satapute, P., Shetti, A., Kulkarni, A. G., and Hiremath, G. (2012). Isolation and characterization of nitrogen fixing Bacillus subtilis strain as-4 from agricultural soil AS-4 from agricultural soil. *Int. J. Recent Sci. Res.* 3, 762–765.

Schneider, O., Sereti, V., Eding, E. H., and Verreth, J. A. J. (2005). Analysis of nutrient flows in integrated intensive aquaculture systems. *Aquac. Eng.* 32, 379–401. doi: 10.1016/j.aquaeng.2004.09.001

Seawright, D. E., Stickney, R. R., and Walker, R. B. (1998). Nutrient dynamics in integrated aquaculture-hydroponics systems. *Aquaculture* 160, 215–237. doi: 10.1016/S0044-8486(97)00168-3

Shahkar, E., Yun, H., Park, G., Jang, I. K., Kyoung Kim, S., Katya, K., et al. (2014). Evaluation of optimum dietary protein level for juvenile whiteleg shrimp (Litopenaeus vannamei). *J. Crustac. Biol.* 34, 552–558. doi: 10.1163/1937240X-00002267

Somerville, C., Cohen, M., Pantanella, E., Stankus, A., and Lovatelli, A. (2014). *Small-Scale Aquaponic Food Production. Integrated Fish and Plant Farming. FAO Fisheries and Aquaculture Technical Paper No. 589*. Rome: FAO.

Stoyanova, S., Sirakov, I., Velichkova, K., and Ali, M. (2019). Effect of feed protein level on water chemical and technological parameters of a recirculating aquaponics system for carp (Cyprinus carpio L.) and lettuce (Lactuca sativa L.) farming. *Turk. J. Fish. Aquat. Sci.* 19, 885–891. doi: 10.4194/1303-2712-v19_10_08

USDA (2007). *Nitrogen Efficiency and Management. Nutrient Management Technical Note No. 6*. Washington DC: NRCS.

Wheatly, M. G. (1999). Calcium homeostasis in crustacea: the evolving role of branchial, renal, digestive and hypodermal epithelia. *J. Exp. Zool.* 283, 620–640. doi: 10.1002/(SICI)1097-010X

Wu, R. (1995). The environmental impact of marine fish culture: towards a sustainable future. *Mar. Pollut. Bull.* 31, 159–166. doi: 10.1016/0025-326X(95)00100-2

Xia, S., Li, Y., Wang, W., Rajkumar, M., Kumaraguru Vasagam, K. P., and Wang, H. (2010). Influence of dietary protein levels on growth, digestibility, digestive enzyme activity and stress tolerance in white-leg shrimp, Litopenaeus vannamei (Boone, 1931), reared in high-density tank trials. *Aquac. Res.* 41, 1845–1854. doi: 10.1111/j.1365-2109.2010.02585.x

Xu, W. J., Morris, T. C., and Samocha, T. M. (2016). Effects of C/N ratio on biofloc development, water quality, and performance of Litopenaeus vannamei juveniles in a biofloc-based, high-density, zero-exchange, outdoor tank system. *Aquaculture* 453, 169–175. doi: 10.1016/j.aquaculture.2015.11.021

Xu, W. J., and Pan, L. Q. (2012). Effects of bioflocs on growth performance, digestive enzyme activity and body composition of juvenile Litopenaeus vannamei in zero-water exchange tanks manipulating C/N ratio in feed. *Aquaculture* 35, 147–152. doi: 10.1016/j.aquaculture.2012.05.022

Xu, W. J., and Pan, L. Q. (2014). Evaluation of dietary protein level on selected parameters of immune and antioxidant systems, and growth performance of juvenile Litopenaeus vannamei reared in zero-water exchange biofloc-based culture tanks. *Aquaculture* 42, 181–188. doi: 10.1016/j.aquaculture.2014.02.003

Xu, W. J., Pan, L. Q., Zhao, D. H., and Huang, J. (2012). Preliminary investigation into the contribution of bioflocs on protein nutrition of Litopenaeus vannamei fed with different dietary protein levels in zero-water exchange culture tanks. *Aquaculture* 35, 147–153. doi: 10.1016/j.aquaculture.2012.04.003

Yang, J., Zhu, B., Ni, X., and He, Y. (2020). Ammonium/nitrate ratio affects the growth and glucosinolates content of pakchoi. *Hortic. Bras.* 38, 246–253. doi: 10.1590/s0102-053620200302

Yang, T., and Kim, H. J. (2019). Nutrient management regime affects water quality, crop growth, and nitrogen use efficiency of aquaponic systems. *Sci. Hortic.* 256:108619. doi: 10.1016/j.scienta.2019.108619

Yang, T., and Kim, H. J. (2020a). Characterizing nutrient composition and concentration in tomato-, basil-, and lettuce-based aquaponic and hydroponic systems. *Water* 12:1259. doi: 10.3390/W12051259

Yang, T., and Kim, H. J. (2020b). Effects of hydraulic loading rate on spatial and temporal water quality characteristics and crop growth and yield in aquaponic systems. *Horticulturae* 6:9. doi: 10.3390/horticulturae6010009

Yun, H., Shahkar, E., Katya, K., Jang, I. K., Kyoung, K. S., and Bai, S. C. (2016). Effects of bioflocs on dietary protein requirement in juvenile whiteleg shrimp, Litopenaeus vannamei. *Aquac. Res.* 47, 3203–3214. doi: 10.1111/are.12772

Zanotto, F. P., and Wheatly, M. G. (1993). The effect of ambient pH on electrolyte regulation during the postmoult period in freshwater crayfish *Procambarus clarkii*. *J. Exp. Biol.* 178, 1–19. doi: 10.1242/jeb.178.1.1

Zanotto, F. P., and Wheatly, M. G. (1995). The effect of water pH on postmolt fluxes of calcium and associated electrolytes in the freshwater crayfish (Procambarus clarkii). *Freshw. Crayfish* 8, 437–450. doi: 10.5869/fc.1995.v8.437

Zhang, J., Lv, J., Dawuda, M. M., Xie, J., Yu, J., Li, J., et al. (2019). Appropriate ammonium-nitrate ratio improves nutrient acumulation and fruit quality in pepper (Capsicum annuum L.). *Agronomy* 9:683. doi: 10.3390/agronomy9110683

Zhao, K., and Feng, L. (2001). *Chinese Halophyte Resources*, 1st Edn. Beijing: China Science Publishing & Media Ltd.

Zhu, S., and Chen, S. (2001). Effects of organic carbon on nitrification rate in fixed film biofilters. *Aquac. Eng.* 25, 1–11. doi: 10.1016/S0144-8609(01)00071-1

Zhu, Y., Qi, B., Hao, Y., Liu, H., Sun, G., Chen, R., et al. (2021). Appropriate NH4+/NO3– ratio triggers plant growth and nutrient uptake of flowering Chinese cabbage by optimizing the pH value of nutrient solution. *Front. Plant Sci.* 12:656144. doi: 10.3389/fpls.2021.656144

Conflict of Interest: The authors declare that the research was conducted in the absence of any commercial or financial relationships that could be construed as a potential conflict of interest.

Publisher's Note: All claims expressed in this article are solely those of the authors and do not necessarily represent those of their affiliated organizations, or those of the publisher, the editors and the reviewers. Any product that may be evaluated in this article, or claim that may be made by its manufacturer, is not guaranteed or endorsed by the publisher.

frontiers in Marine Science

ORIGINAL RESEARCH
published: 28 February 2022
doi: 10.3389/fmars.2022.807989

Antagonistic Activity of Lactic Acid Bacteria Against Pathogenic Vibrios and Their Potential Use as Probiotics in Shrimp (*Penaeus vannamei*) Culture

John Thompson[1], Mark A. Weaver[2], Ingrid Lupatsch[3], Robin J. Shields[1], Sue Plummer[2], Christopher J. Coates[1] and Andrew F. Rowley[1]**

[1] Department of Biosciences, Faculty of Science and Engineering, Swansea University, Swansea, United Kingdom, [2] Cultech Ltd., Port Talbot, United Kingdom, [3] AB Agri Ltd., Peterborough, United Kingdom

Probiotic use in aquaculture settings can be an approach for disease control and dietary supplementation. We assessed the antagonistic effect of culture supernatants of lactic acid bacteria on the growth of known shrimp pathogens, *Vibrio* (*Listonella*) *anguillarum*, *Vibrio alginolyticus,* and *V. harveyi,* using a quantitative microplate bioassay. Supernatants from *Lactobacillus curvatus* subsp. *curvatus, L. plantarum,* and *Pediococcus acidolactici* significantly inhibited the growth of these vibrios. The active component(s) were heat stable (> 100°C) and resistant to freeze-thawing. Most of this inhibitory activity was brought about by the production of an acid pH; however, there was evidence for other factors playing a role. In the search for novel probiotic bacteria, an organism was isolated from the gastrointestinal tract of healthy whiteleg shrimp (*Penaeus vannamei)*—identified tentatively as *Carnobacterium maltaromaticum*. This isolate, however, had less potent vibriocidal activity than the lactic acid bacteria and reduced shrimp survival at a dose of 1×10^7 bacteria/shrimp. During a 28-day feeding trial, juvenile *P. vannamei* fed with *L. plantarum* supplemented diets showed no gross changes in growth parameters compared with the control. We suggest that lactic acid bacteria could be incorporated into biofloc formulations to purge the growth of pathogenic vibrios in pond settings, rather than being fed directly to shrimp.

Keywords: aquaculture, shellfish health, disease, biofloc, competitive exclusion, *Carnobacterium maltaromaticum*, *Vibrio harveyi*, *Vibrio alginolyticus*

OPEN ACCESS

Edited by:
Ying Liu,
Dalian Ocean University, China

Reviewed by:
Vikash Kumar,
Central Inland Fisheries Research Institute (ICAR), India
Jude Juventus Aweya,
Shantou University, China

***Correspondence:**
Christopher J. Coates
c.j.coates@swansea.ac.uk
Andrew F. Rowley
a.f.rowley@swansea.ac.uk

Specialty section:
This article was submitted to Marine Fisheries, Aquaculture and Living Resources, a section of the journal Frontiers in Marine Science

Received: *02 November 2021*
Accepted: *07 February 2022*
Published: *28 February 2022*

Citation:
Thompson J, Weaver MA, Lupatsch I, Shields RJ, Plummer S, Coates CJ and Rowley AF (2022) Antagonistic Activity of Lactic Acid Bacteria Against Pathogenic Vibrios and Their Potential Use as Probiotics in Shrimp (Penaeus vannamei) Culture. Front. Mar. Sci. 9:807989. doi: 10.3389/fmars.2022.807989

INTRODUCTION

Shellfish production is of increasing importance globally to provide a food source for human populations. Shrimp are the main cultured crustaceans with whiteleg (Pacific white) shrimp *Penaeus* (*Litopenaeus*) *vannamei* constituting the largest—4.97 million metric tons yielded in 2018 (FAO, 2020). Shrimp aquaculture has been plagued by disease and epizootics caused by bacterial (e.g., vibrio) and viral (e.g., white spot syndrome virus) pathogens over the last few decades (Naylor et al., 2021; Dhar et al., 2022; Rowley, 2022). To counter these, improvements in shrimp health have been pursued including development of antimicrobials but with their adverse consequences for the development of antibiotic resistance (Chi et al., 2017; Thornber et al., 2020; Sharma et al., 2021), vaccines (Rowley and Pope, 2012; Amatul-Samahah et al., 2020), biofloc technology

(Avnimelech, 2015), and pre/pro-biotics (see Ringø et al., 2020; Butt et al., 2021; Knipe et al., 2021 for recent reviews). In terms of probiotics, research has focused on either seeking beneficial bacteria found naturally in the gastrointestinal (GI) tract of shrimp or employing existing probiotics used in humans including lactic acid-producing bacteria (Kesarcodi-Watson et al., 2008; Ringø et al., 2020).

Lactic acid bacteria are a heterogeneous group of Gram-positive, rod-shaped, non-spore-forming, bacteria that ferment carbon sources to produce organic acids including lactic acid. This group includes a wide range of genera including *Lactobacillus, Lactococcus*, *Leuconostoc, Oenococcus, Pediococcus, Streptococcus,* and *Weissella* (Cohen et al., 2008). These are found in a wide range of environments and in association with both animals and plants. In humans and other terrestrial mammals, they are found on the skin, and in the oral cavity, the gastrointestinal (GI) tract, and the vagina (Barbés, 2008). Lactic acid bacteria are important probiotics in the manufacture of fermented foods. In terms of their potential as probiotics, key species include *Lactobacillus plantarum*, *L. casei*, *L. acidophilus*, *L. brevis*, *L. rhamnosus,* and *Pediococcus acidilactici* (e.g., Gareau et al., 2010; Holzapfel and Wood, 2014; Deng et al., 2022). Members of the genus *Lactobacillus* have been extensively studied with respect to their potential as probiotics to maintain both human (e.g., Gareau et al., 2010; Blum et al., 2022) and animal health (e.g., Ringø et al., 2020; Deng et al., 2022). They produce a wide range of metabolites including bacteriocins (e.g., plantaricin), bacteriocin-like factors, lactic acid and hydrogen peroxide that kill or inhibit the growth of bacteria including those that may be potentially pathogenic to the host (Corr et al., 2007). Furthermore, in some animals, lactobacilli readily adhere to the epithelial cells that line the GI tract, which facilitates their colonization (Altermann et al., 2005).

An increasing number of studies are investigating the potential of lactic acid bacteria as probiotics for shellfish including shrimp (see recent reviews by Ringø et al., 2020; Knipe et al., 2021; Naiel et al., 2021). For example, Castex et al. (2008) explored the commercial application of *P. acidilactici* (Bactocell®) on the GI tract microbiota of *Penaeus stylirostris* and found that the hepatosomatic index was higher in the probiotic group compared to controls, coupled with significant reductions in both total bacterial and vibrio counts after probiotic administration. Similarly, summer syndrome caused by *Vibrio nigripulchritudo* was significantly reduced for shrimp in the probiotic group, which demonstrates the efficacy of probiotics in reducing pathogenic bacteria in culture settings. In other studies, short term administration of *L. plantarum* or *L. acidophilus* in combination with *Saccharomyces cerevisiae* in the diet of *P. vannamei* also act as general immune stimulants that lead to resistance to bacterial infection (e.g., Chiu et al., 2007; Pooljun et al., 2020). Synbiotic preparations of pre- and pro-biotics based on *L. plantarum* have shown promising potential as feed supplements to improve the growth/of *P. vannamei* (Kuo et al., 2021; Prabawati et al., 2022).

Herein, we set out to examine the potential of lactic acid bacteria as probiotics for shrimp with reference to their antagonistic behavior toward several *Vibrio* spp. considered to be pathogens of these animals. In response to evidence that probiotic administration results in significant improvement on growth and feed conversion (e.g., Balcázar et al., 2007), we also investigated whether delivery of a commercial strain of *L. plantarum* used in probiotic preparations for humans in feed has any effect on the growth potential of *P. vannamei.* Finally, we also sought lactic acid bacteria found naturally in the GI tract of juvenile shrimp as putative probiotics for later studies.

MATERIALS AND METHODS

Source of Potential Probiotics for *Penaeus vannamei*

Commercially Available Lactic Acid Bacteria

Three species of lactic acid bacteria commonly used as probiotics in animal studies were selected for screening for anti-*Vibrio* activity, namely, *Lactobacillus plantarum* (NCIMB 30280), *Pediococcus acidilactici* (NCIMB 8018), and *Lactobacillus curvatus* subsp. *curvatus* (NCIMB 9716). *L. plantarum* (from Cultech Ltd., Baglan, United Kingdom), *P. acidolactici,* and *L. curvatus* were stored on slopes of de Man, Rogosa, and Sharpe (MRS) agar (Difco, Becton Dickinson & Co., Oxford, United Kingdom) and grown aerobically on MRS medium at 30°C when required.

Natural Microbiota of Healthy Shrimp

The microbiota of healthy post-larvae and gastrointestinal tract microflora of juvenile *P. vannamei* were screened for potential novel *Lactobacillus*-like probiotic bacterial strains. Six post-larval and juvenile shrimp of sizes 0.5 ± 0.1 and 8 ± 0.5 g, respectively, were sampled. Animals were obtained from the Centre for Sustainable Aquatic Research facility at Swansea University. Whole post-larval shrimp homogenate was prepared (after washing with sterile 3% NaCl [w/v] solution) as their size made removing intact hind gut and hepatopancreas challenging. Juvenile shrimp were dissected aseptically with samples of whole mid-hind gut, including feces, and hepatopancreas taken. Biofilm swabs from the surfaces of shrimp rearing tanks were also tested. Samples were placed in tubes containing 500 μl of sterile 3% NaCl solution before homogenization. Dilutions of the homogenates were performed followed by spread plating on MRS agar (plus 2% NaCl). Plates were incubated under aerobic and anaerobic conditions at 37°C for 72 h. All visually distinct colonies were streaked onto fresh plates. Gram staining and gross colony morphology of isolates were recorded. Initial identification of those Gram-positive isolates obtained from MRS agar plates displaying anti-*Vibrio* activity was made using the API 50 CHL sugar fermentation test (BioMérieux United Kingdom Ltd., Basingstoke, United Kingdom) as per the manufacturer's instructions.

Screening Panel of Putative Bacterial Pathogens of Shrimp

Vibrio spp. were selected based on prior evidence of pathogenicity against crustaceans, particularly shrimp: *Vibrio harveyi* (NCIMB

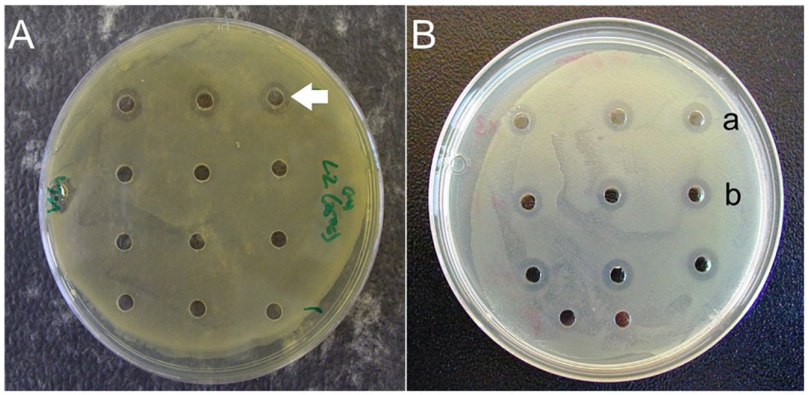

FIGURE 1 | (A) Cell-free culture supernatant antagonistic activity assay against *Vibrio harveyi*. Positive results observed using cell-free supernatant from *Lactobacillus plantarum* (unlabeled arrow). Supernatant in the remaining wells (from other isolates from shrimp GI tracts) displayed no antagonistic activity. **(B).** Cell-free culture supernatant antagonistic activity assay against *V. alginolyticus*. Positive results observed using cell-free supernatant from *L. plantarum* subjected to freezing/thawing (row a) and heating (row b).

1280), *V. alginolyticus* (NCIMB 1339), and *V. anguillarum* (NCIMB 829). All cultures were sourced from NCIMB Ltd. (Aberdeen, United Kingdom) and maintained on tryptic soy agar (TSA) plus 2% NaCl slopes.

Cell-Free Culture Supernatant Antagonism Assay

This qualitative technique determined whether the cell-free culture supernatant of potential probiotics exhibited any antagonistic activity toward *Vibrio* spp. Tryptic soy agar plates (+ 2% NaCl) and tryptic soy broth (TSB, + 2% NaCl) were used to culture the vibrios. Cell-free culture supernatant obtained from incubations of the potential probiotic isolates was tested for antagonistic activity against these bacteria. The strains of lactic acid bacteria were cultured in MRS broth at 30°C for 24 h, and subsequently, they were centrifuged (6,000 × g, 10 min at 25°C) and the supernatant was filter sterilized (0.22 μm). Supernatants were stored at 4°C for no more 24 h prior to assay commencement. *V. harveyi* and *V. anguillarum* were grown in TSB (plus 2% NaCl) at 25°C for 18 h and adjusted to *ca.* 2×10^9 total bacteria.ml^{-1}. Culture (100 μl) was then evenly spread on each plate and 12 equidistant, 4 mm diameter wells were punched into the agar. Forty microliters of the potential probiotic cell-free culture supernatant was added to each well in triplicate (technical replicates). A negative control of the appropriate uninoculated broth was added to the remaining three wells. Each plate was run in duplicate and incubated at 25°C for 24 and 48 h.

The effects of varying the incubation period were assessed by using cell-free supernatant produced from culture samples extracted daily over 7 days. To assess the heat stability of putative anti-*Vibrio* factors, the activity of cell-free culture supernatant (24 h culture) was determined after exposure to temperatures of 65 and 100°C. In addition, to check their stability, the supernatants were also subjected to several cycles of freeze-thawing at –80°C.

Quantification of Microbial Growth Inhibition by Cell-Free Culture Supernatants

The ability of lactic acid bacteria culture supernatants to inhibit the bacterial growth of pathogenic vibrios was quantified using a microplate-based assay. Crustacean pathogens *V. harveyi* and *V. alginolyticus* were cultured in TSB (plus 2% NaCl) at 25°C for 12 h, and 10 ml aliquots were centrifuged (1,000 × g for 5 min at 25°C), washed twice in 3% NaCl solution, and adjusted to *ca.* 1×10^9 cells ml^{-1}.

Cell-free culture supernatants (pH 4.0) of both the commercially available lactobacilli and shrimp isolates were prepared as stated above. Aliquots of these supernatants were also adjusted to pH 6.2 (that of uninoculated MRS broth) and were tested alongside the original supernatants (pH 4.0). Fifty microliters of *V. harveyi* or *V. alginolyticus* suspension were incubated with 100 μl of cell-free culture supernatant at 25°C with shaking for 30 min, in flat-bottomed, 96 well plates. All combinations of cell-free culture supernatant and *Vibrio* were included and run in triplicate on each plate, alongside controls [cell-free culture supernatants and pathogen suspensions were replaced by sterile 3% NaCl solution (w/v)]. A second 96-well plate was prepared with 200 μl of sterile TSB (+ 2% NaCl) per well. Post incubation, 50 μl from each well of the first plate was transferred aseptically to the corresponding wells of the second plate and the OD_{550} was recorded at 60 min intervals over a 24 h period (at 25°C).

Assessment of Pathogenicity of the *Carnobacterium maltaromaticum* Isolate Toward *Penaeus vannamei*

To ascertain if *C. maltaromaticum* was pathogenic to shrimp (and hence its suitability as a probiotic), post larval shrimp were challenged *in vivo* (see section "Results"). Shrimp weighing 1.0 ± 0.2 g (mean ± *S.D.*, two groups each of 10 animals) were

housed in two, 30 l tanks within a closed re-circulating system. Animals of the first group were administered an intramuscular injection of 100 μl sterile 3% NaCl solution, between the second and third pleomeres, and the remaining group was injected with 100 μl *C. maltaromaticum* suspension ($\sim 1 \times 10^7$ viable bacteria per shrimp). No feed was administered during this trial, and the animals were checked at 12 h intervals for mortality changes. At 24, 72, and 96 h post-injection, two shrimp from each group were sacrificed for bacteriology. The small size of the animals made obtaining hemolymph via needle impractical and so the euthanized animals were bisected transversely at the join between the cephalothorax and first abdominal segment (pleomere). The cut surface of the abdominal section was touched onto two MRS agar (plus 2% NaCl) plates, the *ca.* 50 μl of hemolymph deposited was spread aseptically, and the plates were incubated at 25°C (72 h) before being checked for growth. Twenty-four hours after the end of the trial, samples of the tank's surface biofilm were taken and plated (MRS agar plus 2% NaCl) to ascertain whether suspected *C. maltaromaticum* had become a component of the system microbiota.

Lactobacillus plantarum Feed Trial in *Penaeus vannamei*

Two groups each containing 54 post-larval *P. vannamei* (0.5 ± 0.05 g) were used to assess the short term (28 day) effects of the oral administration of *L. plantarum* on growth, feed conversion ratio (FCR) and shrimp survival. Each diet group was housed over three randomly assigned, 30 l tanks (18 animals per tank). One group was fed the control diet and the second group received the same diet top-coated with *L. plantarum* culture. A commercial shrimp maturation diet (Dragon Feeds; 42% protein, 10% lipid, 1 mm pellets) was used as the basis for both treatments. In the case of the *L. plantarum* supplemented diet, a powdered mix of lyophilized *L. plantarum* culture (Cultech Ltd., Baglan, United Kingdom) at a concentration of *ca.* 1.6×10^{11} CFU g^{-1} in skimmed milk powder was top coated onto a commercial diet such that it contained a mass of the probiotic mixture equivalent to 1% (w/w) of the total (final) mass of feed. The viability of *L. plantarum* in the final feed was estimated by spread plating techniques as *ca.* 2×10^8 CFU g^{-1}. The control feed was coated by the same method and contained the equivalent amount of skimmed milk powder. All feed was stored in sealed containers at 4°C until required. Fresh feed was produced halfway through the trial.

Animals were fed twice daily with the feed amount equivalent to *ca*. 7% of tank biomass per day. Prior to feeding, fecal matter and uneaten feed were removed from the tanks, the unconsumed feed was collected separately from the feces, dried at RT and weighed. Five randomly selected animals from each tank were weighed weekly and survival was monitored daily. These values were used to estimate the biomass of each tank and thus the amount of feed required for the subsequent 7 days. Accurate tank biomass determinations were made, via a total count and batch weighing of the animals, at the start of the trial, at the midpoint, and at the end of the trial (28 days). From these data, average values for each tank for individual animal weight and growth rates were determined. Furthermore, to estimate FCR the amount of feed consumed was calculated by subtracting the amount of un-consumed feed from the amount administered.

Statistical Analyses

Analysis of variance (ANOVA) together with a Bonferroni multiple comparisons *post hoc* test was used to determine potential differences between bacterial growth curves. This followed the determination of normal distribution of the data via the application of a Kolmogorov–Smirnov test. Survival data were assessed using a log-rank (Mantel-Cox) curve comparison test. All values are shown as arithmetic means ± 1 standard error of the mean (S.E.M). The reader should refer to figure and table descriptors for respective sample (*n*) sizes.

RESULTS

Antagonistic Behavior of Cell-Free Supernatants of *Lactobacillus plantarum, Pediococcus acidolactici,* and *Lactobacillus curvatus* subsp. *curvatus*

The cell-free culture supernatants of *L. plantarum* and *P. acidilactici* inhibited the growth of *V. harveyi* and *V. anguillarum* producing 1.5–3 mm diameter clearance zones around wells (**Figure 1A**). The supernatant of *L. curvatus* subsp. *curvatus,* however, produced only weak, intermittent interference of *V. anguillarum* growth. Consequently, it was decided not to undertake further testing of *L. curvatus* subsp. *curvatus*. The ability of *L. plantarum* and *P. acidilactici* cell-free culture supernatants to inhibit the growth of *V. harveyi* and *V. anguillarum* was undiminished by heating or freeze-thawing (**Figure 1B**). Interestingly, cell-free culture supernatants of *L. plantarum* or *P. acidilactici* collected over the 7 day growth period produced zones of pathogen inhibition comparable with the 24 h samples.

A microplate reader-based assay was used to fully quantify the interaction between culture supernatants of *L. plantarum* and *P. acidolactici* with vibrios. Cell-free culture supernatant obtained from *L. plantarum* and *P. acidilactici* inhibited the growth of both *V. harveyi* and *V. alginolyticus* over a 24 h period (**Figures 2A–D**). No detectable bacterial growth was observed in any of the wells containing unaltered cell-free culture supernatant at pH 4. Growth did, however, occur in wells when the pH of the cell-free supernatant was adjusted to 6.2 for both lactic acid bacteria. This growth was, however, less than that observed in the appropriate positive controls (*Vibrio* plus MRS broth; pH 6.2). In the case of pH adjusted *L. plantarum* culture supernatant, *V. harveyi* displayed a slight, but not statistically significant decline in growth/cell number after 15 h, when compared with the positive (bacteria-only) control. The effects were more pronounced for *V. alginolyticus*, where growth was significantly lower over the incubation period in wells containing the pH adjusted cell-free supernatant (pH 6.2) in comparison with that in the bacteria-only control (**Figure 2B**). The pH adjusted cell-free culture supernatants of *P. acidilactici* and *L. plantarum*

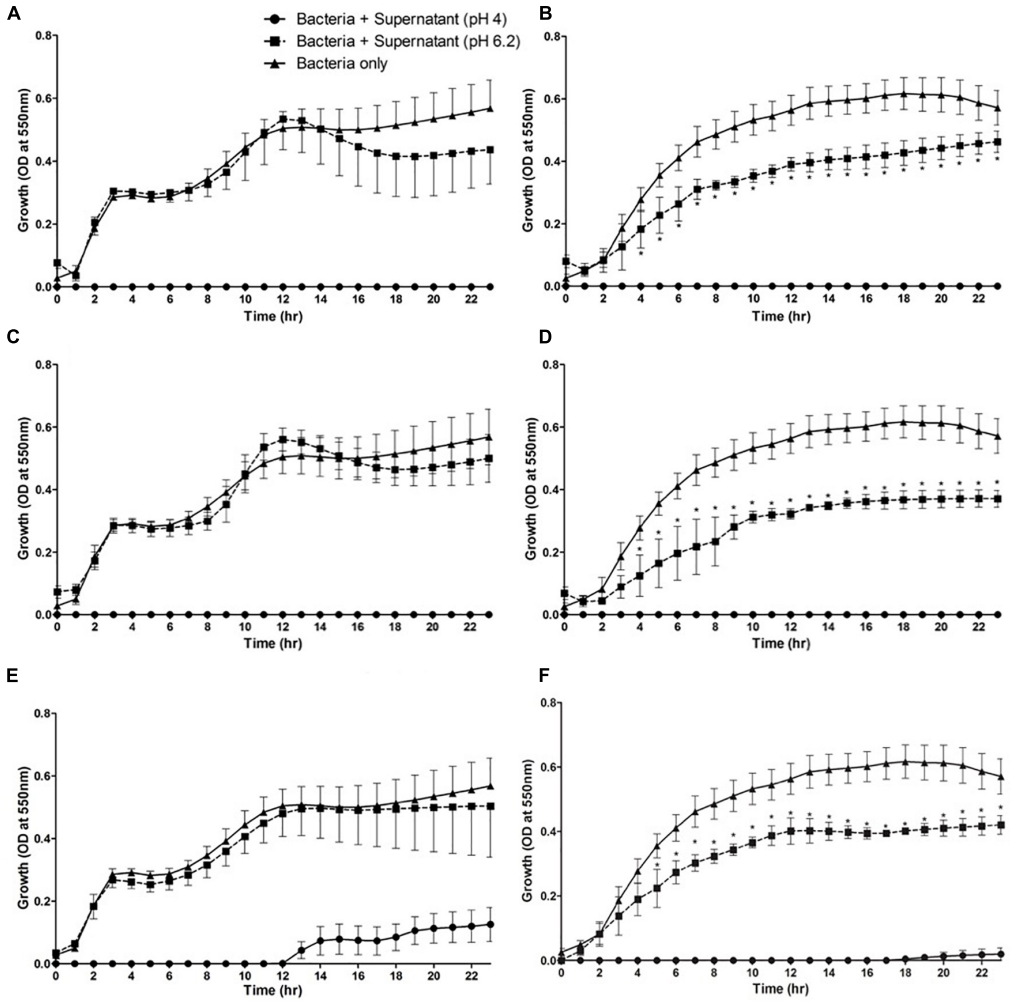

FIGURE 2 | Growth profiles of pathogenic *Vibrio species* in the presence of culture supernatants from lactic acid bacteria *in vitro*. *Vibrio harveyi* **(A,C,E)** and *V. alginolyticus* **(B,D,F)** were incubated in the presence of culture supernatant from *Lactobacillus plantarum* **(A,B)**, *Pediococcus acidilactici* **(C,D)**, and *Carnobacterium maltaromaticum* **(E,F)**. Mean values ± S.E.M, $n = 5$ (per bacterium, 15 in total), $^*P < 0.05$ compared to bacteria alone control and cell-free supernatant of the respective lactic acid bacterium at pH 6.2.

appeared equally ineffective in inhibiting the growth of *V. harveyi* (**Figures 2A,C**). However, both were more effective in their inhibition of *V. alginolyticus* producing statistically significant growth inhibition (**Figures 2B,D**).

Screening of the Microbiota of *Penaeus vannamei* for Potential Novel Lactobacilli-Like Probiotic Bacteria

The isolates from *P. vannamei* (**Table 1**) represent all the colonies observed growing on MRS plates. As the gross morphology of these colonies was highly uniform, all were screened for vibriocidal activity. This screening yielded only two isolates that exhibited potential antagonistic activity toward the selected target *Vibrio* spp. (*V. harveyi* and *V. alginolyticus*) but both had no apparent activity against *V. anguillarum*. The isolates were tentatively identified using the API 50 CHL (V5.1) sugar fermentation test as the lactic acid bacterium, *Carnobacterium maltaromaticum* (97.7% match). The bacteria isolated on MRS media under anaerobic conditions (see **Table 1**) failed to grow after exposure to aerobic conditions and therefore were not tested for anti-*Vibrio* antagonistic behavior.

TABLE 1 | Bacterial isolates from shrimp, *Penaeus vannamei,* and tank biofilms grown on MRS agar.

Source	Number of isolates (CFUs)	
	Aerobic conditions	Anaerobic conditions
Post-larvae	0	6
Juveniles	17	14
Tank biofilm	1	4

As was the case with *L. plantarum* and *P. acidilactici*, the cell-free culture supernatants of *C. maltaromaticum* isolates were

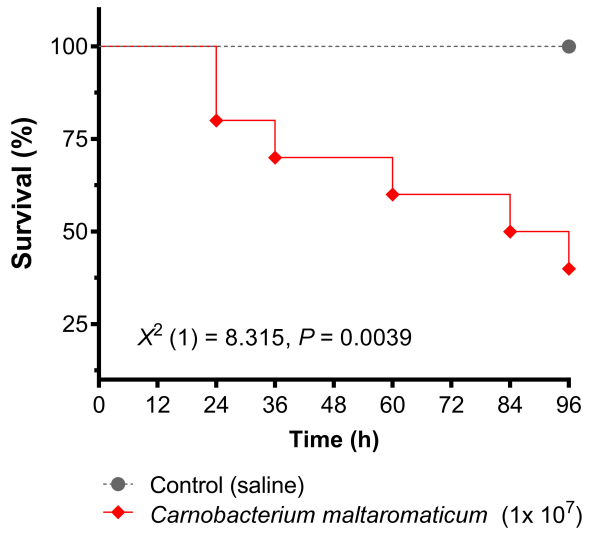

FIGURE 3 | Survival of whiteleg shrimp, *Penaeus vannamei*, over 96 h post inoculation with *Carnobacterium maltaromaticum*. Each shrimp was administered 1 × 10^7 bacteria via intramuscular injection (n = 10 per group, 20 in total). Data were analyzed using the log-rank (Mantel–Cox) curve comparison test.

found to be acidic (*ca.* pH 4) and initially inhibited the growth of both *V. harveyi* and *V. alginolyticus* in the microplate assay (**Figures 2E,F**). This inhibition was not total, however, with vibrio growth occurring after 12 h in the case of *V. harveyi* and 18 h in the case of *V. alginolyticus*. Adjusting the cell-free culture supernatant pH to 6.2 for *C. maltaromaticum* did not interfere with the growth of *V. harveyi* but reduced the growth rate of *V. alginolyticus* in relation to the bacteria only control (**Figure 2F**). Cell-free supernatants of the isolates were found to have no demonstrable inhibitory activity against *V. anguillarum* when using zone of inhibition assays (not shown).

Carnobacterium maltaromaticum Challenge of Shrimp

Exposure of shrimp to 1 × 10^7 CFUs of *C. maltaromaticum* significantly (P = 0.0039) decreased survival (60%) over 96 h (**Figure 3**). Tissue from *C. maltaromaticum*-inoculated shrimp on MRS agar produced large numbers of colonies similar in shape and morphology to the inoculum, implying this bacterium was not effectively cleared by the host's immune defenses. Biofilm samples collected from the tanks containing the *C. maltaromaticum* administered animals were positive for the presence of lactic acid bacteria 24 h after the end of the trial but no further identification of these was carried out and so their identity could be unrelated to the challenge bacteria.

Diet Trials Using *Lactobacillus plantarum*

No measurable beneficial effect was observed in shrimp fed with *L. plantarum* supplemented diets compared with those fed control diets without probiotic. No statistically significant differences were observed between the control and *L. plantarum* supplemented diet groups for any of the performance parameters assessed ($P > 0.05$; **Table 2**).

DISCUSSION

In the last twenty years an increasing number of studies show improvements in growth, digestive enzymes and survival after bacterial challenge, changes in the gut microbiome, and enhanced immune capacity of *P. vannamei* following feeding with lactic acid bacteria alone or in combination with prebiotics, other probiotics, or immune stimulants (Chiu et al., 2007, 2021; Vieira et al., 2008; Kongnum and Hongpattarakere, 2012; Nguyen et al., 2018; Zheng et al., 2018, 2020; Du et al., 2020; Pooljun et al., 2020; Kuo et al., 2021; Prabawati et al., 2022). Most studies report enhanced growth in the presence of probiotics (e.g., Chiu et al., 2021; Kuo et al., 2021), others (Bernal et al., 2017; Nguyen et al., 2018) including our current study, did not find evidence of such improvements. We observed no changes in the recorded parameters (e.g., growth rate, FCR; **Table 2**) between the control and *L. plantarum* diet groups over the 28 day feeding period. It could be argued that the benefits of such probiotic feed may be cumulative and gradual, and therefore, would only become apparent over longer term administration, however, other workers using the same species of shrimp and a variety of probiotic bacteria (*Bacillus subtilis*, *Pseudomonas aestumarina*, *Roseobacter gallaeciensis*, and *V. alginolyticus*) have reported clear benefits in growth parameters over a similar short period (e.g., Balcázar et al., 2007). It could also be argued that the optimal environmental conditions in our recirculating aquaculture system (e.g., temperature, oxygenation, and waste product removal) and formulated shrimp diets produced the ideal growth rates that could not be further improved because of probiotic incorporation. Hence, it would be useful to repeat these trials under field conditions in commercial production sites where our environmental conditions may not be readily maintained.

TABLE 2 | Performance data obtained for post-larval *Penaeus vannamei* fed a commercial shrimp maturation diet and the equivalent diet supplemented with *Lactobacillus plantarum*, for 28 days.

Diet group	Initial weight (g/shrimp)	Final weight (g/shrimp)	Weight gain over trial (g/shrimp)	Feed consumed over trial (g/shrimp)	Feed conversion ratio	Specific growth rate (%)	Survival (%)
Control	0.49 ± 0.03	1.63 ± 0.06	1.13 ± 0.03	1.79 ± 0.05	1.58 ± 0.07	4.27 ± 0.13	94.3 ± 3.4
L. plantarum-supplemented	0.50 ± 0.04	1.66 ± 0.08	1.15 ± 0.05	1.90 ± 0.05	1.65 ± 0.07	4.26 ± 0.13	86.7 ± 3.4

Values represent means ± SE (n = 3; i.e., 3 tanks/treatment).

Our study has shown that all three species of lactic acid bacteria tested (*L. plantarum, P. acidolactici,* and *L. curvatus*) exhibit antagonistic activity to *V. alginolyticus* and *V. harveyi* in the form of inhibitory compounds released into the culture media. The main active component in the inhibitory activity displayed by the lactic acid bacteria was probably the acidic pH. In addition to this, however, there appeared to be secondary component(s) involved in this inhibition. For instance, the pH adjusted (pH 6.2) cell-free culture supernatant of all three strains still significantly inhibited the growth of *V. alginolyticus* compared to the bacteria-only controls. Although the inhibition exhibited was considerably reduced compared to that of the original acidic supernatants, the presence of a secondary inhibitory component separate to organic acids was suggested. Indeed, strains of all three species of the lactic acid bacteria employed in the current study have been found to produce antimicrobial peptides or bacteriocins in addition to lactic acid (Suma et al., 1998; Blom et al., 2001; Jamuna and Jeevaratnam, 2004; Martin-Visscher et al., 2008; Funck et al., 2020). Furthermore, Corr et al. (2007) highlighted the importance of bacteriocin production as an explanation for the antagonistic behavior of lactic acid bacteria in the murine GI tract. In this model, these authors showed that strains of *Lactobacillus salivarius* that can produce bacteriocins were able to protect mice against *Listeria monocytogenes* while strains unable to produce these factors had no such ability.

The cell-free culture supernatant of the putative *C. maltaromaticum* isolate displayed less inhibitory ability toward potential pathogens than that of *L. plantarum* or *P. acidilactici*. Despite this, the fact that it is isolated from the host species, and therefore potentially a constituent of the normal GI tract microbiota, made it worthy of further evaluation. A fundamental question when selecting a potential probiotic is whether it is of benefit to the host organism (Fuller, 1992). Consequently, any candidate micro-organism displaying significant pathogenicity toward the host could not reasonably be forwarded for further study as a probiotic (Decamp and Moriarty, 2006; Kesarcodi-Watson et al., 2008). Our initial susceptibility studies showed that injection of the *C. maltaromaticum*-like isolate from shrimp resulted in a cumulative mortality of 64% after a high challenge dose of *ca.* 1×10^7 viable bacteria shrimp^{-1}. For that reason, together with its limited anti-vibrio activity, we decided not to pursue it further in additional feeding trials.

Whether *C. maltaromaticum, L. plantarum* and *P. acidilactici* could maintain their inhibitory potential *in vivo* within the shrimp's GI tract and benefit the host is an important question. Unless they multiply and colonize the gut, then there is arguably little chance that the anti-vibrio effect seen in the *in vitro* assays would be replicated *in vivo* without constant feeding. Many of the feeding trials of fish and shellfish with lactic acid bacteria suggest that these bacteria do not readily colonize the GI tract of such animals. For instance, Castex et al. (2008) were unable to find viable *P. acidilactici* in the shrimp GI tract within 24 h post-feeding. In another experiment where the authors took hourly samples post-feeding, they found a rapid reduction in *P. acidilactici* numbers. Similarly, Kesselring et al. (2019) fed shrimp the commercial probiotic mix, AquaStar®(a mixture of *P. acidilactici*, *L. reuteri*, *Enterococcus faecium,* and *Bacillus subtilis*) but the beneficial effects of this required continuous or pulse-feeding. Overall, however, despite the apparent lack of long-term colonization by some lactic acid bacteria of the GI tract of shellfish, such as shrimp, there are data implying that such bacteria do act to alter the microbiome (Zheng et al., 2020; Chiu et al., 2021). For example, Zheng et al. (2020) found that diets supplemented with culture supernatants without viable *L. plantarum* were able to modulate the gastrointestinal bacterial microbiome toward the presence of beneficial genera potentially improving the digestive activity and health of such animals. Other approaches of adding probiotics to the rearing water holding shrimp may provide a practical way around the problem of the need for constant feeding with probiotic-containing diets. One such approach could involve the incorporation of probiotic bacteria into the uni- and multi-cellular organisms in biofloc technology that has recently been studied with other bacterial probiotics (Panigrahi et al., 2020).

CONCLUSION

Lactic acid bacteria tested herein produced inhibitory factors that interfered with the growth of several pathogenic vibrios *in vitro*. A short-term trial feeding *L. plantarum* to juvenile shrimp was without significant effects on the growth and survival of such animals. Such results highlight that bacteria screened as potential probiotics using *in vitro* assays do not always demonstrate growth-promoting capacities *in vivo*. Other mechanisms, such as the inclusion of probiotic bacteria in shrimp rearing ponds as part of biofloc technology—recently studied by Panigrahi et al. (2020) and Flores-Valenzuela et al. (2021)—may be an avenue worth pursuing.

DATA AVAILABILITY STATEMENT

The raw data supporting the conclusions of this article will be made available by the authors, without undue reservation.

AUTHOR CONTRIBUTIONS

JT, IL, and AR designed the study with the assistance of all other authors. JT, IL, CC, and AR analyzed the data. AR, CC, and SP acquired the funding. All authors either drafted or edited the manuscript.

FUNDING

JT was supported by the European Social Fund doctoral training grant. AR and CC were supported by the BBSRC/NERC ARCH-UK network grant (BB/P017215/1).

ACKNOWLEDGMENTS

The technical assistance of Alex Keay and Craig Pooley is gratefully acknowledged.

REFERENCES

Altermann, E., Russell, W. M., Azacarate-Peril, M. A., Barrangou, R., Buck, B. L., McAuliffe, O., et al. (2005). Complete genome sequence of the probiotic lactic acid bacterium *Lactobacillus acidophilus* NCFM. *Proc. Natl. Acad. Sci. U.S.A.* 102, 3906–3912. doi: 10.1073/pnas.0409188102

Amatul-Samahah, M. A., Omar, W. H. H. W., Ikhsan, N. F. M., Azmai, M. N. A., and Ina-Salwany, M. Y. (2020). Vaccination trials against vibriosis in shrimp: A review. *Aquaculture Rep*. 18:100471. doi: 10.1016/j.aqrep.2020.100471

Avnimelech, Y. (2015). *Biofloc Technology - a Practical Guide Book*, 3rd. Edn. Baton Rouge: The World Aquaculture Society.

Balcázar, J. L., Rojas-Luna, T., and Cunningham, D. P. (2007). Effect of the addition of four potential probiotic strains on the survival of Pacific white shrimp (*Litopenaeus vannamei*) following immersion challenge with *Vibrio parahaemolyticus*. *J. Invertebr. Pathol.* 96, 147–150. doi: 10.1016/J.JIP.2007.04.008

Barbés, C. (2008). "Lactobacilli," in *Therapeutic Microbiology: Probiotics and Related Strategies*, eds J. Versalovic and M. Wilson (Washington: American Society of Microbiology Press), 19–33.

Bernal, M. G., Marrero, R. M., Campa-Córdova, A. I., and Mazón-Suástegui, J. M. (2017). Probiotic effect of *Streptomyces* strains alone or in combination with *Bacillus* and *Lactobacillus* in juveniles of the white shrimp *Litopenaeus vannamei*. *Aquacult. Int*. 25, 927–939. doi: 10.1007/s10499-016-0085-y

Blom, H., Katla, T., Nissen, H., and Helge, H. (2001). Characterization, production and purification of Carnocin H, a bacteriocin produced by *Carnobacterium* 377. *Curr. Microbiol.* 43, 227–231. doi: 10.1007/s002840010292

Blum, J., Silva, M., Byrne, S. J., Butler, C. A., Adams, G. G., Reynolds, E. C., et al. (2022). Temporal development of infant oral microbiome. *Crit. Rev. Microbiol* 11, 1–13. doi: 10.1080/1040841X.2021.2025042

Butt, U. D., Lin, N., Akter, N., Siddiqui, T., Li, S., and Wu, B. (2021). Overview of latest developments in the role of probiotics, prebiotics and synbiotics in shrimp aquaculture. *Fish Shellfish Immunol*. 114, 263–281. doi: 10.1016/j.fsi.2021.05.003

Castex, M., Chim, L., Pham, D., Lemaire, P., Wabete, N., Nicolas, J.-L., et al. (2008). Probiotic *P. acidilactici* application in shrimp *Litopenaeus stylirostris* culture subject to vibriosis in New Caledonia. *Aquaculture* 275, 182–193. doi: 10.1016/j.aquaculture.2008.01.011

Chi, T. T. K., Clausen, J. H., Van, P. T., Tersbøl, B., and Dalsgaard, A. (2017). Use practices of antimicrobials and other compounds by shrimp and fish farmers in Northern Vietnam. *Aquaculture Rep*. 7, 40–47. doi: 10.1016/j.aqrep.2017.05.003

Chiu, C.-H., Guu, Y.-K., Liu, C.-H., Pan, T.-M., and Cheng, W. (2007). Immune responses and gene expression in white shrimp *Litopenaeus vannamei*, induced by *Lactobacillus plantarum*. *Fish Shellfish Immunol.* 23, 364–377. doi: 10.1016/j.fsi.2008.12.003

Chiu, S. T., Chu, T.-W., Simangunsong, T., Ballantyne, R., Chiu, C.-S., and Liu, C.-H. (2021). Probiotic. *Lactobacillus pentosus* BD6 boost the growth and health status of white shrimp, Litopenaeus vannamei via oral administration. *Fish Shellfish Immunol*. 117, 124–135. doi: 10.1016/j.fsi.2021.07.024

Cohen, D. P. A., Vaughan, E. E., de Vos, W. M., and Zoetendal, E. G. (2008). "Proteomic approaches to study lactic acid bacteria," in *Therapeutic Microbiology: Probiotics and Related Strategies*, eds J. Versalovic and M. Wilson (Washington, USA: American Society of Microbiology Press), 205–221. doi: 10.1128/9781555815462.ch16

Corr, S. C., Riedel, C. U., O'Toole, P. W., and Gahan, C. G. M. (2007). Bacteriocin production as a mechanism for the antiinfective activity of *Lactobacillus salivarius* UCC118. *Proc. Natl. Acad. Sci. U.S.A.* 104, 7617–7621. doi: 10.1073/pnas.0700440104

Decamp, O., and Moriarty, D. J. W. (2006). Probiotics as alternative to antimicrobials: Limitations and potential. *J. World Aquaculture Soc*. 37, 60–62.

Deng, Z. X., Hou, K. W., Zhao, J. C., and Wang, H. F. (2022). The probiotic properties of lactic acid bacteria and their applications in animal husbandry. *Curr. Microbiol.* 79:22. doi: 10.1007/s00284-021-02722-3

Dhar, A. K., Cruz-Flores, R., and Bateman, K. S. (2022). "Viral diseases of crustaceans," in *Invertebrate Pathology*, eds A. F. Rowley, C. J. Coates, and M. M. A. Whitten (Oxford: Oxford University Press), 368–399.

Du, Y., Wang, B., Jiang, K., Wang, M., Zhou, S., Liu, M., et al. (2020). Exploring the influence of the surface proteins on probiotic effects performed by *Lactobacillus pentosus* HC-2 using transcriptome analysis in *Litopenaeus vannamei* midgut. *Fish Shellfish Immunol.* 87, 853–870. doi: 10.1016/j.fsi.2019.02.027

FAO (2020). *Fishery and Aquaculture Statistics 2018*. Rome: FAO, doi: 10.4060/cb12131t

Flores-Valenzuela, E., Miranda-Baeza, A., Rivas-Vega, M. E., Miranda-Arizmendi, V., Beltrán-Ramírez, O., and Emerenciano, M. G. C. (2021). Water quality and productive response of *Litopenaeus vannamei* reared in biofloc with addition of commercial strains of nitrifying bacteria and *Lactobacillus rhamnosus*. *Aquaculture* 542:736869. doi: 10.1016/j.aquaculture.2021.736869

Fuller, R. (1992). "History and development of probiotics," in *Probiotics the Scientific Basis*, ed. R. Fuller (London: Chapman & Hall), 1–8. doi: 10.1007/978-94-011-2364-8_1

Funck, G. D., Marques, J., de, L., Dannenberg, G., da, S., Cruxen, C. E., et al. (2020). Characterization, toxicity and optimization for the growth and production of bacteriocin-like substances by *Lactobacillus curvatus*. *Probiotics Antimicr. Prot*. 12, 91–101. doi: 10.1007/s12602-019-09531-y

Gareau, M. G., Sherman, P. M., and Walker, W. A. (2010). Probiotics and the gut microbiota in intestinal health and disease. *Nat. Rev. Gastroenterol. Hepatol.* 7, 503–514. doi: 10.1038/nrgastro.2010.117

Holzapfel, W. H., and Wood, B. J. B. (2014). *Lactic Acid Bacteria; Biodiversity and Taxonomy*. (New York: John Wiley & Sons) doi: 10.1002/9781118655252

Jamuna, M., and Jeevaratnam, K. (2004). Isolation and partial characterization of bacteriocins from *Pediococcus* species. *Appl. Microbiol. Biotechnol*. 65, 433–439. doi: 10.1007/s00253-004-1576-8

Kesarcodi-Watson, A., Kaspar, H., Lategan, M. J., and Gibson, L. (2008). Probiotics in aquaculture: The need, principles and mechanisms of action and screening processes. *Aquaculture* 274, 1–14. doi: 10.1016/j.aquaculture.2007.11.019

Kesselring, J. C., Gruber, C., Standen, B., and Wein, S. (2019). Continuous and pulse-feeding application of multispecies probiotic bacteria in whiteleg shrimp. *Litopenaeus vannamei*. *J. World Aquacult. Soc*. 50, 1123–1132. doi: 10.1111/jwas.12640

Knipe, H., Temperton, B., Lange, A., Bass, D., and Tyler, C. R. (2021). Probiotics and competitive exclusion of pathogens in shrimp. *Rev. Aquacult*. 13, 324–352. doi: 10.1111/raq.12477

Kongnum, K., and Hongpattarakere, T. (2012). Effect of *Lactobacillus plantarum* isolated from digestive tract of wild shrimp on growth and survival of white shrimp (*Litopenaeus vannamei*) challenged with *Vibrio harveyi*. *Fish Shellfish Immunol.* 32, 170–177. doi: 10.1016/j.fsi.2011.11.008

Kuo, H.-W., Chang, C.-C., and Cheng, W. (2021). Synbiotic combination of prebiotic, cacao pod husk pectin and probiotic, *Lactobacillus plantarum*, improve the immunocompetence and growth of *Litopenaeus vannamei*. *Fish Shellfish Immunol*. 118, 333–342. doi: 10.1016/j.fsi.2021.09.023

Martin-Visscher, L. A., van Belkum, M. J., Garneau-Tsodikova, S., Whittal, R. M., Zheng, J., McMullen, L. M., et al. (2008). Isolation and characterization of carnocyclin A, a novel circular bacteriocin produced by *Carnobacterium maltaromaticum* UAL307. *Appl. Environ. Microbiol*. 74, 4756–4763. doi: 10.1128/AEM.00817-08

Naiel, M. A. E., Farag, M. R., Gewida, A. G. A., et al. (2021). Using lactic acid bacteria as an immunostimulant in cultured shrimp with special reference to *Lactobacillus* spp. *Aquacult. Int*. 29, 219–231. doi: 10.1007/s10499-020-00620-2

Naylor, R. L., Hardy, R. W., Buschmann, A. H., Bush, S. R., Cao, L., Künger, D. H., et al. (2021). A 20-year retrospective review of global aquaculture. *Nature* 591, 551–563. doi: 10.1038/s41586-021-03308-6

Nguyen, T. T. G., Nguyen, T. C., Leekriangsak, M., Pham, T. T., Pham, Q. H., Lueangthuwapranit, C., et al. (2018). Promotion of *Lactobacillus plantarum* on growth and resistance against hepatopancreatic necrosis disease pathogens in white-leg shrimp (*Litopenaeus vannamei*). *Thai J. Vet. Med*. 48, 19–28.

Panigrahi, A., Das, R. R., Sivalumar, M. R., Saravanan, A., Sudheer, N. S., et al. (2020). Bio-augmentation of heterotrophic bacteria in biofloc system improves growth, survival, and immunity of Indian white shrimp *Penaeus indicus*. *Fish Shellfish Immunol*. 98, 477–487. doi: 10.1016/j.fsi.2020.01.021

Pooljun, C., Daorueang, S., Weerachatyanukul, W., Direkbusarakom, S., and Jariyapong, P. (2020). Enhancement of shrimp health and immunity with diets supplemented with combined probiotics: application to *Vibrio parahaemolyticus* infections. *Dis. Aquat. Org.* 140, 37–46. doi: 10.3354/dao03491

Prabawati, E., Hu, S.-Y., Chiu, S.-T., Balantyre, R., Risjani, Y., and Liu, C.-H. (2022). A synbiotic containing prebiotic prepared from a by-product of king oyster mushroom, *Pleurotus eryngii* and probiotic, *Lactobacillus plantarum* incorporated in diet to improve the growth performance and health status of shrimp, *Litopenaeus vannamei*. *Fish Shellfish Immunol*. 120, 155–165. doi: 10.1016/f.fsi.2021.11.031

Ringø, E., Van Doan, H., Lee, S., and Kyu Song, S. (2020). Lactic acid bacteria in shellfish: Possibilities and challenges. *Rev. Fish. Sci. Aquaculture* 28, 139–169. doi: 10.1080/23308249.2019.1683151

Rowley, A. F. (2022). "Bacterial diseases of crustaceans," in *Invertebrate Pathology*, eds A. F. Rowley, C. J. Coates, and M. M. A. Whitten (Oxford: Oxford University Press), 400–435. doi: 10.1093/oso/9780198853756.003.0015

Rowley, A. F., and Pope, E. C. (2012). Vaccines and crustacean aquaculture - A mechanistic exploration. *Aquaculture* 334, 1–11. doi: 10.1016/j.aquaculture.2011.12.011

Sharma, L., Nagpal, R., Jackson, C. R., Patel, D., and Singh, P. (2021). Antibiotic-resistant bacteria and gut microbiome communities associated with wild-caught shrimp from the United States versus imported farm-raised retail shrimp. *Sci. Rep.* 11:3356. doi: 10.1038/s41598-021-82823-y

Suma, K., Misra, M. C., and Varadaraj, M. C. (1998). Plantaricin LP84, a broad spectrum heat-stable bacteriocin of *Lactobacillus plantarum* NCIM 2084 produced in a simple glucose broth medium. *Int. J. Food Microbiol*. 40, 17–25. doi: 10.1016/s0168-1605(98)00010-5

Thornber, K., Verner-Jeffreys, D., Hinchliffe, S., Rahman, M. M., Bass, D., and Tyler, C. R. (2020). Evaluating antimicrobial resistance in the global shrimp industry. *Rev. Aquacult*. 12, 966–986. doi: 10.1111/raq.12367

Vieira, F. D. N., Neto, C. C. B., Mouriño, J. L. P., Jatobá, A., Ramirez, C., Martins, M. L., et al. (2008). Time-related action of *Lactobacillus plantarum* in the bacterial microbiota of shrimp digestive tract and its action as immunostimulant. *Pesquisa Agropecuária Brasileira* 43, 763–769.

Zheng, X., Duan, Y., Dong, H., and Zhang, J. (2020). The effect of *Lactobacillus plantarum* administration on the intestinal microbiota of white leg shrimp *Penaeus vannamei*. *Aquaculture* 526:735331. doi: 10.1016/j.aquaculture.2020.735331

Zheng, X., Duan, Y., Doug, H., and Zhang, J. (2018). Effects of dietary *Lactobacillus plantarum* on growth performance, digestive enzymes and gut morphology of *Litopenaeus vannamei*. *Probiotics Antimicro. Prot*. 10, 504–510. doi: 10.1007/s12602-017-9300-z

Conflict of Interest: MW and SP were employed by the company Cultech Ltd. IL is employed by the company AB Agri Ltd., but not at the time the study was conducted.

The remaining authors declare that the research was conducted in the absence of any commercial or financial relationships that could be construed as a potential conflict of interest.

Publisher's Note: All claims expressed in this article are solely those of the authors and do not necessarily represent those of their affiliated organizations, or those of the publisher, the editors and the reviewers. Any product that may be evaluated in this article, or claim that may be made by its manufacturer, is not guaranteed or endorsed by the publisher.

frontiers | Frontiers in Marine Science

ORIGINAL RESEARCH
published: 20 April 2022
doi: 10.3389/fmars.2022.881016

Metabolic Response in the Gill of *Portunus trituberculatus* Under Short-Term Low Salinity Stress Based on GC-MS Technique

Jiali Wang[1†], Qi Liu[2†], Xinni Zhang[1], Gao Gao[1], Mingming Niu[1], Huan Wang[1,3], Lizhi Chen[2*], Chunlin Wang[1,3], Changkao Mu[1,3] and Fangfang Wang[2]*

[1] School of Marine Science, Ningbo University, Ningbo, China, [2] Aquatic Technology Promotion Station, Sanmen Rural Bureau, Taizhou, China, [3] Key Laboratory of Applied Marine Biotechnology, Ministry of Education, Ningbo University, Ningbo, China

OPEN ACCESS

Edited by:
Xiangli Tian,
Ocean University of China, China

Reviewed by:
Xianliang Meng,
Chinese Academy of Fishery Sciences (CAFS), China
Xugan Wu,
Shanghai Ocean University, China

***Correspondence:**
Huan Wang
wanghuan1@nbu.edu.cn
Lizhi Chen
80079745@qq.com

[†]These authors have contributed equally to this work

Specialty section:
This article was submitted to Marine Fisheries, Aquaculture and Living Resources, a section of the journal Frontiers in Marine Science

Received: *22 February 2022*
Accepted: *29 March 2022*
Published: *20 April 2022*

Citation:
Wang J, Liu Q, Zhang X, Gao G, Niu M, Wang H, Chen L, Wang C, Mu C and Wang F (2022) Metabolic Response in the Gill of Portunus trituberculatus Under Short-Term Low Salinity Stress Based on GC-MS Technique. Front. Mar. Sci. 9:881016. doi: 10.3389/fmars.2022.881016

Salinity is an important factor affecting the survival, growth, and metabolism of marine crustaceans. Low-salt stress will result in the death of swimming crabs. This paper investigates the metabolic response in the gills of *Portunus trituberculatus* under short-term low-salt stress by comparing the metabolic molecules in the four salinity treatment groups (24‰, 16‰, 12‰, and 8‰) by GC-MS technique. In this study, nine common differential metabolites such as pyruvate, malic acid, and phosphoethanolamine were found in the gill tissues of crabs. KEGG enrichment analysis revealed that six metabolic pathways, including the citric acid cycle, pyruvate metabolism, and the HIF-1 signaling system, were significantly impacted by low salt stimulation. According to the findings, salinity 12‰ is a critical node in crab adaptation to low salinity. In the process of adaptation to short-term low-salinity environment, amino acids participated in osmotic regulation, and organic acids such as pyruvate and malic acid were involved in energy metabolism to ensure their energy supply. This research further enriched the theory of osmotic regulation and metabolic mechanism of adaptation to low salt in crustaceans, with the goal of providing guidance for the improvement of culture technique in *Portunus trituberculatus.*

Keywords: ***Portunus trituberculatus*, low salt stress, gills, GC-MS technology, metabolic response**

INTRODUCTION

Portunus trituberculatus, which belongs to the Crustecea, Malacostraca, Decapoda, Portunidae, *Portunus*, is widely distributed in the coastal waters of China, Korea, Japan, and South Asia (Ren et al., 2013). It is an essential mariculture species in China. And salinity as an important environmental factor in aquaculture, is closely related to the geographical distribution (Lv et al., 2019), growth, and reproduction (Chen et al., 2019) of swimming crabs. Although *P. trituberculatus* has a certain degree of wide salinity, sudden decrease of salinity in water or low salinity environment can cause crab death and economic losses (Feng et al., 2019).

Euryhaline crustaceans can maintain osmotic pressure stability *in vivo* through osmoregulation by two mechanisms (Ramaglia et al., 2018): (a) Anisosmotic extracellular regulation. It regulates body fluid osmolality through the ion transporter of gill epithelial cell, including V(H^+)-ATPase, Na^+/K^+-ATPase, $Na^+/K^+/2Cl^-$ cotransporter and so on. (McNamara and Faria, 2012). (b) Intracellular isosmotic regulation. It controls intracellular osmolality and maintains the balance between tissues and hemolymph by adjusting the concentration of osmoregulatory effectors (Lu et al., 2015). For example, crustaceans living in low-salinity environments like estuaries and intertidal zones, can quickly excrete excess amino acids from muscle tissue to prevent cell swelling and rupture, as well as compensate for free amino acids in the hemolymph (Sokolova et al., 2012; Lu et al., 2015). Amino acids produced by intracellular isosmotic regulation have been shown to provide energy to the organism by generating glucose through gluconeogenesis reactions (Ye et al., 2014). Free amino acids like glycine, taurine, alanine, and arginine have been proposed as osmoeffectors in crustaceans in previous studies (Augusto et al., 2007; de Faria et al., 2011).

The study of osmoregulation in *P. trituberculatus* is vital for its culture and artificial breeding, and many studies have been conducted on this topic. The osmotic pressure of crabs decreases with the salinity decreasing, which is proportional to the salinity changes, and the activity of ion transporters (Na^+/K^+-ATPase and carbonic anhydrase) in gills increases with decreasing salinity (Lu et al., 2013). The results of gene expression in *P. trituberculatus* under salinity stress showed that Na^+/K^+-ATPase β-subunit was significantly up-regulated during low salinity challenge, and metabolism and energy genes were significantly up-regulated during high salinity challenge (Xu and Liu, 2011). Based on transcriptome research, Lv et colleagues (Lv et al., 2013) found that differentially expressed genes of swimming crabs under low salt stress were involved in ion transport, amino acid metabolism and synthesis, protein hydrolysis, and carbohydrate metabolism. The expression of miRNAs under low salt stress was also investigated. GO enrichment analysis revealed a significant increase in biological processes such as α-amino acid metabolism and intracellular protein transport (Lv et al., 2016). The process of crab response to low salinity could be divided into early (0-12h), middle (12-48h) and late (48-72h) stages, and the differentially expressed genes in each stage were related to lipid metabolism, energy metabolism and signal transduction, respectively (Gao et al., 2019). Previous research has established that ion transport, amino acid metabolism and carbohydrate metabolism play an important role in osmoregulation.

Following genomics, transcriptomics, and proteomics, metabolomics has become a hotspot in biological research, which can be used to detect the impacts of external environmental stress on the organism (Mazzarelli et al., 2015; Long et al., 2017). Differential metabolites related to osmoregulation such as amino acids, sugars, betaine, and fenugreek were identified in a study for metabolic changes in the muscles of *P. trituberculatus* under low salt stress based on NMR spectroscopy. It was concluded that swimming crabs responds to low salt stress primarily through osmotic pressure regulation, amino acid gluconeogenesis, and energy accumulation (Ye et al., 2014).

In this study, we used the GC-MS technique to compare the metabolic difference molecules in gills of *P. trituberculatus* under four salinity treatments of 24‰, 16‰, 12‰, and 8‰, in order to investigate the metabolic changes in gills of crabs under short-term low salt stress, and finally analyzed the metabolic response of *P. trituberculatus* gills under short-term low salt stress.

MATERIALS

Animals

Swimming crabs (*Portunus trituberculatus*) weighing 5 g ± 0.5 g were acclimated in the laboratory (24 ‰, 28°C) for one week before experimental treatments. The crabs were divided into four groups (each with 60 crabs) and exposed to light hyposalinity challenge (LC, 16 ‰), moderate hyposalinity challenge (MC, 12 ‰), severe hyposalinity challenge (SC, 8 ‰), and non-challenge conditions (NC, 24 ‰) at 28°C. The aquaculture water in the low-salt challenge group was a mixture of ordinary seawater and fresh water. Each treatment was repeated three times with a total of 20 crabs per replicate. As a result, there were 12 buckets in all (4 salinity treatments x 3 repeats). After 48 hours, crabs' posterior gills were extracted and quickly frozen in liquid nitrogen, then stored at -80°C until the metabolic analysis was performed.

Sample Preparation

60 mg of precisely weighed material was put to a 1.5-mL Eppendorf tube. The tube was then filled with two small steel balls, 20 μL of internal standard (0.3 mg/mL 2-chloro-1-phenylalanine methanol solution), and 600 μL of extraction solvent with methanol/water (V: V=4:1). After 2 minutes at -80°C, the samples were ground at 60 Hz for another 2 min. Then 120 μL of chloroform was added, extracted by sonication in an ice-water bath for 10 min and then left at -20°C for 30 min, and centrifuged at 13000 rpm, 4 °C for 10 min, and 200 μL of supernatant was loaded into glass derivatization vials. Quality control samples (QC) were made by combining aliquots from all of the samples into a single sample, with the volume of each QC being the same as the sample. The samples were evaporated with a centrifugal concentrator and drier, and 80 μL of pyridinium methoxamine hydrochloride solution (15 mg/mL) was added to the glass derivatization vial, vortexed and shaken for 2 min, and then subjected to an oxime reaction in a shaking incubator at 37°C for 90 min. The samples were removed, and 80 μL of BSTFA derivatization reagent (with 1% TMCS) and 20 μL of hexane were added. 10 mL of 11 internal standards were added and vortex shaken for 2 min (C8/C9/C10/C12/C14/C16, 0.16 mg/mL; C18/C20/C22/C24/C26, 0.08 mg/mL, all in chloroform configuration). After 30 min at room temperature, the samples were GC-MS examined.

GC-MS

The analytical instrument used for this experiment was a 7890B-5977A GC/MSD gas chromatograph from Agilent Technologies

Inc. (UAS, CA). The chromatographic conditions were a DB-5MS capillary column (30 m×0.25 mm×0.25 μm, Agilent J&W Scientific, Folsom, CA, USA), high purity helium gas (purity not less than 99.999%), the flow rate of 1.0 mL/min, an inlet temperature of 260°C, injection volume of 1 μL, no splitting, and solvent delay of 5 min. Programmed ramp-up: the initial temperature of the column temperature chamber was 60°C, maintained for 0.5 min; programmed ramp-up to 125°C at 8°C/min, 210°C at 5°C/min, 270°C at 10°C/min, 305°C at 20° C/min, maintained for 5 min; mass spectrometry conditions for electron bombardment ion source (EI), ion source temperature The scanning mode was full scan mode (SCAN), mass scan range: m/z 50-500. one QC sample was inserted in every 8 analyzed samples to check the reproducibility of the whole analysis process.

Data Preprocessing and Statistical Analysis

The raw data (.D format) was converted to.CDF format using Chem Station (version E.02.02.1431, Agilent, USA) software, and then the.CDF data were imported into Chroma TOF software (version 4.34, LECO, St Joseph, MI) for processing. The Fiehn and NIST databases were used to annotate metabolites. To produce a "raw data array," sample information, peak names (or retention durations and m/z), and peaks were recovered from raw data by comparing to statistical comparison components in a 3D dataset (.cvs). In all, 1264 peaks were found in all of the samples. All internal standards, as well as any known false positive peaks (due to background noise, chromatographic priming, or BSTFA derivative techniques), were eliminated from the "data set." Each sample's peak area is standardized to the data, multiplied by 10,000, and the peaks of the same metabolite are added together. There were a total of 342 metabolites found.

The data were converted using log2, and the resulting data matrix was then imported into the SIMCA software installation package (14.0, Umetrics, Ume, Sweden). After mean centering and unit variance scaling, principal component analysis (PCA) and orthogonal partial least-squares-discriminant analysis OPLS-DA were used to illustrate the metabolic differences across experimental groups. The 95% confidence interval of the modeled variance is defined by the Hotelling's T2 area, which appears as an ellipse in score plots of the models. The overall contribution of each variable to the OPLS-DA model is ranked by variable importance in the projection (VIP), and variables with VIP > 1 are considered relevant for group discrimination.

To avoid overfitting, the default 7-round cross-validation was used in this investigation, with one/seventh of the samples being omitted from the mathematical model in each round.

Selection of Differential Metabolites

The selection of differential metabolites was based on statistically significant threshold of variable influence on projection (VIP) values derived from the OPLS-DA model and p-values from a two-tailed Student's t-test for normalized peak areas of different groups. VIP values greater than 1.0 and p-values less than 0.05 were considered differential metabolites.

RESULTS

Metabolite Alterations Induced by Low-Salinity Exposure

To summarize the similarities and differences of metabolic phenotypes between LCvsNC, MCvsNC, and SCvsNC crabs separately, we plotted the average metabolic trajectories of PCA for each crab group in the first three PCA diagrams (**Figures 1A–C**). Clearly, compared with LCvsNC groups under light hyposaline stress, the metabolic responses of MCvsNC and SCvsNC groups were more significant. Furthermore, the metabolic alterations in MCvsNC and SCvsNC were more similar.

The OPLS-DA method was used to show the metabolites in gill extracts from low salinity treatment group and normal salinity treatment group (**Figures 1D–F**). The OPLS-DA model had an explanatory ability (R2Y(cum)) close to one and a predictive ability (Q2(cum)) of more than 0.5 for all samples, showing that the model was stable (**Table 1**). To avoid model over-fitting, seven-fold cross-validation and 200 response permutation testing (RPT) were performed to assess the model's quality. In the response ranking test of OPLS-DA model, except for the LC group, the Q2 values of the MCvsNC and SCvsNC groups were smaller than 0, indicating that the OPLS-DA model had high explanatory and predictive power in the MCvsNC and SCvsNC groups (**Figures 1G–I**). To ensure the reliability of the results obtained, further univariate data analysis was performed on the selected metabolites (**Figures 2A–C**). The results showed that most of the changes of metabolic levels were in agreement with the multivariate data analysis. Finally, only univariate statistical results were referred to for the screening of differentials in the LCvsNC group, and both univariate and multivariate statistical analyses could be referred to for the screening of differentials in the MCvsNC and SCvsNC groups.

Differential Metabolite Screening at Various Salinities

The differential metabolites between low salinity treatment groups (LC, MC and SC) and normal salinity treatment group (NC) were screened using a combination of multivariate analysis, univariate analysis, and heat map analysis (**Figure 3**). The screening criteria of LCvsNC group were P-value < 0.05 and VIP value > 1, MCvsNC and SCvsNC groups were P value < 0.05 and VIP value > 1, respectively. The results revealed 18 differential metabolites in the LCvsNC group, including 14 up-regulated metabolites and 4 down-regulated metabolites (**Table 2**), while 36 metabolites changed significantly in the MCvsNC group, including 18 up-regulated metabolites and 18 down-regulated metabolites (**Table 3**). In addition, a total of 46 differential metabolites were found in the SCvsNC group, including 28 up-regulated metabolites and 18 down-regulated metabolites (**Table 4**).

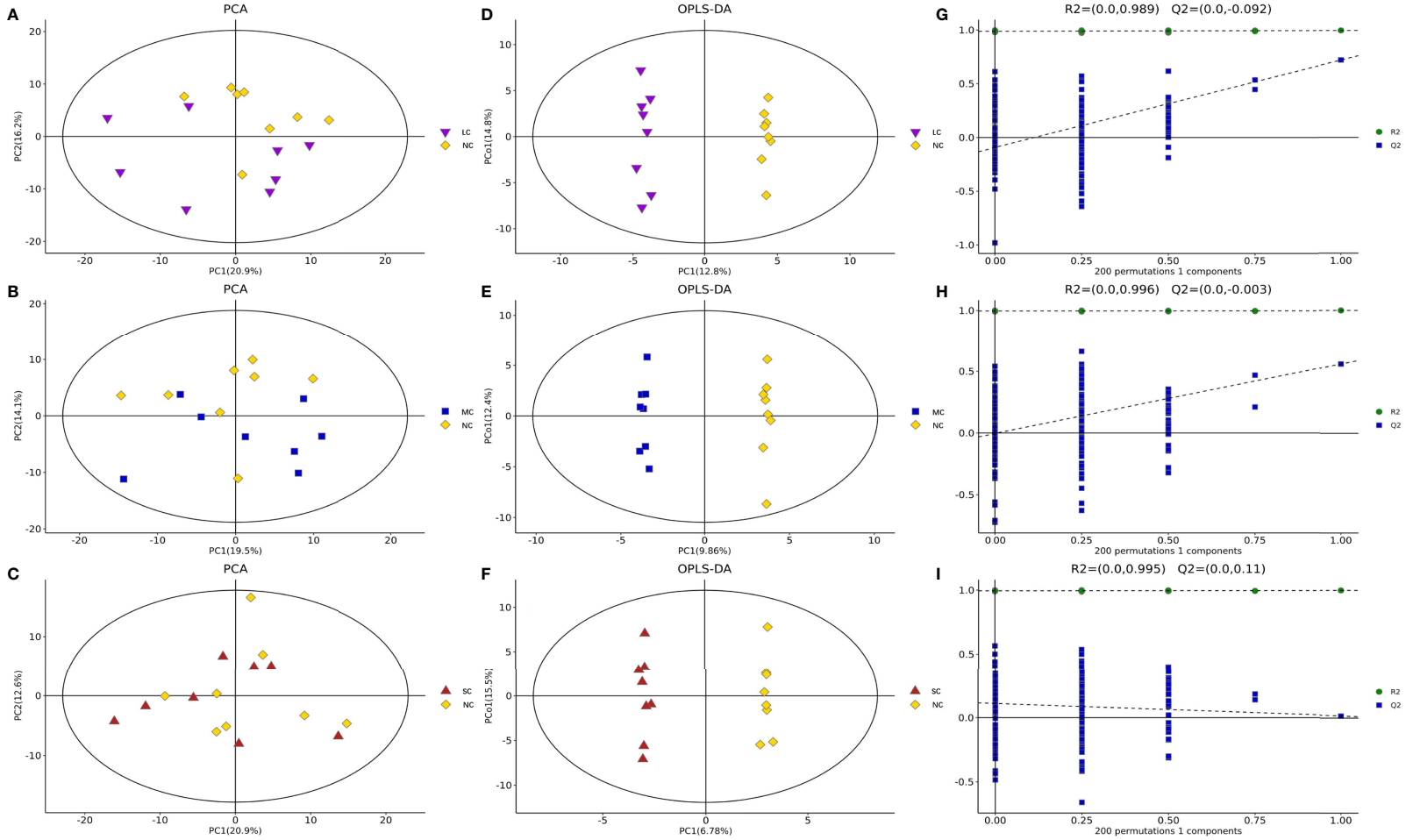

FIGURE 1 | The PCA scores plots, OPLS-DA scores plots and response permutation testing plots for different salinity groups of *P. trituberculatus*. PCA score plot of LCvsNC **(A)**, MCvsNC **(B)** and SCvsNC **(C)**; OPLS-DA scores plots of LCvsNC **(D)**, MCvsNC **(E)** and SCvsNC **(F)**; response permutation testing plots of LCvsNC **(G)**, MCvsNC **(H)** and SCvsNC **(I)**.

TABLE 1 | OPLS Models and corresponding parameters of the 3 groups.

Group	PRE	ORT	N	R2X(cum)	R2Y(cum)	Q2(cum)	R2	Q2
LCvsNC	1	2	16	0.305	0.997	0.0157	0.995	0.11
MCvsNC	1	2	16	0.31	0.998	0.563	0.996	0
SCvsNC	1	2	16	0.365	0.996	0.721	0.989	-0.09

The parameters are explained as follows:1)PRE: Represents the number of principal components during modeling; 2) ORT: Represents the number of sample during modelings; 3) N: Represents the number of samples in modeling; 4) R2X(cum): Represents the cumulative interpretation rate of the model in the X-axis direction (or can be understood as the square of the percentage of the original data information retained in the X-axis direction) during multivariate statistical analysis modeling's, and cum represents the cumulative result of several principal components;5) R2Y(cum): Represents the cumulative interpretation rate of the model in the Y-axis direction (or can be understood as the square of the percentage of the original data information retained in the Y-axis direction);6) Q2(cum): Represents the cumulative prediction rate of the model;7) R2、Q2: Response ranking test parameters, in order to measure whether the model is over-fitting.

According to the classification of these differential metabolites (**Figure 4**), among the up-regulated differential metabolites, the most abundant categories in the LCvsNC group were hydroxy acids and derivatives and fatty acyl species (**Figure 4A**). The most abundant categories in the MCvsNC group were hydroxy acids and derivatives, carboxylic acids and derivatives, and phenols (**Figure 4C**). And the most abundant categories in the SCvsNC group were organooxygen compounds, carboxylic acids and derivatives, and fatty acyl species (**Figure 4E**). Among the down-regulated differential metabolites, there were fewer species in the LCvsNC group (**Figure 4B**). While the most abundant categories in the MCvsNC group were organooxygen compounds, carboxylic acids and derivatives, and fatty acyl species (**Figure 4D**). And the most abundant categories in the SCvsNC group were organooxygen compounds and carboxylic acids and derivatives (**Figure 4F**).

In summary, the number of differential metabolites increased with decreasing salinity. The up-regulated differential metabolites were mainly concentrated in hydroxy acids and their derivatives, carboxylic acids and their derivatives and fatty acyl groups, while the down-regulated differential metabolites were mainly concentrated in organooxygen compounds and carboxylic acids and their derivatives.

Correlation Analysis of Differential Metabolites With Salinity Changes

To find the common effects of different levels of low salt stress on the crab metabolism, we used a Wayne diagram to compare the three groups of differential metabolites (**Figure 5A**). The results showed that there were nine common differential metabolites in the three different treatments, including six common up-regulated metabolites and three common down-regulated metabolites. Among them, the up-regulated metabolites included keto acids and derivatives (pyruvate), hydroxy acids and derivatives (malic acid), fatty acyl (2,4-hexadienedioic acid), organophosphate and derivatives (phosphoethanolamine), imidazopyridine (hypoxanthine) and other classes [4 -(5-methyl-2-furanyl)-2-butanone]. The three down-regulated common differential metabolites included organoxylates (butane-2,3-diol), purine nucleoside (inosine) and other categories (triacontanol). In addition to the nine common differential metabolites mentioned above, there were four common differential metabolites between the LCvsNC and MCvsNC groups and 14 common differential metabolites between the MCvsNC and SCvsNC groups (**Figure 5A**).

Among the nine differential metabolites commonly contained in the three groups, there was a certain potency relationship between the expression of metabolites and salinity. The FC values of the up-regulated differential products like pyruvate, malic acid, phosphoethanolamine, hypoxanthine, and 4 -(5-methyl-2-furanyl)-2-butanone increased with decreasing salinity (**Figure 5B**), that is, the expression of up-regulated differential metabolites increased. The FC values of malic acid and ethanolamine phosphate increased greatly with decreasing salinity, from 2.08 to 4.14 for malic acid and from 2.54 to 4.67 for ethanolamine phosphate. With the decrease of salinity, the FC values of the three common down-regulated differential metabolites decreased, among which the FC value of the triacontanol decreased greatly, and their FC values decreased from 0.46 to 0.20.

The researchers discovered that when salinity reduced, the contents of pyruvate, malic acid, ethanolamine phosphate, hypoxanthine, and 4 -(5-methyl-2-furanyl)-2-butanone increased, while the levels of butane-2,3-diol and inosine decreased (**Figure 5C**). These results suggest that the aforementioned compounds serve as osmoregulators in the gills to help swimming crabs adapt to low salinity.

Analysis of Metabolic Pathways Related to Differential Metabolites at Different Salinities

Metabolic spectrum can reveal individual differential metabolites as well as provide a comprehensive understanding of metabolic pathway induced by salinity reductions.

The metabolic pathway enrichment analysis of the differential metabolites, combined with the p-values obtained from the enrichment analysis and the pathway impact values obtained from the topological analysis, revealed that the LCvsNC group enriched 46 metabolic pathways, of which 17 were significantly affected ($p<0.05$) and 29 were non-significantly affected. The metabolic pathways that were significantly affected included citric acid cycle (TCA cycle), glucagon signaling pathway, pyruvate metabolism, and purine metabolism (**Figure 6A**). The MCvsNC group has 60 metabolic pathways, 21 of which were significantly impacted ($p<0.05$). The significantly affected metabolic pathways included citric acid cycle (TCA cycle), glucagon signaling pathway, glyoxylate and dicarboxylic acid metabolism, glycolysis/gluconeogenesis, pyruvate metabolism, pentose phosphate pathway, HIF-1 signaling pathway glycine, serine and threonine metabolism, etc. (**Figure 6B**). A total of 62 metabolic pathways were enriched in the SCvsNC group, of which 20 metabolic pathways were significantly affected ($p<0.05$), overlapping with most of the metabolic pathways in

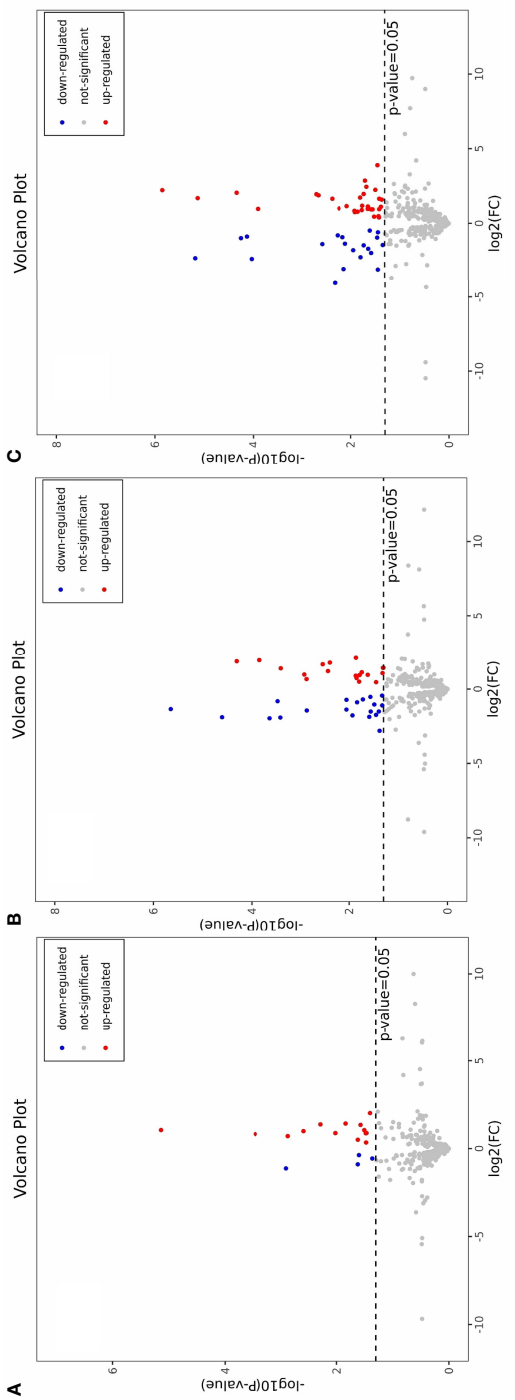

FIGURE 2 | Volcano map of differential metabolites in LCvsNC group **(A)**, MCvsNC group **(B)**, SCvsNC group **(C)**. The red origin represents the differential metabolites that are significantly up-regulated, the blue origin represents the differential metabolites that are significantly down-regulated, and the gray origin represents the insignificant differential metabolites.

the MC group. The significantly affected metabolic pathways included glucagon transmission, citric acid cycle (TCA cycle), glycolysis/gluconeogenesis, galactose metabolism, pyruvate metabolism, glycine, serine and threonine metabolism, alanine, aspartate and glutamate metabolism, and HIF-1 signaling pathway (**Figure 6C**).

The metabolic pathways significantly affected in the 3 groups were analyzed by Wayne diagram (**Figure 7B**), and 6 common differential metabolic pathways were found, including citric acid cycle (TCA cycle), glucagon signaling pathway, HIF-1 signaling pathway, and pyruvate metabolism. These pathways were related to carbohydrate metabolism and signal transduction in *P. trituberculatus*. When the salinity decreased from 16 to 12, the enrichment factors of citric acid cycle (TCA cycle), pyruvate metabolism, glucagon signaling, and HIF-1 signaling pathway increased (**Figures 6A, B**), indicating that the enrichment of energy-related metabolic pathways deepened when the salinity decreased from 16 to 12. When the salinity decreased from 12 to 8, 16 metabolic pathways in the SCvsNC group were the same as those in the MCvsNC group (**Figure 7B**) indicating that the metabolic pathway species of swimming crabs changed little after the salinity decreased to 12. The 16 significantly different metabolic pathways contained five carbohydrate metabolisms and three amino acid or other amino acid metabolisms. The former included TCA cycle, pyruvate metabolism, glyoxylate and dicarboxylic acid metabolism, glycolysis/gluconeogenesis, and pentose phosphate pathways, and the latter included alanine, aspartate and glutamate metabolism, phenylalanine metabolism, glycine, serine and threonine metabolism.

The above results showed that the number of differential metabolic pathways increased with decreasing salinity. The significantly affected differential metabolic pathways in the three experimental groups included TCA cycle and pyruvate metabolism, mainly involving differential metabolites such as citric acid, malic acid, pyruvate and so on. The results imply that TCA cycle and pyruvate metabolism serving as energy supply provided an extremely important role in the osmotic regulation of swimming crabs.

DISCUSSION

Several reports have shown that salinity and its potential changes will affect the survival of aquatic organisms (Charmantier, 1998). Aquatic crustaceans adapt to different salinity environments mainly through the process of osmotic regulation (Romano and Zeng, 2012), and gills are the main sites for the regulation of osmotic pressure and blood ion concentration in crustaceans (Shen et al., 2020). In this study, we used GC-MS techonolgy to investigate the metabolic response of osmotic regulation in gills of *P. trituberculatus* under short-term low salt stress. The result showed that a total of 64 difference metabolites were extracted from gill tissue of swimming crabs using non-targeted metabolomics techniques. And the number of differential metabolites increased significantly with decreasing salinity. According to the results of metabolic pathway enrichment analysis, the number of differential metabolic pathways also

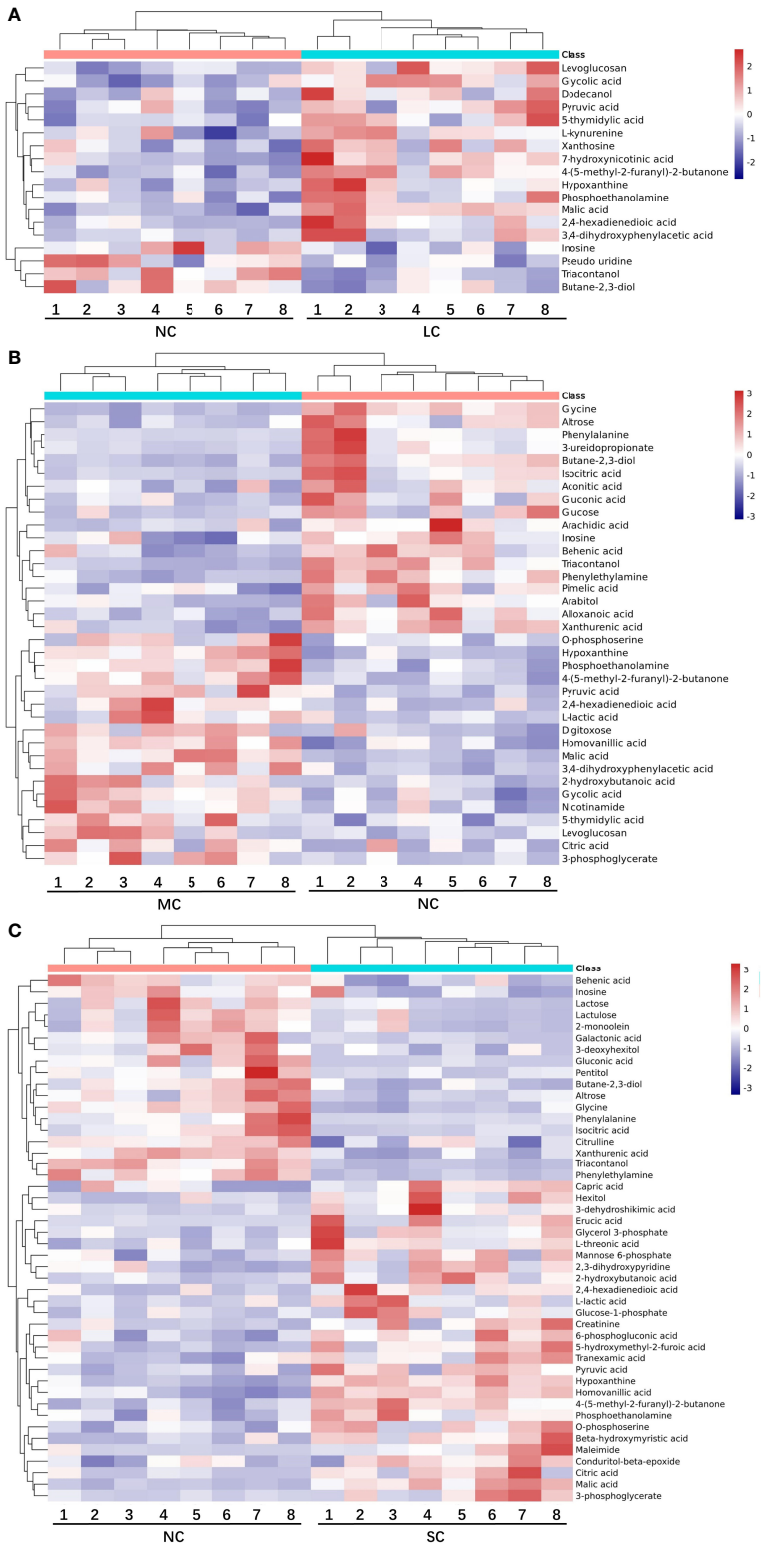

FIGURE 3 | Heat map of differential metabolites in LCvsNC group **(A)**, MCvsNC group **(B)**, SCvsNC group **(C)**. Each gill sample is visualized in a column, and each metabolite is represented by a row. Blue indicates a lower metabolite concentration, while red indicates a higher metabolite level (refer to color scale).

TABLE 2 | Significantly differential metabolites in gills of LCvsNC group.

Up/Down-regulated	Metabolites	RT(min)	P-Value	FC (LC/NC)	AVG (LC)	AVG (NC)
Up-regulated	Hypoxanthine	21.48	0.026809	2.54	30.89	12.17
	7-hydroxynicotinic acid	16.45	0.005188	2.59	0.03	0.01
	2,4-hexadienedioic acid	18.49	0.014524	2.68	0.03	0.01
	Malic acid	14.79	0.000007	2.08	25.24	12.16
	3,4-dihydroxyphenylacetic acid	22.12	0.039541	4.05	1.08	0.27
	Levoglucosan	19.49	0.002588	1.99	0.05	0.03
	4-(5-methyl-2-furanyl)-2-butanone	8.58	0.000350	1.78	28.09	15.82
	Pyruvic acid	6.45	0.031253	2.07	12.71	6.13
	Glycolic acid	6.89	0.001358	1.63	9.69	5.93
	5-thymidylic acid	21.28	0.009561	1.84	0.19	0.10
	Phosphoethanolamine	21.02	0.033279	1.83	2.74	1.50
	Dodecanol	16.70	0.034167	1.84	1.13	0.61
	Xanthosine	32.71	0.024001	1.42	0.09	0.06
	L-kynurenine	28.03	0.033677	1.27	0.23	0.18
Down-regulated	Triacontanol	37.92	0.001262	0.46	0.36	0.78
	Butane-2,3-diol	6.18	0.023958	0.54	9.76	18.17
	Inosine	32.10	0.025091	0.77	0.39	0.50
	Pseudo uridine	29.99	0.043347	0.68	0.10	0.15

RT (min): P-value is used to evaluate whether the difference between the two groups of samples is significant, and the $P < 0.05$ indicates significant difference, and the $P < 0.01$ indicates highly significant difference. FC: The ratio of the average expression of metabolites in the two groups of samples, and FC>1 indicates up-regulated metabolites, and FC<1 indicates down-regulated metabolites.

TABLE 3 | Significantly differential metabolites in gills of MCvsNC group.

Up/Down-regulated	Metabolites	RT(min)	VIP	P-Value	FC (MC/NC)	AVG (MC)	AVG (NC)
Up-regulated	Citric acid	21.79	2.79	0.048516	2.69	1.63	0.61
	Hypoxanthine	21.48	2.65	0.000149	3.87	47.03	12.17
	Malic acid	14.79	2.49	0.000049	3.66	44.55	12.16
	Pyruvic acid	6.45	2.37	0.004059	3.45	21.16	6.13
	3,4-dihydroxyphenylacetic acid	22.12	2.23	0.002898	3.18	0.85	0.27
	3-phosphoglycerate	21.63	2.20	0.013732	4.31	0.10	0.02
	Homovanillic acid	20.73	2.20	0.000408	2.63	0.30	0.12
	Phosphoethanolamine	21.02	1.86	0.003715	2.32	3.47	1.50
	2,4-hexadienedioic acid	18.49	1.72	0.018092	2.19	0.03	0.01
	4-(5-methyl-2-furanyl)-2-butanone	8.58	1.68	0.001227	1.97	31.21	15.82
	L-lactic acid	6.62	1.65	0.049747	2.71	109.65	40.50
	Digitoxose	16.98	1.47	0.016367	1.93	0.39	0.20
	O-phosphoserine	21.72	1.41	0.047674	2.10	0.56	0.27
	Glycolic acid	6.89	1.37	0.001359	1.59	9.45	5.93
	2-hydroxybutanoic acid	7.75	1.33	0.013613	1.86	0.22	0.12
	5-thymidylic acid	21.28	1.30	0.014141	1.68	0.17	0.10
	Levoglucosan	19.49	1.26	0.023880	1.94	0.05	0.03
	Nicotinamide	14.81	1.06	0.015932	1.41	17.20	12.17
Down-regulated	Triacontanol	37.92	2.54	0.000025	0.27	0.21	0.78
	Butane-2,3-diol	6.18	2.52	0.000241	0.26	4.66	18.17
	Phenylalanine	17.90	2.50	0.041504	0.14	0.13	0.93
	Phenylethylamine	16.61	2.49	0.000400	0.26	0.42	1.57
	Glycine	7.68	2.16	0.000002	0.39	71.76	182.93
	Alloxanoic acid	28.94	2.06	0.001375	0.37	0.07	0.19
	3-ureidopropionate	17.90	2.06	0.025677	0.27	0.23	0.84
	Isocitric acid	21.50	2.02	0.011684	0.29	0.32	1.11
	Aconitic acid	19.87	1.81	0.047042	0.47	1.87	4.01
	Altrose	23.20	1.69	0.008798	0.38	0.23	0.60
	Gluconic acid	25.08	1.69	0.035230	0.30	0.19	0.64
	Arachidic acid	31.27	1.67	0.032462	0.49	0.18	0.37
	Xanthurenic acid	29.02	1.58	0.000351	0.57	0.11	0.20
	Glucose	23.19	1.46	0.027423	0.35	0.79	2.26
	Arabitol	19.59	1.41	0.014513	0.54	0.06	0.11
	Behenic acid	32.72	1.40	0.008819	0.61	0.87	1.43
	Pimelic acid	17.38	1.29	0.019016	0.62	0.17	0.27
	Inosine	32.10	1.13	0.026999	0.69	0.35	0.50

RT (min): retention time. VIP is from OPLS DA model, and the larger the VIP, the greater the contribution of the variable to the grouping.

TABLE 4 | Significantly differential metabolites in gills of SCvsNC group.

Up/Down-regulated	Metabolites	RT(min)	VIP	P-Value	FC (SC/NC)	AVG (SC)	AVG (NC)
Up-regulated	Hexitol	25.67	2.51	0.018776	3.91	0.02	0.01
	Hypoxanthine	21.48	2.42	0.000001	4.67	56.81	12.17
	Citric acid	21.79	2.34	0.021288	5.47	3.31	0.61
	Malic acid	14.79	2.23	0.000047	4.14	50.38	12.16
	Beta-hydroxymyristic acid	25.16	2.13	0.002150	3.68	0.03	0.01
	Homovanillic acid	20.73	2.11	0.000008	3.22	0.37	0.12
	5-hydroxymethyl-2-furoic acid	15.97	2.09	0.001948	3.87	0.11	0.03
	Maleimide	7.22	2.05	0.032375	4.73	2.48	0.52
	Capric acid	14.24	1.88	0.042038	2.16	1.42	0.65
	Erucic acid	32.55	1.82	0.035789	14.86	1.02	0.07
	3-phosphoglycerate	21.63	1.78	0.019984	7.27	0.16	0.02
	3-dehydroshikimic acid	20.75	1.67	0.038776	3.14	0.16	0.05
	Pyruvic acid	6.45	1.65	0.004107	3.14	19.23	6.13
	L-lactic acid	6.62	1.56	0.043715	3.01	121.90	40.50
	4-(5-methyl-2-furanyl)-2-butanone	8.58	1.50	0.000127	1.95	30.91	15.82
	2,4-hexadienedioic acid	18.49	1.49	0.022887	2.19	0.03	0.01
	Phosphoethanolamine	21.02	1.44	0.005738	2.00	3.00	1.50
	Creatinine	16.22	1.39	0.015904	3.31	0.58	0.17
	O-phosphoserine	21.72	1.39	0.008458	2.23	0.59	0.27
	Conduritol-beta-epoxide	24.24	1.34	0.028471	1.91	0.01	0.01
	Glycerol 3-phosphate	17.34	1.21	0.022762	1.96	0.12	0.06
	6-phosphogluconic acid	30.69	1.20	0.012460	1.69	0.09	0.05
	2,3-dihydroxypyridine	11.02	1.20	0.026383	1.91	0.18	0.09
	Tranexamic acid	19.19	1.19	0.012207	1.79	0.26	0.14
	L-threonic acid	15.96	1.19	0.014146	1.72	0.77	0.45
	2-hydroxybutanoic acid	7.75	1.19	0.017492	2.27	0.27	0.12
	Glucose-1-phosphate	20.78	1.16	0.038741	1.93	1.47	0.76
	Mannose 6-phosphate	30.14	1.14	0.017228	1.85	0.26	0.14
Down-regulated	Gluconic acid	25.08	2.97	0.004849	0.06	0.04	0.64
	Triacontanol	37.92	2.47	0.000007	0.20	0.15	0.78
	Phenylethylamine	16.61	2.47	0.000095	0.19	0.30	1.57
	Galactonic acid	25.05	2.46	0.007331	0.12	24.72	207.89
	Phenylalanine	17.90	2.42	0.036436	0.12	0.11	0.93
	3-deoxyhexitol	21.67	1.83	0.018792	0.36	0.84	2.35
	Isocitric acid	21.50	1.79	0.011526	0.29	0.32	1.11
	Butane-2,3-diol	6.18	1.77	0.002570	0.38	6.92	18.17
	Lactulose	32.89	1.69	0.026607	0.25	16.25	64.42
	Lactose	33.13	1.62	0.016234	0.21	12.81	62.01
	Citrulline	20.25	1.56	0.006935	0.52	4.91	9.37
	Xanthurenic acid	29.02	1.56	0.000057	0.50	0.10	0.20
	Pentitol	19.00	1.53	0.045742	0.37	0.10	0.26
	Altrose	23.20	1.49	0.007852	0.39	0.23	0.60
	Glycine	7.68	1.48	0.000075	0.54	98.81	182.93
	2-monoolein	33.16	1.40	0.023222	0.31	3.23	10.54
	Behenic acid	32.72	1.30	0.005296	0.57	0.82	1.43
	Inosine	32.10	1.10	0.036592	0.66	0.33	0.50

increased with the decrease in salinity. Especially when the salinity was reduced from 16 to 12, the number of differential metabolic pathways increased greatly, but when the salinity was reduced from 12 to 8, the number and species of differential metabolic pathways did not change obviously. It is suggested that salinity 12 may be an important node for *P. trituberculatus* to adapt to low salinity.

Free amino acids (FAAs) are important cellular osmotic substances and sources of energy supply. They are involved in the regulation of osmotic pressure in aquatic organisms (Sun et al., 2021). Among the differential metabolites screened in this study, the down-regulated amino acids included phenylalanine, glycine, and citrulline. This result may be explained by the fact that low salt stress induced glycine catabolic processes in *P. trituberculatus* (Lv et al., 2013). This result is similar to the conclusion of Nile tilapia and *Litopenaeus vannamei*. In Nile tilapia, the content of phenylalanine increased under acute salinity stress (Liu et al., 2018). And in *Litopenaeus vannamei*, the content of organic osmolytes such as phenylalanine and glycine increased under salinity stress (Gomez-Jimenez et al., 2004). It is suggested that phenylalanine and glycine play a significant role in osmotic regulation. In phenylalanine metabolic pathway (**Figure 7A**), phenylalanine can be metabolized into acetyl-CoA and succinyl-CoA for the TCA cycle, and indirectly participates in energy metabolism. Glycine is the most basic amino acid found in animals, and it is involved in energy metabolism processes such as glycan metabolism and the TCA cycle. Hence, it could be hypothesized that glycine and

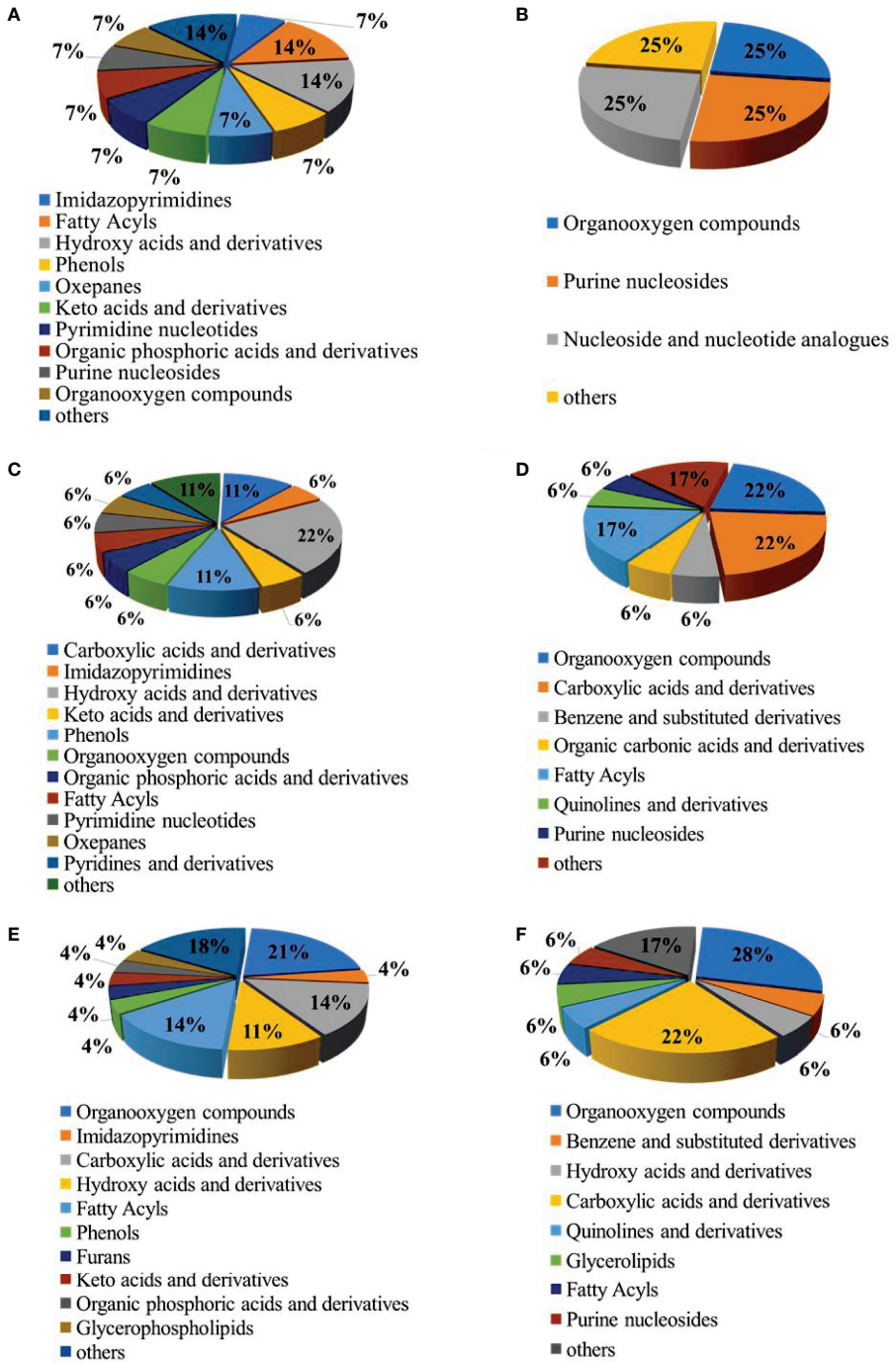

FIGURE 4 | The pie chart of the differential metabolite classification: Up-regulated metabolites in gills of LCvsNC group **(A)**, MCvsNC group **(C)** and SCvsNC group **(E)**; down-regulated metabolites in gills of LCvsNC group**(B)**, MCvsNC group**(D)**and SCvsNC group **(F)**.

phenylalanine are used for energy metabolism in osmotic regulation, causing a decrease in their content in the gills.

Several reports have shown that osmoregulation in crustaceans is an energy-consuming process (Charmantier, 1998; Ye et al., 2009; Mazzarelli et al., 2015; Ramaglia et al., 2018; Huang et al., 2019) and its main modalities include ion transport in gill epithelial cell (Ramaglia et al., 2018), intracellular proteolysis and amino acid release (Sokolova et al., 2012). In comparison to the control NC group, the LC, MC, and SC groups had nine same identical different metabolites, among

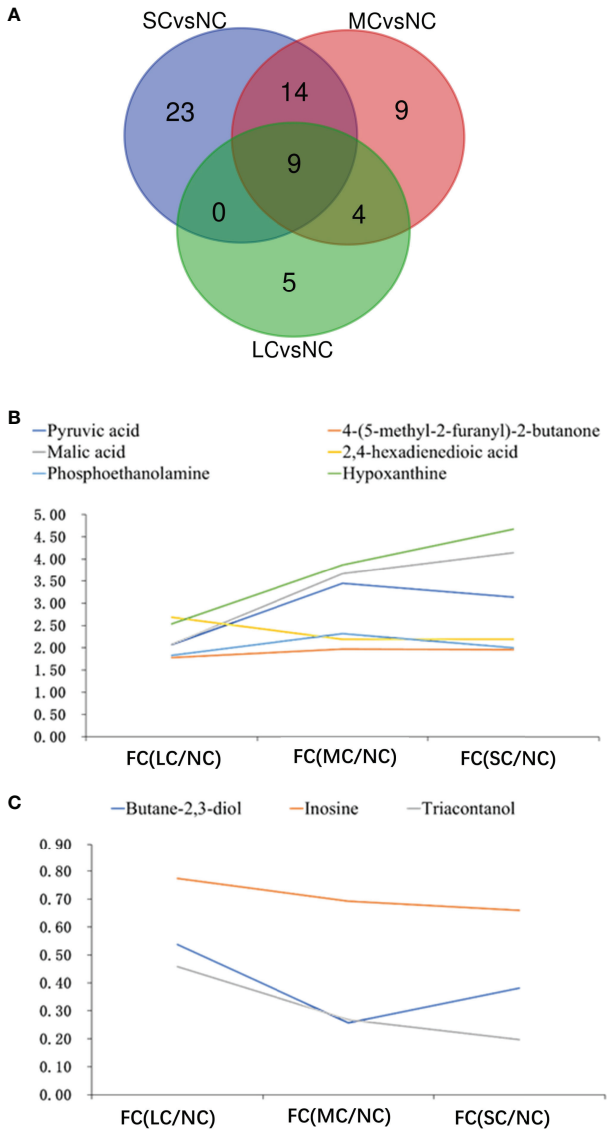

FIGURE 5 | Association analysis of differential metabolites in the three groups: Venn diagram of mutual differential metabolites **(A)**; FC figures of mutual up-regulated metabolites **(B)** and down-regulated metabolites **(C)** in gills. In a, Green circle represents SCvsNC group, red circle represents MCvsNC group, blue circle represents LCvsNC group; the number in the figure represents the amount of different metabolites after intersection.

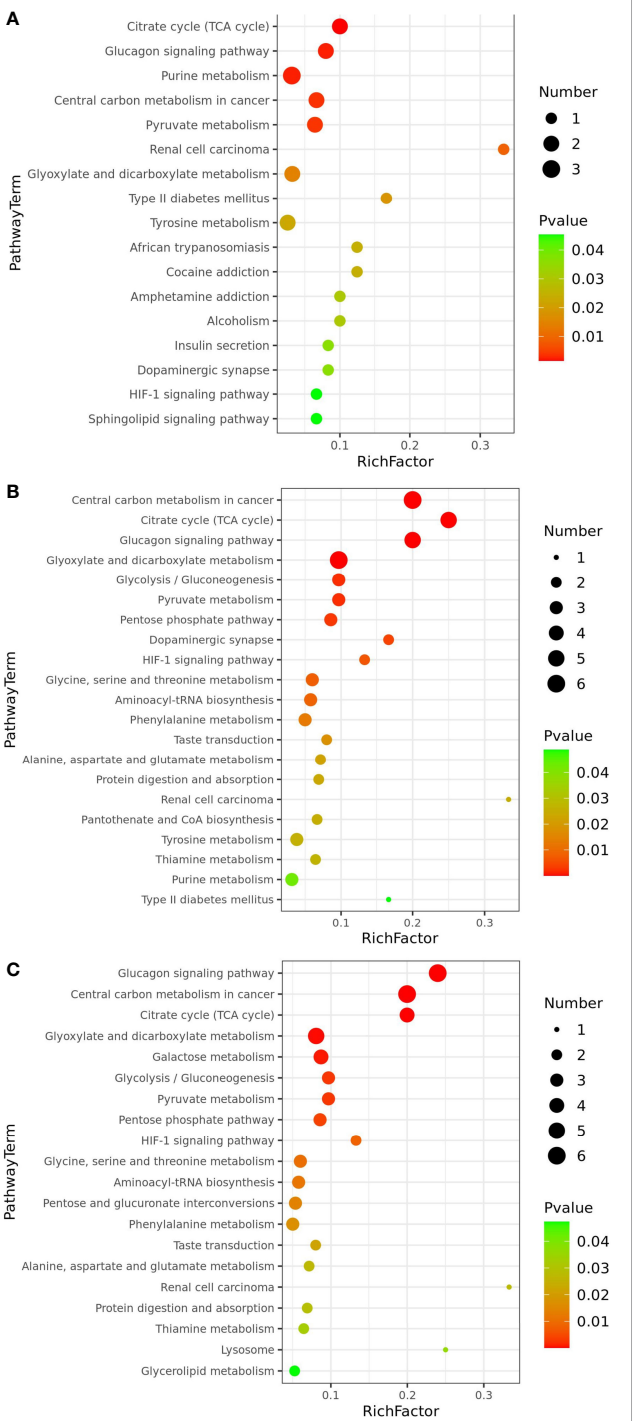

FIGURE 6 | Significantly differential metabolic pathways associated with differential metabolites (p<0.05): LCvsNC group **(A)**, MCvsNC group **(B)** and SCvsNC group **(C)**.

which pyruvate, malic acid, and phosphoethanolamine were up-regulated. The degree of up-regulation increased as salinity decreased. Thus, these organic molecules were essential indicators for gill metabolism of *P. trituberculatus* in response to low salt stress. Furthermore, both the MCvsNC and SCvsNC groups exhibited a significantly different metabolite, lactate, which is the embodiment of cell anaerobic respiration. Pyruvate is oxidatively decarboxylated to produce acetyl-CoA, which links the metabolism of the three major nutrients: sugar, fat and amino acids. Pyruvate and lactate are also jointly involved in the glycolysis/gluconeogenesis process. Glycolysis is an irreversible reaction that produces pyruvate and lactate, which increases their levels in the tissues. These findings suggest that the increase of pyruvate and lactate levels is

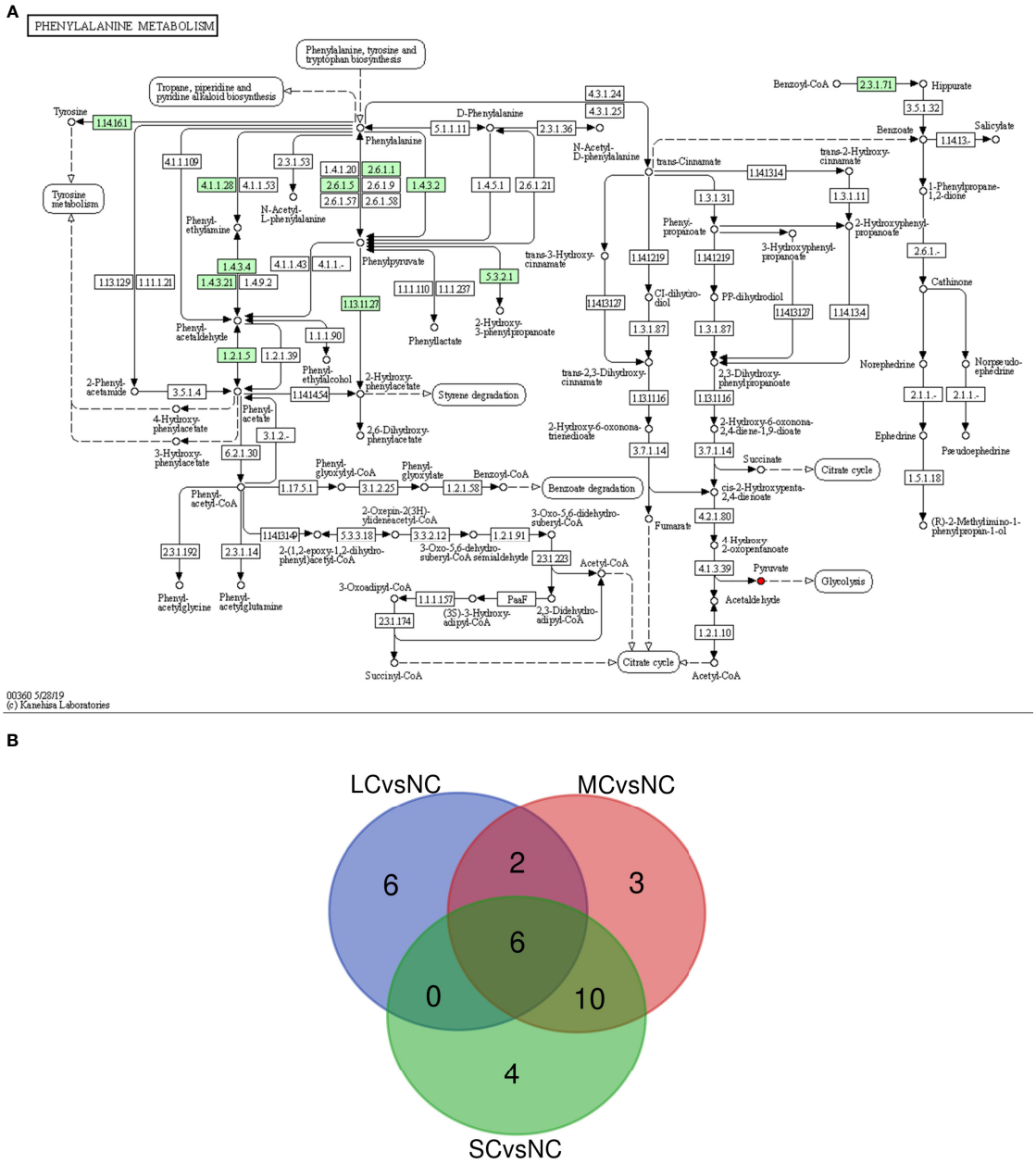

FIGURE 7 | Phenylalanine metabolic pathway **(A)** and Venn diagram of mutual significant metabolic pathways **(B)**. In a, "→" indicates the reaction direction, the small box indicates the enzyme activity, the small circle indicates the compound, the red indicates the up-regulated compound, the blue indicates the down-regulated compound, the large round box indicates the other metabolic pathway, and the dotted arrow indicates the relationship with other metabolic pathways, small green squares indicate enzymes unique to the species. In b, Green circle represents SCvsNC group, red circle represents MCvsNC group, blue circle represents LCvsNC group, the number in the figure represents the amount of different metabolites after intersection.

linked to the energy supply of osmotic regulation. Malic acid is also an important intermediary in the TCA cycle, and it had the highest VIP value of all the up-regulated organic acids in our study, confirming that malic acid is an essential osmoregulatory agent for crabs. It has been found that the content of malic acid increases significantly under salinity stress in plants (Derakhshani et al., 2020; Panda et al., 2021), but the change of malic acid metabolism in crustaceans has not been reported. Pyruvate, lactic acid, and malic acid are critical intermediates of sugar metabolism, which may play a role in the adaptation of *P. trituberculatus* to low salt.

Pyruvate and derivatives have been proven to be essential endogenous ROS scavengers with the potential to reduce inflammation and prevent illnesses induced by oxidative stress

(Kładna et al., 2015). Under low salt stress, the activity of electron transport chain enzymes in the gill mitochondria of Scylla serrata is reduced (Paital and Chainy, 2012), and electrons will escape from the electron transport chain to create ROS (Kim et al., 2006; Kumar et al., 2017), causing oxidative cellular damage (Lushchak, 2011). HIF-1 signaling has been found to accelerate glycolysis, resulting in the massive synthesis of pyruvate, to prevent producing toxic ROS and maintain ATP levels in the body (Kim et al., 2006). Thus, it is proposed that crabs under low salt stress will boost glycolysis by stimulating the HIF-1 signaling pathway, increase the content of pyruvate and lactate levels in tissues and prevent the body from being poisoned by ROS. Besides, among up-regulated differential metabolites, o-phosphatidylserine, a precursor of phosphatidylserine (PS), and phosphoethanolamine increased with decreasing salinity. In the Kennedy pathway, phosphoethanolamine can manufacture the two most prevalent phospholipids in the cell membrane, phosphatidylethanolamine (PE) and phosphatidylcholine (PC) (Fontana et al., 2020). In extensively saline crustaceans, PS can be decarboxylated to form PE, which is further methylated to PC, altering the cell membrane structure for rapid adaptation (Zwingelstein et al., 1998). A considerable rise in PC content was detected in the gills of *Scylla paramamosain* during acute hyposaline stress (Yao et al., 2021). The increased amount of o-phosphoserine and phosphoethanolamine in the gills of *P.trituberculatus* is thought to boost the production of cell membrane phospholipid and protect the osmoregulation function of cell membranes.

CONCLUSION

In this study, the metabolic response in the gills of *Portunus trituberculatus* under various short-term low salinity stress were analyzed, and the number of differential metabolites increased with decreasing salinity. Among the nine common differential metabolites, six metabolites including pyruvate, malic acid and ethanolamine phosphate were up-regulated and three metabolites such as inosine were down-regulated. KEGG enrichment analysis of differential metabolites showed that the number of differential metabolic pathways increased with decreasing salinity. There were 6 common differential metabolic pathways, including pyruvate metabolism, citric acid cycle (TCA cycle), glucagon signaling pathway, and HIF-1 signaling pathway. These metabolic pathways were mainly related to carbohydrate metabolism, signaling and other metabolic processes. In the process of this adaptation, organic acids play a significant role, while carbohydrate metabolism provides energy supply. This research contributes to a better understanding of the metabolic mechanism of osmotic regulation and adaptation to low salinity in crustaceans, with the goal of improving *Portunus trituberculatus* culture technique.

DATA AVAILABILITY STATEMENT

The original contributions presented in the study are included in the article/supplementary material. Further inquiries can be directed to the corresponding authors.

ETHICS STATEMENT

Ethical review and approval was not required for the animal study because the animal subjects used in the present study are crabs, which are invertebrates and are exempt from this requirement.

AUTHOR CONTRIBUTIONS

HW conceived and designed the study. JW, QL, XZ, and FW took samples of experimental animals. JW, QL, XZ, GG, and MN performed and analyzed all the other experiments. JW, QL, and XZ analysed and interpreted results. JW, XZ, GG, MN, LC, CW, and CM checked the paper. JW and QL wrote the manuscript with support from all authors. All authors read and approved the final manuscript.

FUNDING

This work was supported by the National Key R&D Program of China (2020YFD0900203); China Agriculture Research System of MOF and MARA, the K. C.Wong Magna Fund in Ningbo University. The funders had no role in the study design, data collection, and analysis, decision to publish, or preparation of the manuscript

REFERENCES

Augusto, A., Greene, L. J., Laure, H. J., and McNamara, J. C. (2007). The Ontogeny of Isosmotic Intracellular Regulation in the Diadromous, Freshwater Palaemonid Shrimps, *Macrobrachium Amazonicum* and *M. Olfersi* (Decapoda). *J. Crustacean Biol.* 27 (4), 626–634. doi: 10.1651/S-2796.1

Charmantier, G. (1998). Ontogeny of Osmoregulation in Crustaceans: A Review. *Invertebrate Reprod. Dev.* 33 (2-3), 177–190. doi: 10.1080/07924259.1998.9652630

Chen, X., Chen, J., Shen, Y., Bi, Y., Hou, W., Pan, G., et al. (2019). Transcriptional Responses to Low-Salinity Stress in the Gills of Adult Female *Portunus Trituberculatus*. *Comp. Biochem. Physiol. Part D Genomics Proteomics* 29, 86–94. doi: 10.1016/j.cbd.2018.11.001

de Faria, S. C., Augusto, A. S., and McNamara, J. C. (2011). Intra- and Extracellular Osmotic Regulation in the Hololimnetic Caridea and Anomura: A Phylogenetic Perspective on the Conquest of Fresh Water by the Decapod Crustacea. *J. Comp. Physiol. B* 181 (2), 175–186. doi: 10.1007/s00360-010-0522-6

Derakhshani, Z., Bhave, M., and Shah, R. M. (2020). Metabolic Contribution to Salinity Stress Response in Grains of Two Barley Cultivars With Contrasting Salt Tolerance. *Environ. Exp. Bot.* 179, 104229. doi: 10.1016/j.envexpbot.2020.104229

Feng, Y., Zhang, D., Lv, J., Gao, B., Li, J., and Liu, P. (2019). Identification of SNP Markers Correlated With the Tolerance of Low-Salinity Challenge in Swimming Crab (*Portunus Trituberculatus*). *Acta Oceanolog Sin.* 38 (8), 41–47. doi: 10.1007/s13131-019-1428-0

Fontana, D., Mauri, M., Renso, R., Docci, M., Crespiatico, I., Røst, L. M., et al. (2020). ETNK1 Mutations Induce a Mutator Phenotype That can be Reverted With Phosphoethanolamine. *Nat. Commun.* 11 (1), 5938. doi: 10.1038/s41467-020-19721-w

Gao, B., Sun, D., Lv, J., Ren, X., Liu, P., and Li, J. (2019). Transcriptomic Analysis Provides Insight Into the Mechanism of Salinity Adjustment in Swimming Crab *Portunus Trituberculatus*. *Genes Genomics* 41 (8), 961–971. doi: 10.1007/s13258-019-00828-4

Gomez-Jimenez, S., Urias-Reyes, A. A., Vazquez-Ortiz, F., and Hernandez-Watanabe, G. (2004). Ammonia Efflux Rates and Free Amino Acid Levels in *Litopenaeus Vannamei* Postlarvae During Sudden Salinity Changes. *Aquaculture* 233 (1-4), 573–581. doi: 10.1016/j.aquaculture.2003.09.050

Huang, Y. H., Zhang, M., Li, Y. M., Wu, D. L., Liu, Z. Q., Jiang, Q. C., et al. (2019). Effects of Salinity Acclimation on the Growth Performance, Osmoregulation and Energy Metabolism of the Oriental River Prawn, Macrobrachium Nipponense (De Haan). *Aquacult Res.* 50 (2), 685–693. doi: 10.1111/are.13950

Kim, J. W., Tchernyshyov, I., Semenza, G. L., and Dang, C. V. (2006). HIF-1-Mediated Expression of Pyruvate Dehydrogenase Kinase: A Metabolic Switch Required for Cellular Adaptation to Hypoxia. *Cell Metab.* 3 (3), 177–185. doi: 10.1016/j.cmet.2006.02.002

Kładna, A., Marchlewicz, M., Piechowska, T., Kruk, I., and Aboul-Enein, H. Y. (2015). Reactivity of Pyruvic Acid and its Derivatives Towards Reactive Oxygen Species. *Luminescence* 30 (7), 1153–1158. doi: 10.1002/bio.2879

Kumar, V., Khare, T., Sharma, M., and Wani, S. H. (2017). ""ROS-Induced Signaling and Gene Expression in Crops Under Salinity Stress,"," in *Reactive Oxygen Species and Antioxidant Systems in Plants: Role and Regulation Under Abiotic Stress.)*, 159–184. Singapore: Springer Nature. doi: 10.1007/978-981-10-5254-5_7

Liu, Y., Li, E., Xu, C., Su, Y., Qin, J. G., Chen, L., et al. (2018). Brain Transcriptome Profiling Analysis of Nile Tilapia (*Oreochromis Niloticus*) Under Long-Term Hypersaline Stress. *Front. Physiol.* 9. doi: 10.3389/fphys.2018.00219

Long, X., Wu, X., Zhao, L., Ye, H., Cheng, Y., and Zeng, C. (2017). Effects of Salinity on Gonadal Development, Osmoregulation and Metabolism of Adult Male Chinese Mitten Crab, *Eriocheir Sinensis*. *PloS One* 12 (6), e0179036. doi: 10.1371/journal.pone.0179036

Lushchak, V. I. (2011). Environmentally Induced Oxidative Stress in Aquatic Animals. *Aquat Toxicol.* 101 (1), 13–30. doi: 10.1016/j.aquatox.2010.10.006

Lu, J.-Y., Shu, M.-A., Xu, B.-P., Liu, G.-X., Ma, Y.-Z., Guo, X.-L., et al. (2015). Mud Crab *Scylla Paramamosain* Glutamate Dehydrogenase: Molecular Cloning, Tissue Expression and Response to Hyposmotic Stress. *Fish Sci.* 81 (1), 175–186. doi: 10.1007/s12562-014-0828-5

Lu, Y. L., Wang, F., Jia, X. Y., Gao, Q. F., and Dong, S. L. (2013). A Laboratory Simulation of the Effects of Acute Salinity Decrease on Osmoregulation and Hsps Expression in the Swimming Crab, *Portunus Trituberculatus*: Implications for Aquaculture. *Marine Freshwater Behav. Physiol.* 46 (5), 301–311. doi: 10.1080/10236244.2013.832573

Lv, J., Liu, P., Gao, B., and Li, J. (2016). The Identification and Characteristics of Salinity-Related microRNAs in Gills of *Portunus Trituberculatus*. *Cell Stress Chaperones* 21 (1), 63–74. doi: 10.1007/s12192-015-0641-9

Lv, J., Liu, P., Wang, Y., Gao, B., Chen, P., and Li, J. (2013). Transcriptome Analysis of *Portunus Trituberculatus* in Response to Salinity Stress Provides Insights Into the Molecular Basis of Osmoregulation. *PloS One* 8 (12), e82155. doi: 10.1371/journal.pone.0082155

Lv, J., Sun, D., Yan, D., Ti, X., Liu, P., and Li, J. (2019). Quantitative Trait Loci Mapping and Marker Identification for Low Salinity Tolerance Trait in the Swimming Crab (*Portunus Trituberculatus*). *Front. Genet.* 10. doi: 10.3389/fgene.2019.01193

Mazzarelli, C. C., Santos, M. R., Amorim, R. V., and Augusto, A. (2015). Effect of Salinity on the Metabolism and Osmoregulation of Selected Ontogenetic Stages of an Amazon Population of *Macrobrachium Amazonicum* Shrimp (Decapoda, Palaemonidae). *Braz. J. Biol.* 75 (2), 372–379. doi: 10.1590/1519-6984.14413

McNamara, J. C., and Faria, S. C. (2012). Evolution of Osmoregulatory Patterns and Gill Ion Transport Mechanisms in the Decapod Crustacea: A Review. *J. Comp. Physiol. B* 182 (8), 997–1014. doi: 10.1007/s00360-012-0665-8

Paital, B., and Chainy, G. B. (2012). Effects of Salinity on O_2 Consumption, ROS Generation and Oxidative Stress Status of Gill Mitochondria of the Mud Crab *Scylla Serrata*. *Comp. Biochem. Physiol. C Toxicol. Pharmacol.* 155 (2), 228–237. doi: 10.1016/j.cbpc.2011.08.009

Panda, A., Rangani, J., and Parida, A. K. (2021). Unraveling Salt Responsive Metabolites and Metabolic Pathways Using non-Targeted Metabolomics Approach and Elucidation of Salt Tolerance Mechanisms in the Xero-Halophyte *Haloxylon Salicornicum*. *Plant Physiol. Biochem.* 158, 284–296. doi: 10.1016/j.plaphy.2020.11.012

Ramaglia, A. C., de Castro, L. M., and Augusto, A. (2018). Effects of Ocean Acidification and Salinity Variations on the Physiology of Osmoregulating and Osmoconforming Crustaceans. *J. Comp. Physiol. B* 188 (5), 729–738. doi: 10.1007/s00360-018-1167-0

Ren, L. P., Qin, Y., Li, X. C., Sun, Y. N., and Wang, R. X. (2013). Isolation and Characterization of Polymorphic Microsatellite Loci in the Swimming Crab *Portunus Trituberculatus* (Portunidae). *Genet. Mol. Res.* 12 (4), 5911–5915. doi: 10.4238/2013.November.22.19

Romano, N., and Zeng, C. (2012). Osmoregulation in Decapod Crustaceans: Implications to Aquaculture Productivity, Methods for Potential Improvement and Interactions With Elevated Ammonia Exposure. *Aquaculture* 334-337, 12–23. doi: 10.1016/j.aquaculture.2011.12.035

Shen, G., Zhang, X., Gong, J., Wang, Y., Huang, P., Shui, Y., et al. (2020). Transcriptomic Analysis of *Procambarus Clarkii* Affected by "Black May" Disease. *Sci. Rep.* 10 (1), 21225. doi: 10.1038/s41598-020-78191-8

Sokolova, I. M., Frederich, M., Bagwe, R., Lannig, G., and Sukhotin, A. A. (2012). Energy Homeostasis as an Integrative Tool for Assessing Limits of Environmental Stress Tolerance in Aquatic Invertebrates. *Marine Environ. Res.* 79, 1–15. doi: 10.1016/j.marenvres.2012.04.003

Sun, Y. C., Han, S. C., Yao, M. Z., Wang, Y. M., Geng, L. W., Wang, P., et al. (2021). High-Throughput Metabolomics Method Based on Liquid Chromatography-Mass Spectrometry: Insights Into the Underlying Mechanisms of Salinity-Alkalinity Exposure-Induced Metabolites Changes in *Barbus Capito*. *J. Sep Sci.* 44 (2), 497–512. doi: 10.1002/jssc.202000861

Xu, Q., and Liu, Y. (2011). Gene Expression Profiles of the Swimming Crab *Portunus Trituberculatus* Exposed to Salinity Stress. *Marine Biol.* 158 (10), 2161–2172. doi: 10.1007/s00227-011-1721-8

Yao, H., Li, X., Chen, Y., Liang, G., Gao, G., Wang, H., et al. (2021). Metabolic Changes in *Scylla Paramamosain* During Adaptation to an Acute Decrease in Salinity. *Front. Marine Sci.* 8. doi: 10.3389/fmars.2021.734519

Ye, Y., An, Y., Li, R., Mu, C., and Wang, C. (2014). Strategy of Metabolic Phenotype Modulation in *Portunus Trituberculatus* Exposed to Low Salinity. *J. Agric. Food Chem.* 62 (15), 3496–3503. doi: 10.1021/jf405668a

Ye, L., Jiang, S., Zhu, X., Yang, Q., Wen, W., and Wu, K. (2009). Effects of Salinity on Growth and Energy Budget of *Juvenile Penaeus* Monodon. *Aquaculture* 290 (1-2), 140–144. doi: 10.1016/j.aquaculture.2009.01.028

Zwingelstein, G., Bodennec, J., Brichon, G., Abdul-Malak, N., Chapelle, S., and El Babili, M. (1998). Formation of Phospholipid Nitrogenous Bases in Euryhaline Fish and Crustaceans. I. Effects of Salinity and Temperature on Synthesis of Phosphatidylserine and its Decarboxylation. *Comp. Biochem. Physiol. - B Biochem. Mol. Biol.* 120 (3), 467–473. doi: 10.1016/S0305-0491(98)10031-7

Conflict of Interest: The authors declare that the research was conducted in the absence of any commercial or financial relationships that could be construed as a potential conflict of interest.

Publisher's Note: All claims expressed in this article are solely those of the authors and do not necessarily represent those of their affiliated organizations, or those of the publisher, the editors and the reviewers. Any product that may be evaluated in this article, or claim that may be made by its manufacturer, is not guaranteed or endorsed by the publisher.

frontiers | Frontiers in Marine Science

REVIEW
published: 06 May 2022
doi: 10.3389/fmars.2022.886024

Welfare in Farmed Decapod Crustaceans, With Particular Reference to *Penaeus vannamei*

Amaya Albalat[1]*, *Simão Zacarias*[1], *Christopher J. Coates*[2], *Douglas M. Neil*[3] *and Sonia Rey Planellas*[1]

[1] Institute of Aquaculture, University of Stirling, Stirling, United Kingdom, [2] Ryan Institute, School of Natural Sciences, National University of Ireland Galway, Galway, Ireland, [3] Institute of Biodiversity Animal Health and Comparative Medicine, University of Glasgow, Glasgow, United Kingdom

The farming of decapod crustaceans is a key economic driver in many countries, with production reaching around 9.4 million tonnes (USD 69.3 billion) in 2018. These efforts are currently dominated by the farming of Pacific whiteleg shrimp, *Penaeus vannamei*, which translates into approximately 167 billion farmed *P. vannamei* being harvested annually. Further production growth is expected in the future and hence the need for more research into its health and welfare is required. Herein, from an extensive survey of the available literature, we scrutinise farming practices and the challenges associated with the production of *P. vannamei* from an animal-centric welfare perspective (1), we propose potential welfare indicators (2) and we critically review current scientific evidence of sentience in penaeid shrimp among other commercially important decapods (3), since it is plausible that in the near future not only the largest, but in fact all decapod crustaceans will receive welfare protection. This review highlights that despite the wide knowledge on crustacean stress physiology and immunology as well as disease control, still little is known about some key parameters related to the five welfare dimensions. We recommend that further research should focus on developing a systematic integrated welfare assessment encompassing all the different aspects of the crustaceans farming and life cycle up to slaughter. Furthermore, direct and indirect species-specific operational welfare indicators should be developed for all decapod crustaceans currently farmed, similar to the ones suggested in this review for *P. vannamei*.

Keywords: sentience, penaeids, farming, welfare, disease, aquaculture, humane slaughter

OPEN ACCESS

Edited by:
Yangfang Ye,
Ningbo University, China

Reviewed by:
Jitao Li,
Chinese Academy of Fishery Sciences (CAFS), China
Khor Waiho,
University of Malaysia Terengganu, Malaysia

***Correspondence:**
Amaya Albalat
amaya.albalat@stir.ac.uk

Specialty section:
This article was submitted to Marine Fisheries, Aquaculture and Living Resources, a section of the journal Frontiers in Marine Science

Received: *28 February 2022*
Accepted: *11 April 2022*
Published: *06 May 2022*

Citation:
Albalat A, Zacarias S, Coates CJ, Neil DM and Planellas SR (2022) Welfare in Farmed Decapod Crustaceans, With Particular Reference to Penaeus vannamei. Front. Mar. Sci. 9:886024. doi: 10.3389/fmars.2022.886024

1 INTRODUCTION

True prawns belonging to the family Penaeidae comprise more than 400 described species and include commercially extremely valuable species such as the giant tiger prawn (*Penaeus monodon*) and the Pacific whiteleg shrimp (*P. vannamei*, synonym *Lipopenaeus vannamei*). As a typical example of their biology, *P. vannamei* is native to the Eastern Pacific coast from Sonora, Mexico in the North, through Central and South America as far South as Tumbes in Peru, in areas where water temperatures are normally >20°C throughout the year. They occupy tropical marine habitats, where

adults mature at 6-7 months and live and spawn in the open ocean. The larval stages are carried towards the shore by tidal currents, and postlarvae move further inshore to spend their remaining pre-adult stages in coastal estuaries, lagoons or mangrove areas (FAO, 2009).

The artificial rearing of a penaeid species for aquaculture can be traced back to more than 70 years ago with the rearing of Kuruma prawn *P. japonicus* larvae (Hudinaga, 1935; Hudinaga, 1942). However, while initial work was performed in this species, rearing and developmental work especially during the 1960's and 1970's expanded quickly in other geographical areas for various penaeid species (Cummings, 1961; Elwald, 1965; Muthu et al., 1974; Thomas et al., 1974). From a commercial production perspective, the work by Hudinaga (Hudinaga, 1966; Hudinaga, 1967) is considered the basis from which the penaeid shrimp industry developed.

The first captive spawning of *P. vannamei* was achieved in Florida in 1973 from nauplii shipped from a wild-caught mated female from Panama. Following the development of intensive breeding and rearing techniques, the discovery that unilateral eyestalk ablation and adequate nutrition promote maturation, commercial culture of *P. vannamei* began from the mid-1970s in South and Central America and subsequently in mainland United States of America, with strict quarantine laws or bans to prevent importation of exotic pathogens with new stocks. Although a non-indigenous species in Asia, from the beginning of the millennium *P. vannamei* has become the dominant species in penaeid shrimp aquaculture in many Asian countries, notably China, Vietnam, Thailand and India, replacing local species such as *P. monodon*.

In 2018, the total aquaculture production of crustaceans was estimated to be 9.4 million tonnes (USD 69.3 billion) (FAO, 2020). Of this production, more than 50% is accounted for by the farming of *P. vannamei* (4.96 million tonnes) while *P. monodon* production is around 8% (750K tonnes). The main producing countries are now based in the Asia-Pacific region (80% production) led by China, while in Latin America the main producing country is Ecuador with 600K tonnes farmed in 2019. While the production is dominated by these two species, knowledge on rearing methods is available for many penaeid species including *P. aztacus*, *P. chinensis*, *P. merguiensis*, *P. duorarum*, *P. japonicus*, *P. orientalis*, *P. setiferus*, *P. stylirostirs* and *P. indicus* among others (see for example Cook and Murphy, 1969; Heng and Rui-yu, 1994). At the time of writing, the only complete genomes available for the family Penaidae are *P. vannamei* and *P. monodon* (Zhang et al., 2019; Uengwetwanit et al., 2021). However, given the importance of biodiversification from a food security context (Metian et al., 2020) it is possible that this situation will change in the future and necessary tools and SPF-free seed will be available for other species.

While growth in this sector has been very significant, the sector has suffered from a number of production challenges, mostly driven by disease (see *Evaluation of Key Challenges Associated With the Production P. vannamei From a Welfare Perspective*). In fact, the main driver for the introduction of *P. vannamei* to Asia was the perceived differences in its disease susceptibility to white spot syndrome virus (WSSV) compared to *P. monodon* (Funge-Smith and Briggs, 2003). However, incidences of disease in *P. vannamei* have flourished with the development of the industry and major crises have been experienced all over the world (Linda et al., 2005; Kumar et al., 2014). In this context, diseases such as acute hepatopancreatic necrosis disease (AHPND), hepatopancreatic microsporidiosis (HPM), hepatopancreatic haplosporidiosis (HPH), aggregated transformed microvilli (ATM) and covert mortality disease (CMD) have been added to the list of previous known threats to the commercial production of *P. vannamei*, such as white spot disease (WSD), yellow head disease (YHD) and infectious myonecrosis (IMN) (see review Thitamadee et al., 2016). Disease of course plays a significant role in animal welfare. In fact, the word 'dis-ease' refers to a state that lacks 'ease' or well-being. Thus, one of the outcomes of poor welfare is expressed in the form of disease (Butterworth and Weeks, 2009).

1.1 The 'Five Domain Model' as a Framework for Animal Welfare Assessment

While it is clear the importance that disease place within the context of animal welfare, health is only one of the animal welfare pillars within the so-called 'Five Domains Model' (Mellor and Reid, 1994). In this model, good welfare or well-being is described as the state that is manifest in an animal when its (1) nutritional, (2) environmental (physical environment), (3) health, (4) behavioural and (5) mental needs are met. The first four domains focus on the animal's physiological and behavioural needs and encompass pathophysiological disturbances caused by nutritional, environmental and health-related issues. According to Mellor and Beausoleil (2015) once these factors are assessed their anticipated consequences are assigned to the (5) 'mental' domain and it is these affective experiences that determine the animal's welfare state (Mellor et al., 2009). These five domains are essentially equal to the 'five freedoms' formulated by the Farm Animal Welfare Council in a number of countries, including the UK (Mellor and Reid, 1994).

From a more fundamental perspective, the term welfare is intrinsically linked with the absence of suffering, which include anxiety, fear, pain and distress and more recently increasingly linked to the promotion of positive states (Mellor and Beausoleil, 2015). However, these experiences, according to most national and international policy frameworks, only apply to animals that are sentient as non-sentient animals are not capable of feeling.

Therefore, in this review we will evaluate the extent to which the five domains of welfare are being met by current commercial practices in the key penaeid commercial species, *P. vannamei*, and propose future developments that are needed to identify relevant indicators for the evaluation of the welfare of this species when cultured. We will also assess the current evidence for sentience in penaeid and, by extension, other decapod crustacean species, when relevant. We believe these are important considerations *per se* and especially if increased legislative protection on these animals is to be implemented.

2 EVALUATION OF KEY CHALLENGES ASSOCIATED WITH THE PRODUCTION OF *P. VANNAMEI* FROM A WELFARE PERSPECTIVE

2.1 Maturation of Female Broodstock and Current Production Practices: Eyestalk Ablation

In natural environments, *P. vannamei* spawn under specific environmental cues (a combination of optimal water temperature, salinity and dissolved oxygen mainly) stimulating ovary development and spawning by neurosecretory centres (Calderon-Perez et al., 2007). In production systems, parameters such as water temperature, salinity, and dissolved oxygen, nitrogen compounds, photoperiod, light intensity, maturation room and tank characteristics, and diet may be manipulated and adjusted (Browdy, 1998; Whetstone et al., 2002; Jorry, 2012). In general, *P. vannamei* should be held for maturation under specific conditions that include low light (10-30% of natural or artificial light), ideally with a system to control photoperiod (maintained at about 10-12 dark and 12-14 hours light) (Treece and Fox, 1993; FAO, 2003). Noise (particularly loud or intermittent noise), movement and other disturbances should be kept to a minimum level. Maturation tanks should be round (but in Asia square or rectangular tanks are also used), dark-coloured, smooth sided, and of approximately 3-5 m diameter (FAO, 2003). Stocking densities of around 6–15 shrimp m^{-2}, with a male to female ratio of 1:1, 1:1.5 or 1:2 are optimal. Water temperature, salinity, dissolved oxygen, pH, alkalinity and ammonia are usually maintained at the range of 28 – 29 °C, 30 – 35 ppt, ≥4 mg L^{-1}, 8 – 8.2, ≥100 mg L^{-1} $CaCO_3$ and < 1 mg L^{-1} respectively (FAO, 2003). It is also important to make sure that the broodstock have good nutritional status and appropriate size (at least 30 g and >40 g for male and female, respectively), age and origin (i.e., grow-out conditions and genetic background) (Racotta et al., 2003).

The external factors mentioned above are considered to improve success in inducing sufficient egg production to meet commercial schedules, but insufficient to ensure consistent and predictable production scheduling, leading the *P. vannamei* sector to continue reliance on manipulating the endocrine system of penaeids using eyestalk ablation to improve reproductive performance.

Ablation of eyestalks is broadly used in commercial hatcheries as a crude method of hormonal manipulation to induce maturation and spawning in *P. vannamei*. It involves the removal or constriction (through cutting, cauterizing or tying) of one (unilateral) or two (bilateral) eyestalks to reduce the level of gonad inhibiting hormone (GIH/MO-IH) which is produced by the X-organ and sinus gland complex situated in the optic ganglia of the eyestalk (Kang et al., 2014; Wang et al., 2019; Magaña-Gallegos et al., 2021). Eyestalk ablation is important as ovarian maturation of *P. vannamei*, is controlled by GIH hormone and is presumed to inhibit vitellogenesis (Kang et al., 2014). Thus, the eyestalk ablation accelerates ovarian maturation in the female, resulting in spawning (Palacios et al., 1999a). However, from a welfare perspective, both unilateral and bilateral ablations have detrimental effects on females (**Table 1**).

Due to the multiple negative effects associated with ablation (**Table 1**) and concerning the welfare of *P. vannamei* broodstock, predictable maturation and spawning of captive specimens without the use of eyestalk ablation has been considered as a long-term goal for the industry (Quackenbush, 2015). Recent reports have suggested that similar productivity in broodstock can be obtained without eyestalk ablation through the application of husbandry interventions, including pre-maturation conditioning, increased stocking density and/or altered sex ratios (Zacarias et al., 2019). Trials conducted using these practices have demonstrated that rapid maturation and re-maturation of non-ablated *P. vannamei* females can be obtained while maintaining similar production levels of eggs/nauplii compared to ablated females (Zacarias et al., 2019; Zacarias et al., 2021). In addition, genetic background has been

TABLE 1 | Summary of eyestalk ablation effect in Penaeids (includes data from *P. vannamei*, *P. monodon* and *P. stylirostris*).

Eyestalk ablation impact in penaid species	
Reported Effects	**References**
Positive	
Reduce gonad inhibiting hormone	(Treerattrakool et al., 2014; Das et al., 2015)
Induce rapid maturation and spawn	(Chamberlain and Lawrence, 1981; Palacios et al., 1999b)
Negative	
Physiological imbalance	(Palacios et al., 1999b; Das et al., 2015)
Reproductive exhaustion	(Palacios et al., 1999b; Das et al., 2015)
Physical trauma	(Taylor et al., 2004; Bae et al., 2013)
Stress	(Taylor et al., 2004; Bae et al., 2013; Treerattrakool et al., 2014)
Reduction of shrimp hyperglycaemic and moulting inhibiting hormones	(Sainz-Hernández et al., 2008)
High energy demand	(Racotta et al., 2003)
Activation/reduction of immune related genes	(Sainz-Hernández et al., 2008; Bae et al., 2013; Treerattrakool et al., 2014)
Influence on metabolism of macronutrients	(Racotta et al., 2003; Sainz-Hernández et al., 2008)
Alteration of biochemical pathways	(Racotta et al., 2003; Sainz-Hernández et al., 2008)
Weight loss	(Palacios et al., 1999b)
Drop of haemocyanin and glucose in hepatopancreas	(Palacios et al., 1999b)
High broodstock mortality	(Zacarias et al., 2019)
Compromise offspring quality (e.g., decrease robustness to diseases)	(Palacios et al., 1999a; Zacarias et al., 2021)

suggested to play a role in the production without eyestalk ablation. Therefore, ablation of eyestalks may no longer be required, which would represent an important step towards improved animal welfare. As an example, there are a few regular maturation facilities in Central and Latin America (Brazil, Colombia, Ecuador, and México), and Asia (Thailand) that are no longer using eyestalk ablation (Patrick Sorgeloos, 2020. Pers. Comm; Robsons McIntosh, 2020. Pers. Comm.). To support the phase-out of such practice, further studies to quantify the trade-offs from both production and economic perspectives would be very useful for the industry.

2.2 Disease and Stress-Immunity Mechanisms in Farmed Tropical Penaeids

Disease remains the key limiting factor for sustainable food production from crustacean aquaculture and fishing efforts. At the time of writing, 10 out of 11 diseases listed for crustaceans by the World Organisation for Animal Health[1] blight penaeid shrimp aquaculture (listed in **Table 2**). Viral (IHHNV, TSV, WSSV, YHV) pathogens dominated a series of debilitating disease outbreaks across Asia in the 1980s and 1990s, whereas bacterial (*Vibrio parahaemolyticus*) and fungal (*Enterocytozoon hepatopenaei*) pathogens emerged in the 2000s and 2010s (Thitamadee et al., 2016; Shinn et al., 2018; de Souza Valente and Wan, 2021). Substantive financial losses are incurred due to high mortality rates, up to 100% within days-weeks in many cases, and shrimp that survive are usually stunted and deformed, leading to high levels of waste (some features are listed in **Table 2**).

2.2.1 Biological Defences

To prevent, and manage, the spread of disease in decapod aquaculture, extensive efforts have been made to characterise their biological defences (Bachère, 2000; Tassanakajon et al., 2018; Gong and Zhang, 2021). Simply, innate immunity is split across three categories of defence (**Figure 1**): physical barriers (1), cell-directed responses carried out by haemocytes (2), and humoral factors produced by a variety of tissues that recognise, immobilise, and kill pathogens (3). What follows is a synopsis of the major features of decapod innate immunity – the articles cited provide more detail of these topics.

Physical (1). Disease-causing agents need to enter a host for survival, to replicate, and occasionally, complete their lifecycle. The penaeid carapace represents an important biological barrier – cuticle layers formed with chitinous polymers are hardened through the addition of calcium salts (external surface > epicuticle > exocuticle > endocuticle > epidermis > haemocoel > organs). The exoskeleton restricts most pathogens – some fungi and oomycetes are exceptions – to a few sites of entry (Coates et al., 2022); the gastrointestinal, reproductive, and respiratory systems as well as the nephrocomplex (i.e., antennal gland) (De Gryse et al., 2020; Liu et al., 2021). For example, Qi et al. (2017) highlighted the importance of the intestinal barrier in *shrimp*-vibrio antibiosis. The authors interrogated the intestinal transcriptome of *P. vannamei* infected with the causative agent of acute hepatopancreatic necrosis syndrome (AHPNS), namely *V. parahaemolyticus*, to reveal ~2,500 upregulated genes with functions in immunity and cellular restructuring, e.g., pathogen recognition, phenoloxidase activity, antimicrobial peptides.

Cellular (2). Should the physiochemical barriers fail, a heterogenous population of circulating immune cells termed haemocytes (granular, semi-granular and hyaline cells), can intercept the pathogenic intruders, reviewed by Johansson et al. (2000). Crustacean haemocytes perform tissue surveillance and recognise 'non-self' carbohydrate-lipid complexes that coat the surfaces of microbes; β-glucans and mannans for fungi (Vargas-Albores and Yepiz-Plascencia, 2000; Yepiz-Plascencia et al., 2000), lipopolysaccharides (endotoxins) and lipoteichoic acids for Gram-negative and Gram-positive bacteria (Phupet et al., 2018), respectively. Depending on the size of the pathogen (micro vs macro), the numbers of intruders present and the target tissue, haemocytes respond in several well-defined ways (**Figure 1**).

- Phagocytosis – direct ingestion of the microbial target into the cytoplasm and subsequent destruction *via* lysis facilitated mostly by enzymes, reviewed by Liu et al. (2020).
- Degranulation – the release (extra-cellularisation) of cytoplasm-derived granules containing a concoction of anti-infective factors, including antimicrobial peptides, adhesives, and the components of the phenoloxidase cascade (Smith and Söderhäll, 1983). Degranulation precedes nodule/capsule formation.
- Nodule formation – cellular aggregates consisting of numerous microbes (usually bacteria or yeast-like cells), host haemocytes, and melanotic debris. Such nodules are usually sequestered to specific tissues like the hepatopancreas and gills (Smith and Ratcliffe, 1980; Davies et al., 2020).
- Encapsulation – the 'walling off' or 'ensheathment' of microbes, microeukaryotes, parasitoids (too large to phagocytose), and damaged host tissue in recurrent layers of haemocytes. After multiple layers of haemocytes are in place, melanin is used to coat the capsule (van de Braak et al., 2002; Costa et al., 2009).
- Extracellular trap release (ETosis) – discharge of decondensed chromatin embedded with proteinaceous factors. Microbes are caught in the 'chromatin net' and are vulnerable to multiple biocidal agents, including histone-derived peptides and peroxidase (by)products (Ng et al., 2013; Robb et al., 2014).

Humoral (3). There is much coordination and crosstalk between the so called cellular and humoral immune reactions in decapods – wound repair, clot formation (haemostasis) and pro-phenoloxidase activation being key examples (Fontaine and Lightner, 1973; Söderhäll and Smith, 1983; Maningas et al., 2013). A myriad of enzymatic and non-enzymatic factors, including agglutinins, lysins, cytokine-like molecules and antimicrobial peptides (e.g., crustins; Bartlett et al., 2002), are found in the haemolymph of decapods. Many are derived from

[1]World Organisation for Animal Health (OiE) 2022. Aquatics, Crustaceans. Available at: https://www.oie.int/en/what-we-do/animal-health-and-welfare/animal-diseases/?_tax_animal=aquatics%2Ccrustaceans

TABLE 2 | Marked infectious diseases and syndromes of cultured penaeid shrimp.

Disease	Causative agent	OiE listed*	Gross features (and notes)	Reference (not exhaustive)
Abdominal segment deformity disease	Retrovirus-like element (abdominal segment deformity element or ASDE). NLRS, non-long terminal repeat retrotransposons.	-	Twisted and enlarged abdominal segments, with some observations of opaque muscle (necrosis and degeneration).	(Sakaew et al., 2008; Sakaew et al., 2013)
Acute hepatopancreatic necrosis disease [Early mortality syndrome]	*Vibrio parahaemolyticus* isolates	**YES**	The midgut, hepatopancreas and stomach of shrimp visible externally turned brown in infected shrimp. Sloughing of epithelial cells in the tubules of the hepatopancreas. Extensive haemocyte infiltration of tissue, and secondary bacterial septicaemia prior to *in exitus*.	(Lightner et al., 2012; Tran et al., 2013; Kumar et al., 2020)
Aggregated transformed microvilli [White faeces syndrome]	Prokaryotic and microsporidian pathobiome. *Enterocytozoon hepatopenaei* are found in the white faeces of some affected shrimp.	-	Vermiform structures appear in hepatopancreatic tubules and midguts. Extensive sloughing and aggregation of microvilli coincide with the production of white faecal strings.	(Sriurairatana et al., 2014; Tang et al., 2016; Prachumwat et al., 2021)
Covert mortality disease	Covert mortality nodavirus	-	So named due to shrimp dying at the bottom of ponds. Nuclear enlargement in the hepatopancreas, muscle whitening and necrosis	(Zhang et al., 2014; Zhang et al., 2017)
Hepatopancreatic microsporidiosis	*Enterocytozoon hepatopenaei (Agmasoma penaei*)	**YES**	Substantial growth retardation in *P. vannamei* due to disrupted gut epithelium and nutrient absorption. Intracytoplasmic - connective tissue (*A. penaei*) and tubules (*E. hepatopenaei*) of the hepatopancreas.	(Tourtip et al., 2009; Chaijarasphong et al., 2021; Geetha et al. (2022)
Hepatopancreatic haplosporidiosis	*Haplosporidium* sp.	-	Melanisation of the cuticle, hepatopancreas shrinkage (pale and atrophied), reduced growth, and flaccid bodies. Histology revealed tubule epithelia cells contained cytoplasmic multinucleate plasmodia and trophonts.	(Utari et al., 2012; Thitamadee et al., 2016)
Infectious hypodermal and haematopoietic necrosis	Infectious hypodermal and haematopoietic necrosis virus	**YES**	Interferes with developmental stages from eggs to post-larval. The virus infects epidermal and mesodermal tissues. Cuticular deformity, notably a bent rostrum (not always)	(Lightner et al., 1983)
Infectious myonecrosis	Infectious myonecrosis virus	**YES**	Focal to extensive muscle whitening along the abdomen and tail regions. In some shrimp, regions become necrotic and. reddened Lymphoid organs tend to. Be atrophied and enlarged. Rapid onset has been linked to feeding prior to exposure to stress.	Lightner et al., 2004; Poulos et al., 2006; Prasad et al., 2017)
Male reproductive tract degenerative syndrome	Auto-immunity? [some links to temperature, diet, and microbes]	-	Deformed and melanised sperm held in the spermatophores alongside the accumulation of amorphous debris. Dark discolouration is visible externally upon inspection of the shrimp ventrum.	(Talbot et al., 1989; Diamond et al., 2008)
Necrotising hepatopancreatitis	*Hepatobacter penaei*	**YES**	Shell softening, flaccid limbs, discoloured (black) gills, and white, atrophied hepatopancreas. Some shrimp showed reductions in feeding and changes in behaviour.	(Frelier et al., 1993; Nunan et al., 2013)
Taura syndrome	Taura syndrome virus	**YES**	Acute: anorexia, lethargy and erratic swimming. Opaque tail muscle, soft cuticle, and sometimes, reddening of the tail. Transition: melanotic lesions of the cephalothorax and tail cuticle. Chronic: lymphoid organ spheroids (sometimes they appear ectopically).	(Hasson et al., 1995; Bonami et al., 1997; Tumburu et al., 2012)
White head disease	Decapod iridescent virus [1] (Haemocyte iridescent virus)	**YES**	Can target haemocytes, haematopoietic and lymphoid tissues. Whitening of the carapace at the base of the rostrum. Red body discolouration. Atrophy of the hepatopancreas.	(Liao et al., 2020; Qiu et al., 2020)
White spot disease	White spot syndrome virus	**YES**	Shrimp are usually lethargic with reduced levels of feeding and preening, and sometimes, a loose cuticle. Characteristic white, calcified spots can be visible on the dorsum of the carapace. Some have discoloured hepatopancreatic tissue.	(van Hulten et al., 2001; Verbruggen, 2016)

(Continued)

TABLE 2 | Continued

Disease	Causative agent	OiE listed*	Gross features (and notes)	Reference (not exhaustive)
White tail disease	*Macrobrachium rosenbergii* nodavirus Extra small virus	**YES**	Detected in *P. vannamei*, *P. indicus*, and *P. monodon*. Opaqueness and milky/white appearance of the abdomen in larval to juvenile shrimp. Reduced feeding and swimming behaviour is often associated with uropod and telson degeneration.	(Bonami et al., 2005; Ravi et al., 2009; Senapin et al., 2012; Senapin et al., 2013)
Yellow head disease	Yellow head (nido)virus (complex) Gill associated virus	**YES**	Distinct yellowing/bleaching of the cephalothorax/carapace, and enhanced feeding. Abnormally yellow (and soft) hepatopancreas. The virus targets multiple tissues including the gut, antennal gland, nervous tissue, and gonads.	(Wijegoonawardane et al., 2008; Mohr et al., 2015);

**World Organisation for Animal Health (OiE 2022; https://www.oie.int/en/what-we-do/animal-health-and-welfare/animal-diseases/?_tax_animal=aquatics%2Ccrustaceans)*

the haemocytes (e.g., clotting pathway components), while others are released constitutively by diverse tissue types including the hepatopancreas, with the remainder being acute phase (Smith and Chisholm, 1992; Suleiman et al., 2017; Tassanakajon et al., 2018). Arguably, the most identifiable response is the generation of the black/brown pigment melanin from phenoloxidase activities. Melanin itself is microbiostatic and virustatic, whereas the by-products generated from its biogenesis (e.g., oxygenic radicals), are highly toxic (Cerenius et al., 2010; Coates and Talbot, 2018). Multiple enzymes – laccase, tyrosinase, catecholoxidase and haemocyanin – are capable of catalysing simple phenols into quinones, which go on to form melanin (Coates and Costa-Paiva, 2020). These enzymes are usually referred to collectively as phenoloxidases and display multiple immune properties (Cerenius and Söderhäll, 2021).

2.3 Environmental and Biological Conditions During Grow-Out: Health-Stress-Disease Axis in Ponds

The health of farmed fish is inextricably linked to their welfare (Segner et al., 2012), and unsurprisingly, this is also the case for decapod crustaceans such as penaeid shrimps, as illustrated by the Disease triangle in **Figure 2**. There remains a deficit with respect to welfare indicators or standardised reference intervals for monitoring penaeids in captivity, partly because it is

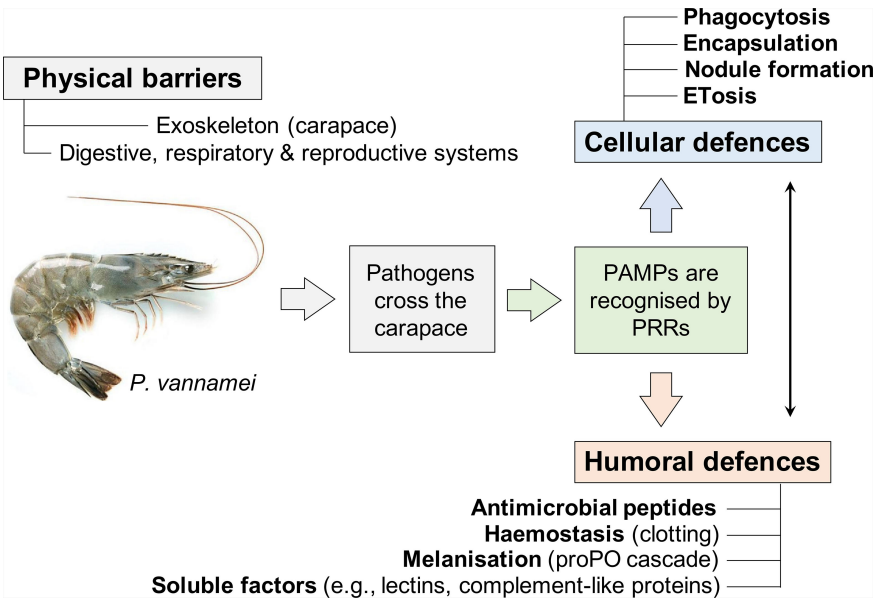

FIGURE 1 | Innate immune defences of penaeid shrimp to infectious disease. Should the disease-causing agents circumvent the physico-chemical barriers, their ligands (pathogen associated molecular patterns, PAMPs) are intercepted by pathogen recognition receptors (PRRs) freely dissolved in the haemolymph or located at the surface of haemocyte plasma membranes. Such recognition triggers a multitude of immune-related cascades including the ingestion of pathogens (phagocytosis), the ensheathment of pathogens – nodules for numerous microparasites, and capsules for larger parasites – and the release of chromatin extracellular traps (ETosis). Bacteria, fungi, and viruses are targeted directly by a series of microbiostatic and microbicidal factors (e.g., lysozyme, lectins) and indirectly by toxic by-products and intermediates of melanogenesis (via the activation of the proPhenoloxidase (proPO) cascade). There is much crosstalk between the cellular and humoral defences (indicated by the black arrow), such as, haemolymph gelation/clotting.

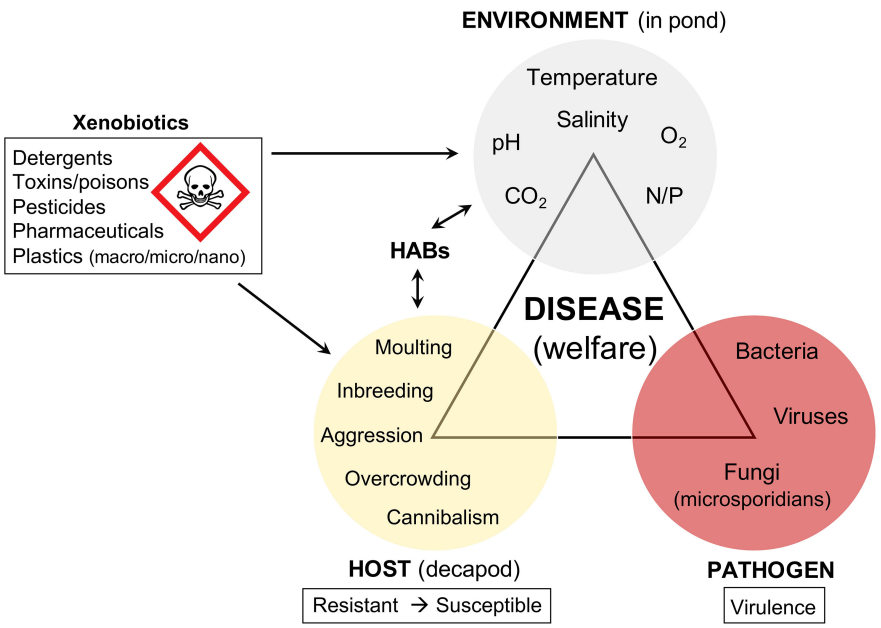

FIGURE 2 | Disease triangle in the context of penaeid welfare (in pond). Growth and maintenance of shrimp under culture conditions poses several challenges for shrimp health and welfare. Susceptible hosts, combined with virulent pathogens and unfavourable environmental conditions encourage disease outbreaks. The presence of immune-modulating xenobiotics, fluctuating abiotic factors leading to hypoxia, hypercapnia, or acidosis can tip the balance in favour of the pathogen(s). HABs, harmful algal blooms; N, nitrogen; P, phosphate.

challenging to define what constitutes a healthy shrimp (Coates and Söderhäll, 2021). Recent efforts have looked to the gut microbiome as a means of measuring 'healthy' penaeids, including immune vigour (Li et al., 2018; Holt et al., 2021). Unsurprisingly, the resident microbes of penaeid tissues are linked to disease and health outcomes – the composition, diversity, and balance between pathobionts and symbionts.

Acute, subacute, prolonged, and chronic perturbations in pond abiotic factors – temperature (Cheng et al., 2005; Rahman et al., 2006), pH (Gunalan et al., 2010), salinity (Li et al., 2008), nitrites (Tseng and Chen, 2004), and hypoxia/hypercapnia (Burgents et al., 2005) – influence decapod susceptibility to disease. Acute stress can stimulate the immune system and tends to have transient impacts on the host, sometimes promoting stress tolerance to subsequent exposure. Prolonged stress, from one or more source (chemical versus physical) can lead to shifts in metabolism, immune dysfunction, and health declines. Imbalances of dissolved oxygen and carbon dioxide in the water (hypoxia, and hypercapnia, respectively) can lead to tissue dysoxia and lactate accumulation – the switch to suboptimal glycolytic metabolism over oxidative phosphorylation. Temperature, pH and dissolved gas content are inextricably linked. As penaeids are ectotherms, temperature extremes outside of their tolerance range can have profound effects on general physiology. Indirectly, higher water temperatures retain less O_2 and increased pCO_2 in the water leads to acidosis. CO_2 can also bind with H_2O in the haemolymph to form H_2CO_3 (carbonic acid) (reviewed by Coates and Söderhäll, 2021; Millard et al., 2021).

From a biological perspective, one of the key questions for both welfare and production is the effects of stocking density. For this reason, there are numerous studies that have assessed the effects of stocking density on *P. vannamei* at different life stages (Froes et al., 2013; Wasielesky et al., 2013; Esparza-Leal et al., 2015) and under different production systems (Cuvin-Aralar et al., 2009; Wasielesky et al., 2013; Durairaj et al., 2018). While most of these studies have concentrated on the impacts from a production perspective there are some studies available on the effects of stocking density on the behaviour of *P. vannamei* (da Costa et al., 2016; Bardera et al., 2021). Results from (da Costa et al., 2016) showed that under aquaria conditions stocking density affects the behaviour of *P. vannamei* juveniles and that there is an optimum animal density that promotes behaviours such as 'searching' and 'feeding'. Dominance hierarchies have been reported and results revealed that at least at the juvenile stage, higher densities (around 25 juveniles m^{-2} compared to 6 and 12 juveniles m^{-2}) maximise feeding behaviour while minimising the effects of dominance. However, the translation of such observations to real productions systems is challenging and therefore studies on real production systems are mainly based on production outputs. In this sense, the effect of stocking density in relation to temperature has been modelled and data indicate the importance of tailoring stocking density based on the production system and temperature as even minor

differences in temperature can produce significant differences in growth and therein profits (Villanueva et al., 2013; Araneda et al., 2020).

In summary, it is difficult to recommend unique values for the main biological factors as they are extremely dependent on the life stage, the actual production system (sometimes associated with different regions) and the environmental conditions the animals experience. However, standardised farming management practices (including animal handling), stable pond/tank conditions (e.g. water quality parameters remaining in ideal range, enough space for shrimp to grow, presence of natural diet and beneficial microbial communities), and routine health checks are necessary to avoid stress, fatalities and financial loss.

3 WELFARE INDICATORS IN DECAPOD CRUSTACEANS

3.1 Current State on Physiological Biomarkers

In decapod crustaceans, as in vertebrates, disturbances in the nutritional, environmental and health welfare domains can lead to allostatic overload (Freire et al., 2020). Allostasis, defined as the adaptive process for actively maintaining stability through change (Sterling and Eyer, 1988) is relevant when trying to establish reference physiological intervals. In this sense, physiological responses that can be measured and that are associated with homeostasis and allostasis could be relevant as direct welfare indicators. The concept of using physiological measures as welfare indicators is particularly relevant for aquatic species where assessing behaviour, pain and suffering is not easy or not possible due to lack of knowledge (Jerez-Cepa and Ruiz-Jarabo, 2021). For these species, the physiological framework is based on the fact that a number of physiological parameters will move outside their allostatic range (overload). These changes must be associated with the different types and degree of stress that the animals experience. Decapod species, like any other organism, respond to stressors by mounting a stress response that involves behavioural and physiological changes at multiple biological levels. The concept of finding suitable biomarkers that can be applied in the context of decapod welfare has been mentioned in few studies (Rosas et al., 2004; Ciaramella et al., 2014; D'Agaro et al., 2014; Wang et al., 2014; Albalat et al., 2019). However, there is little evidence that a concerted effort has been made to establish haematologic biomarkers or reference intervals for decapods, more specifically *Penaeus* spp., in captivity or under cultivation. Tu et al. (2010) trialled some measures – e.g., activities of glutathione-S-transferase, peroxidase and catalase – in *P. monodon* production sites along the Mekong River Delta (Vietnam) and could discriminate between animals reared in intensive systems versus those reared in integrated systems. Producing a suite of biomarkers for decapods is not straightforward as routine measures like cell (haemocyte) counts, protein levels or haemolymph enzyme activity (e.g., lysozyme, phenoloxidase) can fluctuate according to season (Hauton et al., 1997) moult cycle (inter-moult, pre-moult, post-moult; Liu et al., 2004) or even lunar phases (Bautista-Covarrubias et al., 2020).

Rodríguez and Le Moullac (2000) reviewed health control measures of penaeid shrimp and cited 120 mg [protein] mL^{-1} [haemolymph] for laboratory reared *P. vannamei* juveniles. Perhaps some inspiration can be taken from a marine invertebrate often misidentified as a decapod, the Atlantic horseshoe crab *Limulus polyphemus*. Horseshoe crabs are highly valued due to the sensitive endotoxin detection kit (Limulus Amebocyte Lysate) derived from the cellular fraction of their blood (haemolymph), which replaces the rabbit pyrogen test in pharmaceutical and vaccine development (Krisfalusi-Gannon et al., 2018). Because of this commercial sensitivity, reference intervals have been proposed for captive *L. polyphemus ex situ* (Smith et al., 2002) and free-ranging crabs *in situ* (Arnold et al., 2021). As horseshoe crabs suffer from a protein deficiency syndrome in captivity (Smith and Berkson, 2005), an acceptable range is considered ~34 to 112 mg [protein] mL^{-1} [haemolymph] – with most of the soluble protein made up of haemocyanin (>90%; Coates et al., 2012). Haemocyanin comprises >60% of haemolymph protein in most decapods studied to date (e.g., *Nephrops norvegicus*, Coates and Nairn, 2013). Among the numerous cellular and biochemical indicators proposed across the literature, total protein levels and haemocyte counts represent the most likely candidates, in addition to lactate levels, as 'welfare' or 'health' indicators for decapods. These procedures are invasive, but not lethal, in the right hands. Some such measures have been used in an attempt to disentangle 'captivity-associated stress' in crabs (e.g., *Cancer pagurus*; Johnson et al., 2016) and lobsters (e.g., *Homarus gammarus*, Basti et al., 2010; Albalat et al., 2019). Haemolymph biochemical parameter assessment has been trialled with autoanalyzers (haemocytes) and handheld refractometers, e.g., crayfish (*Astacus leptodactylus*) and lobsters (*H. americanus*) (Sepici-Dinçel et al., 2013; Wang and McGaw, 2014).

A condition/welfare index based on both physical appearance and behaviour (e.g. 'vigour') as developed by Albalat et al. (2017) for trawl-caught langoustines *N. norvegicus*, combined with one or more haemolymph measures, would represent a major step forward.

3.2 Operational Welfare Indicators (OWIs): Individual and Group Based, Direct and Indirect and Invasive vs. Non-Invasive

If farmers want to detect welfare problems during the farming of crustaceans, they must have good feasible operational welfare indicators (OWIs) that can be measured quantitatively by staff based at the farms. OWIs must be species- and life stage-specific, minimally invasive, fit for purpose (for production systems and operations) and robust. In **Table 3**, we suggest a list of positive and negative survival and situation-related factors to be observed based on the 5 domains framework suggested by Mellor and Reid (1994) and based on animal (outcomes) and resource (inputs) measures applicable to the crustaceans welfare.

TABLE 3 | List of negative and positive survival and situation related factors to be observed in order to generate the best Operational Welfare Indicators (OWIs) for the species based on the 5 domains framework (adapted from Mellor and Reid, 1994 to crustaceans).

PHYSICAL/FUNCTIONAL DOMAINS							
Survival related factors						**Situation-related factors**	
1. Nutrition		**2. Environment**		**3. Health**		**4. Behaviour**	
Negative	Positive	Negative	Positive	Negative	Positive	Negative	Positive
Restricted food	Enough Food	Uncomfortable environment	Environmental requirements at optimal level	Disease, injury or functional impairment	Healthy, fit and no injury	Behavioural expression restricted	Able to express natural behaviours
Bad quality food	Balanced and varied diet	Environmental requirements at suboptimal levels	Physical features are adequate	Stress			
Diet requirements not met		No physical enrichment					
AFECTIVE EXPERIENCE DOMAINS							
5. Mental states							
Negative Experiences				Positive Experiences			
Overcrowding, Hunger, Malnutrition, Temperature out of ranges, Noise (hearing discomfort)				Homeostasis, good diet, Satiety, Physical comfort, Vigour, Good Health/fitness, Reward, Calmness,			
Repetitive stressors, Injury, Pain, Disease, Fear, Boredom, Anxiety, Panic, Exhaustion				Sociability, Natural Behaviours, Enriched environment			
WELFARE							

Each of the risk factors and stressors during the life cycle of the farmed crustaceans can be assessed by a welfare indicator closely related to the original stressor. For example, acute or unexpected changes in water temperature (the stressor) can lead to changes of the appetite level in the farmed crustaceans. Monitoring and evaluation of the feeding responses is a common OWI potentially related to an environmental stressor (Martins et al., 2012). Real time monitoring of the animals and the environmental parameters is key for the identification of environmental-related welfare issues.

In order to be able to measure the different welfare domains, we present in **Table 4** a list of potential direct (animal) and indirect (environment-based) welfare indicators for *P. vannamei*, that could also be used for other decapod crustaceans as appropriate. Direct individual based OWIs include both physical health and physiological parameters as well as behavioural measures. On the other hand, indirect or resource-based measures include environmental parameters related to water quality, husbandry procedures, type of food and other measures such as predator presence or enclosure design and substrate access (e.g. environmental enrichment such as the background colour of tanks, use of hides and substrates or different feeding methods).

OWIs must be used at different levels depending on the intensity of the intervention needed (Noble et al., 2018). OWIs at the *primary* level of assessment include environmental parameters, visual observations (behaviour and appearance) and sudden changes in relation to them. When this is not sufficient to evaluate the welfare status of the animals then it is necessary to move to a *secondary* level of assessment and use the more invasive handling and laboratory-based OWIs (indicated in orange in **Table 4**) that require physical manipulation of the animals (vigour index or close visual assessment of the damage or disease). If the welfare problem is not solved then the next stage would be the *tertiary* level of assessment where handling and sampling of blood and tissues is required (anaesthetics are recommended for this sampling procedure) with more detailed analysis need to be performed: PCR for disease diagnosis, histopathology, haemolymph sampling for stress parameters or other techniques might be required: behavioural assessment under controlled conditions, etc.

3.3 Other Emerging Operational Welfare Indicators

Biosensors, loggers and early warning systems are: cheap, user-friendly, non-invasive methods for early detection of critical alterations in the farming conditions. They can be automatic systems for behavioral observations or water quality sensors (Barreto et al., 2022). With the use of Artificial Intelligence (AI) and machine learning methods the monitoring of environmental parameters and behaviour can be done automatically, and the decision-making process becomes more accurate (O'Donncha et al., 2021) and autonomous. These methods of precision farming (PF) are being developed for finfish and molluscs with proven success. In shrimp farming, there are examples of monitoring systems to automatically

TABLE 4 | List of potential OWIs to be measured for welfare assessment and their use as a decision support method. Invasive OWIs are highlighted using an asterisk (*).

Operational Welfare Indicators (OWI)	**Group**
Direct animal Based (outcome)	
Individual	
Vigour index (condition factor)*	Stocking density
Behaviour (startle response, feeding response, lethargy, thigmotaxis, activity, swimming)	Behaviour (feeding response, aggression, aggregation, panic response, group activity, swimming and dynamics, dominance)
Haemolymph (protein, stress parameters: glucose, lactate; immune measures: haemocyte counts, lysozyme and phenoloxidase)*	Growth (SGR, FCR)*
Life stage (juvenile, moulting, adult)	Disease and disease control*
Eye damage (eyestalk ablation or others)	
Antennae damage	
External coloration	
Melanosis	
White calcifications	
Milky abdomen	
Uropod/Telson degeneration	
Microbiome (gut)*	
Pathogen screening*	
Indirect environment based (input)	
Water Quality	**Rearing Systems**
Temperature	Water current
Salinity	Light and photoperiod
Oxygen	Noise
Carbon Dioxide	Stocking Density
pH	Tank shape and background colour, furniture, RAS systems
Ammonia/Nitrogen	Predator presence
Nitrite/Nitrate	Environmental Enrichment (positive welfare)
Pollution (heavy metals, organic matter, antibiotics)	
Total Suspended Solids	
Microbiome (water and substrate)	
Pathogens	

record changes in physicochemical water parameters that are processed using AI (Borquez-Lopez et al., 2016). However, AI models could, for example, identify some of the animal-based OWIs in *P. vannamei*, such as body melanosis, antenna and eye damage, and could also monitor their behaviour and assess possible risk factors, based on individual and group behaviour, interaction with environment and social behaviour (aggression, aggregation, feeding responses, etc) (Huang et al., 2019).

Use of rapid on-site testing for disease diagnostics is another emerging health and welfare tool. In general, in aquaculture systems, animal mortality results from complex interactions between genetic background, environmental conditions, stress and opportunistic pathogens, making most laboratory approaches sub-optimal. The on-site testing makes it possible to obtain physiological and behavioural responses to the real environmental conditions and to assess their welfare in relation to those responses (Barreto et al., 2022). Some of those on-site diagnostics are cheap and affordable paper-based diagnostics, widely used for human health (Hu et al., 2014) and recently translated into fish farming[2]. Other advances in welfare indicators are the development of smartphone based diagnostic technologies (Rateni et al., 2017) as well as smartphone applications for visual based diagnostics and the use of cloud metadata[3].

The importance of promoting positive welfare and the need to offer more natural environments for the cultured animals has increased in recent years. The use of environmental enrichment (EE) to increase the complexity on the environment e.g., hiding sites, tanks of various colours and shapes, flows and natural light regimes, life feeding or feeding methods that mimic their natural behaviours, are crucial to promote social interaction, to avoid maladaptive behaviours and to reduce stress related to captive conditions (Arechavala-Lopez et al., 2021). In decapod crustaceans, as observed in fish and other farmed vertebrates, the use of EE could be used to improve their welfare status. EE could be developed on temperature gradients (behavioural prophylaxis) based on thermal preferences and related to their internal emotional states (Rey et al., 2015). Other structural EE are already used for *P. vannamei* such as a dark background colour of the tanks or the rounded shape has been mentioned before.

3.4 Existing Aquaculture Standards Applied to the Farming Practices of *P. vannamei*: Gaps in Welfare Indicators

For the farming of decapod crustaceans and specifically for penaeid shrimp farming the key factors that need to be identified and if necessary revised include feed quality and

[2] https://www.globalseafood.org/advocate/investment-firm-paper-based-disease-test-kits/

[3] https://www.innovationnewsnetwork.com/ensuring-fish-welfare-in-aquaculture-with-new-digital-app/12855/

delivery methods, water quality and flow, stocking density, transport methods and the number of transport events during shrimps' life cycle. The main management practices and interventions to be considered include alternatives to eyestalk ablation for broodstock, grading of juveniles and disease treatments up to point of slaughter. In this way, a good welfare assessment can be achieved for each of the potential stressors, leading to improved husbandry practices.

Most commercial shrimp aquaculture standards use different welfare indicators related to the environment and the health of the animals (input and outcome measures). Few use the 5th domain on the mental status of the animals that should be the main factor to determine the outcome of the welfare status of the animals (**Table 3**).

The Aquaculture Stewardship Council (ASC) Shrimp Standard[4], for example, places a lot of emphasis on the effect of shrimp farming on biodiversity and impacts on the environment, as well as the use of wild fish as an ingredient for feed. Farms are required to measure water quality parameters, as well as, monitor diseases and report during auditing. The use of antibiotics is restricted, and they should be monitored in the water systems. Social aspects of the farming practices are also included. However, no direct animal-based welfare measures and targets are included besides from the routine health checks. No morphological, physiological or behavioural OWIs are required.

Other standards such as the Asian Seafood Improvement Collaborative[5] (ASIC) shrimp standard or the Best Aquaculture Practice[6] (BAP) standards for finfish and crustacean farms are based on best management practices with very general considerations regarding the use of OWIs (stocking densities, feeding, fasting, crowding, and dewatering, water quality, behaviour and condition and testing for disease outbreaks). Humane slaughter techniques are mentioned but with no specifics given. The main issues addressed are environmental, social and those concerning food safety (drug and chemical management, microbial sanitation, hygiene, harvest and transport, biosecurity and traceability). ASIC requirements for shrimp health status are limited to compliance to existing national standards and the stocking densities need to be recorded to monitor and estimate the number of escapes. Mortalities need to be recorded, as well as, the main environmental parameters (temperature, DO, salinity and ammonia). BAP contains a short section on shrimp-specific standards related also to environmental and effluent management (water exchange), as well as, to food safety during harvest and transport (e.g. the use of sulphite solutions as antimelanotic at harvest). It also specifies a maximum biomass limit based on performance measures for health and survival. BAP requires training for staff to provide appropriate levels of husbandry and awareness of these standards.

In Asia, there are also local government standards that address some health and welfare issues, and also focus on animal welfare indicators[7]. These standards contain specific information on best practices and the recommended range of stocking densities for the different culture systems. However, the recommendations on animal welfare are still very general, with no specific animal-based OWIs required.

Therefore, most common shrimp standards are still using very few animal-based OWIs and recommendations are very general, with no guidance on ranges of tolerance or rates for the most common parameters provided. For example, standards should provide guidance on the rates of survival or mortality rates per life stages of shrimp production. Feeding should be focused on nutritional requirements and best feeding practices. Maximum fasting times should be provided, in addition to guidance on crowding prevention techniques and disease prevention and monitoring of relevant parameters. Regulation on humane stunning and slaughter methods and the use of drugs and chemicals, as well as handling standards should be provided. Most of those parameters have been studied and there is sufficient knowledge in the scientific literature to be used in farming protocols and standards. Our review is an example of the amount of knowledge that exists on shrimp farming and mitigation methods.

4 STUNNING AND SLAUGHTER PRACTICES IN RELATION TO SENTIENCE

4.1 Current Scientific Evidence for Sentience in Decapod Crustaceans

Sentience can be defined as having the capacity to feel (Kirkwood, 2006) or following Darwin's definition 'a sentient animal is one for whom feelings matter' (Darwin, 1872). Within the context of this review, we will more specifically align with the Animal Welfare Committee in the UK which has defined sentience as the capacity to experience pain, distress or harm, although as pointed out by other authors this definition lacks the consideration of animals being able to experience positive feelings (Mellor and Beausoleil, 2015; Birch et al., 2021). In any case, the capacity for a living organism to be capable to have feelings such as pain requires a level of awareness and cognitive ability (Broom, 2019). So far, arguments in support of the view that decapod crustaceans have the capacity to feel pain have been made by some authors (Conte et al., 2021; Passantino et al., 2021) while others support the view that the evidence is currently insufficient (Diggles, 2019).

Frameworks to provide scientific evidence of pain in vertebrate species have been proposed and generally agreed for several years (Bateson, 1991). The translation of such frameworks seeking to establish if invertebrates experience pain has been presented by a number of authors (Smith, 1991; Smith and Boyd, 1991; Birch et al., 2021) (**Table 5**).

Upon examining research performed in *P. vannamei*, current evidence of sentience in decapod crustaceans is mainly

[4] https://www.asc-aqua.org/wp-content/uploads/2019/03/ASC-Shrimp-Standard_v1.1_Final.pdf

[5] ASIC: http://www.asicollaborative.org/

[6] BAP: https://bapcertification.org/blog/category/shrimp/

[7] https://asean.org/wp-content/uploads/images/archive/AMAF%2033%20Standard%20on%20ASEAN%20Shrimp%20GAP.pdf

TABLE 5 | Examples of frameworks used to evaluate scientific evidence of sentience in animals.

Criteria emphasis	Description of criteria	
	Smith and Boyd, 1991	**Birch et al., 2021**
Neurological	Possession of receptors sensitive to noxious stimuli, located in functionally useful positions on or in the body, and connected by nervous pathways to the lower parts of a central nervous system	Possession of nociceptors
	Possession of brain centres which are higher in the sense of level of integration of brain processing (especially a structure analogous to the human cerebral cortex)	Possession of integrative brain regions
	Possession of nervous pathways connecting the nociceptive system to the higher brain centres	Connections between nociceptors and integrative brain regions
	Receptors for opioid substances found in the central nervous system, especially the brain.	
Cognitive/ Behaviour	An animal's response to stimuli that would be painful for a human is functionally similar to the human response	Motivational trade-offs that show a balancing of threat against opportunity for reward
	An animal's behavioural response persists, and it shows an unwillingness to resubmit to a painful procedure; the animal can learn to associate apparently non-painful with apparently painful events	Flexible self-protective behaviours in response to injury and threat
		Associative learning that goes beyond habituation and sensitisation
Mixed	Analgesics modify an animal's response to stimuli that would be painful for a human	Responses affected by potential local anaesthetics or analgesics
		Behaviour that shows the animal values local anaesthetics or analgesics when injured

concentrated in what it is known for the largest decapods (crabs, lobsters and crayfish), which do not include penaid species. From a 'neurological perspective', three neutropil areas (terminal medullae, hemiellipsoid bodies and the accessory lobes) are candidates for higher integrative centers (Sandeman and Harzsch, 2016). The terminal medullae and the hemiellipsoid bodies are part of the lateral protocerebrum. Recent research on decapod crustacean brains (supraesophageal ganglia) (Strausfeld et al., 2020) indicate the presence of protocerebral centers in *P. vannamei*. Immunohistochemistry results showed the presence of a substantial lateral protocerebral and optic neuropils and a much reduced anti-DC0-immunereactive centre, the location of which corresponds to the ancestral mushroom body of Stomatopoda and Caridea. This area, therefore, comprises an integrative centre that is associated with the hemiellipsoid body (homologous to insect mushrooms bodies) linked to learning and memory.

From a 'cognitive and behavioural perspective', the little research on *P. vannamei* published to date has mainly focused on feeding behaviour, production practices such as stocking densities and mating behaviour (Yano et al., 1988; Bardera et al., 2020; Bardera et al., 2021). A review by Bardera et al. (2019) highlighted the importance of studying behaviour for the farming/production of *P. vannamei*, but studies on motivational trade-offs, flexible self-protective behaviours in response to injury, threat and associative learning that goes beyond habituation and sensitisation are currently missing. In this regard, recent studies performed in understanding agonistic behaviours in the cultured swimming crab (*Portunus trituberculatus*) (e.g. Su et al., 2021; Wu et al., 2021) and the interaction between animal behaviour and production practices (e.g. Zhang et al., 2021) highlight the importance to factor behavioural aspects in production systems for decapod species.

Finally, from a 'mixed perspective', Taylor et al. (2004) examined the role of a topical anaesthetic (lidocaine) and a coagulation agent in minimising the stress response due to eyestalk ablation in *P. vannamei*. Their results indicate that the application of an anaesthetic significantly improves the elapsed time of feeding onset and their swimming behaviour. On the other hand, the effects of anaesthetics (clove oil/eugenol) have also been examined in a number of decapods, including *P. vannamei* (Parodi et al., 2012; Wycoff et al., 2018; Becker et al., 2021). Results from Wycoff et al. (2018) show that *P. vannamei* was very susceptible to stress and therefore measurements of heart rate, motor nerve activity and sensory rate activity were inconclusive or not possible to perform. However, the study showed that the animals were lethargic within 2 min, and they were inactive to tail pinches within 6 to 12 min when bathed at a eugenol concentration of 200 ppm.

As the number of studies is certainly limited, especially from a cognitive and behavioural perspective it is clear that more fundamental research in this area is needed. However, following the 'precautionary principle' the basic requirement to define current production practices from an animal welfare perspective is relevant. In the case of *P. vannamei*, the demand for increased welfare could potentially be driven not only by stakeholders and certification schemes but also by consumers based in key importing countries, since a very significant proportion of these animals are traded internationally. Therefore, in the next section we evaluate key challenges associated with the stunning and slaughter of *P. vannamei* from an animal welfare perspective.

4.2 Stunning and Slaughter Practices in *P. vannamei*

Partly due to the current lack of welfare protection for decapod crustaceans (see *Current Legislation Relevant to Decapod Crustaceans*); harvesting, stunning and slaughter practices for this group in general, and *P. vannamei* in particular, are not

regulated, or even standardised. Before entering into further detail, it might be relevant to indicate that within the context of this review we have used the terminology of Conte et al. (2021) whereby 'stunning' refers to rendering the animals insensible, and that this process can be reversible or irreversible (in the latter case it should be considered as 'slaughter'). Methods for stunning and slaughter used in decapod crustaceans are varied and include cold shock in air, ice or slurry ice, boiling, freshwater or salt baths, carbon dioxide narcosis, high pressure, mechanical splitting or spiking of the nervous system, dismemberment and electrical stunning as reviewed by Conte et al. (2021). The variety of techniques used not only reflects the absence of legislation but also the fact that decapod species are very diverse in their anatomy and physiology. Decapod crustaceans are held and slaughtered for different ends, e.g., scientific research studies versus food production, and in the latter case, there may be the additional issue of dealing with very large numbers of animals, which is true for *P. vannamei*.

A requirement to use more humane methods of slaughter is now demanded by advocacy bodies, increasingly being mandated by legislative bodies and governments in several parts of the world, and is currently being debated in the UK (see *Current Legislation Relevant to Decapod Crustaceans*). When applied to decapod crustaceans, the majority of methods mentioned above are considered inhumane by the European Union's Scientific Panel on Animal Health and Welfare (Animal Health and Animal Welfare Panel of the European Food Standards Agency, 2005) since most take some time to have an effect and hence have the potential to confer suffering or stress. Methods of rapid dispatch that minimise the potential to inflict suffering and stress, and thus improve welfare, continue to be sought by the crustacean fishery and aquaculture industries. Currently, there is no published information on the commercial slaughter practices for penaeid shrimps, and for that reason it is difficult to ascertain if these are applied correctly to minimise peri-slaughter stress of *P. vannamei* during the harvest process.

A previous study has shown that the use of slurry ice on *P. vannamei* (thought to be the most commonly used slaughter method) renders the animals sedated, accompanied by a reduced cardiac function within seconds (substantial reduction within 30 seconds) (Weineck et al., 2018). Despite a decrease in heart rate, specimens would tail flip within 1 min when exposed to cold water and more importantly, upon transfer to warm water the heart rate increased, indicating that the stunning is reversible. Therefore, although slurry ice proved to be a fast method for stunning, controlling the time and conditions between stunning and slaughter in commercial farms would be very important from a welfare perspective. Regarding electrical stunning, several references are available for the larger decapods (Neil, 2010; Roth and Øines, 2010; Neil, 2012a; Roth and Grimsbø, 2013; Fregin and Bickmeyer, 2016; Roth and Grimsbø, 2016). These studies have shown the effectiveness of electrostunning in rendering these larger decapods insensible rapidly (within 1 second reported) (Roth and Øines, 2010). The effectiveness of electrical stunning in *P. vannamei* was also evaluated recently (Weineck et al., 2018), and was found to be as effective, but less consistent than cold stun in ice slurry.

The choice of slaughter method will also impact post-harvest product quality (Neil, 2012b), and a study performed on *P. vannamei* has shown that the use of slurry ice is more beneficial for post-harvest quality than cold storage and flake ice (Wang et al., 2014). Inappropriate harvesting, stunning and slaughter trigger an acute stress response, which can impact the initial post-mortem metabolism and reduce product freshness (Albalat et al., 2009; Gornik et al., 2010). Furthermore, other stress-related consequences such as extensive autotomy (the casting off a part of the body by an animal under threat) has been reported when crabs were stunned using a low electrical field strength to the whole animal (Roth and Øines, 2010) an effect not reported with higher electrical field strengths (Neil, 2010; Neil, 2012a). Blackening or melanosis development can also be affected if the stunning/slaughter method causes an increase in temperature (Albalat et al., 2022).

5 CURRENT LEGISLATION RELEVANT TO DECAPOD CRUSTACEANS

Countries that protect decapods or place them under some degree of legal protection are Australia, Austria, New Zealand and Norway. Italy and UK do have some partial protection or changes in legislations are being contemplated (in UK).

Australia: In 2004, Australia adopted the Australian Animal Welfare Strategy (AAWS), which explicitly covered 'all sentient animals—that is, those with a capacity to experience suffering and pleasure'. Crustaceans are only protected in some states and by some provisions. These provisions cover cephalopods (Australian Capital Territory) and crustaceans (Australian Capital Territory and New South Wales – for human consumption; Victoria – adult decapods since 1997). However, there is room for improvement in many domains related to animal welfare in general, Australia ranking D on the animal protection index[8]. Animal sentience is still not recognised at the Commonwealth level.

Austria: The Austrian Animal Welfare act of 2004[9] protects crustaceans under national husbandry guidelines. It has been scored as B on the animal protection index[10].

Switzerland: The Animal Welfare Ordinance from 2008[11] protects crustaceans during slaughter and during transport (stunning is required and no ice is allowed during transport)

New Zealand: Animal Welfare act in 1999[12] changed the definition of the NZ animal animal protection act (1960) to cover crabs, lobsters and crayfish.

[8] API: http://api.worldanimalprotection.org/sites/default/files/api_2020_-_australia.pdf

[9] The Federal Act on Animal Welfare (Tierschutzgesetz - TSchG), Federal Law Gazette I 2004/118

[10] https://api.worldanimalprotection.org/sites/default/files/api_2020_-_austria_0.pdf

[11] https://www.globalanimallaw.org/downloads/database/national/switzerland/TSchV-2008-EN-455.1-2011.pdf

[12] https://www.legislation.govt.nz/act/public/1999/0142/latest/DLM49664.html

[13] https://www.regjeringen.no/en/dokumenter/animal-welfare-act/id571188/#:~:text=The%20intention%20of%20this%20Act,welfare%20and%20respect%20for%20animals.&text=The%20Act%20applies%20to%20conditions,squid%2C%20octopi%20and%20honey%20bees

Norway: Legal protection for decapods by the Norwegian Animal Welfare Act (2010)[13] including killing, confining and transport.

The UK government commissioned a report in 2021 to evaluate the current evidence on the welfare status of crustaceans and the potential for them to be sentient (Birch et al., 2021). Following the report DEFRA tabled an amendment to the Animal Welfare (Sentience) Bill was approved in April 2022 and now includes decapod crustaceans and cephalopod molluscs.

Other countries such as Italy have partial protection in some provinces/regions and since 2017 crustaceans cannot be kept on ice in restaurant kitchens (all regions) or boiled alive (in the province of Regno Emilia for example).

6 CONCLUDING REMARKS

Despite the wide knowledge on crustacean nutritional requirements, stress physiology and immunology as well as disease control, still little is known about some key parameters related to the five welfare dimensions, as they might be applied to penaeid shrimp, and some of these gaps have been identified in this review. The main challenges facing the aquaculture of penaeid shrimp such as *P. vannamei* today are still based on improving best management practices (BMPs) taking into consideration different regions/farming systems, the development of species-specific Codes of Good Aquaculture Practices (CAqP), the importance of staff training by continuous professional development courses (CPDs) and the improvement of the monitoring systems both for the aquatic environment and the behaviour, health and welfare of the farmed animals. A systematic integrated welfare assessment encompassing all the different aspects of their farming and life cycle up to slaughter should be implemented in all aquaculture systems to better understand the basic needs of these organisms, to reduce the stressors, which would minimise the effects of stress responses and improve productivity and quality of the final product. The development of the precision farming (PF), with real-time monitoring of the environmental parameters and the possibility of system modelling and machine learning is a step forward for aquaculture systems and the solution for many welfare/stress related issues. Direct and indirect species-specific OWIs should be developed for all decapod crustaceans currently farmed, similar to the ones suggested in this review for *P. vannamei*. Positive welfare using environmental enrichment and better and less invasive husbandry procedures needs to be promoted at all life stages and husbandry practices, from broodstock to slaughter methods.

Understanding sentience in invertebrates is important from an animal and scientific perspective (Rowe, 2018). Moreover, as pointed out by Birch (Birch et al., 2021) evidence of sentience in invertebrates is crucial from a policy perspective. For instance, in the European Union decapod crustaceans were not included in the EU Directive 2010/63/EU on the protection of animals used for scientific purposes, nor other national directives such as the UK's Animal Welfare Act 2006. However, protection of decapod crustaceans has been argued for a number of years and therefore it is possible that the scope of current regulations will be expanded to decapod species. This has already happened in a number of cases such as in the New Zealand's Animal Welfare Act (1999), which includes crabs, lobsters and crayfish, while in Norway legislation includes all decapods as well as some insects (honeybees). Regarding the use of decapod species for scientific purposes, again while there are country- and even institution-specific differences, the requirement for ethical review has been firmly proposed (Rowe, 2018). More research related to crustacean welfare therefore needs to be developed to inform the industry. The new focus on welfare in crustaceans should be seen as an opportunity to boost the farming industry and address the needs of consumers.

AUTHOR CONTRIBUTIONS

All authors listed have made a substantial, direct, and intellectual contribution to the work, and approved it for publication.

ACKNOWLEDGMENTS

CC is joint-lead for WP3 Shellfish Health and Disease as part of the BBSRC/NERC-funded Aquaculture Collaboration Hub UK.

REFERENCES

Albalat, A., Gornik, S. G., Atkinson, R. J., Coombs, G. H., and Neil, D. M. (2009). Effect of Capture Method on the Physiology and Nucleotide Breakdown Products in the Norway Lobster (*Nephrops Norvegicus*). *Mar. Biol. Res.* 5, 441–450. doi: 10.1080/17451000802603637

Albalat, A., Gornik, S., Muangnapoh, C., and Neil, D.M. (2022). Effectiveness and quality evaluation of electrical stunning versus chilling in Norway lobsters (*Nephrops norvegicus*). *Food Control* 138 (9), 108930. doi: /10.1016/j.foodcont.2022.108930

Albalat, A., Johnson, L., Coates, C. J., Dykes, G. C., Hitte, F., Morro, B., et al. (2019). The Effect of Temperature on the Physiological Condition and Immune-Capacity of European Lobsters (*Homarus Gammarus*) During Long-Term Starvation. *Front. Mar. Sci.* 6, 281. doi: 10.3389/fmars.2019.00281

Albalat, A., Sinclair, S., and Neil, D. (2017). Validation of a Vigour Index for Trawl-Caught Norway Lobsters (*Nephrops Norvegicus*) Destined for the Live Market: Underlying Links to Both Physiological Condition and Survivability. *Fish. Res.* 191, 25–29. doi: 10.1016/j.fishres.2017.02.016

Animal Health and Animal Welfare Panel of the European Food Standards Agency [AHAW]. (2005). Aspects of the Biology and Welfare of Animals Used for Experimental and Other Scientific Purposes (EFSA-Q-2004-105). *Annex EFSA J.* 292, 1–136. doi: 10.2903/j.efsa.2005.292

Araneda, M., Gasca-Leyva, E., Vela, M. A., and Dominguez-May, R. (2020). Effects of Temperature and Stocking Density on Intensive Culture of Pacific White Shrimp in Freshwater. *J. Therm. Biol.* 94, 102756. doi: 10.1016/j.jtherbio.2020.102756

Arechavala-Lopez, P., Cabrera-Álvarez, M. J., Maia, C. M., and Saraiva, J. L. (2022). Environmental Enrichment in Fish Aquaculture: A Review of

Fundamental and Practical Aspects. *Rev. Aquac.* 14, 704–728. doi: 10.1111/raq.12620

Arnold, J. E., Hadfield, C. A., Clayton, L. A., Cray, C., Jones, D., and Payton, M. (2021). Development of Methodology and Reference Intervals for the Analysis of the Free-Ranging Atlantic Horseshoe Crab *Limulus Polyphemus* Hemolymph. *Vet. Clin. Pathol.* 50, 259–272. doi: 10.1111/vcp.12983

Bachère, E. (2000). Shrimp Immunity and Disease Control. *Aquaculture* 191, 3–11. doi: 10.1016/S0044-8486(00)00413-0

Bae, S.-H., Okutsu, T., Kang, B. J., and Wilder, M. N. (2013). Alterations of Pattern in Immune Response and Vitellogenesis During Induced Ovarian Development by Unilateral and Bilateral Ablation in *Litopenaeus Vannamei*. *Fish. Sci.* 79, 895–903. doi: 10.1007/s12562-013-0652-3

Bardera, G., Owen, M. A. G., Facanha, F. N., Alcaraz-Calero, J. M., Alexander, M. E., and Sloman, K. A. (2021). The Influence of Density and Dominance on Pacific White Shrimp (*Litopenaeus Vannamei*) Feeding Behaviour. *Aquaculture* 531, 735949. doi: 10.1016/j.aquaculture.2020.735949

Bardera, G., Owen, M. A. G., Façanha, F. N., Sloman, K. A., and Alexander, M. E. (2020). The Influence of Sex on Feeding Behaviour in Pacific White Shrimp (*Litopenaeus Vannamei*). *Appl. Anim. Behav. Sci.* 224, 104946. doi: 10.1016/j.applanim.2020.104946

Bardera, G., Usman, N., Owen, M., Pountney, D., Sloman, K. A., and Alexander, M. E. (2019). The Importance of Behaviour in Improving the Production of Shrimp in Aquaculture. *Rev. Aquac.* 11, 1104–1132. doi: 10.1111/raq.12282

Barreto, M. O., Rey Planellas, S., Yang, Y., Phillips, C., and Descovich, K. (2022). Emerging Indicators of Fish Welfare in Aquaculture. *Rev. Aquac.* 14, 343–361. doi: 10.1111/raq.12601

Bartlett, T. C., Cuthbertson, B. J., Shepard, E. F., Chapman, R. W., Gross, P. S., and Warr, G. W. (2002). Crustins, Homologues of an 11.5-Kda Antibacterial Peptide, From Two Species of Penaeid Shrimp, *Litopenaeus Vannamei* and *Litopenaeus Setiferus*. *Mar. Biotechnol.* 4, 278–293. doi: 10.1007/s10126-002-0020-2

Basti, D., Bricknell, I., Chang, E. S., and Bouchard, D. (2010). Biochemical Reference Intervals for the Resting State in the Adult Lobster *Homarus Americanus*. *J. Shellfish Res.* 29, 1013–1019, 1017.

Bateson, P. (1991). Assessment of Pain in Animals. *Anim. Behav.* 42, 827–839. doi: 10.1016/S0003-3472(05)80127-7

Bautista-Covarrubias, J. C., Zamora-Ibarra, P. A., Apreza-Burgos, E., Rodríguez-Ocampo, A. N., Peraza-Gómez, V., López-Sánchez, J. A., et al. (2020). Immune Response and Oxidative Stress of Shrimp *Litopenaeus Vannamei* at Different Moon Phases. *Fish. Shellfish Immunol.* 106, 591–595. doi: 10.1016/j.fsi.2020.08.040

Becker, A. J., Vaz, L. J., Garcia, L., Wasielesky, J., Heinzmann, B. M., and Baldisserotto, B. (2021). Anesthetic Potential of Different Essential Oils for Two Shrimp Species, *Farfantepenaeus Paulensis* and *Litopenaeus Vannamei* (Decapoda, Crustacea). *Ciec. Rural* 51, 12, e20200793. doi: 10.1590/0103-8478cr20200793

Birch, J. B., Schnell, C., Browning, A., and H. Crump, A. (2021). *Review of the Evidence of Sentience in Cephalopod Molluscs and Decapod Crustaceans, London School of Economics and Political Science* (London, UK: LSE Enterprise Ltd; London School of Economics and Political Science).

Bonami, J.-R., Hasson, K. W., Mari, J., Poulos, B. T., and Lightner, D. V. (1997). Taura Syndrome of Marine Penaeid Shrimp: Characterization of the Viral Agent. *J. Gen. Virol.* 78, 313–319. doi: 10.1099/0022-1317-78-2-313

Bonami, J. R., Shi, Z., Qian, D., and Sri Widada, J. (2005). White Tail Disease of the Giant Freshwater Prawn, *Macrobrachium Rosenbergii*: Separation of the Associated Virions and Characterization of MRNV as a New Type of Nodavirus. *J. Fish. Dis.* 28, 23–31. doi: 10.1111/j.1365-2761.2004.00595.x

Borquez-Lopez, R. A., Martinez-Cordova, L. R., Casillas-Hernandez, R., Lopez-Elias, J. A., Barraza-Guardado, R. H., Ibarra-Gamez, J. C., et al. (2016). Water Quality Index Monitoring for Shrimp Aquaculture Using Open Source Hardware and Fuzzy Inference Systems. *Biotecnia* 19, 3, 45–49. doi: 10.18633/biotecnia.v19i3.449

Broom, D. M. (2019). "Sentience," in *Encyclopedia of Animal Behavior*, *2nd ed.* Ed. J. C. Choe (Oxford: Academic Press), 131–133, pp.

Browdy, C. L. (1998). Recent Developments in Penaeid Broodstock and Seed Production Technologies: Improving the Outlook for Superior Captive Stocks. *Aquaculture* 164, 3–21. doi: 10.1016/S0044-8486(98)00174-4

Burgents, J. E., Burnett, K. G., and Burnett, L. E. (2005). Effects of Hypoxia and Hypercapnic Hypoxia on the Localization and the Elimination of *Vibrio Campbellii* in *Litopenaeus Vannamei*, the Pacific White Shrimp. *Biol. Bull.* 208, 159–168. doi: 10.2307/3593148

Butterworth, A., and Weeks, C. (2009). The Impact of Disease on Welfare. *Welf. Domest. Fowl Other Captive Birds* 9, 189–218. doi: 10.1007/978-90-481-3650-6_8

Calderon-Perez, J. A., Rendon-Rodriguez, S., and Solis-Ibarra, R. (2007). Daily Cycle and Body Characteristics of Mating *Litopenaeus Vannamei* Shrimps (Decapoda: Penaeidae) in the Wild Off Southern Sinaloa, Mexico. *Rev. Biol. Trop.* 55, 189–198. doi: 10.15517/rbt.v55i1.6070

Cerenius, L., Babu, R., Söderhäll, K., and Jiravanichpaisal, P. (2010). *In Vitro* Effects on Bacterial Growth of Phenoloxidase Reaction Products. *J. Invertebr. Pathol.* 103, 21–23. doi: 10.1016/j.jip.2009.09.006

Cerenius, L., and Söderhäll, K. (2021). Immune Properties of Invertebrate Phenoloxidases. *Dev. Comp. Immunol.* 122, 104098. doi: 10.1016/j.dci.2021.104098

Chaijarasphong, T., Munkongwongsiri, N., Stentiford, G. D., Aldama-Cano, D. J., Thansa, K., Flegel, T. W., et al. (2021). The Shrimp Microsporidian *Enterocytozoon Hepatopenaei* (EHP): Biology, Pathology, Diagnostics and Control. *J. Invertebr. Pathol.* 186, 107458. doi: 10.1016/j.jip.2020.107458

Chamberlain, G. W., and Lawrence, A. L. (1981). Maturation, Reproduction, and Growth of *Penaeus Vannamei* and *P Stylirostris* Fed Natural Diets. *J. World Mariculture Soc.* 12, 207–224. doi: 10.1111/j.1749-7345.1981.tb00256.x

Cheng, W., Wang, L.-U., and Chen, J.-C. (2005). Effect of Water Temperature on the Immune Response of White Shrimp *Litopenaeus Vannamei* to *Vibrio Alginolyticus*. *Aquaculture* 250, 592–601. doi: 10.1016/j.aquaculture.2005.04.060

Ciaramella, M. A., Battison, A. L., and Horney, B. (2014). Measurement of Tissue Lipid Reserves in the American Lobster (*Homarus Americanus*): Hemolymph Metabolites as Potential Biomarkers of Nutritional Status. *J. Crust. Biol.* 34, 629–638. doi: 10.1163/1937240X-00002262

Coates, C. J., Bradford, E. L., Krome, C. A., and Nairn, J. (2012). Effect of Temperature on Biochemical and Cellular Properties of Captive *Limulus Polyphemus*. *Aquaculture* 334-337, 30–38. doi: 10.1016/j.aquaculture.2011.12.029

Coates, C. J., and Costa-Paiva, E. M. (2020). "Multifunctional Roles of Hemocyanins," in *Vertebrate and Invertebrate Respiratory Proteins, Lipoproteins and Other Body Fluid Proteins*. Eds. U. Hoeger and J. R. Harris (Cham: Springer International Publishing), pp 233–pp 250.

Coates, C. J., and Nairn, J. (2013). Hemocyanin-Derived Phenoloxidase Activity: A Contributing Factor to Hyperpigmentation in *Nephrops Norvegicus*. *Food Chem.* 140, 361–369. doi: 10.1016/j.foodchem.2013.02.072

Coates, C. J. R., Rowley, A. F., Smith, L. C., and Whitten, M. M. A. (2022). "Host Defences of Invertebrates to Pathogens and Parasites," in *Invertebrate Pathology*. Eds. A. F. Rowley, C. J. Coates and M. A. Miranda (Oxford UK: Oxford University Press).

Coates, C. J., and Söderhäll, K. (2021). The Stress–Immunity Axis in Shellfish. *J. Invertebr. Pathol.* 186, 107492. doi: 10.1016/j.jip.2020.107492

Coates, C. J., and Talbot, J. (2018). Hemocyanin-Derived Phenoloxidase Reaction Products Display Anti-Infective Properties. *Dev. Comp. Immunol.* 86, 47–51. doi: 10.1016/j.dci.2018.04.017

Conte, F., Voslarova, E., Vecerek, V., Elwood, R. W., Coluccio, P., Pugliese, M., et al. (2021). Humane Slaughter of Edible Decapod Crustaceans. *Animals* 11, 1089. doi: 10.3390/ani11041089

Cook, H. L., and Murphy, M. A. (1969). The Culture of Larval Penaeid Shrimp. *Trans. Am. Fish. Soc.* 98, 751–754. doi: 10.1577/1548-8659(1969)98[751:TCOLPS]2.0.CO;2

Costa, A. M., Buglione, C. C., Bezerra, F. L., Martins, P. C. C., and Barracco, M. A. (2009). Immune Assessment of Farm-Reared *Penaeus Vannamei* Shrimp Naturally Infected by Imnv in Ne Brazil. *Aquaculture* 291, 141–146. doi: 10.1016/j.aquaculture.2009.03.013

Cummings, W. C. (1961). Maturation and Spawning of the Pink Shrimp, *Penaeus Duorarum Burkenroad*. *Trans. Am. Fish. Soc.* 90, 462–468. doi: 10.1577/1548-8659(1961)90[462:MASOTP]2.0.CO;2

Cuvin-Aralar, M. L. A., Lazartigue, A. G., and Aralar, E. V. (2009). Cage Culture of the Pacific White Shrimp *Litopenaeus Vannamei* (Boon) at Different Stocking Densities in a Shallow Eutrophic Lake. *Aquac. Res.* 40, 181–187. doi: 10.1111/j.1365-2109.2008.02081.x

da Costa, F. P., Gomes, B., Pereira, S., and Arruda, M. D. (2016). Influence of Stocking Density on the Behaviour of Juvenile *Litopenaeus Vannamei* (Boon). *Aquac. Res.* 47, 912–924. doi: 10.1111/are.12550

D'Agaro, E., Sabbioni, V., Messina, M., Tibaldi, E., Bongiorno, T., Tulli, F., et al. (2014). Effect of Confinement and Starvation on Stress Parameters in the

American Lobster (*Homarus Americanus*). *Ital. J. Anim. Sci.* 13, 3530. doi: 10.4081/ijas.2014.3530

Darwin, C. (1872). *The Expression of the Emotions in Man and Animals*. Ed. J. Murray (London, UK: John Murray).

Das, R., Krishna, G., Priyadarshi, H., P, G.-B., Pavan-Kumar, A., Rajendran, K. V., et al. (2015). Captive Maturation Studies in *Penaeus Monodon* by Gih Silencing Using Constitutively Expressed Long Hairpin Rna. *Aquaculture* 448, 512–520. doi: 10.1016/j.aquaculture.2015.06.036

Davies, C. E., Malkin, S. H., Thomas, J. E., Batista, F. M., Rowley, A. F., and Coates, C. J. (2020). Mycosis is a Disease State Encountered Rarely in Shore Crabs, *Carcinus Maenas*. *Pathog. (Basel Switzerland)* 9, 462. doi: 10.3390/pathogens9060462

De Gryse, G. M. A., Khuong, T. V., Descamps, B., Van Den Broeck, W., Vanhove, C., Cornillie, P., et al. (2020). The Shrimp Nephrocomplex Serves as a Major Portal of Pathogen Entry and is Involved in the Molting Process. *Proc. Natl. Acad. Sci.* 117, 28374–28383. doi: 10.1073/pnas.2013518117

de Souza Valente, C., and Wan, A. H. L. (2021). *Vibrio* and Major Commercially Important Vibriosis Diseases in Decapod Crustaceans. *J. Invertebr. Pathol.* 181, 107527. doi: 10.1016/j.jip.2020.107527

Diamond, S., Powell, A., Shields, R. J., and Rowley, A. F. (2008). Is Spermatophore Melanisation in Captive Shrimp (*Litopenaeus Vannamei*) a Result of an Auto-Immune Response? *Aquaculture* 285, 14–18. doi: 10.1016/j.aquaculture.2008.08.029

Diggles, B. K. (2019). Review of Some Scientific Issues Related to Crustacean Welfare. *ICES J. Mar. Sci.* 76, 66–81. doi: 10.1093/icesjms/fsy058

Durairaj, K., Velmurugan, P., Senthilkumar, P., Vetriselvan, P., Manimekalan, A., and Oh, B. T. (2018). *In-Vivo* Study on Effect of Stocking Density on Growth and Production of Marine Prawn *Litopenaeus Vannamei*. *Indian J. Geo-Mar. Sci.* 47, 1228–1236.

Elwald, J. J. (1965). The Laboratory Rearing of Pink Shrimp, *Penaeus Duorarum Burkenroad*. *Bull. Mar. Sci. Gulf Caribb.* 15, 436–449.

Esparza-Leal, H. M., Cardozo, A. P., and Wasielesky, W. (2015). Performance of *Litopenaeus Vannamei* Postlarvae Reared in Indoor Nursery Tanks at High Stocking Density in Clear-Water Versus Biofloc System. *Aquacult. Eng.* 68, 28–34. doi: 10.1016/j.aquaeng.2015.07.004

FAO. (2003). *Health Management and Biosecurity Maintenance in White Shrimp (Penaeus Vannamei) Hatcheries in Latin America* (Rome, Italy: Food and Agriculture Organization of the United Nations).

FAO. (2009). "Penaeus Vannamei," in *Cultured Aquatic Species Fact Sheets*. Eds. M. Briggs, C. Valerio and N. Michael (Rome, Italy: Food and Agriculture Organisation of the United Nations).

FAO. (2020). *The State of World Fisheries and Aquaculture 2020, Sustainability in Action* (Rome: FAO).

Fontaine, C. T., and Lightner, D. V. (1973). Observations on the Process of Wound Repair in Penaeid Shrimp. *J. Invertebr. Pathol.* 22, 23–33. doi: 10.1016/0022-2011(73)90005-0

Fregin, T., and Bickmeyer, U. (2016). Electrophysiological Investigation of Different Methods of Anesthesia in Lobster and Crayfish. *PloS One* 11, e0162894. doi: 10.1371/journal.pone.0162894

Freire, C. A., Cuenca, A. L. R., Leite, R. D., Prado, A. C., Rios, L. P., Stakowian, N., et al. (2020). Biomarkers of Homeostasis, Allostasis, and Allostatic Overload in Decapod Crustaceans of Distinct Habitats and Osmoregulatory Strategies: An Empirical Approach. *Comp. Biochem. Physiol. Part A: Mol. Integr. Physiol.* 248, 110750. doi: 10.1016/j.cbpa.2020.110750

Frelier, P. F., Loy, J. K., and Kruppenbach, B. (1993). Transmission of Necrotizing Hepatopancreatitis in *Penaeus Vannamei*. *J. Invertebr. Pathol.* 61, 44–48. doi: 10.1006/jipa.1993.1008

Froes, C., Foes, G., Krummenauer, D., Poersch, L. H., and Wasielesky, W. (2013). Stocking Density at Rearing Phase for White Shrimp Farmed in a Biofloc System. *Pesqui. Agropecu. Bras.* 48, 878–884. doi: 10.1590/S0100-204X2013000800010

Funge-Smith, S., and Briggs, M. (2003). "The Introduction of Penaeus Vannamei and P Stylirostris Into the Asia-Pacific Region," in *International Mechanisms for the Control and Responsible Use of Alien Species in Aquatic Ecosystems* (Rome, Italy: Food and Agriculture Organisation of the United Nations (FAO)) 26–29.

Geetha, R., Avunje, S., Solanki, H. G., Priyadharshini, R., Vinoth, S., Anand, P. R., et al. (2022). Farm-Level Economic Cost of *Enterocytozoon Hepatopenaei* (EHP) to Indian *Penaeus Vannamei* Shrimp Farming. *Aquaculture* 548, 737685. doi: 10.1016/j.aquaculture.2021.737685

Gong, Y., and Zhang, X. (2021). Rnai-Based Antiviral Immunity of Shrimp. *Dev. Comp. Immunol.* 115, 103907. doi: 10.1016/j.dci.2020.103907

Gornik, S. G., Albalat, A., Atkinson, R. J., Coombs, G. H., and Neil, D. M. (2010). The Influence of Defined Ante-Mortem Stressors on the Early Post-Mortem Biochemical Processes in the Abdominal Muscle of the Norway Lobster, *Nephrops Norvegicus* (Linnaeu). *Mar. Biol. Res.* 6, 223–238. doi: 10.1080/17451000903147468

Gunalan, B., Soundarapandian, P., and Dinakaran, G. K. (2010). The Effect of Temperature and Ph on WSSV Infection in Cultured Marine Shrimp *Penaeus Monodon* (Fabricius). *Middle-East J. Sci. Res.* 5, 28–33.

Hasson, K. W., Lightner, D. V., Poulos, B. T., Redman, R. M., White, B. L., Brock, J. A., et al. (1995). Taura Syndrome in *Penaeus Vannamei*: Demonstration of a Viral Etiology. *Dis. Aquat. Org.* 23, 115–126. doi: 10.3354/dao023115

Hauton, C., Hawkins, L., and Williams, J. (1997). *In Situ* Variability in Phenoloxidase Activity in the Shore Crab, *Carcinus Maenas* (L.). *Comp. Biochem. Physiol. Part B: Biochem. Mol. Biol.* 117, 267–271. doi: 10.1016/S0305-0491(97)00050-3

Heng, L., and Rui-yu, L. (1994). Comparative Studies on the Larval Development of the Penaeid Shrimps, *Penaeus Chinensis*, *P Merguiensis* and *P Penicillatus*. *Chin. J. Oceanol. Limnol.* 12, 295–307. doi: 10.1007/BF02850489

Holt, C. C., Bass, D., Stentiford, G. D., and van der Giezen, M. (2021). Understanding the Role of the Shrimp Gut Microbiome in Health and Disease. *J. Invertebr. Pathol.* 186, 107387. doi: 10.1016/j.jip.2020.107387

Huang, S., Kuang, Y., Chang, C., Hung, C., Tsai, C., and Feng, K. (2019). AIo Ts for Smart Shrimp Farming *International SoC Design Conference*, Jeju, South Korea: ISOCC, 17–18, pp.

Hudinaga, M. (1935). *Studies on the Development of Penaeus Japonicus Bate: 1st Report* (Hayatomo, Japan: Hayatomo Fishery Institute).

Hudinaga, M. G. K. K. (1942). *Reproduction, Development and Rearing of Penaeus Japonicus Bate* (Tokyo: National Research Council of Japan).

Hudinaga, M. K. J. (1966). Studies on Food and Growth of Larval Stage of a Prawn, *Penaeus Japonicus*, With Reference to the Application to Practical Mass Culture. *Inf. Bull. Planktol. Jpn.* 13, 83–94.

Hudinaga, M., and Kittaka, J. (1967). The Large Scale Production of the Young Kuruma Prawn, Penaeus Japonicus Bate. *Inf. Bull. Planktol. Jpn. (Commemoration No. Dr. Y. Matsue's 60th Birthday)*, 35–46.

Hu, J., Wang, S., Wang, L., Li, F., Pingguan-Murphy, B., Lu, T. J., et al. (2014). Advances in Paper-Based Point-of-Care Diagnostics. *Biosens. Bioelectron.* 54, 585–597. doi: 10.1016/j.bios.2013.10.075

Jerez-Cepa, I., and Ruiz-Jarabo, I. (2021). Physiology: An Important Tool to Assess the Welfare of Aquatic Animals. *Biology* 10, 61. doi: 10.3390/biology10010061

Johansson, M. W., Keyser, P., Sritunyalucksana, K., and Söderhäll, K. (2000). Crustacean Haemocytes and Haematopoiesis. *Aquaculture* 191, 45–52. doi: 10.1016/S0044-8486(00)00418-X

Johnson, L., Coates, C. J., Albalat, A., Todd, K., and Neil, D. (2016). Temperature-Dependent Morbidity of 'Nicked' Edible Crab, *Cancer Pagurus*. *Fish. Res.* 175, 127–131. doi: 10.1016/j.fishres.2015.11.024

Jorry, D. C. (2012). "Marine Shrimps," in *Aquaculture: Farming Aquatic Animals and Plants*. Eds. J. S. Lucas and P. C. Southgate (Australia: John Wiley & sons), 382–418, pp.

Kang, B. J., Okutsu, T., Tsutsui, N., Shinji, J., Bae, S.-H., and Wilder, M. N. (2014). Dynamics of Vitellogenin and Vitellogenesis-Inhibiting Hormone Levels in Adult and Subadult Whiteleg Shrimp, *Litopenaeus Vannamei*: Relation to Molting and Eyestalk Ablation1. *Biol. Reprod.* 90, 1, 1–10. doi: 10.1095/biolreprod.113.112243

Kirkwood, J. K. (2006). "The Distribution of the Capacity for Sentience in the Animal Kingdom," in *Animals, Ethics and Trade: The Challenge of Animal Sentience*. Eds. J. Turner and J. D'Silva (Petersfield: Compassion in World Farming Trust), 12–26, pp.

Krisfalusi-Gannon, J., Ali, W., Dellinger, K., Robertson, L., Brady, T. E., Goddard, M. K. M., et al. (2018). The Role of Horseshoe Crabs in the Biomedical Industry and Recent Trends Impacting Species Sustainability. *Front. Mar. Sci.* 5, 185. doi: 10.3389/fmars.2018.00185

Kumar, B. K., Deekshit, V. K., Raj, J. R. M., Rai, P., Shivanagowda, B. M., Karunasagar, I., et al. (2014). Diversity of *Vibrio Parahaemolyticus* Associated With Disease Outbreak Among Cultured *Litopenaeus Vannamei* (Pacific White Shrimp) in India. *Aquaculture* 433, 247–251. doi: 10.1016/j.aquaculture.2014.06.016

Kumar, V., Roy, S., Baruah, K., Van Haver, D., Impens, F., and Bossier, P. (2020). Environmental Conditions Steer Phenotypic Switching in Acute

Hepatopancreatic Necrosis Disease-Causing *Vibrio Parahaemolyticus*, Affecting Piravp/Pirbvp Toxins Production. *Environ. Microbiol.* 22, 4212–4230. doi: 10.1111/1462-2920.14903

Liao, X., Wang, C., Wang, B., Qin, H., Hu, S., Wang, P., et al. (2020). Comparative Transcriptome Analysis of *Litopenaeus Vannamei* Reveals That Triosephosphate Isomerase-Like Genes Play an Important Role During Decapod Iridescent Virus 1 Infection. *Front. Immunol.* 11, 1904. doi: 10.3389/fimmu.2020.01904

Li, E., Chen, L., Zeng, C., Yu, N., Xiong, Z., Chen, X., et al. (2008). Comparison of Digestive and Antioxidant Enzymes Activities, Haemolymph Oxyhemocyanin Contents and Hepatopancreas Histology of White Shrimp, *Litopenaeus Vannamei*, at Various Salinities. *Aquaculture* 274, 80–86. doi: 10.1016/j.aquaculture.2007.11.001

Lightner, D. V., Pantoja, C. R., Poulos, B. T., Tang, K. F. J., Redman, R. M., Andrade, T. P. D., et al. (2004). Infectious Myonecrosis: New Disease in Pacific White Shrimp. *Glob Aquac Advocate* 7, 85.

Lightner, D. V., Redman, R. M., and Bell, T. A. (1983). Infectious Hypodermal and Hematopoietic Necrosis, a Newly Recognized Virus Disease of Penaeid Shrimp. *J. Invertebr. Pathol.* 42, 62–70. doi: 10.1016/0022-2011(83)90202-1

Lightner, D. V., Redman, R. M., Pantoja, C. R., Noble, B. L., and Loc, T. (2012). Early Mortality Syndrome Affects Shrimp in Asia. (Portsmouth, U.S.A.: Global Seafood Alliance) 40.

Linda, N., Wiwat, S.-o., Supapon, C., and Timothy, W. F. (2005). Taura Syndrome Virus (TSV) in Thailand and its Relationship to TSV in China and the Americas. *Dis. Aquat. Org.* 63, 101–106. doi: 10.3354/dao063101

Liu, F., Li, S., Yu, Y., Zhang, C., and Li, F. (2021). Antennal Gland of Shrimp as an Entry for WSSW Infection. *Aquaculture* 530, 735932. doi: 10.1016/j.aquaculture.2020.735932

Liu, C.-H., Yeh, S.-T., Cheng, S.-Y., and Chen, J.-C. (2004). The Immune Response of the White Shrimp *Litopenaeus Vannamei* and its Susceptibility to Vibrio Infection in Relation With the Moult Cycle. *Fish. Shellfish Immunol.* 16, 151–161. doi: 10.1016/S1050-4648(03)00058-5

Liu, S., Zheng, S.-C., Li, Y.-L., Li, J., and Liu, H.-P. (2020). Hemocyte-Mediated Phagocytosis in Crustaceans. *Front. Immunol.* 11, 268. doi: 10.3389/fimmu.2020.00268

Li, E., Xu, C., Wang, X., Wang, S., Zhao, Q., Zhang, M., et al. (2018). Gut Microbiota and its Modulation for Healthy Farming of Pacific White Shrimp *Litopenaeus Vannamei*. *Rev. Fish. Sci. Aquac.* 26, 381–399. doi: 10.1080/23308249.2018.1440530

Magaña-Gallegos, E., Arévalo, M., Cuzon, G., and Gaxiola, G. (2021). Effects of Using the Biofloc System and Eyestalk Ablation on Reproductive Performance and Egg Quality of *Litopenaeus Vannamei* (Boon) (Decapoda: Dendrobranchiata: Penaeidae). *Anim. Reprod. Sci.* 228, 106749. doi: 10.1016/j.anireprosci.2021.106749

Maningas, M. B. B., Kondo, H., and Hirono, I. (2013). Molecular Mechanisms of the Shrimp Clotting System. *Fish. Shellfish Immunol.* 34, 968–972. doi: 10.1016/j.fsi.2012.09.018

Martins, C. I. M., Galhardo, L., Noble, C., Damsgård, B., Spedicato, M. T., Zupa, W., et al. (2012). Behavioural Indicators of Welfare in Farmed Fish. *Fish. Physiol. Biochem.* 38, 17–41. doi: 10.1007/s10695-011-9518-8

Mellor, D. J., and Beausoleil, N. J. (2015). Extending the 'Five Domains' Model for Animal Welfare Assessment to Incorporate Positive Welfare States. *Anim. Welf.* 24, 241. doi: 10.7120/09627286.24.3.241

Mellor, D. J., Patterson-Kane, E., and Stafford, K. J. (2009). *The Sciences of Animal Welfare* (Oxford, UK: Wiley-Blackwell).

Mellor, D., and Reid, C. (1994). Concepts of Animal Well-Being and Predicting the Impact of Procedures on Experimental Animals. *Improv. Well-Being Anim. Res. Environ.*, 3–18. https://www.wellbeingintlstudiesrepository.org/exprawel/7/

Metian, M., Troell, M., Christensen, V., Steenbeek, J., and Pouil, S. (2020). Mapping Diversity of Species in Global Aquaculture. *Rev. Aquac.* 12, 1090–1100. doi: 10.1111/raq.12374

Millard, R. S., Ellis, R. P., Bateman, K. S., Bickley, L. K., Tyler, C. R., van Aerle, R., et al. (2021). How Do Abiotic Environmental Conditions Influence Shrimp Susceptibility to Disease? A Critical Analysis Focussed on White Spot Disease. *J. Invertebr. Pathol.* 186, 107369. doi: 10.1016/j.jip.2020.107369

Mohr, P. G., Moody, N. J., Hoad, J., Williams, L. M., Bowater, R. O., Cummins, D. M., et al. (2015). New Yellow Head Virus Genotype (Yhv7) in Giant Tiger Shrimp *Penaeus Monodon* Indigenous to Northern Australia. *Dis. Aquat. Org.* 115, 263–268. doi: 10.3354/dao02894

Muthu, M. S., Pillai, N. N., and George, K. V. (1974). On the Spawning and Rearing of *Penaeus Indicus* in the Laboratory With a Note on the Eggs and Larvae. *Indian J. Fish.* 21, 571–574.

Neil, D. M. (2010). *The Effect of the Crustastun™ on Nerve Activity in Crabs and Lobsters* (Glasgow, UK: University of Glasgow).

Neil, D. M. (2012a). "The Effect of the Crustastun™ on Nerve Activity in Two Commercially Important Decapod Crustaceans," in *The Edible Brown Cancer Pagurus and the European Lobster Homarus Gammarus* (Glasgow, UK: University of Glasgow).

Neil, D. M. (2012b). Ensuring Crustacean Product Quality in the Post-Harvest Phase. *J. Invertebr. Pathol.* 110, 267–275. doi: 10.1016/j.jip.2012.03.009

Ng, T. H., Chang, S.-H., Wu, M.-H., and Wang, H.-C. (2013). Shrimp Hemocytes Release Extracellular Traps That Kill Bacteria. *Dev. Comp. Immunol.* 41, 644–651. doi: 10.1016/j.dci.2013.06.014

Noble, C., Gismervik, K., Iversen, M. H., Kolarevic, J., Nilsson, J., Stien, L. H., et al. (2018). *Welfare Indicators for Farmed Atlantic Salmon: Tools for Assessing Fish Welfare* (Tromsø, Norway: Nofima).

Nunan, L. M., Pantoja, C. R., Gomez-Jimenez, S., and Lightner, D. V. (2013). *Candidatus Hepatobacter Penaei*: An Intracellular Pathogenic Enteric Bacterium in the Hepatopancreas of the Marine Shrimp *Penaeus Vannamei* (Crustacea: Decapoda). *Appl. Environ. Microbiol.* 79, 1407–1409. doi: 10.1128/AEM.02425-12

O'Donncha, F., Stockwell, C. L., Planellas, S. R., Micallef, G., Palmes, P., Webb, C., et al. (2021). Data Driven Insight Into Fish Behaviour and Their Use for Precision Aquaculture. *Front. Anim. Sci.* 30, 695054. doi: 10.3389/fanim.2021.695054

Palacios, E., Carrefio, D., Rodríguez-Jaramillo, M. C., and Racotta, I. S. (1999a). Effect of Eyestalk Ablation on Maturation, Larval Performance, and Biochemistry of White Pacific Shrimp, *Penaeus Vannamei*, Broodstock. *J. Appl. Aquac.* 9, 1–23. doi: 10.1300/J028v09n03_01

Palacios, E., Perez-Rostro, C. I., Ramirez, J. L., Ibarra, A. M., and Racotta, I. S. (1999b). Reproductive Exhaustion in Shrimp (*Penaeus Vannamei*) Reflected in Larval Biochemical Composition, Survival and Growth. *Aquaculture* 171, 309–321. doi: 10.1016/S0044-8486(98)00393-7

Parodi, T. V., Cunha, M. A., Heldwein, C. G., de Souza, D. M., Martins, Á. C., Garcia, L., et al. (2012). The Anesthetic Efficacy of Eugenol and the Essential Oils of *Lippia Alba* and *Aloysia Triphylla* in Post-Larvae and Sub-Adults of *Litopenaeus Vannamei* (Crustacea, Penaeidae). *Comp. Biochem. Physiol. Part C: Toxicol. Pharmacol.* 155, 462–468. doi: 10.1016/j.cbpc.2011.12.003

Passantino, A., Elwood, R. W., and Coluccio, P. (2021). Why Protect Decapod Crustaceans Used as Models in Biomedical Research and in Ecotoxicology? Ethical and Legislative Considerations. *Animals* 11, 73. doi: 10.3390/ani11010073

Phupet, B., Pitakpornpreecha, T., Baowubon, N., Runsaeng, P., and Utarabhand, P. (2018). Lipopolysaccharide- and β-1,3-Glucan-Binding Protein From *Litopenaeus Vannamei*: Purification, Cloning and Contribution in Shrimp Defense Immunity *via* Phenoloxidase Activation. *Dev. Comp. Immunol.* 81, 167–179. doi: 10.1016/j.dci.2017.11.016

Poulos, B. T., Tang, K. F. J., Pantoja, C. R., Bonami, J. R., and Lightner, D. V. (2006). Purification and Characterization of Infectious Myonecrosis Virus of Penaeid Shrimp. *J. Gen. Virol.* 87, 987–996. doi: 10.1099/vir.0.81127-0

Prachumwat, A., Munkongwongsiri, N., Eamsaard, W., Lertsiri, K., Flegel, T. W., Stentiford, G. D., et al. (2021). A Potential Prokaryotic and Microsporidian Pathobiome That may Cause Shrimp White Feces Syndrome (WFS). *bioRxiv* 2005, 2023.445355. doi: 10.1101/2021.05.23.445355

Prasad, K. P., Shyam, K. U., Banu, H., Jeena, K., and Krishnan, R. (2017). Infectious Myonecrosis Virus (IMNV) – an Alarming Viral Pathogen to Penaeid Shrimps. *Aquaculture* 477, 99–105. doi: 10.1016/j.aquaculture.2016.12.021

Qiu, L., Chen, X., Guo, X.-M., Gao, W., Zhao, R.-H., Zhang, Q.-L., et al. (2020). A Taqman Probe Based Real-Time Pcr for the Detection of Decapod Iridescent Virus 1. *J. Invertebr. Pathol.* 173, 107367. doi: 10.1016/j.jip.2020.107367

Qi, C., Wang, L., Liu, M., Jiang, K., Wang, M., Zhao, W., et al. (2017). Transcriptomic and Morphological Analyses of *Litopenaeus Vannamei* Intestinal Barrier in Response to *Vibrio Paraheamolyticus* Infection Reveals Immune Response Signatures and Structural Disruption. *Fish. Shellfish Immunol.* 70, 437–450. doi: 10.1016/j.fsi.2017.09.004

Quackenbush, L. S. (2015). Yolk Synthesis in the Marine Shrimp, *Penaeus Vannamei*. *Am. Zool.* 41, 458–464. doi: 10.1093/icb/41.3.458

Racotta, I. S., Palacios, E., and Ibarra, A. M. (2003). Shrimp Larval Quality in Relation to Broodstock Condition. *Aquaculture* 227, 107–130. doi: 10.1016/S0044-8486(03)00498-8

Rahman, M., Escobedo-Bonilla, C. M., Corteel, M., Dantas-Lima, J. J., Wille, M., Sanz, V. A., et al. (2006). Effect of High Water Temperature (33 °C) on the Clinical and Virological Outcome of Experimental Infections With White Spot Syndrome Virus (WSSV) in Specific Pathogen-Free (SPF) *Litopenaeus Vannamei*. *Aquaculture* 261, 842–849. doi: 10.1016/j.aquaculture.2006.09.007

Rateni, G., Dario, P., and Cavallo, F. (2017). Smartphone-Based Food Diagnostic Technologies: A Review. *Sensors* 17, 1453. doi: 10.3390/s17061453

Ravi, M., Basha, A. N., Sarathi, M., Idalia, H. R., Widada, J. S., Bonami, J., et al. (2009). Studies on the Occurrence of White Tail Disease (WTD) Caused by Mrnv and Xsv in Hatchery-Reared Post-Larvae of *Penaeus Indicus* and *P Monodon*. *Aquaculture* 292, 117–120. doi: 10.1016/j.aquaculture.2009.03.051

Rey, S., Digka, N., and MacKenzie, S. (2015). Animal Personality Relates to Thermal Preference in Wild-Type Zebrafish, *Danio Rerio*. *Zebrafish* 12, 243–249. doi: 10.1089/zeb.2014.1076

Robb, C. T., Dyrynda, E. A., Gray, R. D., Rossi, A. G., and Smith, V. J. (2014). Invertebrate Extracellular Phagocyte Traps Show That Chromatin is an Ancient Defence Weapon. *Nat. Commun.* 5, 4627. doi: 10.1038/ncomms5627

Rodríguez, J., and Le Moullac, G. (2000). State of the Art of Immunological Tools and Health Control of Penaeid Shrimp. *Aquaculture* 191, 109–119. doi: 10.1016/S0044-8486(00)00421-X

Rosas, C., Cooper, E., Pascual, C., Brito, R., Gelabert, R., Moreno, T., et al. (2004). Indicators of Physiological and Immunological Status of *Litopenaeus Setiferus* Wild Populations (Crustacea, Penaeidae). *Mar. Biol.* 145, 401–413. doi: 10.1007/s00227-004-1321-y

Roth, B., and Øines, S. (2010). Stunning and Killing of Edible Crabs (*Cancer Pagurus*). *Anim. Welf.* 19, 287–294.

Roth, B., and Grimsbø, E. (2013). *Electrical Stunning of Edible Crabs. Nofima Rapportserie* (Tromsø, Norway: Nofima), 8 p.

Roth, B., and Grimsbø, E. (2016). Electrical Stunning of Edible Crabs (*Cancer Pagurus*): From Single Experiments to Commercial Practice. *Anim. Welf.* 25, 489–497. doi: 10.7120/09627286.25.4.489

Rowe, A. (2018). Should Scientific Research Involving Decapod Crustaceans Require Ethical Review? *J. Agric. Environ. Ethics* 31, 625–634. doi: 10.1007/s10806-018-9750-7

Sainz-Hernández, J. C., Racotta, I. S., Dumas, S., and Hernández-López, J. (2008). Effect of Unilateral and Bilateral Eyestalk Ablation in *Litopenaeus Vannamei* Male and Female on Several Metabolic and Immunologic Variables. *Aquaculture* 283, 188–193. doi: 10.1016/j.aquaculture.2008.07.002

Sakaew, W., Pratoomthai, B., Anantasomboon, G., Asuvapongpatana, S., Sriurairattana, S., and Withyachumnarnkul, B. (2008). Abdominal Segment Deformity Disease (ASDD) of the Whiteleg Shrimp *Penaeus Vannamei* Reared in Thailand. *Aquaculture* 284, 46–52. doi: 10.1016/j.aquaculture.2008.07.041

Sakaew, W., Pratoomthai, B., Pongtippatee, P., Flegel, T. W., and Withyachumnarnkul, B. (2013). Discovery and Partial Characterization of a non-LTR Retrotransposon That may be Associated With Abdominal Segment Deformity Disease (ASDD) in the Whiteleg Shrimp *Penaeus* (*Litopenaeus*) *Vannamei*. *BMC Vet. Res.* 9, 189. doi: 10.1186/1746-6148-9-189

Sandeman, DCK, M., and Harzsch, S. (2016). "Adaptive Trends in Malacostracan Brain Form and Function Relate to Behavior," in *Nervous Systems and Control of Behavior (Natural History of Crustacea) Oxford*. Ed. C. Derby (New York: Thiel TOUP), pp 11–pp 48.

Segner, H., Sundh, H., Buchmann, K., Douxfils, J., Sundell, K. S., Mathieu, C., et al. (2012). Health of Farmed Fish: Its Relation to Fish Welfare and its Utility as Welfare Indicator. *Fish. Physiol. Biochem.* 38, 85–105. doi: 10.1007/s10695-011-9517-9

Senapin, S., Jaengsanong, C., Phiwsaiya, K., Prasertsri, S., Laisutisan, K., Chuchird, N., et al. (2012). Infections of MRNV (*Macrobrachium Rosenbergii* Nodavirus) in Cultivated Whiteleg Shrimp *Penaeus Vannamei* in Asia. *Aquaculture* 338-341, 41–46. doi: 10.1016/j.aquaculture.2012.01.019

Senapin, S., Phiwsaiya, K., Gangnonngiw, W., Briggs, M., Sithigorngul, P., and Flegel, T. W. (2013). Dual Infections of Imnv and MRNV in Cultivated *Penaeus Vannamei* From Indonesia. *Aquaculture* 372-375, 70–73. doi: 10.1016/j.aquaculture.2012.10.027

Sepici-Dinçel, A., Alparslan, Z. N., Benli, AÇ. K., Selvi, M., Sarıkaya, R., Özkul, İ. A., et al. (2013). Hemolymph Biochemical Parameters Reference Intervals and Total Hemocyte Counts of Narrow Clawed Crayfish *Astacus Leptodactylus* (Eschscholt). *Ecol. Indic.* 24, 305–309. doi: 10.1016/j.ecolind.2012.07.002

Shinn, A. P. P., Griffith, J., Trong, D., Vu, T. Q., Jiravanichpaisal, N. T., and P. Briggs, M. (2018). Asian Shrimp Production and the Economic Costs of Disease. *Asian Fish. Sci.* 31S, 29–58. doi: 10.33997/j.afs.2018.31.S1.003

Smith, J. A. (1991). A Question of Pain in Invertebrates. *ILAR J.* 33, 25–31. doi: 10.1093/ilar.33.1-2.25

Smith, S. A., and Berkson, J. (2005). Laboratory Culture and Maintenance of the Horseshoe Crab (*Limulus Polyphemus*). *Lab. Anim.* 34, 27–34. doi: 10.1038/laban0705-27

Smith, S. A., Berkson, J. M., and Barratt, R. A. (2002). "Horseshoe Crab (Limulus Polyphemus) Hemolymph, Biochemical and Immunological Parameters," in *Proceedings of the 33rd Annual Conference of the International Association for Aquatic Animal Medicine* Stamford, U.S.A.: International Association for Aquatic Animal Medicine Proceedings Online.

Smith, J. A., and Boyd, K. M. (1991). "Lives in the Balance," in *The Ethics of Using Animals in Biomedical Research: The Report of a Working Party of the Institute of Medical Ethics*. Eds. J. A. Smith and K. M. Boyd (Oxford: Oxford university press).

Smith, V. J., and Chisholm, J. R. S. (1992). Non-Cellular Immunity in Crustaceans. *Fish. Shellfish Immunol.* 2, 1–31. doi: 10.1016/S1050-4648(06)80024-0

Smith, V. J., and Ratcliffe, N. A. (1980). Cellular Defense Reactions of the Shore Crab, *Carcinus Maenas: In Vivo* Hemocytic and Histopathological Responses to Injected Bacteria. *J. Invertebr. Pathol.* 35, 65–74. doi: 10.1016/0022-2011(80)90085-3

Smith, V. J., and Söderhäll, K. (1983). Induction of Degranulation and Lysis of Haemocytes in the Freshwater Crayfish, *Astacus Astacus* by Components of the Prophenoloxidase Activating System *In Vitro*. *Cell Tissue Res.* 233, 295–303. doi: 10.1007/BF00238297

Söderhäll, K., and Smith, V. J. (1983). Separation of the Haemocyte Populations of *Carcinus Maenas* and Other Marine Decapods, and Prophenoloxidase Distribution. *Dev. Comp. Immunol.* 7, 229–239. doi: 10.1016/0145-305X(83)90004-6

Sriurairatana, S., Boonyawiwat, V., Gangnonngiw, W., Laosutthipong, C., Hiranchan, J., and Flegel, T. W. (2014). White Feces Syndrome of Shrimp Arises From Transformation, Sloughing and Aggregation of Hepatopancreatic Microvilli Into Vermiform Bodies Superficially Resembling Gregarines. *PloS One* 9, e99170. doi: 10.1371/journal.pone.0099170

Sterling, P., and Eyer, J. (1988). "Allostasis: A New Paradigm to Explain Arousal Pathology," in *Handbook of Life Stress, Cognition and Health*. Eds. S. Fisher and J. Reason (Hoboken, U.S.A.: John Wiley & Sons), pp. 629–649.

Strausfeld, N. J., Wolff, G. H., and Sayre, M. E. (2020). Mushroom Body Evolution Demonstrates Homology and Divergence Across Pancrustacea. *Elife* 9, e52411. doi: 10.7554/eLife.52411.sa2

Suleiman, S., Smith, V. J., and Dyrynda, E. A. (2017). Unusual Tissue Distribution of Carcinin, an Antibacterial Crustin, in the Crab, *Carcinus Maenas*, Reveals its Multi-Functionality. *Dev. Comp. Immunol.* 76, 274–284. doi: 10.1016/j.dci.2017.06.010

Su, X. P., Zhu, B. S., and Wang, F. (2021). Feeding Strategy Changes Boldness and Agonistic Behaviour in the Swimming Crab (*Portunus Trituberculatus*). *Aquac. Res.* 53, 2, 419–430. doi: 10.1111/are.15583

Talbot, P., Howard, D., Leung-Trujillo, J., Lee, T. W., Li, W. Y., Ro, H., et al. (1989). Characterization of Male Reproductive Tract Degenerative Syndrome in Captive Penaeid Shrimp (*Penaeus Setiferus*). *Aquaculture* 78, 365–377. doi: 10.1016/0044-8486(89)90112-9

Tang, K. F. J., Han, J. E., Aranguren, L. F., White-Noble, B., Schmidt, M. M., Piamsomboon, P., et al. (2016). Dense Populations of the Microsporidian *Enterocytozoon Hepatopenaei* (EHP) in Feces of *Penaeus Vannamei* Exhibiting White Feces Syndrome and Pathways of Their Transmission to Healthy Shrimp. *J. Invertebr. Pathol.* 140, 1–7. doi: 10.1016/j.jip.2016.08.004

Tassanakajon, A., Rimphanitchayakit, V., Visetnan, S., Amparyup, P., Somboonwiwat, K., Charoensapsri, W., et al. (2018). Shrimp Humoral Responses Against Pathogens: Antimicrobial Peptides and Melanization. *Dev. Comp. Immunol.* 80, 81–93. doi: 10.1016/j.dci.2017.05.009

Taylor, J., Vinatea, L., Ozorio, R., Schuweitzer, R., and Andreatta, E. R. (2004). Minimizing the Effects of Stress During Eyestalk Ablation of *Litopenaeus Vannamei* Females With Topical Anesthetic and a Coagulating Agent. *Aquaculture* 233, 173–179. doi: 10.1016/j.aquaculture.2003.09.034

Thitamadee, S., Prachumwat, A., Srisala, J., Jaroenlak, P., Salachan, P. V., Sritunyalucksana, K., et al. (2016). Review of Current Disease Threats for Cultivated Penaeid Shrimp in Asia. *Aquaculture* 452, 69–87. doi: 10.1016/j.aquaculture.2015.10.028

Thomas, M. M., Kathirvel, M., and Pillai, N. N. (1974). Spawning and Rearing of the Penaeid Prawn, *Metapenaeus Affinis* (H. Milne Edwards) in the Laboratory. *Indian J. Fish.* 21, 543–556.

Tourtip, S., Wongtripop, S., Stentiford, G. D., Bateman, K. S., Sriurairatana, S., Chavadej, J., et al. (2009). *Enterocytozoon Hepatopenaei* Sp. Nov. (Microsporida: Enterocytozoonidae), a Parasite of the Black Tiger Shrimp *Penaeus Monodon* (Decapoda: Penaeidae): Fine Structure and Phylogenetic Relationships. *J. Invertebr. Pathol.* 102, 21–29. doi: 10.1016/j.jip.2009.06.004

Tran, L., Nunan, L., Redman, R. M., Mohney, L. L., Pantoja, C. R., Fitzsimmons, K., et al. (2013). Determination of the Infectious Nature of the Agent of Acute Hepatopancreatic Necrosis Syndrome Affecting Penaeid Shrimp. *Dis. Aquat. Org.* 105, 45–55. doi: 10.3354/dao02621

Treece, G. D., and Fox, J. M. (1993). *Design, Operation and Training Manual for an Intensive Culture Shrimp Hatchery With Emphasis on Penaeus Monodon and Penaeus Vannamei* (Texas, U.S.A.: Texas ARM University Sea Grant College Program).

Treerattrakool, S., Boonchoy, C., Urtgam, S., Panyim, S., and Udomkit, A. (2014). Functional Characterization of Recombinant Gonad-Inhibiting Hormone (GIH) and Implication of Antibody Neutralization on Induction of Ovarian Maturation in Marine Shrimp. *Aquaculture* 428-429, 166–173. doi: 10.1016/j.aquaculture.2014.03.009

Tseng, I. T., and Chen, J.-C. (2004). The Immune Response of White Shrimp *Litopenaeus Vannamei* and its Susceptibility to *Vibrio Alginolyticus* Under Nitrite Stress. *Fish. Shellfish Immunol.* 17, 325–333. doi: 10.1016/j.fsi.2004.04.010

Tumburu, L., Shepard, E. F., Strand, A. E., and Browdy, C. L. (2012). Effects of Endosulfan Exposure and Taura Syndrome Virus Infection on the Survival and Molting of the Marine Penaeid Shrimp. *Litopenaeus Vannamei Chemosphere* 86, 912–918. doi: 10.1016/j.chemosphere.2011.10.057

Tu, H. T., Silvestre, F., Wang, N., Thome, J.-P., Phuong, N. T., and Kestemont, P. (2010). A Multi-Biomarker Approach to Assess the Impact of Farming Systems on Black Tiger Shrimp (*Penaeus Monodon*). *Chemosphere* 81, 1204–1211. doi: 10.1016/j.chemosphere.2010.09.039

Uengwetwanit, T., Pootakham, W., Nookaew, I., Sonthirod, C., Angthong, P., Sittikankaew, K., et al. (2021). A Chromosome-Level Assembly of the Black Tiger Shrimp (*Penaeus Monodon*) Genome Facilitates the Identification of Growth-Associated Genes. *Mol. Ecol. Resour.* 21, 1620–1640. doi: 10.1111/1755-0998.13357

Utari, H. B., Senapin, S., Jaengsanong, C., Flegel, T. W., and Kruatrachue, M. (2012). A Haplosporidian Parasite Associated With High Mortality and Slow Growth in Penaeus (*Litopenaeus Vannamei*) Cultured in Indonesia. *Aquaculture* 366-367, 85–89. doi: 10.1016/j.aquaculture.2012.09.005

van de Braak, C. B. T., Botterblom, M. H. A., Taverne, N., van Muiswinkel, W. B., Rombout, J. H. W. M., and van der Knaap, W. P. W. (2002). The Roles of Haemocytes and the Lymphoid Organ in the Clearance of Injected Vibrio Bacteria in *Penaeus Monodon* Shrimp. *Fish. Shellfish Immunol.* 13, 293–309. doi: 10.1006/fsim.2002.0409

van Hulten, M. C. W., Witteveldt, J., Snippe, M., and Vlak, J. M. (2001). White Spot Syndrome Virus Envelope Protein Vp28 is Involved in the Systemic Infection of Shrimp. *Virology* 285, 228–233. doi: 10.1006/viro.2001.0928

Vargas-Albores, F., and Yepiz-Plascencia, G. (2000). Beta Glucan Binding Protein and its Role in Shrimp Immune Response. *Aquaculture* 191, 13–21. doi: 10.1016/S0044-8486(00)00416-6

Verbruggen, B. (2016). *Generating Genomic Resources for Two Crustacean Species and Their Application to the Study of White Spot Disease* (Exeter, UK: E-thesis University of Exeter). Available at: https://ethos.bl.uk/OrderDetails.do?uin=uk.bl.ethos.702288.

Villanueva, R. R., Araneda, M. E., Vela, M., and Seijo, J. C. (2013). Selecting Stocking Density in Different Climatic Seasons: A Decision Theory Approach to Intensive Aquaculture. *Aquaculture* 384, 25–34. doi: 10.1016/j.aquaculture.2012.12.014

Wang, Z. K., Luan, S., Meng, X. H., Cao, B. X., Luo, K., and Kong, J. (2019). Comparative Transcriptomic Characterization of the Eyestalk in Pacific White Shrimp (*Litopenaeus Vannamei*) During Ovarian Maturation. *Gen. Comp. Endocrinol.* 274, 60–72. doi: 10.1016/j.ygcen.2019.01.002

Wang, G., and Mcgaw, I. J. (2014). Use of Serum Protein Concentration as an Indicator of Quality and Physiological Condition in the Lobster *Homarus Americanus* (Milne-Edward). *J. Shellfish Res. 33* 805-813, 809. doi: 10.2983/035.033.0315

Wang, Q., Zhang, B., and Wang, B. (2014). Effect Os Slurry Ice Treatment on the Quality of Fresh *Litopenaeus Vannamei*. *Mod. Food Sci. Technol.* 30, 134–140.

Wasielesky, W., Froes, C., Foes, G., Krummenauer, D., Lara, G., and Poersch, L. (2013). Nursery of *Litopenaeus Vannamei* Reared in a Biofloc System: The Effect of Stocking Densities and Compensatory Growth. *J. Shellfish Res.* 32, 799–806. doi: 10.2983/035.032.0323

Weineck, K., Ray, A. J., Fleckenstein, L. J., Medley, M., Dzubuk, N., Piana, E., et al. (2018). Physiological Changes as a Measure of Crustacean Welfare Under Different Standardized Stunning Techniques: Cooling and Electroshock. *Animals* 8, 158. doi: 10.3390/ani8090158

Whetstone, J. M. T., Treece, G. D., Browdy, C. L., and Stokes, A. D. (2002). Opportunities and Constraints in Marine Shrimp Farming. *South. Reg. Aquac. Center* 2006, 1–8.

Wijegoonawardane, P. K. M., Cowley, J. A., Phan, T., Hodgson, R. A. J., Nielsen, L., Kiatpathomchai, W., et al. (2008). Genetic Diversity in the Yellow Head Nidovirus Complex. *Virology* 380, 213–225. doi: 10.1016/j.virol.2008.07.005

Wu, B., Zhao, C. P., Xiong, Z. T., Mu, C. K., Xu, S. L., and Wang, D. L. (2021). Analysis of the Agonistic Behaviour and Behavioural Pattern of Portunus Trituberculatus. *Aquac. Res. 52* 5, 2233–2242. doi: 10.1111/are.15075

Wycoff, S. J., Weineck, K., Conlin, S., Suryadevara, C., Grau, E., Bradley, A., et al. (2018). Effects of Clove Oil (Eugenol) on Proprioceptive Neurons, Heart Rate, and Behavior in Model Crustaceans. *Biol. Fac. Publ.* 145, 1–21.

Yano, I., Kanna, R. A., Oyama, R. N., and Wyban, J. A. (1988). Mating Behaviour in the Penaeid Shrimp *Penaeus Vannamei*. *Mar. Biol.* 97, 171–175. doi: 10.1007/BF00391299

Yepiz-Plascencia, G., Galván, T. G., Vargas-albores, F., and García-bañuelos, M. (2000). Synthesis of Hemolymph High-Density Lipoprotein [Beta]-Glucan Binding Protein by *Penaeus Vannamei* Shrimp Hepatopancreas. *Mar. Biotechnol.* 2, 485–492. doi: 10.1007/s101260000030

Zacarias, S., Carboni, S., Davie, A., and Little, D. C. (2019). Reproductive Performance and Offspring Quality of non-Ablated Pacific White Shrimp (*Litopenaeus Vannamei*) Under Intensive Commercial Scale Conditions. *Aquaculture* 503, 460–466. doi: 10.1016/j.aquaculture.2019.01.018

Zacarias, S., Fegan, D., Wangsoontorn, S., Yamuen, N., Limakom, T., Carboni, S., et al. (2021). Increased Robustness of Postlarvae and Juveniles From non-Ablated Pacific Whiteleg Shrimp, *Penaeus Vannamei*, Broodstock Post-Challenged With Pathogenic Isolates of *Vibrio Parahaemolyticus* (VPAHPND) and White Spot Disease (WSD). *Aquaculture* 532, 736033. doi: 10.1016/j.aquaculture.2020.736033

Zhang, Q., Liu, Q., Liu, S., Yang, H., Liu, S., Zhu, L., et al. (2014). A New Nodavirus is Associated With Covert Mortality Disease of Shrimp. *J. Gen. Virol.* 95, 2700–2709. doi: 10.1099/vir.0.070078-0

Zhang, Q., Xu, T., Wan, X., Liu, S., Wang, X., Li, X., et al. (2017). Prevalence and Distribution of Covert Mortality Nodavirus (CMNV) in Cultured Crustacean. *Virus Res.* 233, 113–119. doi: 10.1016/j.virusres.2017.03.013

Zhang, X., Yuan, J., Sun, Y., Li, S., Gao, Y., Yu, Y., et al. (2019). Penaeid Shrimp Genome Provides Insights Into Benthic Adaptation and Frequent Molting. *Nat. Commun.* 10, 1–14. doi: 10.1038/s41467-018-08197-4

Zhang, H. Z., Zhu, B. S., Yu, L. Y., Liu, D. P., Wang, F., and Lu, Y. L. (2021). Selection of Shelter Shape by Swimming Crab (*Portunus Trituberculatus*). *Aquac. Rep.* 21, 100908. doi: 10.1016/j.aqrep.2021.100908

Conflict of Interest: The authors declare that the research was conducted in the absence of any commercial or financial relationships that could be construed as a potential conflict of interest.

frontiers | Frontiers in Marine Science

ORIGINAL RESEARCH
published: 31 May 2022
doi: 10.3389/fmars.2022.918449

A Discontinuous Individual Growth Model of Swimming Crab *Portunus trituberculatus* and Its Application in the Nutrient Dynamic Simulation in an Intensive Mariculture Pond

Shipeng Dong[1,2], *Xian Xu*[1,2], *Fan Lin*[3], *Liye Yu*[1,2], *Hongwei Shan*[1] *and Fang Wang*[1,2*]

[1] Key Laboratory of Mariculture, Ministry of Education, Ocean University of China, Qingdao, China, [2] Function Laboratory for Marine Fisheries Science and Food Production Processes, Qingdao National Laboratory for Marine Science and Technology, Qingdao, China, [3] Yellow Sea Fisheries Research Institute, Chinese Academy of Fishery Sciences, Qingdao, China

OPEN ACCESS

Edited by:
Yangfang Ye,
Ningbo University, China

Reviewed by:
Yongxu Cheng,
Shanghai Ocean University, China
Jia-Song Zhang,
South China Sea Fisheries Research Institute (CAFS), China

***Correspondence:**
Fang Wang
wangfang249@ouc.edu.cn

Specialty section:
This article was submitted to Marine Fisheries, Aquaculture and Living Resources, a section of the journal Frontiers in Marine Science

Received: 12 April 2022
Accepted: 03 May 2022
Published: 31 May 2022

Citation:
Dong S, Xu X, Lin F, Yu L, Shan H and Wang F (2022) A Discontinuous Individual Growth Model of Swimming Crab Portunus trituberculatus and Its Application in the Nutrient Dynamic Simulation in an Intensive Mariculture Pond. Front. Mar. Sci. 9:918449. doi: 10.3389/fmars.2022.918449

Environmental problems such as organic pollution and eutrophication caused by highly intensive mariculture activities constrain the sustainable and healthy development of industry. Therefore, it is necessary to quantify the nutrient dynamics of aquaculture animals in order to reduce the risk of environmental pollution. In this study, a discontinuous individual growth model of *Portunus trituberculatus* in an intensive mariculture pond of *P. trituberculatus–Penaeus japonicus–Sinonovacula constricta* was constructed based on a dynamic energy budget theory combined with the index of condition factor. This model better predicted the growth and molting behavior of *P. trituberculatus*, and an acceptable fit was obtained through model parameterization using the Add-my-Pet (AmP) method (mean relative error = 0.058, symmetric mean squared error = 0.007). Ten molts were simulated over 180 days and generally coincided with the recorded molt time points. Based on this model and *P. trituberculatus* populations, the dynamic processes of carbon, nitrogen, and phosphorus in ingestion, respiration, excretion, feces, residual feed, dead crabs, seeding, molt, and harvest were simulated. The carbon, nitrogen, and phosphorus ingested during the 180-day culture period were 4,938.57 kg ha^{-1}, 1,255.88 kg ha^{-1}, and 244.16 kg ha^{-1}, respectively. Carbon, nitrogen, and phosphorus removal by harvest accounted for 1.06%, 1.03% and 0.62% of the total ingestion, respectively, while carbon, nitrogen, and phosphorus removal by dead crabs accounted for 6.84%, 6.63%, and 4.04%, respectively, and carbon, nitrogen, and phosphorus released from residual feed into the water accounted for 41.43% of the total feed. The accurate simulation of molting behavior and nutrient dynamics in this study provides a theoretical basis for molting risk prevention and environmental stress assessment of *P. trituberculatus* and provides basic modules and data support for the construction of the integrated mariculture ecosystem model.

Keywords: intensive mariculture pond, nutrient dynamic simulation, discontinuous growth model, *Portunus trituberculatus* populations, molt, condition factor

INTRODUCTION

In order to secure fish supplies and reduce the global food crisis caused by the COVID-19 epidemic, intensive farming activities continue to increase around the world (Trottet et al., 2021). Intensive aquaculture involves high-density stocking and feeding of exogenous feed. The residual feed, feces, and excretion can have adverse effects on the aquaculture water bodies and the surrounding aquatic environment (e.g., water eutrophication, reduction of aquatic plant, and animal diversity) (Folke et al., 1988; Roy et al., 2020), and may also lead to food safety problems (e.g., drug residues and spread of pathogens) (Fan et al., 2011). Due to overfishing and resource decline in China, the degree of intensive mariculture of *P. trituberculatus* is increasing and the annual yield exceeds 100,000 tons (China Fishery Statistics Yearbook, 2022). In order to reduce the negative impact of intensive aquaculture activities on the environment, improve aquaculture yield and ecological benefits, and maintain sustainable development of the industry, it is necessary to construct a reasonable integrated multi-trophic aquaculture model for *P. trituberculatus* (Largo et al., 2016; Knowler et al., 2020).

As a method of long-term stable integrated aquaculture, polyculture of crab, shrimp, and shellfish reduces eutrophication and purifies water through shrimp and shellfish feeding on residual bait and feces, and shellfish filtering phytoplankton and suspended matter (Gao et al., 2008; Chang et al., 2020). In order to improve the complementarity between allotment species and main animals in terms of food and ecological niches, it is necessary to understand the growth of the animals and their impact on the environment during the aquaculture process (Reid et al., 2020). The assessment of the environmental impact of *P. trituberculatus* aquaculture has been reported in numerous papers (Zhang et al., 2015; Feng et al., 2018), but their feeding and metabolic activities have been neglected and nutrient dynamics have not been quantified well enough to accurately guide farm production. Continuous monitoring of the physiological dynamics of aquatic animals in the field is time-consuming and laborious. Because of this, individual growth models, which can reproduce the dynamics of each physiological activity in combination with environmental conditions, may be useful tools (Reid et al., 2020; Dong et al., 2022).

A dynamic energy budget (DEB) model is an individual growth model based on the physical and chemical properties of energy metabolism, which can reflect the universal laws of biological energy metabolism (Kooijman, 1986). The model not only quantifies the energy used for growth and the energy distribution throughout the life history stages (including shell and gonadal development) but can also be easily applied to the study of different species and waters (Ren and Ross, 2001; Kooijman, 2010; Sousa et al., 2010). DEB models are increasingly applied to aquatic bioenergetics and population dynamics studies to provide guidance for aquaculture and fisheries management (Spillman et al., 2008; Ren and Schiel, 2008; Orestis et al., 2019). They have been used to study some crustaceans, including the molting behavior of swimming crab *Liocarcinus depurator*, which provides the basis for their application to *P. trituberculatus* in this study (Campos et al., 2009; Talbot et al., 2019; Yang et al., 2020). However, the previous DEB model for *P. trituberculatus* only simulated growth during a single molt period, which has limited application in real production (Talbot et al., 2019).

The purpose of this study was to establish a DEB model for *P. trituberculatus* and simulate its nutrient (carbon, nitrogen, and phosphorus) dynamics based on the model, with the goal of providing important information for environmental assessment and integrated mariculture model management of *P. trituberculatus* in an intensive mariculture pond. In addition, we discussed the possibility of applying the model to carbon sink value estimation and ecosystem modeling in the future.

MATERIAL AND METHODS

DEB Model

The DEB model describes the energy allocation process of biological growth and reproduction as having three parts: 1) structural body (V), which is related to body length, metabolism, and structural maintenance; 2) storage energy (E), which is the assimilated energy that first enters a reserve compartment; and 3) energy for development and reproduction (E_R), which determines reproduction (Kooijman, 1986). Individuals ingest food in an amount proportional to the surface area of the organism and it is then converted into reserves through digestion and absorption at a constant efficiency. Stored energy comes from these reserves and is used for growth, reproduction, and maintenance of life activities based on the k-rule (Kooijman, 2010). The maintenance of structural material takes priority over growth and growth stops when food is insufficient and reserves are low.

Most standard DEB models assume continuous growth in structural volume but crustaceans are molt-growing species that initiate molting when nutrient accumulation and growth and development reach a certain level. This makes application of the DEB model to crustaceans somewhat challenging. Two key pieces of information are required to understand crustacean molt dynamics: the molt increment (MI) (i.e., the magnitude of the increase in size at molt) and the intermolt period (IP) (i.e., the length of time between two successive molts) (Chang et al., 2012). The primary factor influencing crustacean molting is the number of nutrients accumulated in the body (Abuhagr et al., 2014), and this can be assessed *via* indicators such as body weight and condition factors (Roberto and Defeo, 2002; Sharawy et al., 2019). MI and IP can be obtained from the pre- and post-molt lengths predicted by the DEB model if a threshold for nutrient accumulation at the start of the molt is available. In this study, we used condition factor (CF) (i.e., the ratio of body weight to the third power of carapace width) as an indicator of nutrient accumulation in *P. trituberculatus* to initiate molting, extending the DEB model for carapace width growth simulation (**Table 1**). When CF does not reach the molting threshold (k_{CF}), body weight will increase with the aquaculture period but carapace width will not grow. When CF reaches the

TABLE 1 | Equations describing the discontinuous individual growth model of the swimming crab *Portunus trituberculatus*.

Definition	Equation
DEB standard model	
Temperature dependence	$k(T) = k_0 \cdot \exp\left\{\frac{T_A}{T_1} - \frac{T_A}{T}\right\}$
Ingestion rate	$J_x = k(T) \cdot \{J_{xm}\} \cdot f \cdot V^{2/3}$
Assimilation rate	$P_A = AE \cdot J_X = k(T) \cdot f \cdot \{P_{Am}\} \cdot V^{2/3}$
Catabolic rate	$P_C = k(T)\frac{\frac{E}{V}}{[E_G] + \kappa \cdot \frac{E}{V}}\left(\frac{[E_G] \cdot \{P_{Am}\} \cdot V^{2/3}}{[E_M]} + [P_M] \cdot V\right)$
Maintenance rate	$P_M = k(T) \cdot [P_M] \cdot V$
Maturity maintenance rate	$P_J = k(T) \cdot \min(V, V_P) \cdot [P_M] \cdot \left(\frac{1-\kappa}{\kappa}\right)$
Reserve dynamic	$\frac{dE}{dt} = P_A - P_C$
Reproductive reserve dynamic	$\frac{dE_R}{dt} = (1-\kappa) \cdot P_c - P_J$
Biovolume growth	$\frac{dV}{dt} = \frac{\kappa \cdot P_C - P_M}{[E_G]}$
Volume	$V = \frac{E_V}{[E_G]}$
Carapace width	$CW = \frac{V^{1/3}}{\delta_m}$
Wet weight	$WW = \frac{E}{\mu_E} + \frac{\kappa_R \cdot E_R}{\mu_E} + V \cdot \rho$
Molting model	
Condition factor	$CF = \frac{WW}{CW^3} \times 100\%$
Carapace width	$\begin{cases} CW_t = CW_{t-1} & \text{if } CF < k_{CF} \\ CW_t = CW_t & \text{if } CF \geq k_{CF} \end{cases}$

molting threshold, molting occurs and the carapace width grows to the width simulated by the DEB model. According to observed data, the k_{CF} was 45% for the first 40 days and 30% for days 40 – 180.

Model Parameterisation

The parameters of the swimming crab DEB model were estimated according to the Add-my-Pet (AmP) procedure (Marques et al., 2019). The data required for parameterization included zero-variate data, univariate data, and pseudo-data. Zero-variate and univariate data were obtained from previous studies and surveys.

The physiological rate in the DEB model is temperature dependent and follows the Arrhenius relationship. The Arrhenius temperature (T_A) can be obtained from physiological experimental data describing the relationship between respiration and temperature and was estimated to be 6270 K (Dai et al., 2014; see **Figure A1**). Zero variate data related to the development and reproduction of *P. trituberculatus* were mainly obtained from fishery surveys along the Chinese coast (Dong, 2012). Univariate data for carapace width- wet weight, carapace width-age, and wet weight-age were obtained from pond aquaculture observation (Gao et al., 2016; Che et al., 2019).

Based on the completeness scale proposed by Lika et al. (2011), we assigned a completeness score of 2.5 to the data available for *P. trituberculatus*. Mean relative error (MRE) and symmetric mean squared error (SMSE) were used to assess the overall goodness of fit. The goodness-of-fit of model predictions were assessed by estimating the relative error for each zero-variate data point and univariate data set (Marques et al., 2019).

Model Application Experiment

The experimental *P. trituberculatus–Penaeus japonicus–Sinonovacula constricta* integrated multi-trophic aquaculture pond used in this study was located in Zhoushan City, Zhejiang Province, China (24°35′N, 112°7′E), and was 1.33 ha in area, with an average water depth of 1.2 m during the study period. *P. trituberculatus* with a carapace width of 0.74 ± 0.05 cm were stocked to a density of 7.5 kg·ha^{-1}. The experiment was carried out over 180 d, from June 2020 to November 2021. The water temperature in the pond was recorded continuously by a water temperature recorders (HOBO-MX2201, America). During the experiment, iced trash fish were provided daily at 17:50 and the feed level was recorded. Water was changed 1-2 times per month. The salinity range was 14.5 to 19.0. The water temperatures and feed levels are shown in **Figure A2**.

Carbon (C) and nitrogen (N) content in crab feed and feces were determined using an elemental analyzer. The samples were digested using the $HClO_4$-H_2SO_4 method. The phosphorus (P) content in feed and feces was determined using a flow injection analyzer. The energy content of the crab feed was determined using a PARR1281 oxygen bomb calorimeter.

After seeding, the growth and molting of crabs in the pond were monitored twice daily and the molting time was recorded. After molt, 30 – 50 crabs were removed and their wet weight, carapace width, and shell weight were measured. The C, N, and P contents of ground and mixed crabs were analyzed using method described above.

Simulation of Nutrient Dynamics Associated With *P. trituberculatus* Aquaculture

The simulation of nutrients dynamics associated with *P. trituberculatus* included the dynamic processes of ingestion, respiration, excretion, and feces, as well as the nutrient content of seeding, residual feed, dead crab release, molt, and harvest. The simulation of dynamic physiological processes takes into account the general temperature dependence of chemical (enzymatic) processes (Gillooly et al., 2001). Nutrient quantification based on the DEB model was scaled up to the population level based on the aquaculture density of the swimming crabs. The population density of *P. trituberculatus* was calculated as:

$$\frac{dMN}{dt} = -\delta_r \cdot MN \quad (1)$$

where MN represents the density of the swimming crabs (ind ha^{-1}), and δ_r represents their mortality (0.0253 d^{-1}).

The ingestion rate (J_x) of *P. trituberculatus* has been calculated using the individual growth model (**Table 1**). The food intake of *P. trituberculatus* was calculated according to equation (2):

$$\text{Ingestion} = \frac{J_x}{EN_{food}} \cdot MN \cdot 10^{-6} \quad (2)$$

where J_x represents the ingestion rate, which is calculated based on the DEB model and EN_{food} represents the energy content of the crab feed (20.08 J mg^{-1}). The intake of C, N, and P by *P. trituberculatus* were calculated as (kg ha^{-1} d^{-1}):

$$C_{Inge} = \text{Ingestion} \cdot C_{food} \quad (3)$$

$$N_{Inge} = \text{Ingestion} \cdot N_{food} \quad (4)$$

$$P_{Inge} = \text{Ingestion} \cdot P_{food} \quad (5)$$

where C_{food}, N_{food}, and P_{food} represent the C, N, and P contents of the crab feed (36.61%, 9.31%, and 1.81%, respectively).

In intensive aquaculture, exogenous feed is typically provided in large quantities and adjusted to the culture period. The unconsumed food was calculated according to equation (6):

$$Food_{wast} = Food_w - \text{Ingestion} \quad (6)$$

where $Food_w$ represents the daily crab feeding level (kg d^{-1} ha^{-1}). The C, N, and P content of unconsumed food (kg d^{-1} ha^{-1}) were calculated as:

$$C_{wast} = Food_{wast} \cdot C_{food} \quad (7)$$

$$N_{wast} = Food_{wast} \cdot N_{food} \quad (8)$$

$$P_{wast} = Food_{wast} \cdot P_{food} \quad (9)$$

Swimming crabs also affect the environment through respiration and excretion. Respiration rate is proportional to the catabolic rate (P_c, J d^{-1}), (Pouvreau et al., 2006). The amount of C released through respiration by *P. trituberculatus* was calculated as (kg ha^{-1} d^{-1}):

$$C_{resp} = \frac{P_C}{\eta} \cdot 0.375 \cdot MN \cdot 10^{-6} \quad (10)$$

where η is a constant for converting oxygen to energy equivalents and equals 14.3 J mg^{-1} O_2 (Gnaiger and Forstner, 1983) and 0.375 is the ratio of molecular weights used to transform O_2 in C. The amount of N and P released through excretion was calculated as (kg ha^{-1} d^{-1}):

$$N_{excr} = JmgC^{-1} \cdot \left(\frac{N}{C}\right)_{crab} \cdot (P_M + (1-\kappa_R) \cdot \left[(1-\kappa) \cdot P_C - P_J\right] + P_J + \frac{[E_G]-[E_V]}{[E_G]} \cdot (\kappa \cdot P_C - P_J)) \cdot MN \cdot 10^{-6} \quad (11)$$

$$P_{excr} = N_{excr} \cdot \left(\frac{P}{N}\right)_{excr} \quad (12)$$

where JmgC is the ratio of carbon to energy value of the crab feed (55 J mg C^{-1}).$(\frac{N}{C})_{crab}$represents the ratio of nitrogen and carbon in crab (0.247 mg N mg C^{-1}) and $(\frac{P}{N})_{excr}$ represents the ratio of phosphorus and nitrogen in excreta (0.0653 mg P mg N^{-1}).*P. trituberculatus* feces is the main source of nutrients in pond sediment. The fecal wastes were calculated as (kg ha^{-1} d^{-1}):

$$\text{Egestion} = \frac{(1-ae) \cdot J_x}{EN_{food}} \cdot MN \cdot 10^{-6} \quad (13)$$

where ae represents the assimilation efficiency (0.8). The amount of C, N, and P released into the pond by the crab feces was calculated as (kg ha^{-1} d^{-1}):

$$C_{egest} = \text{Egestion} \cdot C_{food} \quad (14)$$

$$N_{egest} = \text{Egestion} \cdot N_{food} \quad (15)$$

$$N_{egest} = \text{Egestion} \cdot N_{food} \quad (16)$$

Dead crabs need to be removed daily to prevent them from remaining decomposing in the water column and causing deterioration of the water quality. Based on their mortality rate, the C, N, and P contents of dead *P. trituberculatus* were calculated as (kg ha^{-1}):

$$C_{death} = WW \cdot \delta_r \cdot C_{crab} \cdot MN \cdot 10^{-6} \quad (17)$$

$$N_{death} = WW \cdot \delta_r \cdot N_{crab} \cdot MN \cdot 10^{-6} \quad (18)$$

$$P_{death} = WW \cdot \delta_r \cdot P_{crab} \cdot MN \cdot 10^{-6} \quad (19)$$

where C_{crab}, N_{crab}, and P_{crab} represent the C, N, and P contents of the crab (6.16%, 1.52%, and 0.18%, respectively).

Nitrogen and phosphorus levels in the water are also influenced by *P. trituberculatus* molting. Ten molts were simulated in this study, and the amounts of N and P released during each molt were estimated using the following equations (kg ha^{-1}):

$$N_{molt} = WW \cdot \delta_S \cdot N_{shell} \cdot MN \cdot 10^{-6} \quad (20)$$

$$P_{molt} = WW \cdot \delta_S \cdot P_{shell} \cdot MN \cdot 10^{-6} \quad (21)$$

where δ_S represents the ratio of shell weight to body weight (9.82%). N_{shell} and P_{shell} represent the N and P contents of crab shells (7.15% and 0.55%, respectively).

The C, N, and P contents of *P. trituberculatus* seeding and harvest were calculated as (kg ha^{-1}):

$$C_{seed} = MN_0 \cdot WW_0 \cdot C_{crab} \cdot 10^{-6} \quad (22)$$

$$N_{seed} = MN_0 \cdot WW_0 \cdot N_{crab} \cdot 10^{-6} \quad (23)$$

$$P_{seed} = MN_0 \cdot WW_0 \cdot P_{crab} \cdot 10^{-6} \quad (24)$$

$$C_{harv} = MN_{180} \cdot WW_{180} \cdot C_{crab} \cdot 10^{-6} \quad (25)$$

$$N_{harv} = MN_{180} \cdot WW_{180} \cdot N_{crab} \cdot 10^{-6} \quad (26)$$

$$P_{harv} = MN_{180} \cdot WW_{180} \cdot P_{crab} \cdot 10^{-6} \quad (27)$$

where MN_0 and WW_0 represent the density and wet weight of crab at the time of seeding, respectively. MN_{180} and WW_{180} represent the density and wet weight of crab at the time of harvest, respectively.

RESULTS

Model Parameters

The results of the predicted zero-variate values for swimming crab based on the AmP procedure are listed in **Table 2**. The DEB parameters were estimated at a reference temperature of 20°C (**Table 3**). The parameter estimation resulted in acceptable goodness-of-fit with MRE = 0.058 and SMSE = 0.007. The model underestimated the age at birth and life span and overestimated the length at end acceleration and ultimate length. The predicted value of the ultimate reproduction rate was in general agreement with the observed value. (http://www.bio.vu.nl/thb/deb/deblab/add_my_pet/entries_web/Portunus_trituberculatus/Portunus_trituberculatus_res)

Model Validation

Simulated and observed growth conditions and the molting behavior of swimming crabs from June to November are shown in **Figure 1**. The simulation was generally consistent with the observed results, indicating that the model accurately simulated the variation in wet weight and carapace width of *P. trituberculatus*. Ten molts were simulated over 180 days and this was equal to the number of molts observed and generally coincided with the recorded molt time points. The simulated molting cycle time lengthened with each stage, from 4 days for juvenile crabs in stages I – II (Observed days: 4), 12 days for juveniles in stages V – VI (Observed days: 11), and 38 days for adults in stages X – XI (Observed days: 36) (**Figure 1A**).

Simulation of Carbon, Nitrogen, and Phosphorus Dynamics Associated With *P. trituberculatus* Aquaculture

The simulation of nutrients dynamics associated with *P. trituberculatus* aquaculture (ingestion, respiration, excretion and feces) is shown in **Figure 2**. The dynamics of C, N, and P involved showed an overall trend of rising and then falling, with a maximum in August. In addition, the trend fluctuated significantly in August due to the high temperature.

The C, N, and P released during molts are shown in **Table 4**. The highest N and P release occurred during the ninth molt, and prior to the last molt, N and P release increased with the number of molts. The total amount of nitrogen and phosphorus released during the last five molts was close to 90% of the total release.

Figure 3 shows the C, N, and P fluxes associated with *P. trituberculatus* aquaculture over the six months rearing cycle including seeding and harvest. The C, N, and P introduced at seeding were 0.46 kg ha^{-1}, 0.11 kg ha^{-1} and 0.01 kg ha^{-1}, respectively.

TABLE 3 | The parameter values of the DEB model for swimming crab *Portunus trituberculatus* at 20°C.

symbol	value	unit	parameter
$[E_G]$	4445	J cm^{-3}	volume-specific costs for structure
$[E_V]$	3556	J cm^{-3}	volume-specific energy of structure
$[E_M]$	42113	J cm^{-3}	maximum storage density
k	0.99	–	fraction of catabolic flux to growth and maintenance
k_R	0.95	–	fraction of reproductive reserves
δ_M	0.4284	–	shape coefficient
$\{J_{Xm}\}$	6062	J cm^{-2} d^{-1}	maximum feeding rate per unit body surface area
$\{P_{AM}\}$	4805	J cm^{-2} d^{-1}	maximum surface area-specific assimilation rate
$[P_M]$	434	J cm^{-3} d^{-1}	volume-specific maintenance rate
T_1	293	K	reference temperature
T_A	6270	K	Arrhenius temperature
k_0	1	–	reference physiological reaction rate at 293K
μ_E	48200	J g^{-1}	energy content of reserves
ρ	1	g cm^{-3}	volume-specific wet flesh weight

The C, N, and P ingested during the 180-day culture period were 4,938.57 kg ha^{-1}, 1,255.88 kg ha^{-1}, and 244.16 kg ha^{-1}, respectively, of which approximately 1.06%, 1.03%, and 0.62% were removed by harvest and 6.84%, 6.63%, and 4.04% were removed by dead crabs. Overall, 44.46% of the N and 28.43% of the P were released as excretion, feces, and molts. The C, N, and P released from the residual feed accounted for 41.43% of the total feed. The C, N, and P released into the water (excluding dead crabs and harvest) during the 180-day aquaculture period were 4,480.53 kg ha^{-1}, 1,446.60 kg ha^{-1}, and 242.09 kg ha^{-1}, respectively.

DISCUSSION

The Discontinuous Individual Growth Model

Traditionally, the parameterization of the DEB model relies on a large number of physiological experiments on individuals held in standard conditions including controlled temperature (Ren and Schiel, 2008; Serpa et al., 2013). As an economically important farmed crab in China, studies on *P. trituberculatus* have focused on biological surveys, genetic breeding, and farming techniques (Lv et al., 2014; Wang et al., 2018; Duan et al., 2021), lacking sufficient physiological information (e.g., starvation experiments). The AmP procedure allows us to estimate parameters for a species for which limited physiological data is available (Lika et al., 2011; Ren et al., 2020) because it allows us to estimate model parameters according to biological (zero-variate data) and growth characteristics (univariate data). Complete zero-variate data include age, length at birth, weight,

TABLE 2 | Zero-variate data used for estimating parameters of the swimming crab *Portunus trituberculatus* DEB model. Observed data and relative error (RE) are specified.

Symbol	Unit	Obervation	Prediction	parameter	RE	Reference
a_b	d	7.0	6.5	age at birth	0.067	(Dong, 2012)
a_m	d	730	720	life span	0.014	(Dong, 2012)
L_j	cm	0.383	0.394	length at end acceleration	0.028	(Gao et al., 2016)
L_i	cm	25.0	26.2	ultimate length	0.047	(Wiki)
R_i	#d^{-1}	7296	7154	ultimate reproduction rate	0.019	(Dong, 2012)

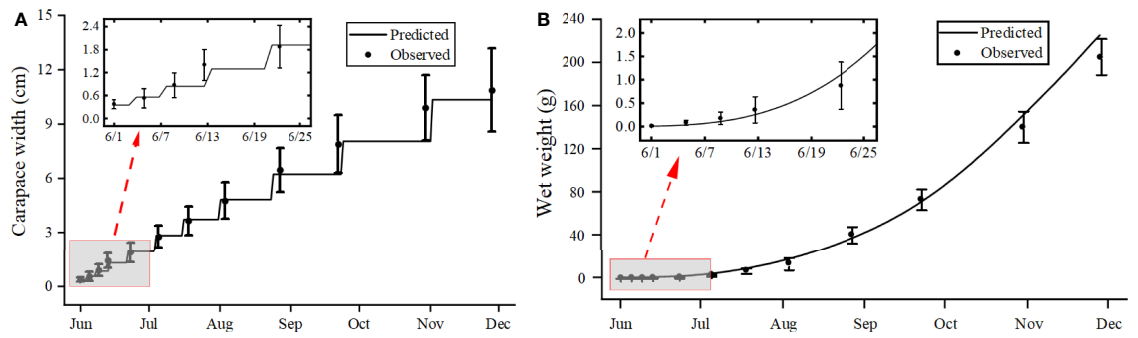

FIGURE 1 | Comparison of observations (circles with bars for standard deviation) and simulations (lines) of carapace width **(A)** and wet weight **(B)** of the swimming crab *Portunus trituberculatus*.

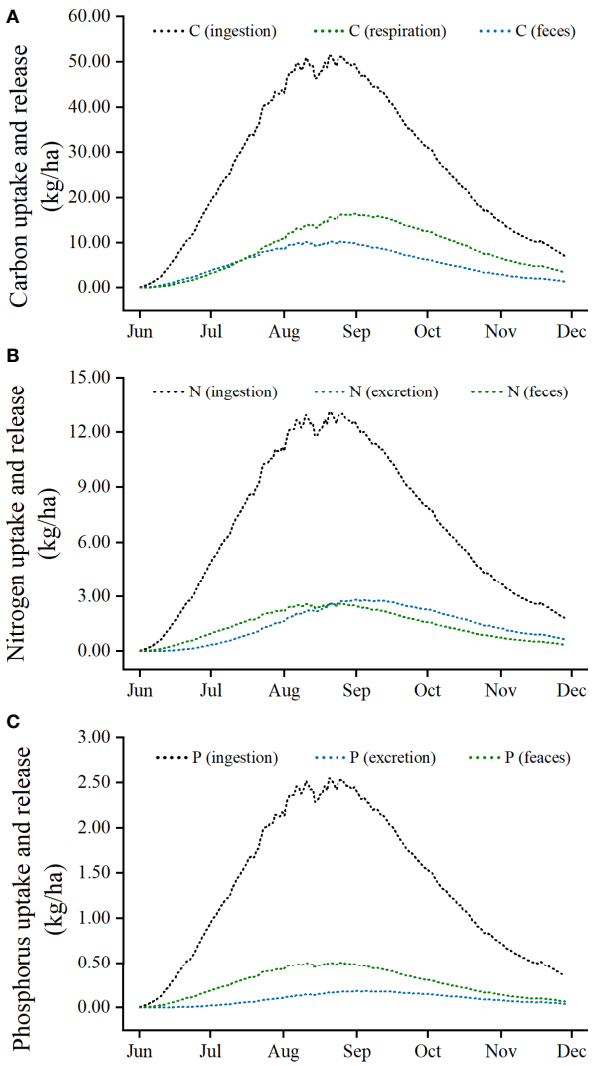

FIGURE 2 | Simulation of carbon **(A)**, nitrogen **(B)**, and phosphorus **(C)** dynamics associated with *Portunus trituberculatus* aquaculture.

maturation temperature, lifespan, ultimate length, and ultimate weight. Inadequate accumulation of relevant knowledge may affect the accuracy of some of these parameters (Marques et al., 2018). Another advantage of the AmP method is that MRE and SMSE can be used to check the veracity of the data (Marques et al., 2019) and the simulated and predicted values of the parameters in this study show a high match (**Table 2**), indicating that the model parameters are reasonable and valid.

More than 1,000 papers have been published on DEB theory (https://www.zotero.org/groups/500643/deb_library/library), which is widely used in aquaculture for finfish, bivalves, shrimp (Cheng et al., 2018; Dambrine et al., 2020; Yang et al., 2020), and swimming crab *L. depurator* (Talbot et al., 2019). This study showed that the DEB model can be applied to *P. trituberculatus* in integrated aquaculture ponds (**Figure 1**). The DEB model predicts individual growth based on food and water temperature dynamics. In the DEB model, food condition f (range: 0 – 1) is used to represent food availability (density and mass), whereas typically the unstable food condition of bivalves, which is usually set to a fixed value in models of finfish, shrimp, and other cast-feeding farming animals, is used (Campos et al., 2009; Ren et al., 2020). This study included values of f ranging from the lowest food scenario ($f = 0$) to arbitrary feeding ($f = 1$), and the results show that the most growth occurred at f = 1, indicating adequate and high-quality feed in the experimental pond (Haberle et al., 2020). DEB theory uses the Arrhenius equation to describe the effect of changing temperature on the rate of individual physiological responses (Kooijman, 2010). *P. trituberculatus* is a eurythermic species but temperature changes have a large effect on its metabolism (Lu et al., 2015). Although the water temperature in the experimental ponds fluctuated within 10°C, the temperature dependence function of the *P. trituberculatus* DEB model showed a significant difference in August (high temperature: 29.1 – 30.70 °C) and November (low temperature: 21.70 – 24.40 °C) (**Figure A3**).

The molting period of crustaceans is often accompanied by unstable ingestion and metabolism, cannibalism, and other phenomena (Su et al., 2019). During the molting period, good feed and water quality and nutrient supplementation can help ensure a successful molt. This makes molting prediction an important prerequisite for crustacean aquaculture management (Lemos and Weissman, 2020; Liu et al., 2021). The application of

TABLE 4 | Carbon, nitrogen, and phosphorus released during the molting of *Portunus trituberculatus*.

Period	I – II	II – III	III – IV	IV – V	V – VI	VI – VII	VII – VIII	VIII – IX	IX – X	X – XI
Nitrogen release (g ha^{-1} $180d^{-1}$)	33	121	413	1166	2936	5067	7506	9352	9565	7900
Phosphorus release (g ha^{-1} $180d^{-1}$)	3	9	32	90	226	390	577	719	736	608

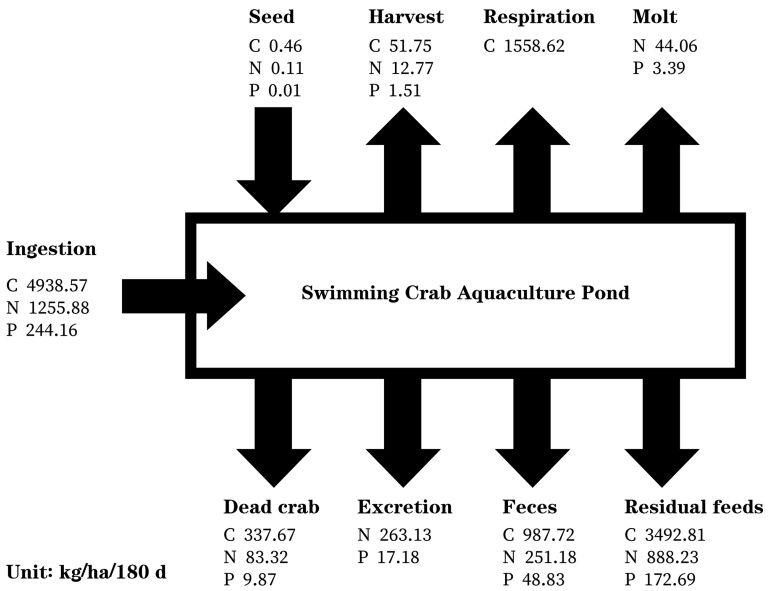

FIGURE 3 | Carbon (C), nitrogen (N), and phosphorus (P) budgets associated with *Portunus trituberculatus* aquaculture over the six months rearing cycle.

a discontinuous growth model based on mathematical functions and probability statistics to *P. trituberculatus* showed satisfactory results (Wang, 2017). The discontinuous growth and periodic loss of calcified structures due to molt make a growth modeling approach based on individual physiological and ecological characteristics inappropriate for crustaceans and most studies ignore molting behavior (Campos et al., 2009; Yang et al., 2020). In the swimming crab DEB model, Talbot et al. (2019) substituted wet weight for structural volume and established a logical relationship with physiological rates in the standard model to complete molt predictions within a single molt cycle. As a comprehensive index to determine the physiological and nutritional states of animals, the condition factor has been used as an important predictor of molt in crustaceans such as penaeid shrimp (*Farfantepenaeus aztecus*, *F. brasiliensis*, *F. duorarum*, and *F. notialis*), brown shrimp (*Crangon crangon*) and Chinese mitten crab (*Eriocheir sinensis*) (Roberto and Defeo, 2002; Chen et al., 2016; Sharawy et al., 2019). The results of this study showed that the growth model of *P. trituberculatus* could accurately predict molt (**Figure 1A**), but molt was also influenced by the environment (temperature, precipitation, etc.). Because these environmental factors are uncontrollable outside of experimental settings, the stability of the model needs further validation. In addition, shell mineralization in shrimp and crabs can play a role in carbon sequestration (Troell et al., 2009), and the successful simulation of molting behavior can provide a reference for carbon sink value estimation of crustaceans.

Nutrient Dynamics Simulation

By using the ecologically complementary habits of different farming organisms and making full use of system materials and energy, the integrated aquaculture model helps to improve economic efficiency and reduce farming pollution (Troell et al., 2003). In China, the shrimp-crab and shrimp-crab-shellfish integrated aquaculture model has become the main farming model for *P. trituberculatus*. However, the existing studies on intensive ponds of *P. trituberculatus* have focused on the overall static carbon, nitrogen, and phosphorus budget and have not quantified nutrient dynamics associated with the aquaculture process (Dong et al., 2013; Zhang et al., 2016). Considering that the simulation of nutrient dynamics at the population level is more meaningful than at the individual level, this study combined the DEB model with the crab density to model the population dynamics of *P. trituberculatus* (**Figure A3**) and simulated the related nutrient dynamic processes (**Figure 2**). The patterns of carbon, nitrogen, and phosphorus uptake and release caused by the ingestion and metabolism of the swimming crabs in the experiment were determined by density changes and fluctuated in July and August due to the frequency of hot weather in summer that reduced physiological activity (Lu et al., 2015).

The assessment of the carbon, nitrogen, and phosphorus budget in the ecosystem is an effective method to evaluate nutrient utilization, energy conversion efficiency and pollution levels in aquaculture ponds (Guo et al., 2017). The results showed that ≤ 8% of the carbon, nitrogen, and phosphorus in feed was converted to swimming crab (including harvested and dead crabs), with most of the remainder being released into the aquaculture environment in the form of excretion, feces, and molts. Meanwhile, 41% of the nutrients in the feed were not consumed by *P. trituberculatus* and was discharged into the aquaculture water environment in the form of residual feed, resulting in 4,480.53 kg ha^{-1}, 1,446.60 kg ha^{-1} and 242.09 kg ha^{-1} of carbon, nitrogen, and phosphorus being retained in the water. Aquaculture discharges can raise the nutrient load of nearby waters and lead to water eutrophication (Herbeck et al., 2013). We have combined Japanese shrimp and razor clams in the *P. trituberculatus* aquaculture system to improve food resource utilization, increase farm production, and reduce the negative environmental impact of farming activities. Of course, assessing the carrying capacity and proportion of farming organisms in an integrated aquaculture system requires long-term dynamic simulation and analysis. In a follow-up study, we will couple the simulation of *P. trituberculatus* nutrient dynamics to an ecosystem model for ecosystem-level assessment of carrying capacity and environmental pollution to provide scientific and precise management information for integrated aquaculture activities.

CONCLUSIONS

The discontinuous growth model established in this study will accurately relay the growth and molting behavior of *P. trituberculatus*, and provide support for a series of techniques such as seeding, feeding, water quality control, and molting management in intensive mariculture. The assessment of nutrient dynamics, in combination with population dynamics and physiological activities, can provide technical guidance for integrated aquaculture practices and help achieve environmental and economic sustainability. This model can not only be used independently for mariculture assessment but can also be combined into an ecological model of an integrated multi-trophic aquaculture ecosystem in order to assess the potential impacts of aquaculture on a larger spatial scale.

DATA AVAILABILITY STATEMENT

The original contributions presented in the study are included in the article/**Supplementary Material**. Further inquiries can be directed to the corresponding author.

AUTHOR CONTRIBUTIONS

SD, XX, and FL designed the experiments and wrote the manuscript. LY and HS performed the experiments. FW supervised and validated the manuscript. All authors contributed to the article and approved the submitted version.

FUNDING

This study was funded by the National Key Research and Development Program of China (2019YFD0900402) and the Yellow River Delta Industry Leading Talents Project.

SUPPLEMENTARY MATERIAL

The Supplementary Material for this article can be found online at: https://www.frontiersin.org/articles/10.3389/fmars.2022.918449/full#supplementary-material

REFERENCES

Abuhagr, A. M., Blindert, J. L., Nimitkul, S., Zander, I. A., LaBere, S. M., Chang, S. A., et al. (2014). Molt Regulation in Green and Red Color Morphs of the Crab *Carcinus Maenas*: Gene Expression of Molt-Inhibiting Hormone Signaling Components. *J. Exp. Biol.* 217, 976–808. doi: 10.1242/jeb.093385

Campos, J., Veer, H., Freitas, V., and Kooijman, S. (2009). Contribution of Different Generations of the Brown Shrimp Crangon Crangon (L.) in the Dutch Wadden Sea to Commercial Fisheries: A Dynamic Energy Budget Approach. *J. Sea. Res.* 62, 106–113. doi: 10.1016/j.seares.2009.07.007

Chang, Z. Q., Neori, A., He, Y. Y., Li, J. T., Qiao, L., Preston, S. I., et al. (2020). Development and Current State of Seawater Shrimp Farming, With an Emphasis on Integrated Multi-Trophic Pond Aquaculture Farms, in China - a Review. *Rev. Aquacult.* 12, 2544–2558. doi: 10.1111/raq.12457

Chang, Y. J., Sun, C. L., Chen, Y., and Yeh, S. Z. (2012). Modelling the Growth of Crustacean Species. *Rev. Fish. Biol. Fisher.* 22, 157–187. doi: 10.1007/s11160-011-9228-4

Che, J., Liu, M. M., Hou, W. J., Dong, Z. G., Yang, S., Cheng, Y. X., et al. (2019). Growth and Gonadal Development of Pond-Reared Male Swimming Crab, *Portunus Trituberculatus*. *Chin. J. Zool.* 54, 347–361. doi: 10.13859/j.cjz.201903005

Cheng, M., Tan, A., Rinaldi, A., Giacoletti, A., Sarà, G., and Williams, G. A. (2018). Predicting Effective Aquaculture in Subtropical Waters: A Dynamic Energy Budget Model for the Green Lipped Mussel, *Perna Viridis*. *Aquaculture* 495, 749–756. doi: 10.1016/j.aquaculture.2018.04.008

Chen, J., Yue, W. C., Chen, X. W., Ci, Y. J., Huang, Z., Wang, J., et al. (2016). Observation on Individual Molting, Growth and Association Analysis With Relative Gene Expression in Chinese Mitten Crab (*Eriocheir Sinensis*). *Chin. J. Zool.* 51, 1059–1070. doi: 10.13859/j.cjz.201606014

China Fishery Statistics Yearbook. (2022). Department of Agriculture, Fisheries Bureau. China Fishery Statistics Yearbook. Beijing, China: Agricultural Press.

Dai, C., Wang, F., Fang, Z. H., and Dong, S. L. (2014). Effects of Temperature on the Respiratory Metabolism and Activities of Related Enzymes of Swimming Crab *Portunus Trituberculatus*. *Prog. Fish. Sci.* 35, 90–96. doi: 10.3969/j.issn.1000-7075.2014.02.013

Dambrine, C., Huret, M., Woillez, M., Pecquerie, L., Allal, F., Servili, A., et al. (2020). Contribution of a Bioenergetics Model to Investigate the Growth and Survival of European Seabass in the Bay of Biscay E English Channel Area. *Ecol. Model.* 423, 109007. doi: 10.1016/j.ecolmodel.2020.109007

Dong, Z. G. (2012). *The Study on Morphology, Biochemistry, Molecular Phylogeography and Genetic Diversity of the Swimming Crab Along Portunus Trituberculatus China Coast* (Ph.D. Dissertation. Shanghai: Shanghai Ocean University).

Dong, J., Tian, X. L., Dong, S. L., Zhang, K., Feng, J., and He, R. P. (2013). Study on Nitrogen and Phosphorus Budget in Polyculture Systems of *Litopenaeus Vannamei* and *Portunus Trituberculatus*. *Periodic. Ocean. Univ. China* 43, 16–24. doi: 10.16441/j.cnki.hdxb.2013.12.003

Dong, S. P., Wang, F., Zhang, D. X., Yu, L. Y., Pu, W. J., and Shang, Y. K. (2022). Growth Performance and Ecological Services Evaluation of Razor Clams Based on Dynamic Energy Budget Model. *J. Environ. Manage.* 306, 114392. doi: 10.1016/j.jenvman.2021.114392

Duan, H. B., Mao, S., Xia, Q., Ge, H. X., Liu, M. M., Li, W. Q., et al. (2021). Comparisons of Growth Performance, Gonadal Development and Nutritional Composition Among Monosex and Mixed-Sex Culture Modes in the Swimming Crab (*Portunustrituberculatus*). *Aquac. Res.* 52, 3403–3414. doi: 10.1111/are.15185

Fan, L. M., Wu, W., Hu, G. D., Qu, J. H., Meng, S. L., Qiu, L. P., et al. (2011). Preliminary Exploration on Assessment of Intensive Pond Ecosystem Health. *Chin. Agric. Sci. Bull.* 27, 395–399. doi: 10.1016/S1671-2927(11)60313-1

Feng, J., Tian, X. L., Dong, S. L., He, R. P., Zhang, K., Zhang, D. X., et al. (2018). Comparative Analysis of the Energy Fluxes and Trophic Structure of Polyculture Ecosystems of *Portunus Trituberculatus* Based on Ecopath Model. *Aquaculture* 496, 185–196. doi: 10.1016/j.aquaculture.2018.07.020

Folke, C., Kautsky, N., Berg, H., Jansson, Å., and Troell, M. (1988). The Ecological Footprint Concept for Sustainable Seafood Production—a Review. *Ecol. Appl.* 8, 63–71. doi: 10.1016/j.aquaculture.2018.07.020

Gao, T. L., Wang, Y. F., Bao, X. N., Ren, Z. M., Mu, C. K., and Wang, C. L. (2016). Study on the Characteristics of Molting and Growth of *Portunus Trituberculatus* Cultured in Single Individual Basket. *J. Biol.* 33, 41–46. doi: 10.3969/j.issn.2095-1736.2016.03.041

Gao, Q. F., Xu, W. Z., Liu, X. S., Cheung, S. G., and Shin, P. K. S. (2008). Seasonal Changes in C, N and P Budgets of Green-Lipped Mussels *Perna Viridis* and Removal of Nutrients From Fish Farming in Hong Kong. *Mar. Ecol. Prog. Ser.* 353, 137–146. doi: 10.3354/meps07162

Gillooly, J. F., Brown, J. H., West, G. B., Savage, V. M., and Charnov, E. L. (2001). Effects of Size and Temperature on Metabolic Rate. *Science* 293, 2248–2251. doi: 10.1126/science.1061967

Gnaiger, E., and Forstner, H. (1983). *Polarographic Oxygen Sensors: Aquatic and Physiological Applications* (Berlin: Springer), XII, 370 pp.

Guo, K., Zhao, W., Jiang, Z. Q., and Dong, S. L. (2017). A Study of Organic Carbon, Nitrogen and Phosphorus Budget in Jellyfish-Shellfish-Fish-Prawn Polyculture Ponds. *Aquac. Res.* 48, 68–76. doi: 10.1111/are.12861

Haberle, J., Marn, N., Gecek, S., and Klanjek, S. (2020). Dynamic Energy Budget of Endemic and Critically Endangered Bivalve Pinna Nobilis: A Mechanistic Model for Informed Conservation. *Ecol. Model* 434, 109207. doi: 10.1016/j.ecolmodel.2020.109207

Herbeck, L. S., Unger, D., Wu, Y., and Jennerjahn, T. C. (2013). Effluent, Nutrient and Organic Matter Export From Shrimp and Fish Ponds Causing Eutrophication in Coastal and Back-Reef Waters of NE Hainan, Tropical China. *Cont. Shelf. Res.* 57, 92–104. doi: 10.1016/j.csr.2012.05.006

Knowler, D., Chopin, T., Martinez-Espineira, R., Neori, A., Nobre, A., Noce, A., et al. (2020). The Economics of Integrated Multi-Trophic Aquaculture: Where are We Now and Where Do We Need to Go? *Rev. Aquacult.* 12, 1–16. doi: 10.1111/raq.12399

Kooijman, S. A. L. M. (1986). "Population Dynamics on the Basis of Budgets," in *The Dynamics of Physiologically Structured Populations, 68*. Eds. J. A. J. Metz and O. Diekmann (Heidelberg/Berlin/NY: Springer-Verlag), 266–297.

Kooijman, S. A. L. M. (2010). *Dynamic Energy Budget Theory for Metabolic Organisation* (Cambridge: Cambridge University Press).

Largo, D. B., Diola, A. G., and Marababol, M. S. (2016). Development of an Integrated Multi-Trophic Aquaculture (IMTA) System for Tropical Marine Species in Southern Cebu, Central Philippines. *Aquacult. Rep.* 3, 67–76. doi: 10.1016/j.aqrep.2015.12.006

Lemos, D., and Weissman, D. (2020). Moulting in the Grow-Out of Farmed Shrimp: A Review. *Rev. Aquacult.* 13, 5–17. doi: 10.1111/raq.12461

Lika, K., Kearney, M. R., Freitas, V., van der Veer, H. W., van der Meer, J., Wijsman, J. W. M., et al. (2011). The "Covariation Method" for Estimating the Parameters of the Standard Dynamic Energy Budget Model I: Philosophy and Approach. *J. Sea. Res.* 66, 270–277. doi: 10.1016/j.seares.2011.07.010

Liu, S., Wang, X., Bu, X., Zhang, C., and Chen, L. (2021). Influences of Dietary Vitamin D3 on Growth, Antioxidant Capacity, Immunity and Molting of Chinese Mitten Crab (*Eriocheir Sinensis*) Larvae. *J. Steroid. Biochem.* 210, 105862. doi: 10.1016/j.seares.2011.09.004

Lu, Y. L., Wang, F., and Dong, S. L. (2015). Energy Response of Swimming Crab *Portunus Trituberculatus* to Thermal Variation: Implication for Crab Transport Method. *Aquaculture* 441, 64–71. doi: 10.1016/j.aquaculture.2015.02.022

Lv, J. J., Liu, P., Gao, B. Q., Wang, Y., Wang, Z., Chen, P., et al. (2014). Transcriptome Analysis of the *Portunus Trituberculatus: De Novo* Assembly, Growth-Related Gene Identification and Marker Discovery. *PloS One* 9, e94055. doi: 10.1371/journal.pone.0094055

Marques, G. M., Augustine, S., Lika, K., Pecquerie, L., Domingos, T., and Kooijman, S. A. L. M. (2018). The Amp Project: Comparing Species on the Basis of Dynamic Energy Budget Parameters. *Plos. Comput. Biol.* 14, e1006100. doi: 10.1371/journal.pone.0094055

Marques, G. M., Lika, K., Augustine, S., Pecquerie, L., and Kooijman, S. A. L. M. (2019). Fitting Multiple Models to Multiple Data Sets. *J. Sea. Res.* 143, 48–56. doi: 10.1016/j.seares.2018.07.004

Orestis, S. Z., Nikos, P., and Konstadia, L. (2019). A DEB Model for European Sea Bass (*Dicentrarchus Labrax*): Parameterisation and Application in Aquaculture. *J. Sea. Res.* 143, 262–271. doi: 10.1016/j.seares.2018.05.008

Pouvreau, S., Bourlès, Y., Lefebvre, S., Gangnery, A., and Alunno-Bruscia, M. (2006). Application of a Dynamic Energy Budget Model to the Pacific Oyster, *Crassostrea Gigas*, Reared Under Various Environmental Conditions. *J. Sea. Res.* 56, 156–167. doi: 10.1016/j.seares.2006.03.007

Reid, G. K., Lefebvre, S., Filgueira, R., Robinson, S. M. C., Broch, O. J., Dumas, A., et al. (2020). Performance Measures and Models for Open-Water Integrated Multi-Trophic Aquaculture. *Rev. Aquacult.* 12, 47–75. doi: 10.1111/raq.12304

Ren, J. S., Jin, X. S., Yang, T., Kooijman, S., and Shan, X. J. (2020). A Dynamic Energy Budget Model for Small Yellow Croaker *Larimichthys Polyactis*: Parameterisation and Application in its Main Geographic Distribution Waters. *Ecol. Model.* 427, 109051. doi: 10.1016/j.ecolmodel.2020.109051

Ren, J. S., and Ross, A. H. (2001). A Dynamic Energy Budget Model of the Pacific Oyster *Crassostrea Gigas*. Ecol. *Model.* 142, 105–120. doi: 10.1016/S0304-3800(01)00282-4

Ren, J. S., and Schiel, D. R. (2008). A Dynamic Energy Budget Model: Parameterisation and Application to the Pacific Oyster *Crassostrea Gigas* in New Zealand Waters. *J. Exp. Mar. Biol. Ecol.* 361, 42–48. doi: 10.1016/j.jembe.2008.04.012

Roberto, P. C., and Defeo, O. (2002). Morphometric Relationships of Penaeid Shrimps in a Coastal Lagoon: Spatio-Temporal Variability and Management Implications. *Estuar. Coast.* 25, 282–287. doi: 10.1007/BF02691315

Roy, K., Vrba, J., Kaushik, S. J., and Mraz, J. (2020). Feed-Based Common Carp Farming and Eutrophication: Is There a Reason for Concern? *Rev. Aquacult.* 12, 1–23. doi: 10.1111/raq.12407

Serpa, D., Ferreira, P. P., Ferreira, H., Fonseca, L., Dinis, M. T., and Duarte, P. (2013). Modelling the Growth of White Seabream (*Diplodus Sargus*) and Gilthead Seabream (*Sparus Aurata*) in Semi-Intensive Earth Production Ponds Using the Dynamic Energy Budget Approach. *J. Sea. Res.* 76, 135–145. doi: 10.1016/j.seares.2012.08.003

Sharawy, Z. Z., Hufnagl, M., and Temming, A. (2019). A Condition Index Based on Dry Weight as a Tool to Estimate *in-Situ* Moult Increments of Decapod Shrimp: Investigating the Effects of Sex, Year and Measuring Methods in Brown Shrimp (*Crangon Crangon*). *J. Sea. Res.* 152, 101762. doi: 10.1016/j.seares.2019.05.004

Sousa, T., Domingos, T., Poggiale, J. C., Poggiale, J. C., and Kooijman, S. A. L. M. (2010). Dynamic Energy Budget Theory Restores Coherence in Biology. *Philos. T. R. Soc. B.* 365, 3413–3428. doi: 10.1098/rstb.2010.0166

Spillman, C. M., Hamilton, D. P., Hipsey, M. R., and Imberger, J. (2008). A Spatially Resolved Model of Seasonal Variations in Phytoplankton and Clam (*Tapes Philippinarum*) Biomass in Barbamarco Lagoon, Italy. *Estuar. Coast. Shelf. S.* 79, 187–203. doi: 10.1016/j.ecss.2008.03.020

Su, X., Liu, J., Wang, F., Wang, Q., and Liu, D. (2019). Effect of Temperature on Agonistic Behavior and Energy Metabolism of the Swimming Crab (*Portunus Trituberculatus*). *Aquaculture* 516, 734573. doi: 10.1016/j.aquaculture.2019.734573

Talbot, S. E., Widdicombe, S., Hauton, C., and Bruggeman, J. (2019). Adapting the Dynamic Energy Budget (DEB) Approach to Include non-Continuous Growth

(Moulting) and Provide Better Predictions of Biological Performance in Crustaceans. *ICES. J. Mar. Sci.* 76, 192–205. doi: 10.1093/icesjms/fsy164

Troell, M., Halling, C., Neori, A., Chopin, T., Buschmann, A. H., Kautsky, N., et al. (2003). Integrated Mariculture: Asking the Right Questions. *Aquaculture* 226, 59–90. doi: 10.1016/S0044-8486(03)00469-1

Troell, M., Joyce, A., Chopin, T., Neori, A., Buschmann, A. H., and Fang, J. G. (2009). Ecological Engineering in Aquaculture — Potential for Integrated Multi-Trophic Aquaculture (IMTA) in Marine Offshore Systems. *Aquaculture* 297, 1–9. doi: 10.1016/j.aquaculture.2009.09.010

Trottet, A., George, C., Drillet, G., and Lauro, F. M. (2021). Aquaculture in Coastal Urbanized Areas: A Comparative Review of the Challenges Posed by Harmful Algal Blooms. *Crit. Rev. Env. Sci. Tec.* 1—42. doi: 10.1080/10643389.2021.1897372

Wang, X. G. (2017). *Growth Characteristics of Portunus Trituberculatus in Zhejiang Fishing Ground* (M. Sc. Dissertation. Zhejiang: Zhejiang Ocean University).

Wang, Y. B., Gao, L., and Chen, Y. X. (2018). Assessment of *Portunus* (*Portunus*) *Trituberculatus* (Mier) Stock in the Northern East China Sea. *Indian. J. Fish.* 65, 28–35. doi: 10.21077/ijf.2018.65.4.81039-03

Yang, T., Ren, J. S., Kooijman, S., Shan, X., and Gorfine, H. (2020). A Dynamic Energy Budget Model of *Fenneropenaeus Chinensis* With Applications for Aquaculture and Stock Enhancement. *Ecol. Model.* 431, 109186. doi: 10.1016/j.ecolmodel.2020.109186

Zhang, K., Tian, X. L., Dong, S. L., Dong, J., Feng, J., He, R. P., et al. (2015). Nitrogen and Phosphorus Budgets of Polyculture System of *Portunus Trituberculatus*, *Litopenaeus Vanname* and *Ruditapes Philippinarum*. *Periodic. Ocean. Univ. China* 45, 44–53. doi: 10.16441/j.cnki.hdxb.20140063

Zhang, K., Tian, X. L., Dong, S. L., Feng, J., and He, R. P. (2016). An Experimental Study on the Budget of Organic Carbon in Polyculture Systems of Swimming Crab With White Shrimp and Short-Necked Clam. *Aquaculture* 451, 58–64. doi: 10.1016/j.aquaculture.2015.08.029

Conflict of Interest: The authors declare that the research was conducted in the absence of any commercial or financial relationships that could be construed as a potential conflict of interest.

Publisher's Note: All claims expressed in this article are solely those of the authors and do not necessarily represent those of their affiliated organizations, or those of the publisher, the editors and the reviewers. Any product that may be evaluated in this article, or claim that may be made by its manufacturer, is not guaranteed or endorsed by the publisher.

frontiers | Frontiers in Marine Science

DATA REPORT
published: 13 June 2022
doi: 10.3389/fmars.2022.922188

Full-Length Transcriptome Construction of the Blue Crab *Callinectes sapidus*

Baoquan Gao[1,2], *Jianjian Lv*[1,2], *Xianliang Meng*[1,2], *Jitao Li*[1,2], *Yukun Li*[1], *Ping Liu*[1,2]* *and Jian Li*[1,2]

[1] *Key Laboratory of Sustainable Development of Marine Fisheries, Ministry of Agriculture, Yellow Sea Fisheries Research Institute, Chinese Academy of Fishery Sciences, Qingdao, China,* [2] *Laboratory for Marine Fisheries and Aquaculture, Qingdao National Laboratory for Marine Science and Technology, Qingdao, China*

Keywords: blue crab, *Callinectes sapidus*, full-length transcriptome, PacBio sequencing, ISO-seq

OPEN ACCESS

Edited by:
Yangfang Ye,
Ningbo University, China

Reviewed by:
Hongbo Jiang,
Shenyang Agricultural University, China
Yuquan Li,
Qingdao Agricultural University, China
Qi Liu,
Dalian Ocean University, China

****Correspondence:***
Ping Liu
liuping@ysfri.ac.cn

Specialty section:
This article was submitted to Marine Fisheries, Aquaculture and Living Resources, a section of the journal Frontiers in Marine Science

Received: *17 April 2022*
Accepted: *09 May 2022*
Published: *13 June 2022*

Citation:
Gao B, Lv J, Meng X, Li J, Li Y, Liu P and Li J (2022) Full-Length Transcriptome Construction of the Blue Crab Callinectes sapidus. Front. Mar. Sci. 9:922188. doi: 10.3389/fmars.2022.922188

BACKGROUND

The blue crab *Callinectes sapidus* is native to the western Atlantic Ocean from Uruguay toNova Scotia (Millikin and Williams, 1984; Johnson, 2015) where it represents a commercially valuable shellfish product (Mancinelli et al., 2017). The blue crab is the target of several large recreational and commercial fisheries ($219 million annually in the U.S.) (National Marine Fisheries Service, 2016), and playing important roles in the ecologically environments they inhabit (Roegner and Watson, 2020). Considering their economic and ecological significance, several studies have been conducted to explore the mechanism of spawning, soft shell crab culture, and physiological processes in blue crab. For example, Bembe et al. studied the optimal temperature and photoperiod for the spawning of blue crabs (Bembe et al., 2017). Spitznagel et al. (2019) investigated the risk factors for mortality and reovirus infection in aquaculture production of soft-shell blue crabs. Further, Roegner and Watson (2020) reported *de novo* transcriptome assembly and functional annotation for adult blue crab Y-organs; they also performed Illumina sequencing for differential gene expression analysis between Y-organs of intermolt and premolt crabs. Yednock et al. (2015) used RNA-Seq to examine short-term transcriptomic responses in two tissues from juvenile blue crabs exposed to crude oil in a laboratory exposure experiment. The genome assembly at the chromosome level of blue crab has been completed, resulting in a 985Mb assembly with a scaffold N50 of 153kb, 88% (888/1013)of which were complete and single copies by arthropod BUSCO (Benchmarking Universal Single-Copy Orthologs) (Bachvaroff et al., 2021).

Single molecule real-time (SMRT) sequencing can generate kilobase-sized sequencing reads, facilitating the assembly of FL transcripts (Eid et al., 2009; Sharon et al., 2013). The FL transcriptome has a lot of advantages. First, FL transcript sequences can be directly obtained to provide detailed information pertaining to the transcriptome of sequenced species. Second, various alternative splicing events can be detected. Besides, new functional genes can be discovered, and perfectideal genome annotation is feasible.

Herein we used Pacific Biosciences (PacBio) SMRT sequencing to report, for the first time, the FL transcriptome of *C. sapidus*. Based on the obtained data, we conducted some important studies, including transcript functional annotation, coding sequence (CDS) prediction, lncRNA prediction, transcription factor (TF) prediction, and simple sequence repeat (SSR) analysis. FL transcriptome

database can prove valuable for studying, for example, the genetic evolution, genetic breeding, and physiological mechanisms of *C. sapidus*.

DATA DESCRIPTION

Sample Collection and RNA Sample Preparation

Six healthy adult *C. sapidus* (223.4 ± 18.4 g) were purchased from an aquatic product market. The crabs were reared for a week in an indoor closed seawater tank (water, 10,000-L; temperature, 19°C; salinity, 30 ppt; pH 8.0). Subsequently, the hemocyte, eyestalk, muscle, hepatopancreas, heart, stomach, gill, and thymus were extracted from three randomly chosen crabs, respectively. These samples were frozen in liquid nitrogen. Total RNA was extracted separately using TRIzol (Invitrogen, USA). RNA quality was assessed by NanoDrop 2000 spectrophotometer (Thermo Fisher Scientific, USA), and a mixed pool sample was used for single molecule FL transcriptome sequencing.

Library Preparation and SMRT Sequencing

The cDNA sequencing library was constructed using the aforementioned mixed pool sample, which was sequenced on a single PacBio SMRT cell. Briefly, first- and second-strand cDNA was generated from mRNA using the SMARTerTM PCR cDNA Synthesis Kit (Pacific Biosciences, USA), and >4-Kb size selection was performed using BluePippin® (Sage Science, USA). Subsequently, >4-Kb cDNA was mixed in equal amounts with non-size-selected cDNA. SMRTbellTM hairpin adapters were ligated after a round of PCR and end-repair. On exonuclease digestion, a cDNA library was obtained.

PacBio Long Read Processing

With minFullPass = 1 and minPredictedAccuracy = 0.80, subreads were processed into error-corrected reads of insert using the Iso-seq pipeline (Pacific Biosciences, Menlo Park, CA, USA). By searching for the polyA tail signal and 5'- and 3'-cDNA primers in reads of insert, FL, and FL non-chimeric (FLNC) reads were identified. Iterative clustering for error correction was used to obtain FLNC consensus isoforms. The LoRDEC software was employed to correct polished consensus isoforms using Illumina short-read RNA-seq data (Salmela and Rivals, 2014). The CD-HIT software was used to remove redundancy of high-quality transcripts (Fu et al., 2012). Gene function was annotated by BLAST v2.2.26 (Altschul et al., 1997) based on the databases of NR (Li et al., 2002), GO (Michael et al., 2000), NT, Pfam, KOG/COG (Tatusov et al., 2003), KEGG (Kanehisa et al., 2004), and Swiss-Prot (Bairoch and Apweiler, 2000).

Predicting Gene Structure of Isoforms

To identify protein CDSs from cDNAs, we applied the ANGEL pipeline (Shimizu et al., 2006). Animal TFDB 2.0 was used to analyze TFs (Zhang et al., 2015). CNCI (Sun et al., 2013), CPC (Kong et al., 2007), Pfam (Finn et al., 2016), and PLEK (Li et al., 2014) were used for lncRNA prediction. SSRs of the transcriptome were identified using MISA (http://pgrc.ipk-gatersleben.de/misa.html).

RESULTS

Data Summary

In total, we obtained 17.19 Gb of subreads, including 6,986,978 subreads with the average length of 2,461 bp and the N50 length of 3,079 bp. Further, 368,306 circular consensus sequence reads were extracted, including 279,032 FLNC reads with the mean length of 3,010 bp. In addition, 142,291 consensus reads were obtained with their mean length of 3,072 bp. Polished transcripts were corrected by Illumina short reads; 142,291 high-quality transcripts with mean length of 3,087 bp were obtained for subsequent analyses. On subjecting high-quality transcripts to redundancy removal, we obtained 66,780 genes. The length of 1,147 (1.72%), 951 (1.42%), 7,580 (11.35%), 22,709 (34.00%), and 34,393 (51.50%) genes was 1–500 bp, 500–1000 bp, 1–2 kbp, 2–3 kbp, and >3 kbp, respectively (**Table 1**). In total, 13,626 genes have at least two transcripts (**Supplementary Table 1**).

TABLE 1 | Reads and annotation statistics for the ISO-seq transcripts.

Type	Subreads	consensus reads	Transcripts corrected by Illumina RNA-seq data	CD-HIT transcripts
Reads number and length distribution				
Total_reads_number	6,986,978	142,291	142,291	66,780
Average_length(bp)	2,461	3,072	3,087	———
<500 bp	1,006,131	1,749	1,737	1,147
500-1,000 bp	463,323	1,620	1,606	951
1,000-2,000 bp	1,230,491	19,441	18,959	7,580
2,000-3,000 bp	2,324,191	60,555	61,079	22,709
>3,000 bp	1,962,842	58,926	58,910	34,393
Annotaion				
Functional				
GO	35,853 (53.69%)			
NR	49,602 (74.28%)			
KEGG	47,373 (70.94%)			
Swissprot	43,233 (64.74%)			
KOG	38,168 (57.15%)			
Pfam	35,853 (53.69%)			
NT	24,946 (37.36%)			
Annotated_in_all	15,955 (23.89%)			
At_least_in_one	52,970 (79.32%)			
Structural				
CDS	65,345			
TF	1,740			
SSR	119,404			
LncRNA	10,271			

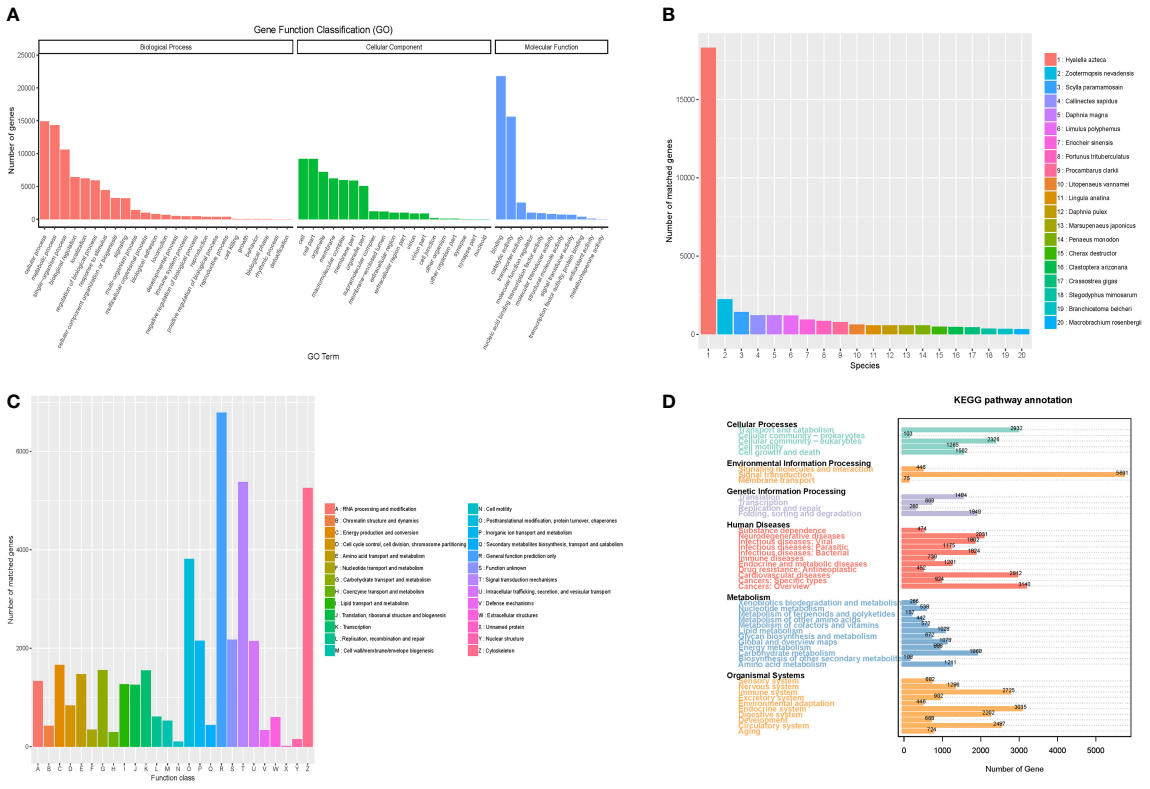

FIGURE 1 | Characterization of functional annotation. **(A)** GO functional annotations. **(B)** NR functional annotations. **(C)** KOG functional annotations. **(D)** KEGG functional annotations.

Gene Annotations

We observed that 52,970 (79.32%) genes were successfully annotated by aligning to one or more of the seven databases, and 15,955 (23.89%) genes were annotated in all the seven aforementioned databases. Furthermore, 35,853 (53.69%) genes were annotated in GO, 49,602 (74.28%) in NR, 47,373 (70.94%) in KEGG, 43,233 (64.74%) in Swiss-Prot, 38,168 (57.15%) in KOG, 35,853 (53.69%) in Pfam, and 24,946 (37.36%) in NT (**Table 1**), respectively.

The genes were assigned to 55 GO terms belonging to the following three main categories: cellular component, molecular function, and biological process. For biological process, most GO terms were enriched in cellular process (14,923, 41.62%), metabolic process (14,337, 39.99%), and single-organism process (10,618, 29.62%). For cellular component, the most abundant GO terms were cell (9,175, 25.59%), cell part (9,175, 25.59%), and organelle (6,197, 20.12%). Binding (21,792, 60.78%), catalytic activity (15,608, 43.53%), and transporter activity (2,522, 7.03%) represented the activity categories of molecular function (**Figure 1A**). Approximately 18,310 (36.91%) genes were aligned to *Hyalella azteca*, followed by *Zootermopsis nevadensis* (2,236, 4.51%) and *Scylla paramamosain* (1,426, 2.87%), by sequence alignment on the basis of the NR database (**Figure 1B**). With regard to KOG annotation, genes were divided into 26 subcategories, such as function R (general function prediction only), function T (signal transduction mechanisms), and function Z (cytoskeleton) (**Figure 1C**). In total, 357 pathways were derived from the KEGG database, and the pathway with the most genes was "metabolism" (116, 32.49%). The highest number of genes were involved in "signal transduction" (5,691, 12.01%), followed by "cardiovascular diseases" (3,140, 6.63%) (**Figure 1D**).

CDS, TF, lncRNA Prediction and SSR Analyses

Using ANGEL, 65,345 CDSs were identified, including 33,461 complete CDSs (**Supplementary Figure 1A**). Besides, 142,291 high-quality transcripts were predicted to be TFs by searching the hidden Markov models of all the TFs in animal TFDB 2.0, which comprise 55 TF families. **Supplementary Figure 1B** shows the distribution of the top 30 TF families. In total, 10,271 lncRNA transcripts were predicted by all four computational approaches (**Supplementary Figure 1C**). Collectively, 88.04% lncRNAs were <4,000-nt long, and most were 2,000–3,000-nt long. Further, 142,291 high-quality transcripts were subjected to SSR analysis, including 119,404 SSRs. The numbers of mono-, di-, tri-, tetra-, penta-, and hexanucleotides were 26,035, 30,524, 22,474, 2,508, 433, and 115, respectively (**Supplementary Figure 1D**).

Reuse Potential

To the best of our knowledge, this is the first study to report the FL transcriptome of *C. sapidus*. The transcriptome data reported

herein should support further studies on *C. sapidus* genetics and genomic information. Moreover, our data should be valuable to chromosome-level genome studies of *C. sapidus* and other related species.

DATA AVAILABILITY STATEMENT

The datasets presented in this study can be found in online repositories. The names of the repository/repositories and accession number(s) can be found below: https://ngdc.cncb.ac.cn/, CRA006442 https://figshare.com/articles/dataset/Full-length_Transcriptome_of_the_blue_crab_Callinectes_sapidus/19608261.

ETHICS STATEMENT

The relevant national and international guidelines were followed during the conductance of the animal experiments and the Yellow Sea Fisheries Research Institute approved the experiments. Endangered or protected species were not involved in this study.

AUTHOR CONTRIBUTIONS

BG and JJL designed the experiment. XM raised Carb. JTL collected Carb tissue samples. YL uploaded data in CNCB-NGDC. BG drafted the manuscript. JL and PL revised the manuscript. All authors contributed to the article and approved the submitted version.

FUNDING

This study was supported by National Marine Genetic Resource Center, Central Public-interest Scientific Institution Basal Research Fund, CAFS (NO. 2020TD46& NO.2021GH05).

SUPPLEMENTARY MATERIAL

The Supplementary Material for this article can be found online at: https://www.frontiersin.org/articles/10.3389/fmars.2022.922188/full#supplementary-material

REFERENCES

Altschul, S. F., Madden, T. L., Schaffer, A. A., and Zhang, J. N. (1997). Gapped BLAST and PSI-BLAST: A New Generation of Protein Database Search Programs. *Nucleic Acids Res.* 25, 3389–3402. doi: 10.1093/nar/25.17.3389

Bachvaroff, T. R., Mcdonald, R. C., Plough, L. V., and Chung, J. S. (2021). Chromosome-Level Genome Assembly of the Blue Crab, *Callinectes Sapidus*. *G3* 11 (9), jkab212. doi: 10.1093/g3journal/jkab212

Bairoch, A., and Apweiler, R. (2000). The SWISS-PROT Protein Sequence Database and its Supplement TrEMBL in 2000. *Nucleic Acids Res.* 28 (1), 45–48. doi: 10.1093/nar/28.1.45

Bembe, S., Liang, D., and Chung, J. S. (2017). Optimal Temperature and Photoperiod for the Spawning of Blue Crab, *Callinectes Sapidus*, in Captivity. *Aquaculture Res.* 48 (11), 5498–5505. doi: 10.1111/are.13366

Eid, J., Fehr, A., Gray, J., Luong, K., Lyle, J., Otto, G., et al. (2009). Real-Time DNA Sequencing From Single Polymerase Molecules. *Science* 323, 133–138. doi: 10.1126/science.1162986

Finn, R. D., Coggill, P., Eberhardt, R. Y., Eddy, S. R., Mistry, J., Mitchell, A. L., et al. (2016). The Pfam Protein Families Database: Towards a More Sustainable Future. Nucleic Acids Research. *Database Issue* 44, 279–285. doi: 10.1093/nar/gkv1344

Fu, L., Niu, B., Zhu, Z., Wu, S., and Li, W. (2012). CD-HIT: Accelerated for Clustering the Next-Generation Sequencing Data. *Bioinformatics* 28 (23), 3150. doi: 10.1093/bioinformatics/bts565

Johnson, D. S. (2015). The Savory Swimmer Swims North: A Northern Range Extension of the Blue Crab *Callinectes Sapidus*? *J. Crust. Biol.* 35, 105–110. doi: 10.1163/1937240X-00002293

Kanehisa, M., Goto, S., Kawashima, S., Okuno, Y., and Hattori, M. (2004). The KEGG Resource for Deciphering the Genome. *Nucleic Acids Res.* 32 (1), 277–280. doi: 10.1093/nar/gkh063

Kong, L., Zhang, Y., Ye, Z. Q., Liu, X. Q., Zhao, S. Q., Wei, L., et al. (2007). CPC: Assess the Protein-Coding Potential of Transcripts Using Sequence Features and Support Vector Machine. *Nucleic Acids Res.* 36, 345–349. doi: 10.1093/nar/gkm391

Li, W., Jaroszewski, L., and Godzik, A. (2002). Tolerating Some Redundancy Significantly Speeds Up Clustering of Large Protein Databases. *Bioinformatics* 18 (1), 77–82. doi: 10.1093/bioinformatics/18.1.77

Li, A. M., Zhang, J. Y., and Zhou, J. Y. (2014). PLEK: A Tool for Predicting Long non-Coding RNAs and Messenger RNAs Based on an Improved K-Mer Scheme. *BMC Bioinf.* 15, 311. doi: 10.1186/1471-2105-15-311

Mancinelli, G., Chainho, P., Cilenti, L., Falco, S., Kapiris, K., Katselis, G., et al. (2017). On the Atlantic Blue Crab (*Callinectes Sapidus* Rathbun 1896) in Southern European Coastal Waters: Time to Turn a Threat Into a Resource? *Fish. Res.* 194, 1–8. doi: 10.1016/j.fishres.2017.05.002

Michael, A., Catherine, A. B., Judith, A. B., David, B., Butler, H., Cherry, J. M., et al. (2000). Gene Ontology: Tool for the Unification of Biology. *Nat. Genet.* 25 (1), 25–29. doi: 10.1038/75556

Millikin, M. R., and Williams, A. B. (1984) *Synopsis of Biological Data on Blue Crab Callinectes Sapidus Rathbun*. FAO Fisheries Synopsis 138, NOAA Technical Report, NMFS 1, 43 pp.

National Marine Fisheries Service. (2016) *Fisheries of the United States 2015. U.S. Department of Commerce, NOAA Current Fishery Statistics No. 2015* (Silver Spring). Available at: https://www.st.nmfs.noaa.gov/commercial-fisheries/fus/fus15/index.

Roegner, M. E., and Watson, R. D. (2020). *De Novo* Transcriptome Assembly and Functional Annotation for Y-Organs of the Blue Crab (*Callinectes Sapidus*), and Analysis of Differentially Expressed Genes During Pre-Molt. *General* and. *Comp. Endocrinol.* 298, 113567. doi: 10.1016/j.ygcen.2020.113567

Salmela, L., and Rivals, E. (2014). LoRDEC: Accurate and Efficient Long Read Error Correction. *Bioinformatics* 30 (24), 3506–3514. doi: 10.1093/bioinformatics/btu538

Sharon, D., Tilgner, H., Grubert, F., and Snyder, M. (2013). A Single-Molecule Long-Read Survey of the Human Transcriptome. *Nat. Biotechnol.* 31, 1009–1014. doi: 10.1038/nbt.2705

Shimizu, K., Adachi, J., and Muraoka, Y. (2006). ANGLE: A Sequencing Errors Resistant Program for Predicting Protein Coding Regions in Unfinished cDNA. *J. Bioinf. Comput. Biol.* 4 (3), 649–664. doi: 10.1142/S0219720006002260

Spitznagel, M. I., Small, H. J., Lively, J. A., Shields, J. D., and Schott, E. J. (2019). Investigating Risk Factors for Mortality and Reovirus Infection in Aquaculture Production of Soft-Shell Blue Crabs (*Callinectes Sapidus*). *Aquaculture* 502, 289–295. doi: 10.1016/j.aquaculture.2018.12.051

Sun, L., Luo, H. T., Bu, D. C., Zhao, G. G., Yu, K. T., Zhang, C. H., et al. (2013). Utilizing Sequence Intrinsic Composition to Classify Protein-Coding and Long Non-Coding Transcripts. *Nucleic Acids Res.* 41 (17), 166. doi: 10.1093/nar/gkt646

Tatusov, R. L., Fedorova, N. D., Jackson, J. D., Jacobs, A. R., Kiryutin, B., Koonin, E. V., et al. (2003). The COG Database: An Updated Version Includes Eukaryotes. *BMC Bioinf.* 4 (1), 41. doi: 10.1186/1471-2105-4-41

Yednock, B. K., Sullivan, T. J., and Neigel, J. E. (2015). *De Novo* Assembly of a Transcriptome From Juvenile Blue Crabs (*Callinectes Sapidus*) Following Exposure to Surrogate Macondo Crude Oil. *BMC Genomics* 16, 521. doi: 10.1186/s12864-015-1739-2

Zhang, H. M., Liu, T., Liu, C. J., Song, S. Y., Zhang, X. T., Liu, W., et al. (2015). AnimalTFDB 2.0: A Resource for Expression, Prediction and Functional Study of Animal Transcription Factors. *Nucleic Acids Res.* 43, 76–81. doi: 10.1093/nar/gku887

Conflict of Interest: The authors declare that the research was conducted in the absence of any commercial or financial relationships that could be construed as a potential conflict of interest.

Publisher's Note: All claims expressed in this article are solely those of the authors and do not necessarily represent those of their affiliated organizations, or those of the publisher, the editors and the reviewers. Any product that may be evaluated in this article, or claim that may be made by its manufacturer, is not guaranteed or endorsed by the publisher.

frontiers | Frontiers in Marine Science

ORIGINAL RESEARCH
published: 15 June 2022
doi: 10.3389/fmars.2022.909827

Molecular Characterization and Expression Analysis of Glutaredoxin 5 in Black Tiger Shrimp (*Penaeus monodon*) and Correlation Analysis Between the SNPs of *PmGrx5* and Ammonia-N Stress Tolerance Trait

Rui Fan[1,2], *Shigui Jiang*[1], *Yundong Li*[1], *Qibin Yang*[1,3], *Song Jiang*[1], *Jianhua Huang*[1], *Lishi Yang*[1], *Xu Chen*[1,3] *and Falin Zhou*[1,3]*

[1] Key Laboratory of South China Sea Fishery Resources Exploitation and Utilization, South China Sea Fisheries Research Institute (CAFS), Guangzhou, China, [2] College of Fisheries and Life Science, Shanghai Ocean University, Shanghai, China, [3] South China Sea Fisheries Research Institute, Chinese Academy of Fishery Sciences, Tropical Fisheries Research and Development Center, Sanya Tropical Fisheries Research Institute, Sanya, China

OPEN ACCESS

Edited by:
Xiangli Tian,
Ocean University of China, China

Reviewed by:
Shuang Zhang,
Guangdong Ocean University, China
Huan Wang,
Ningbo University, China

***Correspondence:**
Falin Zhou
zhoufalin0925@163.com

Specialty section:
This article was submitted to Marine Fisheries, Aquaculture and Living Resources, a section of the journal Frontiers in Marine Science

Received: 31 March 2022
Accepted: 16 May 2022
Published: 15 June 2022

Citation:
Fan R, Jiang S, Li Y, Yang Q, Jiang S, Huang J, Yang L, Chen X and Zhou F (2022) Molecular Characterization and Expression Analysis of Glutaredoxin 5 in Black Tiger Shrimp (Penaeus monodon) and Correlation Analysis Between the SNPs of PmGrx5 and Ammonia-N Stress Tolerance Trait. Front. Mar. Sci. 9:909827. doi: 10.3389/fmars.2022.909827

Glutaredoxins (Grxs) are glutathione-dependent oxidoreductases that belong to the thioredoxin (Trx) superfamily and are an essential part of the redox system in living organisms. However, there is a serious lack of sequence information and functional validation associated with Grxs in crustaceans. In this study, a new Grx gene (*PmGrx5*) was identified and characterized in black tiger shrimp (*Penaeus monodon*). The full-length cDNA of *PmGrx5* is 787 bp and consists of 114 bp 5′-UTR, 232 bp 3′-UTR, and 441 bp ORF, encoding a hypothetical protein of 146 amino acids. The putative PmGrx5 protein is 16.27 kDa with a theoretical isoelectric point of 5.90. Sequence alignment showed that *PmGrx5* had the highest amino acid sequence homology with Grx5 from *Penaeus vannamei* at 98.63% and clustered with Grx5 from other crustaceans. Quantitative real-time PCR (qRT-PCR) analysis showed that *PmGrx5* was expressed in all tissues examined, with a higher expression in the testis, stomach, lymphoid organ, and gill. *PmGrx5* was continuously expressed during development, with the highest expression in zoea I. Ammonia-N stress and bacterial infection both differentially upregulated *PmGrx5* expression in the hepatopancreas and gill. In addition, when *PmGrx5* was inhibited, the expression of some other antioxidant enzymes was upregulated at the beginning of ammonia-N stress, but as the stress time increased, the expression of antioxidant enzymes was inhibited, the expression of apoptotic genes was increased, and the GSH content was significantly reduced. Inhibition of *PmGrx5* led to a greater risk of oxidative damage in shrimp. In addition, the relationship between SNPs in exons of the PmGrx5 gene and tolerance to ammonia-N stress was identified and analysed. A total of nine SNPs were successfully identified, eight of which were significantly associated with ammonia and nitrogen stress tolerance trait in shrimp ($P < 0.05$). The present study shows that

PmGrx5 is involved in redox regulation and plays an important role in shrimp resistance to marine environmental stresses. Meanwhile, this study will provide a basis for molecular marker breeding in shrimp.

Keywords: glutaredoxin, *Penaeus monodon*, ammonia-N stress, innate immunity, SNPs

INTRODUCTION

Black tiger shrimp (*Penaeus monodon*) is currently the third most cultured shrimp in the world, accounting for approximately 8% of total crustacean farming production and is an important part of the mariculture economic industry (FAO, 2020). However, due to the deteriorating marine environment, especially in coastal areas, black tiger shrimp farming is often exposed to viral attacks and bacterial infections, resulting in high mortality rates and huge economic losses (Li et al., 2018). A good marine environment is a prerequisite for the sustainable development of the mariculture industry. Adverse environmental factors can upset the original physiological balance in organisms, and prolonged environmental stress can cause irreversible damage to organs and tissues and even lead to the death of organisms (Dunier and Siwicki, 1994; Chen et al., 1994; Chen and Chen, 2002). Ammonia-N is one of the most important environmental factors in mariculture, and ammonia-N stress is the most common environmental challenge faced by mariculture organisms (Liu et al., 2021). Ammonia-N stress usually causes oxidative stress in crustaceans, which disrupts redox homeostasis in crustaceans and ultimately leads to the production of excess reactive oxygen species (ROS). ROS are a class of single-electron reduction products of oxygen atoms in the body, mainly produced during mitochondrial oxidative phosphorylation and during cellular defense against exogenous compounds, which cause oxidative damage to biological macromolecules such as proteins and deoxyribonucleotides (Nathan and Cunningham-Bussel, 2013). Crustaceans can use a variety of redox systems in their bodies to eliminate excess ROS in order to protect themselves (Bu et al., 2017). Therefore, the study of redox systems is fundamental and necessary for mariculture management and shrimp breeding.

Glutaredoxins (Grxs), also known as thioltransferase, are heat-stable, small molecular weight enzymes that are an essential part of the redox system in living organisms (Holmgren et al., 2005). In the classification of proteins, Grxs are classified as a thioredoxin (Trx) superfamily (Carvalho et al., 2006). On the one hand, the members of the Trx superfamily all have a similar tertiary structure. The typical Trx structure is a centrally located four β-strands surrounded by three α-helices (Pan and Bardwell, 2006). However, the folding pattern of Grxs is subtly different from the typical Trx structure: its central four β-strands are surrounded by five α-helices (Chi et al., 2018). On the other hand, Grxs and Trxs have many of the same or similar functions in living organisms. The main role of Grxs is to use glutathione (GSH) to maintain redox homeostasis in living organisms. Glutathione (GSH) is a small molecular peptide consisting of the amino acids glutamate, cysteine, and glycine and is the main determinant of the redox state of cells. Classically, Grxs regulate the glutathionylation or deglutathionylation of proteins in an organism, thus keeping the GSH to GSSG ratio within normal limits. Because Grxs are required to recognize only the glutathione fraction of the substrate and not the substrate itself, Grxs are more flexible than Trxs in terms of substrate selection and reaction catalysis mechanism (Holmgren, 1979). Grxs were first identified in 1976 in *Escherichia coli* with a deficiency in Trx activity (Holmgren, 1979). Depending on the sequence of the central active sites, typical Grxs can be divided into two types: the dithiol Grxs, which contain Cys-Pro-Tyr-Cys as the catalytic sites; and the monothiol Grxs, which contain Cys-Gly-Phe-Ser as the catalytic sites and contain only one N-terminal cysteine residue. The monothiol Grxs can be further classified into two types: one type contains only a Grx structural domain and the other type contains a Trx structural domain at its N-terminal end with multiple Grx structural domains attached (Lillig et al., 2008). Notably, the second monothiol Grxs are currently only found in eukaryotes (Eklund et al., 1984; Couturier et al., 2009). The mechanism of action of the two Grxs differs somewhat, but both can use cysteine to accomplish reversible regulation of protein glutathionylation (Lillig et al., 2008).

In recent years, as studies have progressed, more other types of Grxs have been discovered. Plants are now known to possess the greatest quantities and types of Grxs, with the active site Cys-Cys-X-X being unique to plants (Verma et al., 2021). Grxs have been shown to be involved in a number of physiological processes in plants, mainly developmental regulation, stress resistance, and environmental adaptation (Xing et al., 2005; Cheng, 2008; Wang et al., 2009), and play an important role in plant growth and resistance to adverse factors. In addition, Grxs of photosynthetic organisms possess more complex structures and more diverse types. For example, a new type of complex Grx linking multiple proteins at the N-terminus has been identified in cyanobacteria (Mondal et al., 2019). The types and quantities of Grxs in animals are far less than in plants, but they still play a very crucial role. In mammals, Grxs have been reported to be involved in iron–sulfur cluster coordination, antioxidative stress, cell growth, and apoptosis (Hiroaki et al., 2003; Potamitou and Arne, 2004; Bräutigam et al., 2013). As Grxs have been found to function in a variety of human pathological processes, their development as drug targets is equally of interest (Levin et al., 2018). In aquatic organisms, Grxs have been reported to have important effects on embryonic development, brain and heart development, and innate immunity (Bräutigam et al., 2011; Bräutigam et al., 2013; Berndt et al., 2014; Omeka et al., 2019). However, few studies on Grxs in crustaceans have been reported. In this study, the full-length cDNA of Grx5 (*PmGrx5*) from *P.*

monodon was cloned for the first time and analyzed for its mRNA expression during development and in different tissues. To determine whether *PmGrx5* is involved in other physiological activities, we observed the expression of *PmGrx5* after injection with various pathogenic bacteria and under ammonia-N stress, as well as physiological changes after *PmGrx5* was disturbed. In addition, we screened for the SNP markers of *PmGrx5* associated with the ammonia-N stress tolerance trait. This study aims to lay the foundation for further exploring the role of Grx5 in natural immune regulation and resistance to ammonia-N stress.

MATERIALS AND METHODS

Experimental Shrimps

All shrimps used in this study were from the experimental base of the South China Sea Fisheries Research Institute in Shenzhen (Guangdong, China) and from a mixed culture pool of different families. The shrimps used for RNA interference weighed 7.01 ± 0.8 g and were 5.12 ± 0.69 cm in length, the shrimps used for the analysis of SNPs weighed 1.71 ± 0.31 g and were 2.53 ± 0.32 cm in length, while the rest of the experimental shrimps weighed 15.08 ± 1.20 g and were 12.37 ± 0.57 cm in length. We kept the shrimps in plastic cylinders filled with aerated filtered seawater under salinity- (29‰), temperature- (26°C ± 2°C), and pH-controlled (7.5–7.8) conditions for 1 week. During the temporary feeding period, we fed the shrimps once a day with compound feed (8.32% moisture, 48.65% crude protein, 5.70% crude fat, and 11.89% ash) until 24 h before treatment.

Sample Collection

To test the *PmGrx5* expression in different tissues, 14 kinds of tissues, namely, the testis, ovary, brain, eyestalk nerve, thoracic nerve, abdominal nerve, epidermis, gill, heart, muscle, stomach, intestine, hepatopancreas, and lymphoid organ, were dissected from three random healthy untreated shrimps. To test the *PmGrx5* expression during the developmental period, we collected samples from a total of 14 different developmental stages, from oosperm to post-larvae (Gürel, 2005). All the above samples were preserved in the RNAlater solution (Ambion, USA) at 4°C for 24 h and then moved to −80°C until used.

Ammonia-N Stress

To test the *PmGrx5* expression under ammonia-N stress, first, we determined the 96-h median lethal concentration (96-h LC_{50}) and the safe concentration (SC) through an acute ammonia-N stress pre-experiment. A total of 180 shrimps were used for the pre-experiment. In a plastic cylinder of 200 L filtered seawater (salinity 29‰, temperature 26°C ± 2°C, pH 7.5–7.8) aerated continuously using an air stone, 30 shrimps per cylinder were placed separately. The seawater was replenished daily. Six concentrations of ammonia-N, i.e., 0, 20, 40, 60, 80, and 100 mg/L, were prepared by applying NH_4Cl per cylinder to seawater until the required concentration was reached. Mortality was registered every 3 h during the pre-experiment. After completion, 96-h LC_{50} and SC were computed by linear regression, which were 29.47 and 2.95 mg/L, respectively (Li et al., 2012; Zhou et al., 2017).

The shrimp sizes and experimental conditions of the formal experiment were similar to those of the pre-experiment. Experimental shrimps were randomly divided into three treatments (control, 96-h LC_{50}, and SC), each having three replicates with 30 shrimps per replicate. During the experiment, no feed was supplied to the shrimps. Shrimp survival was monitored and reported every 3 h, and the dead shrimps were instantly pulled from the cylinders. At 0, 3, 6, 12, 24, 48, 72, and 96 h after ammonia-N stress, three shrimps were chosen for each duplication. Since the gill is the first barrier to the water environment and the hepatopancreas is the most important detoxification and metabolic organ of the shrimp (Rőszer, 2014; Rowley, 2016), these were chosen as representative target organs to detect the expression of *PmGrx5* under ammonia-N stress. The hepatopancreas and gills of the shrimps were immediately dissected and preserved for 24 h at 4°C in the RNAlater solution (Ambion, USA) and then moved to −80°C until used.

Bacteria Challenge Experiment *In Vivo*

To test the *PmGrx5* expression after the immune challenge, the experimental shrimps were randomly divided into four treatments (control, *Staphylococcus aureus*, *Vibrio harveyi*, and *Vibrio anguillarum*) with three replicates per treatment and 25 shrimps per replicate. The Key Laboratory of South China Sea Fishery Resources Extraction & Utilization supplied those three kinds of bacteria. According to a previous study, 100 μl sterile phosphate buffer solution (PBS, pH 7.4) was injected into the shrimps in the control group, and 100 μl (1.0×10^8 CFU/ml) of the corresponding bacterial solution was injected into the shrimps in the other three treatment groups, respectively (Qin et al., 2019). Each shrimp in the second abdominal segment was inserted intramuscularly. Shrimp survival was monitored and reported every 3 h, and the dead shrimps were instantly pulled from the cylinders. From each replication, three shrimps were picked at 0, 3, 6, 12, 24, 48, and 72 h after the injection. In addition, the hepatopancreas is the most important immune and phagocytic organ of the shrimp (Rőszer, 2014). In *P. monodon*, it has been found that after phagocytosis of pathogenic *Vibrio* cell fragments, hepatopancreatic cells can release bacterial antigens into the hemolymph (Alday et al., 2002). We, therefore, chose the gill and the hepatopancreas as representative target organs to detect *PmGrx5* under bacterial infection. The hepatopancreas and gills of the shrimps were immediately dissected and preserved for 24 h at 4°C in the RNAlater solution (Ambion, USA) and then moved to −80°C until used.

Extraction of RNA and Synthesis of cDNA

For the quantification experiments, the total RNA of all samples obtained above was harvested according to the instructions of the HiPure Fibrous RNA Plus Kit (Megan, China). In addition, the total RNA of 14 different tissues was harvested in conjunction with the instructions of the RNeasy Mini Kit (Qiagen, Germany) for cloning the full-length cDNA of *PmGrx5*. The purity and

quantity of total RNA were calculated by measuring the ultraviolet absorbance ratio at 260/280 nm using a NanoDrop 2000 device (Thermo Scientific, USA). Agarose gel electrophoresis (1%) was used to assess the integrity of total RNA. Total RNA for two different purposes was immediately synthesized into the corresponding cDNA according to the instructions of the Evo M-MLV RT Kit with gDNA Clean for qPCR (AG, China) and HiScript-TS 5′/3′ RACE Kit (Vazyme, China), respectively. The synthetic cDNA was preserved at −80°C until used.

Cloning the Full-Length cDNA of *PmGrx5*

The partial fragment of *PmGrx5* was filtered and determined by the NCBI database BLAST on the basis of the cDNA library of *P. monodon* in our laboratory. The primers were constructed by Premier 6.0 based on the identified fragment, and the *PmGrx5* open reading frame (ORF) was expanded by PCR technology. The PCR program was run in three steps: 95°C for 3 min; 35 cycles of 95°C for 15 s, 55°C for 15 s, and 72°C for 15 s; and completed in an ultimate duration of 5 min at 72°C. In 25 μl of the reaction mixture consisting of 1 μl of forward primer, 1 μl of reverse primer, 1 μl of cDNA template, 12.5 μl of double-distilled water, and 12.5 μl of 2× Taq Plus Master Mix II (Vazyme, China), PCR amplification was done.

The 3′ and 5′ end nested PCR primers were constructed by Premier 6.0 according to the *PmGrx5* ORF. The first-round PCR program was run in three steps: 95°C for 3 min; 35 cycles of 95°C for 30 s, 60°C for 30 s, and 72°C for 1 min; and completed in an ultimate duration of 10 min at 72°C. In 50 μl of the reaction mixture consisting of 2 μl of a mixture of UPM long primers and short primers, 2 μl of first-round specific primer, 3 μl of cDNA template, and 43 μl of Mix Green (Tsingke, China), the first-round PCR amplification was done. The second-round PCR program was run in three steps: 95°C for 3 min; 35 cycles of 95°C for 30 s, 55°C for 30 s, and 72°C for 1 min; and completed in an ultimate duration for 10 min at 72°C. In 50 μl of the reaction mixture consisting of 2 μl of NUP, 2 μl of second-round specific primer, 3 μl of first-round PCR product, and 43 μl of Mix Green (Tsingke, China), the second-round PCR amplification was done.

All PCR products were cloned into pEASY®-T1 Cloning Vector (TransGen, China), sequencing a positive monoclonal colony. Lastly, the RACE technology obtained the full-length cDNA of *PmGrx5*. RuiBiotech (Guangzhou, China) was responsible for the synthesis of all primers and the sequencing of all PCR products mentioned above. All the primers above are shown in **Table 1**.

Bioinformatics Analysis of *PmGrx5*

The ORF and its corresponding amino acid sequences of *PmGrx5* were predicted using the ORF Finder (https://www.ncbi.nlm.nih.gov/orffinder). The nucleotide sequences and the protein sequences were analyzed using BLAST (https://blast.ncbi.nlm.nih.gov/Blast.cgi?CMD=Web&PAGE_TYPE=BlastHome). Protein domains were predicted using SMART (http://smart.embl-heidelberg.de/). Signal peptides were predicted using the SignalP-5.0 Server (http://www.cbs.dtu.dk/services/SignalP/). The O-glycosylation sites were predicted using the YinOYang 1.2 Server (http://www.cbs.dtu.dk/services/YinOYang/). The N-glycosylation sites were predicted using the NetNGlyc 1.0 Server (http://www.cbs.dtu.dk/services/NetNGlyc/). The phosphorylation sites were predicted using the NetPhos 3.1 Server (http://www.cbs.dtu.dk/services/NetPhos/). The N-myristoylation sites were predicted using the Motif Scan (https://myhits.sib.swiss/cgi-bin/motif_scan). The protein secondary structure was predicted using SOPMA (https://npsa-prabi.ibcp.fr/cgi-bin/npsa_automat.pl?page=/NPSA/npsa_sopma.html). The protein tertiary structure was predicted using the SWISS-MODEL (https://swissmodel.expasy.org/). Molecular mass and theoretical isoelectric point were predicted using Expasy (https://web.expasy.org/compute_pi/). The nucleotide and protein sequences of Grx5 from different species were downloaded from the NCBI database (https://www.ncbi.nlm.nih.gov/). With the ClustalX 1.83 software, multiple sequence alignment was conducted. The phylogenetic tree with 1,000 bootstrap trial replicates was built by the MEGA-X software. The Grx protein interaction networks were built by the STRING database (https://cn.string-db.org/).

mRNA Expression by Quantitative Real-Time PCR Analysis

The expression levels of *PmGrx5* and related genes in all samples collected in this experiment were detected by quantitative real-time PCR (qRT-PCR). The qRT-PCR primers were constructed by Premier 6.0. In *P. monodon*, elongation factor 1α (*EF-1α*), as a housekeeping gene, has been used as an internal control for all qRT-PCR experiments to normalize the cDNA quantity (Arun et al., 2002; Soonthornchai et al., 2010; Amornrat and Montip, 2010). *EF-1α* was used as the reference gene in this study. The *PmEF-1α* gene from the genomic sequence was deposited in GenBank (MG775229.1). All primers were synthesized by RuiBiotech (Guangzhou, China) and shown in **Table 1**. A Roche LightCycler® 480II was used for the qRT-PCR. The program was run in six steps: 95°C for 30 s, 40 cycles of 94°C for 5 s and 60°C for 30 s, 95°C for 5 s, 60°C for 1 min, 95°C for 1 min, and completed in an ultimate duration for 30 s at 50°C. In 12.5 μl of the reaction mixture consisting of 0.5 μl of forward primer, 0.5 μl of reverse primer, 1 μl of cDNA template (50 ng/μl), 6.25 μl of SYBR Green Premix Pro Taq (AG, China), and 4.25 μl of double-distilled water, PCR amplification was done. The PCR data were analyzed using the $2^{-\Delta\Delta CT}$ method. Statistical analyses were conducted using IBM SPSS Statistics 26.0. One-way ANOVA, followed by Tukey's multiple range test, estimated the statistical differences. When $P < 0.05$, the difference was considered significant. The test data were shown as mean ± standard deviation (SD).

Ammonia-N Stress on *PmGrx5*-Interfered Shrimps

The double-stranded RNA (dsRNA) for *PmGrx5* (dsGrx5) and the green fluorescent protein (*GFP*, as a non-specific negative control) gene (dsGFP) were synthesized using the T7 RiboMAX

TABLE 1 | PCR primers used in this experiment.

Primer name	Nucleotide sequence (5′ → 3′)	Purpose
PmGrx5-F1	TCTTGCCGAAGTTACATCATTACCT	ORF validation
PmGrx5-R1	CTCATCAATCAACTCTCCGCTCTGA	ORF validation
PmGrx5-F2	AATGTGTTGGCAGATGACAGTGTTC	ORF validation
PmGrx5-R2	AAAGACAAGCCTTGTACCCAAACAT	ORF validation
UPM long primer	CTAATACGACTCACTATAGGGCAAGCAGTGGTATCAACGCAGAGT	Universal primer of RACE
UPM short primer	CTAATACGACTCACTATAGGGC	Universal primer of RACE
NUP	AAGCAGTGGTATCAACGCAGAGT	Universal primer of RACE
PmGrx5-3′ first-round	ATGTTCTCGGCTGTAAAGTTCGCTAGGG	3′ RACE
PmGrx5-3′ second-round	TGGCAGATGACAGTGTTCGACAAGGAAT	3′ RACE
PmGrx5-5′ first-round	TCTGCCAACACATTGTGAGCATCGTAGT	5′ RACE
PmGrx5-5′ second-round	CTGCAATATCTCAGAAACCCAGTTACCG	5′ RACE
EF-1α-qF	AAGCCAGGTATGGTTGTCAACTTT	Reference gene
EF-1α-qR	CGTGGTGCATCTCCACAGACT	Reference gene
PmGrx5-qF	GGAGACTTTGTTGGTGGGTGTGA	qRT-PCR
PmGrx5-qR	TGCTCTAATAAGGCTGAGGTGATGC	qRT-PCR
PmTrx-qF	TCCTCCGTCCTTCGTGTCTCTTCCT	qRT-PCR
PmTrx-qR	ACCAGGTGGCGTAGAAGTCGATGAC	qRT-PCR
PmPrx1-qF	TACCCTTTGGATTTCACCTTTGTC	qRT-PCR
PmPrx1-qR	ATTGATTGTTACCTGACGGAGATT	qRT-PCR
PmCAT-qF	CGAGGATTTGCTGTGAAGTTTT	qRT-PCR
PmCAT-qR	ATGAAGGAAGGGAATAGAATAGGAT	qRT-PCR
PmCYC-qF	GGTGACATCGAGAAGGGCAAGAAGA	qRT-PCR
PmCYC-qR	CCTTGGACTTGTTGGCGTCTGTGTA	qRT-PCR
PmIAP-qF	ATGGAGCCCTGTATTGAG	qRT-PCR
PmIAP-qR	GTGGATGGAGAACTGGAA	qRT-PCR
iGFP-F	ATGGTGAGCAAGGGCGAGGAG	dsRNA
iT7GFP-F	TAATACGACTCACTATAGGATGGTGAGCAAGGGCGAGGAG	dsRNA
iGFP-R	TCAAAGATCTACCATGTACAGCTCGT	dsRNA
iT7GFP-R	TAATACGACTCACTATAGGTCAAAGATCTACCATGTACAGCTCGT	dsRNA
iPmGrx5-F	TGTCCAGGCGTAAACACTTTC	dsRNA
iT7PmGrx5-F	TAATACGACTCACTATAGGTGTCCAGGCGTAAACACTTTC	dsRNA
iPmGrx5-R	TCTAATAAGGCTGAGGTGATGC	dsRNA
iT7PmGrx5-R	TAATACGACTCACTATAGGTCTAATAAGGCTGAGGTGATGC	dsRNA
PmGrx5-exon1-F	ACTGAGCCTCCTTCAACCC	Identification of SNPs
PmGrx5-exon1-R	TAATTCCTTACTGACCGACAAA	Identification of SNPs
PmGrx5-exon2-F	TATCCCTGTGAGGCTTTGA	Identification of SNPs
PmGrx5-exon2-R	CTTAGCCACAAAGGAGTCAAT	Identification of SNPs
PmGrx5-exon3-F	ACCTGTGGCACAAGTTTAA	Identification of SNPs
PmGrx5-exon3-R	GCATACATCCTGCTTTCAT	Identification of SNPs

Express RNAi kit (Promega, USA). The primers used to synthesize the dsRNA for the *PmGrx5* and the *GFP* gene are shown in **Table 1**. The purity and quantity of the dsRNA were calculated by measuring the ultraviolet absorbance ratio at 260/280 nm using a NanoDrop 2000 device (Thermo Scientific, USA). Agarose gel electrophoresis (1%) was used to assess the integrity of the dsRNA. The synthetic dsRNA was preserved at −80°C until used.

First, the *PmGrx5* expression was measured by qRT-PCR to determine the interference efficiency of dsGrx5. The concentration of dsRNA was diluted to 1 μg/μl using PBS buffer before the *in-vivo* injection. We divided the experimental shrimps into two groups of three replicates each, with five shrimps in each replicate. We injected dsGrx5 or dsGFP dilution (3 μg per gram of shrimp weight) at the second ventral segment of each shrimp. The dsGFP-injected shrimps were the control group and the dsGrx5-injected shrimps were the experimental group. Due to the importance of the hepatopancreas and the multiple previous reports on the use of the hepatopancreas as the target organ for RNA interference in crustaceans (Alday et al., 2002; Rőszer, 2014; Rowley, 2016; Zheng et al., 2018; Zheng et al., 2021; Jie et al., 2022), therefore, in this study, 24 h after injection, we selected three shrimps from each replicate and immediately collected the shrimp hepatopancreas, following the same procedure provided in the *mRNA Expression by Quantitative Real-Time PCR Analysis* section.

After determining that the interference efficiency of dsRNA was significant, we again divided the experimental shrimps into two groups with three replicates of 40 shrimps each. Injections were carried out as above. Twenty-four hours after the injection, the *PmGrx5*-interfered and dsGFP-injected shrimps were subjected to 48 h of acute ammonia-N stress using 96-h LC_{50}. Sampling was done at 0, 3, 6, 12, 24, and 48 h post-stress. At each time point, we selected three shrimps from each replicate and immediately collected the shrimp hepatopancreas: one part was stored in RNAlater solution (Ambion, USA) at 4°C for 24 h and then moved to −80°C until used, and the other part was stored directly in liquid nitrogen until used.

Similar to the steps provided in the *Extraction of RNA and Synthesis of cDNA* and *mRNA Expression by Quantitative Real-Time PCR Analysis* sections, the same procedures were followed

to analyze the relative expression levels of various related genes such as *PmTrx*, *PmPrx1*, *PmCAT*, *PmCYC*, and *PmIAP* in *PmGrx5*-interfered shrimps and dsGFP-injected shrimps. The specific primers for the above genes are shown in **Table 1**. As Grx5 is a glutathione-dependent oxidoreductase, samples stored directly in liquid nitrogen were assayed using reduced glutathione (GSH) assay kit (Nanjing Jiancheng Bioengineering Institute, China). Three replicates of each sample were assayed and statistically analyzed according to the kit's instructions.

Correlation Analysis Between the SNPs of *PmGrx5* and Ammonia-N Stress Tolerance Trait

Seven hundred healthy juvenile shrimps were selected for the ammonia-N stress experiment (using the same method provided in the *Ammonia-N Stress* section). The first 70 shrimps to die were considered to be the sensitive group and the last 70 shrimps to die and those still alive were considered to be the resistant group. Samples were stored in ethanol and used to extract the DNA. The DNA was extracted from the samples using the MagPure Tissue/Blood DNA LQ Kit (Megan, China).

The NCBI database was used to predict the exonic region of *PmGrx5*. Based on the results, Premier 6.0 was used to design the primers that span the exonic regions to amplify the DNA sequence of the samples. The PCR reaction system consisted of the following: 1 μl of forward primer, 1 μl of reverse primer, 2 μl of DNA template, and 21 μl of Mix Green (Tsingke, China). The PCR procedure was as follows: firstly, 98°C for 2 min, followed by 35 cycles of 98°C for 10 s, 55°C for 15 s, and 72°C for 1 min, and finally 72°C for 10 min. Tsingke Biotechnology was responsible for the synthesis of all the above primers and the sequencing of the PCR products (Guangzhou, China), and the above primers are shown in **Table 1**.

The DNA sequences of each sample were examined using DNAMAN and Chromas to identify the SNPs of *PmGrx5*. Genetic parameters were calculated using WPS Office, including observed heterozygosity (H_o), expected heterozygosity (H_e), effective allele number (N_e), minimum allele frequency (MAF), polymorphism information content (PIC), and Hardy–Weinberg equilibrium (HWE). The χ^2 test using SPSS 26.0 was used to analyze the correlation between the SNPs of *PmGrx5* and ammonia-N stress tolerance trait, and $P < 0.05$ was considered to be a significant difference.

RESULTS

Bioinformatics Results for *PmGrx5*

As seen in **Figure 1A**, the full-length cDNA of *PmGrx5* (GenBank accession number: ON086315) was 787 bp, which included 114 bp 5′-UTR, 232 bp 3′-UTR, a poly-A tail, and 441 bp ORF, encoding a 146 amino acid putative protein. The putative PmGrx5 protein was 16.27 kDa with a theoretical isoelectric point of 5.90. The putative PmGrx5 protein contained only one Grx structural domain. The active center sequence of the *PmGrx5* domain was C-G-F-S (54–57 aa), which was a typical characteristic of the currently known Grx5 proteins. These features suggested that *PmGrx5* was a new member of the monothiol Grxs. According to the putative secondary structure, the proportions of α-helix, extended strand, β-turn, and random coil were 45.21%, 8.90%, 8.90%, and 36.99%, respectively. The putative tertiary structure of PmGrx5 is shown in **Figure 1B**.

As shown in **Figure 2A**, the Grx5 of eight arthropod species was selected for comparison with *PmGrx5*. The results of the multiple sequence alignment showed that in the Grx5 of all the selected species, their amino acid sequences showed a high degree of similarity. In terms of basic structure and function, their Grx5 all contained a similar Grx structural domain, and the signature active center site, C-G-F-S, was highly conserved. In addition, *PmGrx5* has the highest homology to Grx5 in crustaceans. In particular, in *Penaeus*, *PmGrx5* has 98.63% and 94.52% homology with the Grx5 of *Penaeus vannamei* and *Penaeus japonicus*, respectively. *PmGrx5* has the lowest homology with the Grx5 of *Armadillidium vulgare* at 65.47%. In *Chionoecetes opilio*, *Homarus americanus*, *Amphibalanus amphitrite*, *Portunus trituberculatus* and *Limulus polyphemus*, the homology of Grx5 to *PmGrx5* was 77.69%, 75.17%, 73.60%, 71.22%, and 68.99% in this order.

Grx amino acid sequences from 31 different species, including Grx3 and Grx5, were selected using the minimal evolution method of MEGA-X to construct a Grx phylogenetic tree. As shown in **Figure 2B**, both Grx3 and Grx5 were independently aggregated. Grx3 and Grx5 of most species had one to multiple Grx structural domains and the active center site was C-G-F-S, which are typical monothiol Grxs. However, the Grx3 domains of prokaryotes and plants were clustered separately and did not have the active center site C-G-F-S, showing significant differences and signaling evolutionary distancing and separation. The phylogenetic tree showed that vertebrates, including mammals, fish, and amphibians, have Grx3 and Grx5 clustered separately. The same was true for invertebrates and fungi, including *Saccharomyces cerevisiae*, crustaceans, and insects, and Grx3 and Grx5 from fungi were closer to the invertebrate group. Of these, PmGrx3 was the closest phylogenetically to Grx3 from *P. vannamei* and clustered with Grx3 from other crustaceans. The same was observed in the phylogeny of Grx5.

The amino acid sequence of *PmGrx5* was used to construct a protein interaction network based on the STRING database. As the crustacean Grx was rarely studied, the human genome was chosen as the template for the construction. As shown in **Figure 3**, the main proteins predicted to interact with Grx5 were BolA-like protein 1 (BOLA1), BolA-like protein 3 (BOLA3), frataxin (FXN), glutaredoxin 2 (Grx2), iron–sulfur cluster co-chaperone protein (HSCB), iron–sulfur cluster assembly factor (IBA57), iron–sulfur cluster assembly 1 (ISCA1), iron–sulfur cluster assembly 2 (ISCA2), iron–sulfur cluster assembly enzyme (ISCU), and iron–sulfur cluster scaffold protein (NFU1). The main function of these proteins was to regulate the iron–sulfur cluster and redox status in the organism.

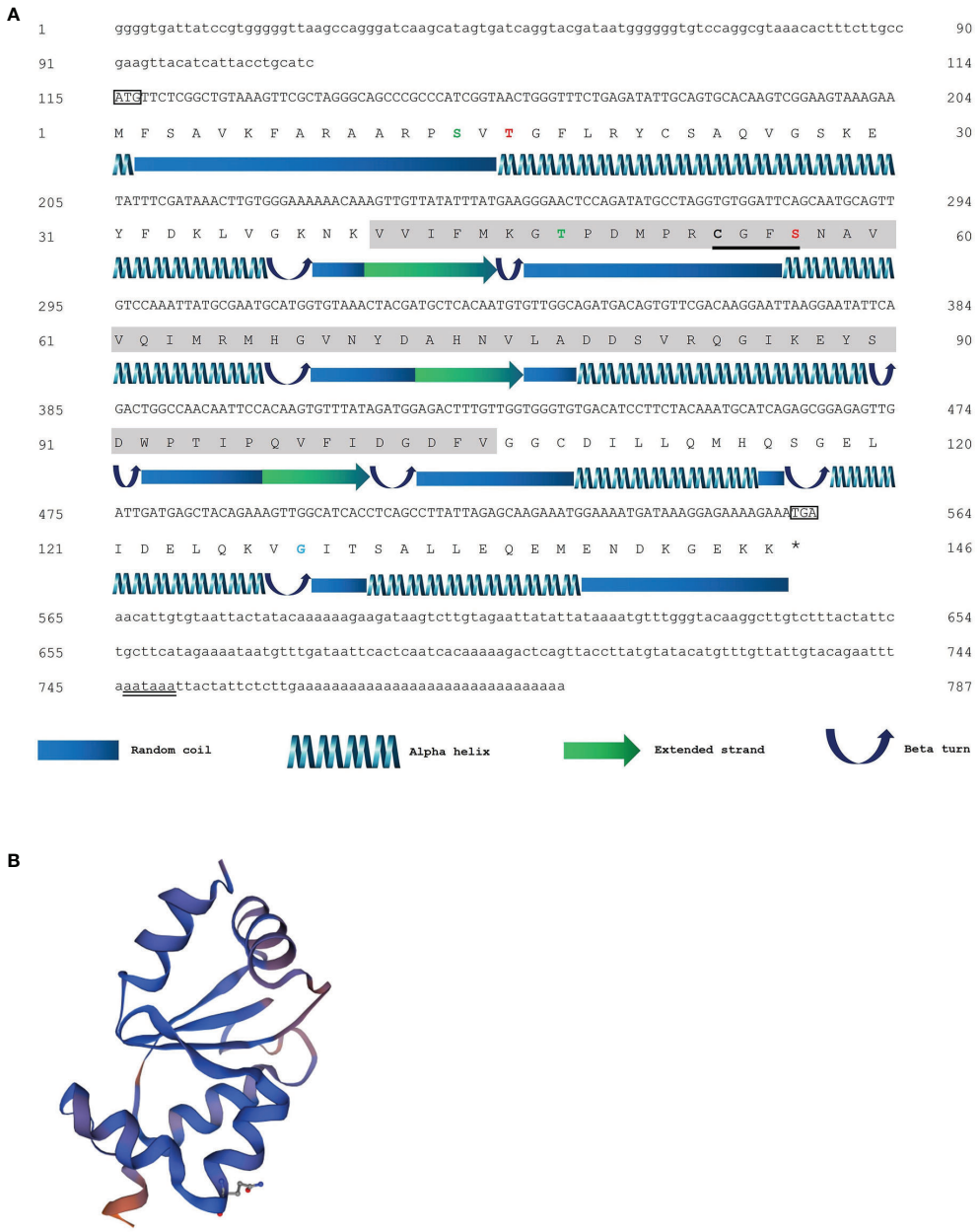

FIGURE 1 | **(A)** The sequence of nucleotides, the deduced sequence of amino acids, and the putative secondary structure of *PmGrx5*. The initiation codon "ATG" and the termination codon "TAA" are marked in the rectangular box. The polyadenylation signal sequence (AATAAA) is marked using a double underline. The gray region indicates the predicted glutaredoxin (Grx) structural domain. The active center sequence (C-G-F-S) of the Grx domains is marked using a single underline. Cys residues are marked in bold. The phosphorylation sites, glycosylation sites, and N-myristoylation sites are highlighted in green, red, and blue, respectively. The legend of the predicted secondary structure is annotated at the bottom of the image. **(B)** The putative tertiary structure of *PmGrx5*.

mRNA Expression of *PmGrx5* in Different Tissues

As shown in **Figure 4**, qRT-PCR results showed that *PmGrx5* was expressed in all tissues examined. *PmGrx5* expression was higher in the testis, stomach, lymphoid organ, and gill ($P < 0.05$). *PmGrx5* expression was lower in the eyestalk nerves, brain, abdominal nerves, and ovary.

mRNA Expression of *PmGrx5* During the Developmental Period

The qRT-PCR results showed that *PmGrx5* was expressed with some regularity in all early developmental stages in black tiger shrimp (**Figure 5**). The expression of *PmGrx5* increased rapidly when development entered nauplius I. Throughout the nauplius stage, the expression of *PmGrx5* showed a gradual

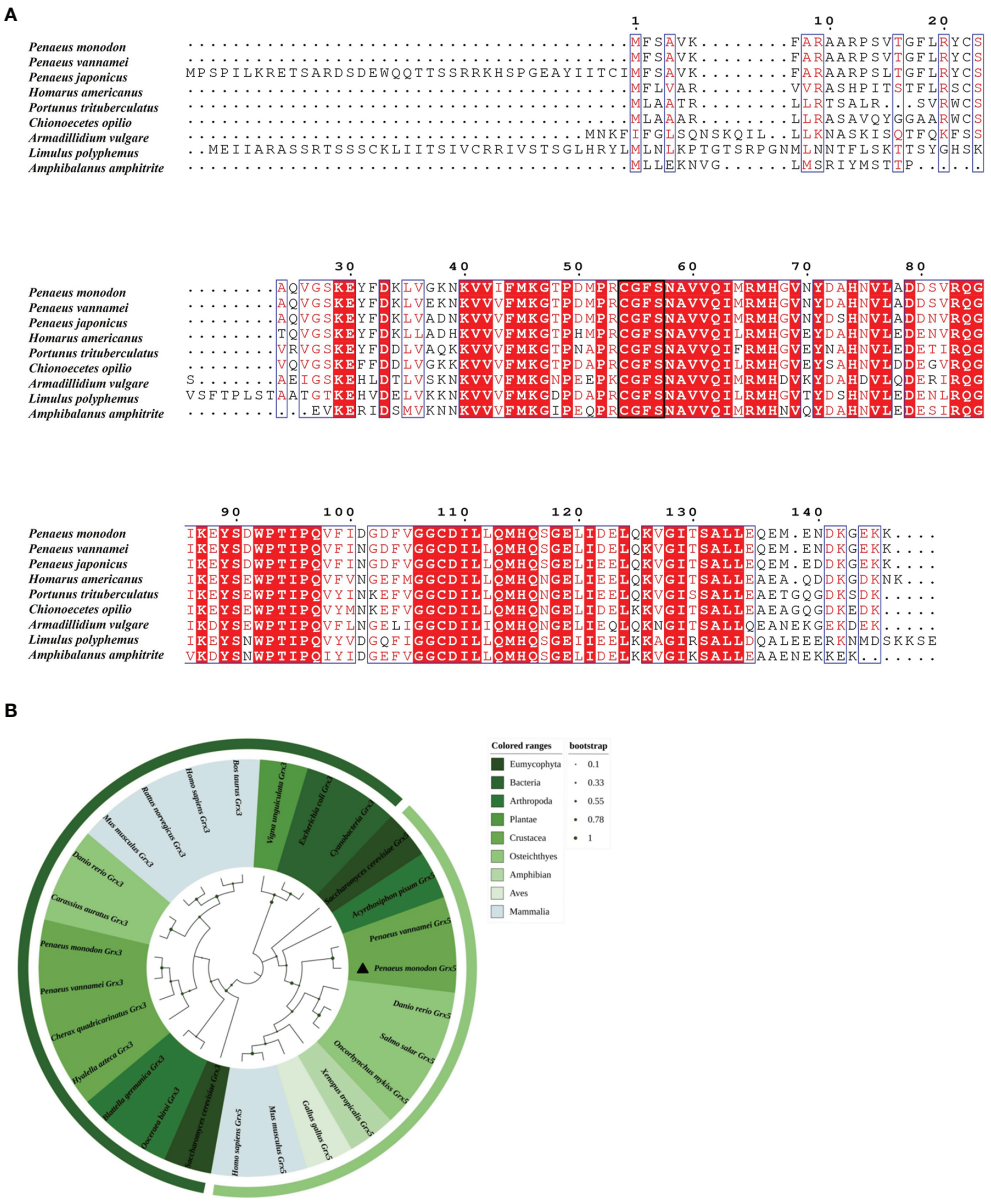

FIGURE 2 | **(A)** Multiple sequence alignment of Grx5 from nine arthropod species. Red regions indicate conserved amino acid residues. Red letters indicate similar residues. Conserved active sites C-G-F-S are highlighted in a black box. The results of the amino acid sequence counts are shown at the top of each row. **(B)** A phylogenetic tree of mono-mercapto Grxs of various species based on amino acid sequences. Bootstrap support values corresponding to each branch are indicated by the dark green dots. The dimensions and corresponding values of the dark green dots are indicated on the right side of the picture. The corresponding species in different colors are shown on the right side of the picture. The dark green outermost arcs indicate the branches of the Grx3 protein. The light green outermost arc indicates the branch of the Grx5 protein. *PmGrx5* is marked with a triangle. The scientific names of all the above species and their NCBI sequence numbers are shown below: *Amphibalanus amphitrite* (KAF0307822.1), *Acyrthosiphon pisum* (AK341132.1), *Armadillidium vulgare* (RXG69803.1), *Blattella germanica* (PSN36174.1), *Bos taurus* (NP_001030273.1), *Carassius auratus* (XP_026078075.1), *Chionoecetes opilio* (KAG0717517.1), *Cherax quadricarinatus* (AEL23128.1), *Cyanobacteria* (WP_190627512.1), *Danio rerio* (NP_001005950.1), *Danio rerio* (BC059659.1), *Escherichia coli* (SYX47894.1), *Gallus gallus* (AJ720261.1), *Homarus americanus* (XP_042230596.1), *Hyalella azteca* (KAA0195653.1), *Homo sapiens* (AAH05289.1), *Homo sapiens* (AB223038.1), *Limulus polyphemus* (XP_013786644.1), *Mus musculus* (NP_075629.2), *Mus musculus* (AK013761.1), *Ooceraea biroi* (EZA62809.1), *Oncorhynchus mykiss* (BT073697.1), *Penaeus monodon* (MZ827442), *Penaeus japonicus* (XP_042868605.1), *Portunus trituberculatus* (MPC08028.1), *Penaeus vannamei* (XP_027209771.1), *Penaeus vannamei* (XP_027214062.1), *Penaeus vannamei* (XM_027358261.1), *Rattus norvegicus* (AAH86381.1), *Saccharomyces cerevisiae* (GFP69319.1), *Saccharomyces cerevisiae* (NM_001183873.1), *Salmo salar* (BT048738.1), *Vigna unguiculata* (QCE13504.1), and *Xenopus tropicalis* (BC075374.1).

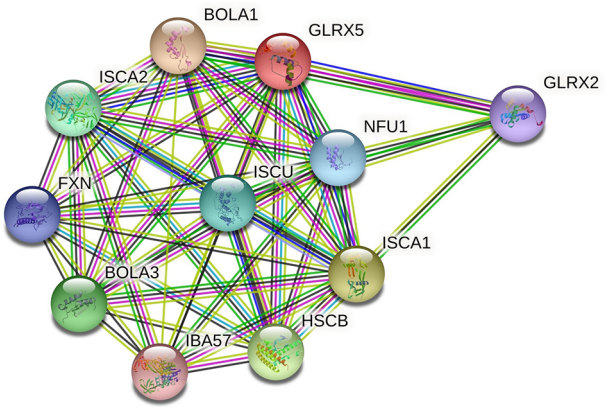

FIGURE 3 | Grx5 protein interaction networks. The red dots represent the target protein Grx5. Other colored dots represent proteins that interact with Grx5. The names of all proteins are abbreviated to the top right of the dots.

decrease and increase and reached a peak at zoea I, which was also the highest expression value throughout the early developmental stages ($P < 0.05$). From mysis II until the development of post-larva, the expression of *PmGrx5* showed a similar trend to the previous stage and finally peaked again at post-larva.

Analysis of *PmGrx5* Transcription for the Hepatopancreas and Gill After Bacterial Challenge

Figure 6 shows the qRT-PCR results for the PmGrx3 expression in the hepatopancreas and gill at different time intervals after multiple pathogenic bacteria injections. In the hepatopancreas,

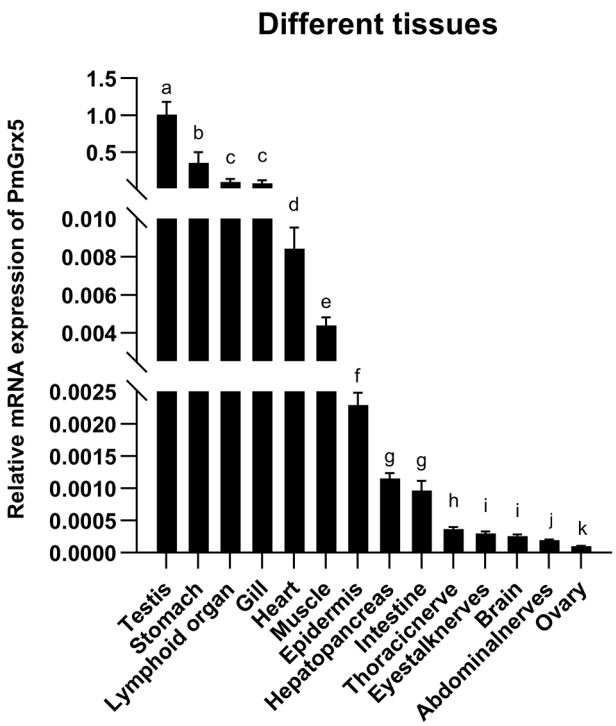

FIGURE 4 | mRNA expression levels of *PmGrx5* in different tissues. The data are presented as mean ± SD ($n = 3$). Different letters denote significant differences ($P < 0.05$).

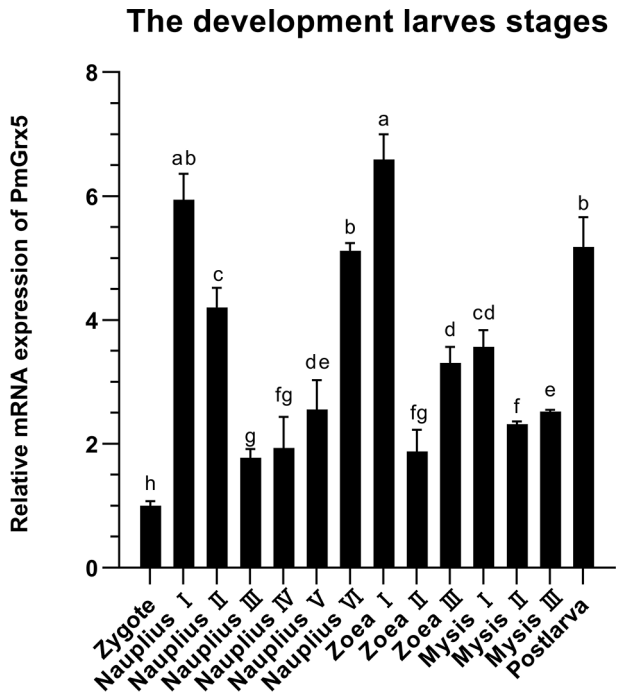

FIGURE 5 | mRNA expression levels of *PmGrx5* during the developmental period. The data are presented as mean ± SD (n = 3). Different letters denote significant differences ($P < 0.05$).

the *PmGrx5* expression was highly significantly upregulated 6 h after *S. aureus* injection compared to the control ($P < 0.05$). A peak was reached 72 h after injection ($P < 0.05$). The *PmGrx5* expression was significantly upregulated, then significantly downregulated, and finally significantly upregulated again within 72 h after *V. harveyi* injection ($P < 0.05$). Within 72 h of *V. anguillarum* injection, the *PmGrx5* expression was only significantly upregulated at 3 h post-injection compared to the control group ($P < 0.05$), with no significant changes at other time points. In the gill, the *PmGrx5* expression was highly significantly upregulated ($P < 0.05$) at 3 h after *S. aureus* injection compared to the control, then plateaued and was significantly upregulated again after 24 h of injection ($P < 0.05$). The expression pattern of *PmGrx5* in the gill was similar to that in the hepatopancreas within 72 h after *V. harveyi* or *V. anguillarum* injection.

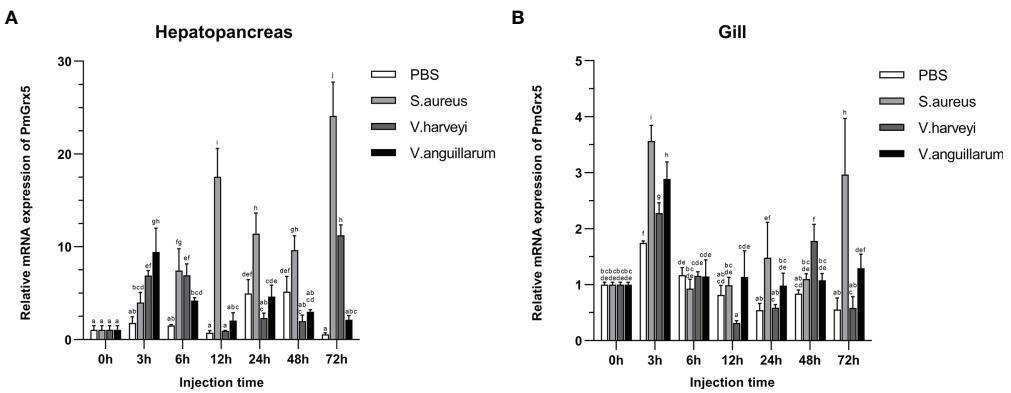

FIGURE 6 | mRNA expression levels of *PmGrx5* in the hepatopancreas **(A)** and gill **(B)** at different time intervals after multiple pathogenic bacteria injections. The data are presented as mean ± SD (n = 3). Different letters denote significant differences ($P < 0.05$).

Analysis of *PmGrx5* Transcription for Hepatopancreas and Gill Under Ammonia-N Stress

Figure 7 shows the qRT-PCR results of *PmGrx5* expression in the hepatopancreas and gill at different time intervals under different levels of ammonia-N stress. From the results, it can be seen that the expression of *PmGrx5* in the hepatopancreas and gill had a similar pattern at 96 h SC, with a gradual increase followed by a decrease over 96 h after ammonia stress. *PmGrx5* peaked at 12 h in the hepatopancreas and at 24 h in the gill, and both produced a fluctuation in elevated expression at 72 h ($P < 0.05$). At 96-h LC_{50}, the trend in *PmGrx5* expression in the hepatopancreas was similar to that at 96-h SC concentrations, except that the response was not as strong as in the former. In the gill, however, the situation was completely different. At 96-h LC_{50}, the expression of *PmGrx5* was not significantly higher in the gill compared to the control and was even consistently lower than in the control and the 96-h SC group.

The Interference Efficiency of dsGrx5 in the Hepatopancreas

As shown in **Figure 8A**, dsGrx5 could significantly inhibit the *PmGrx5* expression in the hepatopancreas ($P < 0.05$), satisfying the requirements of this experiment. As shown in **Figure 8B**, ammonia-N stress was applied to all experimental groups 24 h after dsRNA injection. The *PmGrx5* expression in the dsGFP-injected group was significantly higher than that in the dsGrx5-injected group within 48 h after ammonia-N stress ($P < 0.05$), which demonstrated that dsGrx5 could significantly exert its inhibitory effect within 72 h after injection.

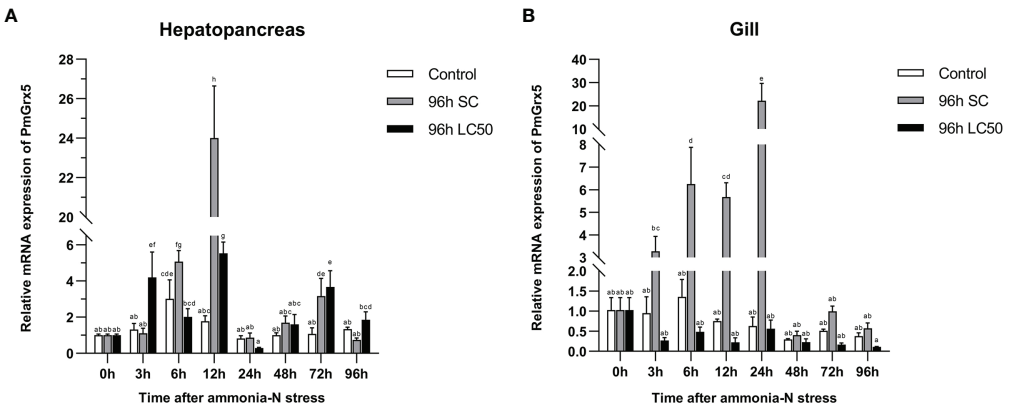

FIGURE 7 | mRNA expression levels of *PmGrx5* in the hepatopancreas **(A)** and gill **(B)** at different time intervals under different concentrations of ammonia-N stress. The data are presented as mean ± SD ($n = 3$). Different letters denote significant differences ($P < 0.05$).

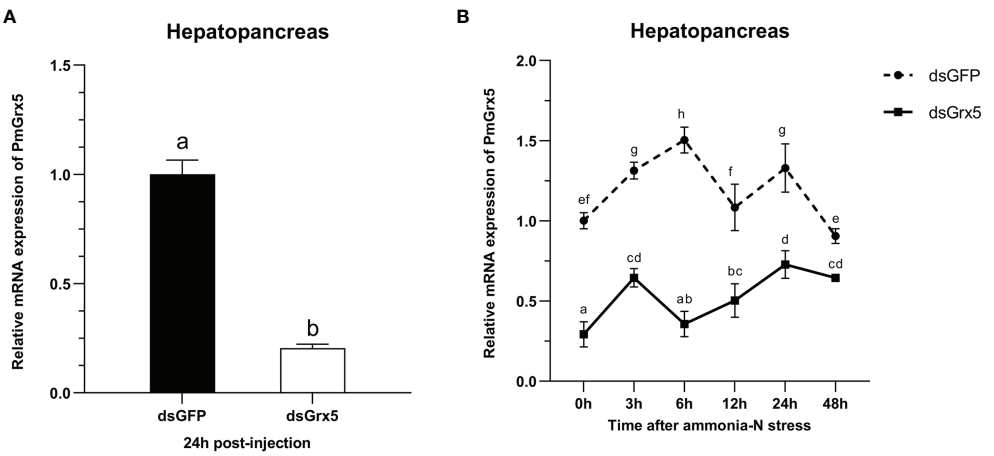

FIGURE 8 | **(A)** mRNA expression levels of *PmGrx5* in the hepatopancreas at 24 h after dsRNA injection. **(B)** Expression profile of *PmGrx5* in the hepatopancreas of dsRNA-injected shrimps within 48 h under ammonia-N stress. The data are presented as mean ± SD ($n = 3$). Different letters denote significant differences ($P < 0.05$).

mRNA Expression of Genes in the Hepatopancreas of dsRNA-Injected Shrimps Under Ammonia-N Stress

As shown in **Figure 9A**, the *PmTrx* expression in the dsGFP-injected group was gradually upregulated and then downregulated within 48 h under ammonia-N stress, reaching a peak at 12 h ($P < 0.05$). Compared with the control group, the *PmTrx* expression in the *PmGrx5*-interfered group showed a similar trend, but its response was stronger, showing significant up- or downregulation ($P < 0.05$).

As shown in **Figure 9B**, the *PmPrx1* expression in the dsGFP-injected group was significantly higher at 3 h after ammonia-N stress ($P < 0.05$), then gradually decreased and finally significantly upregulated again at 48 h after ammonia-N stress ($P < 0.05$). The expression trend of *PmPrx1* in the *PmGrx5*-interfered group was similar to that in the control group from 3

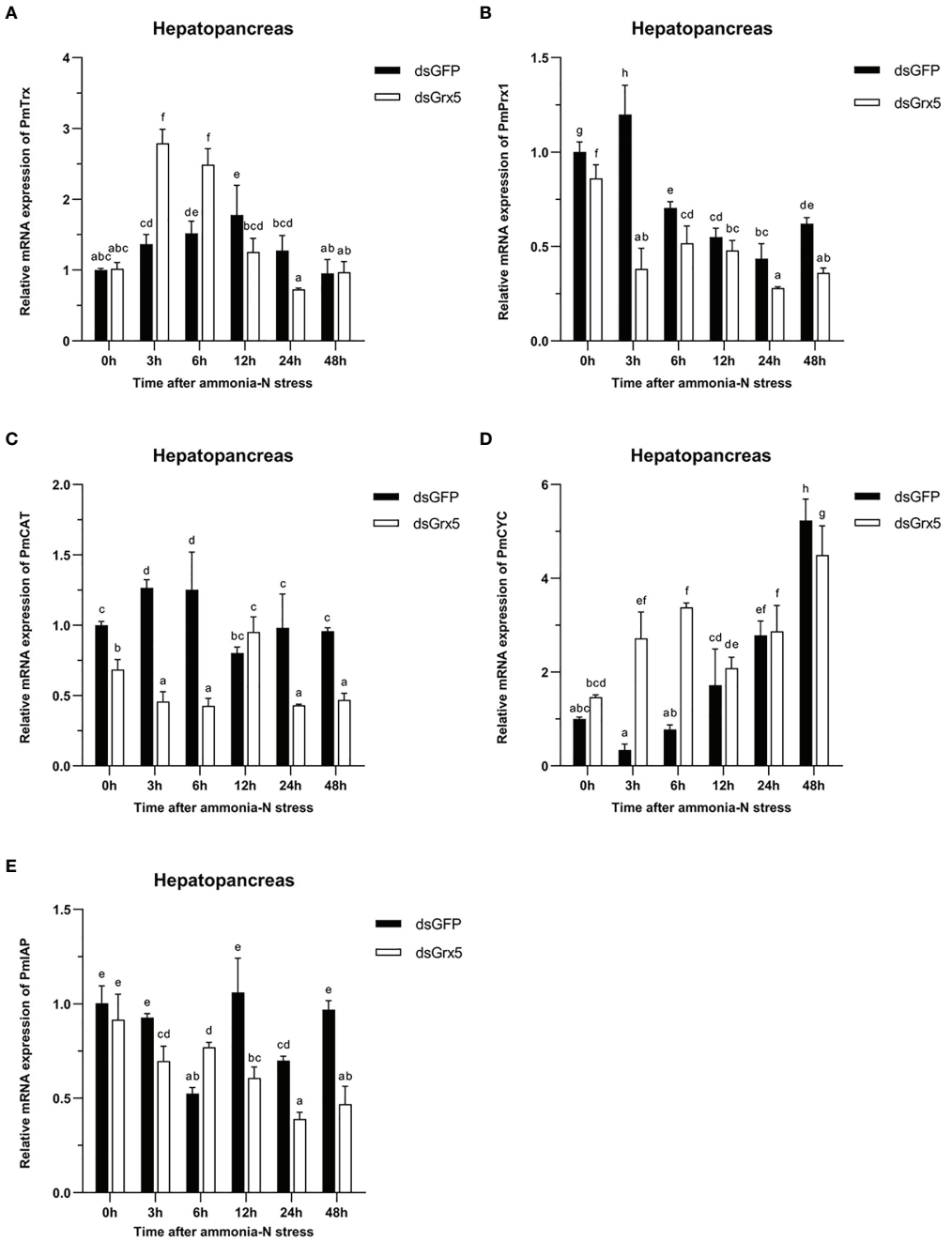

FIGURE 9 | Expression profiles of five genes [*PmTrx* **(A),** *PmPrx1* **(B)**, *PmCAT* **(C)**, *PmCYC* **(D)**, and *PmIAP* **(E)**] in the hepatopancreas of dsRNA-injected shrimps under ammonia-N stress. The data are presented as mean ± SD ($n = 3$). Different letters denote significant differences ($P < 0.05$).

to 48 h after ammonia-N stress. However, the expression level of *PmPrx1* in the *PmGrx5*-interfered group was significantly lower than that in the control group at all time points ($P < 0.05$), except at 12 h after ammonia-N stress, when it was also lower but not significant.

As shown in **Figure 9C**, the *PmCAT* expression in the dsGFP-injected group was significantly increased within 6 h under ammonia-N stress ($P < 0.05$). Its expression decreased significantly at 12 h after ammonia-N stress ($P < 0.05$) and then stabilized. The *PmCAT* expression in the *PmGrx5*-interfered group showed significant upregulation only at 12 h after ammonia nitrogen stress ($P < 0.05$). At the rest of the time points, its expression level was always significantly lower than the initial level and that in the control ($P < 0.05$).

As shown in **Figure 9D**, the *PmCYC* expression in the dsGFP-injected group gradually increased 3 h after ammonia-N stress and reached a maximum at 48 h ($P < 0.05$). The *PmCYC* expression in the *PmGrx5*-interfered group was first significantly upregulated within 48 h after ammonia-N stress and significantly decreased at 12 h, then gradually increased again, also reaching a peak at 48 h ($P < 0.05$). The *PmCYC* expression in the *PmGrx5*-interfered group was significantly higher than that in the control group at 3–6 h after ammonia-N stress ($P < 0.05$). The expression pattern of *PmCYC* in the control and experimental groups was similar during the 12–48-h period after ammonia-N stress.

As shown in **Figure 9E**, the *PmIAP* expression in the dsGFP-injected group was significantly reduced only at 6 and 24 h after ammonia-N stress ($P < 0.05$). In contrast, the *PmIAP* expression level in the *PmGrx5*-interfered group was gradually reduced overall, accompanied by non-significant fluctuations. The *PmIAP* expression level in the *PmGrx5*-interfered group was significantly lower than that in the control group except for 6 h after ammonia-N stress ($P < 0.05$).

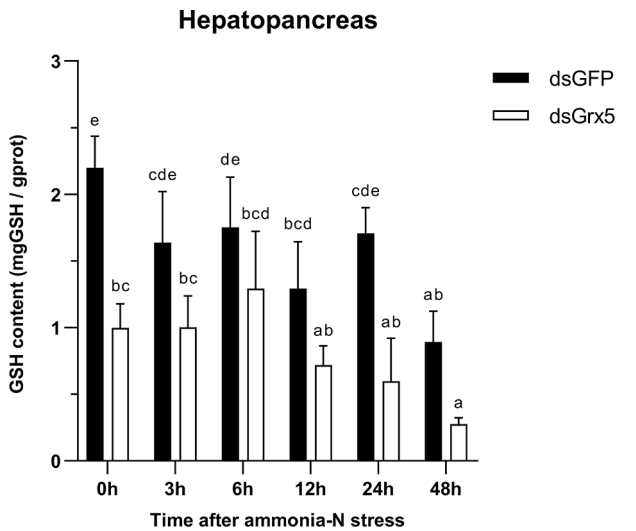

FIGURE 10 | Changes in GSH content in the hepatopancreas of dsRNA-injected shrimps under ammonia-N stress. The data are presented as mean ± SD ($n = 3$). Different letters denote significant differences ($P < 0.05$).

GSH Content in the Hepatopancreas of dsRNA-Injected Shrimps Under Ammonia-N Stress

As shown in **Figure 10**, GSH content in the hepatopancreas of dsGFP-injected shrimps remained essentially flat with no significant changes within 24 h after ammonia-N stress and finally decreased significantly at 48 h ($P < 0.05$). The trend in GSH content in the hepatopancreas of *PmGrx5*-interfered shrimps was similar to that of dsGFP-injected shrimps, but it was always significantly lower than that of dsGFP-injected shrimps ($P < 0.05$).

Correlation Analysis Between the SNPs of *PmGrx5* and Ammonia-N Stress Tolerance Trait

In this study, a total of nine SNPs were identified on the exons of *PmGrx5*. The specific information of the SNPs of *PmGrx5* is shown in **Table 2**. Sequencing maps of the SNPs of *PmGrx5* are shown in **Figure 11**. Analysis of the polymorphic parameters (**Table 3**) showed that H_o for the nine SNPs ranged from 0.0000 to 0.4500, H_e from 0.0072 to 0.4994, N_e from 1.0072 to 1.9976, and MAF from 0.0036 to 0.4821. PmGrx5-E187, PmGrx5-E1134, PmGrx5-E3684, and PmGrx5-E3718 showed low polymorphisms (PIC < 0.2500), and the remaining five SNPs showed moderate polymorphisms (0.2500 < PIC < 0.5000). HWE results showed that PmGrx5-E1134 significantly ($P < 0.05$) deviated from HWE, PmGrx5-E1222 and PmGrx5-E2297 were highly significant ($P < 0.01$) deviating from HWE, and the remaining six SNPs were in HWE.

Correlation analysis between the SNPs of *PmGrx5* and ammonia-N stress tolerance trait is shown in **Table 4**. Except for PmGrx5-E3718, which was not significantly correlated with the ammonia-N stress tolerance trait, the allele distribution of the remaining SNPs was significantly different between the sensitive and resistant groups ($P < 0.05$).

DISCUSSION

Grx5, a small molecule of monothiol Grx, has been previously studied in bacteria, yeast, *Arabidopsis thaliana*, zebrafish, and human, mainly (Camaschella et al., 2007; Oh et al., 2012; Shakamuri et al., 2012; Mapolelo et al., 2013; Petry et al.,

TABLE 2 | Specific information of the SNPs of *PmGrx5*.

SNPs	Position	Type of base mutation	Type of protein mutation
PmGrx5-E169	Exon 1 (69 bp)	c.-46C>G	–
PmGrx5-E187	Exon 1 (87 bp)	c.-28T>C	–
PmGrx5-E1134	Exon 1 (134 bp)	c.20T>C	Mm p.Phe7Ser
PmGrx5-E1222	Exon 1 (222 bp)	c.108G>T	Sm p.Val36=
PmGrx5-E1241	Exon 1 (241 bp)	c.127A>G	Mm p.Ile43Val
PmGrx5-E2297	Exon 2 (297 bp)	c.183C>G	Sm p.Val61=
PmGrx5-E3679	Exon 3 (679 bp)	c.*125A>T	–
PmGrx5-E3684	Exon 3 (684 bp)	c.*129A>C	–
PmGrx5-E3718	Exon 3 (718 bp)	c.*163T>C	–

*Mm, missense mutation; Sm, synonymous mutation. *Meaning of the symbols in Table 2 (Dunnen et al., 2016).*

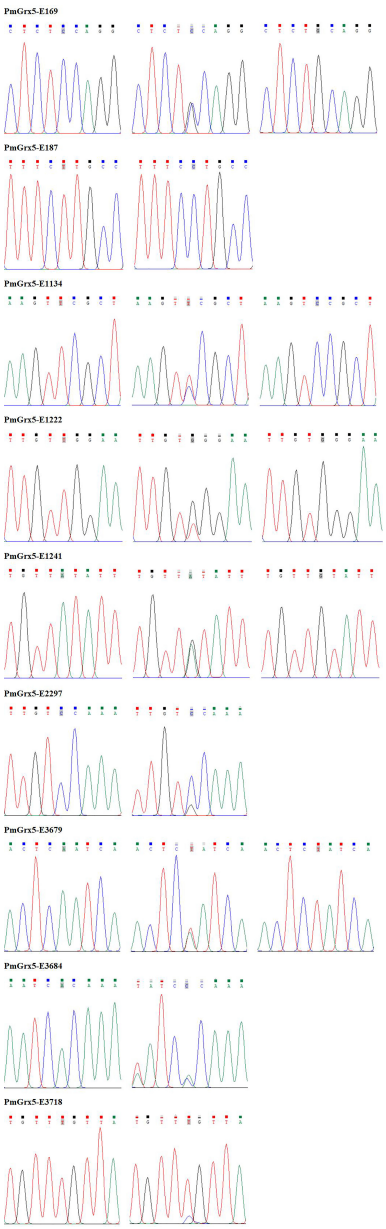

FIGURE 11 | Sequencing maps of the SNPs of *PmGrx5*.

2018). In this study, a new full-length cDNA for Grx5, *PmGrx5*, was successfully cloned for the first time in crustaceans. In the predicted amino acid sequence, there is a unique Grx structural domain containing an active center sequence C-G-F-S, which is typical of the monothiol Grx domain. There are two main types of monothiol Grxs: one contains only one Grx structural domain and the other contains an N-terminal Trx structural domain and one to three Grx structural domains. *PmGrx5* belongs to the former group, while PmGrx3, which is also a monothiol Grx, belongs to the latter group. The difference in the number and complexity of the structural domains in their amino acid sequences predicts their evolutionary differences and potentially different functions. The amino acid sequences of Grx5 from eight species were selected for multiple comparisons with *PmGrx5*. The Grx5 of all nine species was a monothiol Grx and all had the active center sequence C-G-F-S, indicating that C-G-F-S is highly conserved between species. Phylogenetic analysis showed that *PmGrx5* clustered with PvGrx5 with 98.63% amino acid sequence homology, which is highly conserved and predicts that Grx5 may play a similar role in crustaceans. The main function of the protein predicted to interact with Grx5 is to regulate the iron–sulfur cluster and redox state in the organism. Iron–sulfur clusters are a class of cofactors essential to living organisms and have a variety of functions such

TABLE 3 | Polymorphic parameters of the SNPs of *PmGrx5*.

SNPs	H_o	H_e	N_e	MAF	PIC	HWE
PmGrx5-E169	0.4500	0.4484	1.8127	0.3393	0.3478	0.9990
PmGrx5-E187	0.0000	0.1326	1.1529	0.0714	0.1238	0.0679
PmGrx5-E1134	0.2143	0.2746	1.3786	0.1643	0.2369	0.0342
PmGrx5-E1222	0.3143	0.4362	1.7737	0.3214	0.3411	0.0042
PmGrx5-E1241	0.5071	0.4994	1.9976	0.4821	0.3747	0.9831
PmGrx5-E2297	0.4071	0.3243	1.4799	0.2036	0.2717	0.0005
PmGrx5-E3679	0.2571	0.3024	1.4335	0.1857	0.2567	0.2078
PmGrx5-E3684	0.0429	0.0419	1.0437	0.0214	0.0410	0.9669
PmGrx5-E3718	0.0071	0.0072	1.0072	0.0036	0.0071	0.9991

SNPs, single nucleotide polymorphisms; H_o, observed heterozygosity; H_e, expected heterozygosity; N_e, effective number; MAF, minimum allele frequency; PIC, polymorphism information content; HWE, Hardy–Weinberg equilibrium.

TABLE 4 | Correlation analysis between the SNPs of *PmGrx5* and ammonia-N stress tolerance trait.

SNPs	Genotype	Genotype frequencies		χ^2 value	*P*-value
		Sensitivity	Resistance		
PmGrx5-E169	CC	0.5000	0.3714	9.591	0.008267*
	CG	0.3571	0.5429		
	GG	0.1429	0.0857		
PmGrx5-E187	TT	0.8571	1.0000	20.192	0.000007*
	CC	0.1429	0.0000		
PmGrx5-E1134	TT	0.6857	0.7714	13.133	0.001406*
	TC	0.2143	0.2143		
	CC	0.1000	0.0143		
PmGrx5-E1222	TT	0.1000	0.2286	19.572	0.000056*
	TG	0.2286	0.4000		
	GG	0.6714	0.3714		
PmGrx5-E1241	AA	0.1714	0.3571	26.053	0.000002*
	AG	0.4857	0.5286		
	GG	0.3429	0.1143		
PmGrx5-E2297	CC	0.6818	0.3571	17.384	0.000031*
	CG	0.3182	0.6429		
PmGrx5-E3679	AA	0.6714	0.7000	14.122	0.000858*
	AT	0.2286	0.2857		
	TT	0.1000	0.0143		
PmGrx5-E3684	AA	1.0000	0.9143	12.042	0.000520*
	AC	0.0000	0.0857		
PmGrx5-E3718	TT	1.0000	0.9857	2.000	0.157278
	TC	0.0000	0.0143		

**Denotes significant correlation ($P < 0.05$).*

as transferring and catalyzing electrons (Glaser and Glaser, 2020). Therefore, iron–sulfur clusters are also an important component in the regulation of the redox state of cells. It has been demonstrated in several species that monosulfhydryl glutathione with the active site CGFS possesses a good ability to bind iron–sulfur clusters (Herrero and de la Torre-Ruiz, 2007), and it is considered to be an intermediate carrier for the delivery of iron–sulfur clusters to a variety of apolipoprotein target proteins (Shakamuri et al., 2012). Furthermore, inhibition of Grx5 expression in zebrafish results in the inability to synthesize iron–sulfur clusters properly in fish cells. In contrast, injection of Grx5 from other species into zebrafish, such as yeast, mice, and human, respectively, restored the normal synthesis of iron–sulfur clusters in their cells (Wingert et al., 2005). This result suggests that, at least in the physiological processes involved in iron–sulfur cluster synthesis, the function of Grx5 is conserved across multiple species.

In this study, the tissue distribution of *PmGrx5* in crustaceans was examined for the first time. *PmGrx5* was expressed in all tissues, indicating a wide range of biological functions. However, the expression of *PmGrx5* varied greatly in different tissues, with the highest expression in the testis, stomach, lymphoid organ, and gill. In mice, the expression of Grx3, a monothiol Grx, was also the highest in the testis (Cheng et al., 2011). Meanwhile, the expression of dithiol Grx2 was increased during human sperm development. In addition, Grx2b and Grx2c were protein isoforms specific to the human testis (Lönn et al., 2008). Although their exact mechanism and role had not been

proven, Grxs were closely associated with the development of the mammalian testis and sperm, and it was hypothesized that *PmGrx5* performed a similar function. The stomach, lymphoid organ, and gill were all important components of the crustacean immune system. The stomach and gill were the first barriers for crustaceans against external environmental stressors and pathogens (Rowley, 2016). Among crustaceans, the lymphoid organ, currently found only, was considered to be the main immune organ that exerts phagocytosis (Rusaini, 2010). This suggested that *PmGrx5* may play an important role in the immune role played by shrimps.

PmGrx5 was expressed continuously throughout the early developmental period in *P. monodon*. It was easy to see from **Figure 6** that the expression of *PmGrx5* increased each time the shrimps developed to a new stage and that the highest expression was found in the early stage of each stage. The greatest expression of *PmGrx5* was found in nauplius I and zoea I. Early development was a very complex and rapid process, and as a eukaryote that did not rely on photosynthesis, this process required mitochondrial energy supply. The iron–sulfur cluster was one of the key components of the energy production process of the mitochondrial respiratory chain (Beinert, 2000). It is inferred that as a monothiol Grx, *PmGrx5* may be involved in the assembly and transfer of iron–sulfur clusters (Bandyopadhyay et al., 2008) during the early development of *P. monodon*, thus promoting smooth development. In mammals, the monothiol Grx has been shown to be essential for embryonic development and post-embryonic growth (Cheng et al., 2011). In plants, the Grxs17 homolog (a monothiol Grx) is also required for post-embryonic growth (Knuesting et al., 2015).

To verify whether *PmGrx5* was involved in the immune response of *P. monodon* to bacterial infection, one Gram-positive (*S. aureus*) and two Gram-negative (*V. harveyi* and *V. anguillarum*) strains were selected for *in-vivo* injection in this study. *PmGrx5* produced varying degrees of immune response to all three bacteria within 72 h of injection compared to the control group. At 3 h after injection, the expression of *PmGrx5* was significantly upregulated in all three treatment groups in the gill, while the expression of *PmGrx5* was significantly upregulated in the group injected with Gram-negative bacteria only in the hepatopancreas. This phenomenon suggested that *PmGrx5* was more sensitive to Gram-positive bacteria in the gill. However, the relative expression of *PmGrx5* in the hepatopancreas was higher than that in the gill in all three treatment groups, suggesting that *PmGrx5* in the hepatopancreas played a more important role in the defense of shrimp against pathogens than in the gill, the outer barrier organ of immunity. The same phenomenon was found in *Litopenaeus vannamei*, where the response of LvGrx3 (a monothiol Grx) was more sensitive in the gill than in the hepatopancreas after LPS injection, but the highest relative expression of lvgrx3 was detected in the hepatopancreas (Zheng et al., 2021).

Ammonia-N is one of the most common aquatic environmental stressors. Ammonia-N in water consists of non-ionic ammonia nitrogen (NH_3-N) and ionic ammonia nitrogen (NH_4^+-N) (Randall and Tsui, 2002). Excess ammonia-N induces the production of ROS/RNS, which exacerbates oxidative damage in the organism (Ching et al., 2009; Bu et al., 2017). Excess ammonia-N in the environment is toxic to aquatic organisms, and crustaceans are no exception. It had been shown that prolonged ammonia-N stress could lead to oxidative damage and inflammation in aquatic organisms, which in turn would lead to reduced immunity and increased susceptibility to pathogens and mortality (Cheng et al., 2015; Zhang et al., 2015; Shi et al., 2019; Liu et al., 2021). The hepatopancreas is the most important organ for ammonia and nitrogen metabolism. The gill is the first immune defense barrier for shrimp in direct contact with the aquatic environment (Shi et al., 2019). In the present study, the expression of *PmGrx5* was significantly upregulated in the hepatopancreas and gill of the 96-h SC group relative to the control group during 96 h of ammonia-N stress. The 96-h LC_{50} group also showed significant upregulation of *PmGrx5* in the hepatopancreas, but the relative expression was not as strong as that of the 96-h SC group. However, the expression of *PmGrx5* in the hepatopancreas of the 96-h LC_{50} group was even consistently lower than that of the control and the 96-h SC group. The above results suggested that both high and low concentrations of ammonia-N induced *PmGrx5* in response to ammonia-N stress in shrimp and resisted ammonia-N stress by significantly upregulating *PmGrx5* expression. However, as the gill was directly exposed to the environment, a high concentration of ammonia-N may severely disrupt the normal function of the gill. Also, the response of *PmGrx5* in the hepatopancreas under a high concentration of ammonia-N was much less sensitive than that under a low concentration of ammonia-N. Similar results were reported in PmChi4 and PmGrx3 in *P. monodon* and lvGrx2 in *L. vannamei* (Zhou et al., 2017; Zheng et al., 2018; Fan et al., 2021). The above results suggested that within a certain period of time, shrimps can use their own defense system to counteract the adverse effects of ammonia-N stress, but the normal functions of the gill and hepatopancreas of shrimps could be impaired under a high concentration of ammonia-N.

Furthermore, to better validate the defense mechanism of *PmGrx5* in shrimp coping with ammonia stress in the marine environment, we significantly inhibited the expression of *PmGrx5* using dsRNA. The results showed that dsRNA could significantly exert its disrupting effect at least 72 h after injection. We selected *PmTrx* and *PmPrx1*, which are in the same Trx superfamily as *PmGrx5*, and analyzed their expression after *PmGrx5* expression was suppressed. Within 6 h of ammonia-N stress, the expression of *PmTrx* in the *PmGrx5*-interfered group showed significant upregulation compared to the dsGFP-injected group. It had been previously demonstrated that Grx compensated for the functional defects of *E. coli* Trx mutant strains, and therefore, Grx and Trx overlapped in some functions in the cell (Holmgren, 1979). Shrimps may replace the absence of *PmGrx5* by upregulating *PmTrx* during the initial phase of ammonia-N stress. The opposite was true for *PmPrx1*, which was significantly less expressed in the *PmGrx5*-interfered group than in the dsGFP-injected group. It was hypothesized that there was a dependence of *PmPrx1* on *PmGrx5* and that the inability of *PmPrx1* to be expressed properly exacerbated oxidative damage in the organism (Zhao and Wang, 2012). A similar situation was observed in *PmCAT*, where the dsGFP-injected group

upregulated *PmCAT* (a peroxidase) after 3 h under ammonia-N stress to counteract oxidative damage, while the *PmGrx5*-interfered group failed to do so. CYC was an enzyme that played a crucial role in apoptosis (Hu and Yao, 2016). Initially, ammonia-N stress activated the apoptotic pathway and induced massive expression of *PmCYC* in the *PmGrx5*-interfered group. With the prolongation of ammonia-N stress, *PmCYC* showed a gradual upregulation trend in both groups, while *PmIAP* (an anti-apoptotic enzyme) was significantly inhibited in the *PmGrx5*-interfered group. At the same time, the GSH content was also significantly reduced. The above results suggested that when *PmGrx5* was inhibited, the organism would upregulate similar function genes to protect itself under ammonia-N stress. However, as the stress time increased, the expression of antioxidant enzymes was inhibited, and the expression of apoptotic genes was increased. The inhibition of *PmGrx5* led to a greater risk of oxidative damage to the shrimp.

In this study, direct sequencing was applied for the first time in *PmGrx5* for locus typing, and nine SNPs were successfully obtained. Of the nine SNPs, PmGrx5-E1161, PmGrx5-E1249, and PmGrx5-E2324 deviated significantly from the Hardy–Weinberg equilibrium ($P < 0.05$). On the one hand, artificial selection affects allele frequencies; on the other hand, the samples in this study are extreme populations, which also have an impact on the allele frequency distribution. PmGrx5-E1134, PmGrx5-E1222, PmGrx5-E1241, and PmGrx5-E2297 are located on the ORF. PmGrx5-E1134 and PmGrx5-E1241 are missense mutations that result in mutations from phenylalanine (Phe) and isoleucine (Ile) to serine (Ser) and valine (Val). Phe, Ile, and Val are non-polar amino acids, whereas Ser is a polar amino acid. This may be one of the factors contributing to the altered tolerance to ammonia-N stress in shrimp. PmGrx5-E169, PmGrx5-E187, PmGrx5-E3679, PmGrx5-E3684, and PmGrx5-E3718 are located in the UTR. Although the UTR does not directly alter the structure and function of the protein, promoters, enhancers, and transcription factor binding sites are often located in the untranslated region and, therefore, may affect the translation efficiency or stability of the mRNA (Zhang et al., 2021). In the present study, except for PmGrx5-E3745, the remaining SNPs were significantly correlated with the strength of ammonia nitrogen stress tolerance in shrimp ($P < 0.05$), and the exact mode of influence needs to be further investigated.

In conclusion, the cDNA of *PmGrx5* was cloned and identified as a member of the Trx superfamily, and *PmGrx5* was expressed in all tissues and throughout the developmental stages of *P. monodon*. Both ammonia-N stress and bacterial infection significantly induced the mRNA expression level of *PmGrx5* in the hepatopancreas and gill of the shrimp, suggesting that *PmGrx5* plays an important role in the defense mechanism of the shrimp against marine environmental stress and pathogen infection. Inhibition of *PmGrx5* expression under ammonia-N stress significantly affected the expression levels of other antioxidant enzymes and apoptotic genes, leading to a greater risk of oxidative damage in shrimp. In addition, this study identified SNPs in the exonic region of *PmGrx5* and analyzed their correlation with ammonia-N stress tolerance trait in shrimp. This study will lay the foundation for further research on the role of Grx5 in crustacean innate immunity and molecular marker breeding.

DATA AVAILABILITY STATEMENT

The datasets presented in this study can be found in online repositories. The names of the repository/repositories and accession number(s) can be found below: https://www.ncbi.nlm.nih.gov/, ON086315.

ETHICS STATEMENT

The animal study was reviewed and approved by the Animal Care and Use Committee of the South China Sea Fisheries Research Institute.

AUTHOR CONTRIBUTIONS

RF, SGJ, YL, and FZ: conceptualization. RF, QY, SJ, JH, LY, and XC: methodology. RF and FZ: data curation. RF: writing—original draft preparation. FZ: writing—review and editing. All authors contributed to the article and approved the submitted version.

FUNDING

This work was supported by the Research and Development Projects in Key Areas of Guangdong Province (2021B0202003); China Agriculture Research System of MOF and MARA (CARS-48); Central Public-interest Scientific Institution Basal Research Fund, CAFS (No. 2020TD30); and Central Public Interest Scientific Institution Basal Research Fund, South China Sea Fisheries Research Institute, CAFS (Nos. 2020ZD01, 2021SD13).

REFERENCES

Alday, V., Roque, A., and Turnbull, J. F. (2002). Clearing Mechanisms of Vibrio Vulnificus Biotype I in the Black Tiger Shrimp *Penaeus Monodon*. *Dis. Aquat. Organism.* 48, 91–99. doi: 10.3354/dao048091

Amornrat, T., and Montip, T. (2010). Boonsirm Withyachumnarnkul. Characterization of Candidate Genes Involved in Growth of Black Tiger Shrimp *Penaeus Monodon*. *Aquaculture* 307, 150–156. doi: 10.1016/j.aquaculture.2010.07.008

Arun, K. D., Michelle, M. R., and Kurt, R. K. (2002). Quantitative Assay for Measuring the Taura Syndrome Virus and Yellow Head Virus Load in Shrimp by Real-Time RT-PCR Using SYBR Green Chemistry. *J. Virol. Methods* 104, 69–82. doi: 10.1016/S0166-0934(02)00042-3

Bandyopadhyay, S., Gama, F., Molina-Navarro, M. M., Gualberto, J. M., Claxton, R., Naik, S. G., et al. (2008). Chloroplast Monothiol Glutaredoxins as Scaffold Proteins for the Assembly and Delivery of [2Fe-2S] Clusters. *EMBO J.* 27, 1122–1133. doi: 10.1038/emboj.2008.50

Beinert, H. (2000). Iron-Sulfur Proteins: Ancient Structures, Still Full of Surprises. *J. Biol. Inorgan. Chem.* 5, 2–15. doi: 10.1007/s007750050002

Berndt, C., Poschmann, G., Stühler, K., Holmgren, A., and Bräutigam, L. (2014). Zebrafish Heart Development is Regulated *via* Glutaredoxin 2 Dependent Migration and Survival of Neural Crest Cells. *Redox Biol.* 2, 673–678. doi: 10.1016/j.redox.2014.04.012

Bräutigam, L., Johansson, C., Kubsch, B., McDonough, M. A., Bill, E., Holmgren, A., et al. (2013). An Unusual Mode of Iron-Sulfur-Cluster Coordination in a Teleost Glutaredoxin. *Biochem. Biophys. Res. Commun.* 436, 491–496. doi: 10.1016/j.bbrc.2013.05.132

Bräutigam, L., Schütte, L. D., Godoy, J. R., Prozorovski, T., Gellert, M., Hauptmann, G., et al. (2011). Vertebrate-Specific Glutaredoxin is Essential for Brain Development. *Proc. Natl. Acad. Sci. U. S. A.* 108, 20532–20537. doi: 10.1073/pnas.1110085108

Bu, R., Wang, P., Zhao, C., Bao, W., and Qiu, L. (2017). Gene Characteristics, Immune and Stress Responses of PmPrx1 in Black Tiger Shrimp (*Penaeus Monodon*): Insights From Exposure to Pathogenic Bacteria and Toxic Environmental Stressors. *Dev. Comp. Immunol.* 77, 1–16. doi: 10.1016/j.dci.2017.07.002

Camaschella, C., Campanella, A., De, F. L., Boschetto, L., Merlini, R., Silvestri, L., et al. (2007). The Human Counterpart of Zebrafish Shiraz Shows Sideroblastic-Like Microcytic Anemia and Iron Overload. *Blood* 110, 1353–1358. doi: 10.1182/blood-2007-02-072520

Carvalho, A. P., Fernandes, P. A., and Ramos, M. J. (2006). Similarities and Differences in the Thioredoxin Superfamily. *Prog. Biophys. Mol. Biol.* 91, 229–248. doi: 10.1016/j.pbiomolbio.2005.06.012

Chen, S. M., and Chen, J. C. (2002). Effects of pH on Survival, Growth, Molting and Feeding of Giant Freshwater Prawn *Macrobrachium Rosenbergii*. *Aquaculture* 218, 613–623. doi: 10.1016/S0044-8486(02)00265-X

Cheng, N. (2008). AtGRX4, an Arabidopsis Chloroplastic Monothiol Glutaredoxin, is Able to Suppress Yeast Grx5 Mutant Phenotypes and Respond to Oxidative Stress. *FEBS Lett.* 582, 848–854. doi: 10.1016/j.febslet.2008.02.006

Cheng, C., Yang, F., Ling, R., Liao, S., Miao, Y., Ye, C., et al. (2015). Effects of Ammonia Exposure on Apoptosis, Oxidative Stress and Immune Response in Pufferfish (*Takifugu Obscurus*). *Aquat. Toxicol.* 164, 61–71. doi: 10.1016/j.aquatox.2015.04.004

Cheng, N., Zhang, W., Chen, W., Jin, J., Cui, X., Butte, N. F., et al. (2011). A Mammalian Monothiol Glutaredoxin, Grx3, is Critical for Cell Cycle Progression During Embryogenesis. *FEBS J.* 278, 2525–2539. doi: 10.1111/j.1742-4658.2011.08178.x

Chen, J. C., Lin, M. N., Ting, Y. Y., and Lin, J. N. (1994). Survival, Haemolymph Osmolality and Tissue Water of *Penaeus Chinensis* Juveniles Acclimated to Different Salinity and Temperature Levels. *Comp. Biochem. Physiol. Part A. Physiol.* 110, 253–258. doi: 10.1016/0300-9629(94)00164-O

Ching, B., Chew, S. F., Wong, W. P., and Ip, Y. K. (2009). Environmental Ammonia Exposure Induces Oxidative Stress in Gills and Brain of *Boleophthalmus Boddarti* (Mudskipper). *Aquat. Toxicol.* 95, 203–212. doi: 10.1016/j.aquatox.2009.09.004

Chi, C., Tang, Y., Zhang, J., Dai, Y., Abdalla, M., Chen, Y., et al. (2018). Structural and Biochemical Insights Into the Multiple Functions of Yeast Grx3. *J. Mol. Biol.* 430, 1235–1248. doi: 10.1016/j.jmb.2018.02.024

Couturier, J., Jacquot, J., and Rouhier, N. (2009). Evolution and Diversity of Glutaredoxins in Photosynthetic Organisms. *Cell. Mol. Life Sci.* 66, 2539–2557. doi: 10.1007/s00018-009-0054-y

Dunier, M., and Siwicki, A. K. (1993). Effects of Pesticides and Other Organic Pollutants in the Aquatic Environment on Immunity of Fish: A Review. *Fish. Shellfish. Immunol.* 3, 423–438. doi: 10.1006/fsim.1993.1042

Dunnen, J., Dalgleish, R., Maglott, D., Hart, R., Greenblatt, M., Jordan, J., Roux, A., Smith, T., Antonarakis, S., Taschner, P, et al. (2016). HGVS Recommendations for the Description of Sequence Variants: 2016 Update. Human Mutation, 37, 564–569. doi: 10.1002/humu.22981

Eklund, H., Cambillau, C., Sjöberg, B. M., Holmgren, A., Jörnvall, H., Höög, J. O., et al. (1984). Conformational and Functional Similarities Between Glutaredoxin and Thioredoxins. *EMBO J.* 3, 1443–1449. doi: 10.1002/j.1460-2075.1984.tb01994.x

Fan, R., Li, Y., Jiang, S., Jiang, S., Yang, Q., Yang, L., et al. (2021). cDNA Cloning and Expression Analysis of Glutaredoxin 3 in Black Tiger Shrimp *Penaeus Monodon*. *Aquacul. Int.* 29, 2661–2679. doi: 10.1007/S10499-021-00774-7

FAO (2020). *State of World Fishneries and Aquaculture 2020: Sustainability in Action* (Rome). doi: 10.4060/ca9229en

Glaser, J. R., and Glaser, E. M. (2020). Stereology, Morphometry, and Mapping: The Whole is Greater Than the Sum of Its Parts. *J. Chem. Neuroanat.* 20, 115–126. doi: 10.1016/S0891-0618(00)00073-9

Gürel, T. (2005). The Larval Development of Penaeus semisulcatus (de Hann, 1850) (Decapoda: Penaeidae). *J. Fisheries Aquatic Sci.* 22, 195–199. doi: 10.12714/egejfas.2005.22.1.5000156908

Herrero, E., and de la Torre-Ruiz, M. A. (2007). Monothiol Glutaredoxins: A Common Domain for Multiple Functions. *Cell. Mol. Life Sci.: CMLS.* 64, 1518–1530. doi: 10.1007/s00018-007-6554-8

Hiroaki, M., Yoshito, I., Hajime, N., Junji, Y., Koji, S., and Takahito, K. (2003). Glutaredoxin Exerts an Antiapoptotic Effect by Regulating the Redox State of Akt. *J. Biol. Chem.* 278, 50226–50233. doi: 10.1074/jbc.m310171200

Holmgren, A. (1979). Glutathione-Dependent Synthesis of Deoxyribonucleotides. Characterization of the Enzymatic Mechanism of Escherichia Coli Glutaredoxin. *J. Biol. Chem.* 254, 3672–3678. doi: 10.1016/S0021-9258(18)50814-0

Holmgren, A., Johansson, C., Berndt, C., Lönn, M. E., Hudemann, C., and Lillig, C. H. (2005). Thiol Redox Control *via* Thioredoxin and Glutaredoxin Systems. *Biochem. Soc. Trans.* 33, 1375–1377. doi: 10.1042/bst20051375

Hu, W., and Yao, C. (2016). Molecular and Immune Response Characterizations of a Novel AIF and Cytochrome C in Litopenaeus Vannamei Defending Against WSSV Infection. *Fish. Shellfish. Immunol.* 56, 84–95. doi: 10.1016/j.fsi.2016.06.050

Jie, Y., Luo, Z., Xie, J., Cheng, C., Ma, H., Liu, G., et al. (2022). Characterization of Phosphofructokinase (PFK) From Mud Crab *Scylla Paramamosain* and its Role in Mud Crab Dicistrovirus-1 Proliferation. *Fish. Shellfish. Immunol.* 124, 39–46. doi: 10.1016/J.FSI.2022.03.042

Knuesting, J., Riondet, C., Maria, C., Kruse, I., Bécuwe, N., König, N., et al. (2015). Arabidopsis Glutaredoxin S17 and its Partner, the Nuclear Factor Y Subunit C11/negative Cofactor 2α, Contribute to Maintenance of the Shoot Apical Meristem Under Long-Day Photoperiod. *Plant Physiol.* 167, 1643–1658. doi: 10.1104/pp.15.00049

Levin, A., Nair, D., Qureshi, A. R., Bárány, P., Heimburger, O., Anderstam, B., et al. (2018). Serum Glutaredoxin Activity as a Marker of Oxidative Stress in Chronic Kidney Disease: A Pilot Study. *Nephron* 140, 249–256. doi: 10.1159/000492500

Lillig, C. H., Berndt, C., and Holmgren, A. (2008). Glutaredoxin Systems. *BBA-General. Subj.* 1780, 1304–1317. doi: 10.1016/j.bbagen.2008.06.003

Liu, M., Guo, H., Liu, B., Zhu, K., Guo, L., Liu, B., et al. (2021). Gill Oxidative Damage Caused by Acute Ammonia Stress was Reduced Through the HIF-1α/NF-κb Signaling Pathway in Golden Pompano (*Trachinotus Ovatus*). *Ecotoxicol. Environ. Saf.* 222, 112504. doi: 10.1016/J.ECOENV.2021.112504

Li, Y., Yang, Q., Su, T., Zhou, F., Yang, L., and Huang, J. (2012). The toxicity of ammonia-N on Penaeus monodon and immune parameters. *J. Shanghai Ocean Univ.* 21, 358–362.

Li, Y., Zhou, F., Huang, J., Yang, L., Jiang, S., Yang, Q., et al. (2018). Transcriptome Reveals Involvement of Immune Defense, Oxidative Imbalance, and Apoptosis in Ammonia-Stress Response of the Black Tiger Shrimp (*Penaeus Monodon*). *Fish. Shellfish. Immunol.* 83, 162–170. doi: 10.1016/j.fsi.2018.09.026

Lönn, M. E., Hudemann, C., Berndt, C., Cherkasov, V., Capani, F., Holmgren, A., et al. (2008). Expression Pattern of Human Glutaredoxin 2 Isoforms: Identification and Characterization of Two Testis/Cancer Cell-Specific Isoforms. *Antiox. Redox Signaling* 10, 547–557. doi: 10.1089/ars.2007.1821

Mapolelo, D. T., Zhang, B., Randeniya, S., Albetel, A., Li, H., Couturier, J., et al. (2013). Monothiol Glutaredoxins and A-Type Proteins: Partners in Fe-S Cluster Trafficking. *Dalton. Trans.* 42, 3107–3115. doi: 10.1039/C2DT32263C

Mondal, S., Kumar, V., and Singh, S. P. (2019). Phylogenetic Distribution and Structural Analyses of Cyanobacterial Glutaredoxins (Grxs). *Comput. Biol. Chem.* 84, 107141. doi: 10.1016/j.compbiolchem.2019.107141

Nathan, C., and Cunningham-Bussel, A. (2013). Beyond Oxidative Stress: An Immunologist's Guide to Reactive Oxygen Species. *Nat. Rev. Immunol.* 13, 349–361. doi: 10.1038/nri3423

Oh, Y., Hong, S., Yeon, J., Cha, M., and Kim, I. (2012). Interaction Between Saccharomyces Cerevisiae Glutaredoxin 5 and SPT10 and Their *In Vivo* Functions. *Free Radical Biol. Med.* 52, 1519–1530. doi: 10.1016/j.freeradbiomed.2012.01.032

Omeka, W. K. M., Liyanage, D. S., Yang, H., and Lee, J. (2019). Glutaredoxin 2 From Big Belly Seahorse (*Hippocampus Abdominalis*) and its Potential Involvement in Cellular Redox Homeostasis and Host Immune Responses. *Fish. Shellfish. Immunol.* 95, 411–421. doi: 10.1016/j.fsi.2019.09.071

Pan, J. L., and Bardwell, J. C. (2006). The Origami of Thioredoxin-Like Folds. *Protein Sci.* 15, 2217–2227. doi: 10.1110/ps.062268106

Petry, S. F., Sun, L. M., Knapp, A., Reinl, S., and Linn, T. (2018). Distinct Shift in Beta-Cell Glutaredoxin 5 Expression Is Mediated by Hypoxia and Lipotoxicity Both *In Vivo* and *In Vitro*. *Front. Endocrinol.* 9. doi: 10.3389/fendo.2018.00084

Potamitou, F. A., and Arne, H. (2004). Glutaredoxins: Glutathione-Dependent Redox Enzymes With Functions Far Beyond a Simple Thioredoxin Backup System. *Antiox. Redox Signaling* 6, 63–74. doi: 10.1089/152308604771978354

Qin, Y., Jiang, S., Huang, J., Zhou, F., Yang, Q., Jiang, S., et al. (2019). C-type lectin response to bacterial infection and ammonia nitrogen stress in tiger shrimp (Penaeus monodon). *Fish and Shellfish Immunology* 90, 188–198. doi: 10.1016/j.fsi.2019.04.034

Rőszer, T. (2014). The Invertebrate Midintestinal Gland ("Hepatopancreas") is an Evolutionary Forerunner in the Integration of Immunity and Metabolism. *Cell Tissue Res.* 358, 685–695. doi: 10.1007/s00441-014-1985-7

Randall, D. J., and Tsui, T. K. N. (2002). Ammonia Toxicity in Fish. *Mar. pollut. Bull.* 45, 17–23. doi: 10.1016/S0025-326X(02)00227-8

Rowley, A. F. (2016). The Immune System of Crustaceans. *Encyclo. Immunobiol.* 1, 437–453. doi: 10.1016/B978-0-12-374279-7.12005-3

Rusaini, L. O. (2010). Insight Into the Lymphoid Organ of Penaeid Prawns: A Review. *Fish. Shellfish. Immunol.* 29, 367–377. doi: 10.1016/j.fsi.2010.05.011

Shakamuri, P., Zhang, B., and Johnson, M. K. (2012). Monothiol Glutaredoxins Function in Storing and Transporting $[Fe_2S_2]$ Clusters Assembled on IscU Scaffold Proteins. *J. Am. Chem. Soc.* 134, 15213–15216. doi: 10.1021/JA306061X

Shi, M., Jiang, S., Li, Y., Yang, Q., Jiang, S., Yang, L., et al. (2019). Comprehensive Expression Analysis of the Beta Integrin From Penaeus Monodon Indicating its Participation in Innate Immunity and Ammonia Nitrogen Stress Response. *Fish. Shellfish. Immunol.* 98, 887–898. doi: 10.1016/j.fsi.2019.11.049

Soonthornchai, W., Rungrassamee, W., Karoonuthaisiri, N., Jarayabhand, P., Klinbunga, S., Söderhäll, K., et al. (2010). Expression of Immune-Related Genes in the Digestive Organ of Shrimp, Penaeus Monodon, After an Oral Infection by *Vibrio Harveyi*. *Dev. Comp. Immunol.* 34, 19–28. doi: 10.1016/j.dci.2009.07.007

Verma, P. K., Verma, S., and Tripathi, R. D. (2021). Pandey Nalini,Chakrabarty Debasis. CC-Type Glutaredoxin, OsGrx_C7 Plays a Crucial Role in Enhancing Protection Against Salt Stress in Rice. *J. Biotechnol.* 329, 192–203. doi: 10.1016/j.jbiotec.2021.02.008

Wang, Z., Xing, S., Birkenbihl, R. P., and Zachgo, S. (2009). Conserved Functions of Arabidopsis and Rice CC-Type Glutaredoxins in Flower Development and Pathogen Response. *(Special. Issue.: Redox Biol. I.). Mol. Plant* 2, 323–335. doi: 10.1093/mp/ssn078

Wingert, R. A., Galloway, J. L., Barut, B., Foott, H., Fraenkel, P., Axe, J. L., et al. (2005). Deficiency of Glutaredoxin 5 Reveals Fe-S Clusters are Required for Vertebrate Haem Synthesis. *Nature* 436, 1035–1039. doi: 10.1038/nature03887

Xing, S., Rosso, M. G., and Zachgo, S. (2005). ROXY1, a Member of the Plant Glutaredoxin Family, is Required for Petal Development in Arabidopsis Thaliana. *Development* 132, 1555–1565. doi: 10.1242/dev.01725

Zhang, L., Li, Y., Wu, M., Ouyang, H., and Shi, R. (2021). The SNP Polymorphisms Associated With WSSV-Resistance of Prophenoloxidase in Red Swamp Crayfish (*Procambarus Clarkii*) and Its Immune Response Against White Spot Syndrome Virus (WSSV). *Aquaculture* 530, 735787. doi: 10.1016/j.aquaculture.2020.735787

Zhang, Y., Ye, C., Wang, A., Zhu, X., Chen, C., Xian, J., et al. (2015). Isolated and Combined Exposure to Ammonia and Nitrite in Giant Freshwater Pawn (*Macrobrachium Rosenbergii*): Effects on the Oxidative Stress, Antioxidant Enzymatic Activities and Apoptosis in Haemocytes. *Ecotoxicology* 24, 1601–1610. doi: 10.1007/s10646-015-1477-x

Zhao, F., and Wang, Q. (2012). The Protective Effect of Peroxiredoxin II on Oxidative Stress Induced Apoptosis in Pancreatic β-Cells. *Cell Biosci.* 2, 22. doi: 10.1186/2045-3701-2-22

Zheng, P., Wang, L., Wang, A., Zhang, X., Ye, J., Wang, D., et al. (2018). cDNA Cloning and Expression Analysis of Glutaredoxin (Grx) 2 in the Pacific White Shrimp *Litopenaeus Vannamei*. *Fish. Shellfish. Immunol.* 86, 662–671. doi: 10.1016/j.fsi.2018.12.011

Zheng, P., Zhang, X., Wang, D., Li, J., Zhang, Z., Lu, Y., et al. (2021). Molecular Characterization and Expression Analysis of a Novel Glutaredoxin 3 Gene in Pacific White Shrimp (*Litopenaeus Vannamei*). *Front. Mar. Sci.* 8. doi: 10.3389/FMARS.2021.687377

Zhou, K., Zhou, F., Huang, J., Yang, Q., Jiang, S., Qiu, L., et al. (2017). Characterization and Expression Analysis of a Chitinase Gene (PmChi -4) From Black Tiger Shrimp (*Penaeus Monodon*) Under Pathogen Infection and Ambient Ammonia Nitrogen Stress. *Fish. Shellfish. Immunol.* 62, 31–40. doi: 10.1016/j.fsi.2017.01.012

Conflict of Interest: The authors declare that the research was conducted in the absence of any commercial or financial relationships that could be construed as a potential conflict of interest.

Publisher's Note: All claims expressed in this article are solely those of the authors and do not necessarily represent those of their affiliated organizations, or those of the publisher, the editors and the reviewers. Any product that may be evaluated in this article, or claim that may be made by its manufacturer, is not guaranteed or endorsed by the publisher.

frontiers | Frontiers in Marine Science

TYPE Original Research
PUBLISHED 15 August 2022
DOI 10.3389/fmars.2022.884244

OPEN ACCESS

EDITED BY
Xiangli Tian,
Ocean University of China, China

REVIEWED BY
Vikash Kumar,
Central Inland Fisheries Research Institute (ICAR), India
Thavasimuthu Citarasu,
Manonmaniam Sundaranar University, India

*CORRESPONDENCE
Mouna Jlidi
jlidimanno@yahoo.fr
Mamdouh Ben Ali
mamdouh.benali@cbs.rnrt.tn

SPECIALTY SECTION
This article was submitted to Marine Fisheries, Aquaculture and Living Resources, a section of the journal Frontiers in Marine Science

RECEIVED 06 March 2022
ACCEPTED 27 June 2022
PUBLISHED 15 August 2022

CITATION
Jlidi M, Akremi I, Ibrahim AH, Brabra W, Ali MB and Ali MB (2022) Probiotic properties of *Bacillus* strains isolated from the gastrointestinal tract against pathogenic Vibriosis. *Front. Mar. Sci.* 9:884244. doi: 10.3389/fmars.2022.884244

Probiotic properties of *Bacillus* strains isolated from the gastrointestinal tract against pathogenic Vibriosis

Mouna Jlidi[1,2]*, Ismahen Akremi[1,2], Adel Haj Ibrahim[1], Wided Brabra[1,2], Manel Ben Ali[1,2] and Mamdouh Ben Ali[1,2]*

[1]Laboratory of Microbial Biotechnology and Engineering Enzymes (LBMIE), Center of Biotechnology of Sfax (CBS), University of Sfax, Sfax, Tunisia, [2]Astrum Biotech, Business Incubator, Center of Biotechnology of Sfax (CBS), University of Sfax, Sfax, Tunisia

Vibriosis is one of the major diseases leading to massive fish mortality. Probiotics may provide a potential alternative method to protect fish from pathogens and to promote a balanced environment minimizing the use of antibiotics and chemotherapy. The aims of this study were to (i) isolate and purify marine spore-former strains from Sardine and shrimp intestine, (ii) screen for bacteria with potential probiotic properties, and (iii) carry out their *in vitro* safety assessment using a subtractive procedure. Among 108 spore-former strains, five strains exhibited a strong antibacterial activity against Vibriosis such as *Vibrio harveyi* and *Vibrio anguillarum*. These selected strains were unaffected by high-temperature and gastrointestinal conditions; produced amylase, protease, and lipase activities; and showed high percentages of auto-aggregation and co-aggregation with pathogens, as well as a strong adhesion to fish mucus. Partial 16S rDNA gene sequencing and MALDI-TOF MS revealed that isolates are *Bacillus amyloliquefaciens* or *Bacillus subtilis*. All of them were susceptible to antibiotics, while hydrolic enzymes and virulence factors were not detected for *B. subtilis* S17. In conclusion, based on their proprieties and their safety assessment, *B. subtilis* S17 could serve as a potential probiotic candidate for aquaculture.

KEYWORDS

Vibriosis, probiotic, *Bacillus* spp., safety assessment, adhesion

1 Introduction

Intensive aquaculture is known to cause stressful conditions related to stocking densities and high feeding. Such practices enhance the probability of disease outbreaks mainly at larval and early fry stages. Outbreaks are habitually caused by a wide range of pathogenic bacteria. Vibriosis is one of the major diseases leading to poor growth, low

immunity, and high mortality and therefore massive economic losses for the aquaculture sector (Meidong et al., 2017; Kaktcham et al., 2018; Ghanei-Motlagh et al., 2020; Makridis et al., 2021). Several *Vibrio* species have been concerned with marine animals' health problems. Recent studies showed that *Vibrio alginolyticus*, *V. harveyi*, and *V. parahaemolyticus* are the most potent species infecting farms (Daniels and Shafaie, 2000; Yılmaz et al., 2021). To sort out these problems, traditional methods such as vaccines and antibiotics are widely used. Nevertheless, the widespread use of antibiotics leads to the appearance and emergence of resistant bacteria and affect the aquatic environment (water and sediment contamination) (Caruffo et al., 2015; Medina et al., 2020; Makridis et al., 2021). Recently, probiotics have emerged as a good and effective alternative to ban or minimize the antibiotic use and control diseases (Balcazar et al., 2007; Meidong et al., 2017; Emam and Dunlap, 2020). Probiotics are defined as live microorganisms which beneficially affect the health of the host when consumed in adequate concentrations (Fuller, 1989; FAO/WHO/OIE, 2006; Pinto et al., 2020). Their potential benefits on the host are attributed to improve the immune system and enhance digestion and growth promotion by producing enzymes. Other beneficial effects include water remediation and secretion of inhibitory substances which confer resistance to intestinal pathogens and prevent their intestinal adhesion, and lead to better health properties (Verschuere et al., 2000; Balcázar et al., 2006; Balcazar et al., 2007; Fernandes and Kerkar, 2019; Medina et al., 2020; Khan et al., 2021). A large number of bacteria are classified as probiotics, but the most widely used in aquaculture are *Lactobacillus* and *Bacillus*. However, *Bacillus* species have attracted much more attention due to non-toxic and non-pathogenic compound production and their sporulation ability, which gives them protection against stressed conditions (heat, gastrointestinal tract (GIT) compared to other probiotics (Barbosa et al., 2005; Cao et al., 2019; Kuebutornye et al., 2019; Emam and Dunlap, 2020; Amoah et al., 2021). To exert and endure the benefits of probiotics within the host, several properties should be investigated for probiotic strain screening, including antagonism against fish pathogens, being kept alive in GIT, resistance to storage conditions, secretion of exogenous enzymes, and being safe (Fuller, 1989; Muñoz-Atienza et al., 2014; Cao et al., 2019; Zhou et al., 2019; Ghanei-Motlagh et al., 2020). Generally, probiotics are isolated from the indigenous and exogenous microbiota of aquatic animals (Balcázar et al., 2006; do Vale Pereira et al., 2017). However, the search for a putative probiotic should continue as the increase demand for sustainable and environment-friendly aquaculture.

In this study, we used Sardine and shrimp intestine, an untapped source of novel microorganism, as a source of potential probiotic bacteria. Hence, we have isolated, selected, and identified potential probiotic bacteria for aquaculture based on subtractive screening by means of several physiologic criteria and safety assessment.

2 Materials and methods

2.1 Pathogen collection and culture conditions

All *Vibrio* used as indicators (*Vibrio anguillarum* CECT4344; *V. alginolyticus*; *V. fischeri*; *V. harveyi* Lg 10/6, Lg 14/01, Lg 26/01, Lg 48/01, Lg 13/04, Lg 34/04, and Lg 35/03; *V. parahaemolyticus*; *V. proteolyticus*; *V. vulnificus*, and *V. splendidus* provided by The Microbiology Department of the University of Malaga) were isolated from diseased fish. They were potent causative agents of fish infection. Each strain was cultured in Tryptone Soya Agar (TSA) (Oxoid Ltd., Hampshire, UK) supplemented with NaCl 1.5% (w/v) at 28°C. Stock cultures in Tryptone Soy Broth (TSB) were stored at -80°C and -20°C in 1.5% NaCl with 15% glycerol to provide stable inoculum throughout the study (Midhun et al., 2018).

2.2 Sampling procedure and isolation of spore-forming bacteria

Bacteria used in this study were isolated from intestines of Sardine (*Sardina pilchardus*) and shrimp (*Penaeus kerathurus*). Intestines were washed with sterile saline solution, and content was aseptically removed. One gram from each intestine sample was homogenized in 9 ml phosphate-buffered saline (PBS, pH = 7.2). Selection of spore-forming isolates was by heat treatment. The homogenates were diluted in buffered peptone water (up to 10^{-3}) and incubated at 65°C for 30 min. One hundred-microliter aliquots of appropriate serial dilutions were spread onto Difco sporulation medium (DSM) for 48h at 28°C. Colonies obtained were picked and purified. Pure isolates in TSB were stored in 1.5% NaCl with 15% glycerol at -20°C and -80°C until further routine use (Barbosa et al., 2005).

All isolates were then investigated for catalase activity by the suspension of a fresh single colony in 3% of hydrogen peroxide. Air bubble production was considered as a positive result.

2.3 Antimicrobial activity

2.3.1 Colony overlay method

The preliminary screening for antimicrobial activity of spore-forming isolates was done by the colony overlay method described by Alonso et al. (2019). Both indicators and isolates were grown in TSB containing 1.5% NaCl and incubated overnight at 28°C. In order to form a bacterial lawn, 100 µl *Vibrio spp*. Culture (10^5 CFU/ml) was spread in TSA plates using a sterile cotton-tipped swab. Drops of isolate cultures were dispensed onto the plates once dried. After incubation at 28°C for 24 h, antimicrobial activity was assessed by observing the

presence of inhibition zones around colonies and represented as scores as described by Midhun et al. (2017). Based on cumulative scores, promising antagonistic spore-forming bacteria against indicators were selected. Further, the strong *Vibrio inhibitory* spore-forming bacteria were confirmed through cell-free supernatants (CFSs).

2.3.2 Extracellular antimicrobial assay

The extracellular antimicrobial activity of cell-free supernatants was determined using a microtiter plate and an agar well diffusion test (ADT). Briefly, selected strains were cultured in TSB containing 1.5% NaCl incubated at 28°C for 24 h at 150 rpm. CFS was obtained by centrifugation of overnight cultures (10^7 CFU/ml) at 8,000×g at 4°C for 20 min and filter sterilized through 0.22-µm pore-size filters.

The inhibitory activity was evaluated in a 96-well microtiter plate by inoculation of pathogenic bacteria culture (10 µl, 10^5 CFU/ml) with TSB fresh medium (150 µl) and sterilized CFS (50 µl) in each well. Controls were inoculated with pathogenic bacteria only in 200 µl fresh TSB. The absorbance at 600 nm was used to measure the inhibition efficiency (IE) during 24 h by the following formula:

$$IE = (\textbf{OD in presence of CFS of isolates})/(\textbf{OD of pathogen only})$$

where IE<1 indicates inhibition of pathogenic bacteria by isolates, IE = 1 indicates no inhibition, and IE >1 indicates growth promotion (Mukherjee and Ghosh, 2016).

Besides, antibacterial activity using ADT was assayed as described by Cintas et al. (1995) with some modifications. Plates were seeded with indicators (100 µl, 10^5 CFU/ml). Fifty microliters of CFS was placed into wells (6 mm of diameter) cut in TSB with 1.5% NaCl and 0.8% agar (w/v). After 2 h at 4°C, the plates were incubated under 24 h at 28°C then antimicrobial activity was defined by the presence of a clear inhibitory zone around the wells. Further, neutralization was obtained using 1 N sodium hydroxide to pH = 7. To determine the nature and thermostability of the antimicrobial compounds, the supernatant was treated with proteinase K at 10 mg/ml (AppliChem GmbH, Darmstadt, Germany) and then heated at 100°C for 10 min. After treatments, samples were assayed for residual antimicrobial activity by an ADT using *Vibrio anguillarum* CECT4344 and *V. harveyi* Lg26/01 as indicators.

2.4 Preparation of vegetative cells, spores, and sporulation efficiency

For the preparation of vegetative cells, each selected strain was grown in TSB with 1.5% NaCl and taken from logarithmic-phase cells.

Sporulation of isolates was induced by exhaustion of nutrients in DSM. In fact, overnight cultures of selected strains in TSB with 1.5% NaCl were inoculated to DSM broth and incubated 28°C at 150 rpm for 24 and 48 h. After inoculation, cultures were diluted and plated in TSA in order to determine viable and heat-resistant cells before and after heat treatment (80°C, 20 min), respectively. Sporulation efficiency was determined by quantifying viable cells before and after heating (Barbosa et al., 2005; Prieto et al., 2014; Zhou et al., 2019; Santos et al., 2021).

2.5 Screening of probiotic properties of spore-forming isolates

2.5.1. Evaluation of extracellular enzymes

The extracellular enzyme production of selected bacteria was performed by plate assay according to Hmani et al. (2017) with some modifications. Protease and amylase production was determined using Luria-Bertani (LB) agar plates supplemented with 1% skimmed milk and 1% starch, respectively. Culture plates were spot inoculated and incubated for 24 h at 28°C. The clear zone around the colonies revealed a proteinase production. After plates were flooded with iodine, yellow discoloration appeared, indicating amylase production. For lipase activity, strains were spotted onto LB plates containing 1% olive oil and 1% rhodamine. Lipase activity was observed by zone of clearance surrounding colonies.

2.5.2 Biofilm production

The ability to produce biofilm was determined by the crystal violet assay as described by Midhun et al. (2017) with modifications. Selected strains were inoculated into 10 ml of LB broth containing 1% glucose and incubated at 28°C for 24 h. Cultures were diluted to an OD600 of ~0.1. Each well of a sterile 96-well flat-bottom polystyrene plate (orange scientific) was filled with 200 µl of diluted culture. *Escherichia coli* DH5α and *Staphylococcus aureus* ATCC 6538 were used as negative and positive biofilm-forming strains, respectively, and sterile LB broth was considered as blank to check the sterility and non-specific attachment. After incubation, excess medium from each well was removed by tapping. The wells were washed twice with 250 µl of PBS (pH = 7.2) to eliminate floating bacteria. The adherent bacteria were fixed at 60°C for 1 h and stained with 150 µl of 0.2% crystal violet prepared in 20% EtOH (v/v). The stained bound bacteria were released by adding 200 µl of glacial acetic acid. After incubation for 1 h at room temperature, the absorbance at 570 nm was determined using a microplate reader. The wells of isolates in which OD values are higher than those in blank wells were considered to be biofilm producers.).

2.5.3 Resistance to high temperature, pH, and bile salts

The resistance of selected strains to high temperatures required by the fish feed process was assessed according to Kuebutornye et al. (2020)

with modifications. Briefly, an overnight culture was harvested. The pellets were resuspended in PBS and exposed to elevated temperatures (80°C, 90°C, and 100°C) for 5 and 10 min, respectively. Viable counts were determined by the spread plate method after incubation at 28°C for 24 h.

The tolerance of vegetative cells and spores to low pH and bile salt was assayed as described by Barbosa et al. (2005) and Hmani et al. (2017) with modifications. Essentially, ~10^8 to 10^9 bacterial cells ml^{-1} were resuspended in TSB broth containing bile salts (0%–5%, sodium cholate 50%, sodium deoxycholate 50%) (Bio Basic, Markham, Canada) or in TSB broth adjusted to pH 1, 2, 3, and 7.3 (control) with concentrated HCl. Aliquots were taken immediately and after 3 h for low pH and after 6 h for bile salt tolerance. Viable counts were determined by the spread plate method on TSA after incubation at 28°C for 24 h.

2.5.4 Auto-aggregation and co-aggregation assays

Auto-aggregation assay was performed according to Meidong et al. (2018). Overnight cultures grown were centrifuged, washed twice, and resuspended in PBS followed by turbidity measurement to obtain OD600~1(A0). The bacterial suspensions were vortexed for 10 s and kept undisturbed at 28°C for 5 h and after 24 h. Then each hour OD600 of the upper suspensions (At) was measured. The auto-aggregation percentage (%Agg) was expressed as:

$$\%\,\mathbf{Agg} = 1 - (\mathbf{At}/\mathbf{A0}) \times 100$$

where At represents the OD600 at time t = 1, 2, 3, 4, 5, and 24 h and A0 the OD600 at t = 0.

In the co-aggregation assay, the suspension of isolated strains and fish pathogens was prepared similarly to the auto-aggregation analysis above. Equal volumes of tested strains and pathogens were mixed and incubated at 28°C for 6 h. The OD600 of the mixtures and controls (unmixed cultures of tested strains and pathogens) were measured after incubation. Co-aggregation (Co-agg) was calculated as:

$$\%\ \mathbf{Co-agg} = [(\mathbf{Apat} + \mathbf{Aisolate}) - 2(\mathbf{Amix})/(\mathbf{Apat} + \mathbf{Aisolate})] \times 100$$

where Apat and Aisolate represent the OD600 of each bacterial suspension alone and Amix represents the OD600 of mixed suspension pathogen and isolated strains (Meidong et al., 2018).

2.5.5 Adhesion assay *in vitro*

2.5.5.1 Mucus preparation and characterization

Mucus was isolated from the skin and intestine of gilt-head bream (*Sparus aurata*) according to Balcázar et al. (2008). The skin mucus was collected by scraping the dorsolateral surfaces of fish using a cell scarper. The intestine was removed and scraped to collect intestinal mucus. All mucus were homogenized in PBS and centrifuged three times at 120,000× g for 15 min at 4°C to remove cellular materials and particulate. Then the samples were adjusted to a protein concentration of 1 mg/ml in PBS. The protein concentration was determined according to Beltrán et al. (2017) and Midhun et al. (2018). The mucus preparations were filter sterilized by a 0.22-µm-size Millipore filter and finally stored at -20°C until use.

2.5.5.2 Adhesion and growth on fish mucus

Adhesion ability was evaluated according to Li et al. (2020) with some modifications. Briefly, 100 µl of skin and intestinal mucus was immobilized on a polystyrene microtiter plate by overnight incubation at 4°C. To remove excess mucus, wells were washed twice with 250 µl of PBS. Overnight-grown bacteria (vegetative cells or spores) were centrifuged at 6,000 g for 15 min, washed twice, and resuspended in PBS with fluorescein isothiocyanate (FITC) (100 µg/ml) at 28°C for 1 h in the dark. Labelled bacteria were washed three times with PBS. Then, 100 µl of the labelled bacterial suspension (10^8 CFU/ml) was added to each well. Plates were incubated at 28°C for 1 h and then washed with PBS to remove unbound bacteria. The bound bacteria were lysed with 200 µl of 1% sodium dodecyl sulphate (SDS) in 0.1 M NaOH at 60°C for 1 h. The fluorescence intensity was measured with the excitation and emission spectrum of 485 nm/530 nm by spectrophotometry. Adhesion was calculated using the formula:

$$\%\,\mathbf{Adhesion} = \mathbf{A}/\mathbf{A0} \times 100$$

where A is the fluorescence of adhering bacteria and A0 is the fluorescence of initial bacteria.

Moreover, to determine whether the observed bacterial adhesion was due to non-specific adhesion or cell surface hydrophobicity, adhesion assays to bovine serum albumin (BSA) and polystyrene were performed as described above.

The ability of the strain to establish and persist in the gut is essential. For this purpose, the growth of the strain in the intestine and skin mucus was evaluated. In fact, the skin and intestinal mucus were inoculated with the bacterial suspension and spores (10^6 CFU/mL) and incubated at 28°C for 24 h. Colony-forming units (CFU/mL) were counted. Sterilized mucus-inoculated plates served as controls (Midhun et al., 2017).

2.6 Identification of selected spore formers

The selected spore formers were identified using molecular identification targeting 16S rRNA genes and matrix-assisted laser desorption ionization-time-of-flight mass spectrometry (MALDI-TOF MS) (Ultraflex III, Bruker Daltonics, Bremen, Germany).

Total bacterial DNA was extracted using the InstaGene Matrix resin (Bio-Rad Laboratories Inc., Hercules, CA, USA). PCR amplification was performed using primers 27F and 1492R (Table 1). PCR reaction was prepared as follows: 25 µl of MyTaq Mix (Bioline, London, UK), l µl of each primer (0.7 µmol), and l µl of purified DNA (~50 ng). The samples were amplified under the following conditions: initial denaturation at 97°C for 1 min, followed by 35 cycles of denaturation (95°C for 15 s), annealing (48 for 15 s), and elongation (72°C for 10 s), ending with a final extension step at 72°C for 7 min. The corresponding species identity was obtained by comparative sequence analysis against available sequence data in the National Centre for Biotechnology Information (NCBI) database.

A single colony of selected strains was also analysed by MALDI-TOF MS as described by Altakhis et al. (2021). Bruker Flex Control software was used to run measurements of MALDI-TOF MS which were expressed as score. Based on the report of Bruker software, results of identification were reliable only when the scores generated were ≥1.7 (Han et al., 2021).

2.7 *In vitro* safety assay

2.7.1 Antibiotic resistance

The antibiotic susceptibility of selected strains was determined by broth microdilution test as described by Araújo et al. (2015). The antibiotics used were ampicillin (0.12–8 µg/ml), vancomycin (0.5–32 µg/ml), gentamicin (2–128 µg/ml), kanamycin (4–256 µg/ml), streptomycin (4–256 µg/ml), erythromycin (0.12–8 µg/ml), clindamycin (0.25–16 µg/ml), tetracycline (0.5–32 µg/ml), and chloramphenicol (1–64 µg/ml). A single colony was suspended in 5 ml of saline solution (0.85% NaCl) to reach an optical density of 0.5 McFarland Scale (10^8 CFU/ml) and diluted in TSB. Fifty microliters of strain suspension was inoculated with each well containing 50 µl of the different antibiotic concentrations. The inoculated plaques were incubated at 28°C for 18 h; the minimum inhibitory concentrations (MICs) were read as the lowest concentration of antibiotics inhibiting the growth of bacteria and were compared according to EFSA (Muñoz-Atienza et al., 2013). Resistance was defined when the MICs of strains are higher than the respective breakpoint. *Staphylococcus aureus* CECT794 and *Enterococcus faecalis* CECT795 were used as controls.

2.7.2 Production of hydrolic enzymes

Haemolysis activity was investigated as previously described by Muñoz-Atienza et al., 2014 (Eaton and Gasson, 2001). Briefly, selected strains previously cultured in TSB with 1.5%NaCl were streaked on horse blood agar plates (bioMérieux, Marcy l'Etoile, France). After 1–2 days at 28°C, the presence of clear zones or green zones of hydrolysis around the colonies revealed β-haemolysis or α-haemolysis, respectively; the absence of clear zones around colonies means γ-haemolysis. *Enterococcus faecalis* P4 was used as positive control.

Gelatinase production was determined as described by Eaton and Gasson (Eaton et al,. 2001). Selected strains grown in TSB broth at 28 C for 16 h were streaked on Todd–Hewitt (Oxoid) agar plates (1.5%, w/v) with 30 g/l gelatin. After overnight incubation, the plates were placed at 4°C for 5 h before examination. The presence of zone of turbidity (protein hydrolysis) around the colonies revealed the activity. *Enterococcus faecalis* P4 was used as positive control.

The ability of selected strains to hydrolyse primary and secondary bile salts was determined according to Araújo et al. (2015) with some modifications. Briefly, 10 µl of cultures grown

TABLE 1 Oligonucleotide primers used in this study.

Target gene	Primer	5′–3′ sequence	Annealingtemperature	Reference
16S rDNA	27F	AGA GTTTGATCCTGGCTCAG	48	(Araújo et al., 2015)
	1492R	CGGTTACCTTGTTACGACTT		
hdc	CL1	CCWGGWAAWATWGGWAATGGWTA	48	
	JV17HC	AGACCATACACCATAACCTT		
ldc	CAD2-F	CAYRTNCCNGGNCAYAA	53	
	CAS2-R	GGDATNCCNGGNGGRTA		
odc	3	GTNTTYAAYGCNGAYAARACNTAYTTYGT	52	
	16	TACRCARAATACTCCNGGNGGRTANGG		
tdc	TD5	CAAATGGAAGAAGAAGTAGG	48	
	TD2	ACATAGTCAACCATRTTGAA		
sfp	sfp-F	ATGAAGATTTACGGAATTTA	46	(Hsieh et al., 2004)
	sfp-R	TTATAAAAGCTCTTCGTACG		
cesA	CER1	ATCATAAAGGTGCGAACAAGA	52	(Horwood et al., 2004)
	EMT1	AAGATCAACCGAATGCAACTG		
ces B	EM1-F	GACAAGAGAAATTTCTACGAGCAAGTACAAT	60	(Ehling-Schulz et al., 2004)
	EM1-R	GCAGCCTTCCAATTACTCCTTCTGCCACAGT		

in TSB broth was spotted onto TSB agar plates supplemented with 0.5% (w/v) sodium salts of taurocholate or taurodeoxycholate (Sigma-Aldrich, St. Louis, MO, USA) and 0.05% (w/v) L-cysteine (Merck) and incubated at 30°C for 72 h under anaerobic conditions (AnaeroGen, Oxoid). The presence of opaque halos of precipitated deconjugated bile acids around the colonies was considered as a positive result. Fresh faecal slurry of a healthy adult cow was used as the positive control.

2.7.3 PCR detection of potential virulence factors

Detection of genes encoding histidine decarboxylase (*hdc*), tyrosine decarboxylase (*tdc*), ornithine decarboxylase (*odc*), lysine decarboxylase (*ldc*), surfactin synthetase (*sfp*), and creolise synthetase (*cesA*, *cesB*) was carried out by PCR. *Lactobacillus* sp. 30a, *L. brevis* CECT4121, and *Bacillus cereus* 4086 were used as positive controls. PCR amplifications were performed as previously described by Araújo et al. (2015).

2.8 Statistical analysis

Data were expressed as means ± standard error of the mean (SEM). A statistical analysis of the data was performed using the software package SPSS 19.0. One-way analysis of variance (ANOVA) means and Tukey and Duncan's tests were applied. Significant differences were accepted to be significant when $P< 0.05$.

3 Results

3.1 Isolation of spore former strains and screening for antimicrobial activity

A total of 108 colonies were isolated and purified from sardine and shrimp intestine (47 from *Sardina pilchardus* and 61 from *Penaeus kerathurus*). All isolated strains were found to be Gram-positive, catalase positive. Out of 108 isolates, only 20 showed antagonistic activities by the colony overlay method presented as scores (Table 2). Cumulative maximum and minimum scores were 25 and 2, respectively. All 20 exerted direct antimicrobial activity against, at least, two of the indicators (Figure 1). Strain S17 showed a strong antagonistic activity against all tested pathogens.

Based on the total score, the strong pathogen inhibitory strains (Cm4, Cm5, Z1, S17, and C211) were selected and analysed for extracellular antimicrobial activity assay and for various probiotic potentials.

The inhibition of selected strain CFSs was substantiated by IE values varying in reference time (Figure 2). In majority of hours, inhibition of pathogens was more than 20% for *Vibrio anguillarum* (Va) and 30% for *V. harveyi* Lg26/01(Vh3). Moreover, lower inhibition was observed during the initial phase (between 2 and 6 h). On other hand, antibacterial activity of CFS and its nature was as described in Figure 3 and Supplementary Figure S1. All CFSs of selected strains were able to inhibit pathogenic bacteria. The antimicrobial activity of CFS exerted by all these strains withstood after adjustment of pH but disappeared, partially or completely, after heat and proteinase K treatments, thus confirming the proteinaceous nature of the antimicrobial compounds.

3.2 Sporulation efficiency

All selected strains showed different sporulation efficiencies (Figure 4) and showed spore titres in order of 10^7–10^8 spores/ml. The sporulation of S17 and Z1 had the highest rate at 18% and 20% after 24 h and 89% and 92% after 48 h, respectively, while Cm5 had the lowest at 14% and 84% after 24 h and 48 h, respectively.

3.3 Probiotic properties of selected spore-forming bacteria

3.3.1 Evaluation of extracellular enzymes and biofilm production

Extracellular enzyme production is wide-ranging among selected strains. The S17 strain exhibited the highest protease and amylase activities. Lipase activity was detected with Cm5, Z1, and C211 (Supplementary Table S1). Further, lipase activity was not detected in sardine isolates. Finally, all the selected strains were able to form biofilm. Among them, S17 had the strongest ability followed by C211 (Figure 5).

3.3.2 Tolerance to high temperature and pH and bile salt

Vegetative cells and spores were tested for resistance to high temperature, various pH, and bile concentrations.

Selected strains gave promising results after exposure to high temperatures (80°C, 90°C, 100°C for 5 and 10 min). High viability (above 80%) was observed in all selected vegetative cells after exposure to various temperatures compared to control (spore formers without exposure to high temperatures). However, there were no significant differences at different times of exposure among various temperatures for Z1 and S17. At last, the strains Cm4 and C211 had a significant decrease in viability (Supplementary Figure S2).

For the vegetative cells, all selected strains remained viable after 3 h of exposure to pH 2.0 and pH 3.0, but none could tolerate exposure to pH 1.0 (Table 3). Among all tested strains, S17 was found to have the highest resistance to acid conditions, while Cm5 and Z1 showed the lowest acid tolerance. Tested strains also withstood (0.5%–5%) bile concentrations after a 3-h

TABLE 2 Direct antimicrobial activity against fish pathogens.

Biotope	Isolates	Va	Val	Vf	Vh1	Vh2	Vh3	Vh4	Vh5	Vh6	Vh7	Vp	Vpr	Vv	Vs	Total score
Shrimp intestine	**Cm1**	0	0	0	0	0	0	0	0	0	2	0	0	0	0	2
	Cm2	1	0	0	0	0	0	0	0	0	1	0	0	0	0	2
	Cm4	4	0	3	0	0	2	1	1	0	2	2	1	2	0	18
	Cm5	4	0	3	1	2	2	2	1	0	2	2	1	2	0	22
	Cm6	1	0	1	0	0	0	0	0	0	0	0	0	0	0	2
	Z1	4	1	3	0	2	3	1	1	0	1	2	1	2	0	21
	Z3	0	0	1	0	0	0	0	0	0	0	1	1	0	0	3
	C10	0	0	1	0	1	0	0	0	0	0	0	0	0	0	2
	C11	0	0	0	0	0	2	0	0	0	0	0	0	0	0	2
	C20	0	0	0	1	2	1	2	0	0	2	0	0	0	0	8
	C211	3	0	2	0	1	3	2	1	1	0	1	0	3	0	17
Sardine intestine	**S1**	1	0	0	1	1	1	1	1	0	0	0	0	0	0	6
	s2	1	0	0	1	0	1	0	0	0	0	0	0	0	0	3
	S3	1	0	0	1	0	1	0	0	0	0	0	0	0	0	3
	S4	1	0	0	1	0	1	0	0	0	1	0	0	0	0	4
	S6	1	0	0	1	0	1	0	0	0	1	0	0	0	0	4
	S9	0	1	3	0	0	0	0	0	0	0	0	0	0	0	4
	S10	1	0	0	0	0	1	0	0	0	0	0	0	0	0	2
	S14	0	0	2	0	1	0	1	0	0	0	0	0	0	0	4
	S17	3	1	4	1	2	3	2	2	1	1	2	1	2	0	25

Zones of inhibition (halo diameter) were presented as scores; 0 (0–5 mm), 1 (low,6–10 mm), 2 (moderate, 11–20 mm), 3 (high, 21–24 mm) and 4 (very high, ≥25 mm. 0—no antagonistic activity. All indicator strains were assayed at least twice. Va, *Vibrio anguillarum* CECT4344; Val, *V. alginolyticus*; Vf, *V. fischerie*; Vh1, *V. harveyi* Lg 10/6; Vh2, *V. harveyi* Lg 14/01, Vh3, *V.harveyi* Lg 26/01; Vh4, *V. harveyi* Lg 48/01; Vh5, *V. harveyi* Lg 13/04; Vh6, *V. harveyi* Lg 34/04; Vh7, *V. harveyi* Lg 35/03; Vp, *V. parahaemolyticus*; Vpr, *V. proteolyticus*; Vv, *V. vulnificus*; Vs, *V. splendidus*.

exposure. Thus, S17 showed the highest tolerance to 5% of bile salt, whereas strain CJ3 exhibited the lowest tolerance. However, all spores of tested strains demonstrated significantly high tolerance to gastric and intestinal conditions after a 3-h exposure (Figure 6). Noteworthily, all spores could tolerate exposure to pH 1.0 and remain viable compared to vegetative cells in the same condition.

3.3.3 Auto-aggregation and co-aggregation assays

As seen in Table 4, auto-aggregation for selected strains increased with the incubation period and varied from 4% to 92%. All selected strains revealed low auto-aggregation ability (<50%) at the first 3 h. Nonetheless, a significant increase was observed after 24 h. Among them, S17 and C211 exhibited the strongest auto-aggregation ability (92%; 90%, respectively) after 24 h of incubation.

In addition, all tested strains were able to co-aggregate with pathogens significantly, showing co-aggregation percentages above 55% (Figure 7). Among the isolates, S17 showed the highest percentage of co-aggregation against *V. fischeri* (81%), *V. harveyi* Lg48/01 (79%), and *V. harveyi* Lg26/01 (67%) after 6 h of incubation. S17 also presented a strong ability to co-aggregate against *V. anguillarum* with more than 74%, followed by Cm4 and Cm5.

3.3.4 Adhesion and growth on fish mucus

The adhesion ability of the tested strains (vegetative cells) to mucus is shown in Table 5. All tested strains were highly capable of binding to intestinal mucus (44.7 to 58.3%) but less to skin mucus (10.6% to 29.4%). S17 showed the highest, both skin and intestinal mucus adhesion with more than 29% and 58%, respectively. The adhesion ability of spores was found to be lower than that of its vegetative cells for skin and intestinal mucus (Figure 8A). All the spores were more able for adhesion to intestinal mucus than skin mucus, ranging from 8% to 60%. All tested strains (vegetative cells and spores) adhered significantly less to BSA (5% to 37%) and polystyrene (19% to 50%) compared to skin and intestinal mucus.

All tested strains (vegetative cells and spores) were able to grow in fish mucus collected from the skin and intestine of *S. aurata* (Figure 8B). The growth of vegetative cells was found to be higher than that of their spores for skin and intestinal mucus. Interestingly, growth of vegetative cells on intestinal mucus was observed to be higher compared to growth on skin mucus. The significantly highest growth was observed for S17, for both skin and intestinal mucus, respectively.

3.4 Identification and *in vitro* safety assay

The selected strains were subjected to partial 16S rDNA gene sequencing and MALDI-TOF MS. According to these methods,

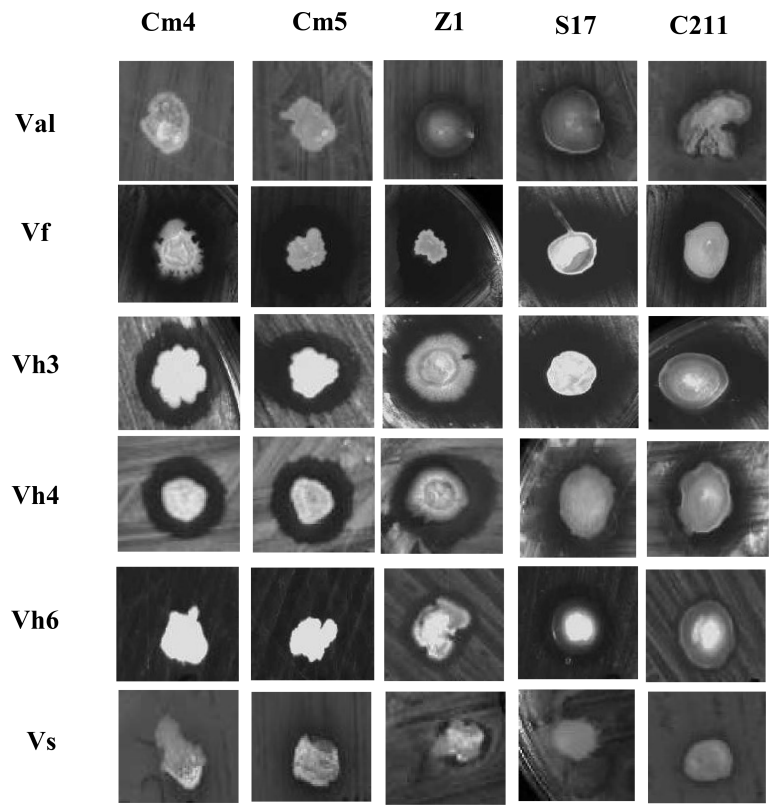

FIGURE 1
Pictorial overview of antimicrobial activities of selected strains against indicators Vibrios (colony overlay method).Val, *V.alginolyticus;* Vf, *V.fischerie;* Vh3, *V. harveyi* Lg 26/01; Vh4, *V. harveyi* Lg 48/01; Vh6, *V. harveyi* Lg 34/04 and Vs, *V. spendidus*.

all selected strains were identified as *Bacillus* spp. The isolates were identified as *B. subtilis* (Cm4, Cm5, S17, and C211) and *B. amyloliquefaciens* (Z1) by MALDI-TOF MS (Table 6) which was confirmed by PCR. In addition, all selected spore formers were found to be susceptible to tested antibiotics.

All strains exhibited haemolysis on blood agar (β-haemolytic) except S17, which was negative for haemolytic activity (γ-haemolytic) (Supplementary Table 2). More analysis revealed that Z1 and C211 were found to exhibit bile salt deconjugation, and all selected isolates showed gelatinase production except S17 (Supplementary Table S2). Furthermore, PCR screening for the presence of biogenic amines and toxins showed that none of the tested strains encoded any of the virulence genes searched *hdc*, *tdc*, *odc*, *sfp*, *cesA*, or *cesB*, with the exception of *ldc* which was detected in Cm4 and C211 (Supplementary Table 2).

4. Discussion

During the past decades, aquaculture production has faced many threats due to the outbreak of diseases, i.e., Vibriosis (Yılmaz et al., 2021). In order to control or prevent fish pathogens, probiotics are used as a viable and friendly alternative (Balcázar et al., 2008; Kavitha et al., 2018; Khan et al., 2021). Gastrointestinal microbiota is considered as the best source to isolate and select potential probiotics. Indeed, fish and shrimp intestine constitute a dynamic ecosystem containing diverse unexplored microorganisms and playing a crucial role in animal health (Romero et al., 2014; Zhou et al., 2014; Kuebutornye et al., 2020; Medina et al., 2020). Numerous studies assumed that probiotics from target marine animals and from the same ecological niche of pathogens would be more effective (Midhun et al., 2017; Kuebutornye et al., 2020; Yamashita et al., 2020; Santos et al., 2021). In the present investigation, spore-former strains were isolated from sardine and shrimp intestine and were evaluated for their probiotic potential and their safety to select the most putative as probiotic for aquaculture.

An initial prescreening was carried out based on antimicrobial activity against Vibriosis which is one of major pathogens in aquaculture. From 108 isolates, only 20 showed antagonistic activity by the colony overlay method against, at least, two of tested Vibriosis such as *V. harveyi*, *V. anguillarum*,

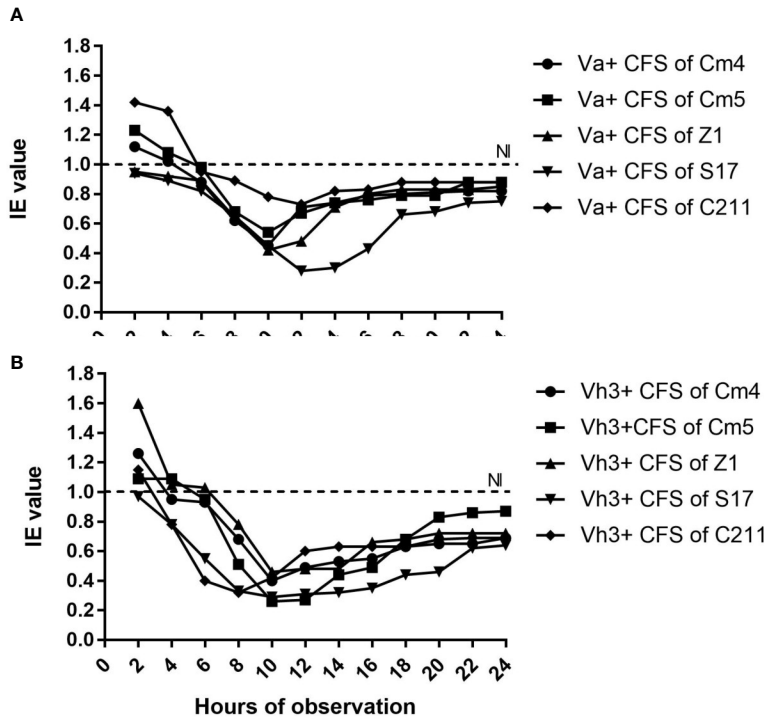

FIGURE 2
Inhibition efficiency (IE) of selected strains against **(A)** *Vibrio anguillarum* CECT4344 (Va) and **(B)** *V.harveyi* Lg 26/01 (Vh3) as a function of time. *IE˃1 indicated growth promotion of pathogen, IE=1indicated no inhibition (NI) and IE<1 indicated inhibition of pathogen by CFS of selected strains.

and *V. fischeri*. Previous studies indicated that *Bacillus* species, including *B. pumilus* (Lei et al., 2015), *B. amyloliquefaciens* (Cai et al., 2019; Medina et al., 2020), and *B. subtilis* (Zhou et al., 2019), exhibited antagonistic activity against Vibriosis (Amoah et al., 2021). Similar studies also reported that some *Bacillus* inhibit the growth of various *Vibrio* species (*V. harveyi*, *V. alginolyticus*, *V. vulnificus*, and *V. parahaemolyticus*) (Prieto et al., 2014; Meidong et al., 2018; Li et al., 2019; Zhou et al., 2019). Later on, selected strains with promising direct antimicrobial activity were tested for extracellular inhibitory activity by ADT and microtiters. In this respect, only five strains were found to produce proteinaceous compounds and *B. subtilis* S17 showed the strongest antagonistic activity against all tested *Vibrio* species. In fact, the antibacterial activity of selected strains is probably explained by the production of inhibitory components such as organic acids, hydrogen peroxide, and bacteriocins or by competition for adhesion sites and/or nutrients in the intestine (Pinto et al., 2020; Santos et al., 2021). Hence, published reports revealed that the antibacterial substances not only inhibit pathogen's growth but also increase the resistance of the host against pathogens (Verschuere et al., 2000; Guo et al., 2016; Midhun et al., 2017; Samson et al., 2020; Khan et al., 2021).

Unlike lactic acid bacteria, *Bacillus* sp. is considered to be a very stable strain due to its sporulation ability. Their endospores are resistant to harsh conditions, including high temperature, UV and acidity, drought, freezing, radiation, and rising oxygen levels. Relatively, *Bacillus* spores are able to survive throughout the simulation of GIT (Barbosa et al., 2005; Kuebutornye et al., 2020). In this present work, the sporulation rates of selected strains were more than 80% after 48 h of incubation. However, the differences in sporulation rates observed among the bacilli tested may be due to a different mechanism of sporulation process (Barbosa et al., 2005; Prieto et al., 2014; Banerjee and Ray, 2017).

Probiotics not only reduce the risk of fish infection in aquaculture by inhibiting the growth of pathogens but also could promote animal health. Several studies report that *Bacillus* sp. is able to produce digestive enzymes, including amylase, protease, lipase, cellulose, and xylanase (Hmani et al., 2017; Midhun et al., 2017). The present study confirms the ability of selected bacterial strains to produce extracellular enzymes including amylase, protease, and lipase. Indeed, these enzymes facilitate the digestion of fish diet and can help and improve the growth rate. Therefore, application of probiotics capable of producing enzymes is gaining attention to promote a

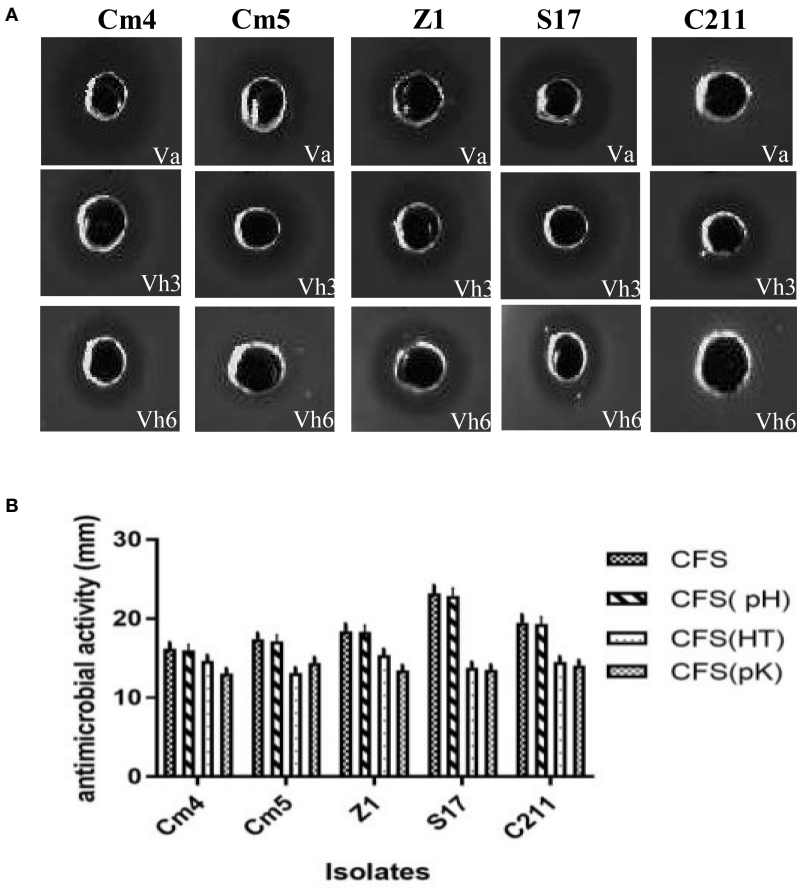

FIGURE 3
(A) Pictorial overview of antibacterial activity of selected strains against indicators (VA, *Vibrio anguillarum* CECT4344; Vh3, *Vibrio harveyi* Lg 26/01and Vh4, *V. harveyi* Lg 34/04) and **(B)** nature of their antagonistic activity against *Vibrio anguillarum* CECT4344 using agar well-diffusion method. *CFS: supernatant without any treatment, CFS (pH): pH neutralization treatment, CFS (HT): heat treatment at 100 ° C, CFS (pK): proteolytic enzyme treatment.

nutritional benefit in cultivable fish (Benhamed et al., 2014; Sharifuzzaman et al., 2018).

Moreover, biofilm is a complex and heterogenic aggregation of microorganisms. The probiotic biofilm has many benefits to host intestinal health including increasing the gut resistance by producing secondary metabolites, increasing the colonization efficiency, protecting the gut epithelium by competing with pathogenic strains for adherence sites, and inducing immune reactions to the gut pathogens in the host (Midhun et al., 2017; Banerjee and Ray, 2017; Midhun et al., 2017; Chauhan and Singh, 2019). In this study, all selected strains were capable of forming biofilm at high levels. Among them, strains S17 and C211 had the strongest ability to form biofilm.

During the production of animal feed production, heat treatment is considered as an essential process to get rid of vegetative cells (Banerjee and Ray, 2017; Kuebutornye et al., 2020). In this report, all tested strains showed higher survivability percentages above 80% during heat treatment (80°C, 90°C, 100°C) which were mentioned on previous findings (Kuebutornye et al., 2020; Amoah et al., 2021). Furthermore, probiotics are intended to colonize the GIT of fish and to restore the balance of intestinal microflora. The candidate strains should tolerate GIT conditions. In fact, ingested probiotic strains need to survive the acidity of stomach and fish bile in the small intestine. Moreover, bile plays an important role in the mechanism (specific and non-specific) of defence in the gut. Hence, probiotic strains are required to tolerate bile salts which are so toxic for bacteria due to their effect on the structure of the membrane (Ramesh et al., 2015; Egerton et al., 2018; Feng et al., 2019; Samson et al., 2020). In the present study, the vegetative cells and spores of selected strains were tested in GIT conditions. No vegetative cells could tolerate pH 1.0 while the majority of tested cells withstand a low pH above 1.0 and a wide range of bile concentrations up to 5%. Previous studies have reported the ability of some strains of *Bacillus* to survive the stomach and

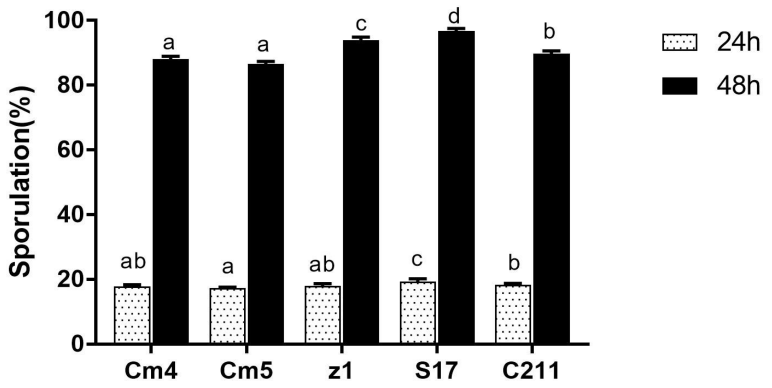

FIGURE 4
Sporulation efficiency of selected strains. The sporulation is expressed as the percentage of spores relative to vegetative cells after 24 h (white bar) and 48 h (black bar). Data are presented as (mean ± SD, n=3) with different superscript letters denoting a significant differences ($p<0.05$).

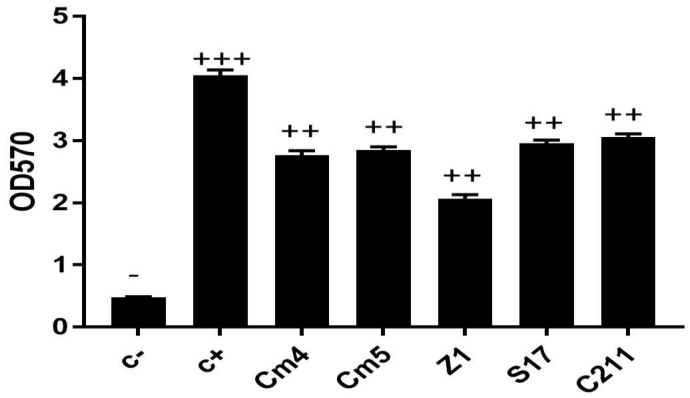

FIGURE 5
Biofilm production of selected strains. The ability of biofilm production is classified as follows: OD570 < 1, non-biofilm (-); 1< OD570 < 2, weak (+); 2< OD570 < 4, medium (+ +) and OD570>4, strong biofilm (+ + +).

TABLE 3 Tolerance of vegetative cells and spores at different pH conditions for 3 h at 28°C (log CFU/mL, SD*).

Viable count (log CFU/ml) Strains	Vegetative cells				spores			
	7.3	1	2	3	7.3	1	2	3
Cm4	9.84 ± 0.01^{c}	ND	6.85 ± 0.02^{c}	6.94 ± 0.01^{c}	7.92 ± 0.01^{b}	7.84 ± 0.01^{b}	7.84 ± 0.01^{b}	7.86 ± 0.03^{b}
Cm5	9.46 ± 0.01^{b}	ND	5.65 ± 0.03^{b}	5.61 ± 0.01^{a}	7.47 ± 0.01^{a}	7.29 ± 0^{a}	7.36 ± 0.02^{a}	7.41 ± 0.05^{a}
Z1	8.78 ± 0^{a}	ND	5.32 ± 0.02^{a}	5.69 ± 0.09^{a}	8.5 ± 0.02^{c}	8.31 ± 0.05^{c}	8.38 ± 0.03^{c}	8.41 ± 0.05^{c}
S17	9.63 ± 0.07^{b}	ND	8.46 ± 0.01^{d}	8.85 ± 0.01^{d}	8.56 ± 0.08^{c}	8.53 ± 0.05^{d}	8.55 ± 0.05^{d}	8.55 ± 0.05^{d}
C211	9.89 ± 0.01^{c}	ND	5.51 ± 0.03^{b}	6.13 ± 0.13^{b}	8.42 ± 0.02^{c}	8.28 ± 0^{c}	8.3 ± 0^{c}	8.32 ± 0.02^{c}

**Bacterial levels were determined by plate count on TSB. Data are presented as (mean ± SD, n = 3) with different superscript letters denoting a significant difference ($p< 0.05$). ND, not detected.*

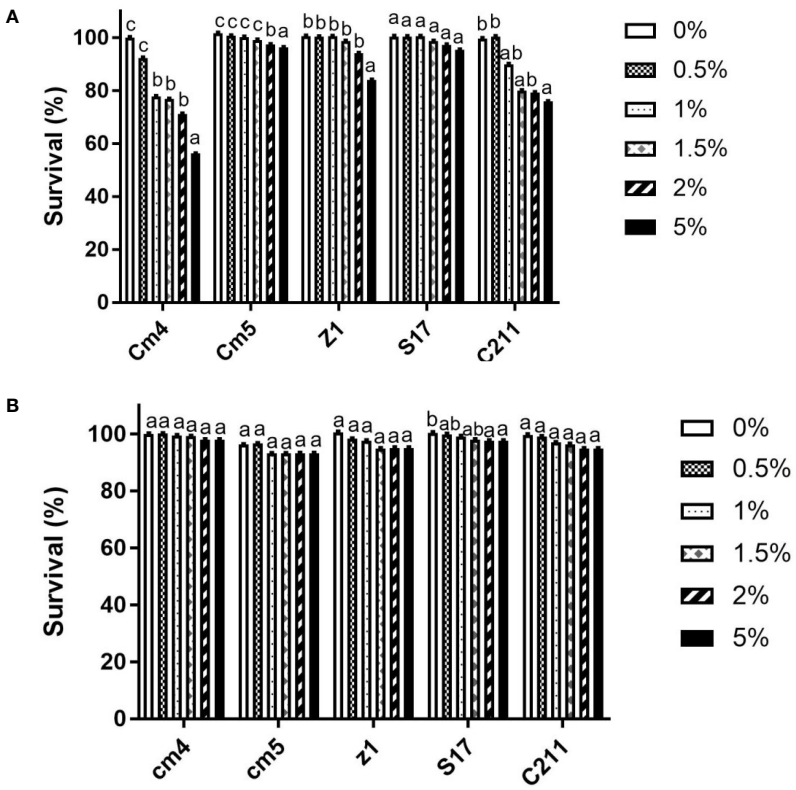

FIGURE 6
Tolerance of vegetative cells **(A)** and spores **(B)** at different bile concentrations for 3h at 28°C (log CFU/mL, SD*). Data are presented as (mean ± SD, n=3) with different superscript letters denoting a significant differences ($p<0.05$).

intestinal environment where they could work effectively (Shinde et al., 2019; Medina et al., 2020), whereas a small reduction of spore count of tested strains was observed and could be due to their germination (Barbosa et al., 2005; Sahoo et al., 2015). This finding suggests that those can be used as probiotic as they could tolerate the harsh gastric acid and toxic bile.

Determination of bacterial cell surface properties, i.e., hydrophobicity, auto-aggregation, and co-aggregation, is an indirect method for the adhesion ability of probiotic strains. Further, aggregating probiotic bacteria may help not only adhesion and colonization of the GIT but also the modulation of the immune system (Balakrishna, 2013; Dutta et al., 2018; Kaktcham et al., 2018; Khan et al., 2021). In the current study, all tested strains showed auto-aggregation ability ranging from 4% to 92% after 24 h of incubation. Among them, S17 and C211 exhibited high auto-aggregation ability (92%; 90%, respectively), in accordance with previous findings (Meidong et al., 2017; Khan et al., 2021; Amoah et al., 2021). Moreover, a co-aggregation assay was developed to quantify

TABLE 4 Auto-aggregation of the isolate strains after 24 h.

Strains	Auto-aggregation					
	1 h	2 h	3 h	4 h	5 h	24 h
Cm4	4.02 ± 0.18^{a}	41.77 ± 2.03^{b}	45.86 ± 2.16^{a}	53.68 ± 2.45^{a}	58.54 ± 2.65^{a}	60.52 ± 2.76^{a}
Cm5	11.4 ± 0.51^{b}	19.81 ± 0.89^{a}	47.04 ± 2.27^{a}	78.95 ± 3.82^{b}	79.48 ± 3.76^{b}	88.74 ± 4.4^{b}
Z1	17.21 ± 0.72^{c}	34.04 ± 1.57^{b}	42.98 ± 2.09^{a}	54.95 ± 2.49^{a}	77.46 ± 3.68^{b}	83.93 ± 4.08^{b}
S17	21.43 ± 0.65^{c}	36.8 ± 1.67^{b}	44.33 ± 1.97^{a}	47.04 ± 2.19^{a}	77.63 ± 3.51^{b}	91.94 ± 4.21^{b}
C211	28.79 ± 1.31^{d}	37.43 ± 1.69^{b}	41.48 ± 1.69^{a}	81.01 ± 3.87^{b}	87.37 ± 4.13^{b}	90.14 ± 4.36^{b}

Data are presented as (mean ± SD, n = 3) with different superscript letters denoting a significant difference ($p< 0.05$).

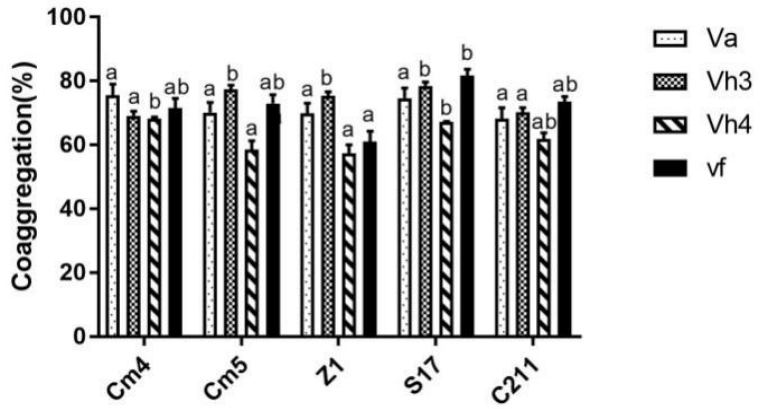

FIGURE 7
Co-aggregation percentages of selected strains with pathogens after 6h.Va, *Vibrio anguillarum* CECT4344; Vh3, *V. harveyi* Lg 26/01; Vh4, *V. harveyi* Lg 48/01; Vf, *V. fischerie*. Data are presented as mean ± SD (n=3) with different superscript letters denoting a significant differences ($p<0.05$).

inter-bacterial adherence (Dutta et al., 2018; Rungsirivanich et al., 2020). Co-aggregation capacity is considered as a way to exclude pathogens from the host. According to different investigations, co-aggregation ability can increase the competition of an epithelial cell's receptor and may protect GIT against undesired microorganisms (Balakrishna, 2013; Dutta et al., 2018; Kaktcham et al., 2018; Meidong et al., 2018; Rungsirivanich et al., 2020). In the present study, all strains tested were able to co-aggregate with pathogens, showing inhibition percentages above 55%. The result also points out that strain S17 showed the highest percentage of co-aggregation against *Vibrio fischeri* (81%), *V. harveyi* Lg48/01 (79%), and *V. harveyi* Lg26/01 (67%) after 6 h of incubation. Dutta **et al.** found that *B. subtilis* LR3H1A and *B. tequilensis* LR3F3P showed a strong co-aggregation with several pathogens (Khan et al., 2021).

The adhesion of probiotic strains to mucus is required and is considered as an important criterion for probiotic selection. Adherence to GIT is the first step in probiotic strains for colonization, stimulation of the immune system, and antagonistic activity. Upon ingestion in GIT, probiotic strains have to attach to the border of microvilli or to the mucus to prevent the colon sweep. Cell adhesion is a complex process which involves contact between the membrane of bacterial cell and surface (Mbozo et al., 2017; Dutta et al., 2018; Rungsirivanich et al., 2020; Gutiérrez Falcón et al., 2021). In fact, many factors including electrostatic interactions, hydrophobicity, steric forces, components of the surface, pH of the milieu, and viscosity are involved (Balcázar et al., 2008; Muñoz-Atienza et al., 2014; Chauhan and Singh, 2019). In this study, all tested strains (vegetative cells and spores) were highly capable of binding to the intestinal mucus but less to skin mucus. This higher adhesion capacity may be due to the presence of specific receptors on the intestinal mucus or may be related to mucus composition (Balcázar et al., 2008). However, all tested *Bacillus* adhered less to polystyrene and BSA compared to intestinal mucus. This binding may involve specific interactions. Similar results were reported by Balcázar et al. and Muñoz-Atienza et al. (Balcázar et al., 2008; Muñoz-Atienza et al., 2014). Once probiotic strains adhered, the next step involved their mucus growth in order to establish in the

TABLE 5 Adhesion of selected strains to fish mucus.

Strains	% adhesion			
	SM	IM	BSA	Polystyrene
Cm4	13.88 ± 0.53^{b}	58.33 ± 1.19^{b}	7.32 ± 0.18^{b}	29.89 ± 0.35^{a}
Cm5	17.04 ± 0.81^{c}	53.25 ± 2.22^{b}	19.55 ± 0.28^{c}	45.34 ± 2.2^{c}
z1	15.4 ± 0.44^{bc}	44.74 ± 1.15^{a}	4.71 ± 0.18^{a}	31.21 ± 1.2^{a}
S17	29.41 ± 0.59^{d}	55.56 ± 2.6^{b}	36.58 ± 0.4^{d}	40.74 ± 0.87^{b}
C211	10.58 ± 0.37^{a}	56.2 ± 1.03^{b}	16.56 ± 0.63^{c}	50.05 ± 0.51^{c}

Data are presented as mean ± SD (n = 3) with different superscript letters denoting a significant difference (p< 0.05). SM, skin mucus; IM, intestinal mucus.

TABLE 6 Identification of selected spore formers.

Isolate	Top best matched species	MALDI-TOF MS	Score value
Cm4	*Bacillus subtilis*	*Bacillus subtilis*	1.78
Cm5	*Bacillus subtilis*	*Bacillus subtilis*	1.8
Z1	*Bacillus amyloliquefaciens*	*Bacillus amyloliquefaciens*	1.84
S17	*Bacillus subtilis*	*Bacillus subtilis*	2.10
C211	*Bacillus subtilis*	*Bacillus subtilis*	1.96

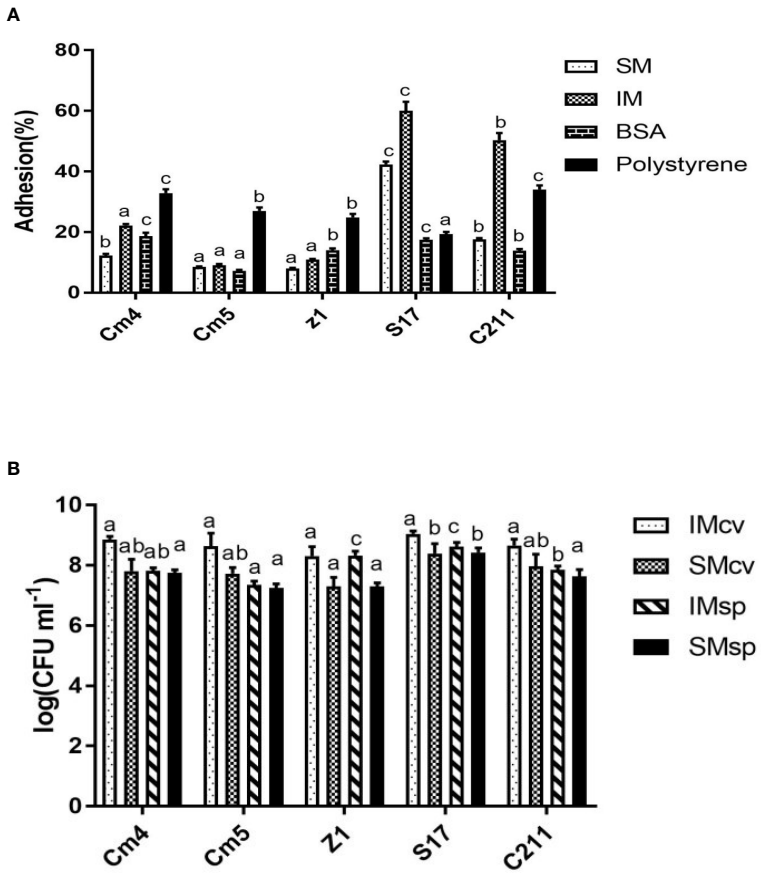

FIGURE 8
(A) Adhesions of spores to fish mucus, BSA and polystyrene and **(B)** Growth of selected strains on intestinal and skin mucus of *Sparus aurata*. Data are presented as mean ± SD (n=3) with different superscript letters denoting a significant differences ($p<0.05$). * IM, intestinal mucus; SM, skin mucus; cv, vegetative cells; sp, spores.

intestine of marine animals (Mbozo et al., 2017). In the present investigation, all vegetative cells and spores of tested strains grew well in the skin and intestine mucus of *S. aurata*, which indicates that our probiotic strains will be able to bind, establish, and remain in the intestine.

Safety assessment is an important precondition for probiotic evaluation. Before the use of probiotics, it is mandatory to confirm that no pathogenic and harmful effects may occur in marine hosts (Verschuere et al., 2000; Medina et al., 2020; Pinto et al., 2020). In the current investigation, all selected stains were found to be susceptible to tested antibiotics demanded by EFSA. This result may ensure the inability and scarcity to transfer antibiotic resistance genes to gut bacteria, thus assuring their safety for aquaculture application (Gutiérrez Falcón et al., 2021). Regarding hydrolic enzymes and virulence factors, S17 did not show haemolytic activity (γ-haemolytic), gelatinase production, and bile salt deconjugation. In addition, S17 appeared to be free of studied virulence factors. Our results are in accordance with the previous study (Hsieh et al., 2004; Shinde et al., 2019). With this regard, candidate probiotic S17 may be considered as a safe strain.

5 Conclusions

In the present study, 108 spore-former strains were isolated from sardine and shrimp intestine. Among all tested strains, only *B. subtilis* S17 possesses suitable probiotic potential for Vibriosis control based on antimicrobial activity, heat and GIT tolerances, extracellular enzyme production, adhesion ability, and safety assessment. Afterward, *in vivo* evaluation studies are required to determine its real-life applications.

Data availability statement

The datasets presented in this study can be found in online repositories. The names of the repository/repositories and

accession number(s) can be found below: https://www.ncbi.nlm.nih.gov/, MZ378829.

Author contributions

MJ, IA and MamBA designed the study. MJ conducted the study, analysed the data, and wrote the manuscript. AH, WB, and ManBA participated in its organization and helped to draft the manuscript. MJ and MamBA revised the manuscript. All authors have read and agreed to the published version of the manuscript.

Funding

This study was supported by a grant from Astrum biotech the Ministry for Higher Education and Scientific Research, Tunisia.

Conflict of interest

The authors declare that the research was conducted in the absence of any commercial or financial relationships that could be construed as a potential conflict of interest.

Publisher's note

All claims expressed in this article are solely those of the authors and do not necessarily represent those of their affiliated organizations, or those of the publisher, the editors and the reviewers. Any product that may be evaluated in this article, or claim that may be made by its manufacturer, is not guaranteed or endorsed by the publisher.

Supplementary material

The Supplementary Material for this article can be found online at: https://www.frontiersin.org/articles/10.3389/fmars.2022.884244/full#supplementary-material

References

Alonso, S., Castro, M. C., Berdasco, M., de la Banda, I. G., Moreno-Ventas, X., and de Rojas, A. H. (2019). Isolation and partial characterization of lactic acid bacteria from the gut microbiota of marine fishes for potential application as probiotics in aquaculture. *Probiotics. antimicrob. proteins.* 11 (2), 569–579. doi: 10.1007/s12602-018-9439-2

Altakhis, M., Pillidge, C. J., Osborn, A. M., Torley, P. J., and Kaur, M. (2021). Assessment of the potential use of MALDI-TOF MS for the identification of bacteria associated with chilled vacuum-packaged lamb meat. *Meat. Science.* 177, 108508. doi: 10.1016/j.meatsci.2021.108508

Amoah, K., X-h, D., Tan, B.-p., Zhang, S., Kuebutornye, F. K. A., Chi, S.-y., et al. (2021). *In vitro* assessment of the safety and potential probiotic characteristics of three bacillus strains isolated from the intestine of hybrid grouper (Epinephelus fuscoguttatus♀× e. lanceolatus♂). *Front. Vet. Science.* 8. doi: 10.3389/fvets.2021.675962

Araújo, C., Muñoz-Atienza, E., Nahuelquín, Y., Poeta, P., Igrejas, G., Hernández, P. E., et al. (2015). Inhibition of fish pathogens by the microbiota from rainbow trout (Oncorhynchus mykiss, walbaum) and rearing environment. *Anaerobe.* 32, 7–14. doi: 10.1016/j.anaerobe.2014.11.001

Balakrishna, A. (2013). *In vitro* evaluation of adhesion and aggregation abilities of four potential probiotic strains isolated from guppy (Poecilia reticulata). *Braz. Arch. Biol. Technol.* 56 (5), 793–800. doi: 10.1590/S1516-89132013000500010

Balcázar, J. L., De Blas, I., Ruiz-Zarzuela, I., Cunningham, D., Vendrell, D., and Muzquiz, J. L. (2006). The role of probiotics in aquaculture. *Vet. Microbiol.* 114 (3-4), 173–186. doi: 10.1016/j.vetmic.2006.01.009

Balcazar, J. L., De Blas, I., Ruiz-Zarzuela, I., Vendrell, D., Girones, O., and Muzquiz, J. L. (2007). Sequencing of variable regions of the 16S rRNA gene for identification of lactic acid bacteria isolated from the intestinal microbiota of healthy salmonids. *Comp. immunol. Microbiol. Infect. diseases.* 30 (2), 111–118. doi: 10.1016/j.cimid.2006.12.001

Balcázar, J. L., Vendrell, D., de Blas, I., Ruiz-Zarzuela, I., Muzquiz, J. L., and Girones, O. (2008). Characterization of probiotic properties of lactic acid bacteria isolated from intestinal microbiota of fish. *Aquaculture* 278 (1-4), 188–191. doi: 10.1016/j.aquaculture.2008.03.014

Banerjee, G., and Ray, A. K. (2017). The advancement of probiotics research and its application in fish farming industries. *Res. Vet. Sci.* 115, 66–77. doi: 10.1016/j.rvsc.2017.01.016

Barbosa, T. M., Serra, C. R., La Ragione, R. M., Woodward, M. J., and Henriques, A. O. (2005). Screening for bacillus isolates in the broiler gastrointestinal tract. *Appl. Environ. Microbiol.* 71 (2), 968–978. doi: 10.1128/AEM.71.2.968-978.2005

Beltrán, J. M. G., Espinosa, C., Guardiola, F. A., and Esteban, MÁ. (2017). Dietary dehydrated lemon peel improves the immune but not the antioxidant status of gilthead seabream (Sparus aurata l.). *Fish. shellfish. Immunol.* 64, 426–436. doi: 10.1016/j.fsi.2017.03.042

Benhamed, S., Guardiola, F. A., Mars, M., and Esteban, MÁ. (2014). Pathogen bacteria adhesion to skin mucus of fishes. *Vet. Microbiol.* 171 (1-2), 1–12. doi: 10.1016/j.vetmic.2014.03.008

Cai, Y., Yuan, W., Wang, S., Guo, W., Li, A., Wu, Y., et al. (2019). *In vitro* screening of putative probiotics and their dual beneficial effects: To white shrimp (Litopenaeus vannamei) post larvae and to the rearing water. *Aquaculture.* 498, 61–71. doi: 10.1016/j.aquaculture.2018.08.024

Cao, L., Pan, L., Gong, L., Yang, Y., He, H., Li, Y., et al. (2019). Interaction of a novel bacillus velezensis (BvL03) against aeromonas hydrophila in vitro and *in vivo* in grass carp. *Appl. Microbiol. Biotechnol.* 103 (21-22), 8987–8999. doi: 10.1007/s00253-019-10096-7

Caruffo, M., Navarrete, N., Salgado, O., Díaz, A., López, P., García, K., et al. (2015). Potential probiotic yeasts isolated from the fish gut protect zebrafish (Danio rerio) from a vibrio anguillarum challenge. *Front. Microbiol.* 6. doi: 10.3389/fmicb.2015.01093

Chauhan, A., and Singh, R. (2019). Probiotics in aquaculture: a promising emerging alternative approach. *Symbiosis.* 77 (2), 99–113. doi: 10.1007/s13199-018-0580-1

Cintas, L. M., Rodriguez, J. M., Fernandez, M. F., Sletten, K., Nes, I. F., Hernandez, P. E., et al. (1995). Isolation and characterization of pediocin L50, a new bacteriocin from pediococcus acidilactici with a broad inhibitory spectrum. *Appl. Environ. Microbiol.* 61 (7), 2643–2648. doi: 10.1128/aem.61.7.2643-2648.1995

Daniels, N. A., and Shafaie, A. (2000). A review of pathogenic vibrio infections for clinicians. *Infections Med.* 17 (10), 665–685. doi: 17.10/infectmed.200.665-685

do Vale Pereira, G., da Cunha, D., Pedreira Mourino, J., Rodiles, A., Jaramillo-Torres, A., and Merrifield, D. (2017). Characterization of microbiota in arapaima gigas intestine and isolation of potential probiotic bacteria. *J. Appl. Microbiol.* 123 (5), 1298–1311. doi: 10.1111/jam.13572

Dutta, D., Banerjee, S., Mukherjee, A., and Ghosh, K. (2018). Potential gut adherent probiotic bacteria isolated from rohu, labeo rohita (Actinopterygil : Cypriniformes:Cyprinidae): Characterisation, exo-enzyme production, pathogen inhibition, cell surface hydrophobicity, and biofilm formation. *Acta Ichthyologica Piscatoria.* 48 (3), 221-233. doi: 10.3750/AIEP/02251

Eaton, T. J., and Gasson, M. J. (2001). Molecular screening of enterococcus virulence determinants and potential for genetic exchange between food and medical isolates. *Appl. Environ. Microbiol.* 67 (4), 1628–1635. doi: 10.1128/AEM.67.4.1628-1635.2001

Egerton, S., Culloty, S., Whooley, J., Stanton, C., and Ross, R. P. (2018). The gut microbiota of marine fish. *Front. Microbiol.* 9. doi: 10.3389/fmicb.2018.00873

Ehling-Schulz, M., Fricker, M., and Scherer, S. (2004). Identification of emetic toxin producing bacillus cereus strains by a novel molecular assay. *FEMS Microbiol. letters.* 232 (2), 189–195. doi: 10.1016/S0378-1097(04)00066-7

Emam, A. M., and Dunlap, C. A. (2020). Genomic and phenotypic characterization of bacillus velezensis AMB-y1; a potential probiotic to control pathogens in aquaculture. *Antonie van Leeuwenhoek* 113 (12), 2041–2052. doi: 10.1007/s10482-020-01476-5

FAO/WHO/OIE (2006). *Expert consultation on antimicrobial use in aquaculture and antimicrobial resistance*.

Feng, P., Ye, Z., Kakade, A., Virk, A., Li, X., and Liu, P. (2019). A review on gut remediation of selected environmental contaminants: Possible roles of probiotics and gut microbiota. *Nutrients.* 11 (1), 22. doi: 10.3390/nu11010022

Fernandes, S., and Kerkar, S. (2019). Bacterial probiotics over antibiotics: A boon to aquaculture. *Adv. Biol. Sci. Res. Elsevier,*, 2021 (13), 1572–1584. doi: 10.1016/B978-0-12-817497-5.00014-8

Fuller, R. (1989). Probiotics in man and animals. *J. Appl. bacteriol.* 66 (5), 365–378. doi: 10.1111/j.1365-2672.1989.tb05105.x

Ghanei-Motlagh, R., Mohammadian, T., Gharibi, D., Menanteau-Ledouble, S., Mahmoudi, E., Khosravi, M., et al. (2020). Quorum quenching properties and probiotic potentials of intestinal associated bacteria in Asian Sea bass lates calcarifer. *Mar. Drugs* 18 (1), 23. doi: 10.3390/md18010023

Guo, X., Chen, D.-D., Peng, K.-S., Cui, Z.-W., Zhang, X.-J., Li, S., et al. (2016). Identification and characterization of bacillus subtilis from grass carp (Ctenopharynodon idellus) for use as probiotic additives in aquatic feed. *Fish. Shellfish. Immunol.* 52, 74–84. doi: 10.1016/j.fsi.2016.03.017

Gutiérrez Falcón, A., Padilla, D., Real, F., Ramos Sosa, M. J., Acosta-Hernández, B., Sánchez Henao, A., et al. (2021). Screening of new potential probiotics strains against photobacterium damselae subsp. piscicida for marine aquaculture. *Animals.* 11 (7), 2029. doi: 10.3390/ani11072029

Han, S.-S., Jeong, Y.-S., and Choi, S.-K. (2021). Current scenario and challenges in the direct identification of microorganisms using MALDI TOF MS. *Microorganisms.* 9 (9), 1917. doi: 10.3390/microorganisms9091917

Hmani, H., Daoud, L., Jlidi, M., Jalleli, K., Ali, M. B., Brahim, A. H., et al. (2017). Ali MB. a bacillus subtilis strain as probiotic in poultry: selection based on *in vitro* functional properties and enzymatic potentialities. *J. Ind. Microbiol. Biotechnol.* 44 (8), 1157–1166. doi: 10.1007/s10295-017-1944-x

Horwood, P. F., Burgess, G. W., and Jane Oakey, H. (2004). Evidence for non-ribosomal peptide synthetase production of cereulide (the emetic toxin) in bacillus cereus. *FEMS Microbiol. letters.* 236 (2), 319–324. doi: 10.1111/j.1574-6968.2004.tb09664.x

Hsieh, F.-C., Li, M.-C., Lin, T.-C., and Kao, S.-S. (2004). Rapid detection and characterization of surfactin-producing bacillus subtilis and closely related species based on PCR. *Curr. Microbiol.* 49 (3), 186–191. doi: 10.1007/s00284-004-4314-7

Kaktcham, P. M., Temgoua, J.-B., Zambou, F. N., Diaz-Ruiz, G., Wacher, C., and de Lourdes Pérez-Chabela, M. (2018). *In vitro* evaluation of the probiotic and safety properties of bacteriocinogenic and non-bacteriocinogenic lactic acid bacteria from the intestines of Nile tilapia and common carp for their use as probiotics in aquaculture. *Probiotics. antimicrob. proteins.* 10 (1), 98–109. doi: 10.1007/s12602-017-9312-8

Kavitha, M., Raja, M., and Perumal, P. (2018). Evaluation of probiotic potential of bacillus spp. isolated from the digestive tract of freshwater fish labeo calbasu (Hamilton, 1822). *Aquacult. Rep.* 11, 59–69. doi: 10.1016/j.aqrep.2018.07.001

Khan, M. I. R., Choudhury, T. G., Kamilya, D., Monsang, S. J., and Parhi, J. (2021). Characterization of bacillus spp. isolated from intestine of labeo rohita–towards identifying novel probiotics for aquaculture. *Aquacult. Res.* 52 (2), 822–830. doi: 10.1111/are.14937

Khan, M. I. R., Kamilya, D., Choudhury, T. G., Tripathy, P. S., and Rathore, G. (2021). Deciphering the probiotic potential of bacillus amyloliquefaciens COFCAU_P1 isolated from the intestine of labeo rohita through in vitro and genetic assessment. *Probiotics. Antimicrob. Proteins*, 1–13. doi: 10.1007/s12602-021-09788-2

Kuebutornye, F. K. A., Abarike, E. D., and Lu, Y. (2019). A review on the application of bacillus as probiotics in aquaculture. *Fish. Shellfish. Immunol.* 87, 820–828. doi: 10.1016/j.fsi.2019.02.010

Kuebutornye, F. K., Abarike, E. D., Lu, Y., Hlordzi, V., Sakyi, M. E., Afriyie, G., et al. (2020). Mechanisms and the role of probiotic bacillus in mitigating fish pathogens in aquaculture. *Fish. Physiol. Biochem.*, 2020 (46), 819-841. doi: 10.1007/s10695-019-00754-y

Kuebutornye, F. K., Lu, Y., Abarike, E. D., Wang, Z., Li, Y., and Sakyi, M. E. (2020). *In vitro* assessment of the probiotic characteristics of three bacillus species from the gut of Nile tilapia, oreochromis niloticus. *Probiotics. antimicrob. proteins.* 12 (2), 412–424. doi: 10.1007/s12602-019-09562-5

Lei, X., Piao, X., Ru, Y., Zhang, H., Péron, A., and Zhang, H. (2015). Effect of bacillus amyloliquefaciens based direct-fed microbial on performance, nutrient utilization, intestinal morphology and cecal microflora in broiler chickens. *Asian-Australasian J. Anim. Sci.* 28 (2), 239. doi: 10.5713/ajas.14.0330

Li, X., Ringø, E., Hoseinifar, S. H., Lauzon, H. L., Birkbeck, H., and Yang, D. (2019). The adherence and colonization of microorganisms in fish gastrointestinal tract. *Rev. Aquaculture.* 11 (3), 603–618. doi: 10.1111/raq.12248

Li, M., Wang, Y., Cui, H., Li, Y., Sun, Y., and Qiu, H.-J. (2020). Characterization of lactic acid bacteria isolated from the gastrointestinal tract of a wild boar as potential probiotics. *Front. vet. science.* 7. doi: 10.3389/fvets.2020.00049

Makridis, P., Kokou, F., Bournakas, C., Papandroulakis, N., and Sarropoulou, E. (2021). Isolation of phaeobacter sp. from larvae of atlantic bonito (Sarda sarda) in a mesocosmos unit, and its use for the rearing of european seabass larvae (Dicentrarchus labrax l.). *Microorganisms.* 9 (1), 128. doi: 10.3390/microorganisms9010128

Mbozo, A. B. V., Kobawila, S. C., Anyogu, A., Awamaria, B., Louembe, D., Sutherland, J. P., et al. (2017). Investigation of the diversity and safety of the predominant bacillus pumilus sensu lato and other bacillus species involved in the alkaline fermentation of cassava leaves for the production of ntoba mbodi. *Food control.* 82, 154–162. doi: 10.1016/j.foodcont.2017.06.018

Medina, M., Sotil, G., Flores, V., Fernández, C., and Sandoval, N. (2020). *In vitro* assessment of some probiotic properties and inhibitory activity against yersinia ruckeri of bacteria isolated from rainbow trout oncorhynchus mykiss (Walbaum). *Aquacult. Rep.* 18, 100447. doi: 10.1016/j.aqrep.2020.100447

Meidong, R., Doolgindachbaporn, S., Jamjan, W., Sakai, K., Tashiro, Y., Okugawa, Y., et al. (2017). A novel probiotic bacillus siamensis B44v isolated from Thai pickled vegetables (Phak-dong) for potential use as a feed supplement in aquaculture. *J. Gen. Appl. Microbiol.* 63 (4), 246–253. doi: 10.2323/jgam.2016.12.002

Meidong, R., Khotchanalekha, K., Doolgindachbaporn, S., Nagasawa, T., Nakao, M., Sakai, K., et al. (2018). Evaluation of probiotic bacillus aerius B81e isolated from healthy hybrid catfish on growth, disease resistance and innate immunity of pla-mong pangasius bocourti. *Fish. shellfish. Immunol.* 73, 1–10. doi: 10.1016/j.fsi.2017.11.032

Midhun, S. J., Neethu, S., Vysakh, A., Arun, D., Radhakrishnan, E., and Jyothis, M. (2017). Antibacterial activity and probiotic characterization of autochthonous paenibacillus polymyxa isolated from anabas testudineus (Bloch, 1792). *Microb. pathog.* 113, 403–411. doi: 10.1016/j.micpath.2017.11.019

Midhun, S. J., Neethu, S., Vysakh, A., Radhakrishnan, E., and Jyothis, M. (2018). Antagonism against fish pathogens by cellular Components/Preparations of bacillus coagulans (MTCC-9872) and it's *In vitro* probiotic characterisation. *Curr. Microbiol.* 75 (9), 1174–1181. doi: 10.1007/s00284-018-1506-0

Midhun, S. J., Neethu, S., Vysakh, A., Sunil, M., Radhakrishnan, E., and Jyothis, M. (2017). Antibacterial activity of autochthonous bacteria isolated from anabas testudineus (Bloch, 1792) and it's *in vitro* probiotic characterization. *Microb. pathog.* 113, 312–320. doi: 10.1016/j.micpath.2017.10.058

Mukherjee, A., and Ghosh, K. (2016). Antagonism against fish pathogens by cellular components and verification of probiotic properties in autochthonous bacteria isolated from the gut of an Indian major carp, catla catla (H amilton). *Aquacult. Res.* 47 (7), 2243–2255. doi: 10.1111/are.12676

Muñoz-Atienza, E., Araújo, C., Magadán, S., Hernández, P. E., Herranz, C., Santos, Y., et al. (2014). *In vitro* and *in vivo* evaluation of lactic acid bacteria of aquatic origin as probiotics for turbot (Scophthalmus maximus l.) farming. *Fish. shellfish. Immunol.* 41 (2), 570–580. doi: 10.1016/j.fsi.2014.10.007

Muñoz-Atienza, E., Gómez-Sala, B., Araújo, C., Campanero, C., Del Campo, R., Hernández, P. E., et al. (2013). Antimicrobial activity, antibiotic susceptibility and virulence factors of lactic acid bacteria of aquatic origin intended for use as probiotics in aquaculture. *BMC Microbiol.* 13 (1), 15. doi: 10.1186/1471-2180-13-15

Nayak, S. (2010). Probiotics and immunity: a fish perspective. *Fish. shellfish. Immunol.* 29 (1), 2–14. doi: 10.1016/j.fsi.2010.02.017

Pinto, A., Barbosa, J., Albano, H., Isidro, J., and Teixeira, P. (2020). Screening of bacteriocinogenic lactic acid bacteria and their characterization as potential probiotics. *Microorganisms* 8 (3), 393. doi: 10.3390/microorganisms8030393

Prieto, M., O'Sullivan, L., Tan, S., McLoughlin, P., Hughes, H., Gutierrez, M., et al. (2014). *In vitro* assessment of marine bacillus for use as livestock probiotics. *Mar. Drugs* 12 (5), 2422–2445. doi: 10.3390/md12052422

Ramesh, D., Vinothkanna, A., Rai, A. K., and Vignesh, V. S. (2015). Isolation of potential probiotic bacillus spp. and assessment of their subcellular components to induce immune responses in labeo rohita against aeromonas hydrophila. *Fish. shellfish. Immunol.* 45 (2), 268–276. doi: 10.1016/j.fsi.2015.04.018

Romero, J., Ringø, E., and Merrifield, D. L. (2014). "The gut microbiota of fish," in *Aquaculture nutrition: Gut health, probiotics and prebiotics* Oxford, (Wiley-Blackwell Publishing), 101, 75–100. doi: 10.1002/9781118897263.ch4

Rungsirivanich, P., Supandee, W., Futui, W., Chumsai-Na-Ayudhya, V., Yodsombat, C., and Thongwai, N. (2020). Culturable bacterial community on leaves of Assam tea (Camellia sinensis var. assamica) in Thailand and human probiotic potential of isolated bacillus spp. *Microorganisms* 8 (10), 1585. doi: 10.3390/microorganisms8101585

Sahoo, T. K., Jena, P. K., Nagar, N., Patel, A. K., and Seshadri, S. (2015). *In vitro* evaluation of probiotic properties of lactic acid bacteria from the gut of labeo rohita and catla catla. *Probiotics. antimicrob. proteins.* 7 (2), 126–136. doi: 10.1007/s12602-015-9184-8

Samson, J. S., Choresca, C. H., and Quiazon, K. M. A. (2020). Selection and screening of bacteria from African night crawler, eudrilus eugeniae (Kinberg, 1867) as potential probiotics in aquaculture. *World J. Microbiol. Biotechnol.* 36 (1), 16. doi: 10.1007/s11274-019-2793-8

Santos, R. A., Oliva-Teles, A., Pousão-Ferreira, P., Jerusik, R., Saavedra, M. J., Enes, P., et al. (2021). Isolation and characterization of fish-gut bacillus spp. as source of natural antimicrobial compounds to fight aquaculture bacterial diseases. *Mar. Biotechnol.* 23 (2), 276–293. doi: 10.1007/s10126-021-10022-x

Sharifuzzaman, S., Rahman, H., Austin, D. A., and Austin, B. (2018). Properties of probiotics kocuria SM1 and rhodococcus SM2 isolated from fish guts. *Probiotics. antimicrob. proteins.* 10 (3), 534–542. doi: 10.1007/s12602-017-9290-x

Shinde, T., Vemuri, R., Shastri, M. D., Perera, A. P., Tristram, S., Stanley, R., et al. (2019). Probiotic bacillus coagulans MTCC5856 spores exhibit excellent *in vitro* functional efficacy in simulated gastric survival, mucosal adhesion and immunomodulation. *J. Funct. foods.* 52, 100–108. doi: 10.1016/j.jff.2018.10.031

Verschuere, L., Rombaut, G., Sorgeloos, P., and Verstraete, W. (2000). Probiotic bacteria as biological control agents in aquaculture. *Microbiol. Mol. Biol. Rev.* 64 (4), 655–671. doi: 10.1128/MMBR.64.4.655-671.2000

Yamashita, M. M., Ferrarezi, J. V., GdV, P., Bandeira, G., Côrrea da Silva, B., SA, P., et al. (2020). Autochthonous vs allochthonous probiotic strains to rhamdia quelen. *MicrobialPathogenesis* 139, 103897. doi: 10.1016/j.micpath.2019.103897

Yılmaz, S., Yılmaz, E., Dawood, M. A., Ringø, E., Ahmadifar, E., and Abdel-Latif, H. M. (2021). Probiotics, prebiotics, and synbiotics used to control vibriosis in fish: A review. *Aquaculture* 737514, 73–75. doi: 10.1016/j.aquaculture.2021.737514

Zhou, S., Song, D., Zhou, X., Mao, X., Zhou, X., Wang, S., et al. (2019). Characterization of bacillus subtilis from gastrointestinal tract of hybrid hulong grouper (Epinephelus fuscoguttatus× e. lanceolatus) and its effects as probiotic additives. *Fish. shellfish. Immunol.* 84, 1115–1124. doi: 10.1016/j.fsi.2018.10.058

Zhou, Z., Yao, B., Romero, J., Waines, P., Ringø, E., Emery, M., et al. (2014). "Methodological approaches used to assess fish gastrointestinal communities," in *Aquaculture nutrition: gut health, probiotics and prebiotics Oxford*, vol. 101. (Wiley-Blackwell Publishing), 27. doi: 10.1002/9781118897263.ch5

Advantages of publishing in Frontiers

OPEN ACCESS
Articles are free to read for greatest visibility and readership

FAST PUBLICATION
Around 90 days from submission to decision

HIGH QUALITY PEER-REVIEW
Rigorous, collaborative, and constructive peer-review

TRANSPARENT PEER-REVIEW
Editors and reviewers acknowledged by name on published articles

Frontiers
Avenue du Tribunal-Fédéral 34
1005 Lausanne | Switzerland

Visit us: www.frontiersin.org
Contact us: frontiersin.org/about/contact

REPRODUCIBILITY OF RESEARCH
Support open data and methods to enhance research reproducibility

DIGITAL PUBLISHING
Articles designed for optimal readership across devices

FOLLOW US
@frontiersin

IMPACT METRICS
Advanced article metrics track visibility across digital media

EXTENSIVE PROMOTION
Marketing and promotion of impactful research

LOOP RESEARCH NETWORK
Our network increases your article's readership